

Smart Innovation, Systems and Technologies 202

Yuzo Iano · Rangel Arthur ·  
Osamu Saotome · Guillermo Kemper ·  
Ana Carolina Borges Monteiro *Editors*



# Proceedings of the 5th Brazilian Technology Symposium

Emerging Trends, Issues, and Challenges  
in the Brazilian Technology, Volume 2

AES  
International

 Springer

# **Smart Innovation, Systems and Technologies**

Volume 202

## **Series Editors**

Robert J. Howlett, Bournemouth University and KES International,  
Shoreham-by-sea, UK

Lakhmi C. Jain, Faculty of Engineering and Information Technology,  
Centre for Artificial Intelligence, University of Technology Sydney,  
Sydney, NSW, Australia

The Smart Innovation, Systems and Technologies book series encompasses the topics of knowledge, intelligence, innovation and sustainability. The aim of the series is to make available a platform for the publication of books on all aspects of single and multi-disciplinary research on these themes in order to make the latest results available in a readily-accessible form. Volumes on interdisciplinary research combining two or more of these areas is particularly sought.

The series covers systems and paradigms that employ knowledge and intelligence in a broad sense. Its scope is systems having embedded knowledge and intelligence, which may be applied to the solution of world problems in industry, the environment and the community. It also focusses on the knowledge-transfer methodologies and innovation strategies employed to make this happen effectively. The combination of intelligent systems tools and a broad range of applications introduces a need for a synergy of disciplines from science, technology, business and the humanities. The series will include conference proceedings, edited collections, monographs, handbooks, reference books, and other relevant types of book in areas of science and technology where smart systems and technologies can offer innovative solutions.

High quality content is an essential feature for all book proposals accepted for the series. It is expected that editors of all accepted volumes will ensure that contributions are subjected to an appropriate level of reviewing process and adhere to KES quality principles.

Indexed by SCOPUS, EI Compendex, INSPEC, WTI Frankfurt eG, zbMATH, Japanese Science and Technology Agency (JST), SCImago, DBLP.

All books published in the series are submitted for consideration in Web of Science.

More information about this series at <http://www.springer.com/series/8767>

Yuzo Iano · Rangel Arthur ·  
Osamu Saotome · Guillermo Kemper ·  
Ana Carolina Borges Monteiro  
Editors

# Proceedings of the 5th Brazilian Technology Symposium

Emerging Trends, Issues, and Challenges  
in the Brazilian Technology, Volume 2

 Springer


*Editors*

Yuzo Iano  
School of Electrical and Computer  
Engineering  
UNICAMP  
Limeira, São Paulo, Brazil

Rangel Arthur  
School of Technology  
UNICAMP  
Campinas, São Paulo, Brazil

Osamu Saotome  
Divisão de Engenharia Eletrônica  
Instituto Tecnológico de Aeronáutica  
São José dos Campos, São Paulo, Brazil

Guillermo Kemper  
Universidad Peruana de Ciencias Aplicada  
Lima, Peru

Ana Carolina Borges Monteiro   
School of Electrical and Computer  
Engineering  
UNICAMP  
Campinas, Brazil

*Associate-Editors*

Reinaldo Padilha França  
School of Electrical and Computer  
Engineering  
UNICAMP  
Campinas, São Paulo, Brazil

Diego Pajuelo Castro  
School of Electrical and Computer  
Engineering  
UNICAMP  
Campinas, São Paulo, Brazil

ISSN 2190-3018

ISSN 2190-3026 (electronic)

Smart Innovation, Systems and Technologies

ISBN 978-3-030-57565-6

ISBN 978-3-030-57566-3 (eBook)

<https://doi.org/10.1007/978-3-030-57566-3>

© The Editor(s) (if applicable) and The Author(s), under exclusive license to Springer Nature Switzerland AG 2021

This work is subject to copyright. All rights are solely and exclusively licensed by the Publisher, whether the whole or part of the material is concerned, specifically the rights of translation, reprinting, reuse of illustrations, recitation, broadcasting, reproduction on microfilms or in any other physical way, and transmission or information storage and retrieval, electronic adaptation, computer software, or by similar or dissimilar methodology now known or hereafter developed.

The use of general descriptive names, registered names, trademarks, service marks, etc. in this publication does not imply, even in the absence of a specific statement, that such names are exempt from the relevant protective laws and regulations and therefore free for general use.

The publisher, the authors and the editors are safe to assume that the advice and information in this book are believed to be true and accurate at the date of publication. Neither the publisher nor the authors or the editors give a warranty, expressed or implied, with respect to the material contained herein or for any errors or omissions that may have been made. The publisher remains neutral with regard to jurisdictional claims in published maps and institutional affiliations.

This Springer imprint is published by the registered company Springer Nature Switzerland AG  
The registered company address is: Gewerbestrasse 11, 6330 Cham, Switzerland

# Committees

## Organizing and Executive Committee

Yuzo Iano, LCV/DECOM/FEEC/UNICAMP, General Chair BTSym & WSGE  
Osamu Saotome, ITA, Associate-General Chair BTSym  
Rangel Arthur, FT/UNICAMP, Vice-General Chair BTSym  
Carlos Arturo Raymundo Ibáñez, UPC, Associate-General Chair BTSym  
Guillermo Leopoldo Kemper Vásquez, UPC, Associate-General Chair BTSym  
Fernando Hashimoto, DMU/UNICAMP, Associate-General Chair BTSym  
Rogério Bazi, PUC-Campinas, Associate-General Chair BTSym  
Gabriel Gomes de Oliveira, LCV/DECOM/FEEC/UNICAMP, Technical Program  
and Finance Chair  
Ana Carolina Borges Monteiro, LCV/DECOM/FEEC/UNICAMP, Proceedings  
Chair  
Reinaldo Padilha França, LCV/DECOM/FEEC/UNICAMP, Proceedings Chair  
Telmo Cardoso Lustosa, LCV/DECOM/FEEC/UNICAMP, Local Arrangements  
Chair  
Alysson Gomes de Oliveira, LCV/DECOM/FEEC/UNICAMP, Marketing Chair  
Diego Arturo Pajuelo Castro, LCV/DECOM/FEEC/UNICAMP, Proceedings Chair  
David Minango, LCV/DECOM/FEEC/UNICAMP, Registration Chair  
Lisber Arana, LCV/DECOM/FEEC/UNICAMP, Institutional Relationship Chair  
Alex R. Ruelas, LCV/DECOM/FEEC/UNICAMP, Institutional Relationship Chair  
Abel Dueñas Rodríguez, LCV/DECOM/FEEC/UNICAMP, Media Chair

## Scientific and Academic Committee

Osamu Saotome, ITA  
Luiz César Martini, DECOM/FEEC/UNICAMP  
David Bianchini, PUC-Campinas

Luis Geraldo Pedroso Meloni, DECOM/FEEC/UNICAMP  
 Ana Cláudia Seixas, PUC-Campinas Cláudia Seixas  
 Cristiano Akamine, Universidade Presbiteriana Mackenzie PUC-Campinas  
 Celso Iwata Frison, PUC/Minas-Poços de Caldas  
 Luiz Vicente Figueira de Mello Filho, Universidade Presbiteriana Mackenzie  
 Guillermo Leopoldo Kemper Vásquez, USMP & UNI-INICTEL  
 Lia Toledo Moreira Mota, PUC-Campinas  
 Lucas Heitzmann Gabrielli, DECOM/FEEC/UNICAMP  
 Edgard Luciano Oliveira da Silva, EST/UEA  
 Talía Simões dos Santos, FT/UNICAMP  
 Janito Vaqueiro Ferreira, DMC/FEM/UNICAMP  
 Vlademir de Jesus Silva Oliveira, UNEMAT/Sinop  
 Navid Razmjoo, Tafresh University, Tafresh, Iran  
 Hugo Enrique Hernandez Figueroa, DECOM/FEEC/UNICAMP  
 Antônio José da Silva Neto, IPRJ/UERJ  
 Bruno Sanches Masiero, DECOM/FEEC/UNICAMP  
 Marcos Antonio do Nascimento Guimarães, UNIP/CAMPINAS, JUNDIAÍ  
 Alessandra Akkari, Universidade Presbiteriana Mackenzie  
 Maria Thereza de Moraes Gomes Rosa, Universidade Presbiteriana Mackenzie  
 Angela del Pilar Flores Granados, FEA/UNICAMP  
 Paolo Bacega, Faculdade Anhanguera  
 Marcos Fernando Espindola, IFSP São Paulo  
 Polyane Alves Santos, Instituto Federal Da Bahia  
 Vicente Idalberto Becerra Sablón, USF/UNIMEP  
 Grimaldo Wilfredo Quispe Santivañez, UNAAT, Tarma, Perú  
 Jessie Leila Bravo Jaico, UNPRG, Lambayeque, Perú  
 Ernesto Karlo Celi Arévalo, UNPRG, Lambayeque, Perú  
 Nestor Adolfo Mamani Macedo - UNMSM, Lima, Perú  
 Luz María Paucar-Menacho, UNS, Ancash, Perú  
 Edwin Alberto Valencia Castillo, UNC, Cajamarca, Perú  
 Christian Del Carpio, UPC, Lima, Perú  
 Gustavo Huaman Bustamante, Inictel/UNI, Lima, Perú  
 Itamar Salazar Reque, Inictel/UNI, Lima, Perú

## **Technical Reviewers Committee**

Rangel Arthur, INOVA/FT/UNICAMP  
 Ana Carolina Borges Monteiro, LCV/DECOM/FEEC/UNICAMP  
 Reinaldo Padilha França, LCV/DECOM/FEEC/UNICAMP  
 Adão Boava - Universidade Federal de Santa Catarina, UFSC  
 Amilton Lamas, PUC-Campinas  
 Agord de Matos Pinto Júnior, DESIF/FEEC/UNICAMP  
 Angela del Pilar Flores Granados, FEA/UNICAMP

Joaquim Marcos Santa Rita da Silva, Instituto Nacional de Telecomunicações  
Alysson Gomes de Oliveira, LCV/DECOM/FEEC/UNICAMP  
José Alexandre Nalon, Centro Universitário Salesiano São Paulo, UNISAL  
Murilo Cesar Perin Briganti, LCV/DECOM/FEEC/UNICAMP  
Luigi Ciambarella Filho, Universidade Veiga de Almeida/Develop Biotechnology  
Lucas Alves, LCV/DECOM/FEEC/UNICAMP  
Ingrid Araujo Sampaio, Universidade Estadual de Campinas  
Denise Helena Lombardo Ferreira, PUC-Campinas  
Hermes José Loschi, LCV/DECOM/FEEC/UNICAMP  
Daniel Rodrigues Ferraz Izario, LCV/DECOM/FEEC/UNICAMP  
Mariana Carvalho, DCA/FEEC/UNICAMP  
Diego Pajuelo, LCV/DECOM/FEEC/UNICAMP  
Douglas Aguiar do Nascimento, LCV/DECOM/FEEC/UNICAMP  
Edson José Gonçalves, LCV/DECOM/FEEC/UNICAMP  
Alessandra Akkari, Universidade Presbiteriana Mackenzie  
Polyane Alves Santos, Instituto Federal Da Bahia  
Kelem Christine Pereira Jordão, LCV/DECOM/FEEC/UNICAMP  
Josué Marcos de Moura Cardoso, LCV/DECOM/FEEC/UNICAMP  
Giovanni Moura de Holanda, FITec, Technological Innovations, Brazil  
Euclides Lourenço Chuma, LCV/DECOM/FEEC/UNICAMP  
Gabriel Gomes de Oliveira, LCV/DECOM/FEEC/UNICAMP  
José Yauri, DCA/FEEC/UNICAMP  
Julío Humberto León Ruiz, LCV/DECOM/FEEC/UNICAMP  
Navid Razmjoo, Tafresh University, Tafresh, Iran  
Antônio José da Silva Neto, IPRJ/UERJ  
Raphael Ronald, CTI (Centro de Tecnologia da Informação)  
Raquel Jahara Lobosco, UFRJ/Macaé  
Necasio Gomes Costa, UFRJ  
Claudia Maria Moraes Santos, UNIVAP  
Vitor Chaves de Oliveira, IFSP São Paulo/Mackenzie  
Gustavo Mesones, UPC, Lima, Perú  
Julio Ronceros, UPC, Lima, Perú  
Kalun Lau, UPC, Lima, Perú  
Manuel Márquez, UPC, Lima, Perú  
Mirko Klusmann, UPC, Lima, Perú  
Nikolai Vinces Ramos, UPC, Lima, Perú  
Sergio Salas, UPC, Lima, Perú

## **Sponsor**

Beta Telecommunications



# Foreword

It is with great satisfaction that I write this foreword to the book, Proceedings of the 5th Brazilian Technology Symposium (BTSym'19), held at the Mackenzie Presbyterian University, SP, Brazil, in October 2019. This event is in its fifth edition and has consolidated to become an excellent opportunity for researchers, teachers, and students to present and discuss the results of their research works.

The 2019 edition of BTSym is characterized by the broad scope of exposed areas, with papers dealing with current and important topics for Brazilian and world technological development, including subjects related to the various branches of human, engineering, smart and sustainable future of cities, architecture, biomedical, and computer science.

Events such as BTSym are an essential part of the research and innovation process. Firstly, these events contribute to the promotion of research activities, which are key to a country's technological development. The dissemination of research results, as promoted by BTSym, contributes to the transformation of research findings into technological innovation. In addition, these events facilitate the sharing of findings, eventually leading to the formation of research networks, which accelerate the achievement of new results.

Therefore, I congratulate the BTSym General Chair, Prof. Dr. Yuzo Iano, and his group of collaborators for the important initiative of organizing the BTSym 2019 and for providing the opportunity for authors to present their work to a wide audience through this publication.

Finally, I congratulate the authors for the high-quality research papers and scientific experiments presented in this proceedings.

Reinaldo Padilha França  
Researcher and Associate-Editor  
University of Campinas  
Campinas, Brazil

# Preface

This book contains the Proceedings of the 5th Brazilian Technology Symposium, an event held in Campinas, SP, Brazil, in October 2019. This book was divided into two parts: the first part on Emerging Trends in Health, Natural and Physical Sciences and the second part on Emerging Trends in Humans and Urban Sciences.

The Brazilian Technology Symposium is an excellent forum for presentations and discussions of the latest results of projects and development research, in several areas of knowledge, in scientific and technological scope, including smart designs, sustainability, inclusion, future technologies, architecture and urbanism, computer science, information science, industrial design, aerospace engineering, agricultural engineering, biomedical engineering, civil engineering, control, and automation engineering, production engineering, electrical engineering, mechanical engineering, naval and oceanic engineering, nuclear engineering, chemical engineering, probability, and statistics.

This event seeks to bring together researchers, students, and professionals from the industrial and academic sectors, seeking to create and/or strengthen the linkages between issues of joint interest. Participants were invited to submit research papers with methodologies and results achieved in scientific level research projects, completion of course work for graduation, dissertations, and theses.

The 56 full chapters accepted for this book were selected from 210 submissions, and in each case, the authors were shepherded by an experienced researcher, with a rigorous peer review process. Among the main topics covered in this book, we can highlight health, medicine, chemistry, physics, physiology, cytology, histology, hematology, gynecology, virology, dermatology, pathology, health care, molecular biology, microbiology, biochemistry, biomedicine, clinical analysis, diagnostic methods, people management, ergonomics, agriculture, agronomy, food, fuel, transport, bioeconomics, natural resources, environment, energy, hydraulics, technology, languages, statistical methods, digital image processing, digital signal

processing, CNN, deep learning, e-Health, m-Health, simulation, IoT, telemedicine, wearable technology, artificial intelligence, and much more.

We hope you enjoy and take advantage of this book and feel motivated to submit your papers in future to Brazilian Technology Symposium.

Campinas, Brazil

Ana Carolina Borges Monteiro  
Proceedings Chair of Brazilian Technology Symposium

# Acknowledgments

Our appreciation goes to a lot of colleagues and friends who assisted in the development of this book, Proceedings of the 5th Brazilian Technology Symposium (BTSym'19).

First of all, I would like to thank all the members of the Organizing and Executive Committee, for the commitment throughout the year, several meetings were held, and many challenges were overcome for the accomplishment of the BTSym 2019.

Also, and with great merit, I would like to thank all the members of the Scientific and Academic Committee and Technical Reviewers Committee, for their excellent work, which was essential to ensure the quality of our peer review process, and collaborating with the visibility and technical quality of the BTSym 2019.

The Brazilian Technology Symposium is an event created by the Laboratory of Visual Communications of the Faculty of Electrical and Computer Engineering of the University of Campinas (UNICAMP). In this way, I would like to thank the Mackenzie Presbyterian University, especially for the support and hosting of the BTSym 2019, which was critical for the success of their accomplishment.

Beta Telecommunications played a crucial role in holding the BTSym 2019, in the same way as the Pro-Rector of Extension and Culture at the University of Campinas, especially Prof. Fernando Augusto de Almeida Hashimoto, due to financial support from it, and it was possible to consolidate with quality many BTSym 2019 organization aspects, which ensured the quality to support the authors and speakers.

Finally, I thank all the authors for their participation in the BTSym 2019. I sincerely hope to have provided an experience that was very useful and enriching in the personal and professional lives of everyone, and my special thanks go to Prof. Rangel Arthur. Due to the continuous support in activities that enrich the academic environment through research directed to innovative technological development.

He is a generous, charismatic, dedicated, determined, and fair person, being an excellent fellow in academic research that certainly contributes a lot to BTSym, who has a lot to thank Prof Rangel Arthur for.

Prof. Yuzo Iano  
General Chair of Brazilian Technology Symposium

# Contents

<b>Emerging Trends in Health, Natural and Physical Sciences</b>	
<b>Algorithm Oriented to the Detection of the Level of Blood Filling in Venipuncture Tubes Based on Digital Image Processing . . . . .</b>	<b>3</b>
Jorge Castillo, Nelson Apfata, and Guillermo Kemper	
<b>Computational Fluid Dynamics Analysis of Blood Rheology . . . . .</b>	<b>17</b>
Guilherme S. Souza, Enzo D. Giustina, Marcus V. Carvalho, and Raquel J. Lobosco	
<b>Wearable Technology for Presumptive Diagnosis of High Blood Pressure Based on Risk Factors . . . . .</b>	<b>25</b>
Eithel Josue Meza Prada, Helgar Miguel Angel Herrera Agullar, Jimmy Armas-Aguirre, and Paola A. Gonzalez	
<b>Cytology and Hematology: A Review of the Fundamental Principles . . .</b>	<b>35</b>
Ana Carolina Borges Monteiro, Yuzo Iano, Reinaldo Padilha França, and Rangel Arthur	
<b>Hematology: A Review of the Main Methodologies of Clinical Analyses . . . . .</b>	<b>49</b>
Ana Carolina Borges Monteiro, Yuzo Iano, Reinaldo Padilha França, and Rangel Arthur	
<b>An Algorithm Oriented at Obtaining the Molecular Weight and Concentration of DNA Samples in Agarose Gel Images . . . . .</b>	<b>61</b>
Christian del Carpio, Marcelo Garcia, Julio Elías, David Laván, and Guillermo Kemper	
<b>Classification of Dermoscopy Skin Images with the Application of Deep Learning Techniques . . . . .</b>	<b>73</b>
Pablo David Minango Negrete, Yuzo Iano, Ana Carolina Borges Monteiro, Reinaldo Padilha França, Gabriel Gomes de Oliveira, and Diego Pajuelo	

**Association Between Human Papillomavirus Infection and Anus Cancer Precursor Lesions: A Review . . . . . 83**  
 Ana Carolina Borges Monteiro, Yuzo Iano, Reinaldo Padilha França, Rangel Arthur, Pablo David Minango Negrete, Diego Pajuelo, Gabriel Gomes de Oliveira, and Lisber Arana Hisnostroza

**A New Approach for ECG Recording in Rats: An Autonomic Nervous System Analysis . . . . . 91**  
 Raphael Santos do Nascimento, Fernando da Silva Fiorin, Adair Roberto Soares Santos, Luiz Fernando Freire Royes, and Jefferson Luiz Brum Marques

**Algorithm for Detection of Raising Eyebrows and Jaw Clenching Artifacts in EEG Signals Using Neurosky Mindwave Headset . . . . . 99**  
 Luis Vélez and Guillermo Kemper

**Correspondence Between TOVA Test Results and Characteristics of EEG Signals Acquired Through the Muse Sensor in Positions AF7–AF8 . . . . . 111**  
 Ober Castillo, Simy Sotomayor, Guillermo Kemper, and Vincent Clement

**Mobile Robot to Assist in Therapies for Children with Autism . . . . . 121**  
 Madai Keila Taype Mateo and Grimaldo Wilfredo Quispe Santivañez

**A Smart Home Control Prototype Using a P300-Based Brain–Computer Interface for Post-stroke Patients . . . . . 131**  
 Sergio A. Cortez, Christian Flores, and Javier Andreu-Perez

**Electronic Ecomap as an Instrument to Improve Physician–Family Interaction in Preventive Medicine . . . . . 141**  
 Néstor Mamani-Macedo, Julio Raime, Luzmila Pro, Jaime Pariona, and Olga Solano

**Intelligent Management Model in an IoT Environment Applied for the Healthcare Sector . . . . . 149**  
 Jessie Bravo and Roger Alarcón

**Evaluation Method of Variables and Indicators for Surgery Block Process Using Process Mining and Data Visualization . . . . . 159**  
 Piero Rojas-Candio, Arturo Villantoy-Pasapera, Jimmy Armas-Aguirre, and Santiago Aguirre-Mayorga

**A Technological Solution to Identify the Level of Risk to Be Diagnosed with Type 2 Diabetes Mellitus Using Wearables . . . . . 169**  
 Daniela Nuño, Ernesto Rodríguez, Jimmy Armas, and Paola Gonzalez

**Mamey Apple Peel for Cr<sup>3+</sup> Removal from Contaminated Waters . . . . . 177**  
 Nathali Cotrina and Ricardo Vejarano

**Method of Estimating River Levels with Reflective Tapes Using Artificial Vision Techniques** . . . . . 191  
 Lidia E. López Huamán, Marco Paul E. Apolinario Lainez, and Samuel G. Huamán Bustamante

**Design and Implementation of a Hydro-Energetic System in Water Distribution Networks** . . . . . 201  
 Lenin Jiménez, Cecilia Luna, Manuel Quiñones-Cuenca, and Holger Benavides

**Hydraulic Fill Assessment Model Using Weathered Granitoids Based on Analytical Solutions to Mitigate Rock Mass Instability in Conventional Underground Mining** . . . . . 215  
 Cristhian Portocarrero-Urdanivia, Angela Ochoa-Cuentas, Luis Arauzo-Gallardo, and Carlos Raymundo

**A Study on Investigations Carried Out in Dams from the Perspective of Risk Analysis** . . . . . 225  
 Gabriel Gomes de Oliveira, Yuzo Iano, Ana Carolina Borges Monteiro, Reinaldo Padilha França, Diego Pajuelo, and Pablo David Minango Negrete

**Numerical Simulation of Hydrodynamic Conditions in Rivers Facing Extreme Events Due to the “El Niño” Phenomenon** . . . . . 235  
 Gabriela Alvarez, Alvaro Moreno, Emanuel Guzmán, and Sissi Santos

**Dynamic Amplification Factor Proposal for Seismic Resistant Design of Tall Buildings with Rigid Core Structural System** . . . . . 245  
 Eder Quezada, Yaneth Serrano, and Guillermo Huaco

**A Mechanical Development of a Dry Cell to Obtain HHO from Water Electrolysis** . . . . . 257  
 Gustavo Salazar, Wilmer Solis, and Leonardo Vines

**An Automated System for the Stage of Hydrolysis and Filtration in the Extraction of Pectin from the Cocoa Shell** . . . . . 267  
 Maritza Ccencho, Valeria Quijada, and Leonardo Vines

**Automatic Leaf Segmentation from Images Taken Under Uncontrolled Conditions Using Convolutional Neural Networks** . . . . . 277  
 Itamar Franco Salazar-Reque and Samuel Gustavo Huamán Bustamante

**Method of Anomalies Detection in Persea Americana Leaves with Thermal and NGRDI Imagery** . . . . . 287  
 Bruno D. Rivadeneyra Bustamante and Samuel G. Huamán Bustamante

**Development of a Machine to Control the Level of Washing in Panca Chili Seeds** . . . . . 297  
 Anthony De La Cruz, Jaime Cardenas, and Leonardo Vines



<b>Bacteriological Contaminants Detection in Some Consumed Raw Vegetables Based on Spectrometry in Ayacucho Town, Peru</b> . . . . .	309
José Yauri, Manuel Lagos, Rousell Vidalón, Julio Cárdenas, Kay Jerí, Lisber Arana, and Yuzo Iano	
<b>Feasibility in Using Banana Flour in Bread Production: Centesimal and Sensory Analysis</b> . . . . .	321
Nathália Rafaela Santos de Carvalho, Maria Thereza de Moraes Gomes Rosa, Isabela Francabandiera Tornizielo, and Daniela Helena Pelegrine Guimarães	
<b>Spectral Behavior of Maize, Rice, Soy, and Oat Crops Using Multi-spectral Images from Sentinel-2</b> . . . . .	327
Lady Angulo and Sergio Pamboukian	
<b>Emerging Trends in Humans and Urban Sciences</b>	
<b>Production Process of Bioethanol Fuel Using Supported <i>Saccharomyces Cerevisiae</i> Cells</b> . . . . .	339
L. C. Fardelone, T. S. Bella de Jesus, G. P. Valença, J. R. Nunhez, J. A. R. Rodrigues, and P. J. S. Moran	
<b>An Automatic Biodiesel Decanting System for the Optimization of Glycerin Separation Time by Applying Electric Field and Temperature</b> . . . . .	349
Kevin Bulnes, Diego Paredes, and Leonardo Vincés	
<b>Prototype Proposal for Control and Inspection of Gas Stations</b> . . . . .	357
Lucas Eder de Araújo Sousa, Felipe Silveira Stopiglia, Luiz Vicente Figueira de Mello Filho, Daniela Helena Pelegrine Guimarães, and Maria Thereza de Moraes Gomes Rosa	
<b>Modeling of Solid-Liquid Equilibrium in Nitrobenzene and Para-Xylene Mixtures</b> . . . . .	367
Michelli Fontana, Caroline dos Santos Ribas, Paulo Henrique Schuck, Rafael Lopes Turino, and André Zuber	
<b>X-Ray Characterization of TiO<sub>2</sub> Obtained by Chemical Route for Photocatalysis</b> . . . . .	377
Tiago Siqueira Lima, Wesley Rafael Penteadó, André Luis de Castro Peixoto, and Ademir Geraldo Cavallari Costalonga	
<b>Co-authors Networks in Adsorption Refrigeration and Air-Conditioning with Solar Energy</b> . . . . .	383
Carla Abregú Marcos, Abraham Soplá Maslucán, Miguel Cano Lengua, and José C. Alvarez	

**Microsimulation of Public Transport Stops for the Optimization of Waiting Times for Users Using the Social Force Model . . . . .** 391  
Francis Mendoza, Mayling Tong, Manuel Silvera,  
and Fernando Campos

**Mathematical Model for the Improvement of Vertical Traffic at Universities . . . . .** 401  
Julio C. Lazo Lozano and Grimaldo Wilfredo Quispe Santivañez

**A Novel Dataset for the Transport Sector in a Province of Peru . . . . .** 409  
Miguel Arango Guerrero and Pedro Shiguihara Juárez

**Development of a Mobile Application for English Language Learning Through Corrective Feedback . . . . .** 417  
Adriana Guanuche, Gustavo Caiza, Osana Eiriz, and Roberto Espí

**Influence of the Chinese Culture on the Negotiation Process Peru-China . . . . .** 427  
Nicole Alexandra Acevedo Cueva

**Phone Calls Speech-to-Text: A Comparison Between APIs for the Portuguese Language . . . . .** 437  
Nilton M. Iinuma and Massaki de O. Igarashi

**Production of Cantonese Lexical Tones by Native Speakers of Brazilian Portuguese: A Comparative Analysis . . . . .** 447  
João Vítor Possamai de Menezes and Adriano Vilela Barbosa

**Smart Campus IoT Guidance System for Visitors Based on Bayesian Filters . . . . .** 463  
Alvaro Aspilcueta Narvaez, Dennis Núñez Fernández,  
Segundo Gamarra Quispe, and Domingo Lazo Ochoa

**Research of the Academic Performance of University Students Through Statistical Models . . . . .** 473  
Olga Solano Dávila, Luis Nuñez Lira, Olga Bolaños Solano,  
and Néstor Mamani-Macedo

**Model of Sustainable Digital Transformation Focused on Organizational and Technological Culture for Academic Management in Public Higher Education . . . . .** 483  
Jessie Bravo, Janet Aquino, Roger Alarcón, and Nilton Germán

**University of Brasilia’s Potential for Bioeconomy Services and Innovation . . . . .** 493  
Flávio Duque Estrada Soares Pereira and Wagner Augusto Fischer

**A Proposal for Modeling of the Management of Talent Recruitment and Training in Peruvian Sports Centers . . . . .** 505  
Arturo Laredo, Luzmila Pro Concepcion, and Nestor Mamani-Macedo

**Mentoring Process: An Assessment of Career, Psychosocial Functions and Mentor Role Model . . . . . 515**  
Neusa Maria Bastos Fernandes dos Santos, Mariana Juer,  
Igor Polezi Munhoz, Alessandra Cristina Santos Akkari,  
Rodrigo Guimarães Motta, and Marianna Konyosi Miyashiro

**Compensation Program: A Quantitative Study of the Top Management Team’s Level of Knowledge and Satisfaction . . . . . 527**  
Neusa Maria Bastos Fernandes dos Santos, Rafael Maia Chagas,  
Alessandra Cristina Santos Akkari, Igor Polezi Munhoz,  
Fernando Fukunaga, and Ligia Kaori Matsumoto Hirano

**Physical Ergonomics Applied to the Administrative Sector and the Factory Floor: The Case of a Food Industry . . . . . 537**  
Kélvyn Santos Aguiar, Maria Thereza de Moraes Gomes Rosa,  
Luiz Vicente Figueira de Mello Filho, João Carlos Gabriel,  
and Alessandra Cristina Santos Akkari

**Evaluation of Illuminance in Workplace: A Case Study on the Production of Multicolored Self-adhesive . . . . . 547**  
Wellingtânia Domingos Dias, Taciana Ramos Luz,  
and Meinhard Sesselmann

**Smart City: A Qualitative Reflection of How the Intelligence Concept with Effective Ethics Procedures Applied to the Urban Territory Can Effectively Contribute to Mitigate the Corruption Process and Illicit Economy Markets . . . . . 557**  
Kelem Christine Pereira Jordão, David Bianchini, Yuzo Iano,  
Ana Carolina Borges Monteiro, and Reinaldo Padilha França

**A Discussion of the Challenges Small Towns Face in Reaching the Promising Scenario of Electronic Government Intelligent Cities . . . . . 571**  
Valéria Sueli Reis, Yuzo Iano, Gabriel Gomes de Oliveira,  
Telmo C. Lustosa, Mauro A. S. Miranda, Odair dos Santos Mesquita,  
Ana Carolina Borges Monteiro, and Reinaldo Padilha França

# **Emerging Trends in Health, Natural and Physical Sciences**

# Algorithm Oriented to the Detection of the Level of Blood Filling in Venipuncture Tubes Based on Digital Image Processing



Jorge Castillo , Nelson Apfata , and Guillermo Kemper 

**Abstract** This article proposes an algorithm oriented to the detection of the level of blood filling in patients, with detection capacity in millimeters. The objective of the software is to detect the amount of blood stored into the venipuncture tube and avoid coagulation problems due to excess fluid. It also aims to avoid blood levels below that required, depending on the type of analysis to be performed. The algorithm acquires images from a camera positioned in a rectangular structure located within an enclosure, which has its own internal lighting to ensure adequate segmentation of the pixels of the region of interest. The algorithm consists of an image improvement stage based on gamma correction, followed by a segmentation stage of the area of pixels of interest, which is based on thresholding by HSI model, in addition to filtering to accentuate the contrast between the level of filling and staining, and as a penultimate stage, the location of the filling level due to changes in the vertical tonality of the image. Finally, the level of blood contained in the tube is obtained from the detection of the number of pixels that make up the vertical dimension of the tube filling. This number of pixels is then converted to physical dimensions expressed in millimeters. The validation results show an average percentage error of 0.96% by the proposed algorithm.

**Keywords** Blood draw · Filling level · Detection · Image processing · Venipuncture tube

---

J. Castillo · N. Apfata · G. Kemper (✉)  
Universidad Peruana de Ciencias Aplicadas, Av. Prolongación Primavera 2390, Santiago de Surco, Lima, Peru  
e-mail: [guillermo.kemper@upc.pe](mailto:guillermo.kemper@upc.pe)

J. Castillo  
e-mail: [u201320068@upc.edu.pe](mailto:u201320068@upc.edu.pe)

N. Apfata  
e-mail: [u201517081@upc.edu.pe](mailto:u201517081@upc.edu.pe)

## 1 Introduction

The extraction of blood either with the use of a syringe or a venipuncture tube is performed manually, which generates that the amount of blood stored is calculated empirically or visually by the extractor, which is the large percentage of clinical decisions based in laboratory tests.

The Ministry of Health of Peru (MINSA) in its Technical Health Standard of the Clinical Pathology Services Production Unit has as a general objective to establish the criteria for the organization and operation of the Clinical Pathology UPS, of public health services and private for proper management in it [1]. On the management control of the Clinical Pathology UPS, quality management policies, programs, and procedures must be developed where documents such as corrective actions, quality records, among others must be used [1]. This is the reason why the development of new ways of monitoring processes within Clinical Pathology is necessary since the laws of the Peruvian State promote them. The problem appears when the venipuncture tube is filled with excess or defect over its indicated capacity for each type of test to be performed since it must be experienced enough to be precise with the amount of blood drawn. With this problem, the entities or persons in charge of blood collection do not have control over the failures they make during the extraction or the times in which the patient was wrongly performed.

Some works related to the detection of liquid level by digital image processing (not necessarily blood) have been found in the scientific literature. In [2], it is proposed a multiple bottle filling system for industrial application, in which the liquid is filled depending on the color of the bottle. Liquids can be filled with a single system. The experimental setup is designed to fill two liquids, depending on the color of the bottles, using the Siemens S7-1200 programmable logic controller [2]. On the other hand, in [3], it is proposed a machine that estimates the automatic insulin dosing by digital image processing. The equipment allows improving the accuracy of insulin dosing in a syringe that is usually done manually and inaccurately by using an enclosure that contains an endless screw, couplers, and stepper motors. Also, we found a robot that automates blood collection by venipuncture called Veebot; this machine keeps the registration of the complete process of blood extraction, as the temporal data and images. It automates the process of blood extraction, meaning the camera seeks for the vein and extracts the blood itself; it acquires the start and end time, level of filling of the tube. This machine is not commercial and is expensive as well [4]. VenusPro by Vasculogic is a machine that does exactly the same as the Veebot, so it fulfills the same cost and commercial expectations [5].

The algorithm proposed in this work is entirely in the processing of images; the results shown at the end show that the method used obtains results consistent with those measured with a measuring instrument with sensitivity in millimeters.

## 2 Description of the Proposed Algorithm

Figure 1 shows the block diagram of the proposed detection algorithm. In general, the algorithm summary follows the following steps. The process begins with the improvement of the image of the venipuncture tube, which consists of gamma correction in order to generate greater contrast in the red, green, and blue tones. After that, the segmentation of the object or region of pixels of interest is performed; for this, the original image is transformed to the HSI model, in which a component is chosen where the background of the image and the area of pixels of interest are differentiated. Notoriously, the image component is also chosen where there is greater contrast between tube filling and bloodstain. Once segmented the object, the image is filtered, first uniformizing it and then looking for changes of hue in the vertical, and as a penultimate step, the horizontal projections are obtained to find the local maximums in this and find the position of the filling level. Finally, a conversion of the number of pixels in the vertical component into a real dimension is made.

### 2.1 Image Enhancement

For the detection of the level of filling of the tube, it is necessary to differentiate the portion of the pixel area of the tube that is blood and stain on the wall; for this, it is necessary to generate contrast in dark areas; this was obtained with the gamma correction.

#### 2.1.1 Gamma Correction

In this part, you get an image with greater contrast in the area of pixels that represents blood. The variation of the image in hue depends on the gamma factor as can be seen in Fig. 2, so an appropriate value was chosen that generates contrast in low tones.

The correction of each component is expressed as:

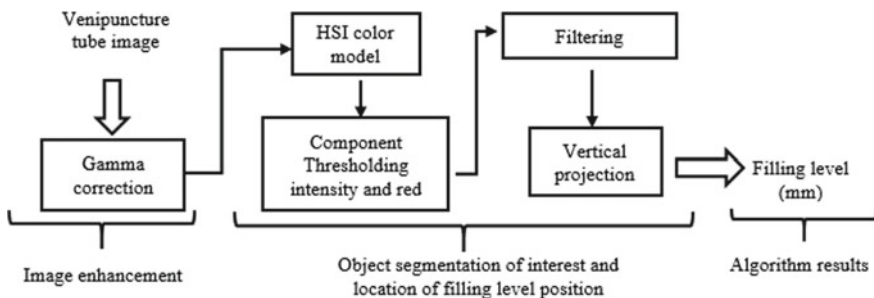


Fig. 1 Block diagram of the proposed algorithm

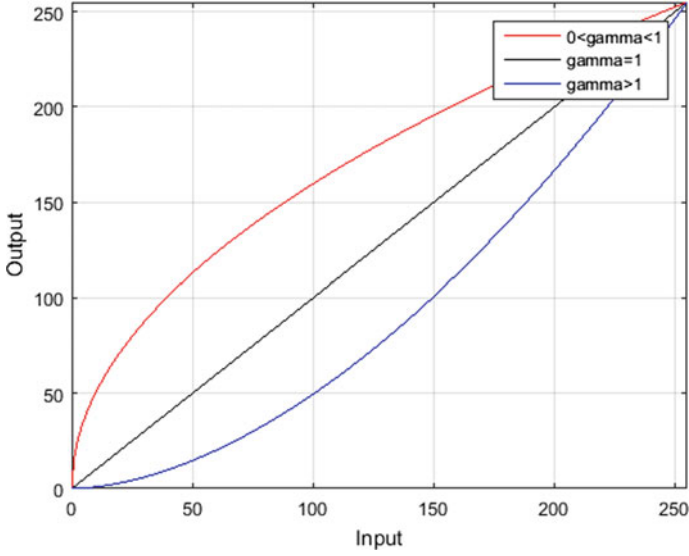


Fig. 2 Gamma correction correspondence function

$$I1'_R(x, y) = I_R(x, y)^\gamma \quad (1)$$

$$I'_R(x, y) = \text{round}\left(\frac{255 \times I1'_R(x, y)}{I1'_{R\max}}\right) \quad (2)$$

$$I1'_G(x, y) = I_G(x, y)^\gamma \quad (3)$$

$$I'_G(x, y) = \text{round}\left(\frac{255 \times I1'_G(x, y)}{I1'_{G\max}}\right) \quad (4)$$

$$I1'_B(x, y) = I_B(x, y)^\gamma \quad (5)$$

$$I'_B(x, y) = \text{round}\left(\frac{255 \times I1'_B(x, y)}{I1'_{B\max}}\right) \quad (6)$$

where  $I1'_{R\max}$ ,  $I1'_{G\max}$  y  $I1'_{B\max}$  satisfy the following conditions:

$$I1'_{R\max} \geq I'_R(x, y) \forall (x, y) \quad (7)$$

$$I1'_{G\max} \geq I'_G(x, y) \forall (x, y) \quad (8)$$

$$I1'_{B\max} \geq I'_B(x, y) \forall (x, y) \quad (9)$$



Likewise:

$I_R(x, y)$ ,  $I_G(x, y)$ ,  $I_B(x, y)$ : Image in its three red, green, and blue components respectively of the input image.

$I'_R(x, y)$ ,  $I'_G(x, y)$ ,  $I'_B(x, y)$ : Image resulting from the red, green, and blue components.

$\gamma$ : Gamma factor.

The results obtained can be visualized in Fig. 3, 4, 5 and 6 (after applying  $\gamma = 0.4$ ). The gamma value used response to the contrast tests applied for the segmentation of the venipuncture tube.



**Fig. 3** **a** Original red image component, **b** red component after gamma correction (0.4)



**Fig. 4** **a** Original green image component, **b** green component after gamma correction (0.4)



**Fig. 5** **a** Original blue image component, **b** blue component after gamma correction (0.4)



**Fig. 6** **a** Original image, **b** image after gamma correction (0.4)

## 2.2 Segmentation of Object of Interest

After obtaining an image where a contrast between what is blood and stain is visualized on the tube wall, only the part that represents blood is segmented; for this, the following steps are followed.

### 2.2.1 HSI Model

In this part, the background is separated from the area of pixels that represents the tube; for this, the transformation is carried out to the HSI model (Hue and saturation that represent the component of color and intensity that represents the lighting of the image) [6]. The results obtained can be visualized in Fig. 7.

Where the tube and the bottom differ more in the intensity component.



**Fig. 7** **a** Intensity component, **b** saturation component

### 2.2.2 Thresholding by the Intensity and Red Component

At this point, the tube is separated from the bottom based on the appropriate model in item Sect. 2.2.1 in the intensity component. Therefore, a histogram of the intensity of the image is made, which can be seen in Fig. 8.

The most coherent threshold for separating the bottom of the tube is 190, which is visualized in Fig. 8 with a marker, separating the object of interest; the bottom tube is removed in the red component in Fig. 3b where the greatest contrast between filling and stain is found in the tube; the result is displayed in Fig. 9.

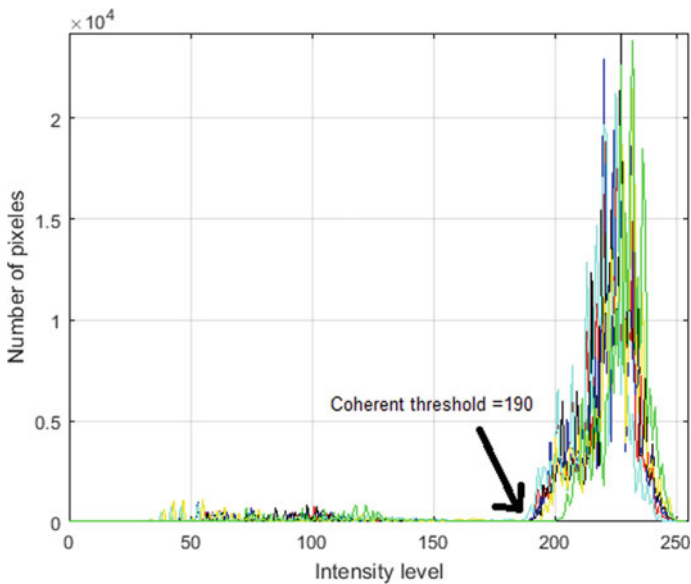


**Fig. 8** Intensity histogram of several images, with threshold indicator (190)



**Fig. 9** Resulting image after tube segmentation

### 2.2.3 Image Filtering

For this step, the image of Fig. 8 was filtered with an averaging mask  $F_{\text{mean}}$  described in the following expression [7]:

$$F_{\text{mean}} = \frac{1}{36} \times \begin{bmatrix} 1 & \dots & 1 \\ \vdots & \ddots & \vdots \\ 1 & \dots & 1 \end{bmatrix}_{6 \times 6} \quad (10)$$

After that, filtering is applied through the convolution between the image in Fig. 9 and the averaging mask  $F_{\text{mean}}$  with the aim of standardizing the areas where shades that do not belong to it (such as the light reflection) can occur by the curvature of the tube. The result of the image can be visualized in Fig. 10.

Once the filtered image is obtained, the aim is to highlight the vertical changes in the hue component. For this, a Sobel mask [8] is used, which can be expressed as:

$$M_{\text{sh}} = \begin{bmatrix} -1 & -2 & -1 \\ 0 & 0 & 0 \\ 1 & 2 & 1 \end{bmatrix} \quad (11)$$

Figure 11 shows the result of the filtering.

Since the image in Fig. 11 is not very useful in this condition, thresholding is performed. In this case, a threshold value of 5 was chosen since it allowed obtain the best results (see Fig. 12).



**Fig. 10** Image after filtering with an averaging mask



**Fig. 11** Image after applying the Sobel mask

#### 2.2.4 Horizontal Projection

Horizontal projections [9] were used to locate positions where there are changes in hue in the vertical direction of the image, which can be seen in Fig. 13. Local maximums are considered if they exceed half the maximum vertical projection because this represents half of the projection in the diameter of the tube.

Having obtained the local maximums, which in the case of Fig. 13 were in the vertical positions 181, 346 and three near 467, which can be seen with orange markers.

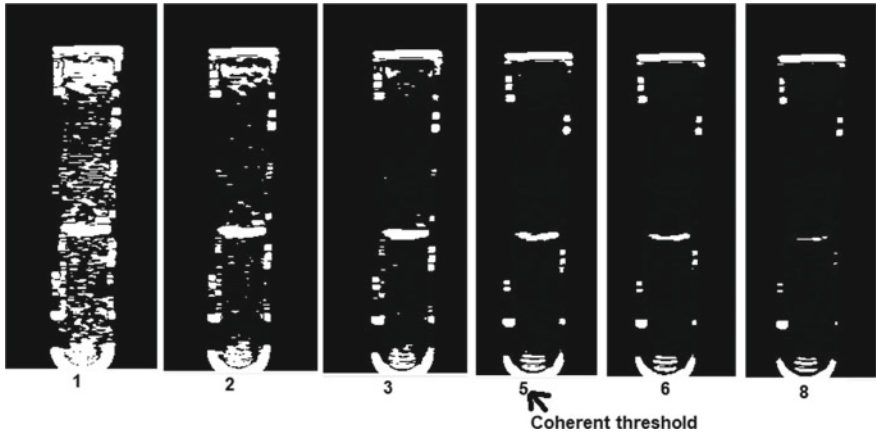


Fig. 12 Image after binarization by several thresholds

After that, the search for the local maximum that meets the following conditions is carried out. First, it should not be very close to the lower and upper position in the vertical tube. Second, we look for that position that does not have other very close local maxima such as that of Fig. 13 at the bottom; the only point that meets these conditions is at position 346 for the case, which represents the position of the fill level.

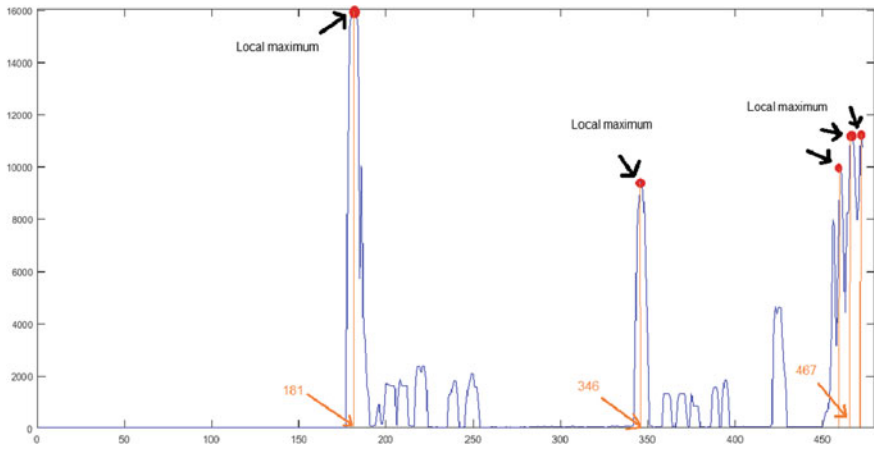


Fig. 13 Horizontal image projection with local maximum markers

### 3 Results

To obtain the filling level, the number of pixels in the vertical component is scaled to a real measurement, which follows the following expression:

$$D_{(\text{mm})} = N_{\text{pixels}} \times d_{\text{pixel}} \quad (12)$$

where

$D_{(\text{mm})}$  Tube filling level in millimeters.

$N_{\text{pixels}}$  Number of pixels in the vertical from the filling level to the bottom of the tube.

$d_{\text{pixel}}$  Dimension of a pixel in millimeters.

The validation of the proposed detection algorithm was based on measurement with a metric sensitivity instrument in millimeters since no contact can be made with the sample.

The procedure consists of detecting at the level of a blood sample tube to be able to determine if it is adequate in terms of its content for the respective laboratory tests. For this, several tests were performed for the calculation of percentage error, which is expressed as:

$$E_p = \left| \frac{V_v - V_a}{V_v} \right| \times 100\% \quad (13)$$

where

$E_p$  Percentage error

$V_v$  True value

$V_a$  Approximate value

$V_v - V_a$  Absolute error.

The result of these tests can be visualized in Fig. 14.

### 4 Conclusions

Analyzing the results, a maximum percentage error of 4.26%, average of 0.96% and a minimum of 0% were obtained, regarding the absolute error were maximum 1.96 mm, average 0.41 mm and minimum of 0 mm, based on these data, it can be indicated that the detection algorithm sometimes fails in more than 1 mm near the relative 5%, in addition, the average relative error indicates satisfactory, however, that it could be improved. The results with high errors were witnessed when the images obtained are immediately placed in an upright position, which causes the bloodstain to be very similar to the content. In summary, a blood level detection algorithm in venipuncture tubes was developed successfully with an average error of 0.96% which is considered adequate for the purpose of this investigation. On the other hand, when waiting for 4–5 s in a vertical position of the tube to obtain the image, the results were better than those obtained in the tests; given this limitation,

it is recommended to perform a vertical position vibration of the tube before image acquisition for better and faster results. It should be noted that this research is a small part of a more extensive development so that only the development of the blood level detection algorithm is explained here. The advantage of this research is that it can be used as the basis of a more complex algorithm for better image acquisition, using neural networks, among other methods.

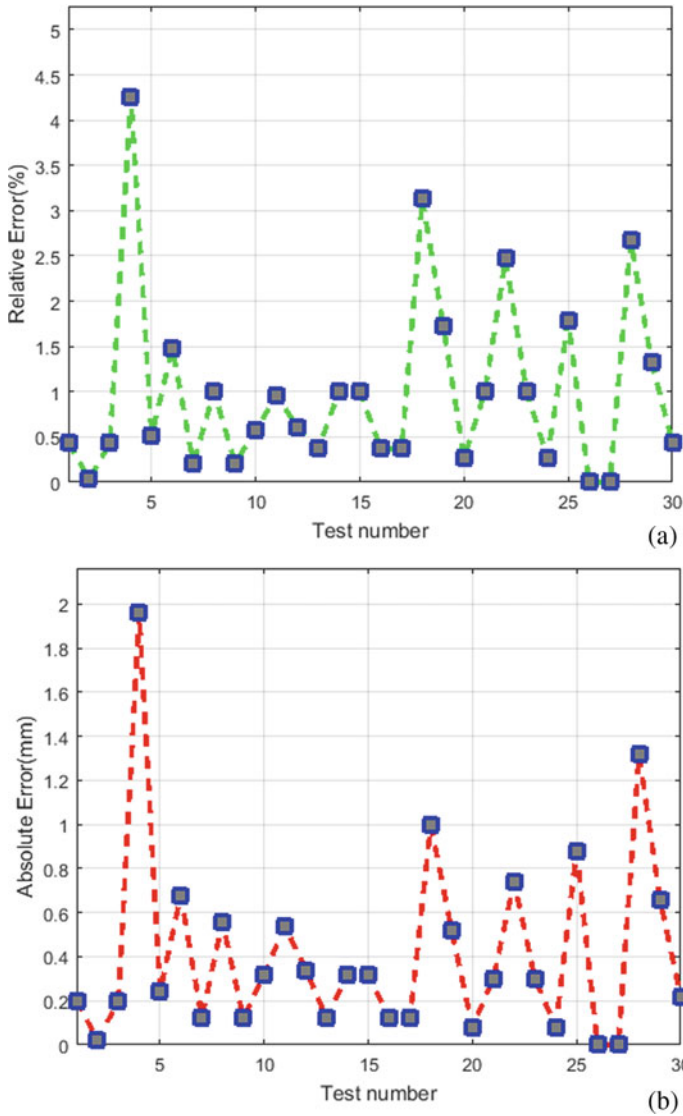


**Fig. 14** **a** Percentage error of calculation of the level of detection of the algorithm, **b** absolute error







## References

1. Peru. Ministerio de Salud. Dirección General de Salud de las Personas. Dirección de Servicios de Salud, Norma técnica de salud de la unidad productora de servicios de patología clínica. Recovered from [http://www.diresaapurimac.gob.pe/media/attachments/2018/09/07/nts\\_072\\_minsa\\_dgsp\\_upss\\_patologia\\_clinica.pdf](http://www.diresaapurimac.gob.pe/media/attachments/2018/09/07/nts_072_minsa_dgsp_upss_patologia_clinica.pdf) (2009)
2. Pannu, J., Kulkarni, R., Ranjana, M.: On the automated multiple liquid bottle filling system. In: International Conference on Circuit, Power and Computing Technologies (2016)
3. Alarcon, M., Torobeo, D., Lau, K., Kemper, G.: An electronic equipment for automatic insulin dosage based on digital image processing (2017)
4. Veebot: Robot Draws Blood. <http://www.veebot.com/solutions.html> (2019)
5. VascoLogic: VenousPro. <http://vasculogic.com/about-vasculogic.html> (2019)
6. Saravanan, G., Yamuna, G., Nandhini, S.: Real time implementation of RGB to HSV/HSI/HSL and its reverse color space models. Commun. Signal Proces. (2016)
7. Oré, G., Vasquez, A., Soto, J., Kemper, G.: Measuring the level of mildew in quinoa plantations based on digital image processing. In: Proceedings of the 3rd Brazilian Technology Symposium, Junio 2019
8. Israni, S., Jain, S.: Edge detection of license plate using Sobel operator. In: International Conference on Electrical, Electronics, and Optimization Techniques, Marzo 2016
9. Pan Z., Wang M.: A new method of shredded paper image stitching and restoration. In: Computing Technology, Intelligent Technology, Industrial Information Integration (2017)

# Computational Fluid Dynamics Analysis of Blood Rheology



Guilherme S. Souza , Enzo D. Giustina , Marcus V. Carvalho ,  
and Raquel J. Lobosco 

**Abstract** Computational fluid dynamics can be an auxiliary tool for the diagnostic and treatment of cardiovascular diseases. Thrombosis and atherosclerosis are pathologies that affect the delivery of blood to the neck and head. One of the most affected by these pathologies is the carotid sinus. The objective of this paper is to improve the accuracy of blood flow simulations, in order to avoid using in vivo experiments on developments of new technologies and treatments. To reproduce flow characteristics, the numerical model used is based on the average dimensions of many angiograms. The geometry and the correct rheological model are crucial to the fidelity of the physical phenomenon. The blood as a non-Newtonian fluid was modeled with the Casson and Carreau-Yasuda Model. Using the open-source software OpenFOAM for the numerical simulations integrating the rheoTool facilities, non-Newtonian models and Newtonian assumptions were compared.

**Keywords** Blood · Rheology · OpenFOAM · Artery

## 1 Introduction

The study of blood behavior is a fundamental field of biotechnology development. According to clinical observations, bifurcation regions and curvatures are more sensitive to pathological alterations. The carotid sinus (a region in the carotid artery where

---

G. S. Souza (✉) · E. D. Giustina · M. V. Carvalho · R. J. Lobosco  
Federal University of Rio de Janeiro, Macaé, Brazil  
e-mail: [gui.eng.santos@gmail.com](mailto:gui.eng.santos@gmail.com)

E. D. Giustina  
e-mail: [enzodellag@gmail.com](mailto:enzodellag@gmail.com)

M. V. Carvalho  
e-mail: [mvpascavalho@peb.ufrj.br](mailto:mvpascavalho@peb.ufrj.br)

R. J. Lobosco  
e-mail: [rlobosco@macae.ufrj.br](mailto:rlobosco@macae.ufrj.br)

a bifurcation occurs) is most affected by arteriosclerosis lesions [1]. Therefore, the hemodynamic study is important for a better understanding of arteriosclerosis and its relation with the blood flow [2]. In addition, it is important to mention that in vivo precise measures of some parameters are extremely difficult, such as shear rate. Consequently, numerical simulations turn in a great ally in the development of new technologies devices and research development in the area [2].

There is no consensus in which the rheological model better represents the blood viscosity due to its complex rheology. The most used fluid models are the power law, Casson, and Carreau-Yasuda [3]. Some researchers argue that the Newtonian behavior hypothesis is a good assumption [1, 4] for large arteries and the non-Newtonian behavior is more important for capillaries and small vessels. Since the shear stress in the vessel walls has great relation with atherosclerosis, it would also be relevant to investigate non-Newtonian behaviors in large arteries [2]. However, none of those models considers its viscoelasticity.

In order to improve the computational fluid dynamics, CFD, simulations of blood flow, this study reproduced some cases implemented by Carvalho [5] and integrated different boundary conditions in the rheoFoam tool, an external solver for simulating complex fluids at OpenFOAM package. This package allows a viscoelastic treatment for non-Newtonian fluids.

## 2 Methodology

### 2.1 Mesh

The similarity between the geometry model and the real artery is a crucial parameter. In this work, the geometry is based on the model used by Bharadvaj [6], Ku et al. [7], Gijssen et al. [8], which was developed by fifty-seven angiograms of twenty-two adults and thirty-five children, which such data, used in this research, come from to the studies referenced.

The flow characteristics were analyzed in the internal carotid in the regions depicted in Fig. 1; the planes S1 to S5 are divided by horizontal and vertical sections; A-A and B-B, respectively, note that the diameter of the vessel increases until its maximum value in S1, where it starts to decrease afterward.

### 2.2 Boundary Conditions

Two different values of inlet velocity were implemented. At first, we have used a steady velocity of 0.09 m/s with a parabolic radial distribution, just like M. V. P. Carvalho, in order to be able to compare the data from the rheoTool solver with previous results.

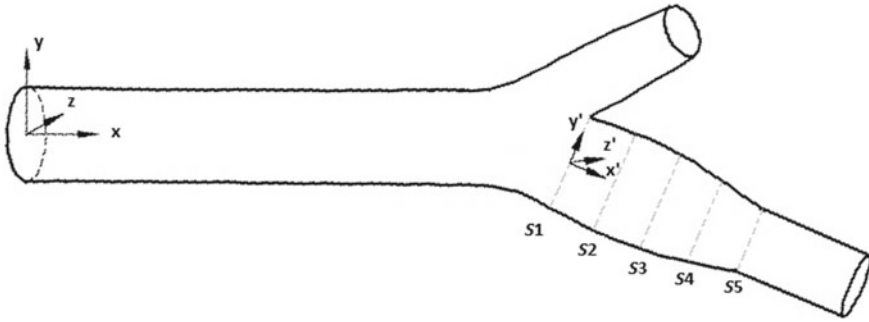


**Fig. 1** Geometry used at Gijzen et al. [8]

The second condition was based on the work of Wiwatanapataphee et al. [9] to reproduce this flow velocity variation on time. The periodical velocity disturbance was used in this study to mimic the influence of the heart pulsation characteristics on the flow. The Fourier transform was used to get the velocity function used in the simulations.

The speed is assumed to be directly proportional to the flow rate, when the section's area is constant (Fig. 2).

The normalized function of the sign shown in Fig. 7 was implemented as an oscillatory regime in blood flow. The interval from 0 to 0.45 s is the diastole and 0.45 to 0.8 s the systole. The sign function multiplied for the maximum velocity in the common carotid results in the approximated velocity function that was used as the boundary conditions.

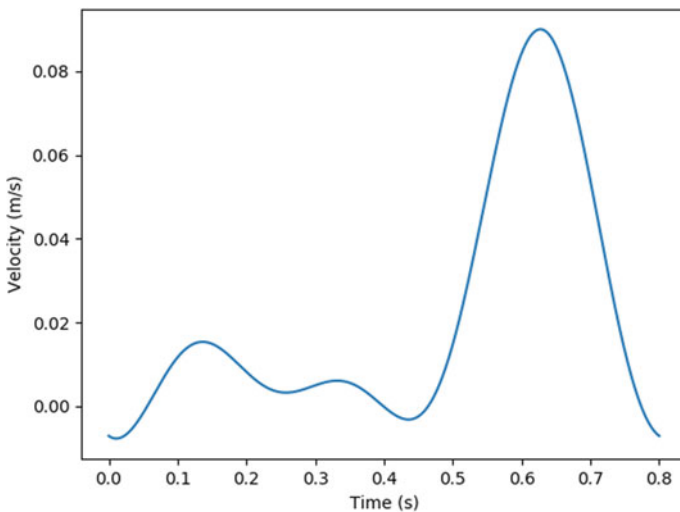


**Fig. 2** Speed profile with 0.089 m/s [10] as maximum speed

The velocity distribution has a parabolic profile and the pressure on the inlet, and the outlets are constant. In the outlet, the atmospheric pressure resembles the experiments made by Ku et al. [7]. For all the simulations, it was considered a stress-free condition at both exits and a no-slip condition in the vessel walls.

### 3 Results

A comparison of the relative error between the computational and experimental results can be seen graphically in Fig. 3. Each section cut represents the sections S1, S2, S3, S4, and S5. The relative error values, like the one shown in Fig. 3 for the Yasuda model, are measured in Table 1.

Figure 4 shows a comparison in the velocity profile, and the dots are the experimental results.

Table 1 presents the statistic comparison. The mean deviation of Yasuda’s rheological model using rheoTool package from the experimental result was 0.007365 while it was 0.0082734 m/s, reproducing the simulations of Carvalho and Lobosco [5]. The standard deviation in the same case was 0.004945 on rheoFoam while it was 0.005604. Those results mean that using the rheoTool package, the precision and accuracy were improved.

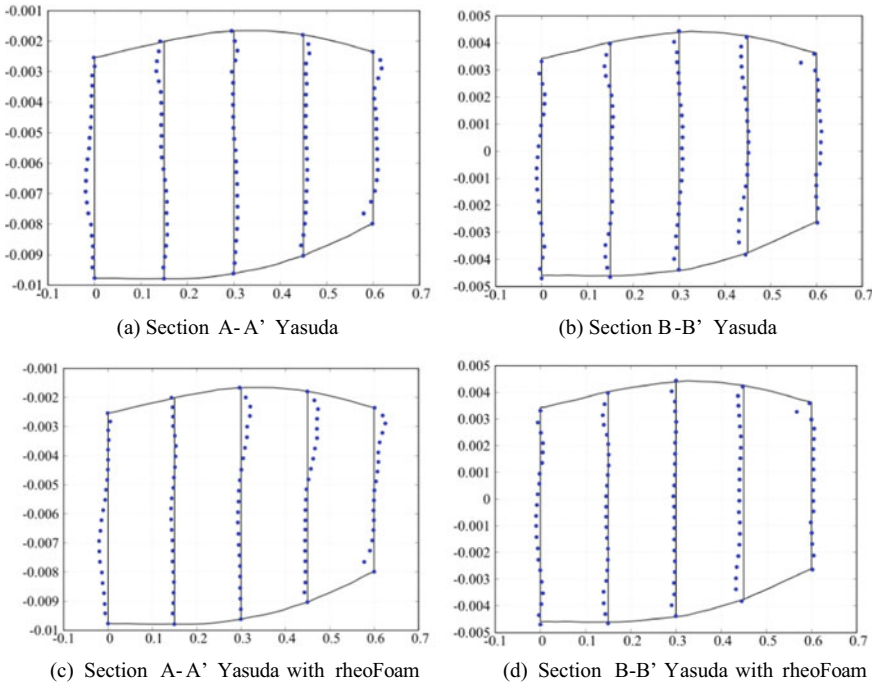


**Fig. 3** Graphics comparing the deviation of simulation from the experiment on each section on computational simulation and the experimental result

**Table 1** Statistic comparison of the differences in computational results and experimental

Rheologic model	Solver	Mean	Standard deviation
Yasuda	Non-NewtonianIcoFoam	-0.008273	0.005604
	rheoFoam	-0.007365	0.004945
	<sup>a</sup> rheoFoam	0.011122	0.017199
Newtonian	Non-NewtonianIcoFoam	-0.004181	0.006717

<sup>a</sup>The oscillatory regime was used on simulation, but the experimental was a steady flow

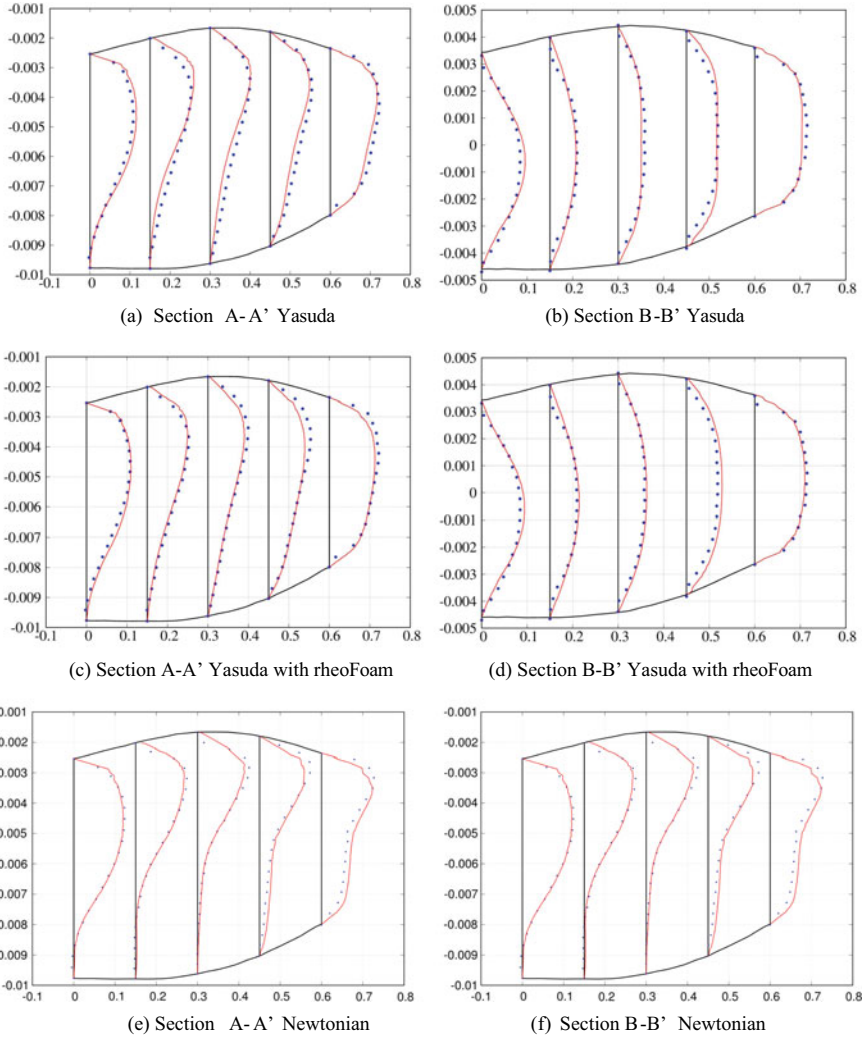


**Fig. 4** Graphics comparing the velocity on each section on computational simulation and the experimental results

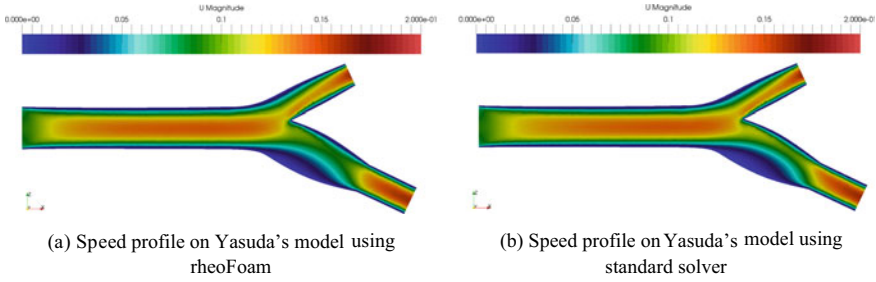


**Fig. 5** Illustration of velocity magnitude

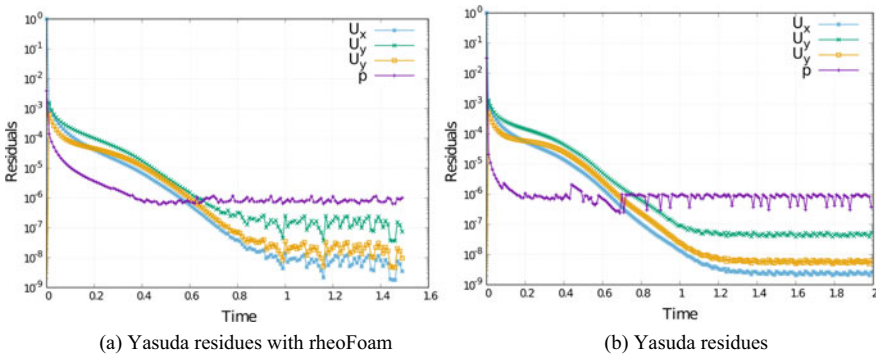


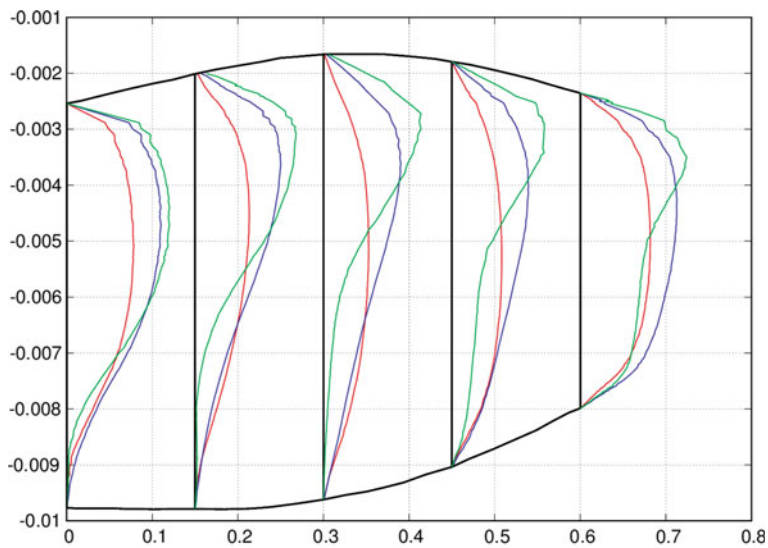
**Fig. 6** Graphics of residues of pressure (purple) and the velocity components  $x$  (blue),  $y$  (green) and  $z$  (yellow) on a logarithm scale

An illustration of the numerical velocity profile can be seen in Fig. 5 while Fig. 6 shows the computational numerical residues.

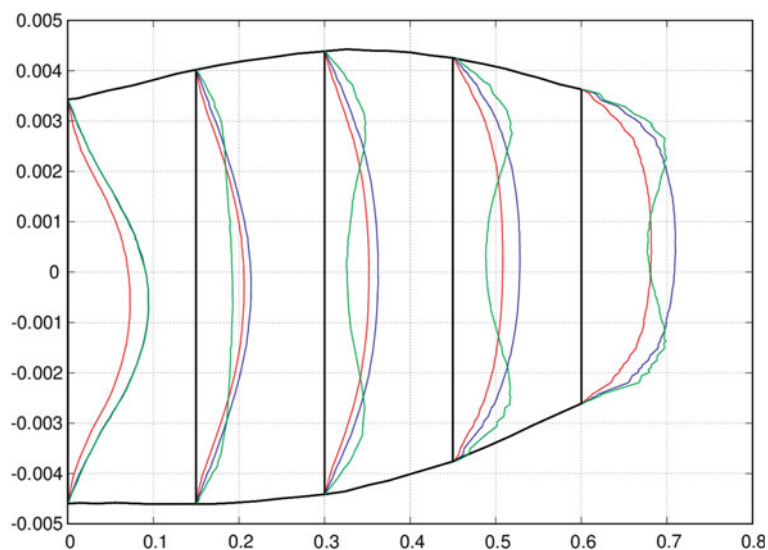
The results which are shown in Fig. 5 allow a comparison between the oscillatory velocity profile and the steady-state flow. Both models, the Newtonian and non-Newtonian can be compared in the graph.

Figure 7 compares the velocity profiles obtained from simulations with different fluid dynamic models applied. As can be seen, Newtonian and non-Newtonian steady-state hypotheses present substantial differences, and these results agree with the results stated at [2, 7], which non-Newtonian approaches are preferable.

Comparing the steady-state and oscillatory velocity profiles for non-Newtonian models, it can be seen that the oscillatory condition has a more uniform profile. This difference would be due to the periodic disturbance of the velocity in oscillatory conditions, which do not allow the velocity to achieve the fully developed velocity magnitude in the steady-state condition.



(a) Section A-A' velocity profile



(b) Section B-B' velocity profile

**Fig. 7** Graphics of velocity profile adopting the Newtonian model (green), Yasuda's model (blue), both on steady flow and Yasuda's model (red) simulating the heart beating on systoles



## 4 Conclusion

The oscillatory boundary condition highly impacts the results of the simulation, showing that steady flow models may be inadequate. The rheoFoam improves the accuracy of the simulation. The results shown in this paper are not definitive, because of some simplification in the vessel wall conditions and unconsidered viscoelastic characteristics; therefore, the result contributes to the progress of the numerical research of complex fluids in arteries.

## References

1. Resch, M., Perktold, K., Peter, R.O.: Three-dimensional numerical analysis of pulsatile flow and wall shear stress in the carotid artery bifurcation. *J. Biomech.* **24**(6), 409–420 (1991)
2. Boyd, J., Buick, J.M., Green S.: Analysis of the casson and carreau-yasuda non-newtonian blood models in steady and oscillatory flows using the lattice boltzmann method. *Phys. Fluids* **24**(6), 093–103 (2007)
3. Shibeshi, S.S., Collins, W.E.: The rheology of blood flow in a branched arterial system. *Appl. Rheol.* **15**(6), 398 (2005)
4. Shibeshi, S.S., Collins, W.E.: A numerical study of blood flow using mixture theory. *Int. J. Eng. Sci.* **76**, 56–72 (2014)
5. Carvalho, M.V.P., Lobosco, R.J.: An ´alise reol´ogica do escoamento sangu´ineo na bifurca¸cao da art´eria car´otida com uso do openfoam
6. Mabon, R.F., Bharadvaj, B.K., Giddens, D.P.: Steady flow in a model of the human carotid bifurcation. Part i: laser-doppler anemometer measurements. *J. Biomech.* **15**(5), 349–378 (1982)
7. Ku, D.N., et al.: Hemodynamics of the normal human carotid bifurcation: in vitro and in vivo studies. *Ultrasound Med. Biol.* **11**(1), 13–26 (1985)
8. Gijssen, F.N.V., Frank, J.H., Janssen, J.D.: The influence of the non-newtonian properties of blood on the flow in large arteries: steady flow in a carotid bifurcation model. *J. Biomech.* **32**(6), 601–608 (1999)
9. Wiwatanapataphee, T.S.B., Wu, Y.H., Nuntadilok, B.: Effect of branchings on blood flow in the system of human coronary arteries. *Math. Biosci. Eng.* **9**(1), 199–214 (2012)
10. Wegent, F., Strecker, C., Weiller, C., Harloff, A., Zech, T., Markl, M.: Comparison of blood flow velocity quantification by 4d flow mr imaging with ultrasound at the carotid bifurcation. *AJNR Am. J. Neuroradiol.* **34**, 14071413 (2013)

# Wearable Technology for Presumptive Diagnosis of High Blood Pressure Based on Risk Factors



Eithel Josue Meza Prada , Helgar Miguel Angel Herrera Agullar , Jimmy Armas-Aguirre , and Paola A. Gonzalez 

**Abstract** In this paper, we propose a technological solution integrated to a wearable device that allows measuring some physiological variables such as body mass index (BMI), steps walked in a determined day, burned calories, blood pressure and other risk factors associated with the Framingham's score. The objective of this article is to identify the evolutionary pattern of the Framingham's score each day in order to determine a presumptive diagnosis of high blood pressure. The technological solution was validated in the social insurance of a public hospital in Lima, Perú. The preliminary results obtained in a diagnostic test show a sensitivity level of 83.33%, a level of precision better than a traditional Framingham's score for presumptive diagnosis of high blood pressure. Our proposal contributes to the patient's awareness about the bad routine habits related to lifestyle and promotes the empowerment of data in order to make some changes that influence on the reduction of cardiovascular disease risk.

**Keywords** Physiological variable · Presumptive diagnosis · Risk factor · Framingham's score · Wearable device

---

E. J. M. Prada · H. M. A. H. Agullar (✉) · J. Armas-Aguirre  
Universidad Peruana de Ciencias Aplicadas, Av. Prolongación Primavera 2390, Santiago de Surco, Lima, Peru  
e-mail: [u201516110@upc.edu.pe](mailto:u201516110@upc.edu.pe)

E. J. M. Prada  
e-mail: [u201213904@upc.edu.pe](mailto:u201213904@upc.edu.pe)

J. Armas-Aguirre  
e-mail: [jimmy.arms@upc.pe](mailto:jimmy.arms@upc.pe)

P. A. Gonzalez  
Rowe School of Business, Faculty of Management, Dalhousie University, Halifax, NS, Canada  
e-mail: [paola.gonzalez@dal.ca](mailto:paola.gonzalez@dal.ca)

# 1 Introduction

The modern world is characterized by the automation of processes, in the day-to-day work of the people. This is evidenced by the marked change in the style of life of each individual, both in the form of feed as in the sedentary lifestyle product of technological advance that automates activities that involved in the past physical activity. This leads to the appearance of cardiovascular diseases due to the excess of the sedentary lifestyle.

According to the report of the institute of statistics and informatics (INEI) issued in the year 2018, indicates that in Peru, the number of people of 15 years overdiagnosed as hypertensive each year is approximately 13% of the population and its growth occurs at a rate of 1% each year [1].

Hypertension is a condition in which the blood vessels have a consistently high voltage, which can damage the walls of the arteries. An artery is each of the vessels that carry blood with oxygen from the heart toward the capillaries of the body. High blood pressure and cardiovascular diseases (CVD) are closely related since high blood pressure is the nexus to identify people at high risk for heart attacks due to the fact that there is a close relationship between blood pressure and cardiovascular health; while more boost a person's blood pressure, it is very likely that the health of your heart is in trouble. It is for this reason that people with blood pressure levels too high are candidates for heart attacks.

According to the research of the World Health Organization (WHO) with respect to the year 2016, two of the ten leading causes of death in the world were due to ischemic heart disease and stroke, which are classified as CVD [2]. The CVD refers to a set of disorder of the blood vessels of the heart and today are the main cause of death throughout the world.

According to the information of the guide for the prevention, detection, evaluation and management of hypertension in adults, major causes of hypertension are attributable to factors of genetic predisposition, overweight, physical condition and sodium intake [3]. Despite the fact that the main risk factors are more related to genetic predisposition and nutritional factors, it is important to know and to control some risk factors associated with the lifestyle in order to reduce the risk of hypertensive patients.

This article contributes to the emerging development of technologies committed to health care through an integrated technological solution to a portable device, which measured the variables considered as major risk factors associated with high blood pressure according to the Framingham score, by means of a portable device in order to analyze the behavior of that score with the passage of time in order to generate a guide to health education that enables the user to obtain possible values for that score in the future and can generate changes in your lifestyle to help the prevention of arterial hypertension.

## 2 Literary Review

During the planning stage, it is considered the review of related articles to various fields. On the one hand, an analysis was made of the factors related to hypertension. On the other hand, we reviewed the portable technologies emerging in the market.

### 2.1 Variables Related to Hypertension

According to the medical documentation, points out that there are multiple variables that influence arterial hypertension; for our case study, the following variables were considered to be obtained by means of the portable device: The person's age [4], BMI (Weight/height) [5, 6], calories burned in a determine day [7], steps walked in a determined day [8], measured arterial pressure in sedentary [9], consumption of alcohol [10], consumption of tobacco [11], sodium level in the blood [12], predisposition in hypertensive parents [13].

In [4], the author argues that as the years go by a person tends to increase your blood pressure due to aging and stretches of arterial walls. In patients older than 65 years of age, the prevalence of hypertension is located between 60 and 70%.

In [5, 6], the author argues in his research that excess body fat contributes to the increase in blood pressure. It is estimated that for every 10 kilos obtained, an increase in blood pressure amounts to between 2 and 3 mm Hg. The appropriate levels of BMI for each person must be between 18.5 and 24.9 kg/m<sup>2</sup>.

In [7], the author argues that the basal metabolism is the set of chemical reactions that causes the body to function optimally. Therefore, each action that the body can generate is related to the consumption of calories. The number of calories burned a day ideal for maintaining good blood pressure levels depends on a certain way of the action of the basal metabolism but the main factors are the completion of exercises or any other type of physical activity.

In [8], the author argues that it is important to establish an exercise program that combines activities such as running, dancing, nothing or walking during each week. It is recommended to combine activities such as walking daily between 20 and 30 min a day to get to reduce blood pressure values at adequate levels.

In [9], the author describes the two types of arterial pressures and marks the importance of the difference in values between the two, as shown in Table 1.

In [10], the author argues that alcohol is a factor that can lead to obstruction of the blood vessels due to the release of salts and hormones in the blood, which has an impact on the proper cardiac function. It is estimated that alcohol intake between 0.75 and 1 grams of ethanol/kg produces an increase in blood pressure.

In [11], the author is based on preliminary studies that describe the damage caused by the components of tobacco and smoke generated physiopathological alterations involved in complications associated with the acceleration of atherosclerosis and vascular disorders and endothelial cells observed in a tobacco smoker.

**Table 1** Arterial pressure categories

Category	Description
Normal blood pressure	120–139 mmHg systolic and 80–89 mmHg diastolic
Mild hypertension	140–159 mmHg systolic and 90–99 mmHg diastolic
Medium-serious hypertension	160–179 mmHg systolic and 100–109 mmHg diastolic
Serious hypertension	>180 mmHg systolic and >110 mmHg diastolic

In [12], the author demonstrates the direct relationship between blood pressure and salt consumption through development of an experiment taken over four weeks in a sample of 500 hypertensive patients that consisted in the reduction of 0.5 g of salt; the outcome of this case study obtained a decrease of 20% of the figures related to blood pressure in 60% of patients. Therefore, it concludes that the restriction of Salinas decreases the incidence of secondary factors such as hypocalcemia induced by thiazide diuretics that affect blood pressure levels.

In [13], the author argues that despite the fact that the determinants of hypertension are not known, there are epidemiological studies that have shown that about 30% of the 40 the variation in blood pressure of the population is determined by genetic factors.

## 2.2 Portable Technologies

Portable devices are all kinds of accessories are easy to integrate into the clothing or body of each user. Among them is with smart clothing, fibers to collect electromagnetic signals, healthy watches among others. To carry out the measurements of arterial pressures were evaluated the main portable devices whose measurement values have been certified by specialized institutions. Figure 1 detailed the reason for the election of the portable device ‘Smartwatch Skmei Jam,’

## 3 Technological Solution

This proposal consists in a technological solution based on the Framingham’s score, a scheme was validated by the medical community for the identification of risk factors associated with cardiovascular disease and hypertension, which unlike the traditional score through a form, allows the collection of data more precisely through a portable device non-invasive. Then it will be explained in detail of each one of the phases.





















FEATURES/ DEVICES	 OM-RON BLOOD PRESSURE MONITOR	 SMARTBAND LYN WO M4	 SMARTWATCH SKMEI JAM
MEASURING ACCURACY	±0,5mmHg	N.A	±5 mmHg
COMPATABILITY OS	NA		
MEASURING PARAMETERS	 Blood Pressure	 Heart Rate  Sleep Quality  Step Count  Calories Burn  Distance Travelled	 Heart Rate  Sleep Quality  Step Count  Blood Pressure  Calories Burn  Distance Travelled
VALIDATION	 International Society of Hypertension		

Fig. 1 Devices portable evaluation

### 3.1 Phase 1: The Physiological Data Collection of the User Through the Portable Device

Portable devices allow recording and storing physiological data and these are obtained through the discovery of services available from each device in specific. During the day, the portable device will record the data obtained by the daily activities of the person to be stored and classified in an object for each variable defined. For the distance traveled, steps walked and calories burned will evaluate the data obtained throughout the day; in the case of blood pressure, the indicator which allows the correct evaluation and reliability of the sample is the state at rest, so the user will only be assessed such data when the user is at rest.

### 3.2 Phase 2: The Reception of the Data Through the Mobile Application by Means of a Bluetooth Communication Protocol

Developed a mobile application that allows communication and reception of the data with the portable device via Bluetooth. The software consumes the services offered by the portable device through reading requests to the services available during the connection to the device. The acquisition of the data is carried out through a text format for data exchange (JSON).

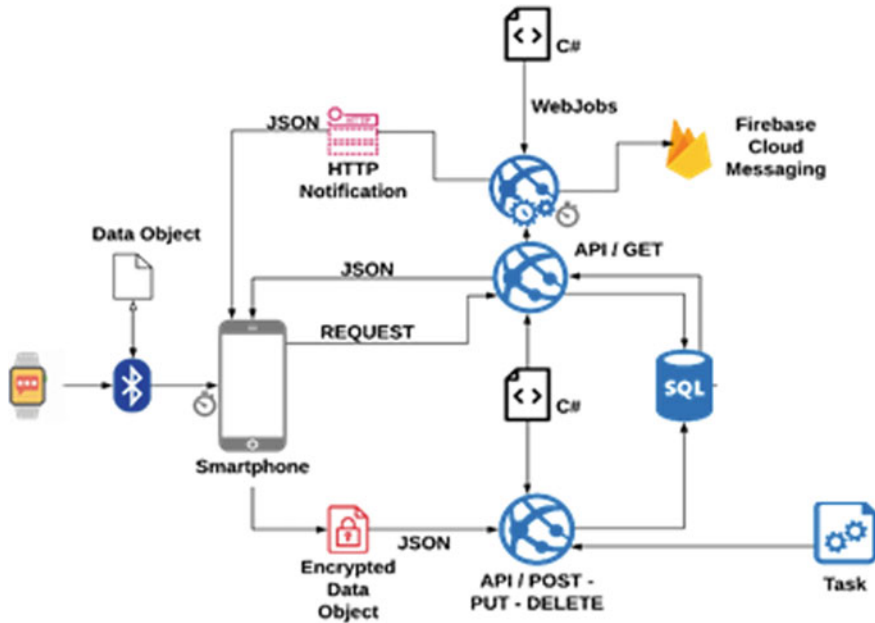


Fig. 2 Data communication diagram

### 3.3 Phase 3: The Sending of Data from the Mobile Application to the Database Engine of SQL Azure Hosted in the Cloud

As part of the development of software, it is contemplated two communication services developed in C# and deployed as App Services on Azure with communication to the storage services. These services enable communication software with the database in the cloud through HTTPS requests: GET and POST. At the end of the data collection during the day, the software performs a POST request to the service and inserts the information from the user on our storage service. GET requests shall facilitate the procurement and display of user data. Figure 2 shows the data communication diagram.

### 3.4 Phase 4: The Process of Generation of Reports of Educational Health Based on the Framingham's Score

Once registered, the data for each patient in the technological solution will generate a daily educational health report which will show the levels obtained by the patient in each parameter that has been analyzed. This allows the patient to see the variance of

your score over time and be aware of certain changes in your lifestyle, thus reducing the probability of being hypertensive patients in the future.

## 4 Validation

### 4.1 Test Scenario

The validation of the proposed model was carried out with social insurance patients from EsSalud who was diagnosed as diabetic and had a high risk of acquiring high blood pressure at some time in their lives. The population sampling included 25 patients who used the traditional model of the discard of cardiovascular diseases based on a questionnaire of the main risk factors according to the Framingham's score and the new proposed model that proposes to calculate certain parameters such as the distance traveled and the average for all arterial pressures throughout the day from a portable device. For the traditional method, each question receives a certain score according to the age and gender of the patient. In this way can be calculated if the patient has a low probability, medium, or high to be hypertensive. For both methods, most of the parameters were similar, in contrast to the question whether or not the patient performs a physical activity, whose question is very subjective, and blood pressure field of the traditional method considered only blood pressure at the time that the patient receives the query on the part of the doctor.

### 4.2 Comparison Between Two Models

The traditional model, after applying the questionnaire, determined that 19 people (76%) stated that if carried out physical activity into your daily routine, while six people (24%) stated that they did not physical activity every day. Instead of that, the proposed model dictated that 18 people (72.00%) were not engaged in physical activity, 5 people (20.00%) had little physical activity, and 2 people (8.00%) carried out an adequate physical activity. Table 2 shows the Framingham score in both models of physiological risk analysis for the 25 diabetic patients surveyed.

The 25 patients analyzed in both models went through a more comprehensive monitoring and greater reliability on the part of the medical community for the measurement of blood pressure on how to final disposal of diagnosis of high blood pressure.

**Table 2** The number of patients according to the risk level of arterial hypertension

Method	Low risk	Medium risk	Serious risk
Traditional model	4 (16%)	7 (28%)	14 (56%)
Proposed model	2 (8%)	8 (32%)	15 (60%)



This monitoring is known as ambulatory blood pressure monitoring (MAP), a method that involves the use of an assistive technology device oscillometric measurement of high precision that the patient carries with it during the 24 h a day and it performs multiple measurements of blood pressure throughout the day.

Finally, in order to validate our proposal, these metrics are important to foresee whether a person is diagnosed as a hypertensive patient:

- True positives: Are events in which the patient presented a high risk of being hypertensive and after monitoring by MAP was diagnosed as a hypertensive patient.
- False positives: Are the events in which the patient presented a high risk of being hypertensive, but after the monitoring by MAP was not diagnosed as a hypertensive patient.
- False negatives: Are the events in which the patient presented a risk to medium or low to be hypertensive, but after the monitoring by MAP was diagnosed as a hypertensive patient.
- True negatives: Are the events in which the patient presented a risk to medium or low high to be hypertensive, and after the monitoring by MAP was not diagnosed as a hypertensive patient.
- Sensitivity: It is defined as the capacity of a diagnostic test to properly identify an individual with a high probability of being hypertensive and then confirm the existence of the disease. This is calculated as follows:

$$\text{Sensitivity} = \frac{\text{TP}}{\text{TP} + \text{FN}} \quad (1)$$

- Specificity: It is defined as the capacity of a diagnostic test to properly identify an individual with a high probability of not being hypertensive and then confirms the absence of the disease. This is calculated as follows:

$$\text{Specificity} = \frac{\text{TN}}{\text{TN} + \text{FP}} \quad (2)$$

### 4.3 Discussion of the Results

Table 3 shows the assessment of validity from both models. From a population of 25 diabetic patients, it is determined that six patients were diagnosed as hypertensive. By using the traditional model, it was identified that the levels of sensitivity and specificity were 66.67% and 47.37%, respectively. On the other hand, the proposed model was identified that levels of sensitivity and specificity were 83.33% and 47.37%, respectively.

**Table 3** Assessment of validity of both models

Validity and reliability assessment of the test	Traditional model	Proposed model
True positive (TP)	4 (16%)	5 (20%)
False positive (FP)	10 (40%)	10 (40%)
False negatives (FN)	2 (8%)	1 (4%)
True negatives (TN)	9 (36%)	9 (36%)

## 5 Conclusions

This work proposed a technological solution to analyze the probability of being a hypertensive patient through the use of the Framingham score. This solution proposes to calculate some risk factors such as the number of steps walked and the average arterial pressure value throughout the day via the portable device.

Despite the fact that the experiment was carried out with a small number of patients, it can be concluded that the proposed model has a better degree of accuracy in terms of sensitivity than the traditional model, although in terms of specificity both have the same results.

On the other hand, this technological solution aims to raise awareness of patients in the importance of lifestyle changes in order to reduce the amount of punctuations and prevent be hypertensive patients. In addition, it allows doctors to carry out real-time control of arterial pressures of their patients and identify whether they are complying with the health objectives proposed.

## References

1. Instituto Nacional de Estadística e Informática, INEI: Encuesta Demográfica y de salud familiar. [https://proyectos.inei.gob.pe/endes/2018/ppr/Indicadores\\_de\\_Resultados\\_de\\_los\\_Programas\\_Presupuestales\\_ENDES\\_Primer\\_Semestre\\_2018.pdf](https://proyectos.inei.gob.pe/endes/2018/ppr/Indicadores_de_Resultados_de_los_Programas_Presupuestales_ENDES_Primer_Semestre_2018.pdf). Last accessed 09 Sept 2019 (2018)
2. Organización Mundial de la Salud, OMS: Las 10 principales causas de defunción. <https://www.who.int/es/news-room/fact-sheets/detail/the-top-10-causes-of-death> (2018)
3. Mendis, S., Lindholm, L.H., Mancia, G., et al.: World Health Organization (WHO) and International Society of Hypertension (ISH) risk prediction charts: assessment of cardiovascular risk for prevention and control of cardiovascular disease in low and middle-income countries. *J. Hypertens.* **25**, 1578–1582 (2007)
4. Kovesdy, C.P., Alrifai, A., Gosmanova, E.O., et al.: Age and outcomes associated with BP in patients with incident CKD. *Clin. J. Am. Soc. Nephrol.* **11**, 821–831 (2016)
5. Neovius, M., Rasmussen, F.: Evaluation of BMI-based classification of adolescent overweight and obesity: choice of percentage body fat cutoffs exerts a large influence. *The COMPASS Study. Eur. J. Clin. Nutr.* **62**, 1201–1207 (2008)
6. Dong, J.Y., Zhang, Z.L., Wang, P.Y., et al.: Effects of high-protein diets on body weight, glycaemic control, blood lipids and blood pressure in type 2 diabetes: meta-analysis of randomised controlled trials. *Br. J. Nutr.* **110**, 781–789 (2013)

7. Mertens, I.L., Van Gaal, L.F.: Overweight, obesity, and blood pressure: the effects of modest weight reduction. *Obes. Res.* **8**, 270–278 (2000)
8. Whelton, S.P., Chin, A., Xin, X., et al.: Effect of aerobic exercise on blood pressure: a meta-analysis of randomized, controlled trials. *Ann. Int. Med.* **136**, 493–503 (2002)
9. Thomopoulos, C., Parati, G., Zanchetti, A.: Effects of blood pressure lowering on outcome incidence in hypertension: 7. Effects of more versus less intensive blood pressure lowering and different achieved blood pressure levels—updated overview and meta-analyses of randomized trials. *J. Hypertens.* **34**, 613–622 (2016)
10. Xin, X., He, J., Frontini, M.G., et al.: Effects of alcohol reduction on blood pressure: a meta-analysis of randomized controlled trials. *Hypertension* **38**, 1112–1117 (2001)
11. Meade, T.W., Imeson, J., Stirling, Y.: Effects of changes in smoking and other characteristics on clotting factors and the risk of ischaemic heart disease. *Lancet* **ii**, 986–988 (1987)
12. Zemel, M.B., Gualdoni, S.M., Sowers, J.R.: Sodium excretion and plasma renin activity in normotensive and hypertensive black adults as affected by dietary calcium and sodium. *J. Hypertens.* **4**(Suppl 6), S343–S345 (1986)
13. Kunes, J., Zicha, J.: The interaction of genetic and environmental factors in the etiology of hypertension. *Physiol. Res.* **58**(Suppl 2), S33–S41 (2009)

# Cytology and Hematology: A Review of the Fundamental Principles



Ana Carolina Borges Monteiro , Yuzo Iano , Reinaldo Padilha França , and Rangel Arthur 

**Abstract** Since ancient times, human beings have been looking for alternative methods to detect and diagnose diseases, mainly by assessing patients' body fluids. The creation of the microscope contributed to the development of modern techniques of clinical analysis, as this instrument allowed the visualization of structures invisible to the naked eye and opened the door to various types of scientific research. Based on this, it is essential to develop studies that synthesize the fundamental information on hematology and cytology, in order to support future research as well as assist in the academic training of professionals in the medical fields.

**Keywords** Blood cells · Hematology · Blood count · Hematological devices · Cellular biology

## 1 Introduction

The cells are described as functional and structural units defined as the smallest part of a living organism. The cells that make up a living organism are all the same, with the same genetic load; however, due to the natural process of cell differentiation, they present variations in shape and performance according to the function they perform

---

A. C. Borges Monteiro (✉) · Y. Iano · R. Padilha França  
School of Electrical and Computer Engineering (FEEC), University of Campinas, UNICAMP, Av. Albert Einstein - 400, Barão Geraldo, Campinas, SP, Brazil  
e-mail: [monteiro@decom.fee.unicamp.br](mailto:monteiro@decom.fee.unicamp.br)

Y. Iano  
e-mail: [yuzo@decom.fee.unicamp.br](mailto:yuzo@decom.fee.unicamp.br)

R. Padilha França  
e-mail: [padilha@decom.fee.unicamp.br](mailto:padilha@decom.fee.unicamp.br)

R. Arthur  
School of Technology (FT), School of Technology, University of Campinas, UNICAMP, R. Paschoal Marmo - 1888, Jardim Nova Italia, Limeira, SP, Brazil  
e-mail: [rangel@ft.unicamp.br](mailto:rangel@ft.unicamp.br)

© The Editor(s) (if applicable) and The Author(s), under exclusive license to Springer Nature Switzerland AG 2021

Y. Iano et al. (eds.), *Proceedings of the 5th Brazilian Technology Symposium*, Smart Innovation, Systems and Technologies 202, [https://doi.org/10.1007/978-3-030-57566-3\\_4](https://doi.org/10.1007/978-3-030-57566-3_4)

in the organism. This division of tasks between cells is a strategy for saving energy and increasing efficiency in carrying out biological functions [1].

The cells have the same biological function that are grouped together and form a tissue, which in turn form the organs (brain, lungs, intestines, heart). A grouping of organs creates a system (neurological system, respiratory system, digestive system, cardiovascular system). The set of systems originates organisms, such as plants, insects, parasites, and even the human body. This entire process must take place in an extremely precise and harmonic way. Otherwise, the changes will be so drastic that they are incompatible with life [2].

Cells are organisms susceptible to changes in the environment in which they are. According to Darwin's theory, over time, there may be climate changes and/or shortages of nutrients, consequently, such factors stimulate physiological changes to organisms [3]. In this way, only the organisms that are able to adapt are able to survive [2].

The human body has about 100 trillion cells, consisting mainly of carbon, oxygen, hydrogen, calcium, phosphorus, and nitrogen [1, 4]. About 70% of the human organism is formed by hydrogen and oxygen, which are responsible for the formation of water. The other 30% are responsible for the constitution of carbon-based compounds, which are called organic compounds [5, 6].

Cell classification is done in two distinct types: prokaryotes and eukaryotes. The prokaryotic cells (from the Greek, *pro* = first; *carium* = nucleus) are small (1–5  $\mu\text{m}$ ), have a cell wall, responsible for mechanical protection, and have genetic material dispersed by the cytoplasm, that is, they do not present—they have a nuclear envelope [2, 7]. These cells include bacteria and blue algae, being formed by only a single cell, that is, they are classified as unicellular [2, 7, 8].

Eukaryotic cells (from Greek, *eu* = true; *carium* = nucleus) have more complex genetic material, being formed by DNA and RNA, which are organized in the cytoplasm through the cell envelope. Eukaryotic cells are responsible for the formation of more complex organisms, that is, those formed by more than one cell (multicellular organisms). Among these organisms, it is possible to mention: vertebrate and invertebrate animals and plants. In addition, the cytoplasm of eukaryotic cells has compartments that have different molecules responsible for performing specialized functions [2, 7].

These cells have a more complex structure, being composed of several structures such as cell membranes, nuclear envelope, nucleus, cytoplasm, peroxisomes, lysosomes, endoplasmic reticulum, mitochondria, Golgi complex, cytoskeleton, plasma membrane, and cytoplasmic deposit [2, 7]. However, such discoveries could only be made through the invention of the optical microscope.

Thus, the objective of the present study is to carry out a bibliographic review regarding cytology and hematology, in order to easily explain the synthesis of blood cells as well as their biological functions.

## 2 Methodology

The present study is based on the collection of information from 27 bibliographic sources in the medical literature that addresses the subject of cytology and hematology. These sources were chosen because they have an emphasis on blood cell synthesis.

## 3 Results and Discussion

The first notion of microscopy appeared around the year 1595, through the works of the Dutchman Zacharias Janssen, a glasses manufacturer who, through the union of two lenses on the same axis, noticed the presence of small structures in objects. Later, in the year 1665, Robert Hooke, using an ocular lens and an objective lens, built the first microscope. This work originated in the book *Micrographia*, where different living beings observed under microscopy have been described [4].

For 50 years, the Dutchman Anton van Leeuwenhoek, burned lenses and built high-quality microscopes for his time. In this way, Leeuwenhoek was the first to describe the various forms of bacteria in a drop of water from a lake, with his findings constantly being sent to the Royal Society of London. Later, through the scraping of his own teeth and water from washing a pepper, Leeuwenhoek described the presence of bacterial structures. The Royal Society, after analyzing the letters, sent Robert Hooke, who confirmed the veracity of the observations made by him [4].

Human eyes are capable of detecting variations in intensity and in the length of light waves. This human capacity has been expanded through advances in the field of microscopy, which have allowed for increased resolution as well as the use of techniques that compensate for the transparency of cells. Cellular components are generally transparent, with the exception of some cytoplasmic pigments capable of absorbing certain wavelengths of light. Living cells have low absorption of these wavelengths, as they have a high concentration of water, so even when dehydrated this problem persists. To compensate for this limitation, dyes are used that selectively stain the different cellular structures. These dyes are made up of compounds capable of absorbing specific wavelengths [8, 9].

The resolution limit of the microscope is responsible for providing the details observed in the images generated from a sample. In this way, it has no relation to the capacity of increasing the size of the analyzed image. Thus, it is determined by the shortest distance between two points [3]. It is important to note that the increased capacity is valid only when accompanied by a parallel increase in the equipment's resolving power. Thus, the resolution limit is dependent on the ocular and objective lenses, which are unable to add details. Thus, ocular lenses are totally dependent on objective lenses, as they are responsible for increasing the size of the image (Fig. 1) [3, 9].

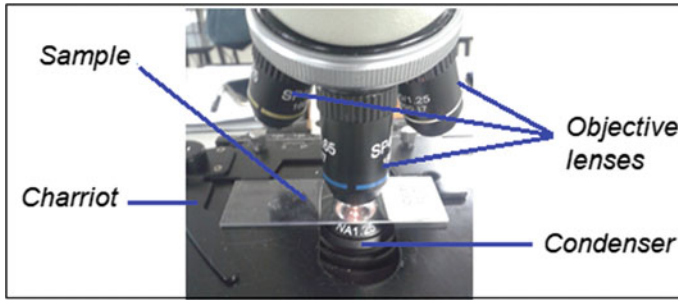


**Fig. 1** Microscope structure—sample analysis example

In Eq. 1, it is possible to note the instrument's resolution limit (RL) of the objective lens. In this context, the microscope resolution limit is totally dependent on the numerical aperture (NP) coming from the objective lenses, and it is also necessary to consider the length of light applied to the sample.

$$NP = k \times \lambda AN \quad (1)$$

where  $k$  is a constant estimated in seconds, being numerically represented by 0.61 and  $\lambda$  (lamina) is the wavelength of the light used. Due to the greater sensitivity of human eyes to the wavelength of the yellow–green band, the value of  $0.55 \mu\text{m}$  is used in the calculation of the resolution limit. Through this formula, it is notable that the resolution limit is directly proportional to the wavelength of the light used, and it is also inversely proportional to the numerical aperture of the objective lens [2, 3, 9].

The creation of the first microscope opened the door to the development of techniques used in the areas of clinical analysis. Clinical analyses date back to the age of Hippocrates, the father of medicine. At that time, the color, odor, taste, and texture of biological fluids were important tools for patients' clinical diagnoses [2, 8].

Later, with the creation of the microscope, it was possible to correlate the physical characteristics of biological fluids with their microscopic constitution of the analyzed samples. In other words, it was understood that the human organism is formed by cells and can be attacked by fungi, bacteria, and parasites. The characterization of the morphology and after of the physiology of blood cells was essential (and still is) for the conclusion of several types of human pathologies [2, 8].

Human blood represents approximately 7% of a person's total body weight, with its constitution corresponding to 55% of the plasma and 45% of blood cells. Among the diverse functions performed by the blood, it is possible to mention: basic acid balance, excretion of metabolites, transport of gases and nutrients to organs and tissues, distribution of hormones, osmotic balance, and temperature regulation [2, 7–9].

The function of transporting substances such as plasma proteins, water, amino acids, glucose, hormones, immunoglobulins (IG), albumin, components of the coagulation cascade, among others, is the responsibility of the plasma. Plasma is the liquid part of the blood, disregarding any and all types of cells. Plasma is of great importance for coagulation analysis, while serum is characterized by being a plasma

with the absence of coagulation factors. The serum is widely used for biochemical tests, such as glucose measurement, renal markers, liver enzymes, pregnancy tests, hepatitis, HIV, among others [2, 8, 9].

The solid portion of the blood is made up of blood cells, which are called erythrocytes, leukocytes, and platelets. The main function of these elements is homeostasis of the body, tissue repair, blood clotting, and defense of the body against various types of etiological agents, which are usually: viruses, bacteria, and intestinal parasites. However, the discovery of all blood elements as well as their respective functions is the result of the invention of instruments capable of increasing the size of cells and ethylene agents hundreds of times [7–9].

### ***3.1 Hematopoiesis***

The synthesis of human blood, uterine life begins at the same time. During the embryonic phase, the first blood cells are synthesized by the yolk sac. Later, when the fetus begins to develop, the synthesis of blood elements becomes a liver and splenic function. When the individual reaches adulthood, the bone marrow takes on the task of producing blood cells. This is because this region is composed of hematopoietic tissue with controlled and orchestrated conditions for the formation of each precursor cell. It is important to note that any of the blood cells come from the stem cell, which resides inside the bone marrow [10–13].

The entire process of blood cell formation is called hematopoiesis and occurs within the bone marrow from a mother cell also known as a stem cell. The main characteristic of this cell is to be of the pluripotent type, that is, it has the capacity to originate different blood cell lines, be they erythrocytes, leukocytes, or platelets (Fig. 2). However, for these syntheses, several coordinated actions are necessary that generate orchestrated responses that culminate in processes of duplication, differentiation, and maturation. It is important to note that many sanguineous cells end their maturation process in the bloodstream or in lymphoid organs [14, 15].

The stem cell is a cell capable of self-duplication, giving rise to daughter cells. The daughter cells are the Colony Forming Units (CFU), as they have the genetic information necessary for the formation of a cell series. The hematopoiesis process is characterized by the participation of regulatory and stimulating factors such as cytokines, erythropoietin (regulator of erythropoiesis), thrombopoietin (regulator of thrombocytopenia), Granulocyte Colony-Stimulating Factor (G-CSF), Monocyte Colony-Stimulating Factor (M-CSF), Macrophage Colony-Stimulating Factor (M-CSF), IL-3 (multiple colony-stimulating factors) and interleukins IL-2, IL-4, and IL-6 [12, 13, 16].



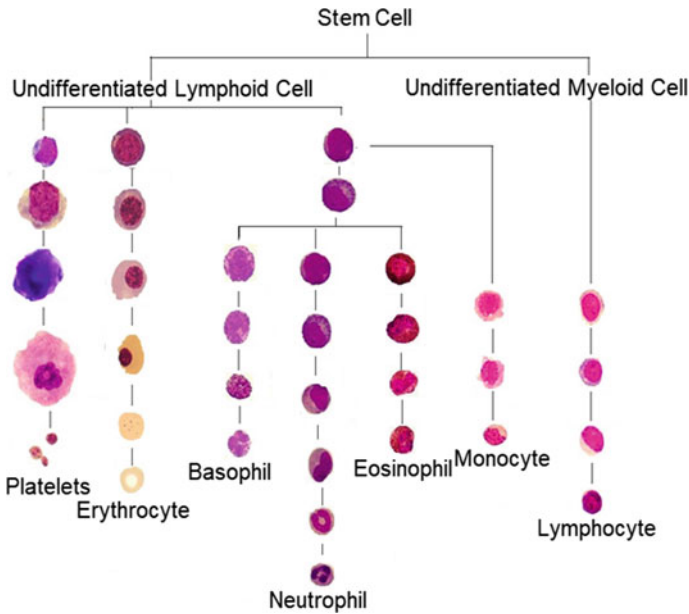


**Fig. 2** Hematopoiesis

During the embryonic phase, the yolk sac is responsible for the formation of the first blood cells; later, during fetal development, this function is transferred to the liver and spleen. During adulthood, the inside of the bone marrow consists of hematopoietic tissue (or hematopoiesis), which resides inside long bones and in the axial skeleton. Inside the bone marrow, there is a network of venous sinusoids around an arteriole and central veins, which permeate the developing cells. All blood cells are derived from bone marrow stem cells. Thus, the bone marrow presents a suitable microenvironment for the development of hematopoietic cells and for the proliferation of primitive cells and progenitor cells [10–12].

Cytokines are glycoproteins that act in low concentrations on re-receptors, producing signals that control the cell cycle, maturation and cell functions. Generally, they are responsible for the regulation of more than one cell line and show an additive and synergistic effect with other growth factors, modulating the expression of regulatory genes producing cytokines [12, 13].

### 3.1.1 Erythrocytes

In the literature and in the medical routine, erythrocytes receive other nomenclatures such as red blood cells (RBC) and erythrocytes. The main morphological characteristics of these cells are the absence of a cell nucleus, a biconcave disk shape, and formation based on a tetramer, that is, two  $\alpha$  chains and two  $\beta$  chains, which carry out the transport of oxygen through the connection of the oxygen molecule to each of the iron molecules [17, 18]. The gas exchange process occurs when the erythrocytes reach the lungs, at that moment there is the formation of oxyhemoglobin (oxygen molecules linked to the iron molecules present inside each red cell). Upon reaching the tissues, this iron–oxygen bond is broken due to the pressure difference. In this way, red blood cells deposit oxygen molecules and remove carbon dioxide from tissues. The binding of carbon dioxide to iron is called carboxyhemoglobin. Subsequently, the dioxide is transported to the lungs or dissolved in the plasma [17–20].

The erythrocytes originate in the bone marrow, being formed through the cell maturation processes of the following cells: proerythroblast, basophilic erythroblast, polychromatic erythroblast, orthochromatic erythroblast, and reticulocyte. By differentiating the pluripotential cell (Stem cell) and erythropoietin stimuli, proerythroblasts are created [13, 19, 20].

The final stages of the maturation process are characterized by the formation of reticulocytes, which are also called young red blood cells. The reticulocytes have mitochondria, an irregular shape, and several remaining organelles inside. The most striking feature of cell maturation is the reticulocytes leaving the bone marrow into the bloodstream, where within 72 h, their cell nucleus expels, giving rise to erythrocytes [13, 20].

### 3.1.2 Leukocytes

The body's innate immune response and adaptive immune response are the results of the action of leukocytes. Both in the literature and in the medical routine, leukocytes are also called white blood cells (WBC). These cells are classified into two major groups: granulocytes and agranulocytes. Granulocytic leukocytes are defense cells characterized by the presence of granules dispersed in the cytoplasm. These granules exert anti-inflammatory and antimicrobial action. Another morphological characteristic of these cells is the presence of a variable number of lobes. Thus, granulocyte cells are also called polymorphonuclear cells. The leukocytes that fit these characteristics are neutrophils, eosinophils, and basophils. In turn, leukocytes classified as agranulocytes do not have granules visible under optical microscopy generally used in the routine of several clinical analysis laboratories. Another striking morphological feature is the presence of only one lobule. In view of this, these leukocytes are also called monomorphonuclear nomenclature. Agranulocyte leukocytes are lymphocytes and monocytes [17, 18].

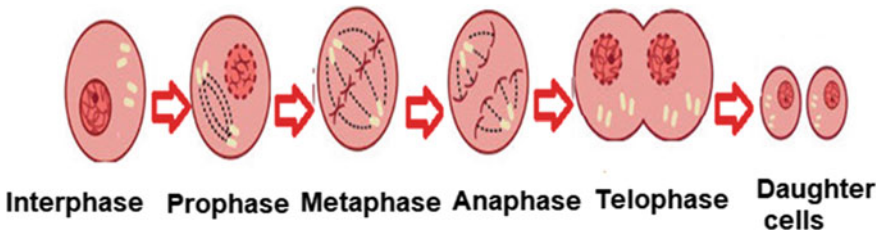


**Fig. 3** Mitosis phases

The synthesis of leukocytes occurs during hematopoiesis, where the leukocyte precursor cells of the granulocytic series (neutrophils, eosinophils, and basophils) start the process of producing proteins and cytoplasmic granules. In this context, the primary granules are characterized by blue staining and are responsible for the conversion of precursor cells called myeloblasts to promyelocytes. Subsequently, specific granules appear, which are responsible for the progression to myelocytes of the type: neutrophils, eosinophils, and basophils [19, 21].

The leukocytes resulting from the process of determining the granulocytic lineage are indivisible by mitosis (The phases of mitosis can be seen in Fig. 3). In addition, these cells have a segmented nucleus, the ability to phagocyte particles, the destruction of microorganisms and motility. It is important to note that depending on the leukocyte lineage, when it reaches the maturation process, it has the ability to cross the wall of venules in order to destroy invading agents and rebuild damaged tissues [13, 21].

### Neutrophils

After determining the production of the neutrophil lineage, the cell maturation sequence is myeloblast, promyelocyte, myelocyte, metamyelocyte, rod neutrophil, and segmented neutrophil, with the production of neutrophils stimulated by G-CSF. An adult human being produces more than  $1 \times 10^{11}$  neutrophils per day, so neutrophils make up about 70% of blood cells. In addition, after leaving the inside of the bone marrow, each neutrophil survives an average of 6 h in the bloodstream [12, 13, 19].

Until the metamyelocyte phase, the cells are contained within the bone marrow; however, from the neutrophil rod stage, cells are released into the bloodstream. The rod neutrophils measure about 12  $\mu\text{m}$ , with a horseshoe-shaped nucleus or stick, remaining in this stage until the segmentation of the lobes undergoes. When found in abundance in the bloodstream, these cells indicate the presence of infection and/or acute inflammation [12, 13, 19].

Segmented neutrophils, in turn, are characterized by a spherical shape with an approximate diameter of 12–15  $\mu\text{m}$ , and the nucleus is segmented from 3 to 5 connected lobes. Mature neutrophils have primary and secondary granules; however,

secondary granules are more numerous, about twice as many as primary granules. The primary granules are azurophilic, have positive peroxidase, and measure about 500 nm. These granules are made up of a large amount of lysosomal enzymes (a lysosome, elastase, proteinase 3—and  $\alpha$ —antitrypsin), and bactericidal factors are formerly known as cationic proteins (defensins, bactericidal factors and bactericidal protein to increase permeability). In turn, the secondary granules are smaller, measuring about 200 nm and contain lactoferrin, lysozyme, and protein-bound to B12 and other proteins [13, 19].

Classified as phagocytic cells, neutrophils have the primary function of identifying, ingesting, and destroying microorganisms. The host's defense responses consist of sequential stages of recognition and activation of phagocytes and the destruction of microorganisms. Neutrophils spend less than 48 h in the bloodstream before migrating to the tissues, being the first cells to reach the sites of infection and/or inflammation. Thus, through direct contact with protein secretion, and the presence of receptors for antibodies and complements, these cells are able to recruit and mediate other cells of different lineages to the site of inflammation and/or infection. After the defense action, these cells undergo programmed cell death (apoptosis) [12, 21].

## Eosinophil

The maturation phases of eosinophils follow a similar line to that of neutrophils, is described through the following stages: eosinophil myeloblast, promyelocyte, myelocyte, and mature eosinophil, which suffer the action of G-CSF, IL-3, and IL-5, responsible for eosinophil maturation) [13, 21].

Mature eosinophils represent about 2–3% of leukocytes and act on innate and acquired immunity, being present in the mucous membranes of the respiratory, gastrointestinal, and genito-urinary tracts, and may increase in number due to the recruitment of these blood cells in inflammatory and/or infectious conditions. Classified as granulocytic cells, eosinophils have cytoplasmic granules that contain enzymes responsible for damaging the cell walls of parasites or acting against allergic responses. These granules contain basic proteins that bind to acidic dyes like eosin [21, 22].

Eosinophilic granules and their myeloid precursors are abundant in peroxidases and lysosomal enzymes; however, eosinophil peroxidase is genetically different from neutrophils, conferring less bactericidal action when compared to neutrophils. Thus, the cellular function of eosinophils is directly linked to the storage of proteins, such as major basic protein, eosinophil cationic protein, and eosinophil-derived neurotoxin [12, 20].

The larger basic proteins represent more than half of the granule proteins and have cytotoxic activity against parasitic infections. They also induce the release of histamine by basophils and mast cells, this process acts in the negative regulation of allergic and inflammatory processes. The other basic proteins can cause the formation of transmembrane pores capable of causing tissue damage [11–13].

## Basophils

Basophils are granulocytic cells that act on innate and acquired immunity. Its granules are filled by various inflammatory and antimicrobial mediators, thus being responsible for the immune responses against allergic reactions. Despite the structural and functional similarities with mast cells, basophils originate from other progenitor cells: promyelocyte, basophilic myelocyte, basophilic metamyelocytes, basophilic, and basophilic rod. The entire process of development and maturation occurs inside the bone marrow, with only the mature basophil being released into the bloodstream [12, 19].

These cells represent less than 1% of the leukocytes in the blood. The granules of the basophils are abundant and dense, capable of preventing complete visualization of the nucleus under an optical microscope and have an affinity for basic dyes. In addition, they are able to synthesize several mediators. Although they are not normally present in the tissues, basophils can be recruited to some inflammatory sites. Like mast cells, basophils express receptors for immunoglobulin G (IgG) and immunoglobulin E (IgE) and can be stimulated by binding the antigen to the IgE on its surface [12, 15].

## Monocytes

Monocytes are classified as agranulocytic cells, originating from the following lineage: monoblast, pro monocyte, monocytes, and macrophages. The functions of monocytes are the removal of dead or senescent cells, removal of foreign particles, processing, and presentation of antigens in immunological reactions and participation in acute and chronic inflammatory reactions. They also have an important role in the formation of atheromatous plaque (related to atherosclerosis) and in the destruction of both microorganisms and neoplastic cells and grafts [22, 23].

Monocytes are characterized by acquiring their functional maturity in the tissues in the form of macrophages. There are two possibilities after the monocytes leave the medulla: either the cells are housed in the marginal compartment of blood vessels (adhered to endothelial cells) or are released into the bloodstream [22, 24].

These cells are the largest leukocytes, measuring 15–20  $\mu\text{m}$  in diameter; however, they are responsible for forming only a small portion of the total blood cell population. The monocyte nucleus is euchromatic being relatively large and irregular, having the characteristic of invagination on one side. Next to this nuclear invagination, this cell contains a prominent Golgi complex and vesicles. Monocytes are actively phagocytic cells, containing numerous lysosomes. They are also highly mobile and with a well-developed cytoskeleton. In turn, the cytoplasm is light in color [23, 24].

## Lymphocytes

Lymphocytes are the second most numerous type of leukocytes in adults, while during childhood they are the most numerous type of blood leukocytes. They are formed through the following lineage: undifferentiated lymphoid cell, lymphoblast, pro-lymphocyte, medium lymphocyte, small lymphocyte, and plasmocyte [25, 26].

Most circulating lymphocytes have a small size of 6–8  $\mu\text{m}$  in diameter and increased cytoplasmic volume. Often, this change occurs as a result of antigenic stimulation. These cells are found in extravascular tissues (including lymphoid tissue), being classified as the only leukocyte that returns to the circulation. The lifespan of lymphocytes varies from a few days to many years. Long-lived lymphocytes play an important role in maintaining immune memory [25].

Blood lymphocytes are a heterogeneous collection, mainly of B and T cells, and consist of different subsets and stages of activity and maturity. About 85% of all lymphocytes circulating in the blood are T cells. Primary immunodeficiency diseases can cause molecular damage to T and B lymphocytes. Included as lymphocytes are Natural Killer Cells (NK). NK cells are morphologically similar to T cells [26].

B lymphocytes and T lymphocytes have a rounded nucleus with dense color, surrounded by a sparse cytoplasm, which is hardly visible under optical microscopy. In the electron microscope, few cytoplasmic organelles can be seen, except for a small number of mitochondria, isolated ribosomes, scarce ER profiles, and occasional lysosomes. These cells become mobile when they come into contact with solid surfaces and can pass between endothelial cells to exit or reenter the vascular system. Thus, they migrate widely within the various tissues, including the epithelia [26, 27].

### 3.1.3 Platelets

Platelets are cytoplasmic fragments of megakaryocytes produced in the bone marrow. Because they are fragments, these cells have no nucleus and are therefore anucleated. They have a discoid shape of about 2–4  $\mu\text{m}$  in diameter and a very complex internal structure divided into four zones: peripheral zone, sol-gel zone, organelle zone, and membrane system. The interior of the platelet is able to communicate with the external environment due to the presence of a channel system known as the open canalicular system. This communication is important, as it guarantees the release of molecules stored in platelets [13, 19, 20].

Platelets have significantly reduced blood circulation time, taking an average of 10 days to remove. These cell fragments are removed from the circulation by the reticuloendothelial cells of the liver and spleen. These cells have important functions for the maintenance of our bodies. When, for example, a lesion occurs in a blood vessel, they clump together, forming a plug, and release substances that ensure that more platelets move to the site. In addition, they participate in the coagulation cascade, releasing important substances that guarantee the formation of a clot. It is worth noting that platelets also have enzymes that contribute to the removal of the clot [13, 19, 20].

## 4 Conclusions

Cells are the fundamental units of life on Earth, having undergone countless changes since their emergence. These changes allowed the evolution of living beings to the form and function they currently have. This evolution was due to the specialization of cell groups to perform specific functions aimed at ensuring the balance of life of organisms. Among these developments, there was the appearance of blood cells, which are divided into three basic types: erythrocytes, leukocytes, and platelets, which are responsible for the transport of gases throughout the body, defense against antigens, blood clotting, among other functions.

The importance of the classification of blood cell types is that through this knowledge it is possible to detect and carry out treatment of types of blood disease in which blood components are affected such as anemia derivations through red blood cells, immune thrombocytopenic derivations through platelets, leukemia derivations by white blood cells, among other several hematological diseases, such as types of hemoglobinopathies and hereditary coagulopathies, in the same way, that it is possible to detect several types of related disorders and diseases.

## References

1. Farah, S.B.: DNA: Segredos e Mistérios. In: DNA: segredos e misterios (2007)
2. Junqueira, L.C., Carneiro, J.: *Biologia Celular e Molecular*, 9ª edição. Guanabara Koogan, Rio de Janeiro (2012)
3. Koss, L.G., Gompel, C.: *Introdução à Citopatologia Ginecológica com Correlações Histológicas Clínicas*. Editora Roca (2006)
4. Karp, G.: *Biologia Celular e Molecular: Conceitos e experimentos*, 3ª edição, pp. 53–54. Barueri, SP (2005)
5. Weiss, T.F.: *Cellular Biophysics*. MIT Press, Cambridge, Mass (2017)
6. Darwin, C.: *A Origem das Espécies*. Sumaré, Martin Claret (2014)
7. Junqueira, L.C., Carneiro, J.: *Histologia Básica*. Rio de Janeiro, Brazil, Guarabara Koogan (2013)
8. Murray, P.R., Rosenthal, K.S., Pfaller, M.A.: *Microbiologia médica*. Elsevier Health Sciences (2017)
9. De Robertis, E., Hib, J.: *De Robertis Bases da Biologia Celular e Molecular*. 4ª. Guanabara Koogan, São Paulo (2006)
10. Molinaro, E., Caputo, L., Amendoeira, R.: *Métodos Para a Formação de Profissionais em Laboratórios de Saúde*. Fio Cruz, Rio de Janeiro (2009)
11. Verrastro, T., Lorenzi, T.F., Neto, S.W.: *Hematologia e Hemoterapia: Fundamentos de Morfologia, Patologia e Clínica*. Atheneu, Rio de Janeiro (2005)
12. Delves, P.J., et al.: *Essential Immunology*. Wiley (2017)
13. Monteiro, A.C.B.: *Proposta de uma metodologia de segmentação de imagens para detecção e contagem de hemácias e leucócitos através do algoritmo WT-MO*. Dissertation, State University of Campinas, UNICAMP—SP, Brazil (2019)
14. Abbot Laboratorie De México S.A.: *Atlas Com Interpretacion Histogramas Y Escatergramas*. E.G, Buenos Aires (2002)
15. Fischbach, F.T., Dunning, M.B.: *A Manual of Laboratory and Diagnostic Tests*. Lippincott Williams & Wilkins (2009)

16. Abbas, A.K., Lichtman, A.H.H., Pillai, S.: Cellular and Molecular Immunology. Elsevier Health Sciences (2014)
17. Monteiro, A.C.B., Iano, Y., França, R.P., Arthur, R., Estrela, V.V.: A Comparative study between methodologies based on the hough transform and watershed transform on the blood cell count. In: Brazilian Technology Symposium, pp. 65–78. Springer, Cham (2018)
18. Monteiro, A.C.B., Iano, Y., França, R.P., Arthur, R.: Methodology of high accuracy, sensitivity and specificity in the counts of erythrocytes and leukocytes in blood smear images. In: Brazilian Technology Symposium, pp. 79–90. Springer, Cham (2018)
19. Souza, M.H.L., Rêgo, M.M.S.: Princípios de Hematologia e Hemoterapia. Alfa Rio (2009)
20. Da Silva, P.H., Hashimoto, Y., Alves, H.B.: Hematologia Laboratorial. Revinter, Rio de Janeiro (2009)
21. Murphy, K., Travers, P., Walport, M.: Janeway's Immunobiology, 8th edn. Garland Science, New York (2012)
22. Rodak, B.F., Caar, J.H.: Clinical Hematology Atlas. Elsevier Health Sciences (2015)
23. Nemer, A.S.A., Neves, F.J., Ferreira, J.E.S.: Manual De Solicitação e Interpretação de Exames Laboratoriais. Revinter (2010)
24. Standring, S. (ed.): Gray's Anatomia: A Base Anatômica da Prática Clínica. Elsevier, Brasil (2010)
25. Erichsen, E.S., et al.: Medicina Laboratorial Para o Clínico. Elsevier (2015)
26. Da Silva, P.H., et al.: Hematologia Laboratorial: Teoria e Procedimentos. Artmed Editora (2015)
27. Failace, R.: Hemograma: Manual de Interpretação. Artmed Editora (2015)



# Hematology: A Review of the Main Methodologies of Clinical Analyses



Ana Carolina Borges Monteiro , Yuzo Iano , Reinaldo Padilha França , and Rangel Arthur 

**Abstract** Human blood is composed of liquid and solid elements, blood cells being extremely important for the assessment of the patient's health status. Blood consists of plasma and cellular elements, which include blood cells and cellular fragments. Erythrocytes are blood cells containing a large amount of hemoglobin which is the pigment responsible for the transport of oxygen, being numerous and the most found in our blood. Leukocytes are colorless cells whose main function is to defend our organism, still emphasizing that there is not only one type of leukocyte, but it is possible to identify five distinct types. In this scenario, the exam that analyzes blood cells is called a blood count, and for this reason, it is the most requested laboratory exam in the medical routine. Based on this, explaining the methodologies of this exam as well as performing its interpretation is essential to support scientific research and provide a background for health professionals in academic training.

**Keywords** Blood cells · Hematology · Blood count · Hematological devices · Cellular biology

---

A. C. Borges Monteiro (✉) · Y. Iano · R. P. França  
School of Electrical and Computer Engineering (FEEC), University of Campinas – UNICAMP,  
Av. Albert Einstein - 400, Barão Geraldo, Campinas, SP, Brazil  
e-mail: [monteiro@decom.fee.unicamp.br](mailto:monteiro@decom.fee.unicamp.br)

Y. Iano  
e-mail: [yuzo@decom.fee.unicamp.br](mailto:yuzo@decom.fee.unicamp.br)

R. P. França  
e-mail: [padilha@decom.fee.unicamp.br](mailto:padilha@decom.fee.unicamp.br)

R. Arthur  
School of Technology (FT), University of Campinas – UNICAMP, R. Paschoal Marmo - 1888,  
Jardim Nova Italia, Limeira, SP, Brazil  
e-mail: [rangel@ft.unicamp.br](mailto:rangel@ft.unicamp.br)

## 1 Introduction

The blood count is a laboratory test that is highly requested in the medical routine, as it directly provides the diagnosis of pathologies or is used as an indicator for the detection of various diseases. This exam is formed by the erythrogram, leukogram and platelet, which evaluate the quantity and morphology of erythrocytes, leukocytes, and platelets, respectively [1].

The erythrogram is the part of the blood count responsible for evaluating the total number of erythrocytes (RBC), hemoglobin (Hb), hematocrit (Htc), and hematimetric indices: Mean Corpuscular Volume (MCV), Mean Corpuscular Hemoglobin (MCH) and Hemoglobin Concentration Mean Corpuscular (CHCM). The total erythrocyte count is used to detect hematological disorders. Reductions in the number of red blood cells are called erythropenia, which is a strong indication of the presence of anemia or blood loss. On the other hand, erythrocytosis is characterized by an increase in the production of erythrocytes, either by genetic or external factors, is responsible for the appearance of polycythemias [1, 2].

Anemias can be classified either of genetic origin (falciform anemia, thalassemia, spherocytosis anemia, among others) or by food deficit (iron deficiency anemia, megaloblastic anemia, among others). Both types inspire care and medical follow-up, as food anemias cause indisposition, decrease in work performance, pallor and vertigo. In turn, genetic anemias need lifelong care, as they are responsible for pain crises, hospitalizations and the need for periodic blood transfusions. Some types of polycythemia are of genetic origin and, like genetic anemias, need continuous care, as it is characterized by the exacerbated production of erythrocytes, causing damage to the organism such as infarction and strokes [3–5].

Hemoglobin is a protein present inside erythrocytes, being responsible for the reddish pigmentation of cells and for the transport of  $O_2$  and  $CO_2$  to tissues, through the association of these gases with iron molecules. The hematocrit, in turn, expresses in percentage the amount of blood cells present in the plasma [6].

Hematimetric indices are dependent on the values of hemoglobin, hematocrit and RBC, with the function of assessing the color and size of erythrocytes. The size of the erythrocytes is evaluated through the MCV, which classifies these cells into normocytic, microcytic and macrocytic. Normocytic red blood cells are those that are normal in size, while microcytes are smaller in size and macrocytes are larger in volume than those expressed by reference values. Both HCM and CHCM are responsible for evaluating the erythrocyte staining according to the parameters: normal coloration, insufficient staining or exacerbated staining, being classified into normochromic, hypochromic and hyperchromic, respectively [7].

It is important to emphasize that the decrease of just one parameter is not enough to conclude a diagnosis of anemia or leukemia. The confirmation of these pathologies depends on biochemical or cytochemical tests for the adequate conclusion of the hematological disorder subtype found. However, the suspicion of these pathologies is often detected through the blood count, which usually presents changes in more than one of the analyzed parameters [8]. Healthy patients have an RBC count

within the reference values, and the erythrocytes are classified as normocytic and normochromic. However, patients with iron deficiency anemia, for example, have a reduction in the total RBC count associated with microcytic and hypochromic red blood cells [9].

The leukogram is the part of the blood count with the function of evaluating the granulocyte and agranulocyte leukocytes through the quantitative evaluation of the total count and by the differential count of the leukocytes. The total WBC count indicates or rules out the presence of inflammations and/or infections from different sources. The decrease in the total leukocyte count is called leukopenia and occurs in cases of patients undergoing cancer treatment or in cases of a sedentary lifestyle. In turn, leukocytosis is represented by the increase in the amount of leukocytes, due to the presence of allergies; parasitic, viral or bacterial infections, or leukemias [10–12].

The differential leukocyte count, evaluates the amount of each leukocyte: neutrophils, eosinophils, basophils, monocytes and lymphocytes. Neutrophils are the most abundant blood cells, representing about 70% of the total circulating blood cells. The quantitative increase in neutrophils is called neutrophilia, indicating the presence of acute bacterial infections. However, neutrophilia is also present in exams of patients with burns, myocardial infarction, postoperative period, stress, use of glucocorticoids and intense physical exercises [11, 12].

Neutrophilia is divided into two types: neutrophilia with a left shift and neutrophilia with a right shift. The left shift is a condition present in cases of acute infections, when there is the release of a large amount of neutrophil rods into the bloodstream. In turn, the deviation to the right is characterized by the presence of segmented or hypersegmented neutrophils (more than 5 lobes), being indicative of chronic infections. The decrease in the amount of neutrophils is called neutropenia and may indicate, spinal infiltration, immunosuppression by the human immunodeficiency virus (HIV), alcoholism, food deficit, radiation exposure or use of cytotoxic drugs [13].

Eosinophils are cells that act mainly in the intestines, epithelium and the respiratory system. Thus, eosinophilia is characterized by the numerical increase of these cells, which is indicative of intestinal infections by helminths (schistosomiasis, hookworm, ascariasis, among others), dermatitis, dermatoses, acute myeloid leukemia, chronic myeloid leukemia, pernicious anemia or allergic processes respiratory. However, the decrease (eosinophilia) or the absence of eosinophils in the bloodstream is normal. Thus, eosinopenia is usually due to the administration of adrenocortical or corticoid hormones [13, 14].

Basophils are cells little present in the bloodstream; however, they play an important role during allergic reactions through the release of IgE and histamines. Basophilia is a process where there is a greater number of circulating basophils, being indicative of allergic reactions or the presence of leukemias. Basopenia, in turn, is not classified as a pathological process [3, 14].

Monocytes, on the other hand, are largely related to phagocytosis processes. Thus, the increase in the production and release of these cells is called monocytosis. This increase is suggestive of tissue repairs or indicates the presence of chronic infections. However, monocytopenia is indicative of decreased monocyte production and release

and is often associated with the lifestyle of the patient who is exposed to stress. All leukocytes present variations in their amounts according to the patient's age [14, 15].

Lymphocytes are blood cells active in the processes of viral infections. The increase in the number of these cells in the bloodstream (lymphocytosis) is directly related to the presence of viral pathologies such as hepatitis, HIV, rubella, among others [11–14]. The decrease in the amount of lymphocytes (lymphopenia) can be interpreted such as chronic HIV, acute stress or the presence of liver cirrhosis. It is important to note that lymphocytosis is a normal condition during childhood. Like lymphocytes, other blood cells undergo changes in their amounts according to the stage of life [16].

Thrombocytopenia occurs when the patient has a reasonable drop in the normal number of platelets. This analysis can be done after counting platelets in a blood sample. When a patient has thrombocytopenia, bleeding occurs more easily, as well as the appearance of purple spots on the body. The patient may also have blood in the stool, bloody vomiting, pain in the joints and muscles and have a weakness.

Thrombocytosis occurs when a patient has a high number of platelets in the blood, the number is greater than 1,000,000 platelets per  $\text{mm}^3$ . Thrombocytosis can be further classified into primary and secondary. The primary is related to myeloproliferative diseases (related to the abnormal production of blood cells), and the secondary is triggered by some underlying disease, such as infections and anemias [6].

However, in order to arrive at such quantifications of red blood cells and platelets, specific methodologies for each cell type are employed. Thus, the present study aims to present in a clear and brief way the main methodologies for total and differential blood cell counts.

## 2 Methodology

Considering the need to gather fundamental information regarding basic concepts of hematology, this study brought together the main concepts present in the literature regarding hematology, explaining from blood cells to the comparison between the methodologies employed.

## 3 Results and Discussion

Regardless of the methodology used to perform the complete blood count, this test must be performed by collecting 4 ml of venous blood collected in a tube containing EDTA anticoagulant (“Ethylenediaminetetraacetic acid”) or heparin, which can be collected with or without fasting of the patient. The samples must avoid the presence of hemolysis (ruptured erythrocytes causing a lower count in the total amount of red blood cells), lipemia (presence of fat in the form of triglycerides which makes it

difficult to read results by colorimetric methods), clots (resulting in lower counts of platelets), use of antibiotics, anti-inflammatory and antiallergic agents hours before the exam (decreases the amount of leukocytes, being able to mask infectious or allergic conditions) and avoid smoking 2 h before the exam (change in hemoglobin rates, hematocrit and indexes hematimetric) [15].

Currently, the blood count can be performed using two methodologies: manual and automated, which are used according to the needs of each clinical analysis laboratory. Both the manual methodology and the automated methodology must be carried out with the help of a health professional such as doctors, pharmacists, biologists, biomedical and hematologists [1, 5].

The manual methodology is more dependent on the health professional to be performed, so the time taken to perform the exam is greater. It is also important to consider that mainly in underdeveloped and developing countries, health professionals are often subjected to long working hours. This reality directly impacts the accuracy of the results released. This is because in the manual methodology it is necessary to count blood cells one by one under optical microscopy. The biggest advantage of the manual methodology is the cost. This technique depends on low-cost reagents and instruments, thus being more present in small laboratories and/or in countries with low per capita income [1, 5].

The automated methodology has a higher cost, especially when applied to low-income populations, since the cost of acquisition, maintenance and reagents are passed on to the patient at the time of payment for the exam. However, the investment is worthwhile, as there is the less direct interaction between the health professional and the patient's blood. Thus, there is less chance of accidents involving blood samples. When such an accident occurs, the professional is exposed to a high risk of infection with Hepatitis types B, C, D, HIV, Syphilis, Malaria, Chagas disease, among others. Other benefits are the speed and accuracy of the results obtained, after all, the equipment is not subject to stress, fatigue and personal problems like a human [1, 5, 10].

### ***3.1 Manual Erythrogram***

The total erythrocyte count in a Neubauer chamber is performed by means of a 1:200 dilution, where 20  $\mu$ l of whole blood is deposited in a test tube in 4 ml Hayen's liquid (sodium citrate diluted in physiological solution) with subsequent homogenization. Subsequently, part of this solution is transferred to the Neubauer chamber, which is covered by a glass coverslip and analyzed under optical microscopy, where erythrocytes will be counted under the objective lens at 400 $\times$  magnification [10, 16].

It is also necessary to make a blood smear, by sliding a few microliters of blood on a glass slide and later using dyes, which allow the visualization of cellular structures. These dyes have the function of staining the nuclear and cytoplasmic structures of blood cells. There is a wide variety of dyes; however, the most used for blood smears are Leishman and panoptic. Only the final portion of the slide is used for counting,

as the anterior portions have clustered and/or overlapping cells, preventing reliable counting. This blood smear is used to analyze the red cell morphology and staining [16].

Quantitative and morphological analyzes of blood cells are fundamental parameters for the detection of anemia, since the vast majority of them result in anisocytosis (variation in shape), such as sickle cell anemia (sickle-shaped red blood cells), spherocytosis anemia (red blood cells with a circle format), hereditary ellipsis (elongated red blood cells), among others. Through the blood smear, it is also possible to identify blood parasites in the acute phase, such as leishmaniasis, nasturtium and malaria, among others. It is important to emphasize that it is only necessary to make a single blood smear during the entire blood count analysis process, with the same slide used for the analysis of red blood cells, leukocytes and platelets [17, 18].

The erythrocytes are responsible for the transport of oxygen, since inside these cells there is a protein called hemoglobin, which in addition to giving the blood a red color it binds to oxygen, which allows red blood cells to transport and distribute oxygen gas from the lungs to inside the cells of the body. The importance of analyzing these cells goes from both ends, related to the increase in the number of erythrocytes, is considered polyglobulia (known as polycythemia), is normally not clinically relevant; however, its reduction in relation to the level of red blood cells is considered hypoglobulia, which is a sign of anemia [18, 19].

Although in addition to assessing erythrocytes and hemoglobin, the eritrogram also performs a hematocrit check, which it is related to the volume of erythrocytes found in the centrifuged blood, since through that there is a possibility in determining the ratio between red blood cells and plasma, relative to the liquid part of the blood [15].

The determination of hematocrit consists of filling 2/3 of a glass capillary with whole blood. Subsequently, one end of the capillary must be sealed by means of heat sources or the use of mass, in order to prevent the escape of blood. This capillary must be placed in a microhematocrit centrifuge at a rotation of 1500 rpm (rotations per minute) for 5 min. After centrifugation, there is the separation of whole blood in 2 phases: a lighter one, formed by plasma, and another more dense, formed by the sedimentation of blood cells. To read the result, it is necessary to measure in millimeters the size of the sediment formed at the bottom of the capillary [6, 19].

Hemoglobin, in turn, can be determined using equipment called a spectrophotometer. Several methodologies are available in the market for the quantification of hemoglobin, with variations both in the time spent to perform the exam and in the amount of sample needed and reagents used during the process. The most used methodology for the measurement of hemoglobin is the cyanomethoglobin method, which uses Drabkin's liquid. This liquid can be composed of potassium ferrocyanide ( $K_3FeCN_6$ ) potassium cyanide (KCN) or anhydrous potassium phosphate ( $KH_2PO_4$ ) [5, 20, 21].

Upon contact with Drabkin's liquid, red blood cells are hemolyzed, with the release of free Hb, which in turn is converted to methemoglobin (iron hemoglobin in the iron form). Due to the action of potassium cyanide, methemoglobin is transformed into cyanomethemoglobin, a stable compound that absorbs light at 540 nm. The

hemoglobin concentration of the sample is calculated from a commercial hemoglobin standard, pre-determined by the manufacturer [5, 20, 21].

The hematimetric indices, in turn, are determined by means of mathematical formulas depending on the values obtained for total RBC, hemoglobin and hematocrit [5, 22]. Equation 1 is used to determine the MCV:

$$MCV = Htc \times 10RBC \quad (1)$$

where Htc represents the hematocrit value obtained by centrifuging whole blood, and RBC indicates the total red blood cell count obtained by automated equipment or by manual counting in a Neubauer chamber. The result is expressed between 80–90 fl, which indicates the absence of pathologies [5, 22]. In Eq. 2, the HMC determination is presented:

$$MCH = Hb \times 10RBC \quad (2)$$

where Hb indicates hemoglobin concentration and RBC is the total red blood cell count. The reference value is given between 26 and 34 picograms. CMCH, through Eq. 3:

$$CMCH = Hb \times 100Htc \quad (3)$$

where Hb represents hemoglobin and Htc the hematocrit [5, 22]. The reference value is expressed as

$$31.5 - \frac{36g}{dL} \quad (4)$$

### 3.2 *Manual Leukogram*

The leukogram assesses white blood cells (WBC), called leukocytes, the defense cells responsible for fighting invading agents. Leukocytes are actually a group of different cells, with different functions in the immune system. Some leukocytes directly attack the invader, others produce antibodies, others only make the identification, and so on; this test helps in the diagnosis of viral, bacterial or parasitic infections, spinal dysplasias, leukemias and lymphomas [4].

The counting of WBC is performed through total counting and differential counting, which are counts with different methodologies, but complementary. It is important to note that the counts are expressed in absolute and relative values [23].

The total count of WBC is performed in the Neubauer chamber, through a 1:20 dilution, where 0.4 ml of Turk's liquid and 20  $\mu$ l of whole blood are deposited in a test tube. Turk's liquid can consist of 2% glacial acetic acid or 1% hydrochloric acid,

which can be stained with methylene blue or gentian violet in order to differentiate it from the Hayer liquid [23].

Differential leukocyte counting is performed using a blood smear previously prepared for the evaluation of erythrocytes. In this process, 100 leukocytes present in the final portion of the blood smear slide should be counted. It is necessary to note manually, how many leukocyte subtypes were counted per field. Upon reaching the total of 100 cells counted, the professional must finish the identification and count of the leukocytes and perform the calculations of relative WBC and absolute WBC (value expressed as a percentage) [4, 23].

### 3.3 *Manual Platelet Count*

To manual platelet count is need still taking into account that to make thin smears, dry and stain using the usual methods. Examine under the microscope with an immersion objective. After count 1000 erythrocytes in different fields, noting the number of platelets found [8]. Apply the values in the formula:

$$\text{Number of platelets} \times \frac{\text{Number of erythrocytes per mm}^2}{1000} \quad (5)$$

### 3.4 *Automated Counting*

The automation of the blood count implies greater agility in the performance of the exams and in the release of the reports; however, they are a more expensive methodology when compared to the manual methodology. This methodology is able to count the three cellular types simultaneously. In the 1950s, Coulter Eletronic, Inc introduced the impedance principle for cell counts [1, 15].

The impedance principle is based on the fact that cells, bad conductors of electricity are diluted in an electrically conductive solution. This cell suspension is weighed through an orifice with a diameter around 100  $\mu\text{m}$ , where an electric current passes. This electric current originates from two electrodes: one located on the inside of the orifice and positively charged, and the other located on the outside of the orifice, negatively charged. In this way, each time the cell passes through the hole, it interrupts the electrical current and there is a change in conductance; therefore, each interruption is counted as a particle [1].

The impedance principle, over the years, has been enabled with counters capable of measuring cell volume. Such evolution was the result of the color-relation of the proportionality of the magnitude of the interruption of the electric current (pulses) with the cell volume. Thus, it was observed that small pulses corresponded to small volumes, while large pulses were the result of larger volumes [15].



From this correlation between the magnitude of the electric current and the cell volume, a new concept called the threshold concept was created. The threshold concept is responsible for classifying cells according to their volume, thus allowing the detection of globular volume. The globular volume corresponds to the hematocrit performed on the manual blood count; however, it receives this name because it is performed without the need for microcentrifugation. Both the impedance principle and the threshold concept are responsible for the introduction of multiparameter devices on the market. These devices are capable of performing simultaneous cell counts using separate channels for counting [1, 15].

In the 1960s, the conductivity technique was developed, based on the high-frequency electromagnetic current, which is responsible for providing information regarding the cell volume, the size of the nucleus and the content of the cytoplasmic granulations. Subsequently, in 1970, the techniques of laser beam dispersion (laser light scatter) and hydrodynamic fluid were introduced. Both techniques preserve the leukocyte nuclei and granulations, retracting only the cytoplasmic membrane. These techniques are based on the principles of diffraction, refraction and reflection of the emitted light [15].

However, in these techniques, red blood cells are undetectable. To solve this problem, erythrocytes started to be quantified by means of flow cytometry and hydrodynamic focus, where these cells are counted one by one, through an extremely fine capillary. The red blood cells are then subjected to a laser beam, where the dispersion of the light is analyzed at different angles of deviation. In this context, the cell size is indicated at zero degrees, at  $10^\circ$  the internal structure is indicated and at  $90^\circ$  the leukocytes are identified and their lobularity characteristics and their granulation content [1, 15].

Currently, there are a large number of multiparameter devices, which use impedance, conductivity and scattered light techniques. These technologies can also be associated with the cytochemical characteristics of cells (such as myeloperoxidase) and the use of reagents that perform the analysis of certain cell types. However, before purchasing a hematological device, it is necessary to take into account the following parameters: Automation device versus type of patient attended; number of hemograms per day  $\times$  samples/time spent by the device; cost of each hemogram; quality control; technical assistance; interfacing, training of employees [1, 15].

However, even with the acquisition of hematological equipment, manual hemogram is not a dispensed practice, being recommended for the confirmation of hematological reports of pediatric patients, patients over 75 years of age, cancer patients, patients with suspected leukemia or polycythemia, patients with leukocytosis and patients in severe condition (mainly in a state of hospitalization in the Intensive Care Unit—ICU) [1, 15].

## 4 Conclusions

The manual blood count is an examination that is totally dependent on human performance, which is used for the use of non-automated equipment. It is a cheaper exam, but more time-consuming and less reliable, as it depends on counts and calculations performed by health professionals. It is considered a good alternative for small laboratories, where the demand for tests is small and the cost of acquiring hematological equipment and reagents does not match the cost-benefit of the process.

Over time, the study of blood cells is no longer restricted to just observing the morphology of cells and has started to develop more specific tests, but that does not dispense with the use of conventional microscopy. This test responsible for the analysis of blood cells is called a complete blood count. Thus, review studies are extremely important to fundament and inspire new research, whether they refer to studies of cell biology, molecular biology, histology, cytology, hematology, or even for the creation of medical devices.

## References

1. Failace, R.: Hemograma: Manual de Interpretação. Artmed Editora (2015)
2. Monteiro, A.C.B., Iano, Y., França, R.P.: An improved and fast methodology for automatic detecting and counting of red and white blood cells using watershed transform. In: VIII Simpósio de Instrumentação e Imagens Médicas (SIIM)/VII Simpósio de Processamento de Sinais da UNICAMP (2017)
3. Verrastro, T., Lorenzi, T.F., Neto, S.W.: Hematologia e Hemoterapia: Fundamentos de Morfologia, Patologia e Clínica. Atheneu, Rio de Janeiro (2005)
4. Fischbach, F.T., Dunning, M.B.: A Manual of Laboratory and Diagnostic Tests. Lippincott Williams & Wilkins (2009)
5. Monteiro, A.C.B.: Proposta de uma metodologia de segmentação de imagens para detecção e contagem de hemácias e leucócitos através do algoritmo WT-MO. Dissertation, State University of Campinas – UNICAMP (2019)
6. Nemer, A.S.A., Neves, F.J., Ferreira, J.E.S.: Manual De Solicitação e Interpretação de Exames Laboratoriais. Revinter (2010)
7. Monteiro, A.C.B., Iano, Y., França, R.P., Arthur, R.: Development of a laboratory medical algorithm for simultaneous detection and counting of erythrocytes and leukocytes in digital images of a blood smear. In: Deep Learning Techniques for Biomedical and Health Informatics, pp. 165–186. Academic Press (2020)
8. Erichsen, E.S., et al.: Medicina Laboratorial Para o Clínico. Elsevier (2015)
9. Souza, M.H.L., Rêgo, M.M.S.: Princípios de Hematologia e Hemoterapia. Alfa Rio (2009)
10. Handin, R.I.; Lux, S.E., Stossel, T.P. (ed.): Blood: Principles and Practice of Hematology. Lippincott Williams & Wilkins (2003)
11. Monteiro, A.C.B., Iano, Y., França, R.P., Arthur, R.: Methodology of high accuracy, sensitivity and specificity in the counts of erythrocytes and leukocytes in blood smear images. In: Brazilian Technology Symposium, pp. 79–90. Springer, Cham (2018)
12. Monteiro, A.C.B., Iano, Y., França, R.P., Arthur, R., Estrela, V.V.: A Comparative study between methodologies based on the hough transform and watershed transform on the blood cell count. In: Brazilian Technology Symposium, pp. 65–78. Springer, Cham (2018)
13. Abbas, A.K., Lichtman, A.H.H., Pillai, S.: Cellular and Molecular Immunology. Elsevier Health Sciences (2014)

14. Turgeon, M.L.: *Clinical Hematology: Theory and Procedures*. Lippincott Williams & Wilkins (2005)
15. Da Silva, P.H., et al.: *Hematologia Laboratorial: Teoria e Procedimentos*. Artmed Editora (2015)
16. Mcpherson, R.A., Pincus, M.R.: *Henry's Clinical Diagnosis and Management by Laboratory Methods E-Book*. Elsevier Health Sciences (2017)
17. Keohane, E.M., Otto, C.N., Walenga, J.M.: *Rodak's Hematology-E-Book: Clinical Principles and Applications*. Elsevier Health Sciences (2019)
18. Lazarus, H.M., Schmaier, A.H. (eds.): *Concise Guide to Hematology*. Springer (2018)
19. Cappell, M.S.: *Principles and Practice of Hospital Medicine*. McGraw-Hill Education Medical (2017)
20. Cappellini, M.D.: Advances in hemoglobin disorders. *HemaSphere* **2**(S2), 23 (2018)
21. LABEST: *Hemoglobina. Labtest*, Minas Gerais (2019)
22. Emilse, L.A.M., Cecilia, H., María, T.M., Eugenia, M.M., Alicia, I.B., Lazarte, S.S.: *Blood Res.* (2018)
23. Gulati, G.L., Gatalica, Z., Hyun, B.H.: Benign disorders of leukocytes. In: *Handbook of Hematologic Pathology* (2019)

# An Algorithm Oriented at Obtaining the Molecular Weight and Concentration of DNA Samples in Agarose Gel Images



Christian del Carpio , Marcelo Garcia , Julio Elías , David Laván , and Guillermo Kemper 

**Abstract** This article presents an algorithm for obtaining the weight and concentration of DNA samples from agarose gel images using digital image processing techniques. The purpose of this algorithm is to obtain much more accurate results than the results obtained by experts using their visual sense. The algorithm is based on capturing the DNA samples and comparing them with DNA molecular weight markers using digital image processing techniques to find the concentration, which is the intensity of the samples, and the weight of the samples. The proposed algorithm achieved a moderate “level of agreement” in the results, as calculated by kappa, compared with the expert results of a total of six images, containing 51 DNA samples in total. These DNA samples open source is from flies.

**Keywords** Agarose gel · DNA ladder · DNA · Molecular weight · Image processing

---

C. del Carpio (✉) · M. Garcia · J. Elías · G. Kemper  
Universidad Peruana de Ciencias Aplicadas, Lima, Peru  
e-mail: [pcelcdel@upc.edu.pe](mailto:pcelcdel@upc.edu.pe)

M. Garcia  
e-mail: [u201112135@upc.edu.pe](mailto:u201112135@upc.edu.pe)

J. Elías  
e-mail: [u201111196@upc.edu.pe](mailto:u201111196@upc.edu.pe)

G. Kemper  
e-mail: [guillermo.kemper@upc.pe](mailto:guillermo.kemper@upc.pe)

D. Laván  
Laboratorio de Microgravedad – INICTEL - UNI, Lima, Peru  
e-mail: [dlavan@inictel-uni.edu.pe](mailto:dlavan@inictel-uni.edu.pe)

# 1 Introduction

Recently, interest in the investigation of the genetic expression of DNA using agarose gel images has increased because of the increasing interest in finding explanations about the mutations and diseases that attack genetic information. To prepare the agarose gel using the inserted DNA samples, the gel must undergo electrophoresis. This technique is used to separate the DNA fragments according to their size [1]. Previous studies have proposed different image processing algorithms for calculating the molecular weight and concentration in agarose gels.

Segmentation methods have been proposed that use the histograms of rows and columns to obtain an accurate cut of the samples [2]. “Enhanced fuzzy c-means”, has also been proposed, which is an efficient segmentation algorithm in the case of samples and DNA ladders [3]. Edge detection, geometric diffusion filters, and 2D noise filters have been used for sample detection [4].

Skutkova et al. [5], propose an algorithm to remove most distortions, such as non-uniform noise, brightness, and/or contrast, geometrical disproportion, present in digitized electrophoresis gel images. These distortions affect the detection of the bands present in the image. This method involves the use of signal processing techniques such as Dynamic time warping, peak detection, filters, etc. The algorithm was tested on 50 images, achieving acceptable results.

Abeykoon et al. [6], propose an automated system to analyze and segment the DNA bands using signal and image processing techniques. The proposed algorithm eliminates defects due to noise and double bands present in the images. Ten images were analyzed and compared with the result obtained by the proposed system and three experts who analyzed the images manually. Seven images were correctly detected and three images showed an error of up to 17% of non-detection of the bands. In the three images, the error was due to the presence of doubles, which the algorithm did not detect.

Intarapanich et al. [7], developed an image processing tool that automatically processes DNA gel electrophoresis images. The tool was originally conceived to facilitate large-scale genotyping analysis of sugarcane crops. The software allows for the proper segmentation of DNA bands, even if they are found very close together. Ten images were analyzed to test the tool. The average accuracy of 78% was achieved in the segmentation of the lanes in the 10 images. The software was developed in Java and is available through the “imageJ” framework.

Salazar et al. [8], propose a methodology for processing one-dimensional gel electrophoresis images containing information on insect and parasite antigens. It proposes a maximum and minimum algorithm for the identification of each of the bands contained in the image.

The methods that were reported in the literature generally focused on improving the segmentation of the samples. However, preprocessing the image before segmentation is also important. Normally, the images<sup>1</sup> that are used to conduct these

---

<sup>1</sup>The images that were analyzed in this project were provided by the “Microgravity Laboratory of INICTEL-UNI”.

studies are obtained from the literature because the agarose gels are expensive and time-consuming to prepare.

The present study proposes an algorithm for the automatic and precise calculation of the molecular weight and concentration of DNA in the agarose gel images. The results are compared with the results that were obtained by the experts from INICTEL-UNI to assess the accuracy of the algorithm. The agreement between the results is assessed in terms of Cohen's kappa coefficient which will act as the method that can be used to evaluate the results. Six images were processed by the algorithm, yielding a total of 51 samples.

## 2 Description of the Proposed Algorithm

A flowchart of the proposed method is depicted in Fig. 1 and comprises the following five steps: image acquisition, the region of interest cropping, rotation, segmentation, and counting the molecular weights and concentrations.

### 2.1 Sample Preparation

Three main steps are involved in the preparation of these samples. First, the agarose is mixed with the buffer in an Erlenmeyer flask to prepare it for electrophoresis. This solution is heated and poured into the gel mold, where it is left to cool for 30 min. Further, the agarose gel is taken to an electrophoresis bucket. The bucket is filled with the buffer for electrophoresis, and the DNA samples are placed in wells. Subsequently, the bucket is electrified for approximately 20 min during the electrophoresis process. Finally, the agarose gel is placed in a UV transilluminator to excite the DNA samples.



Fig. 1 Proposed method flowchart

## 2.2 Image Acquisition

All the agarose gel samples were digitized using a Canon 12.1 megapixel digital camera. The images were acquired in the RGB color mode (resolution of 8 bits per component) with a spatial resolution of  $4000 \times 3000$  pixels and are stored in the jpg format. Because the three RGB components exhibit an identical value for each pixel, the grayscale image illustrates a resolution of 8 bits per pixel as shown in Fig. 2.

## 2.3 Region of Interest Cropping

First, the image must be cropped to include only the region that contains the agarose gel. Because the RGB components are known to have the same value throughout the image, only the “R” component can be expressed as  $I_R(x, y)$ .

Equation (1), describes the binarization operation that was applied to the image  $I_R(x, y)$ . The threshold that was used in the study was obtained by conducting various tests on the images in which a good result was observed with a threshold of 50. The resulting image is referred to as  $I_B(x, y)$ , and it is illustrated in Fig. 3. The region of interest takes the value of “1”, whereas the rest of the image takes the value of “0”.

$$I_B(x, y) = \begin{cases} 0, & I_R(x, y) \leq 50 \\ 1, & I_R(x, y) > 50 \end{cases} \quad (1)$$

Further, the coordinates of the region of interest are identified, as can be observed in Fig. 3. The center of the image is precisely the point at which the agarose gel is observed. The cropped image  $I_{R1}(x, y)$  is depicted in Fig. 4.

Fig. 2 The acquired image

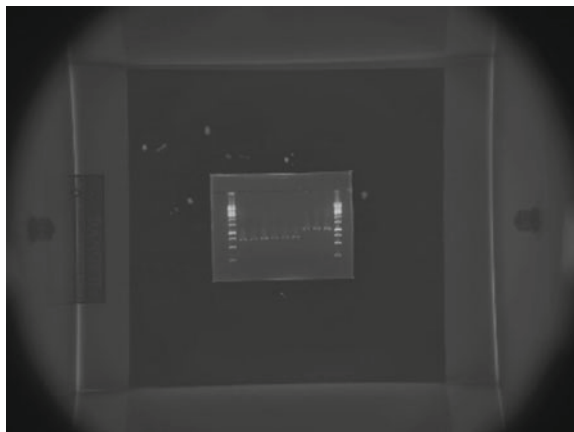




Fig. 3 The binarized acquired image

### 2.4 Rotation

The image  $I_{R1}(x, y)$  will be slightly inclined and must be straightened to avoid any errors during the later stages of processing. The inclination angle  $\theta$  can be measured from the upper left part of the image, as depicted in Fig. 4.

Equations (2) and (3) are used to rotate the agarose gel images shown in Fig. 5. The image  $I_p(w, z)$  is the result of rotating the image  $I_{R1}(x, y)$  using the transformation matrix  $T$ .

$$I_p(w, z) = T\{I_{R1}(x, y)\} \tag{2}$$

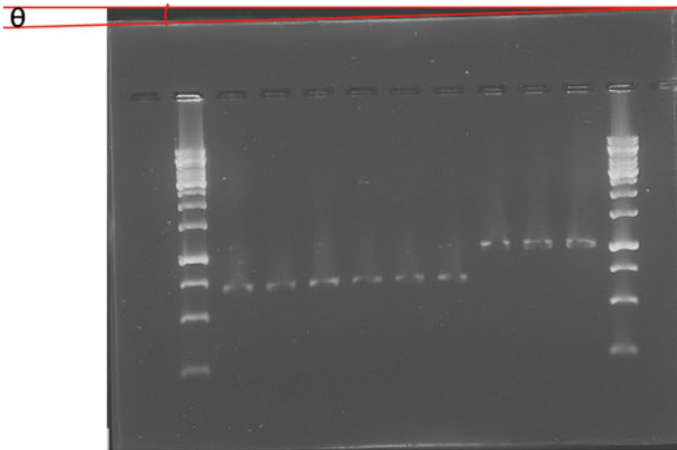


Fig. 4 The agarose gel image



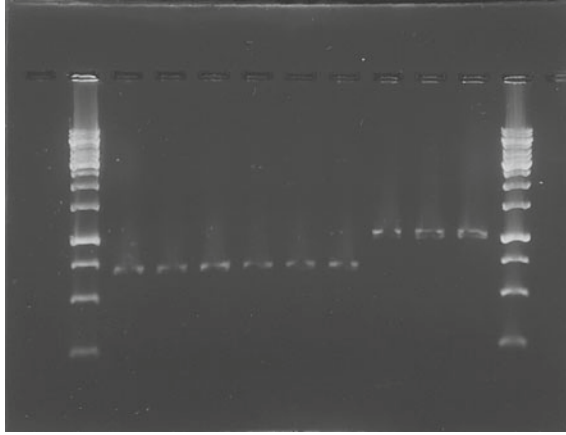


Fig. 5 Image  $I_p(w, z)$  resulting from the rotation process

$$T = \begin{bmatrix} \cos \theta & \sin \theta & 0 \\ -\sin \theta & \cos \theta & 0 \\ 0 & 0 & 1 \end{bmatrix} \quad (3)$$

## 2.5 Segmentation

The rotated image,  $I_p(w, z)$ , is ready to be segmented. All columns of the image are extracted, which are the areas at which the DNA ladders and samples are located.

To improve the segmentation process, the average value of pixels in  $I_p(w, z)$  is calculated according to (4), where  $r_j$  are the gray levels and  $p_j$  is the probability of the occurrence of each gray level. Additionally, the standard derivation is calculated using (5). A range of pixel values is returned; however, the difference between the values can be disregarded for the present purposes. This range of values is denoted as black pixels, which are equal to 0, as described in (6), yielding the image  $I_v(w, z)$ . This image is illustrated in Fig. 6.

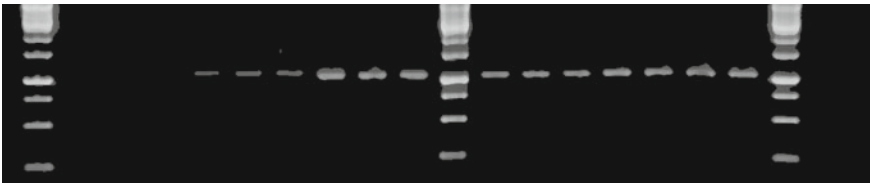


Fig. 6 Image  $I_v(w, z)$  of the agarose gel with the disregarded pixels in black

$$\mu = \sum_{j=0}^{255} r_j \times p_j \quad (4)$$

$$\sigma = \sqrt{\sum_{j=0}^{255} (r_j - \mu)^2 \times p_j} \quad (5)$$

$$I_v(w, z) = \begin{cases} 0, & \mu - \sigma \leq I_p(w, z) \leq \mu + \sigma \\ I_p(w, z), & \text{other case} \end{cases} \quad (6)$$

Further, (7) is used to obtain the horizontal projection  $P_h(z)$ , of image  $I_v(w, z)$ , where  $N$  is the height of the image.

$$P_h(z) = \sum_{w=0}^{N-1} I_v(w, z) \quad (7)$$

The coordinates are obtained from this horizontal projection as shown in Fig. 7, and each lobe that is present in the project is cut out from the image. This results in the segmented columns in  $I_v(w', z')$ , as can be observed in Fig. 8.

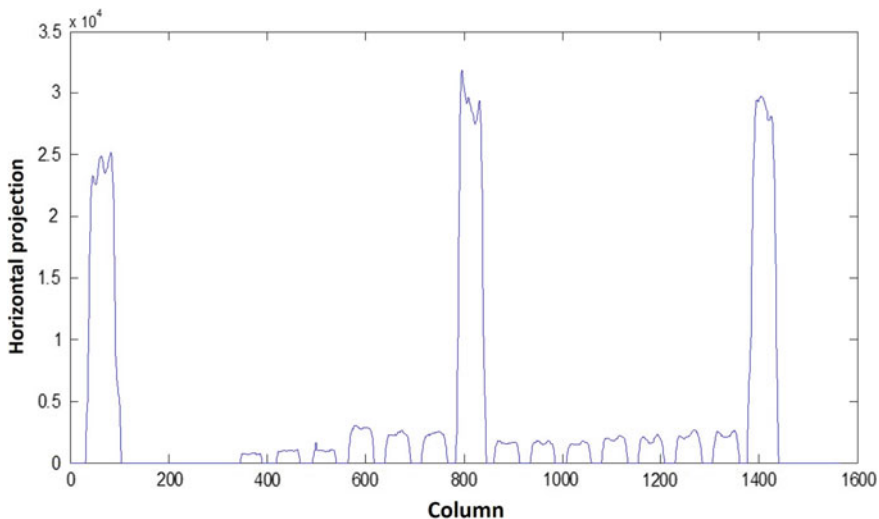
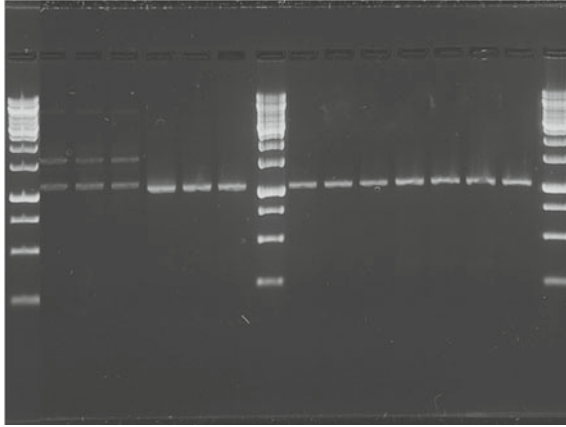


Fig. 7 The horizontal projection of the image



**Fig. 8** Segmented image  $I_v(w', z')$

## 2.6 Calculating Weight and Concentration

To finally estimate the weight and concentration of the samples, the segmented columns of the DNA ladders are processed. An example of a segmented DNA ladder is depicted in Fig. 9.

Equation (8) is used to obtain the vertical projection of each DNA ladder in the image  $I_v(w', z')$ ;  $I_c(g, f)$  is the image of each column of  $I_v(w', z')$ , and  $M$  is the width of each column in the image  $I_c(g, f)$ . Thus, the position of each mark in the DNA ladder is calculated, which allows the weights of the samples to be calculated according to the positions of each DNA sample.



**Fig. 9** The segmented DNA ladder

$$P_t(g) = \sum_{f=0}^{M-1} I_c(g, f) \quad (8)$$

Further, the segmented columns in all the samples from the image are used. The vertical projection in (8) is used again, and only the part of the image that contains the sample is segmented, as depicted in Fig. 10.

Finally, when all the samples have been segmented, the horizontal position of each sample is compared with the position of the marks to estimate the molecular weight of the samples. Figure 11 shows the pixel intensity of the samples and the marks are compared to calculate the concentration.

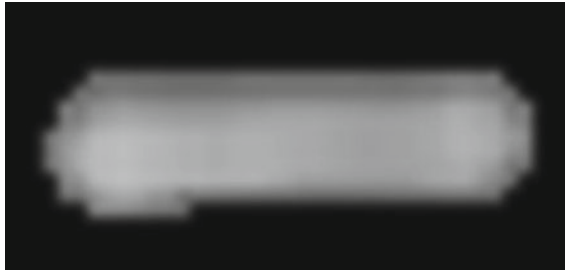


**Fig. 10** The segmented sample

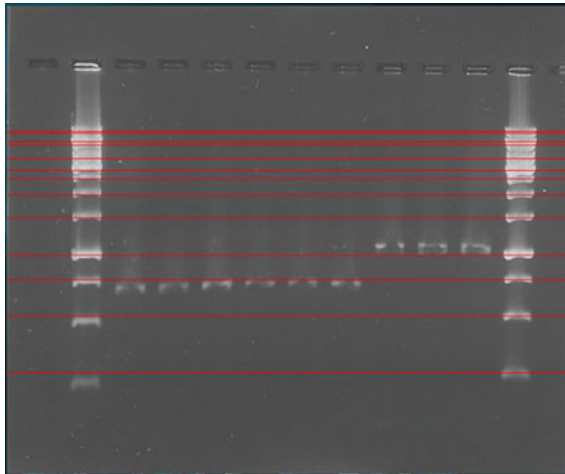


**Fig. 11** Image used to obtain the results

### 3 Results

Six agarose gel images were processed using the algorithm. These images were obtained from six different biopsies.

From these images, we separated all the samples of each image to obtain 51 segmented samples. These samples were compared with the DNA ladder marks according to the image to which they belong to obtain the results. These were compared with the results decided by the experts in molecular biology at the INICTEL-UNI.

It is important to mention that the agarose gel images are open-source DNA of flies.

Cohen’s kappa coefficient is used to validate the algorithm. This measure indicates the level of agreement between two evaluators that can be used to classify a result according to different excluding possibilities. In Table 1, the simplest example is illustrated using only two possibilities.

The kappa coefficient [9]  $k$  is calculated using (9)

$$\kappa = \frac{P_0 - P_e}{1 - P_e} \tag{9}$$

where,  $P_0$  (ratio of observed agreement) and  $P_e$ (ratio of the agreement by chance) are calculated using (10) and (11), respectively.

$$P_0 = \frac{a + d}{n} \tag{10}$$

$$P_e = \frac{s_3 \times s_1 + s_4 \times s_2}{n^2} \tag{11}$$

The table for the kappa coefficient was made and the results are depicted in Table 2.

According to Table 3, which lists the levels of agreement for different kappa coefficients, the agreement obtained with the proposed method is moderate.

**Table 1** The possibilities table

		Method B		
		Positive	Negative	
Method A	Positive	$a$	$c$	$s_3$
	Negative	$b$	$d$	$s_4$
		$s_1$	$s_2$	$n$

**Table 2** Results of the calculation of the Kappa coefficient

		Specialist		Total
		Correct reading	Wrong reading	
Algorithm	Correct reading	48	1	49
	Wrong reading	1	1	2
Total		49	2	51
$P_0 = 0.9608$		$P_e = 0.9245$		$k = 0.4808$

**Table 3** Levels of the agreement to the Kappa coefficient

Kappa coefficient	Level of agreement
<0	Without agreement
0–0.2	Poor agreement
0.2–0.4	Fair agreement
0.4–0.6	Moderate agreement
0.6–0.8	Good agreement
0.8–1.0	Very good agreement

## 4 Conclusions

The study contributes to obtain a better precision of the molecular concentration in DNA samples, as well as to automate the process. The desired result of obtaining a moderate “degree of agreement” as assessed by the kappa index was obtained, the result was 0.4808. However, 51 samples were obtained, an observed agreement ratio of 96.08%, i.e., a precision error in the results of less than 5%, compared to the experts’ results.







## References

1. Ken Academy: Electroforesis en gel. <https://es.khanacademy.org/science/biology/biotech-dna-technology/dna-sequencing-pcr-electrophoresis/a/gel-electrophoresis>. Last accessed 27 Sept 2019 (2018)
2. Caridade, C.M.R., et al.: An automatic Method to identify and extract information of DNA bands in Gel Electrophoresis Images. In: 31st Annual International Conference of the IEEE EMBS (2009)
3. Lee, J.D., et al.: Automatic DNA sequencing for electrophoresis gels using image processing algorithms. *Int. J. Biomed. Sci. Eng.* (2011)
4. Bajla, I., et al.: Improvement of Electrophoretic Gel Image Analysis. Austrian Research Centers Seibersdorf (2001)
5. Skutkova, H., Vitek, M., Krizkova, S., Kizek, R., Provaznik, I.: Preprocessing and classification of electrophoresis gel images using dynamic time warping. *Int. J. Electrochem. Sci.* **8**(2013), 1609–1622 (2013)

6. Abeykoon, A., Dhanapala, M., Yapa, R., Sooriyapathirana, S.: An automated system for analyzing agarose and polyacrylamide gel images. *Ceylon J. Sci. (Bio. Sci.)* **44**(1), 45–54 (2015)
7. Intarapanich, A., Kaewkamnerd, S., Shaw, P., Ukosakit, K., Tragoonrung, S., Tongsim, S.: Automatic DNA diagnosis for 1D gel electrophoresis images using bio-image processing technique. In: *BMC Genomics Volume 16 Supplement 12, 2015: Joint 26th Genome Informatics Workshop and 14th International Conference on Bioinformatics: Genomics (2015)*
8. Salazar, C., Niño, C., Diaz, R.: Color bands detection on a gel electrophoresis image in one dimension applying a location algorithm based on maximums and minimums. *Iteckne* **14**(2), 122–130 (2017). <https://dx.doi.org/10.15332/iteckne.v14i2.1766>
9. Cohen, J.: A coefficient of agreement for nominal scales. *Educ. Psychol. Measur.* **XX**(1) (1960)

# Classification of Dermoscopy Skin Images with the Application of Deep Learning Techniques



Pablo David Minango Negrete , Yuzo Iano ,  
Ana Carolina Borges Monteiro , Reinaldo Padilha França ,  
Gabriel Gomes de Oliveira , and Diego Pajuelo 

**Abstract** The aid-computer assistant is important for the improvement in the diagnostic of skin lesions, principally to detect melanoma, which is the most dangerous skin cancer type. The principal goal of the aid-computer assistant is to detect melanoma in its initial stage because the probability of the five-year survival ratio is over 95%. With the purpose of diagnosed early, in this paper we propose an algorithm based on deep learning to classified dermoscopy images with two types of skin lesions, which are melanoma or malignant cancer and benign cancer. We use AlexNet architecture modified to attend our problem, which was trained twice times with 2000 and 3000 images, divide into three sets (training, validation, and test set). We analyze three types of optimizers in order to improve the process of learning, where the best result was obtained by SGD with an accuracy of 99.79% for the training set, 81.50% for the validation set, and 79.17% for the test set in the scenery of 4000 images.

---

P. D. Minango Negrete (✉) · Y. Iano · A. C. Borges Monteiro · R. Padilha França ·  
G. G. de Oliveira · D. Pajuelo  
School of Electrical and Computer Engineering (FEEC), University of Campinas – UNICAMP,  
Av. Albert Einstein - 400, Barão Geraldo, Campinas, SP, Brazil  
e-mail: [pablodavid218@gmail.com](mailto:pablodavid218@gmail.com)

Y. Iano  
e-mail: [yuzo@decom.fee.unicamp.br](mailto:yuzo@decom.fee.unicamp.br)

A. C. Borges Monteiro  
e-mail: [monteiro@decom.fee.unicamp.br](mailto:monteiro@decom.fee.unicamp.br)

R. Padilha França  
e-mail: [padilha@decom.fee.unicamp.br](mailto:padilha@decom.fee.unicamp.br)

G. G. de Oliveira  
e-mail: [oliveiragomesgabriel@ieee.org](mailto:oliveiragomesgabriel@ieee.org)

D. Pajuelo  
e-mail: [diego.pajuelo.castro@gmail.com](mailto:diego.pajuelo.castro@gmail.com)



**Keywords** Skin cancer · Dermoscopy images · Melanoma · Non-melanoma · AlexNet · Deep learning · CNN

## 1 Introduction

There are several skin lesion types that can be classified in two ways, which are melanoma and nonmelanoma [1], where melanoma is the most dangerous because it is more likely to spread over other parts of the body if not detected, controlled and treated early. Melanoma is developed by melanocytes (cells that give skin color), which begins to grow quickly and out of control [2].

The ultraviolet rays that come from the sun are one of the main factors in the generation of skin cancer because the radiation has enough energy to eliminate an electron (ionize) from an atom or a molecule, this type of radiation can damage the DNA in cells, which in turn may lead to cancer [3].

Melanoma can be developed anywhere of the skin but the most common areas to find melanomas are on the face, neck, and arms, due to are more liable to be exposed directly to sun rays. Likewise, the risk of having melanoma is almost more than 20 times for white people than people with darker skin color. Another risk factor is the first-degree relatives (parents, brothers, sisters, or children) have had melanoma. According to [4], around 10% of all people with melanoma have a family history of the disease.

In Brazil, skin cancer is one of the most common to appear and correspond about 30% of all malignant tumors registered in the country, melanoma barely represents about 3% of neoplastic malignancy, be the gravest because have a higher probability of cause metastasis [5]. Early detection is considered when the melanoma is beginning and in its initial stages when this happens there is an estimated 5-year survival rate of 95% but if the melanoma is in its latest stages the survival rate drops to 14% [2].

Melanoma has an elevated lethality, for this reason, its incidence is low. Brazil has an estimative of 2920 new cases in men and 3340 new cases in women, and most cases are found in the south region. The skin cancer nonmelanoma estimates 85,170 new cases for men and 80,140 for women.

Among men, the skin cancer nonmelanoma is the most incident in the south region (160.08/100 thousand), southeast (89.80/100 thousand), and west-central (69.27/100 thousand), in the other regions, the estimated risk are: northeast (53.75/100 thousand) and north (23.74/100 hundred). Among women, the skin cancer nonmelanoma is the most incident in all regions of the country with an estimated risk of (97.64/100 thousand) in the south region, (95.16/100 thousand) in the southeast, (92.66/100 thousand) in the west-central, (45.59/100 thousand) in the northeast and in the north (27.71/100 hundred) [1].

In the last years, the medical assistant by computer takes an important role over decision making because it aids with a complementary diagnostic over the skin lesions type that the patient has. Recent studies demonstrate acceptable performance

values of classification, segmentation, detection, and recognition over images with different skin lesions.

This performance increases thanks to deep learning algorithms, which have excellent results of accuracy at the moment of classification and recognized patterns in images, several times without the necessity of a previously images processing.

In this paper, we employ AlexNet architecture with the task of classifying images. We analyze three types of optimizers with the purpose to obtain higher values in the accuracy. For training, the architecture uses 2000 and 3000 images divided into three sets (training, validation, and test set).

The paper is organized as follows: Sect. 2, short bibliographic revision is presented. Section 3, the proposed methodology is described. Section 4, experimental results are shown, in Sect. 5 the conclusions are discussed.

## 2 Related Work

Due to the improvement of computers to have more processing power and several services of GPU computing like Colaboratory from Google, Kaggle, AWS from Amazon, etc. Nowadays, it is possible to have higher results of accuracy over different tasks of classification and segmentation of medical images. Deep learning algorithms that employ CNN architecture have shown excellent results, due to databases with a large number of images. However, problems such as an imbalance of classes, wrong labels affect system accuracy.

The principal goal to develop an aid-system to recognize and classify different skin lesions is due to the diagnosis and recognition of the skin lesion are given visually by a dermatologist, and it can be complicated and lead to subjective results.

Sabbaghi et al [6] applied a stacked sparse auto-encoders to discover the latent information features from input image pixel intensities. The high-level learned of features was employed into a classifier for classifying dermoscopy images. In [6], this work did not implement CNN.

The idea of using a pre-trained ConvNet was implemented in [7], where it extracted the features using the filters from a CNN pre-trained on natural images to classified 10 classes of non-dermoscopy skin images. Other techniques of deep learning were successfully applied to skin lesion analysis like the works of Barata et. al [8], Abbas et al [9], and among others.

## 3 Methodology

In this section, we describe the architecture type chosen and which parameters were modified with the purpose to attend our problem of binary classification between benign and malignant cancer. Furthermore, the dataset and implementation aspects are described.

### 3.1 Dataset Description

For our experiments, we use the open dataset of International Skin Imaging Collaboration (ISIC) [10]. This dataset contains about 23,906 images with different skin lesions with their own histopathological diagnostic. Due to the imbalance of classes, we focus on two types of lesions, which are benign and malignant skin cancer, because it is one of the principal’s objectives of this organization try to reduce the mortality caused by malignant skin cancer known as melanoma too. Thus, we use and analyze 1000 and 2000 images for each class, which were chosen randomly.

### 3.2 Architecture Description

The proposed binary classification between benign and malignant cancer is based in AlexNet architecture [11], which is a well-documented and usually used for the convolutional neural networks in image classification problems.

The flow of the AlexNet architecture of the proposed system is shown in Fig. 1, AlexNet consists of five convolutional layers with different sizes of filters or kernels, which have the principal function of decrease the dimensionality of the image and extract the information.

The first block of Fig. 1. is the input of the architecture where the images are resized in  $200 \times 200$  pixels RGB, and for the huge quantity of images is necessary to divide into batches of images in order to not overload the system. The next section of blocks is the convolutional layers where the size of kernels are: C1( $11 \times 11$ ), C2( $5 \times 5$ ) and C3, C4 and C5 ( $3 \times 3$ ).

In each one of these layers, the Rectified Linear Unit (ReLU) is used as function activation, likewise, each block integer the concept of MaxPooling [12] for reducing the number of dimensionalities with the help of a filter which takes the maximum number of the window. The size of these filters is ( $3 \times 3$ ). After each process in convolutional layers, we normalize the output with the BatchNormalization [12], for stabilizes the learning process and try to have a faster convergence.

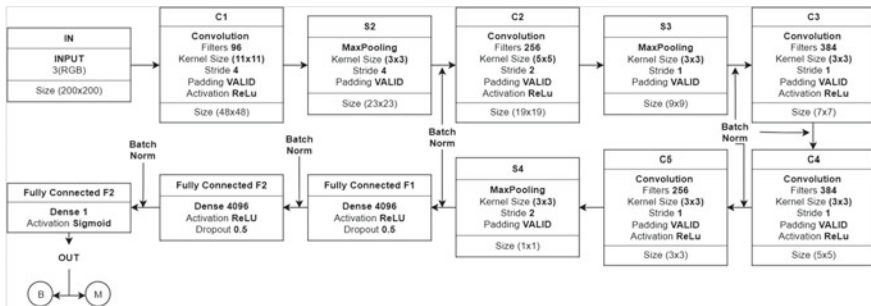


Fig. 1 AlexNet architecture adapted to our problem

The last three blocks correspond to the dense layers, in the F1 and F2 we apply Dropout [12], which permits the probability of turn off certain quantities of neurons randomly, but maybe they activate in the next step with the goal of reducing the overfitting. In the last block, we choose two neurons, which can try to predict the true label of the class. As our problem is a binary classification, a better activation function is a sigmoid because it is the most utilized to predict values between 0 and 1.

For compiling the architecture, we analyze the performance of three types of optimizers, which are Adam, RMSprop [13], and Stochastic Gradient Descent (SGD) [14]. The optimizers have an initial learning rate of 0.001. Binary cross entropy was used as a loss function [15]. Early stopping was applied to interrupt the training; thus, it was monitoring the validation accuracy (AUC) and if do not improve after 10 epochs, the training is stopped and save the best performance.

## 4 Results and Discussion

All experiments presented are trained with AlexNet architecture. They are performed by using Keras package [16] as a deep learning framework in order to build and train the model. For results visualization, we employed the Matplotlib package [17]. All codes are implemented in the Kaggle environment, in its GPU mode, where it works with 13 Gb of Ram and 2 cores.

The dataset employed was random split in three sets, where for the first training of AlexNet, we employed 1400 images for training (700 images for each class), for the validation set 400 images were employed (200 for each class), and for the test set we used 200 images.

The same way for the second training, we increase the number of images in each one set, leaving the experiment thereby with 2400 images of the training set (1200 for each class), 1000 images for validation set (500 for each class) and 600 images for the test set. All sets have the same quantity of images to resolve the problem of imbalanced classes with the purpose of not affect the accuracy of the model.

For the evaluation of our methodology, we use the following metrics in the three sets of data.

- Accuracy represents the correct predictions in each one class, divided for the total numbers of predictions.
- Loss measures the wrongly classified images with respect to the true label.

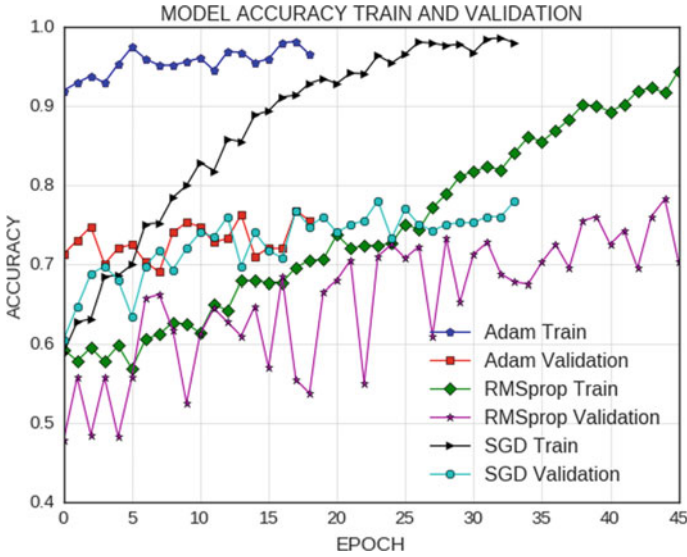
Table 1 shows the performance of the first training of the model, the training values are tested in [18], where we compare with the validation values. The accuracy is not high as the training, the SGD is the optimizer that achieves the better percentage of learning so much for the two sets of data with 97.66% for the training set and 78% for the validation set.

Figure 2 shows the efficiency of the three optimizers, where we note that the better accuracies are attended by the training set, while the validation set attends until 78%

**Table 1** Accuracy and loss comparisons of the different types of optimizers into the training and validation sets

		Adam	RMSprop	SGD
Training	Acc	96.66	87.64	<b>97.66</b>
	Loss	0.0817	0.3141	<b>0.0567</b>
Validation	Acc	75.50	70.25	<b>78.00</b>
	Loss	0.8227	0.7583	<b>0.4360</b>

Bold value represents the better values of the learning



**Fig. 2** Performance of AlexNet architecture, training, and validation accuracy

of learning. It is important to take attention with the loss values because here we appreciate if the model is generalized or it is overfitting. In our case, the optimizer Adam is a clear case of overfitting, however, SGD has an acceptable value of the loss.

Table 2 shows the values obtained in the second training, as the first evaluation, the better optimizer is SGD for both sets of data, we note that the values increased with more images. SGD attends an accuracy of 81.50% in the validation set which improves 3.5% over learning binary classification.

We appreciate that SGD shows a learn most permanent for training and validation set. The other optimizers, the learning is more variable. This is appreciated in the detailed process of training and validation shown in Fig. 3.

After analyzing the performance of these three optimizers with different quantities of images, we proceeded to take SGD which attends better accuracy in the two training for evaluated the learning over the test set. Table 3 shows that when we have more

**Table 2** Accuracy and loss comparisons of the different types of optimizers into the training and validation sets

		Adam	RMSprop	SGD
Training	Acc	97.85	89.72	<b>99.79</b>
	Loss	0.0591	0.2434	<b>0.0120</b>
Validation	Acc	77.70	79.60	<b>81.50</b>
	Loss	0.8047	0.5528	<b>0.4098</b>

Bold value represents the better values of the learning

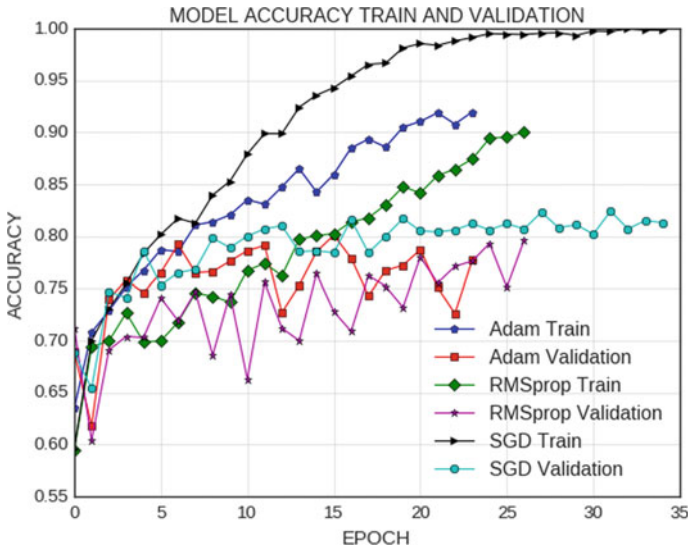


**Fig. 3** Performance of AlexNet architecture, training and validation accuracy

**Table 3** Evaluation of the two training over the test set

		T1	T2
Test	Acc	70.50	79.17
	Loss	0.2950	0.2083

quantity of images the learning is better. In the case of the second training (T2) we obtain an accuracy of learning of 79.19%, which represents an increase of 8.67% in comparison to the first training.

## 5 Conclusion

A modified AlexNet architecture was proposed for aid in the early detection of melanoma skin cancer, which represents a binary classification to identify between skin cancer non-melanoma and melanoma. We tested it with different quantities of images divided into three sets (training, validation and test set), where we observed that SDG is the better optimizer with an attendance of performance in the learning of 99.79% in the training, 81.50% in the validation and 79.17% in the test set. These results were obtained in the second training for 4000 images, stating the potential of the proposal. It is important to take attention in the results on the loss evaluation because in this metric, we can observe if the architecture of our model was generalized the learning or it was fall in the overfitting.

## References









1. INCA: Estimativa 2018 – síntese de resultados e comentários. Available <http://www1.inca.gov.br/estimativa/2018/sintese-de-resultados-comentarios.asp>. Accessed 11 Sept 2019 (2016)
2. Society, A.C.: What is melanoma skin cancer? What is melanoma? Available <https://www.cancer.org/cancer/melanoma-skin-cancer/about/what-is-melanoma.html>. Accessed 11 Sept 2019 (2017)
3. Society, A.C.: Ultraviolet (uv) radiation. Available <https://www.cancer.org/cancer/cancer-causes/radiation-exposure/uv-radiation.html>. Accessed 13 Sept 2019 (2017)
4. Society, A.C.: Melanoma skin cancer risk factors: Melanoma risk factors. Available <https://www.cancer.org/cancer/melanoma-skin-cancer/causes-risks-prevention/risk-factors.html>. Accessed 13 Sept 2019 (2017)
5. INCA: Câncer de pele melanoma. Available <https://www.inca.gov.br/tipos-de-cancer/cancer-de-pele-melanoma>. Accessed 13 Sept 2019 (2018)
6. Sabbaghi, S., Aldeen, M., Garnavi, R.: A deep bag-of-features model for the classification of melanomas in dermoscopy images. In: 2016 38th Annual International Conference of the IEEE Engineering in Medicine and Biology Society (EMBC), Aug 2016, pp. 1369–1372
7. Kawahara, J., Ben Taieb, A., Hamarneh, G.: Deep features to classify skin lesions. In: 2016 IEEE 13th International Symposium on Biomedical Imaging (ISBI), April 2016, pp. 1397–1400
8. Barata, C., Ruela, M., Francisco, M., Mendonça, T., Marques, J.S.: Two systems for the detection of melanomas in dermoscopy images using texture and color features. *IEEE Syst. J.* **8**(3), 965–979 (2014)
9. Abbas, Q., Celebi, M., Serrano, C., García, I.F., Ma, G.: Pattern classification of dermoscopy images: A perceptually uniform model. *Pattern Recogn.* **46**(1), 86–97. Available <http://www.sciencedirect.com/science/article/pii/S0031320312003457> (2013)
10. ISIC Project: Public skin lesion image archive. <https://www.isic-archive.com/#!/topWithHeader/onlyHeaderTop/gallery>, 2018
11. Krizhevsky, A., Sutskever, I., Hinton, G.E.: Imagenet classification with deep convolutional neural networks. *Neural Inf. Process. Syst.* **25**, 01 (2012)
12. Géron, A.: *Hands-On Machine Learning with Scikit-Learn and TensorFlow: Concepts, Tools, and Techniques to Build Intelligent Systems*, 1st edn. O’Reilly Media, Inc. (2017)
13. Kingma, D.P., Ba, J.: Adam: a method for stochastic optimization. In: Cite arxiv:1412.6980Comment: Published as a Conference Paper at the 3rd International Conference for Learning Representations, San Diego (2015). Available <http://arxiv.org/abs/1412.6980>
14. Ruder, S.: An overview of gradient descent optimization algorithms. *CoRR*, vol. abs/1609.04747 (2016). Available <http://arxiv.org/abs/1609.04747>

15. Janocha K., Czarnecki, W.M.: On loss functions for deep neural networks in classification. CoRR, vol. abs/1702.05659, (2017). Available <http://arxiv.org/abs/1702.05659>
16. Chollet, et al.: Keras. <https://keras.io> (2015)
17. Hunter, J.D.: Matplotlib: a 2d graphics environment. Comput. Sci. Eng. **9**(3), 90–95 (2007)
18. Minango, P., Iano, Y., Monteiro, A.C.B., França, R.P., de Oliveira, G.G.: Classification of automatic skin lesions from dermoscopic utilizing deep learning. SET Int. J. Broadcast Eng. ISSN Print 2446-9246 ISSN Online: 2446-9432. <https://doi.org/10.18580/setijbe.2019.14>. Web Link <http://dx.doi.org/10.18580/setijbe.2019.14> (2019)



# Association Between Human Papillomavirus Infection and Anus Cancer Precursor Lesions: A Review



Ana Carolina Borges Monteiro , Yuzo Iano , Reinaldo Padilha França , Rangel Arthur , Pablo David Minango Negrete , Diego Pajuelo , Gabriel Gomes de Oliveira , and Lisber Arana Hisnostrza 

**Abstract** Human papillomavirus, commonly referred to as HPV, is a virus with tropism by differentiating tissues. Its pathogenesis is related to the disorder of genes that inhibit cell apoptosis and cell suppression, this fact favors its action and spread by an organism. Due to these characteristics, HPV is associated with cervical, anus, head, and neck cancer. Based on this, the present work has as objective the accomplishment of a bibliographical revision study of the main characteristics of this virus as well as its effects on the human organism. Studies such as this can be seen as key elements for understanding and preventing this sexually transmitted disease (STD), which has its highest incidence rates in underdeveloped and developing countries, where health and education policies are often scarce or nonexistent.

**Keywords** Human papillomavirus · Cytopathology · Molecular biology · Sexually transmitted disease · Diagnostic methods

## 1 Introduction

Human papillomavirus (HPV) is a 72 capsomer non-enveloped virus belonging to the Papovaviridae family, with a mean diameter of 55 nm. The genome of these

---

A. C. Borges Monteiro (✉) · Y. Iano · R. Padilha França · P. D. M. Negrete · D. Pajuelo · G. G. de Oliveira · L. A. Hisnostrza

School of Electrical and Computer Engineering (FEEC), University of Campinas – UNICAMP, Av. Albert Einstein - 400, Barão Geraldo, Campinas, SP, Brazil  
e-mail: [monteiro@decom.fee.unicamp.com.br](mailto:monteiro@decom.fee.unicamp.com.br)

Y. Iano  
e-mail: [yuzo@decom.fee.unicamp.com.br](mailto:yuzo@decom.fee.unicamp.com.br)

R. Padilha França  
e-mail: [padilha@decom.fee.unicamp.com.br](mailto:padilha@decom.fee.unicamp.com.br)

R. Arthur  
School of Technology (FT), University of Campinas – UNICAMP, R. Paschoal Marmo - 1888, Jardim Nova Italia, Limeira, SP, Brazil

© The Editor(s) (if applicable) and The Author(s), under exclusive license to Springer Nature Switzerland AG 2021

Y. Iano et al. (eds.), *Proceedings of the 5th Brazilian Technology Symposium*, Smart Innovation, Systems and Technologies 202, [https://doi.org/10.1007/978-3-030-57566-3\\_8](https://doi.org/10.1007/978-3-030-57566-3_8)

viruses consists of eight to nine open reading frames and one regulatory region. This virus has double circular deoxyribonucleic acid (DNA) containing about 7900 base pairs and genes encoding eight proteins: E1, E2, E4, E5, E6, E7 (non-structural), and L1 and L2 (structural) that form the viral capsid with icosahedral symmetry. L1 protein when produced in a heterologous expression system has the ability to self-assemble. The genome of this virus is organized into three regions: early region (E), late region (L), and regulatory region (URR). The L1 and L2 genes are responsible for encoding viral capsid proteins and genes, as well as for the coding of proteins involved in viral replication and cell transformation. E1 and E2 genes are involved in viral replication, while E5, E6, and E7 genes encode proteins responsible for this cellular transformation. HPV infections can be divided into two types: cutaneous or mucosal [1, 2].

More than 200 types of HPV are currently described in the literature, which is classified according to their oncogenic potential. Approximately 45 types of this virus infect the male and female anogenital tract epithelium. HPV subtypes can be classified as low risk (types 6, 11, 42, 43, and 44) and high risk (types 16, 18, 31, 33, 35, 39, 45, 46, 51, 52, 56, 58, 59, and 68) [3, 4].

Since the 1970 s, German scientist Harald zur Hausen of the Cancer Research Center (Heidelberg—Germany) has devoted himself to the study of HPV. In her research, there was evidence of the association of subtype 16 Human papillomavirus with biopsies with positive reports of women with cervical cancer. Shortly after this discovery, Hausen also associated subtype HPV 18 with the same pathology. Both subtypes are found in approximately 70% of these biopsies. In the year 2008, Harald zur Hausen won the 2008 Nobel Prize in Medicine for his research on HPV. Based on these findings, further research on this virus has been boosted [3, 4].

This infection is due to unprotected sexual contact, which through micro-abrasions, facilitates the penetration of the virus in the deep layer of epithelial tissue. However, the infection can also occur through direct or indirect contact with lesions on other parts of the body. There is also the possibility of vertical transmission during pregnancy or at delivery. Low-risk oncogenic lesions are manifested as a common wart, genital wart, or condyloma [5].

The classic risk factors for both oncogenic and non-oncogenic development are early onset of sexual intercourse, multiplicity of lifelong sexual partners and high parity (non-surgical births), being young, being a smoker, and being of low socio-economic status, prolonged oral contraceptive use, nutritional deficiencies, human immunodeficiency virus infection (HIV), and other genital infections caused by sexually transmitted agents, such as *Chlamydia trachomatis*, *Herpes simplex virus*) [6].

To understand the oncogenicity of HPV, it is necessary to consider that when the daughter cells immediately enter the G1 phase and are capable of either restarting the cell cycle or performing a temporary or permanent halt. The G1 phase has a checkpoint, G1/S, controlled by the pRb (retinoblastoma protein) pathway. Once the cell passes this point, it is compelled to replicate its DNA. If an incorrect copy of DNA occurs during S or DNA damage, then the cell will not pass the G2/M checkpoint, and gene-induced growth arrest and apoptosis will occur. In this process, several

inhibitor proteins can stop the advance of this cycle, such as p15 and p16, which block fundamental components for cell cycle progressions, such as cyclin-dependent kinases (CDK) and cyclins, preventing the advance of the phase cycle. G1 to S [7, 8].

Other inhibitors are p21, associated with the proto-oncogene ras, and p53, which are responsible for monitoring the quality, integrity of their chromosomes, and the correct execution of the different phases of the cycle. Human cells are equipped with mechanisms for controlling cell division. Mutations in the genetic content of these cells can overcome these defenses and contribute to cancer formation. One such mechanism of action is apoptosis, which occurs when fundamental components are damaged or production system control is unregulated. The development of tumor cells implies an escape from this mechanism. Protein p53, among its many functions, assists the onset of apoptosis, reducing the chance of genetically damaged cells being eliminated by initiating a carcinogenic process. Another mechanism for controlling cell division limits the number of times a given cell reproduces. In this mechanism, the tips of the chromosomes (telomeres) mark the number of divisions, and at the appropriate time initiate senescence and death at the time of telomerase. Activation of this enzyme induces cell immortalization, an indispensable event for carcinogenesis [7, 8].

Within this context in carcinogenesis two classes of genes are fundamental for the development of cancer, because under normal conditions they are responsible for cell cycle control. Proto-oncogenes stimulate, while suppressor genes inhibit the processes of cell division. Collectively, these two classes of genes are responsible for the uncontrolled proliferation found in cancers in humans. When mutations occur, proto-oncogenes become oncogenes, which are carcinogenic and cause excessive cell multiplication. These mutations cause the proto-oncogene to overexpress its growth-stimulating protein or to produce a more active form. In contrast, tumor suppressor genes when inactivated by mutations contribute positively to cancer when. The result of these combinations is the loss of action of functional suppressor genes, which deprives the cell of controls crucial for inhibiting inappropriate growth [7, 8].

Due to the dissemination of information about the incidence of STD, as well as its oncogenicity capacity, there is an increase in condom use among young people in some countries [9]. Therefore, the need to develop bibliographical review studies is noteworthy. Thus, the present study aims to present to the scientific community as well as the general population the main information about HPV that affects the anal regions so that this information is transmitted in a clear, concise, and updated way; after all, HPV in regions anal diseases is as risky as HPV housed in the uterine cervix region, whereas it is less addressed by the general media.

## 2 Methodology

The present study was performed based on the analysis of scientific works related to genital HPV, as well as diagnostic methods of this pathology. These studies were analyzed focusing on scientific publications conducted between 2014 and 2019.

### 3 Results and Discussion

The anal canal is histologically characterized by the presence of a multi-stratified squamous lining. The anal canal is located from the anal border to the pectineal line, which is characterized by being a transition zone between the squamous and non-squamous epithelium. In turn, the area that delimits the anal canal and rectum is made up of transition cells, which resemble the cells that make up the urogenital lining and rectal glandular mucosa. Thus, the appearance of tumors in the distal region of the pectineal line is called squamous cell carcinomas, or epidermoids, which are classified as keratinized. However, those originating from tissues above the dentate line are called epithelioid, which are non-keratinized. Women with cervical cancer are considerably more susceptible to the development of anus or rectal canal cancer [10].

Anal epithelial and anal canal neoplasms, besides presenting differences in embryonic origin, also present different segments for lymphatic drainage, according to their location before the pectineal line. Just above the pectineal line, the lymph flows toward the paravertebral lymph nodes and the perirectal spaces, which are indications for the diagnosis of rectal adenocarcinoma. Just below the pectineal line, lymph flows toward the nodes of the inguinal region, being characteristic for the detection of inguinal adenopathies [11].

Tumor severity and clinical presentation depend on anal size and location. Lesions less than 2 cm are classified as small and have a probability of cure in 80% of cases. However, tumors of 5 cm or more are usually invasive and compromise the lymph nodes, thus presenting less than 50% chance of cure [12].

Just as HPV has tropism in the transitional zones of the cervix, HPV in the anal canal has a preference for the anal transition zone (ZTA). Based on this feature, the anal Pap smear test began. This exam consists of the removal of anal cells for cytological studies by introducing anal swab or endocervical brush in the anal canal. For this, the swab should be introduced between 3 and 4 cm inside the anal canal. This occurs because the length of the anal canal varies from 2.52 to 2.93 cm in women and from 3.27 to 3.4 cm in men. After the introduction, the swab or brush should be rotated 360° around the axis. The material should be uniformly deposited on a glass slide and subsequently fixed and stained properly [13].

The cytological analysis performed on anal smears aims to search for columnar epithelium cells, squamocolumnar cells (coming from the transition zone) and squamous cells. High-grade anal intraepithelial neoplasias (AIS) are considered precursors of anal carcinomas, presenting a high relationship with infection with high oncogenic HPV risk subtypes, mainly by subtypes 16 and 18. These subtypes have their DNA identified between 35 and 90% of tumor cells [13, 14].

The risk of progression is associated with the severity of dysplasia, and HPV virus classification is directly linked to premalignant and malignant lesions, without correlation with the recurrence rate of lesions in the anal region. Thus, the treatment of precursor lesions aims to prevent the evolution of squamous cell carcinoma [15].

AIS are classified as synonymous with severe dysplasia, severe atypia, and in situ carcinoma. This pathology has a higher incidence in squamous cells, being responsible for the cytological picture of binucleation or multinucleation, the presence of koilocytes and atypical paraceratocyte cells in addition to moderate dysplasia. It is noted that most anal carcinomas follow a cytological pattern similar to that found in cervical carcinomas [18].

The biological effects caused by infections with other STDs are related to the presence of persistent inflammation accompanied by damage through oxidative metabolites. Infected cells are prone to increased cytokine secretion. When this infection becomes chronic there is the induction of tissue damage by indirect production of reactive oxygen species, thus triggering the inflammatory cascade. As a consequence of this process, there is a decrease in immunity. In addition, if the patient is a smoker, immunosuppression will be even higher, as nicotine is a determining factor for Langerhans cell depression. Thus, the somatization of immunosuppressor cofactors further facilitates the installation of the HPV virus [18].

The anal canal is more affected than the anal margins, and the transition zone between the anus and rectum is the most affected by tumors. The transition zone has areas of normal rectal mucosa and the presence of squamous epithelium, with the presence of cells of various sizes arranged in arrangements, also has microvilli arranged in columns. This region is affected by high-grade squamous intraepithelial lesions, which are associated with infections caused by high-risk oncogenic HPV subtypes. When untreated, the lesions may progress to invasive carcinoma [17, 18].

About 20% of affected patients are asymptomatic, the others usually have anorectal bleeding or pain usually accompanied by the sensation of mass occupying the rectal region. This symptomatology, however, is often mistakenly mistaken for hemorrhoidal diseases. Anal oncogenic low-risk HPV infection in the latent form initially manifests itself through anal pruritus, with later onset of warts. However, the presence of anal pruritus is not a determining factor for the closure of this diagnosis, since pruritus has a multifactorial etiology such as inflammatory bowel disease, uremia, parasitic diseases, dermatopathies, inadequate hygiene habits, inadequate clothing, the presence of STDs, among others [19].

In turn, high-risk anal oncogenic HPV presents difficulties in its diagnosis, since the lesions are subclinical and their detection is dependent on anoscopy exams. As the lesions are inapparent and usually asymptomatic, the individual seeks medical attention only when the lesions have progressed. Anal border tumors are classified as dermatological lesions and may develop as verrucous carcinoma, Kaposi's sarcoma, Bower's disease, or squamous cell carcinoma. However, those that affect the rectal transition zone or rectal canal are considered malignant and have four origins histological: squamous cell carcinoma, malignant melanoma, adenocarcinoma, and sarcomas [19, 20].

## 4 Diagnostic Methods

The most suitable diagnostic methods for detecting the presence of HPV in the anal region are anoscopy and anal Pap smear. Anoscopy consists of applying 5% acetic acid to the anorectal mucosa for two minutes. Subsequently, the excess is removed with a physiological solution, followed by toluidine blue. The examination should be performed using a colposcope. The result is observed through the presence of ketoacid reactions, which appear in coloration whitish when positive, indicating HPV infection [20].

Polymerase chain reaction (PCR) is a high sensitivity test and is used to prove the existence or the absence of HPV DNA. The PCR reaction is the amplification of viral DNA (HPV) using conserved sequences from specific HPV regions as primers. This test also enables the identification of the HPV genotype by amplifying specific regions for each of the high- or low-grade viruses [21, 22].

Recent studies show that increased expression of miR-16, miR-25, miR-92a, and miR-378 and reduced expression of miR-22, miR-27a, miR-29a, and miR-100 are attributed to viral oncoprotein. E6 or E7. In the future, miRs are expected to be powerful tools for early detection of HPV regardless of their subtype and site of infection [23].

Researchers have developed a methodology for the detection of urine high-risk oncogenic HPV. This technique is based on the detection of virus DNA present in the samples. The results obtained were 90.9% accurate in identifying cervical lesions with abnormal cells [24].

In recent years, there have been a growing number of researches related to pathology detection through the digital processing of medical images [25–27]. In this context, it is expected that in the coming decade's methodologies will be developed that are capable of detecting precursor lesions and cancerous lesions of HPV, similarly to blood cell detection and counting research. These studies have shown high sensitivity, accuracy, specificity, low computational and runtime time consumption, and low cost. Cost reduction is paramount for poor people's access to quality health [25, 26].

In addition, it is important to note that in the not too distant future, the results of cytopathological examinations, patient anamnesis, and data from health institutions can be transmitted and shared by real-time telecommunication channels without data loss and low memory consumption of the devices involved regardless of the type of operating system involved (Android, Windows, Linux, iOS, among others) [27, 28]. Such action is paramount, because the faster the doctor has access to the medical reports, the faster the patient is referred for treatment, and consequently the chances of cure increase.

## 5 Conclusions

The association between HPV and malignant neoplasms shows that this virus is responsible for the precursor lesions that direct individuals to cancer development. However, with recent advances in molecular biology coupled with cytopathology practices, they have led to the possibility of early and more accurate diagnosis of the subtype involved. The classification of the HPV subtype involved in lesions is paramount for the correct management of the disease. Even with such advances, prevention through education focused on adolescents, youth, and adults is the best way to ensure the health of individuals. Only with massive awareness activities can we avoid future HPV complications with other STDs. Importantly, not all STDs are curable, some should only be followed and controlled throughout the patient's life. Such information is often not disseminated as it should. In addition to prevention, the establishment of telemedicine-based data sharing networks is important to promote better treatment and follow-up of patients who live in remote regions or where there is a shortage of professionals specialized in this type of clinical management. In addition, it is necessary to create complex databases that, using artificial intelligence techniques, are able to compile data on cytopathology, molecular biology, dermatoscopy, cytology, and histology of patients affected by HPV. Thus, the medical diagnosis may become increasingly accurate and less likely to fail to identify and classify the HPV subtype; after all, an incorrect medical diagnosis may lead to the patient's death or irreversible damage.

## References






1. Doorbar, J., Egawa, N., Griffin, H., Kranjec, C., Murakami, I.: Human papillomavirus molecular biology and disease association. *Rev. Med. Virol.* **25**, 2–23 (2015)
2. Maxwell, J.H., Khan, S., Ferris, R.L.: The molecular biology of HPV-related head and neck cancer. In: Fakhry, C., D'Souza, G. (eds.) *HPV and Head and Neck Cancers*. Head and Neck Cancer Clinics. Springer, New Delhi (2015)
3. Okami, K.: A new risk factor for head and neck squamous cell carcinoma: human papillomavirus. *Int. J. Clin. Oncol.* **21**(5), 817 (2016)
4. Mammias, I.N., Spandidos, D.A.: Paediatric virology as a new educational initiative: an interview with Nobelist Professor of virology Harald zur Hausen. *Exp. Therap. Med.* **14**(4), 3329–3331 (2017)
5. Jesus, S.P.D., et al.: A high prevalence of human papillomavirus 16 and 18 co-infections in cervical biopsies from southern Brazil. *Braz. J. Microbiol.* **49**, 220–223 (2018)
6. Ribeiro, A.A., Costa, M.C., Alves, R.R.F., Villa, L.L., Saddi, V.A., dos Santos Carneiro, M.A., Rabelo-Santos, S.H.: HPV infection and cervical neoplasia: associated risk factors. *Infect. Agents Cancer* **10**(1), 16 (2015)
7. Cseke, L.J., Kirakosyan, A., Kaufman, P.B., Westfall, M.V.: *Hand-Book of Molecular and Cellular Methods in Biology and Medicine*. CRC Press (2016)
8. Erkekoglu, P.: *Oncogenes and Carcinogenesis* (2019)
9. Abreu, M.N.S., et al.: Conhecimento e percepção sobre o HPV na população com mais de 18 anos da cidade de Ipatinga, MG, Brasil. *Ciência & Saúde Coletiva* **23**, 849–860 (2018)
10. Allen, D.C., Cameron, R.I. (eds.): *Histopathology Specimens: Clinical, Pathological and Laboratory Aspects*. Springer (2017)

11. Minsky, B.D., Guillem, J.G.: Neoplasms of the anus. In: *Holland-Frei Cancer Medicine*, pp. 1–12 (2016)
12. Júnior, J.C.M.: S: Câncer Ano- reto-cólico - Aspectos atuais: I - Câncer Anal. *Rev bras Coloproct* **27**(2), 2109–2223 (2007)
13. Nadal, S.R., et al.: Quanto a escova deve ser introduzida no canal anal para avaliação citológica mais eficaz? *Rev. Assoc. Med. Bras.* **55**(6), 749–751 (2009)
14. Duarte, B.F., da Silva, M.A.B., Germano, S., Leonart, M.S.S.: Anal cancer diagnosis in patients with human papillomavírus (HPV) and human immunodeficiency virus (HIV) coinfection. *Rev. Inst. Adolfo Lutz* **75**, 1710 (2016)
15. Monteiro, A.C.B., da Cruz Pires, D.V.D.: Characterization of the risk factors for anus cancer and its relationship with Human Papillomavirus-es. *Rev Saude em foco* (2015)
16. Chaves, E.B.M., Capp, E., Corleta, H.V.E., Folgieri, H.J.: A citologia na prevenção do câncer anal, vol. 39, no. 11, pp. 532–537. Rio de Janeiro, Femina (2011)
17. Cuevas, M.: *Virus del papiloma humano y salud femenina. Ediciones i* (2019)
18. Magalhães, M.N.: *Carcinoma epidermóide do canal anal* (2016)
19. Cutrim, P.T.: *Papilomavírus humano (hpv) e sua associação entre as le-sões cervical e anal em mulheres* (2017)
20. Darragh, T.M., Palefsky, J.M.: Anal cytology. In: *The Bethesda System for Reporting Cervical Cytology*, pp. 263–285. Springer, Cham (2015)
21. Bernardy, J.P., Bierhals, N.D., Possuelo, L.G., Renner, J.D.P.: Padronização da PCR em tempo real para a genotipagem de HPV 6-11, HPV 16 e HPV 18 utilizando controle interno. *Revista Jovens Pesquisadores* **8**(1), 37–48 (2018)
22. Clifford, G.M., et al.: Comparison of two widely-used HPV detection and genotyping methods: GP5+/6+ PCR followed by reverse line blot hybridization and multiplex type-specific E7 PCR. *J. Clin. Microbiol.* JCM-0061 (2016)
23. Wang, X., et al.: microRNAs are biomarkers of oncogenic human papillomavirus infections. *Proc. Natl. Acad. Sci. U.S.A.* **111**(11), 4262–4267 (2014)
24. Allison, D.B., Olson, M.T., Maleki, Z., Ali, S.Z.: Metastatic urinary tract cancers in pap test: cytomorphologic findings and differential diagnosis. *Diagn. Cytopathol.* **44**(12), 1078–1081 (2016)
25. Monteiro, A.C.B., Iano, Y., França, R.P., Arthur, R.: *Toxoplasmosis Gondii: from discovery to advances in image processing. In Brazilian Technology Symposium*, pp. 91–101. Springer, Cham (2018)
26. Monteiro, A.C.B., Iano, Y., França, R.P., Arthur, R.: *Methodology of high accuracy, sensitivity and specificity in the counts of erythrocytes and leukocytes in blood smear images. In: Brazilian Technology Symposium*, pp. 79–90. Springer, Cham (2018)
27. Padilha, R., Iano, Y., Monteiro, A.C.B., Arthur, R., Estrela, V.V.: *Betterment proposal to multipath fading channels potential to MIMO systems. In: Brazilian Technology Symposium*, pp. 115–130. Springer, Cham (2018)
28. França, R.P., Peluso, M., Monteiro, A.C.B., Iano, Y., Arthur, R., Estrela, V.V.: *Development of a kernel: a deeper look at the architecture of an operating system. In: Brazilian Technology Symposium*, pp. 103–114. Springer, Cham (2018)



# A New Approach for ECG Recording in Rats: An Autonomic Nervous System Analysis



Raphael Santos do Nascimento , Fernando da Silva Fiorin ,  
Adair Roberto Soares Santos , Luiz Fernando Freire Royes ,  
and Jefferson Luiz Brum Marques 

**Abstract** Reliable electrocardiogram (ECG) recording systems in rats become tools remarkably crucial for the drug safety evaluation in experimental physiological methods. However, the currently existing techniques for ECG measurement in rats still impair a better translational that occurs in the autonomic nervous system (ANS) models. For this reason, we developed a new tool for the ECG measurement in rats on the awake state, no surgical procedure, restraint, as well as anesthesia administration and compared to the isoflurane anesthesia administration. The heart rate variability (HRV) method was used to evaluate the ANS status. The findings demonstrated clearly that the isoflurane anesthesia influence the activities sympathetic and parasympathetic of ANS. Therefore, our newly introduced tool showed to be adequate to study cardiac electrical activity in rats.

**Keywords** Electrocardiogram · Autonomic nervous system · Isoflurane · Rat

---

R. S. do Nascimento (✉) · J. L. B. Marques  
Institute of Biomedical Engineering, Federal University of Santa Catarina, Florianopolis, SC,  
Brazil  
e-mail: [raphael\\_caixa@hotmail.com](mailto:raphael_caixa@hotmail.com)

J. L. B. Marques  
e-mail: [jefferson.marques@ufsc.br](mailto:jefferson.marques@ufsc.br)

F. da Silva Fiorin · A. R. S. Santos  
Laboratory of Neurobiology of Pain and Inflammation, Federal University of Santa Catarina,  
Florianopolis, SC, Brazil  
e-mail: [fernandofiorin@hotmail.com](mailto:fernandofiorin@hotmail.com)

A. R. S. Santos  
e-mail: [adair.santos@ufsc.br](mailto:adair.santos@ufsc.br)

L. F. F. Royes  
Laboratory of Exercise Biochemistry, Federal University of Santa Maria, Santa Maria, RS, Brazil  
e-mail: [nandoroyes@yahoo.com.br](mailto:nandoroyes@yahoo.com.br)

# 1 Introduction

Electrocardiogram (ECG) is widely used as a study tool for the understanding of cardiovascular physiology, both clinically and in experimental research animals. In this context, ECG measurement methods explored in rats have contributed actively in the last decade to the pharmaceutical industries in regard to the drug safety evaluation. For this reason, rat models become remarkably useful for the assessment of cardiac pathologies [1]. Importantly, the increasing development of the experimental physiological models using rats is resulting in a more significant demand for less invasive ECG measurement methods. However, currently, existing techniques for recording ECG from rats still require the use of surgical procedures [2], anesthesia administration [3], as well as restraint of animals [4].

In this perspective, recent studies have reported that the use of a telemetry system is the most efficient standard for physiological measurement *in vivo* [5]. The telemetry is a technique in which a transmitter is implanted on small animals, permitting the recording of the signals automated and wireless, where the data are posteriorly received by a receiver outside the home cage of the animals. This method allows the recording to be done in rats over a long period, occurring in a state very close to the animal's natural cardiovascular physiology. Nevertheless, despite this method provides data more optimized and reliable it still possesses many limitations such as a very high cost of implementation, physical size (it requires a minimum bodyweight of the animals for implantation), and external power requirements for its operation [1, 5, 6]. In investigations of the cardiac autonomic nervous system (ANS), these methods described here may affect the natural physiological features, impairing a better translational approach. For example, the surgical procedure for telemetric transmitter implantation in very diseased animals may result in the non-survival of these animals. From the anesthesia administration standpoint, the use of several drugs for cardiovascular evaluation is also sometimes questionable by influences in the divisions sympathetic and parasympathetic of ANS [3, 7].

Indeed, all these conditions presented above reinforce the importance of the development of new approaches to the recording of ECG in rats, which leads to better control of confounders associated with the ANS experimental models. Based on this, the heart rate variability (HRV) analysis has been suggested for examining of the sympathetic and parasympathetic activities of ANS. This is attributed as an acceptable tool for characterizing the influences of cardiac autonomic control on the sinus node, which describes the fluctuations of the intervals among consecutive heartbeats (NN intervals). Epidemiological studies have shown that decreased HRV activity is correlated with a higher risk of mortality and morbidity in cardiac patients [8].

Therefore, considering the use of HRV parameters analysis to evaluate the ANS conditions on the natural animal physiology, we developed a new tool for ECG recording in rats in the awake state, no permit the use of anesthetics, surgical procedures, restraint or any other type of force exerted on the animals. In order to test

the efficacy of the system proposed, we also explored in set the use of isoflurane anesthetics for comparative analysis.

## **2 Materials and Methods**

### ***2.1 Animals***

Five male adult Wistar rats 150 days old (400–475 g) were used in this study. Animals were maintained under controlled laboratory conditions (12 h light-dark cycle, in constant temperature  $22 \pm 2$  °C, 54% relative humidity), with free access to filtered water and ad libitum access to a standard laboratory diet. Animals were randomly housed (maximum 3) in boxes (27 cm × 36 cm × 31 cm), which were covered by shavings and allocated on ventilated racks. All procedures performed on the animals followed the Committee on Care and Use of Experimental Animal Resources of the Federal University of Santa Catarina (protocol number 2712080317).

### ***2.2 Data Acquisition Protocol***

To data recording in the awake state, an electrocardiograph was developed a custom-made jacket to the thoracic circumference of the rats, in which three electrodes were allocated internally to record ECG signals. This was produced from brim with elastane and three fabric velcro tapes. For adaptation in the jacket, the animals were habituated during forty (40) days (60 min/day for each animal) with the jacket in a glass box (30 cm × 20 cm × 23 cm) free to move. The animals were induced to enter inside of the jacket using a feed pellet and with the hands. After the adaptation period, ECG recording has been conducted in anesthetized and awake conditions. Before the beginning of assessments, the animals were allowed 30 min dressed in the jacket. The recording in the anesthetized state was done after the isoflurane administration (2.5% mixed with 100% of oxygen) in the morning period. After the assessments in the anesthetized state, the animals were carefully transferred to their home cage to recovery consciousness (minimum rest of 3 h). In the afternoon period, the animals were evaluated in the awake state on the new device developed.

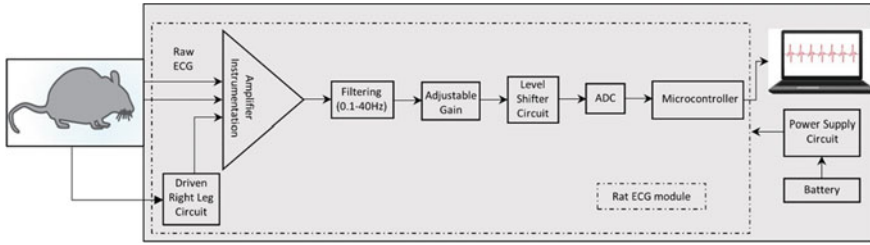


**Fig. 1** General block diagram of the ECG measurement system in rats

### 2.3 Device Architecture

ECG samples were acquired using lead I configuration in the awake and anesthetized condition. The three electrodes included one for the driven right leg for reducing noise. The ECGs were recorded during 8–10 min for each animal, from which was selected a 5-min sample with the lowest noise (e.g., movement artifacts) for processing. The recorded raw signals were amplified by an instrumentation amplifier (INA129, Texas Instruments Inc., Texas, USA) and subsequently filtered by both high-pass (first order, 0.1 Hz) and low-pass (Butterworth, fourth-order, 40 Hz) filters. As this type of signal possesses amplitude in the range millivolts, it was adjusted by a gain circuit before sending it to the digital-to-analog converter. We also used a shifter level circuit allowing only the range accepted by the converter (0–5 V). The signal was digitalized by a 12-bit analog-to-digital converter (ADS1015, Texas Instruments Inc., Texas, USA) at 500 samples/s and sent through I<sup>2</sup>C connection to a microcontroller (Arduino Nano board V.3.0, San Jose, California, USA). The data received by microcontroller were transmitted by USB connection to a computer for storage and off-line HRV analysis. All the devices used in the ECG module were battery-powered (as illustrated in the block diagram in Fig. 1).

### 2.4 Heart Rate Variability

To assess the HRV features in rats, the data were extracted by HRVtool application (HRVtool, Greifswald, MV, Germany, version 1.03) custom-built software using Matlab (MathWorks Inc., Natick, MA, USA, version 8.5). The data were manipulated following the recommendation of the Task Force of the European Society of Cardiology and the North American Society of Pacing and Electrophysiology [8]. The extraction of HRV parameters in the time domain was calculated three components: mean HR (mean heart rate), SDNN (standard deviation of all NN intervals), and RMSSD (square root of the sum of the squares of differences among NN intervals). SDNN represents the contributing to all HRV components during the recorded period, reflecting a measure of overall HRV and RMSSD provides information about

the parasympathetic tone in the short term recording. For the analysis in the frequency domain, data were resampled using cubic spline interpolation to obtain time evenly spaced. Two frequency bands were established: low frequency in the normalized unit (LFnu, 0.2–0.75 Hz) and high frequency in the normalized unit (HFnu, 0.75–3.0 Hz) using fast Fourier transformation (FFT) algorithm [9]. Although there are controversies about the precise reflection of these parameters, both reflect the parasympathetic (LF) and sympathetic (HF) activities, respectively, and the LF/HF ratio demonstrates information about the global sympathetic-vagal balance.

## 2.5 Statistical Analysis

The data analysis was conducted using Paired Students t-tests to evaluate the effects of isoflurane administration in comparison to the new tool developed in awake rats. All data were expressed as the means  $\pm$  standard error of the mean (S.E.M).  $p < 0.01$  and  $p < 0.05$  were considered statistically significant. Statistical analysis was carried out by the GraphPad Prism (GraphPad Software, Inc., San Diego, CA, U.S.A., version 8.0) statistical program.

## 3 Results

The use of anesthesia administration and ECG recording methods in surgical settings for evaluation of ANS has been questioned due to the influence on the sympathetic and parasympathetic activities. In this present study, we tested a new model in the awake and isoflurane-anesthetized state under the same animals and compared the results.

HRV parameters varied in both time and frequency domains in the animals in awake and anesthetized conditions (Fig. 2). The results obtained in the time domain showed that the heart rate was statistically higher ( $p < 0.01$ ; Fig. 2a) in the awake state. On the other hand, the SDNN ( $p > 0.05$ ; Fig. 2b) and RMSSD ( $p > 0.05$ ; Fig. 2c) components did not differ among both the animal states. However, we observed a reduction in the component SDNN, although not statistically significant. Interestingly, we also noted that the HRV parameters recorded in the anesthetized state induced a more significant standard error of the mean in comparison to the awake state, reflecting on all the metrics measured in the time domain. Data analysis of linear HRV metrics in the frequency domain revealed that there were substantial differences on all the evaluated parameters LFnu ( $p < 0.05$ ; Fig. 2d), HFnu ( $p < 0.05$ ; Fig. 2e) and LF/HF ( $p < 0.05$ ; Fig. 2f), respectively, in comparison of animals between both conditions.

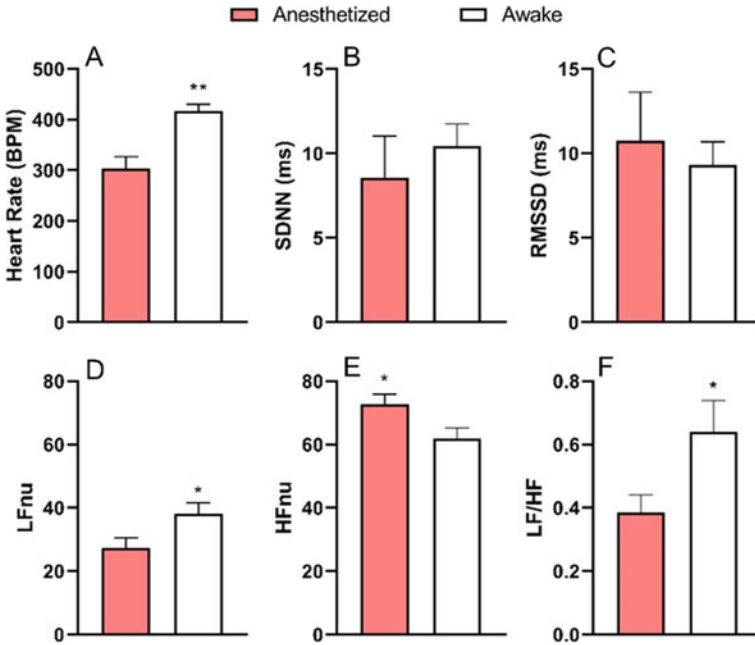


**Fig. 2** Heart rate variability metrics. Data are given as means  $\pm$  standard error of the mean. BPM, beats per minute; ms, milliseconds; nu, normalized units. Data analysis was conducted using the student's paired *t*-tests. \**p* < 0.05 and \*\**p* < 0.01 were considered statistically significant

## 4 Discussion

In this present work, we designed a new tool for non-invasive ECG recording in awake rats, without the use of anesthetics, surgical procedures, restraint, or any other type of force exerted on the animals, evaluating the possible influences on the sympathetic and parasympathetic behaviors of ANS. The findings in our study demonstrated that the proposed system for acquiring ECG signals in rats worked well, providing HRV values more compatible with the natural physiology of rats. Furthermore, our data showed that the use of isoflurane administration in experimental physiological models triggers effects on the ANS activities (sympathetic and parasympathetic).

Due to the experimental physiological models in rats become essential tools to the drug safety assessment, there is a growing interest in the search for models that may record the ECG in rats non-invasively. Although the techniques developed until the present moment have evolved, these still imply effects on the cardiac physiology of animals. For example, the use of isoflurane anesthesia administration for evaluation cardiac is widely used on several models, including physiological monitoring to elicit greater control of prolonging and deepening anesthetic. Nonetheless, our results demonstrated changes in the HRV indexes in both the time and frequency domain measured in the awake and anesthetized conditions. In general, the measure of HRV

evidenced by HR and SDNN parameters, our findings showed low activity compared to the anesthetized state, although SDNN was not statistically significant. These results are consistent with previous studies in rats and mice, which showed low HR after the isoflurane administration in comparison with the awake state [10, 11].

From a parasympathetic tone standpoint (indexed by RMSSD and HFnu), our data indicated activation only in the frequency domain by HFnu, suggesting intense activity on the vagal tone in the anesthetized state. On the other hand, some works showed low activity after the use of this drug [12, 13]. Such discrepancy may be explained by the different ECG models in rats used. Regarding the sympathetic tone (LFnu) and balance sympathetic-vagal (LF/HF), our study showed strong activity on both LFnu and LF/HF components under isoflurane. Similarly, studies reported high activity in rats and dogs [12, 13]. Together, these results indicate that although the global HRV is controlled by sympathetic activity, this may suffer the influence of parasympathetic activity during isoflurane administration.

In this context, the tool presented here comprised a set of solutions for the conventional methods used, which cause effects on the HRV parameters as well as other physiological models. Unlike telemetry, our model may be applied to animals of any size, with low cost for implementation. Although is necessary for an animal adaptation time in the jacket, this may be performed for any experimental cardiac model, even on very diseased animals. In this line thinking, this provides values with smaller experimental errors which may occur by anesthesia administration, surgical procedure, restraint as well as force exerted on the animals.

## 5 Conclusion

In summary, the results found herein regarding the HRV parameters in the time and frequency domain, demonstrated clearly that the isoflurane anesthesia administration in physiological models interferes with the sympathetic and parasympathetic activities of ANS. In this sense, our approach developed for ECG recording is more suitable to explore the cardiac electrical activity features in rats.

**Acknowledgements** The authors gratefully acknowledge the student fellowships from the National Council for Scientific and Technological Development (CNPq) (to R.S.N) and the Coordination of Superior Level Staff Improvement (CAPES) (to F.S.F). A.R.S.S., L.F.F.R, and J.L.B.M are grantees of CNPq research productivity fellowships.

## References

1. Accardi, M.V., et al.: Rat cardiovascular telemetry: Marginal distribution applied to positive control drugs. *J. Pharmacol. Toxicol. Methods* **81**, 120–127 (2016)
2. Silva, L.E.V., et al.: Comparison between spectral analysis and symbolic dynamics for heart rate variability analysis in the rat. *Sci. Rep.* **7**, 8428 (2017)

3. Fenske, S., et al.: Comprehensive multilevel in vivo and in vitro analysis of heart rate fluctuations in mice by ECG telemetry and electrophysiology. *Nat. Protoc.* **11**, 61–86 (2016)
4. Mongue-Din, H., Salmon, A., Fiszman, M.Y., Fromes, Y.: Non-invasive restrained ECG recording in conscious small rodents: a new tool for cardiac electrical activity investigation. *Pflugers Arch.* **454**, 165–171 (2007)
5. Niemeyer, J.E.: Telemetry for small animal physiology. *Lab. Anim.* **45**, 255–257 (2016)
6. Deveney, A., Kjellstrom, A., Forsberg, T., Jackson, D.: A pharmacological validation of radiotelemetry in conscious, freely moving rats. *J. Pharmacol. Toxicol. Methods* **40**, 71–79 (1998)
7. Hildebrandt, I.J., Su, H., Weber, W.A.: Anesthesia and other considerations for in vivo imaging of small animals. *ILAR J.* **49**, 17–26 (2008)
8. Task Force of the European Society of Cardiology & The North American Society of Pacing and Electrophysiology: Heart rate variability: standards of measurement, physiological interpretation, and clinical use. *Eur. Hear. J.* **17**, 354–381 (1996)
9. Cerutti, C., et al.: Autonomic nervous system and cardiovascular variability in rats: a spectral analysis approach. *Am. J. Physiol.* **261**, H1292–H1299 (1991)
10. Stein, A.B., et al.: Effects of anesthesia on echocardiographic assessment of left ventricular structure and function in rats. *Basic Res. Cardiol.* **102**, 28–41 (2007)
11. Pachon, R.E., Scharf, B.A., Vatner, D.E., Vatner, S.F.: Best anesthetics for assessing left ventricular systolic function by echocardiography in mice. *Am. J. Physiol. Hear. Circ. Physiol.* **308**, H1525–H1529 (2015)
12. Kato, K., Wakai, J., Ozawa, K., Sekiguchi, M., Katahira, K.: Different sensitivity to the suppressive effects of isoflurane anesthesia on cardiorespiratory function in SHR/Izm, WKY/Izm, and Crl: CD (SD) rats.: *Exp. Anim.* **65**, 393–402 (2016)
13. Kato, M., et al.: Spectral analysis of heart rate variability during isoflurane anesthesia. *Anesthesiology* **77**, 669–674 (1992)



# Algorithm for Detection of Raising Eyebrows and Jaw Clenching Artifacts in EEG Signals Using Neurosky Mindwave Headset



Luis Vélez  and Guillermo Kemper 

**Abstract** The present work proposes an algorithm to detect and identify the artifact signals produced by the concrete gestural actions of jaw clench and eyebrows raising in the electroencephalography (EEG) signal. Artifacts are signals that manifest in the EEG signal but do not come from the brain but from other sources such as flickering, electrical noise, muscle movements, breathing, and heartbeat. The proposed algorithm makes use of concepts and knowledge in the field of signal processing, such as signal energy, zero crossings, and block processing, to correctly classify the aforementioned artifact signals. The algorithm showed a 90% detection accuracy when evaluated in independent ten-second registers in which the gestural events of interest were induced, then the samples were processed, and the detection was performed. The detection and identification of these devices can be used as commands in a brain-computer interface (BCI) of various applications, such as games, control systems of some type of hardware of special benefit for disabled people, such as a chair wheel, a robot or mechanical arm, a computer pointer control interface, an Internet of things (IoT) control or some communication system.

**Keywords** EEG signals · Brain-computer interface · Neurosky mindwave headset · Artifacts detection

## 1 Introduction

The electroencephalogram (EEG) signal is originated by neurons activities recorded as fluctuations in electric differential potentials obtained from several areas and specific points on the human brain. Commonly, EEG has been used for medical research and medical applications, but in last years there has been a substantial

---

L. Vélez · G. Kemper (✉)

School of Electronic Engineering, Universidad Peruana de Ciencias Aplicadas, Lima, Peru

e-mail: [pcelgkem@upc.edu.pe](mailto:pcelgkem@upc.edu.pe)

L. Vélez

e-mail: [u201315423@upc.edu.pe](mailto:u201315423@upc.edu.pe)

© The Editor(s) (if applicable) and The Author(s), under exclusive license

to Springer Nature Switzerland AG 2021

Y. Iano et al. (eds.), *Proceedings of the 5th Brazilian Technology Symposium*,

Smart Innovation, Systems and Technologies 202,

[https://doi.org/10.1007/978-3-030-57566-3\\_10](https://doi.org/10.1007/978-3-030-57566-3_10)

perspective to use it for non-medical brain–computer interface applications like device control, tools for education, and entertainment industry. The raw EEG signal is usually contaminated by artifacts from different sources such as the heartbeats, eyes blinks, muscle activities, and noise from electrical equipment [1]. Detection of these artifacts is often an important subject in EEG research. Commonly, when electrodes are positioned on central scalp zones containing mainly brain activity, temporoparietal sites that may contain muscle artifacts and frontal sites that may carry strong blinks, eye movement, and other muscle artifacts [2]. Blind source separation (BSS) methods, like independent component analysis (ICA) and canonical correlation analysis (CCA), have also been proposed for EMG artifacts detection and removal [3–5]. Such methods, however, require multi-channel data and long data epochs to produce important results.

The computational complexity is another characteristic that difficults the choice of ICA or CCA for artifact detection in applications that require real-time implementations [6].

Artificial intelligence and machine learning methods, such as neural networks and vector support machines (SVM), are also widely used in the process of extraction and classification artifacts [7, 8]. Although these methods have been giving very good results, they require a long training process of the network and a large number of standard signals, which must be collected from accredited sources, and which will serve as a reference for their optimal operation, in addition to requiring greater computational capacity.

The proposed algorithm correctly extracts and classifies two EMG artifacts of interest (jaw clench and raising eyebrows), with an accuracy of 90%, allowing its use in real-time processing, due to its light computational load, simplicity of implementation and its use with EEG sensors of low cost and a single active channel, promoting the development of multiple applications for brain–computer interfaces (BCI) such as games, manipulation of the computer pointer for people with disabilities of upper limbs, or communication projects in people with disabilities of this faculty. The aim is to detect these two particular artifacts generated by two muscular events: the jaw clenching and eyebrows raising.

The gestures that were made to obtain the artifacts of interest are shown in Figs. 1 and 2, respectively.

## 2 Description of the Proposed Algorithm

It is important to indicate that the framework used in this study corresponds to the development of a computational algorithm. Thus, ethical approval for the experiment in this study was deemed unnecessary by the university, since the research was designed to develop a computational framework with the help of a commercial non-invasive sensor that does not represent any health risk. Likewise we consider that the activities undertaken in the research do not pose risks greater than those ordinarily encountered in daily life.



Fig. 1 Jaw clench artifact gestural

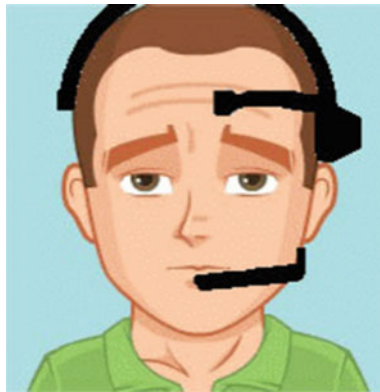


Fig. 2 Eyebrows raising artifact gestural

Figure 3 shows a block diagram of the proposed algorithm. Details of each processing stage are described in the following sections.

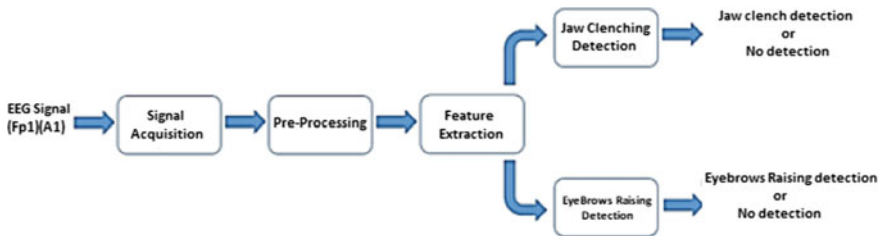
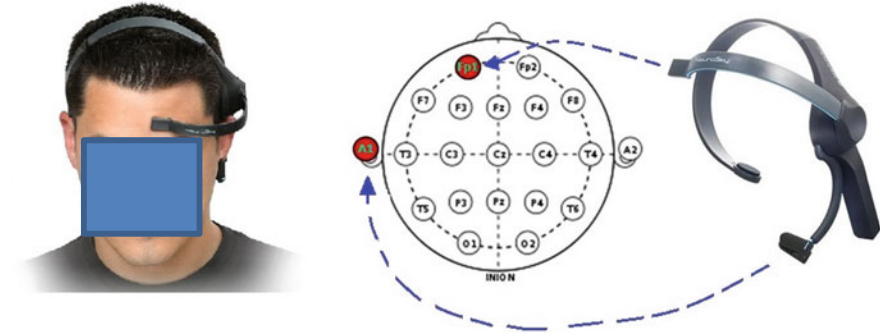


Fig. 3 Block diagram of the proposed algorithm



**Fig. 4** Position of mindwave mobile headset electrodes on the 10–20 international system of electrode placement. Fp1–A1 electrodes

## 2.1 Signal Acquisition

The signals were acquired using an economic BCI mindwave mobile headset from Neurosky. This device is composed of a headset, an ear clip, and a sensor arm. The dry electrode is on the sensor arm which is placed in frontage. According to [9] the 10–20 international system of EEG electrode placement on the human head, this position is around corresponding to the Fp1 position shown in Fig. 4. The reference and ground electrodes are on the ear clip at A1. The diadem also has a Bluetooth module that sends the signals to the computer at a sampling frequency of 512 Hz.

## 2.2 Preprocessing Signal

The aim at this stage was to condition the signals to increase precision in the extraction of characteristics.

Unwanted noise components (coming mainly from the 60 Hz power grid) are removed for signal improvement. For this purpose, an infinite impulse response IIR Butterworth second-order filter with a cutoff frequency of 59 and 61 Hz is used for work like a 60 Hz band stop notch filter. The use of this filter provided the best results in terms of lowering noise and unwanted distortion. The original signal and the filtered signal are showed in Figs. 5 and 6, respectively.

### 2.2.1 Jaw Clench Detection

For the detection of the first artifact jaw clench, Cooper's algorithm was used, which extracts and classifies, combining the concepts of energy and zero crossings in a single operation. Although this algorithm correctly detects the presence of the artifact of interest, in some cases, it gives false detections, so it is combined with the zero-crossing algorithm, additionally, to rule out the erroneous detections, which are fragments confused by their similarity in features with jaw clench.

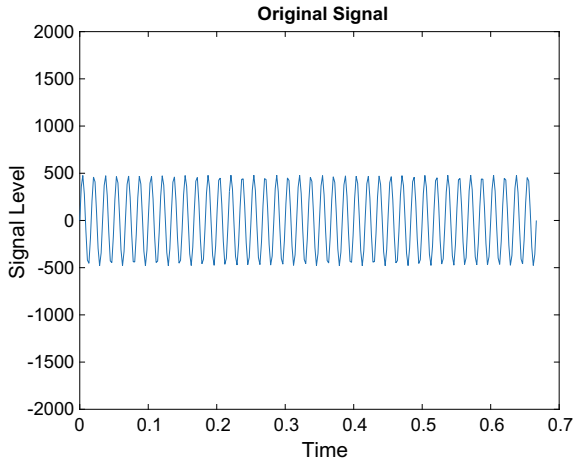


**Fig. 5** Original signal

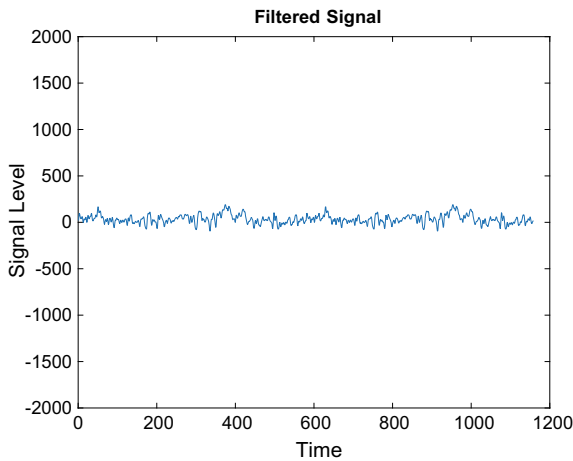


**Fig. 6** Filtered signal with a 60 Hz notch filter

### 2.2.2 Cooper’s Algorithm

*Step 1.* Signal samples are recorded for times of 10 s, and this recording time was chosen for practicality, considering that the signal sample is not so short so that it is possible to perform the gestures, and not so extensive, that it produces a very long processing time. Total samples obtained in 10 s are calculated by applying the following expression:

$$N \text{ samples} = F_s \times T_{\text{record}}$$

$$\begin{aligned}
 N \text{ samples} &= 512 \text{ Hz} \times 10 \text{ s} \\
 N \text{ samples} &= 5120
 \end{aligned}
 \tag{1}$$

*Stage 2.* The signal is divided into a certain number of blocks, with a certain number of samples per block. Finally, 15 samples per block were considered, since, and according to experimental research, it provided a favorable total block density for Cooper's histogram analysis. Total epochs are calculated by applying the following expression:

$$\begin{aligned}
 N \text{ epochs} &= \frac{N \text{ samples}}{\text{samples by Epoch}} \\
 \text{Samples by epoch} &= 15 \\
 N \text{ epochs} &= \frac{5120}{15} \approx 342
 \end{aligned}
 \tag{2}$$

*Stage 3.* The entire signal is traversed, for each of the 342 blocks, and the Cooper parameter of each block is calculated, applying the following expression with the 15 sample values of the evaluated block:

$$C = \sum_{m=0}^L |y[m] \cdot |y[m]| - y[m-1] \cdot |y[m-1]| | \tag{3}$$

where  $y[m]$  is the actual discrete sample analyzed and  $y[m-1]$  is the precedent sample, and  $C$  is the block Cooper value.

*Stage 4.* Start detector. A starting threshold range of  $u_{i\min} = 81,100$  and  $u_{i\max} = 90,000$  is chosen. This threshold range was used because it was experimentally possible to minimize the error in the detection of the event of interest and avoid considering very high values of the Cooper parameter that are reached by noise or other artifacts but never by the jaw clenching. Cooper value of the current block, [blockcooper], is in this threshold range, the 15 samples of the block are saved in the output vector [clench], which will contain the extracted artifact signal, and the final sample of said block is also saved (15th sample) as the starting sample ("ki") of the extracted artifact signal.

*Stage 5.* End detector. An end threshold value of  $u_f = 5000$  is chosen. This threshold value was used because it was experimentally possible to minimize the error in the detection of the event of interest considering Cooper's histogram. It is evaluated if the Cooper value of the block is less than this threshold  $u_f$ , if it is lower, it is saved as the last block and the algorithm is completed. The 15th sample of the final block is also saved as an end sample of the extracted artifact signal ("kf"). Figure 7 shows jaw clench detection using Cooper's algorithm.

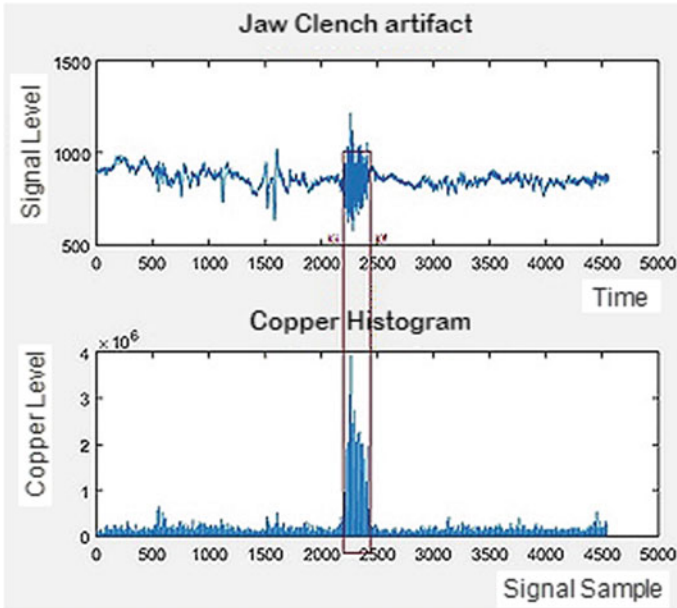


Fig. 7 Jaw clench artifact classification and Cooper’s histogram

### 2.2.3 Zero-Crossing Density Algorithm

Stage 1. The previously extracted fragment is divided into a certain number of blocks, with a certain number of samples per block. Finally, 15 samples per block were considered, since, according to experience, it provided a favorable total block density for the analysis of the calculation of zero crossings.

Stage 2. The entire fragment is traversed, for each of the samples of the signal, and the sign of the present sample is evaluated with the sign of the previous sample, to verify if there is a change of sign between two continuous samples. If this condition exists, it is counted as zero crossing, causing the density to increase by a value of two. All this is done according to the following expression:

$$Z = \sum_{m=0}^{N-1} |\text{sign}[y(m)] - \text{sign}[y(m - 1)]| \tag{4}$$

where  $y(m)$  is the actual discrete sample analyzed,  $y(m - 1)$  is the precedent sample,  $N$  is the total samples, and  $Z$  is the zero-crossing density value.

Stage 3. Classification or discard. A decision threshold value of  $U_z = 150$  is chosen. This threshold value was used because it was experimentally possible to minimize the error in the detection of the event of interest. If the value of zero crossings of the current fragment is greater than the “ $U_z$ ” value, the start samples are saved (“ $K_i$ ”) and end (“ $k_f$ ”) to delimit the artifact, otherwise the fragment is discarded.

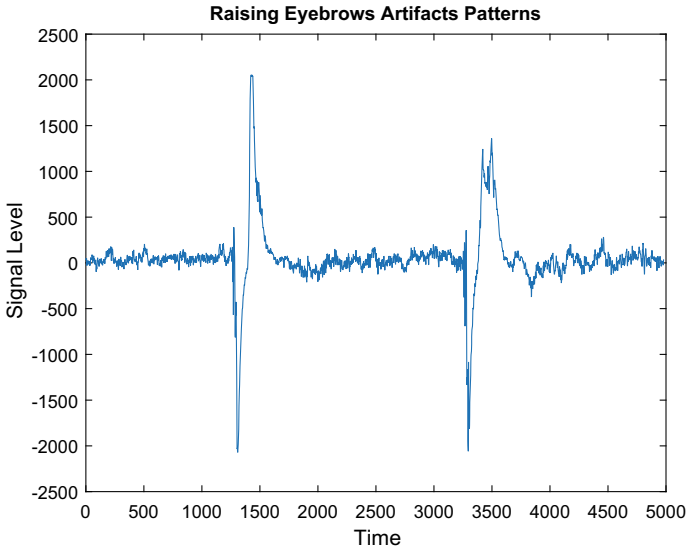


**Fig. 8** Original “eyebrows raising” artifacts signal recorded with Neurosky mindwave headset

#### 2.2.4 Eyebrows Raising Detection

For the detection of the second “raising eyebrows” artifact, the algorithm of calculation of energy by blocks of the signal was used, which extracts the possible fragments that contain the artifact of interest. In the case of this detection, the characteristic is that it has very high energy values in the peaks, and a minimum value of zero crossings, unlike the first artifact that has high values of zero crossings, and low energy levels.

Figure 8 shows two original raising eyebrows artifacts registered by Neurosky mindwave headset in two different times.

#### 2.2.5 Energy Calculation Algorithm Per Signal Blocks

Stage 1. Steps 1 and 2 of the Cooper’s algorithm are performed.

Stage 2. The entire signal is traversed for each of the 342 blocks, and the energy value of each block is calculated. This calculation is performed through the following expression:

$$E_i = \sum_{n=iN}^{iN+N-1} x^2(n) \quad (5)$$



where  $x(n)$  is the discrete sample analyzed,  $i$  is the block number,  $N$  is the block total samples, and  $E_i$  is the energy of the block.

Stage 3. Start detector. A start threshold value of  $u_i = 1.5e8$  was chosen. This threshold value was finally used because it was experimentally possible to minimize the error in the detection of the event of interest after 10 variations, and due to the high energy value of the present artifact in the peaks. If the energy of the current block exceeds this starting threshold, the 15 samples of the block are stored in the output vector [eyebrow], which will contain the possible extracted artifact signal, in addition, the final sample of said block is saved (15th sample) as a start sample of the extracted artifact signal. The peak width counter is increased for subsequent evaluation that will serve to validate the extracted segment.

Stage 4. End detector. An end threshold value of  $u_f = 0.3e8$  was chosen. This threshold value was finally used because it was experimentally possible to minimize the error in the detection of the event of interest after 10 variations. If the energy of the block is less than this end threshold, it is saved as the last block of the extracted signal.

Stage 5. The peak width is evaluated if it is less than a threshold width of 150. This value was considered because the minimum peak width for a rapid brow lift is approximately 160 samples. If it is smaller the extracted signal is discarded, otherwise the algorithm culminates. The 15th sample of the final block is also saved as an end sample of the extracted artifact signal if the discard is not performed. Figure 9 shows eyebrows raising artifact detection.

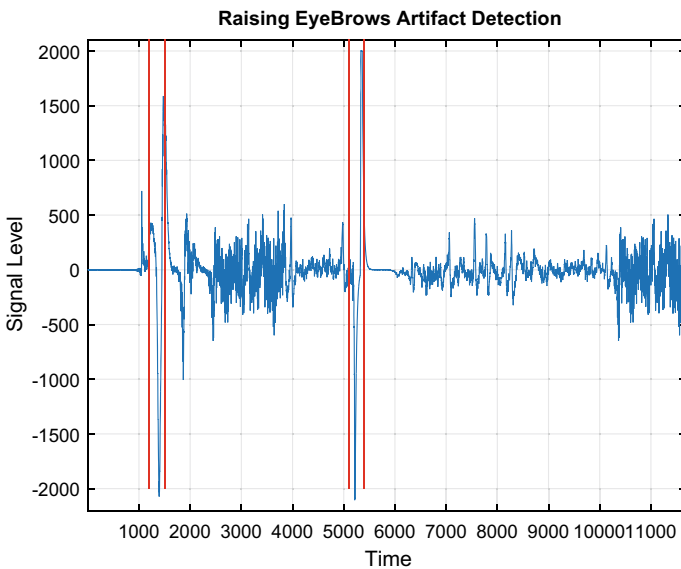


Fig. 9 “Eyebrows raising” artifacts detection

### 3 Results

To evaluate the proposed algorithms, both the eyebrow lift detection and mandibular pressure detection, independent tests were performed to validate the accuracy in detecting these events. Placing and performing the Bluetooth pairing of the Neurosky sensor with the desktop computer and the recording application, made in MATLAB, we made recordings of 10 s, time that was considered adequate to be able to perform one of the gestures with tranquility. After each recording, the recorded signal was analyzed to detect the gesture made. With the results obtained, Table 1 was carried out, and the percentage of error in the detection of each algorithm corresponding to each gestural event was calculated (Figs. 10 and 11).

The goal of this recordings was a concept and preliminary study for later applications, where tests with individuals will be regulated by the respective ethical committee.

**Table 1** Results of the algorithms precision detection

Test number	Jaw clench detection result	Raise eyebrows detection result
1	Right	Right
2	Right	Wrong
3	Right	Right
4	Right	Right
5	Right	Right
6	Right	Right
7	Right	Right
8	Right	Right
9	Right	Right
10	Right	Right
11	Right	Right
12	Right	Right
13	Right	Right
14	Right	Right
15	Right	Right
16	Right	Wrong
17	Right	Right
18	Wrong	Right
19	Right	Right
20	Right	Right

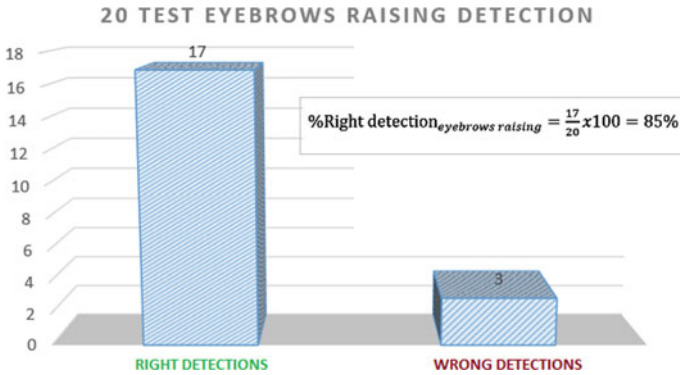


Fig. 10 Detection right rate in eyebrows raising artifact

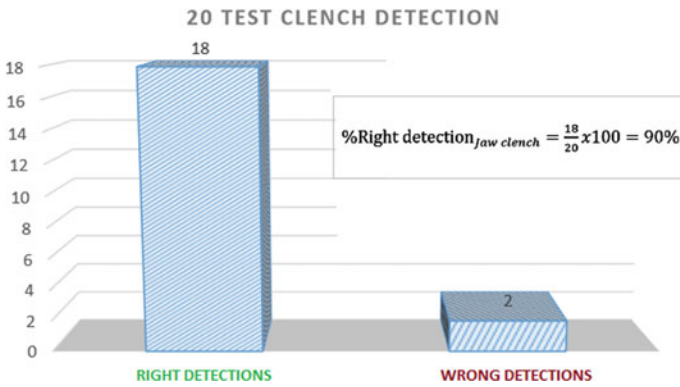


Fig. 11 Detection right rate in jaw clench artifact

## 4 Conclusion

In conclusion, the present work provides a possibility to take advantage of jaw clench and raising eyebrows artifacts, to be used as commands in any system that can be controlled, using simple digital signal processing (DSP) algorithms and of easy implementation. As a factor to take into account, it is that conductive gel should be used in the electrode, since it is very helpful in the noise filter of different frequencies that are introduced in the electrode, and that cannot be suppressed by digital filters.





As future work, these artifacts are planned to be used in a brain–interface system to control the computer mouse pointer, very useful for people with disabilities in the movement of their hands and arms to control it.

## References

1. Matiko, J.W., Beeby, S.P., Tudor, J.: Real time eye blink noise removal from EEG signals using morphological component analysis. In: 2013 35th Annual International Conference of the IEEE Engineering in Medicine and Biology Society (EMBC), pp. 13–16. <https://doi.org/10.1109/embc.2013.6609425> (2013)
2. Delorme, A., Sejnowski, T.J., Makeig, S.: Enhanced detection of artifacts in EEG data using higher-order statistics and independent component analysis. *NeuroImage* **34**, 1443–1449 (2007). <https://doi.org/10.1016/j.neuroimage.2006.11.004>
3. Jafari, A., Gandhi, S., Konuru, S.H., Hairston, W.D., Oates, T., Mohsenin, T.: An EEG artifact identification embedded system using ICA and multi-instance learning. In: 2017 IEEE International Symposium on Circuits and Systems (ISCAS), pp. 1–4. <https://doi.org/10.1109/iscas.2017.8050346> (2017)
4. Loring Z., Dornhege, J.R., Millan, T., Hinterberger, D.J., McFarland, K.M. (eds.): *Toward Brain-Computer Interfacing*. The MIT Press, London (2007)
5. Xia Erkens, I.J., Molina, G.G.: *Artifact detection and correction in neurofeedback and BCI applications* (2008)
6. Islam, M.K., Rastegarnia, A., Yang, Z.D.: Methods for artifact detection and removal from scalp EEG: a review. *Neurophysiologie Clinique/Clin. Neurophys.* **46**, 287–305. <https://doi.org/10.1016/j.neucli.2016.07.002> (2016)
7. Chambayil, B., Singla, R., Jha, R.: EEG eye blink classification using neural network. In: *Proceedings of the World Congress on Engineering*, vol. 1, pp. 2–5 (2010)
8. Kousarrizi, M.R.N., Ghanbari, A.A., Teshnehlab, M., Shorehdeli, M.A., Gharaviri, A.: Feature extraction and classification of EEG signals using wavelet transform, SVM and artificial neural networks for brain computer interfaces. In: 2009 International Joint Conference on Bioinformatics, Systems Biology and Intelligent Computing, pp. 352–355. IEEE (2009). <https://doi.org/10.1109/ijcbs.2009.100>
9. Sanei S., Chambers J.: *EEG Signal Processing*. Wiley (2007)

# Correspondence Between TOVA Test Results and Characteristics of EEG Signals Acquired Through the Muse Sensor in Positions AF7–AF8



Ober Castillo , Simy Sotomayor , Guillermo Kemper ,  
and Vincent Clement 

**Abstract** This paper seeks to study the correspondence between the results of the test of variable of attention (TOVA) and the signals acquired by the Muse electroencephalogram (EEG) in the positions AF7 and AF8 of the cerebral cortex. There are a variety of research papers that estimates an index of attention in which the different characteristics in discrete signals of the brain activity were used. However, many of these results were obtained without contrasting them with standardized tests. Due to this fact, in the present work, the results will be compared with the score of the TOVA, which aims to identify an attention disorder in a person. The indicators obtained from the test are the response time variability, the average response time, and the  $d'$  prime score. During the test, the characteristics of the EEG signals in the alpha, beta, theta, and gamma subbands such as the energy, average power, and standard deviation were extracted. For this purpose, the acquired signals are filtered to reduce the effect of the movement of the muscles near the cerebral cortex and then went through a subband decomposition process by applying transformed wavelet packets. The results show a well-marked correspondence between the parameters of the EEG signal of the indicated subbands and the visual attention indicators provided by TOVA. This correspondence was measured through Pearson's correlation coefficient which had an average result of 0.8.

---

O. Castillo · S. Sotomayor · G. Kemper (✉)  
Universidad Peruana de Ciencias Aplicadas, Av. Prolongación Primavera 2390, Santiago de Surco, Lima, Peru  
e-mail: [pcelgkem@upc.edu.pe](mailto:pcelgkem@upc.edu.pe)

O. Castillo  
e-mail: [u201412884@upc.edu.pe](mailto:u201412884@upc.edu.pe)

S. Sotomayor  
e-mail: [u201412287@upc.edu.pe](mailto:u201412287@upc.edu.pe)

V. Clement  
Martin-Luther University Halle-Wittenberg, Univesrtitätsplatz 010, 06108 Halle (Saale), Germany  
e-mail: [vincent.c.clement@gmail.com](mailto:vincent.c.clement@gmail.com)

**Keywords** Neurofeedback · Mindfulness · Visual attention · Muse · EEG signals · Signal processing · TOVA test

## 1 Introduction

Problems of attention and concentration are the most common in the learning processes of children and adolescents. Fuster conducted a review of the different definitions of attention in which he concludes that it is a mechanism directly related to the activation and selection of cognitive processes. Attention has been divided into different types among which sustained attention is found. Sustained attention is defined as the ability to maintain the focus of attention on a stimulus or activity for a long time [1].

In this context, a tool developed to support the diagnosis of attention deficit hyperactivity disorder (ADHD) is the test of variables of attention—TOVA<sup>®</sup>. This test consists of the presentation of two types of visual stimulation on a conventional screen under certain technical specifications. These stimuli are divided into two, the target stimuli and the nontarget stimuli. Figure 1 shows the TOVA target stimuli on the left and the TOVA nontarget stimuli on the right. During the TOVA test, new stimuli are presented every 2000 ms and are flashed for 100 ms. At the end of the test, the results shown are the average response time of the correct answers (RT), the variability of the correct response times (RTV), and the indicator that relates the committed and the omitted errors ( $D'$ ) [2].

On the other hand, studies on the monitoring of brain activity have associated selective attention to the manifestations of brain activity in the gamma subband. [3]. Other studies provide strong results regarding the relationship of the alpha subband with changes in the attention stimuli [4]. However, very few correspond their results in standardized psychological tests.



**Fig. 1** TOVA stimuli: target (left) and nontarget (right)

Therefore, this research aims to find a correspondence between the electrical activity of the brain and the results of the standardized TOVA attention variables test. Research results reveal a correspondence according to Pearson’s correlation coefficient of 0.84 at electrode AF7 and 0.76 at electrode AF8 between the band  $B_{\beta-H}$  standard deviation and the RT indicator of TOVA.

## 2 Description of the Proposed Algorithm

Figure 2 shows a block diagram of the proposed algorithm. Details of each processing stage are described in the following sections.

**Stage 1.** A database was built from 10 sessions of the test TOVA.

**Stage 2.** The TOVA test was performed with one change in the conditions mentioned above. Behind the monitor where the TOVA test was shown, a movie was projected for distracting stimulus. Seven tests were performed.

These two different conditions in the performance of the TOVA test allowed us to find the relationship between certain physiological changes in brain activity and the parameters of the TOVA test.

### 2.1 EEG Signal

The signal used in this investigation was provided by the electroencephalogram device Muse version 2016, developed by Interaxon Inc. This device has four electrodes in the positions TP9, AF7, AF8, and TP10, according to the international system for the electrode placement 10/10 [5, 6]. The device connects to the PC via Bluetooth 4.0 and delivers 12 bits per sample at a sampling rate of 256 Hz. The brain’s electrical activity is classified in different frequency bands. These frequency signals are encountered from 0.1 Hz up to roughly 100 Hz. According to this, the EEG device needs to enable at least twice the maximum frequency to be analyzed (100 Hz) to match the sampling theorem [7].

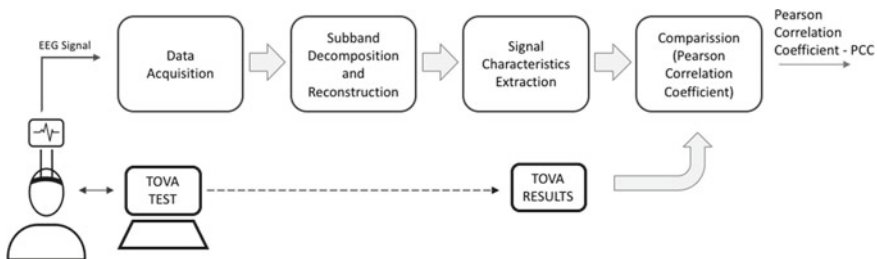


**Fig. 2** Block diagram of the proposed algorithm

## 2.2 Data Acquisition

The signal was acquired for 21.6 min, the duration of the TOVA test. Due to the sampling frequency (256 Hz), 331,776 samples of raw data were obtained for each session and for each electrode. Studies of ADHD reveal that in most cases the characteristics of attention disorders are the product of damage in the prefrontal cortex. This is why the two front electrodes of the Muse (AF7 y AF8) were used [1].

On the other hand, both for the generation of the database (Stage 1) and for the subsequent tests (Stage 2), suitable space for the realization of these tests was prepared and a TOVA test was coded following the specifications that are available in the test manual. Some of these considerations are the size of the stimulus, that should be found in between 15 and 30% of the monitor's size (this is measured diagonally), the displayed stimuli, that should be placed at eye level to the subject, and an eye to monitor the distance of 75 cm [8].

## 2.3 Subband Decomposition Filtering and Reconstruction

In this stage, the acquisition signal of the EEG is separated into four main subbands that were needed in the identification of a correspondence between the TOVA and the EEG signals. These were obtained from the decomposition of the signal in 18 subbands 4 Hz wide as shown in Fig. 3 [9]. For this, a subband decomposition algorithm was developed with the objective of eliminating the bands where the artifacts signals were located and then proceed to the reconstruction of the bands of interest:  $B_{\beta-L}$ ,  $B_{\beta-M}$ ,  $B_{\beta-H}$ ,  $B_{\gamma-L}$ ,  $B_{\gamma-M}$  y  $B_{\gamma-H}$  whose description is in Table 1.

Due to the instability of the EEG signals, and their non-stationary characteristics, it is recommended to use the wavelet packet transform. A wavelet transform is a mathematical tool that allows the extraction of information both in time and frequency. The families of this type of filters that are used for decomposition come from a single function known as "mother wavelet" and its use has been shown to effectively remove the different noises on non-stationary signals [10]. For this investigation, the Daubechies 9 ("db9") family was used, which shows a great correlation with the EEG signal according to Akkar and Hassim, 2017 [11].

To reduce the influence of blinks on the acquisition signal, the averaging filter, the median filter, and the elimination of the band containing more energy during the blink were tested. It was noted that the best method to eliminate intrusive signals in brain activity is to eliminate the band that contains the most components of the signal to be removed. The results of the filters are observed below. Figure 4a shows that the average and median filter affect the entire signal; and, although they reduce the peaks produced by the blinking, much information is lost from the part not affected by these blinks, unlike Fig. 4b, where greater reduction is observed during the blinking and conservation of the signal not affected by them. The bands where the highest energy were produced by the artifacts was removed from the reconstruction process, as shown in Fig. 4; these bands correspond to a bandwidth of de 0–12 Hz, and these are components of the alpha and delta band of brain activity that, for purposes of this paper, they are not of interest in the search of the state of attention.



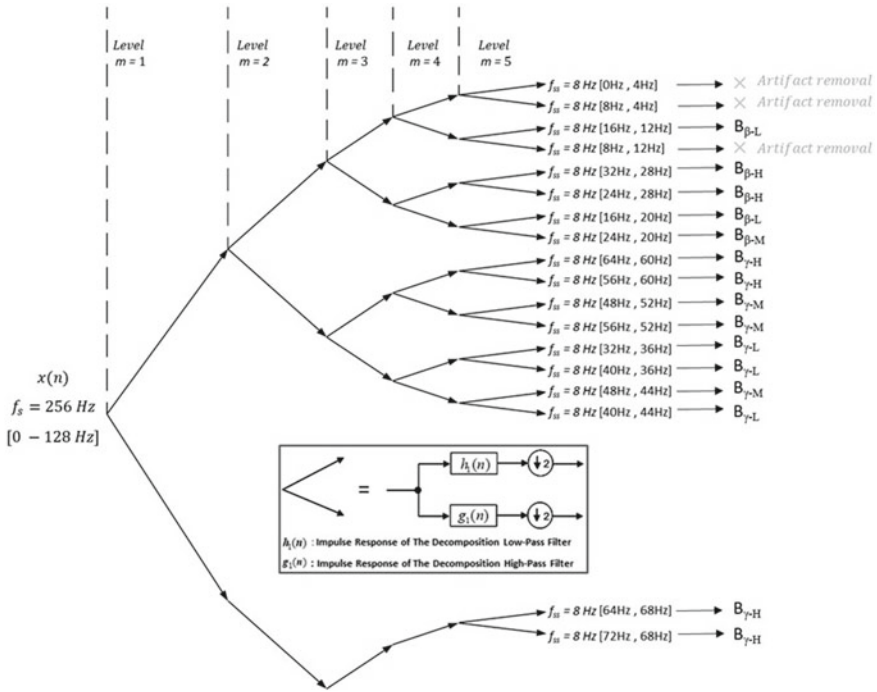


Fig. 3 Wavelet packet decomposition tree used in the proposed method

Table 1 Frequency bands association

Subband	Hz	$i$	Subband	Hz	$i$
$B_{\beta-L}$	12–20	1	$B_{\gamma-M}$	44–56	6
$B_{\beta-M}$	20–24	2	$B_{\gamma-H}$	56–72	7
$B_{\beta-H}$	24–32	3	$B_{\beta}$	12–32	8
$B_{\gamma-L}$	32–44	4	$B_{\gamma}$	32–56	9

### 2.4 Signal Characteristics Extraction

In this stage, the signal characteristics of each subband indicated in Table 1 were extracted. The characteristics extracted were:

Temporary mean power ( $P$ ). To calculate, the vector  $x_i$  was taken, where  $i$  describes the corresponding subband and  $N_i$  the number of elements contained in the vector of the subband  $i$ ; the absolute values added to the square of the  $N_i$  elements contained in the vector were summed to finally divide it by the size of the vector.

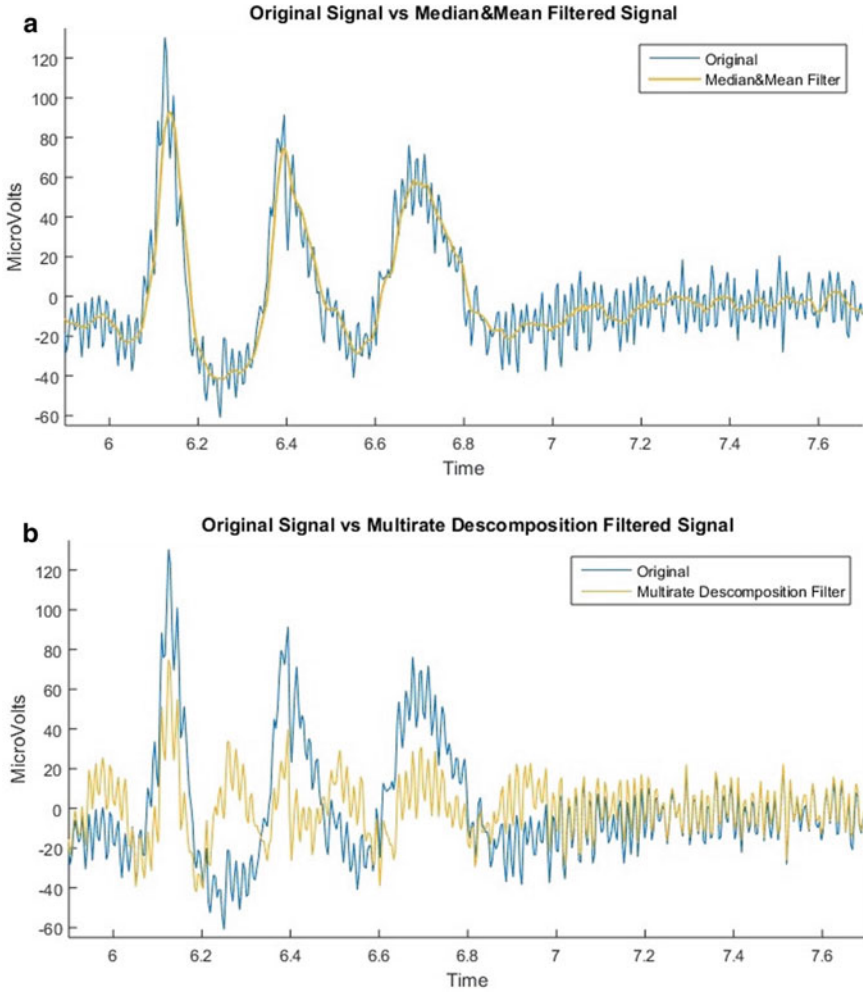


**Fig. 4** **a** Original signal compared to the median and mean filtered signal. **b** Original signal compared to the original signal without  $B_d$

$$P_i = \frac{1}{N_i} \times \sum_{n=1}^{N_i} |x_i(n)|^2 \quad (1)$$

Temporary standard deviation ( $\sigma$ ). To calculate, the sum of the difference between each element and its mean  $\mu_i$  squared was made. Finally, it was divided by the number of elements contained in  $x_i$ .

$$\sigma_i = \sqrt{\frac{\sum_{n=1}^{N_i} (x_i(n) - \mu_i)^2}{N_i}} \quad (2)$$

**Table 2** Mean TOVA results summary

	Optimal TOVA test	Non-optimal TOVA test
RTV	63.60	104.74
RT	344.13	426.18
$d'$	4.55	4.07

The exposed characteristics were applied to all the rebuilt subbands during the performance of the TOVA both for the obtaining of the database (Stage 1) and for the tests TOVA under distracting conditions (Stage 2).

From these results, it was possible to identify the bands in which there was a greater change between the two stages. Within this analysis, the band  $B_{\beta-H}$  was chosen and it was also decided to integrate a new band ( $B_{\Sigma}$ ) defined in Eq. 3.

$$B_{\Sigma} = B_{\beta-L} + B_{\beta-M} + B_{\beta-H} + B_{\gamma-L} + B_{\gamma-M} \quad (3)$$

## 2.5 Comparison

To compare the results of the EEG, the following TOVA parameters were extracted: response time (RT), this parameter reflects the average time required for a correct response to a target stimulus. Response time variability (RTV) corresponds to the variability of the correct response times.  $D$  Prime score ( $d'$ ) indicates the accuracy to discriminate a target stimulus and a nontarget stimulus. This score can be interpreted as “perceptual sensitivity” [12]. Table 2 shows a summary of the results obtained from the TOVA test. The second column corresponds to the average of the tests performed under optimal conditions and the third column, to the average of the tests performed under distracting stimuli.

Each of these parameters was contrasted with the characteristics of the bands selected in the previous point to find some correspondence between both groups.

## 3 Results

Finally, Pearson’s correlation coefficient of the TOVA test with the selected EEG signals was calculated. Ten sessions of Stage 1 and seven sessions of Stage 2 were performed. From there, we needed to remove three sessions on electrode AF7 and one session on electrode AF8 due to an accumulation of values that were far above from the mean. A correlation coefficient was observed between the temporary standard deviation of the  $B_{\beta-H}$  band with the TOVA RT of  $-0.8824$  for the AF7 electrode and  $-0.8071$  para the AF8 electrode, as shown in Fig. 5a.

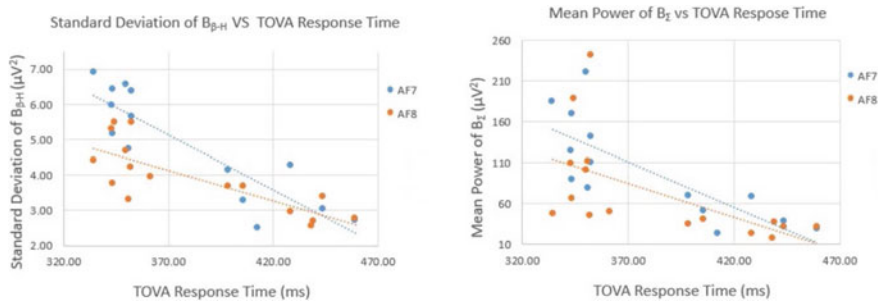


**Fig. 5** **a** Correlation between  $B_{\beta-H}$  and TOVA response time. **b** Correlation between  $B_{\Sigma}$  and TOVA response time

A correlation coefficient between the temporary mean power of the band  $B_{\Sigma}$  and the TOVA RT of  $-0.7817$  for electrode AF7 and  $-0.5154$  for electrode AF8 is also observed in Fig. 5b.

The x-axis shows the TOVA response time in which a higher value corresponds to the slower response toward a stimulus, indicating a lower attention state [12]. The y-axis shows the value of the characteristics extracted from the band obtained in the TOVA tests performed, being the temporary standard deviation in Fig. 5a and the temporary mean power in Fig. 5b. It was found that tests performed in Stage 1, with optimal conditions, tend to have an EEG response of high mean power and standard deviation, and tests performed in Stage 2, with the distracting stimulus, tend to have lower mean power and lower standard deviation.

## 4 Discussion

The existence of a relationship is between the behavior of the physiological activity of the brain and the TOVA results as evidenced by the good correlation between the average response time of the TOVA and the standard deviation of the band  $B_{\beta-H}$ , and this relationship shows that greater response times are manifesting, in inverse proportion, into greater standard deviation of the power in the band  $B_{\beta-H}$ . However, it is important to continue taking data to reinforce this correlation and find other parameters that could also meet this relationship.

For the continuation of this investigation, an analysis will be carried out in smaller window times in the EEG signal to observe in more detail the behavior of the signals throughout the test and, in this way, determine the existence of a greater correlation between the EEG signals and other TOVA parameters.

Furthermore, the AF8 electrode signal shows more reliability in seeking the correspondence between the parameters specified above. This asymmetrical performance between AF7 and AF8 electrodes may be due to not so accurate EEG positioning or degraded electrode. Due to this behavior, AF7 electrode presented samples that were

far above from the mean in three sessions, so they were removed from the analysis: two correspond to a stage 1 session and one to a stage 2 session.

This research allowed us to identify the brain activity band where sustained attention manifests in relation to standardized TOVA test. In the same way, we can build now a characteristic vector in order to feed a neural network for classifying the attention state. The final goal of this research is to develop a neurofeedback therapy device of the attention state.

It is important to indicate that the framework used in this study corresponds to the unique case approach because we attempted to determine a correlated behavior between two parameters. Thus, ethical approval for the experiment in this study was deemed unnecessary by the university, since the research was designed to develop a computational framework. For this, all the data presented were acquired from the first author of this research and did not involve human participation. Additionally, for this study, we use a commercial EEG non-invasive sensor with dry surface electrodes that do not represent any health risk. The activities undertaken in this research do not pose risks greater than those ordinarily encountered in daily life, as well as affecting the preservation of the anonymity.

The goal of these recordings was a concept and preliminary study for later applications, where tests with several persons will be regulated by the respective ethical committee.

## 5 Conclusions

The research carried out shows that sustained attention is manifested in the temporary standard deviation of the  $B_{\beta-H}$  band. This relationship has a behavior inversely proportional to the response time of the TOVA. A lower level of sustained attention corresponds to a longer average response time to the objective stimulation of the TOVA test.

With the results obtained, a behavior of brain activity has been identified during the state of sustained attention, so a K-means classifier will be implemented to develop a neurofeedback therapy that will be used as a tool in psychology studies.

## References

1. Fuster, M.: Human Neuropsychology. The Prefrontal Cortex, pp. 183–235 (2015)
2. Robert, L., Tammy, D., Lawrence, G., Carol, K., Steve, H.: TOVA Variables and Scoring, pp. 4–7. T.O.V.A. Professional Manual (2018)
3. Müller, Matthias, M., Thomas, G, Andreas, K.: Modulation of induced gamma band activity in the human EEG by attention and visual information processing. *Int. J. Psychophysiol.* **38**(3), 283–299 (2000)

4. Sauseng, P., Klimesch, W., Stadler, W., Schabus, M., Doppelmayr, M., Hanslmayr, S., Gruber, W.R., Birbaumer, N.: A shift of visual spatial attention is selectively associated with human EEG alpha activity. *Eur. J. Neurosci.* **22**(11), 2917–2926 (2005)
5. Trans Cranial Technologies. 10/20 System Positioning Manual (2012)
6. Mike, S., Mary Ann, W., Daniel, D.: Epilepsy and Seizures. *The Little Black Book of Neuropsychology: A Syndrome-Based Approach*. Chapter 16, p. 429 (2011)
7. Luc, L.: Nyquist sampling theorem: understanding the illusion of a spinning wheel captured with a video camera, pp. 49(6). Physics Department, Royal Military College of Canada, Physics Education,, 697. (2014)
8. Robert, L., Tammy, D., Lawrence, G., Carol, K., Steve, H.: The T.O.V.A. Test, pp. 2–4. T.O.V.A. Professional Manual (2018)
9. Kemper, G., Ponce, D., Telles, J., Carpio, C.: An algorithm to obtain boat engine RPM from passive sonar signals based on DEMON processing and wavelets packets transform. *J. Electr. Eng. Technol* (2019)
10. Krishnaveni, V., Jayaraman, S., Aravind, S., Hariharasudhan, V., Ramadoss, K.: Automatic identification and removal ocular artifacts from EEG using wavelet transform. *Measur. Sci. Rev.* **6**, Section 2, Nr. 4 (2006)
11. Hanan, A., Faris, J.: Optimal mother wavelet function for EEG signal analyze based on packet wavelet transform. *Int. J. Sci. Eng. Res.* **8**(2) (2017)
12. Robert, L., Tammy, D., Lawrence, G., Carol, K., Steve, H.: TOVA Variables and Scoring. T.O.V.A. Professional Manual, pp. 4–5 (2018)

# Mobile Robot to Assist in Therapies for Children with Autism



Madai Keila Taype Mateo  and Grimaldo Wilfredo Quispe Santivañez 

**Abstract** The increase in the autistic population and rapid technological advances have led to further research on robot-assisted rehabilitation for autism therapy as a practical system aimed at overcoming the distance between autistic patients and their therapists. In this investigation, an interactive mobile robot was developed whose main objective is to perform therapy for children with autism spectrum disorder (ASD) that meets certain qualities that will be chosen by the therapist, so that the robot will be able to give treatment in different approaches of language, speech, and coordination. This mobile robot offers the ease of being manipulated by a geomagnetic router (GRG) glove, RFID cards that allow the display of different expressions (emotions), and SD cards that can save voice recordings or songs according to the therapist.

**Keywords** Autism · Interactive mobile robot · GRG · RFID

## 1 Introduction

Currently, interactive mobile robots are still alien to the Peruvian market because the delay and lack of importance of new implementations for the treatment of children with autism spectrum disorder (ASD) in Peru, specifically in Huancayo, has prevented our country from implementing modern and updated technology in this field. Autism represents a challenge for medicine. It is an early onset of neuropsychological development disorder. It is one of the most serious alterations that affect behavior and communication with stereotyped patterns. Autism spectrum disorder (ASD) is a neurological and developmental condition that begins in childhood and

---

M. K. Taype Mateo

Facultad de Ingeniería, Universidad Continental, Huancayo 15036, Peru  
e-mail: [74895642@continental.edu.pe](mailto:74895642@continental.edu.pe)

G. W. Quispe Santivañez (✉)

Universidad Nacional Autónoma Altoandina de Tarma, Tarma 12651, Peru  
e-mail: [gquispe@unaat.edu.pe](mailto:gquispe@unaat.edu.pe)

© The Editor(s) (if applicable) and The Author(s), under exclusive license to Springer Nature Switzerland AG 2021

Y. Iano et al. (eds.), *Proceedings of the 5th Brazilian Technology Symposium*, Smart Innovation, Systems and Technologies 202, [https://doi.org/10.1007/978-3-030-57566-3\\_12](https://doi.org/10.1007/978-3-030-57566-3_12)

lasts a lifetime. People with ASD present problems that concern difficulties to talk and a scattered vision when communicating with other people [1].

According to [2], the percentage of minors aged 3–11 years with a mental disability, specifically autism, is 0.076% of the current population of Peru. In the Junín region, out of 60 people diagnosed with ASD, 29 are minors aged 3–11 years [3]. This is increasing owing to various circumstances. It is worth noting that within this percentage, the majority of people are of low socioeconomic status, and consequently the various therapies that can be applied are ignored as they can not afford it. Although children with ASD need adequate care and education according to their condition, there has been no progress in projects that provide adequate treatment within the educational field. This research work aims to facilitate progress in the scientific, technological, and educational field with respect to autism therapy in the Junín region, specifically in Huancayo.

Robots can cooperate with humans to perform tasks. The image from science fiction that comes to mind, of humanoid robots or service robots working alongside humans, still invokes a certain sense of surprise and insecurity when performing a joint task. This perception is perhaps influenced by the image of the industrial robot working in manufacturing scenarios. The case of robots for medical applications is especially interesting owing to the aspect of human relations in health issues [4]. Robotics brings together various disciplines such as mechanics, electronics, computer science, artificial intelligence, control engineering, and physics. Other important areas are algebra, programmable automatons, animatronics, and state machines [5]. Medical robots are robots that operate in any of the following scenarios: a surgical environment, rehabilitation scenario, or domestic environment where assistance tasks are performed. The common characteristic that we find in these robots is that apart from collaborating to perform a certain task, these medical robots have a direct physical relationship with human beings, i.e., there is physical contact between the robot and a person. Obviously, this feature conditions the human-machine interface of these robots and makes them different from industrial robots [4].

In recent years, the psychological approach and engineering and robotics advances have been combined to offer an alternative in the treatment of children and adults with ASD, robot-assisted therapy [6]. In this sense, there are therapies given to children with autism from behavioral analysis when they interact with different toys [7]. Also, through therapies driven by mistrust and deception games, children with ASD learned complex social rules from a social robot [8]. The empirical evidence supports the potential use of specific robotic and technological agents for increasing motivation and socially relevant behaviors in some children with ASD [9]. The development of this type of robot-assisted therapies aims at improving basic services to children with ASD from the moment they are diagnosed and throughout their life cycle, with support services for families, allowing parents to live with the affected child as long as possible, without dismantling the family nucleus and thus achieving true integration into society [10].

This work pretends to explore to what extent does the prototype development of an interactive mobile robot for the treatment of children with moderate ASD at the school stage may contribute. The main objective of the research is to design a mobile



robot that will help therapists in their sessions, specifically with speech, language, and music.

## 2 Function

The proposed prototype will fulfill the function of being the therapist's assistant because therapists will make improvements in the therapies for language, speech, and music [11].

Next, the therapies where the robot will assist are explained:

- **Speech:** The therapist is available for therapy with RFID cards because thanks to this the robot can change expressions in six opportunities. With the help of speech, the therapist can interact with the patient when they identify themselves and use expressions.
- **Language:** Here we propose a therapy that is simple for the patient because the robot has an SD card in which words selected by the therapist can be recorded to interact with the patient.
- **Music:** In this therapy, the robot has an SD card, where music selected by the therapist can be recorded.
- **Coordination:** It has a geo-drive control system in the form of geomagnetic router gloves (GRG) that can direct the robot to a specific point.

## 3 Materials and Methods

This project involves systematic creation and development, and the documentation of the design activity can be used to manufacture the product. In terms of existing work, the method standardized by the German association of engineers VDI (Verein Deutscher Ingenieur), VDI2222, was developed [12]. This method can be easily used by designers with or without experience, in addition to seeking optimization in each of its stages, so that the solutions always aim to be the best. Next, a list of research requirements is prepared where the design is analyzed, which will make it easy to interact with the children with the objective of capturing the attention of children with ASD, so that they can learn to socialize through the SD cards (provided in the prototype) in which voice or songs will be transmitted according to the desired treatment. A child will be able to see the changes in the expressions of the robot using the RFID cards.

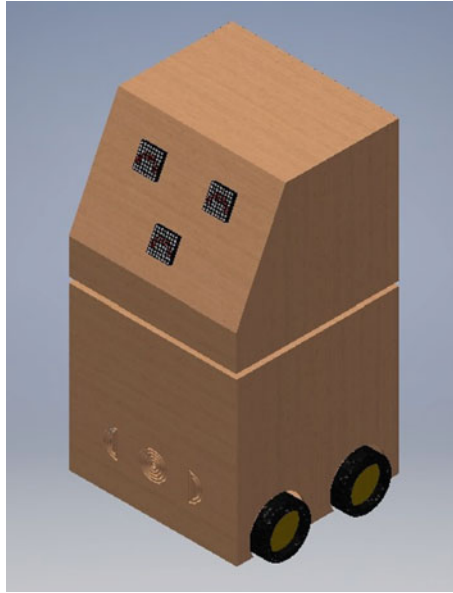


**Fig. 1** Robot assembly–inventor

### ***3.1 Design***

It was achieved by separating the physical from the intangible, it was developed through steps, through which the designs of both software and hardware were obtained to finally assemble them together. The development was carried out using Inventor [13] and Proteus software [14] (Figs. 1, 2, and 3).

### ***3.2 Materials***

The materials used in this work were Arduino mega, accelerometer, L293D Driver, Bluetooth, RFID card reader, SD card reader, speakers,  $8 \times 8$  matrixes, and MDF frame.

### ***3.3 Software Development***

It was based on being able to control the robot by two methods: by an application created for an application, by an accelerometer as well as the RFID cards or by algorithms with the programming of microcontrollers.

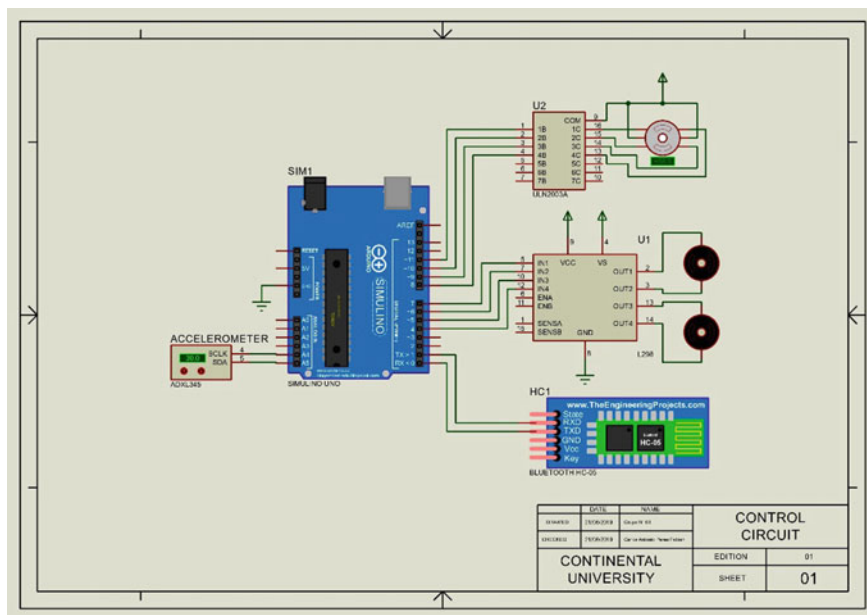
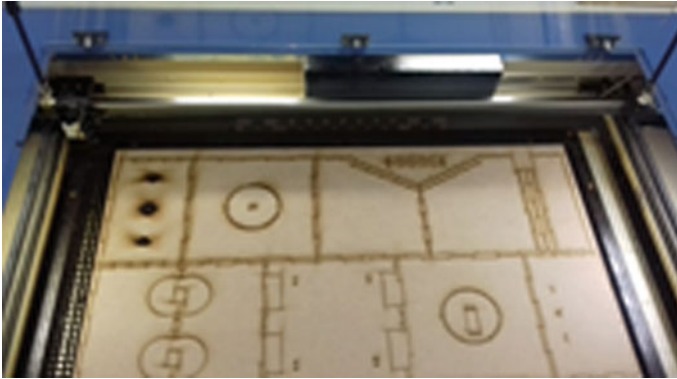


Fig. 2 A complete circuit in proteus



Fig. 3 Geomagnetic router glove (GRG)



**Fig. 4** Laser cutting of the robot design

### ***3.4 Hardware Development***

Hardware was manufactured using easily accessible materials and efficient manipulation. The operation was executed with the AutoCAD program and laser cutting (Fig. 4).

### ***3.5 Flowchart***

This part explains the robot process and its working (Fig. 5).

## **4 Results**

From the fabrication and testing process, an interactive mobile robot with two degrees of freedom was obtained with dimensions of 23 cm  $\times$  23 cm and a height of 48 cm. The total weight of the robot was 2 kg, and the rotation range of the head was from 9° to 180°. The human-machine interface was developed using open-source software and hardware technology that allows cost reduction in the manufacturing of therapeutic robots without degrading their quality. In this case, the software system was built in Arduino. The hardware was implemented with technological components that were compatible with everything that was used. The performance of the interactive robot was evaluated at each stage of the child's cognitive development. The obtained data show that the signals coming from the controller and the commands given by the Arduino do not have communication delay because they are working at the speed of milliseconds. To improve the robot-patient interaction, audio (voice) and music player were incorporated into the robot to listen to and observe the patient's reactions

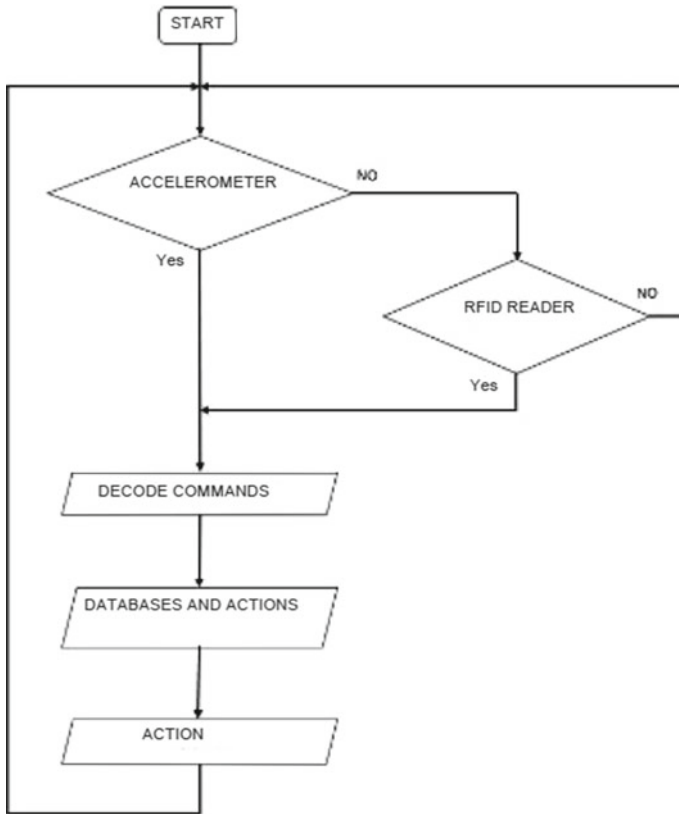


Fig. 5 Flowchart of robot operation

in real-time. It also had an accelerometer installed, which was part of the robot and was placed in the hand of the patient or therapist to observe the robot movement and the obtained interaction. In addition, there was an option of the specialist starting a conversation with the patient to evaluate the degree of attention and understanding that the patient had through the robot. In conclusion, this development has allowed the generation of knowledge about therapeutic social robotics. It has facilitated a new field of application of interactive robots. In this way, the research in this area can take advantage of it and served to implement new ideas in future projects where may be implemented.

## 5 Development Cost

It is known that the robot mentioned as the background is in charge of examining children with and without ASD who learned to socialize with a social robot through

games of mistrust and deception. The cost of this robot for academic use is EUR 5.79,000; within Peru, the cost is PEN 21.83,971. Therefore, it is very expensive, especially in Huancayo. Thus, the robot proposed in this research, which works as a therapist assistant with the objective of treating children with ASD, offers ease of acquisition, as its components are very easy to find in the Peruvian market. Moreover, its maintenance can easily be understood by users, and its cost for academic use in Peru is PEN 2000 (Tables 1, 2, and 3).

**Table 1** Cost of materials

Item	Description	Quantity	Unit	Unit cost	Total cost
1	Accelerometer	1	PEN	15.00	15.00
2	Driver module	1	PEN	20.00	20.00
3	Arduino mega	1	PEN	60.00	60.00
4	Lithium battery	8	PEN	5.00	40.00
5	RFID card	6	PEN	5.00	30.00
6	Servomotor	1	PEN	25.00	25.00
7	RFID reader	1	PEN	15.00	15.00
8	SD card	1	PEN	4.00	4.00
9	Matrix 8 * 8	3	PEN	16.00	48.00
10	Gearmotor	4	PEN	6.00	24.00
			<b>Subtotal</b>	PEN	281.00

**Table 2** Mechanical part cost

Item	Description	Quantity	Unit	Unit cost	Total cost
1	Chassis	1	Und	30	30
2	Bolts	50	Und	15	15
3	Nuts	50	Und	15	15
4	Brackets	4	Und	5	20
			<b>Subtotal</b>	PEN	80.00

**Table 3** Total cost

Item	Description	Quantity	Unit	Subtotal
1	Purchase of electronic part materials	1	Todo	281
2	Purchase of mechanical part materials	1	Todo	80
3	Services	1	Todo	700
		<b>Total</b>	PEN	1061.00

## 6 Conclusion

In this study, we demonstrate the feasibility of manufacturing a mobile robot that makes facial changes, music, and simple and interactive movement. Contributing mainly to therapies as an assistant in the process of improvement in the patient. It exhibits movements that can attract the attention of children being able to move easily and without irregularities. The movement of the head gives realism to its expressions with the design and construction of the interactive mobile robot for the treatment of children with ASD were performed with two degrees of freedom where you can easily interact with the user through the glove where you place the accelerometer, and you can observe the movement of the robot, it is also able to interact with the user by the voice recorded on the SD card, responding with sounds and gestures images by the RFID card. Therefore, the interactive mobile robot is suitable for such treatments.

As future work, we will improve the design of the mechanism to enlarge the arms of the prototype and, also accompany and measure qualitatively the improvements in therapy.

## References

1. Medlineplus.gov.: Trastorno del espectro autista: MedlinePlus en español. Available at <https://medlineplus.gov/spanish/autismspectrumdisorder.html>. Accessed 12 Feb 2020 (2020)
2. Zhang, Y., et al.: ¿Could social robots facilitate children with autism spectrum disorders in learning distrust and deception? 2019. China: s.n. 7, S0747-5632-(19)30148-7 (2019)
3. Discapacidad, Observatorio Nacional de: Conadis. <https://www.conadisperu.gob.pe/observatorio/estadisticas/inscripciones-en-el-registro-nacional-de-la-persona-con-discapacidad-julio-2019/>. Accessed 2 July 2019 (2019)
4. Opensurg, Consorcio. Robotica Medica. Elche: Cytel. 978-84-15413-12-7 (2013)
5. Sánchez Martín, F.M., Milán Rodríguez, F., Salvador Bayarri, J., Palou Redota J., Rodríguez Escovar, F.: Esquena Fernández S, Villavicencio Mavrich H. Historia de la Robótica: de Arquitas de Tarento al Robot Da Vinci (Parte I). *Actas Urol Esp.* **31**(2), 69–76 (2007)
6. Pennisi, P., et al.: Autism and social robotics: a systematic review. *Autism Res.* **9**(2), 165–183 (2015). <https://doi.org/10.1002/aur.1527>
7. Yaser, A.A., et al.: Robotic Trains as an Educational and Therapeutic Tool for Autism Spectrum Disorder Intervention. W. Lepuschitz, Italy (2019)
8. Provenzi L.: Interaction with social robots: Improving gaze toward face but not necessarily joint attention in children with autism spectrum disorder. IRCCS Eugenio Medea, Italia. <https://doi.org/10.3389/fpsyg.2019.01503>
9. Kumazaki, H., et al.: Brief Report: Evaluating the Utility of Varied Technological Agents to Elicit Social Attention from Children with Autism Spectrum Disorders, p. 2018. Springer, Japan (2018)
10. Anys, 40: Autismo. Autismo. <https://www.autismo.com.es/autismo/tratamientos-del-autismo.html>. Accessed 20 May 2019 (1976–2019)
11. Asociación Americana del Habla, L. y. Autismo Diario. Retrieved from <https://autismodiario.org/2017/04/17/desarrollo-la-comunicacion-autismo-traves-la-musica-juego/>. Accessed 17 Apr 2019
12. VDI: A systematic approach to the design of technical systems and products. Guideline 2222 (1986)

13. Autodesk: Inventor 2019 [Software]. Retrieved from <https://latinoamerica.autodesk.com/products/inventor/overview> (2019)
14. LabCenter. (s.f.): Proteus 8.7 [Software]. Retrieved from <https://www.labcenter.com/>



# A Smart Home Control Prototype Using a P300-Based Brain–Computer Interface for Post-stroke Patients



Sergio A. Cortez , Christian Flores , and Javier Andreu-Perez 

**Abstract** In this paper, we present and compare the accuracy of two types of classifiers to be used in a Brain–Computer Interface (BCI) based on the P300 waveforms of three post-stroke patients and six healthy subjects. Multilayer Perceptrons (MLPs) and Support Vector Machines (SVMs) were used for single-trial P300 discrimination in EEG signals recorded from 16 electrodes. The performance of each classifier was obtained using a five-fold cross-validation technique. The classification results reported a maximum accuracy of 91.79% and 89.68% for healthy and disabled subjects, respectively. This approach was compared with our previous work also focused on the P300 waveform classification.

**Keywords** P300 · Multilayered perceptron · Support vector machines · Stroke patients

## 1 Introduction

A Brain–Computer Interface (BCI) is a system that records, analyzes, and classifies brain signals to control an external device or a computer. Also, it allows healthy subjects or patients to communicate through brain activity [1]. The electroencephalographic signals (EEG) are a suitable and common way to register and analyze brain signals while a subject develops different sorts of mental activities. Some of these, such as resting states and cognitive tasks, are specially studied for

---

S. A. Cortez (✉) · C. Flores

Department of Electrical and Computer Engineering, Universidad de Ingeniería y Tecnología,  
Lima, Peru

e-mail: [sergio.cortez@utec.edu.pe](mailto:sergio.cortez@utec.edu.pe)

C. Flores

e-mail: [cflores@utec.edu.pe](mailto:cflores@utec.edu.pe)

J. Andreu-Perez

Department of Computer Science and Electronic Engineering, University of Essex, Colchester,  
UK

e-mail: [javier.andreu@essex.ac.uk](mailto:javier.andreu@essex.ac.uk)

© The Editor(s) (if applicable) and The Author(s), under exclusive license

131

to Springer Nature Switzerland AG 2021

Y. Iano et al. (eds.), *Proceedings of the 5th Brazilian Technology Symposium*,

Smart Innovation, Systems and Technologies 202,

[https://doi.org/10.1007/978-3-030-57566-3\\_13](https://doi.org/10.1007/978-3-030-57566-3_13)

BCI design purposes. Different paradigms such as motor imagery (MI), oddball, and steady-state visual evoked potential (SSVEP) [2], elicit specific potentials that are then used to build BCI systems. Speller is one application of a BCI based on the P300 waveform which is commonly used as an alternative communication way, especially for disabled people. This application uses the oddball paradigm which consists of showing infrequent stimulus (targets) blended with irrelevant stimuli sequences (non-targets). For each target, 300 ms after, the P300 waveform is elicited and can be identified in the EEG [3]. This paradigm requires less training periods than others [4], thereby making it a successful tool for BCI design [5].

In [5], a system for the detection of visual P300 in healthy and disabled subjects was developed. Bayesian Linear Discriminant Analysis (BLDA) was tested for the classification of visual P300. The best classification accuracy was on average 94.97%, and the maximum bit rate reached for the disabled subjects was 25 bits per minute. EEG data in [6] was classified using a Backpropagation Neural Network (BPNN). The authors achieved a score classification of 96.3% and 96.8% for disabled and healthy subjects. The best bit rate was 21.4 and 35.9 bits per minute for disabled and healthy subjects, respectively. A support vector machine (SVM) algorithm and one modification of the speller ( $6 \times 6$  to  $4 \times 10$ ) were proposed in [7] to classify the P300 visual evoked potential. The data from six healthy subjects were analyzed, and the results reported an average accuracy of 75%. In [8], it was developed a P300 BCI system based on ordinal pattern features and Bayesian Linear Discriminant Analysis (BLDA). Their best bit rate was 16.715 bits per minute for disabled subjects and 26.595 bits per minute for healthy subjects. A stepwise linear discriminant analysis (SWLDA) was proposed in [9] to classify P300 waves from a  $6 \times 6$  speller. The results from eight healthy subjects reported an average accuracy of 92%. In [10], a Hidden Markov Model (HMM) was used to classify EEG data of a  $6 \times 6$  speller reaching a classification result of 85% offline and 92.3% online.

About Smart Homes using BCI, in [11], the authors proposed a random forest classifier for P300 classify from three subjects. The best classification accuracy for the subjects was on average 87.5%. A  $6 \times 6$  character speller and icon speller were compared and their performance analyzed in [12] for nine subjects. The authors achieved a score classification of 80% for character speller and 50% for icon speller. A Stepwise Linear Discriminant Analysis (SWLDA) was used to classify EEG data from one subject with Amyotrophic Lateral Sclerosis (ALS) using a  $6 \times 6$  row-column speller to control television in [13]. The classification accuracy was 83%. Regarding Virtual Reality Environments (VRE), [14] proposed to control a smart home application using different speller masks (i.e., music, tv channels, etc.) testing with twelve subjects. Average classification accuracy of 75% was reported.

This work presents a P300-based BCI for post-stroke people and healthy people. The output of this BCI can be used to control home appliances. The aim of this work is to discriminate the presence of the P300 waveform in EEG from 16 channels using Multilayer Perceptron (MLP) and Support Vector Machine (SVM) classifiers. Results outperformed our previous work [15]. This work is presented as follows: In Sect. 2 is presented the experimental procedure including participants, experimental setup, and EEG acquisition. The methods are presented in Sect. 3 which describes preprocessing, feature vectors, and classifiers. The results and discussion are presented in Sect. 4. Finally, we present the conclusions and future work in Sect. 5.

**Table 1** Subjects information

Subject	Age	Gender	Diagnosis
S01	33	Male	Healthy
S02	21	Male	Healthy
S03	20	Male	Healthy
S04	21	Male	Healthy
S05	24	Male	Healthy
S06	29	Male	Healthy
S07	20	Male	Hemorrhagic post-stroke
S08	52	Female	Ischemic post-stroke
S09	55	Male	Ischemic post-stroke

## 2 Experimental Procedure

### 2.1 Participants

The volunteers are grouped by healthy and disabled subjects, aged between 20 and 55. Table 1 shows the age, gender, and medical diagnosis of each volunteer. The six healthy participants (S01 to S06) acted as the control group for the three post-stroke patients (S07 to S09). Subject S08 exhibited limited spoken communication and was able to perform restricted movements of his legs. Subject S07 exhibited reduced spoken communication skills and was able to perform movements with his extremities. Finally, subject S09 was able to perform restricted movements with his hands and arms. The Ethics Committee from the Universidad Peruana Cayetano Heredia issued the ethical approval for the experiment and informed written consent. All participants that opted to participate were also informed about the academic objective of the research, as well as ensured preservation of their anonymity.

### 2.2 Experimental Setup

Six images that are placed in two rows and three columns, above a white background as shown in Fig. 1, were displayed on the screen of a computer. Each image represents an option that provides the subject the capability to interact with another individual or with its surroundings without speaking or moving his arms [5].

The protocol of the experiment, based on Hoffmann's [5], is displayed in Fig. 2. As can be seen, one image (out of six) is flashed in a random sequence during the first 100 ms, and during the next 300 ms, as shown in Fig. 2, a white background is displayed. This process is repeated until the completion of the six images sequence. The group of six images randomly flashed is called one block, and one run represents



**Fig. 1** Display of six images on a computer screen

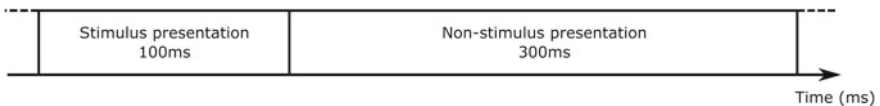


**Fig. 2** Stimuli timing diagram used in each experiment

the interval between 20 and 25 blocks, which are also chosen randomly in each experiment. The database contains four recording sessions per subject, and each session includes six runs. All subjects who participate in this experiment were forbidden to talk and were told to count how many times the image they were told to pay attention to appear on the screen. Each session was separated by one break of 10 min, and two sessions were performed per day.

### **2.3 EEG Acquisition**

The EEG signals were recorded using an electroencephalograph of the brand g.tec. Sixteen bipolar electrodes (Fz, FC1, FC2, C3, Cz, C4, CP1, CP2, P7, P3, Pz, P4, P8, O1, O2, and Oz) were placed in accordance with the international 10/20 system in order to record the brain signals. The ground and reference electrode were placed at the right mastoid and at the left earlobe, respectively. Also, the EEG signals were sampled at 2400 Hz. Figure 3 displays the experiment setup. Furthermore, the C++ programming language and MATLAB R2016a were used to analyze the EEG data.



**Fig. 3** Subject in P300 speller experiments

### 3 Methods

#### 3.1 Preprocessing

A six-order bandpass Butterworth filter with cut-off frequencies 1 and 15 Hz was used to filter the EEG data after it was downsampled from 2400 to 120 Hz. For each electrode, all data samples between 0 and 1000 ms posterior to the beginning of the stimulus were extracted obtaining 120 samples per trial. Artifacts were eliminated by winsorization: each channel signal under the 10th percentile and above 90th percentile was replaced by the 10th percentile or the 90th percentile, respectively [5]. Finally, the data was standardized.

#### 3.2 P300 Classification

**Feature Vectors and Training Matrices** The feature vector construction begins rearranging the data from a single trial. Specifically, the samples of each channel are concatenated with the others in the following way:

$$V = [S_1^1 S_1^2 S_1^3 \dots S_1^{16} S_2^1 S_2^2 \dots S_{120}^{16}]$$

where for a single sample  $S_i^k$ ,  $i$  indicates the channel to which it belongs and  $k$  its position with respect of time. The vectors obtained from all the trials present in the four sessions of a subject are stacked shaping the training and testing matrices. Each

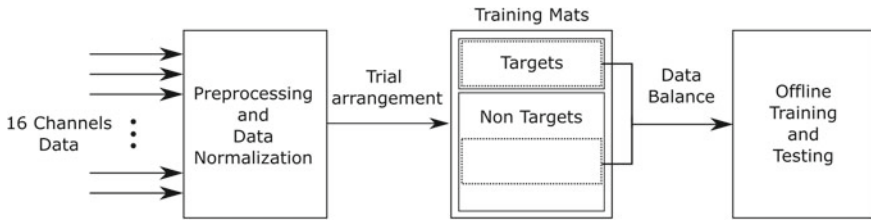


**Fig. 4** EEG signal processing block diagram

trial, and therefore each  $V$ , has a label associated which points out the presence of a P300 waveform in it. When that is the case, the trial is considered as target and when not, non-target.

Since there is an uneven amount of trials target and non-target, due to the experimental procedure for EEG recording, a balanced process is required before training to avoid biasing in classification. The same number of target trials is chosen randomly from a non-target trial pool, resulting in an even-class matrix. Two types of classifiers will use these matrices for their training process: Multilayered Perceptron and Support Vector Machine. The whole process is illustrated in Fig. 4.

**Multilayered Perceptron Architecture** Authors, like [16], had used neural networks to discriminate the presence of ERPs in EEG signals. Multilayer Perceptrons (MLPs) are neural nets that can be described as function approximators [17]. Multiple parameters, like weights and biases, are adjusted in the training stage trying to match known outputs (target or non-target) with specific inputs (trials data). This process results in a model able to predict the class or label of future new inputs with similar characteristics.

The number of inputs, hidden layers, outputs, and total neurons defines MLP architecture. Modifying these can completely change its behavior and could also affect its capacity to find patterns and learn from them [18]. The architecture proposed here for P300 discrimination consists of a net with four hidden layers of 60, 40, 30, and 20 neurons on each, respectively. Each neuron has a hyperbolic tangent sigmoid as its activation function, except for the output one, which is a logistic sigmoid.

**Support Vector Machine** It is a machine learning algorithm for binary classification. The idea behind its classification criteria is the construction of a decision hyper-plane in a high dimensional feature space where input vectors are mapped [19]. This decision boundary can be linear or nonlinear depending on the kernel employed, and it has a direct impact on the model generalization or learning capability. An SVM with a Gaussian or radial basis function (RBF) kernel is trained for P300 discrimination in EEG signals.

**Classifiers Training and Validation** The classification accuracy of each classifier is obtained after fivefold cross-validation. For the MLPs, the inputs were renormalized from  $-1$  to  $1$  before these enter the net. In each subject training stage, the number of epochs used was defined trying to achieve the net full convergence. All subjects

required only 150 epochs except for subjects S03, S04, and S07, which required 300, 2000 and 2500 epochs, respectively. The algorithm used in the MLPs training process was the scaled conjugate gradient backpropagation. The training stage for each MLP took approximately three minutes using an Nvidia GTX 1050 Graphics Processing Unit (GPU) for the calculations; and for the SVM classifiers, it took less than one minute in an Intel Core i7 CPU.

## 4 Results and Discussions

In this section, we compare the performance of the classifiers for all the subjects. Table 2 presents the classification accuracy of the two classifiers in the training and testing stage. It also highlights which of the two classifiers obtained higher results in testing for a single subject. Overall, the performance of each healthy subject was similar and above 80% with the exception of S04. Clearly, the MLP model achieved a higher precision in classification over the SVM one. Nonetheless, both classifiers can be used for the design of a P300 based BCI.

The performance of patients S08 and S09 was similar and even better than most healthy subjects. The P300 waveform in subjects S01 and S08 was apparently easily recognized by the MLP yielding the highest accuracies in classification. However, patient S07 performance was the lowest in comparison with the rest. A possible explanation for this is the patient critical condition (hemorrhagic stroke). Our results show that patients who had suffered ischemic strokes are able to use a BCI based on the P300 paradigm as their average classification accuracy is greater than 80%. In comparison with our previous work [15], both classifiers presented here outperformed the Adaptive Neuro-Fuzzy Inference Systems (ANFIS) ensemble for the healthy subjects (S01, S02, S03, and S06) and post-stroke patients (S08 and S09).

**Table 2** Cross-validated classifiers accuracy

Subject	MLP		RBF SVM	
	Training (%)	Testing (%)	Training (%)	Testing (%)
S01	100	<b>91.79</b>	99.06	91.51
S02	100	<b>80.28</b>	97.27	79.07
S03	100	<b>85.32</b>	97.05	83.90
S04	100	75.70	95.18	<b>78.89</b>
S05	100	<b>84.94</b>	97.60	83.40
S06	100	<b>83.00</b>	97.56	81.65
S07	100	68.73	92.82	<b>69.21</b>
S08	100	<b>89.68</b>	97.68	85.46
S09	100	86.98	98.16	<b>87.43</b>

Bold indicates the two classifiers obtained a higher classification accuracy for a specific subject

## 5 Conclusions and Future Work

A comparison between the SVM and MLP classifiers for P300 discrimination in EEG signals was presented. Both obtained significant results for the two types of subjects present in this study. Patients who had suffered an ischemic stroke seem to be suitable users of a P300-based BCI since their performances were similar to the healthy ones. However, patients with more critical conditions, like the one who had experienced a hemorrhagic stroke, may require another type of classifier with more learning capabilities or a longer training period.

As future work, we intend to validate these classifiers with more post-stroke patients and include amyotrophic lateral sclerosis (ALS) ones. We will also extend the methodology presented in this work by employing deep learning tools and extreme learning machine algorithms.

**Acknowledgements** This work used the database made in a collaborative project between the Universidad Cayetano Heredia and the Universidad de Ingeniería y Tecnología supported by the Programa Nacional de Innovación para la Competitividad y Productividad of Peru, under the grant PIAP-3-P-483-14.

## References

1. Wang, Y.T., Nakanishi, M., Wang, Y., Wei, C.S., Cheng, C.K., Jung, T.P.: An online brain-computer interface based on SSVEPs measured from non-hairbearing areas. *IEEE Trans. Neural Syst. Rehabil. Eng.* **25**, 14–21 (2017)
2. Lotte, F., Bougrain, L., Cichocki, A., Clerc, M., Congedo, M., Rakotomamonjy, A., Yger, F.: A review of classification algorithms for EEG-based brain–computer interfaces: a 10 year update. *J. Neural Eng.* **15**, 031005 (2018)
3. Farwell, L.A., Donchin, E.: Talking off the top of your head: toward a mental prosthesis utilizing event-related brain potentials. *Electroencephalogr. Clin. Neurophys.* (1988)
4. Han-Jeong Hwang, S.C., Kim, S., Im, C.-H.: EEG-based brain–computer interfaces: a thorough literature survey. *J. Human–Comput. Interact.* **29**, 814–826 (2013)
5. Hoffmann, U., Vesin, J.-M., Ebrahimi, T., Diserens, K.: An efficient P300-based brain–computer interface for disabled subjects. *J. Neurosci. Methods* **167**(1), 115–125 (2008)
6. Turnip, A., Soetraprawata, D.: The performance of EEG-P300 classification using backpropagation neural networks. *Mechatron. Electr. Power, Veh. Technol.* **4**(2), 81–88 (2013)
7. He, S., Huang, Q., Li, Y.: Toward improved p 300 speller performance in outdoor environment using polarizer. In: 2016 12th World Congress on Intelligent Control and Automation (WCICA), pp. 3172–3175, June 2016
8. Alhaddad, M.J., Kamel, M.I., Bakheet, D.M.: P300-brain computer interface based on ordinal analysis of time series. In: 2014 International Conference on Computational Science and Computational Intelligence (2014)
9. Krusienski, D.J., Sellers, E.W., Cabestaing, F., Bayouth, S., McFarland, D.J., Vaughan, T.M., Wolpaw, J.R.: A comparison of classification techniques for the p300 speller. *J. Neural Eng.* **3**(4), 299 (2006)
10. Speier, W., Arnold, C., Lu, J., Deshpande, A., Pouratian, N.: Integrating language information with a hidden markov model to improve communication rate in the p300 speller. *IEEE Trans. Neural Syst. Rehabil. Eng.* **22**, 678–684 (2014)



11. Masud, U., Baig, M.I., Akram, F., Kim, T.: A p 300 brain computer interface based intelligent home control system using a random forest classifier. In: 2017 IEEE Symposium Series on Computational Intelligence (SSCI), pp. 1–5, Nov 2017
12. Carabalona, R., Grossi, F., Tessadri, A., Castiglioni, P., Caracciolo, A., de Munari, I.: Light on! real world evaluation of a p300-based brain–computer interface (BCI) for environment control in a smart home. *Ergonomics* **55**(5), 552–563 (2012)
13. Sellers, E.W., Vaughan, T.M., Wolpaw, J.R.: A brain-computer interface for long-term independent home use. *Amyotrophic Lateral Sclerosis* **11**(5), 449–455 (2010)
14. Holzner, C., Guger, C., Edlinger, G., Gronegess, C., Slater, M.: Virtual smart home controlled by thoughts. In: 2009 18th IEEE International Workshops on Enabling Technologies: Infrastructures for Collaborative Enterprises, pp. 236–239, June 2009
15. Achancaray, D., Flores, C., Fonseca, C., Andreu-Perez, J.: A p 300-based brain computer interface for smart home interaction through an ANFIS ensemble. In: 2017 IEEE International Conference on Fuzzy Systems (FUZZ-IEEE), pp. 1–5, July 2017
16. Gupta, L., Molfese, D.L., Tamma, R.: An artificial neural-network approach to ERP classification. *Brain Cogn.* **27**(3), 311–330 (1995)
17. Winston, P.H.: *Artificial Intelligence*, 3rd edn. Addison-Wesley Longman Publishing Co., Inc., Boston, MA, USA (1992)
18. Wu, F.Y., Slater, J.D., Honig, L.S., Ramsay, R.E.: A neural network design for event-related potential diagnosis. *Comput. Biol. Med.* **23**(3), 251–264 (1993)
19. Cortes, C., Vapnik, V.: Support-vector networks. *Mach. Learn.* **20**(3), 273–297 (1995)

# Electronic Ecomap as an Instrument to Improve Physician–Family Interaction in Preventive Medicine



Néstor Mamani-Macedo , Julio Raime , Luzmila Pro , Jaime Pariona , and Olga Solano

**Abstract** According to the World Health Organization (WHO), the main causes of mortality in low-income countries are communicable diseases, maternal and perinatal conditions, and nutritional conditions. The issue arises because early detection requires the implementation of a primary healthcare system. As part of the family record, we have the Ecomap, an instrument for recording family relationships with their environment in their day-to-day activities graphically, whether this comprises people or institutions such as the church and health centers. In Peru, the use of Ecomap has traditionally been in a hard-copy format, which has problems updating because it is handwritten. Given this limitation, a computer application “electronic Ecomap” (e-Ecomap) has been developed, a resource with which healthcare personnel can interact in a user-friendly manner. In an aggregate mode, it will be possible to visualize the families of a community as a whole, highlighting the behavior of the institutions surrounding them. In this manner, it will be possible to prevent the effects of these risks in a generation of psychosocial problems that can later lead to psychosomatic illnesses. Finally, the e-Ecomap will be able to infer the connections of the family with its environment in conjunction with the data registered in the family record.

**Keywords** Electronic ecomap · Family record · Preventive medicine

N. Mamani-Macedo (✉) · J. Raime · O. Solano  
Facultad de Ciencias Matemáticas, Universidad Nacional Mayor de San Marcos, Lima 1, Peru  
e-mail: [nmamanim@unmsm.edu.pe](mailto:nmamanim@unmsm.edu.pe)

J. Raime  
e-mail: [julio.raime@unmsm.edu.pe](mailto:julio.raime@unmsm.edu.pe)

O. Solano  
e-mail: [osolanod@unmsm.edu.pe](mailto:osolanod@unmsm.edu.pe)

L. Pro · J. Pariona  
Facultad de Ingeniería de Sistemas e Informática, Universidad Nacional Mayor de San Marcos,  
Lima 1, Peru  
e-mail: [lproc@unmsm.edu.pe](mailto:lproc@unmsm.edu.pe)

J. Pariona  
e-mail: [jparionaq@unmsm.edu.pe](mailto:jparionaq@unmsm.edu.pe)

## 1 Introduction

During the last twenty years, Peru has shown a steady growth of between 4 and 9%, excluding 2009, given the problems faced in the global economy, 2014, and 2017 because of the decrease in the price of minerals and weather effects such as “El Niño” [1, 2]. Nevertheless, according to Miguel Malo, advisor to the Pan American Health Organization, there is still a need in primary healthcare to close gaps in services; for instance, in the area of chronic diseases, improving the resolution capacity of frequent diseases such as hypertension and diabetes is one such concern [3]. According to the WHO [4], the main causes of death in low-income countries are communicable diseases, maternal and perinatal conditions, and nutritional conditions. Chronic and communicable diseases are multicausal, and the company of family and other external entities, such as the church, health centers, neighborhood associations, and public and private social support institutions is of utmost importance in their treatment.

The Ecomap (ecological map) is a graphic representation that shows all the entities that are involved in the life of an individual or family (ecological system), and its results can be observed in a simple manner. Ann Hartman developed the instrument in 1975 [5], and its use soon spread from social workers to nursing and subsequently to human medicine; at present, it is widely used by primary care physicians. In Peru, an Ecomap is a part of the family record [6], used in a hard-copy format. The purpose of the family record is to facilitate a biopsychosocial approach to a family and its members, assessing their health problems within the economic, social, and environmental context in which the family operates. A genogram provides us with a historical image of the family through and between generations, but the Ecomap locates the family in its current social context, providing a visual map of the connections of the family and its members to the external world. These connections can include, for example, the relationship between family members and their neighborhood or with the public entities of social, cultural, sports, educational, and religious support, among others [7]. In this context, our proposal is to develop an electronic ecomap linked to an electronic family record application.

## 2 Theoretical Framework

### 2.1 *Ecomap*

An Ecomap is an instrument that allows the physician and health team to identify the interrelationships of a family with the environmental and socio-cultural context in which it operates quickly, thereby providing information on the extra-family network of resources. Therefore, it constitutes a complement to the family diagram and visual aid for an understanding of the environment in which the life of families takes place. Its routine use allows for representing the family and its contacts with their supra systems, in other words, with the environment that surrounds the family, namely,

extended family, health systems, work, educational institutions, recreation, religious institutions, friends, neighbors, etc. On one hand, from these contacts or relationships, resources can be obtained that the family can use to meet its objectives in an adequate manner. On the other hand, these contacts can become considerable energy drains, thereby making it difficult for the family to achieve their goals. Hartman [5] described the Ecomap as a picture of the family and its situation, highlighting the connections extra-family positive and negative nature, mapping points of conflict to be mediated. The solution implies finding the resources necessary, internal and external, to mitigate them. Ecomap enables the family doctor to accomplish the following [8–11]:

- Identify extra-family social support resources that are absent and/or present and that may be useful in situations of family crises.
- Detect shortcomings that the family is going through with the goal of working to address them.
- Enhance the doctor–patient-family relationship as well as communication.
- Suspect problems both inside and outside the family, which can be corroborated with the application of other instruments.

In Peru, the Ecomap is currently used in a hard-copy format [6], and healthcare personnel in charge of the family visit must draw the existing relationships between the family and its environment. In this process, the risk of making errors in the drawing is present in addition to the possibility of corrections affecting the ease of reading that an Ecomap must have; in the worst-case scenario, a new format should be used. Consequently, there is an increase in the family visit time, thereby increasing the dissatisfaction of families with the family doctor visit. In addition, when using a printed format, the family’s ecomap has to be redrawn at each visit, which may fall back on the aforementioned errors.

## 2.2 *State-of-the-Art*

Ecomap is a tool used in several countries in the field of family medicine and its electronic implementations are:

- (1) **Design templates** on generic online platforms such as Canva,<sup>1</sup> Smartdraw,<sup>2</sup> and Scribblar<sup>3</sup> that allow for the creation of Ecomaps from scratch or for the customization of any of the predesigned templates.

---

<sup>1</sup><https://www.canva.com/graphs/ecomap/>.

<sup>2</sup><https://cloud.smartdraw.com/>.

<sup>3</sup><https://scribblar.com/>.

- (2) **Standalone applications**, which are tools that allow for the creation of Ecomaps and storing the data in a database; these also use or customize predefined templates. They include Genogram Analytics<sup>4</sup> and Ecotivity<sup>TM5</sup> from WonderWare Inc.

### 2.3 Computer Technology

The following technologies were used for the development of our proposal:

- **SVG (Scalable Vector Graphics)**<sup>6</sup> is an XML language used to draw vector graphics. It can be used to create an image either by specifying all the necessary lines and shapes, by modifying existing images or through a combination of both.
- **MVC (model–view–controller)**<sup>7</sup> is a type of software architecture that separates data from the model, the user interface, and the control logic.
- **JAVA**<sup>8</sup> is an object-oriented programming language that allows for code portability because it runs on a virtual machine (Java virtual machine or JVM). There are currently JVMs for all known platforms.
- **MySQL**<sup>9</sup> is a database management system (DBMS) system for managing data tables.

## 3 Developed Solution

### 3.1 Methodology

The prototyping methodology was used for the development of the software, which is also known as the evolutionary development model [11], beginning with the definition of the global objectives for the software, followed by identifying the known requirements and the areas of the schema for which more detail is required. The construction of the prototype ensures better software quality as well as an appealing interface for users.

To develop the electronic ecomap, the format to be used was first proposed, which should be in accordance with the programming language of the family file application; SVG was selected for its versatility. Subsequently, the Ecomap was integrated with the electronic family record to collect information about family members.

---

<sup>4</sup><http://www.genogramanalytics.com/index.html>.

<sup>5</sup><https://www.interpersonaluniverse.net/>.

<sup>6</sup><https://www.w3.org/Graphics/SVG/>.

<sup>7</sup><https://www.codecademy.com/articles/mvc>.

<sup>8</sup><https://go.java/index.html>.

<sup>9</sup><https://www.mysql.com/>.

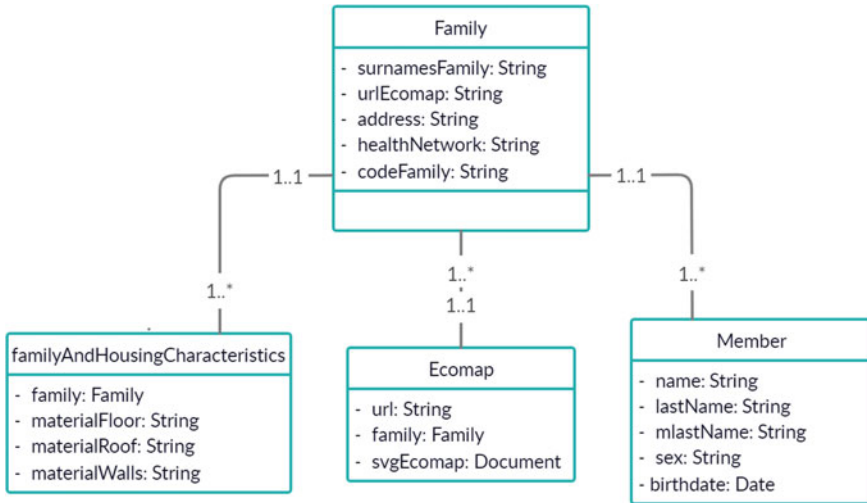
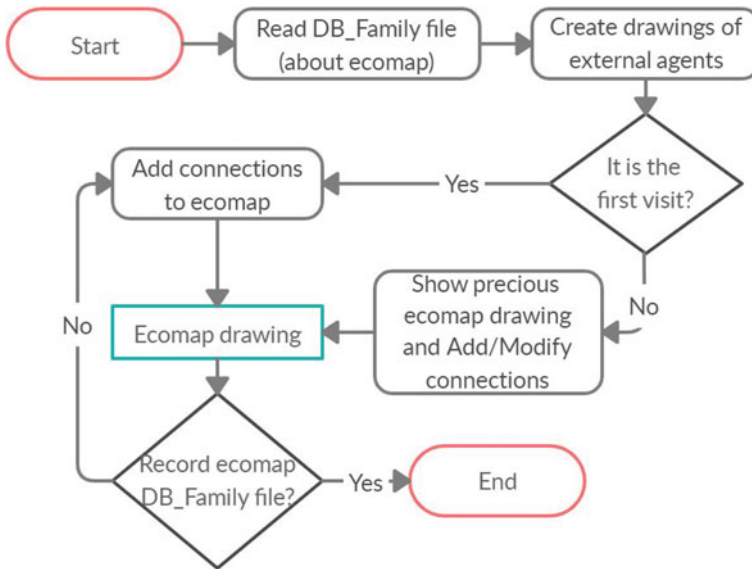


Fig. 1 Main classes that interact with the ecomap

The family record has the family visit as one of its components, with the Ecomap being one of its instruments. Therefore, its implementation could significantly improve the interaction between the family doctor and the family, enhancing confidence with respect to home visits and thus creating a pleasant environment for both of the parties involved.

Figure 1 shows the main system classes that interact with electronic ecomap.

With information captured from the characteristics of the family and home and the member registry, given the risks that each may present, the aim is to infer the connections that the family may maintain with its environment and, by doing so, recommend these connections to the healthcare personnel. To begin with, this information is based on statistics from previous visits or from other families, thereby allowing the system to learn. Figure 2 shows the flow diagram of the process carried out when working with the electronic ecomap. In addition, the developed solution does not require an internet connection, which also facilitates its use in rural or remote areas, such as in the forest or Peruvian highlands, where it is difficult to reach families and help them with respect to the prevention of diseases. The solution developed is in accordance with the needs of the field of preventive medicine and meets the requirements of the Ministry of Health from Perú.



**Fig. 2** Process diagram of the electronic Ecomap

### 3.2 Case Study

To validate our proposal, we use information from the INEI<sup>10</sup> (National Institute of Statistics and Informatics) obtained in the national household survey on living conditions and poverty and choose to analyze the anonymized information of a lower-middle-class family. Family members attend social programs that provide economic assistance. Their relationship with community institutions is stressful; they attend a church where they are required to tithe and shop at their uncles' store, which is close to the neighborhood. The father wants to leave work soon, and the children have missed school four times in the last two months. The family prefers to self-medicate rather than attending a health center. All of the aforementioned generates the following information concerning the connections with their environment:

- Stress with friends and neighbors
- The flow of inputs with social programs
- Stress with community institutions
- The flow of inputs with the church
- The flow of inputs with relatives outside the household
- Weak regarding work
- Weak regarding school
- Weak regarding their interaction with health centers.

Having this information will help build their ecomap as shown in Fig. 3a, with the help of the electronic ecomap.

<sup>10</sup><https://www.inei.gob.pe/>.

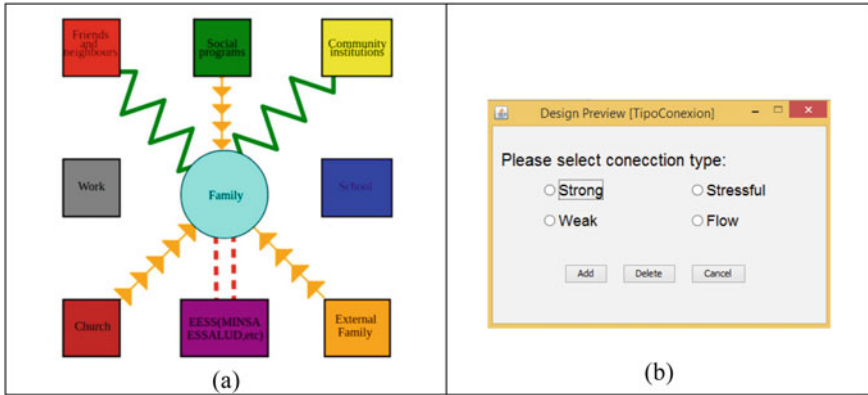


Fig. 3 a Electronic Ecomap and b the menu to select connections

To start creating connections with external agents, one must select the agent with the mouse and click on it; the program will display a dropdown menu of four available options: weak, strong, flow, and stressful as shown in Fig. 3b. By selecting the desired connection(s) and clicking on either “Add” or “Delete,” the Ecomap will update the drawing associated with the selected connection.

## 4 Discussion

The main problem with the family record in the printed format lies in its management, transportation, reading, reliability, and integrity, which are characteristics that must be improved and updated according to state-of-the-art technology. Our research group previously developed the electronic family record and, as an essential part of this, now, we have implemented the electronic ecomap, a virtual version of the ecomap currently used in the hard-copy family record. To safeguard the integrity of the database, using a database that is not visible to anyone but the personnel working on it has been proposed; consequently, readings would only be possible through the electronic family record software.

The electronic family record and the electronic ecomap positively influence the manner in which the family accepts the visit of a family doctor because the visit does not take more time than necessary, which can occur if there are errors in the family record or in the ecomap in the printed format. In addition, the family will be more motivated in the next visit because of the clarification that the main objective of the visit is to help them in preventing diseases and illnesses. There are some other aspects of improvement for the ecomap. One of its main shortcomings is the treatment of the electronic ecomap as an object and not as a mere drawing. Addressing this shortcoming is possible with the use of the object-oriented programming (OOP), through which an ecomap object can be connected with other objects to facilitate



comprehension or help improve the reading of other problems that the family might present. Being able to link the Ecomap with the genogram, for instance, will allow for a greater understanding of the family with respect to external and internal entities that influence the health of the family.

## 5 Conclusion

In the electronic family record, we focus on solving the problems of biopsychosocial problems in the family with its environment. In the electronic ecomap, the positive and negative interactions between the family and all the entities that are involved around it were displayed. In this work, we demonstrate its importance in the area of preventive medicine.

As future work, an electronic signature used by each healthcare staff member will be developed in order to member to verify authenticity, to identify responsible individuals/users for each visiting user, and to determine whether the healthcare personnel signed the electronic ecomap as established. This could help to strengthen the family's trust in the healthcare crew.

## References

1. BCRP: Banco Central de Reserva del Perú. Memoria (2014)
2. BCRP: Banco Central de Reserva del Perú. Memoria (2017)
3. Arroyo, J., Arroyo, J., Velásquez, A., Céspedes, S., Malo, M., Pedroza, J., Saco, A., Zamora, V.: *La Salud Hoy: Problemas y Soluciones*. CENTRUM. PUCP (2015)
4. World Health Organization: The top 10 causes of death. <https://www.who.int/es/news-room/fact-sheets/detail/the-top-10-causes-of-death>. Accessed 30 Nov 2019
5. Hartman, A.: Diagrammatic assessment of family relationships. *Soc. Casework* **59**, 465–476 (1978)
6. Ministerio de Salud del Perú: NTS N°139-MINSA/2018/DGAIN: Norma Técnica de Salud para la Gestión de la Historia Clínica. Resolución Ministerial N° 214-2018/MINSA
7. Jesuit Social Services: Strong Bonds. <http://www.strongbonds.jss.org.au/workers/cultures/ecomaps.pdf>. Last accessed 30 Nov 2019
8. Cox, Ruth P.: *Health-Related Counseling with Families of Diverse Cultures: Family, Health and Cultural Competencies*. Greenwood Press, Westport, CT (2003)
9. Modelo de atención integral de salud basado en familia y comunidad. <https://determinantes.dge.gob.pe/archivos/1880.pdf>
10. El ECOMAPA: medicina familiar, educación continuada para el médico general. <https://encolombia.com/libreria-digital/lmedicina/ecmg/fasciculo-1/ecmg1-recursos2/>
11. Gowtham, V., Manoj, Y., Pooventhiran, G., Praveen, A., Shivaram, R., Kathiresan, A.: Evolutionary models in software engineering. *Int. J. New Technol. Res. (IJNTR)*. **3**(5) (2017). ISSN 2454-4116

# Intelligent Management Model in an IoT Environment Applied for the Healthcare Sector



Jessie Bravo and Roger Alarcón

**Abstract** This work pretends to solve the inadequate management of devices and their integration in an Internet of Things (IoT) environment which limits the performance of the network in a hospital. The objective of the work is to develop an integration plan, based on an intelligent management model of devices in an IoT environment. The model was validated through the digital transformation maturity model and is applied to the cardiology department at the hospital as a part of the integration plan in the healthcare sector.

**Keywords** Internet of Things · Digital transformation maturity model · Healthcare sector

## 1 Introduction

According to the International Telecommunications Union [1], IoT can be defined as a dynamic global infrastructure for the information society with self-configuration capability based on standard communication protocol interconnecting physical and virtual things, which have identities, physical attributes, and virtual personalities; they use smart interfaces and are perfectly integrated inside the information network. It is evident that many problems to overcome exist in the Peruvian Healthcare System. Peruvian Government budget allocates only 2.2% of the Gross Domestic Product (GDP) in healthcare sector; this is much lower only compared to other Latin American countries [2], problems like the scarce infrastructure, which generates a saturation of patients in hospitals and healthcare centers, the poor management of these care centers, which cause an inadequate quality of the service for the patients, the lack

---

J. Bravo (✉) · R. Alarcón  
School of Computer and Informatics Engineering, Pedro Ruiz Gallo Public University,  
Lambayeque, Peru  
e-mail: [jbravo@unprg.edu.pe](mailto:jbravo@unprg.edu.pe)

R. Alarcón  
e-mail: [ralarcong@unprg.edu.pe](mailto:ralarcong@unprg.edu.pe)

of medical staff which doesn't allow a timely patient care, the lack of automation of monitoring and patient control, which creates a lack of immediate action in the face of a patient critical situation.

This work pretends to apply computational intelligence to a device management model in an IoT environment, which allows the improvement of the network performance in the healthcare sector in order to overcome the inefficient management of medical devices and processes.

## 2 State of the Art

Regarding the management of an IoT system, in [3], they clearly indicate that IoT systems and pure network solutions differ one from the other because the latter offer low-level services and support for business administration, and an IoT system is vastly more complex than a communication system.

An IoT proposed architecture model by Kosmatos et al. [4] explains the architecture based on three layers: the RFID's perspective, the smart object's perspective, and the social perspective, but does not consider the response time in real-time and the diversity of technologies of existing connectivity.

In addition, there is a model proposed by the ITU-T [1] consisting of four layers: application, support services, and applications, network, and device with management and security capabilities related to them, approved in 2012. This model does not focus on device management.

The different investigations carried out in this field corroborate these advances. In [5], the IoT benefits the healthcare sector, such as improving availability and accessibility, the ability to personalize content and a cost-effective delivery, being energy consumption one of the critical points, all of this will be achieved through new IoT technologies such as smart portable sensors for health care, body area sensors, advanced generalized health care systems, and big data analysis. In [6] is presented a proposal to improve the Quality of Service (QoS) in terms of throughput of cognitive body area networks by performing a mathematical channel model for off-body communication. In [7], the results of an exhaustive survey of IoT technologies, methods, statistics, and success stories applied to healthcare were presented. Furthermore, [8] carry out an analysis of current solutions in the healthcare sector, proposing a healthcare model where benefits such as a lower labor intensity and a lower operational cost are entailed. In [9] is proposed a generalized monitoring system capable of sending patients' physical signs to remote medical applications in real-time. The system consists of two parts: the data acquisition part and the data transmission part. An IoT implementation in the healthcare sector is proposed by Sokac [10], who designed a Holter monitor that has electrodes and other electronic components integrated into an elastic shirt, and it is able to communicate to a smartphone via Bluetooth, allowing a permanent patient monitoring.

### 3 Proposal

In this paper, an intelligent device management model was developed in an IoT environment, and it was applied to the healthcare sector specifically, taking into account, mainly, computational intelligence, the ITU-T device management architecture, the IoT environment architecture and having the knowledge that achieving network quality of service implies, at least, complying with the following aspects: reliable and consistent connectivity, a device real-time operation, efficient online monitoring, and error detection. For the proposed model elaboration, five dimensions have been taken into account: the device dimension, the network dimension, the manager dimension, the provider dimension, and the user dimension, as shown in Fig. 1.

Furthermore, the security is presented in a transversal way to the model and all of this, from a holistic standpoint, will allow integration into an IoT environment applied to the healthcare sector.

The supplier dimension will allow managing the real-time data generated from several IoT and non-IoT devices, and it will facilitate its access anywhere, at any time.

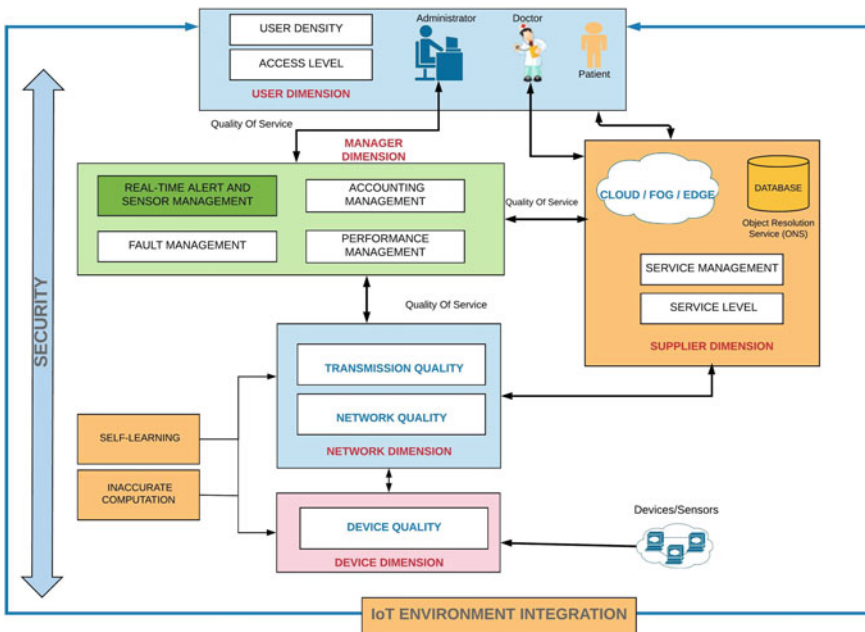


Fig. 1 Smart device management model in the IoT environment

In this dimension, there are three possible ways of storing the information generated by the devices that were considered: Cloud Computing, Fog Computing, and Edge Computing. A Cloud Computing solution is based on data centers with the capacity to process and store large volumes of data, having as a disadvantage that they are generally far away and are slow to respond, and it is also subject to fluctuation that is defined as a variation in the delay of the received packages [11]. Some IoT devices require real-time processing to make decisions and execute immediate actions, also greater mobility and a large number of devices, consequently, in those cases, consider solutions such as Fog Computing and Edge Computing is a necessity [12, 13]. These two architectures can allow the immediate use of the data of the equipment and/or medical sensor, which will deliver better results. For example, glucose values and insulin doses will probably require an immediate response and, therefore, require an automatic analysis and an immediate load in the cloud with Fog Computing or Edge Computing.

As for the device dimension, it is necessary to, first, explain what is understood as a device: physical equipment that can be connected to a network and has some degree of computing and storage capacity. Identification technology will allow the unique identification of the resource.

For this work, a device that interacts directly with users is called a terminal device, such as personal computers, laptops, smartphones, and others. Instead, a device that can help restricted resources to connect to the Internet is called the agent device, such as the wireless sensor networks (WSN) gateway, the RFID reader. The devices that connect directly to the Internet, such as sensors, can also be identified. In this specific case, there are also medical devices, such as tomography, X-ray equipment, ECG, which use the Internet for medical control or self-support. The four types of devices, mainly identified, are:

- Terminal device: a PC, a laptop, a tablet, or a Smartphone.
- Agent device: such as a WSN Gateway, an RFID reader.
- Sensor device: as a temperature, blood pressure, or glucose sensor.
- Medical device: for example, tomography, ECG, X-ray.

The processing capacity is another form of classification, and the devices were classified as basic, regular, high, and the classification is based on their storage memory, the response time, and the energy duration of the device. To achieve the quality of service of the network in this, dimension is necessary to take into account, mainly, the quality of the device: Here, the number of users connected simultaneously to the device must be taken into account, also the device capacity to support a high volume of traffic data and their capacity to work in critical situations.

In the network dimension, the interconnection of the different devices identified in the previous dimension is contemplated, mainly through: Ethernet, WLAN, WSN, RFID, WPAN, WBAN, and WWAN.

In this dimension, in order to achieve an improved quality of service of the network, the following aspects need to be taken into account:

- **Quality of the network:** If the network is capable of supporting applications in real-time if the traffic is prioritized, and the type of data transmitted over the network.
- **Transmission quality:** Aspects such as bandwidth, throughput, latency, jitter, and error rate are measured.

Furthermore, in the device and network dimension, computer intelligence is applied, specifically, machine learning and inaccurate computing that allows the device to make a smart decision and selects how to respond to failure and how to access critical information in real-time that allows an immediate response. The devices must be able to learn from the generated data stored on the Internet in such a way that it will allow immediate access from anywhere. And through inaccurate computing, it will allow prioritizing according to three types of levels: critical, acceptable, and normal and have an adequate response.

The decision trees are the machine learning classification technique that was applied, and the following variables are used in the learning:

- Device type (Medical, Sensor, or Terminal)
- Processing Capacity (Basic, Regular, and High)
- Device priority (Critical, Acceptable, Normal)
- Health condition (Type 0, 1, 2, and 3)
- Network Platform (Ethernet, WLAN, WSN, RFID, WPAN, WBAN, WWAN).

Where the objective is to determine the supplier that best suits each need. The supplier can be Cloud Computing, Fog Computing, and Edge Computing.

In the decision tree, a series of observations are mapped based on the variables mentioned above, and it is determined which would be the best provider, for this the algorithm C5.0 has been used.

As for the user dimension, there are three different roles: patient, doctor, and network administrator. According to the severity of the health condition of the patient, it was classified as:

- Type 0: highest priority requires a real-time monitoring.
- Type 1: requires almost real-time monitoring in every few hours.
- Type 2: requires periodic monitoring, twice a day possibly.
- Type 3: requires monitoring from time to time.

This dimension includes two key aspects to achieve an effective quality of service of the network:

- **The density of users:** The quality of the service will be influenced by the number of users who will use of patient monitoring and follow-up services. The classification is as follows: high-density, medium-density, and low-density.
- **Access level:** There is a necessity to define what rights and privileges those users will have to safeguard the security and privacy of the stored data. The device is important, but the knowledge of who is accessing it, from where the access is coming from, and the time of the access is equally important. Regarding the level of access, the following have been considered: high, medium, and low.

The management dimension is the graphical interface that will allow controlling and monitoring the resources. First, the security management that has been framed as a transversal task immersed in each dimension of the presented model, and second, the alert and sensor management in real-time since this aspect is critical for the medical devices in the context of the proposed model.

The five dimensions defined in a transversal manner include security management, having the need to safeguard the privacy of stored data. To achieve this, aspects of reliability, availability, and integrity in each of the dimensions must be checked. Finally, another considered aspect is, to achieve the integration of existing IoT devices in the healthcare sector to a data network, which will allow improving the service of the hospital that is being studied, mainly in two aspects: real-time patient monitoring and online access to the patient’s clinical information.

### 4 Validation and Discussion

The project was carried out focusing on one of the most relevant departments of the hospital—case study, the cardiology department. The reason is the increase in cardiovascular diseases in the last years. Figure 2 shows the proposed modeling whose validation is further discussed after.

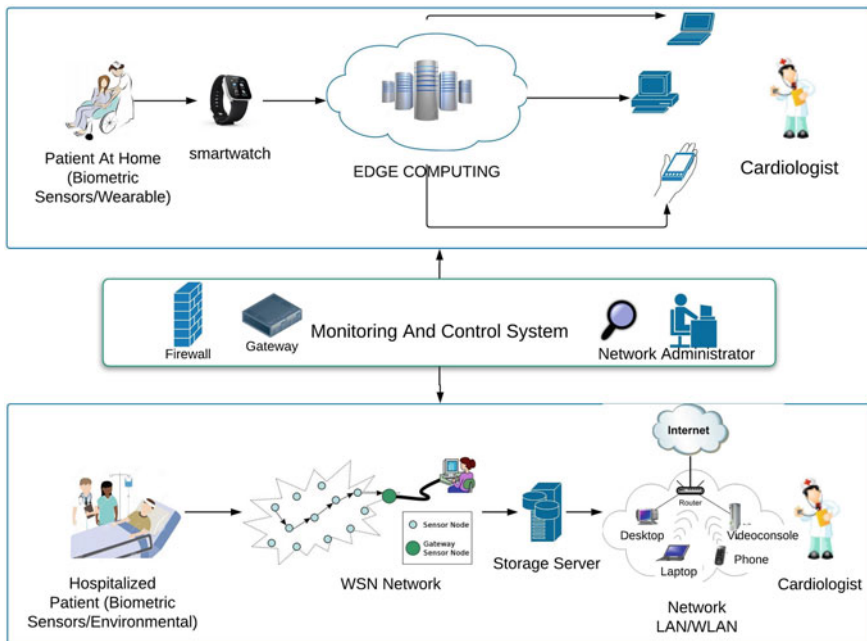


Fig. 2 Model applied to the case study

To corroborate the intelligent management model in an IoT environment in the healthcare sector, to assess whether it is feasible to adopt such a proposal in the organization under study and determine its level of maturity, the application of the maturity model tool was also carried out.

The maturity model suitable for its application is the digital transformation maturity model of an organization and for this purpose [14]. The maturity levels derivate from the model are as follows:

1. **Beginner:** The digital channels are incipient, the web interfaces are not used in an efficient way, and the products or services are not offered through it. Management is still reluctant to change and it is immature in terms of digital culture, and the benefits it generates in the company.
2. **Medium level:** The customer requirements are taken into account but it is still lacking a customer-centric approach, their digital channels are not completely developed, and the mobile channel is inefficient. These companies recognize the necessity of change, and the digital culture is present in some small groups or departments, but it's necessary to be extended to the entire company.
3. **Advanced:** Many innovative initiatives are carried out, which allows the development of digital culture. All channels are fully developed, and the products and services are offered on all channels. The omnichannel experience is complete. The user experience is taking into account, an advanced analysis of the data is applied, and the customer is the priority.
4. **Expert:** The digital transformation is fully applied, and the change is welcome. The customer-centric and omnichannel is approached from the design. Business intelligence is applied at all levels of the company. The digital culture is part of the strategic plan.

The maturity model takes into account three dimensions: The culture and organization, the technology and the business. The following formulas were applied to determine the level of maturity:

For the score calculation in each dimension:

$$Score_{Dimension} = \frac{\sum_{i=1}^n Score_{criteria}}{n} \tag{1}$$

For the score calculation of the model:

$$Score_{Model} = \frac{\sum_{j=1}^{nd} Score_{Dimension}}{nd} \tag{2}$$

**Table 1** Score by dimension

Dimension	Dimension score
Culture and organization	14.67
Technology	7.33
Business	8.67



Table 1 summarizes the scores regards each dimension after applying the validation instrument to the IT staff of our study case.

For the culture and organization level, an *advanced* maturity level is reached, given that the organization has the disposition and the digital culture that is required to adopt the change that is proposed. Regarding the technology dimension, a medium maturity level is reached, since the digital channels are not completely implemented. For the business dimension, the medium maturity level is reached, where employees are involved in the change and the need for the use of analytics for decision making is recognized. The average score of the model is 10.22, this means that the company is in the medium maturity level, so it is concluded that it is feasible to adopt the IoT in our case study.

## 5 Conclusions

The digital transformation maturity model was applied, obtaining an average level of maturity, so it is concluded that the application of the proposal in the place under study is feasible. It was partially exemplified in a private hospital specifically in the area of cardiology demonstrating its contribution and the achievement of the objectives set.

As future work, it is intended to develop a methodology based on each of the dimensions of the proposed model.

## References

1. U.-T. Y.2060: Unión Internacional de las Telecomunicaciones. <https://www.itu.int/rec/T-REC-Y.2060-201206-I/es>. Last accessed 18 Jan 2019
2. Cabani, L.: Diario El Peruano. <https://www.elperuano.pe/noticia-la-gestion-de-recursos-salud-77727.aspx>. Last accessed 10 July 2019
3. Jurado Perez, L., Velásquez Vargas W., Vinuesa Escobar, N.: Estado del Arte de las Arquitecturas de Internet de las Cosas (IoT). In: Academia.edu, pp. 1–48. Springer, Berlin, Heidelberg (2014)
4. Kosmatos, E., Tselikas, N., Boucouvalas, A.: Integrating RFIDs and smart objects into a unified Internet of Things architecture. *Adv. Internet of Things* **1**, 5–12 (2011)
5. Firouzi, F., Farahani, B., Ibrahim, M., Chakrabarty, K.: From EDA to IoT eHealth: promise, challenges. *IEEE Trans. Comput. Aided Des. Integr. Circ. Syst.* **37**(12), 2965–2978 (2018)
6. Ahmed, T., Le Moulllec, Y.: A QoS optimization approach in cognitive body. *Sensors (Basel)* **17**(4), 780 (2017)
7. Castro, D., Coral, W., Cabra, J., Colorado, J., Méndez, D., Trujillo, L.: Survey on IoT solutions applied to healthcare. *DYNA* **84**, 192–200 (2017)
8. Sanmartín Mendoza, P., Ávila Hernández, K., Vilora Núñez, C., Jabba Molinares, D.: Internet de las cosas y la salud centrada en el hogar, *Revista Salud Uninorte* **32**(2), 337–351 (2016)
9. Li, C., Hu, X., Zhang, L.: The IoT-based heart disease monitoring system for pervasive. *Procedia Comput. Sci.* **112**, 2328–2334 (2017)
10. Sokac, M.: A new design for a Holter monitor based on Internet of Things technology. *ResearchGate* 1–5 (2017)

11. Kumar Sahoo, P., Kumar Dehury, C.: Design and implementation of a novel service management framework for IoT devices in cloud. *J. Syst. Softw.* **119**, 149–161 (2016)
12. OpenFog: Reference Architecture for Fog Computing. <http://www.OpenFogConsortium.org>, <http://www.springer.com/Incs>. Last accessed 10 Jan 2019
13. Progress Software Corporation: Progress Open Edge. [https://documentation.progress.com/output/ua/OpenEdge\\_latest/index.html#page/gsdev%2Fgetting-help-using-the-openedge-knowledge-servic.html%23](https://documentation.progress.com/output/ua/OpenEdge_latest/index.html#page/gsdev%2Fgetting-help-using-the-openedge-knowledge-servic.html%23). Last accessed 6 Feb 2018
14. Paradigma: paradigmigital.com. <https://dtma.paradigmigital.com/>. Last accessed 25 Aug 2019

# Evaluation Method of Variables and Indicators for Surgery Block Process Using Process Mining and Data Visualization



Piero Rojas-Candio , Arturo Villantoy-Pasapera , Jimmy Armas-Aguirre , and Santiago Aguirre-Mayorga 

**Abstract** In this paper, we proposed a method that allows us to formulate and evaluate process mining indicators through questions related to the process traceability, and to bring about a clear understanding of the process variables through data visualization techniques. This proposal identifies bottlenecks and violations of policies that arise due to the difficulty of carrying out measurements and analysis for the improvement of process quality assurance and process transformation. The proposal validation was carried out in a health clinic in Lima (Peru) with data obtained from an information system that supports the surgery block process. Finally, the results contribute to the optimization of decision-making by the medical staff involved in the surgery block process.

**Keywords** Process mining · Data visualization · Healthcare · Surgical block · Medical variables

## 1 Introduction

The Social Health Insurance, ‘EsSalud’, is a decentralized public organization whose purpose is to provide coverage to insured people and their right-holders, through the provision of different types of insurance to the population in the face of human’s risks

---

P. Rojas-Candio · A. Villantoy-Pasapera (✉) · J. Armas-Aguirre  
Universidad Peruana de Ciencias Aplicadas (UPC), Lima 15023, Peru  
e-mail: [u201513323@upc.edu.pe](mailto:u201513323@upc.edu.pe)

P. Rojas-Candio  
e-mail: [u201510881@upc.edu.pe](mailto:u201510881@upc.edu.pe)

J. Armas-Aguirre  
e-mail: [jimmy.arms@upc.pe](mailto:jimmy.arms@upc.pe)

S. Aguirre-Mayorga  
Pontificia Universidad Javeriana, Bogotá, Colombia  
e-mail: [saguirre@javeriana.edu.co](mailto:saguirre@javeriana.edu.co)

[1]. This institution provides care to approximately 11,493,000 insured Peruvians, who represent 35.7% of the total population [2]. These insured people are concentrated in a higher proportion in ages from 0 to 14 years, from 25 to 44 years and 65 to more [3]. According to the annual report drawn up in 2017 by this institution, it shows that there is a total of 28,149 complaints registered in the Insured Service information system, which represents 18.8% of the total requests for that system with a 25-day completion time [4]. Also, according to the newspaper *El Comercio*, one of the main reasons for the complaints is due to the lack of access for health services due to the waiting time of care for the insured [5]. EsSalud seeks to propose strategies to reduce these complaints and waiting times, but such investigations involve a higher work effort and use of human resources. The results of the tests do not show to be very effective since the insured may still be dissatisfied because the attention time is still high [6].

In recent years, the development of technology has been enormous, and this is because support for different industries in their organizational processes is vital [7], as in the case in the health sector, which has access to large volumes of data in the information systems they manage to support their business processes. At this point, process mining allows extracting process execution information from the information systems available in an organization to build process models, compare existing models with those built automatically to identify bottlenecks and deviations and to improve business processes [8].

## 2 Literature Review

Given the importance of the proper structuring of this life-saving process, previous studies that applied the discipline of process mining in various industries were reviewed to visualize the results obtained in the case studies and the contribution that the authors presented.

Therefore, as can be seen in Table 1, a comparison of process mining tools made in research was taken as a Ref. [7], since this is aligned with our purpose of identifying an easy-to-use tool that incorporates the disciplines of Process Mining and Data Visualization. The tool chosen in this research is Celonis, for its ease of use and the excellent user experience it provides.

## 3 Proposed Method

### 3.1 Proposal Description

The method to be presented uses the seven activities of [15] because indicators are planned to provide quantitative and real answers about the surgery process based on the specific needs of stakeholders [7], which is mainly designed according to the PM2 methodology. Our method proposes a definition of variables within data visualization

**Table 1** Comparison of process mining tools. [7]

Tool	ProM	Disco	Celonis	QPR Process Analyzer
References	[9–11]	[10, 12]	[10, 13, 14]	[10, 11]
Import type support	MXML, XES	CSV, XLS, MXML, XES y FXL	CSV, XLS	XES
Amount of event logs	Unlimited	5 million events	Unlimited	10 million events
Output model notation	BPMN, Work flow, Petri nets, EPCs, Transition systems	Fuzzy model	Fuzzy model	Work flow
Monthly cost	Free	\$1618	\$598–1929	\$1126
Number of users per license	Unlimited	1	1	1
Support time (Months)	–	Unlimited	Unlimited	1
License	–	X	X	X
Filtering data	X	X	X	–

techniques to understand in depth what is going to be represented graphically and, at the same time, be of interest to those responsible for the surgery block process at a business level. Figure 1 shows the evaluation method.

### 3.2 Stages of the Method

**Objectives and Question Definition** As a start, for this process mining and data visualization project, exploitation of the domain knowledge from the process experts, end-users, clients or administrative staff will be carried out to make a definition of the project scope, goals, and questions related to these goals. The goals of a project are related to improving KPIs related to cost, time, quality, etc. Associated with these goals, performance-driven questions are used to determine how to assess and achieve these goals. Each question can be answered with operational scenarios including one or more process mining features measuring indicators of the process. These indicators are defined to provide quantitative answers based on the specific needs of stakeholders. The output of this stage is a document that contains a GQFI (Goal-Question-Process Mining Feature-Performance Indicator) table.

**Data Extraction** In this stage, event data is extracted related to the patient for process mining. Healthcare data attributes are extracted according to the questions and objectives set. There are three minimum requirements for the control-flow analysis of healthcare data; activity id, information about activities, and timestamps of these activities.

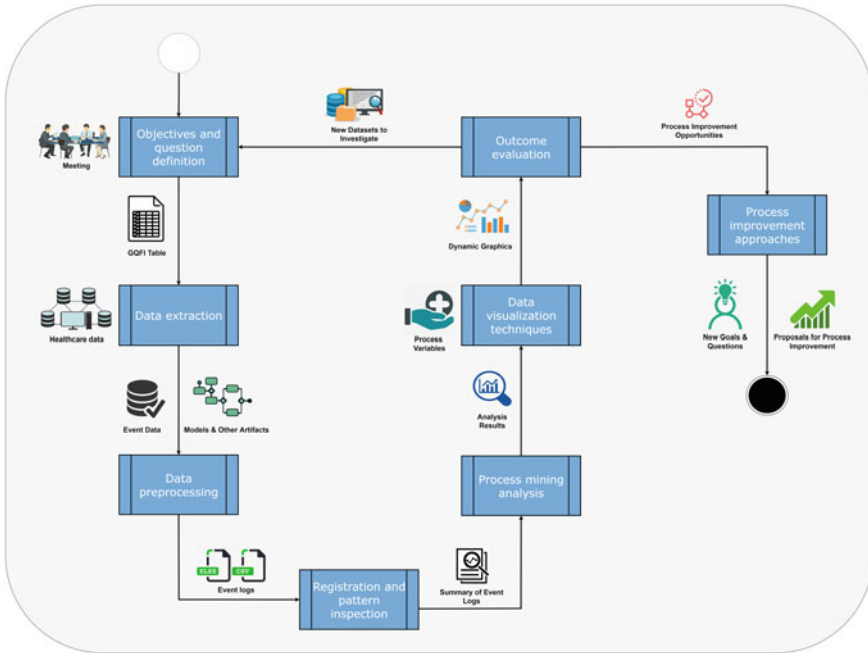


**Fig. 1** Evaluation method of variables and indicators for the surgery block process using process mining and data visualization

**Data Preprocessing** In order to solve data quality issues, such as incorrect, imprecise, missing, and irrelevant data, the extracted event data, according to the GQFI table, must be formatted, filtered, abstracted, or clustered at different levels so that the results are meaningful and valuable. To apply process mining techniques and connect the event log to the model, event data obtained as a query must be expressed in the form of event logs.

**Registration and Pattern Inspection** This stage refers to gaining a first impression of the log and to gathering statistics to create a log and a pattern summary. This inspection consists of the number of cases, events, duration of events, traces of patterns, resources, frequencies and relative frequencies of events. The aim of this stage is to fully understand and visualize the process quickly.

**Process Mining Analysis** Given a discovered or documented process model and an event log related to that process, conformance checking techniques are used to detect and verify inconsistencies related to business process compliance in aspects of quality, time, resources, and costs.

**Data Visualization Techniques** Based on the event logs uploaded into a tool, it is important to consider what is the most important information and how long is the magnitude of your data to represent it graphically. Therefore, it is necessary to decide the most important aspects and characteristics of the uploaded data.

**Outcome Evaluation** At this stage, results related to process mining indicators and medical variables displayed in data visualization graphs are evaluated. After each process mining activity, healthcare data can be divided into smaller sets. New datasets can be investigated in terms of patient attributes, service, department, or doctor information.

**Process Improvement Approaches** In process mining, the improvement is associated with the identification and elimination of bottlenecks, loop reprocessing, prevention of unnecessary states, and understanding of activities that consume more than average time.

## 4 Case Study: Validation

The method presented was validated in a Peruvian network of health centers. The institution allowed us the implementation of pilot planning for the application and validation of the proposed method. The data provided refers to the period from May to August 2018 of a clinic located in Lima, Peru. For the validation of our proposal, we first ran a run through the entire flow of activities of the method that compose it, thanks to the support of the IT area of the health center, since they were responsible for providing information about their process. Likewise, together with a specialist from the surgery block, the indicators and variables related to process mining and data visualization, respectively, were validated.

### 4.1 Data Extraction

Due to the confidentiality of data that the network of clinics is affected to fulfill, this stage of the method was realized by the IT area of the company. For this, said area extracted the information considering the minimum structure of an event log. They consider a unique identification of each patient, the associated activities associated with each patient from their reception to their departure, and the times for each registered activity.

### 4.2 Data Preprocessing

In this activity, the information provided by the IT staff began to be refined because some records were not with the complete data due to possible operational errors generated by the medical team of surgery block. The records associated with this incomplete data were deleted so as not to compromise the project result. The

minimum requirements of an event log were considered so that it can be loaded and used in the Celonis tool.

### ***4.3 Registration and Pattern Inspection***

For this activity, the information processed in the Celonis tool is loaded. After the information is loaded, this tool allows generating an overview of the process. For this view, graphics are generated automatically to have the first impression of it. It was observed that there was an average of 15 cases per day, with a total of 135 events per day. Likewise, it was shown that there was an average of 11 h of execution between the beginning and end of the process without considering the extreme values.

On the other hand, the bottlenecks were obtained that increased the execution time considerably. It is recorded that between reception and preparation of the patient it took 15 h on average. All this information obtained will be useful for review in the following analysis activity.

### ***4.4 Process Mining Analysis***

Figure 2 shows the entire process by using the Celonis tool. This process begins from the patient's entrance to the health center and ends until his or her exit after passing through a recovery due to the surgical operation received.

After having an overview of the process, we perform the discovery of the model by executing the fuzzy miner algorithm in the system. In the first view, under 100% of the connections, the spaghetti effect of the process was shown. Therefore, it was decided, with the process specialist, to work with 99.1% of activities because of these covered variants greater than 1%, while the others were below this percentage.

After the discovery of the model, the process mining feature that refers to the conformity check was continued. For this task, a documented model provided by the process specialist was loaded, and the comparison was made with all traces of the event records. This is aimed at knowing the percentage of affinity between the documented process and the loaded event logs. The result shown by the tool was that there are 75% compliance and a total of 21 violations of the process.

### ***4.5 Data Visualization Techniques***

Figure 3 shows the representations that were used according to each defined variable. It should be noted that four of the nine variables were represented quantitatively because three of them refer to average values, while the remaining is simply the sum of surgeries performed in the process. Regarding the other five variables that were represented graphically, in the variable of surgical care per month, the bar graph was chosen, because the dimension "month of activity" and the measurement "number



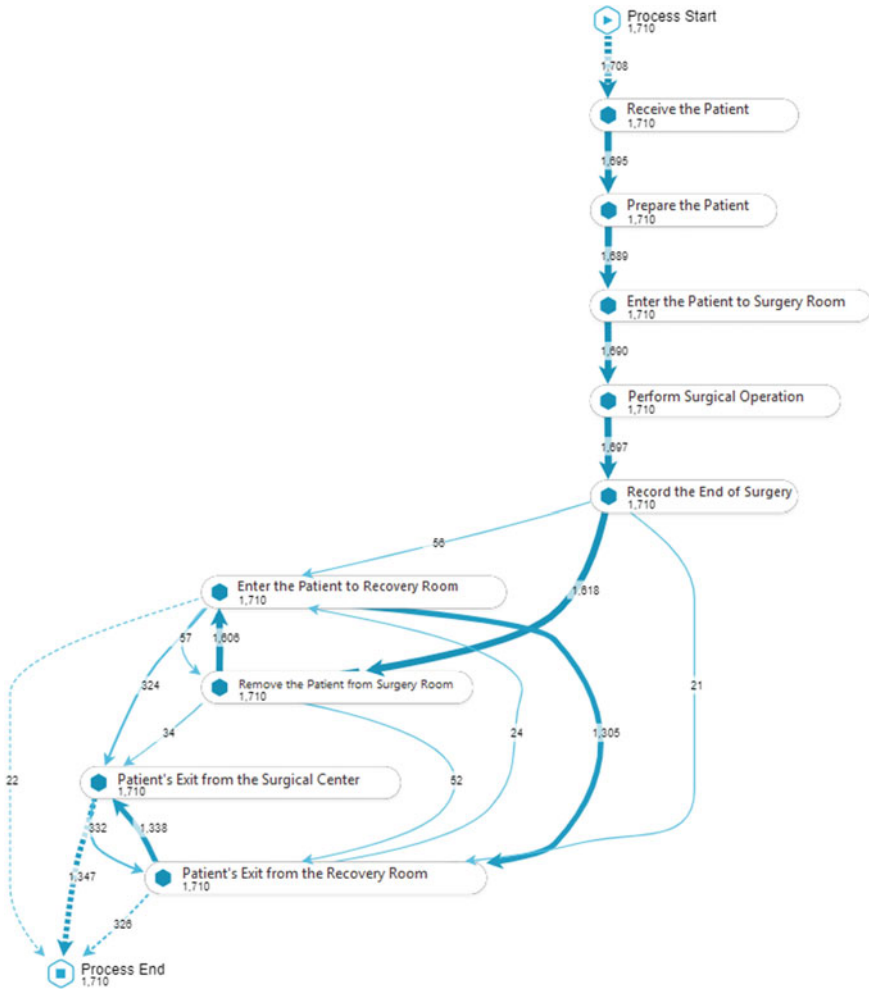


**Fig. 2** Model of the surgery block process discovered in 99.1% of Celonis connections

of surgeries” are necessary without using a legend in that type of graph. Secondly, to evaluate trends by operating room, it was decided to use the donut diagram because it consists of seven operating rooms, and each one is represented on a different scale due to the number of surgeries. Thirdly, to represent the amount of surgical care by type of encounter, a ring diagram was used for the same reason presented previously. Finally, to know the average time in which a surgical operation is performed by type of encounter and by operating room, the bar chart was used as it helps us to easily identify what type of encounter or operating room takes more or less time to perform a surgery.



**Fig. 3** Dynamic graphs made with the information of the surgery Block and using the defined medical variables

### 4.6 Outcome Evaluation

In the inspection phase of records and patterns, a first impression was made of the surgery block process with some indicators automatically generated by the Celonis tool. This allowed us to have a first filter of the cases that we want to review. The important thing to highlight is the following information: the process, from start to finish, has an average duration of approximately 11 h without considering the extreme values. Likewise, a bottleneck was highlighted between the activities of the patient reception and patient preparation. That bottleneck had a value of 15 h, considering the total of the event records.

### 4.7 Process Improvement Approaches

The improvement of adapting the documented model was identified in order to correspond to the findings of the event records in the information systems. This will allow the elimination of future observations in the following process mining projects. Likewise, the need to be able to count on a technology that facilitates the recording of the start or end times of activity was identified. As a proposed solution in the face of incomplete or regularized records of patient-related activities, it is recommended to adopt Bluetooth-based beacon technology.

## 5 Final Remarks

A method of evaluating indicators and variables was used for the surgery block process using process mining and data visualization. The method was executed through operative scenarios in the surgical process in a network of clinics to answer typical and frequent questions for this process. To perform this, 1710 cases were reviewed with a total of 15,390 surgical encounters.

It is validated that the application of the method allowed us to identify bottlenecks, variants, violations, and variances of the process. Also, this model improves the documented process model regarding the records of events of the health center's information systems.

As future work, the development of a tool that supports all the process mining features listed in the GQFI table to respond to all indicators related to those features so that they are evaluated, and new improvements in the health process are proposed.

## References

1. EsSalud Institution: <http://www.essalud.gob.pe/nuestra-institucion/>. Last accessed 01 Sept 2019
2. EsSalud's Institutional Statistics: <http://www.essalud.gob.pe/estadistica-institucional/>. Last accessed 01 Sept 2019
3. EsSalud's Presentation to the Labor and Social Security Commission of the Congress of the Republic. [http://www.congreso.gob.pe/Docs/comisiones2018/Trabajo/files/04\\_09\\_2018\\_exposicion\\_presidenta\\_essalud\\_fiorela\\_molineli\\_situacion\\_financiera\\_de\\_essalud.pdf](http://www.congreso.gob.pe/Docs/comisiones2018/Trabajo/files/04_09_2018_exposicion_presidenta_essalud_fiorela_molineli_situacion_financiera_de_essalud.pdf). Last accessed 01 Sept 2019
4. EsSalud's 2017 Annual Memorandum. [http://www.essalud.gob.pe/downloads/memorias/memoria\\_2017.pdf](http://www.essalud.gob.pe/downloads/memorias/memoria_2017.pdf). Last accessed 01 Sept 2019
5. EsSalud loses more than S/2,900 millions in a year. <https://elcomercio.pe/economia/peru/essalud-pierde-s-2-900-millones-ano-noticia-616248>. Last accessed 01 Sept 2019
6. Interventions to reduce waiting times for access to health services: synthesis of evidence. [http://www.essalud.gob.pe/ietsi/pdfs/direcc\\_invest\\_salud/6\\_intervenc\\_para\\_reduc\\_tiemp\\_espera\\_acceso.pdf](http://www.essalud.gob.pe/ietsi/pdfs/direcc_invest_salud/6_intervenc_para_reduc_tiemp_espera_acceso.pdf). Last accessed 01 Sept 2019
7. Armas, J., Aguirre, S., Coronado, A., Evangelista, M.: Evaluation of operational process variables in healthcare using process mining and data visualization techniques. In: Proceedings of the 17th LACCEI International Multi-conference for Engineering, Education and Technology. Latin American and Caribbean Consortium of Engineering Institutions, Montego Bay (2019)
8. Gurgun Erdogan, T., Tarhan, A.: A goal-driven evaluation method based on process mining for healthcare processes. *Appl. Sci.* **8**(6), 894 (2018)
9. proM 6.7: <http://www.promtools.org/doku.php?id=prom67>. Last accessed 01 Sept 2019
10. van der Aalst, W.: *Process Mining: Data Science in Action*, 2nd edn. Springer, Heidelberg (2016)
11. Ailenei, I.: *Process mining tools: a comparative analysis*. Student thesis: Master. Eindhoven University of Technology, Eindhoven, The Netherlands (2011)
12. Disco: <https://fluxicon.com/disco/>. Last accessed 01 Sept 2019
13. PwC's Finance Digital Day. <https://fdocuments.us/document/finance-digital-day-pwcdk-the-pwcs-process-intelligence-is-an-approach.html>. Last accessed 26 Jan 2020
14. Celonis Operation Guide. [https://help.sap.com/rc/6163e388c6ce431a893758775e8dca41/4.3/en-US/SAP-Process-Mining-by-Celonis-4.3\\_Operation-Guide-1.6.pdf](https://help.sap.com/rc/6163e388c6ce431a893758775e8dca41/4.3/en-US/SAP-Process-Mining-by-Celonis-4.3_Operation-Guide-1.6.pdf). Last accessed 01 Sept 2019

15. R'Bigui, H., Cho, C.: The state-of-the-art of business process mining challenges. *Int. J. Bus. Process Integr. Manage.* **8**(4), 285–303 (2017)

# A Technological Solution to Identify the Level of Risk to Be Diagnosed with Type 2 Diabetes Mellitus Using Wearables



Daniela Nuñovero , Ernesto Rodríguez , Jimmy Armas ,  
and Paola Gonzalez 

**Abstract** This paper proposes a technological solution using a predictive analysis model to identify and reduce the level of risk for type 2 diabetes mellitus (T2DM) through a wearable device. Our proposal is based on previous models that use the auto-classification algorithm together with the addition of new risk factors, which provide a greater contribution to the results of the presumptive diagnosis of the user who wants to check his level of risk. The purpose is the primary prevention of type 2 diabetes mellitus by a non-invasive method composed of the phases: (1) Capture and storage of risk factors; (2) Predictive analysis model; (3) Presumptive results and recommendations; and (4) Preventive treatment. The main contribution is in the development of the proposed application.

**Keywords** Wearable · Primary prevention · Type 2 diabetes mellitus

## 1 Introduction

According to the International Diabetes Federation [1], is estimated that around 425 million people of the world, that is, 8.8% of adults between 20 and 79 years old, suffer diabetes. It is important to mention that more than 50% of these people are not aware that they suffer from this disease, avoiding the possibility of preventing harmful and

---

D. Nuñovero · E. Rodríguez (✉) · J. Armas  
Universidad Peruana de Ciencias Aplicadas (UPC), Av. Primavera 2399 Surco, Lima, Peru  
e-mail: [u20141a651@upc.edu.pe](mailto:u20141a651@upc.edu.pe)

D. Nuñovero  
e-mail: [u201523752@upc.edu.pe](mailto:u201523752@upc.edu.pe)

J. Armas  
e-mail: [jimmy.arms@upc.pe](mailto:jimmy.arms@upc.pe)

P. Gonzalez  
Dalhousie University, 6299 South Street, Halifax, Canada  
e-mail: [paola.gonzalez@dal.ca](mailto:paola.gonzalez@dal.ca)

expensive complications. In 2045, if there is not detection and early prevention of this chronic disease, 629 million people could have diabetes [1]. In addition, in 2017, it was estimated that 10.7% of deaths in the world were due to diabetes, exceeding the percentage of other diseases such as tuberculosis and HIV/AIDS [1].

Diabetes is a chronic disease that occurs when a person has elevated blood glucose levels, because their pancreas stops producing insulin or because the body does not produce it effectively [1]. The predominant type of this disease in the world population is type 2, which is characterized by the inadequate production of insulin and the inability of the body to respond to this hormone, in other words, resistance to it [2]. One of the particularities of type 2 is that it is a chronic disease of slow progression and difficult to determine the exact moment in which it appears [1].

In Peru, 3.3% of the population between 15 and over were diagnosed with diabetes mellitus, where the percentage of people is higher in Metropolitan Lima and the rest of the coast [3]. In addition, according to the National Institute of Health (INS) indicated that 70% of Peruvian adults are suffering from obesity and overweight, being young 42.4% [4]. This information means that the risk of people suffering from this chronic disease is increasing.

For this reason, this paper proposes a technological solution that evaluates risk factors, without the need for laboratory tests or other invasive procedures. From this evaluation, through a predictive analysis model based on the inference of the data, it is possible to be prone as a person can be diagnosed with type 2 diabetes mellitus. From this information, the result is obtained with a percentage of certainty of the risk that the person is suffering from. It is there, where an objective is defined with respect to physical activity, which will be measured through a wearable device. Similarly, the mobile application provides recommendations on how to maintain an adequate diet to reduce the risk of contracting the disease.

## 2 Literature Review

### 2.1 Diabetes Prediction Techniques

In the previous study [5], a prediction model for the diagnosis of T2DM is presented, where three types of algorithms to SAP predictive analytics tool have been compared, in order to validate and determine which one has greater precision.

The first category, decision trees, includes the R-CNR tree algorithm. According to SAP [6], the algorithm allows classifying observations into groups and predicting one or more discrete variables based on other variables. Among the output options, a trend or fill field can be obtained based on two types of analysis (classification and regression). On the other hand, the category of neural networks algorithm includes the R-Nnet neural network. The most representative characteristic of this type is that it does not follow a linear path, because is processed collectively, in parallel through nodes (or neurons) [5]. According to the description provided by SAP [7], the algorithm allows predicting, classifying, and recognizing statistical patterns through library functions. Finally, the classification category includes the native auto-classification algorithm. According to SAP [8], the algorithm is used for binary or categorical classification. In addition, the algorithm detects the type of model and algorithm

used and that best suits based on the target variable that was selected. It also decides whether the input should be continuous or categorical and determines the appropriate classification for these variables. As a result, this allows reducing data preparation and modeling activities.

Performed the tests [9], it is obtained that the “Auto Classification” algorithm has 91.7% accuracy and obtains greater positive results compared to the other evaluated algorithms.

For this reason, it was decided to use it for the solution, in order to improve precision and accuracy. The variables proposed in the previous study will continue to be used and add new ones found in the literature review.

## ***2.2 Technology Platforms***

To choose the platform that best suits the solution, an analysis was carried out under certain criteria defined by Forrester, who is a market researcher, in charge of advising leading business and technology companies. Hence, the Microsoft Azure platform suits very well the requirements and demands of the solution.

## ***2.3 Wearable Device***

For the solution, the wearable device “*Mi band 4*” was used, since it has the characteristics that are required. In addition, this device is focused on capturing information about the user’s physical activity.

# **3 Proposed Technology Solution**

## ***3.1 Description of the Solution***

Using the elements described in the literature review, a technology solution is proposed to identify the presumptive level of user predisposition to be diagnosed with type 2 diabetes mellitus. This proposal solution focuses on two key users: The user that will use in the future, whom we will call the patient; and the doctor.

The solution is governed by two stages: The first is related to the diagnosis of the disease and the second focused on preventive treatment. First, the diagnostic stage focuses on the data collection and storage phases, the execution of a predictive analysis model to identify the presumptive level of patient risk, plus results and recommendations delivery. Secondly, the preventive treatment stage, formed by the monitoring and control phases followed by some feedback from the doctor. Figure 1 depicts the technological solution of the work.

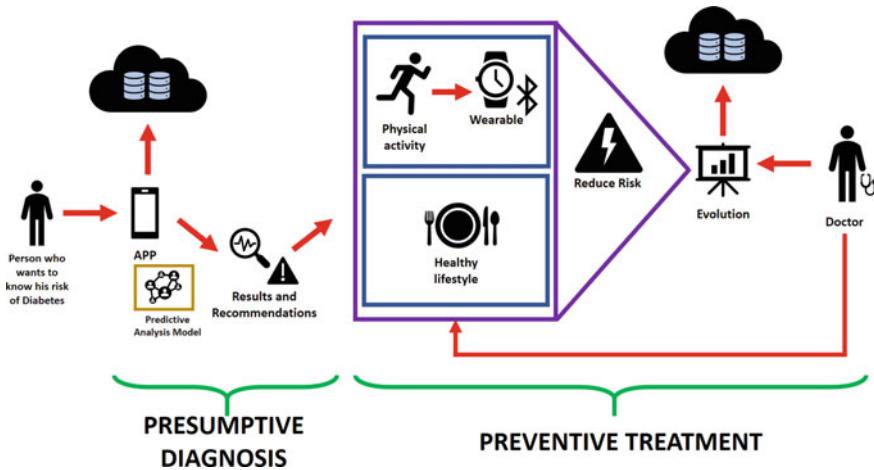


Fig. 1 Proposed technology solution

## 3.2 Stages and Phases of the Solution

### 3.2.1 Diagnosis

- *Risk Factors Collection and Storage.* For this phase, in the future applications, the patient will fill out a form in the application. The form contains Yes/No questions and questions with predefined answers to identify the presence and values of risk factors of the patient, which will later be sent via Web service to an Oracle database.
- *Predictive Analysis Model.* Responses from the form will be automatically sent to the SAP predictive analytics tool and analyzed using the auto-classification algorithm, which will result in a presumptive diagnosis of type 2 diabetes mellitus and stored automatically by the tool on an Oracle database.
- *Results and Recommendations Delivery.* The results of the predictive analysis model will be displayed in the mobile application. After this, a suggestion will be displayed about following a preventive treatment regularly monitored by a doctor in order to reduce the level of predisposition in the medium term.

### 3.2.2 Preventive Treatment

- *Monitoring and control.* In this stage, the wearable device is connected to the mobile application. The wearable, in the future applications, will send information about the physical activity of the user to the mobile application using Bluetooth Low Energy (BLE) technology. This information will be recorded in the database so that at the end of the day, the risk factors information of the patient is up to date. The patient will be able to see a historical evolution of their risk level through a



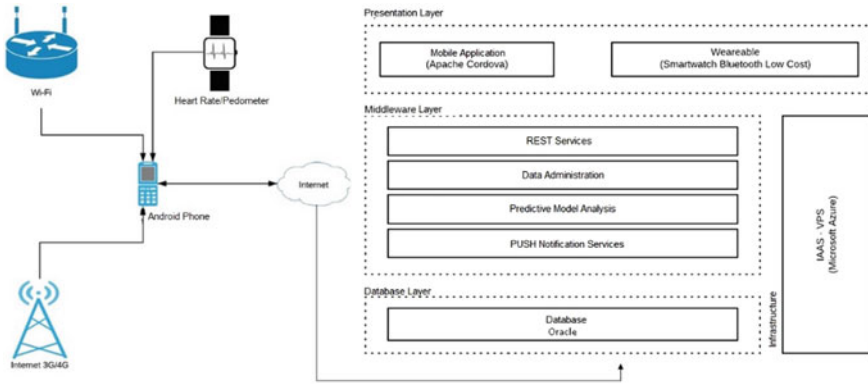


**Fig. 2** Architecture of the proposed technology solution

dashboard in the mobile application, as well as a view with healthy food recipes in order to reduce the patient’s risk.

- *Feedback.* The application is also developed so that a doctor can periodically monitor the patient’s risk level evolution in order to provide constant feedback to the patient without the need to schedule an appointment.

### 3.3 Proposed Architecture

The following architecture will support the proposed stages of the technology solution. This architecture enables the interaction of server components hosted in Microsoft Azure with the mobile application and the wearable device. The architecture shown in Fig. 2 shows how equipment can interact with the mobile app and wearable device, which communicates with the database and predictive analytics model using Web services, both hosted in Azure. It is important to mention that any cloud platform allows deploying Web services that interact with any database that can be used to support this solution.

## 4 Case Study

### 4.1 Implementation

It is essential that the wearable device is associated with the phone and that the mobile is connected to the Internet. The dashboard of the solution is shown in Fig. 3.

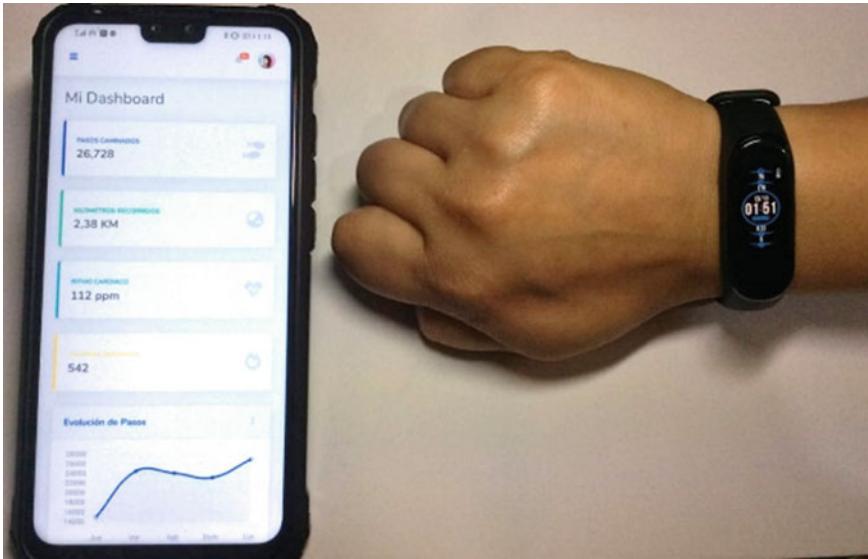


**Fig. 3** Case study

**Risk Factors Collection and Storage** For the implementation of the solution, it was provided with the mobile application so that it could register and enter his data, and then consider the data for the presumptive diagnosis.

**Data Reception in Mobile Application** The information collected will be stored in a database.

**Predictive Analysis Model** After obtaining the respective information with the help of the “SAP Predictive Analytics tool,” it will be analyzed with the auto-classification algorithm, from which it yielded the results composed of a Boolean (1 or 0) value indicating whether or not the user is prone to suffer from the disease, and the percentage of certainty of the result.

**Results and Recommendations Delivery** The results of the predictive analysis model will be shown in the mobile application, along with a recommendation indicating to approach a doctor or specialist for the corresponding tests.

**Preventive Treatment** From the result, it will be possible to decrease the risk shown at baseline. So, the physical activity was measured through the wearable and encouraged to have a much healthier diet.

The goal of this recordings was a concept and preliminary study for later applications, since the research was designed to develop a computational framework, where tests with several persons will be regulated by the respective ethical committee.

## 5 Conclusions

The solution presented serves its purpose by reducing the risk of developing T2DM. We expect that users when using our solution allowed them to feel responsible for their health, letting them notice that a change in their physical activity habits has a great representative impact on their level of risk from T2DM.

As future work, having a historical database with information from people who have previously performed the basal glucose test would be ideal for improving the accuracy and effectiveness of the model results used by the proposed solution. Likewise, we agree that higher samples and time periods are needed on monitored users in order to improve the quality of preventive treatment.

## References

1. International Diabetes Federation (FID): IDF Diabetes Atlas, 8th edn. Bruselas (2017)
2. Organización Mundial de la Salud (OMS): Informe Mundial Sobre La Diabetes. Ginebra (2016)
3. Instituto Nacional de Estadística e Informática: Perú: Enfermedades No Transmisibles y Transmisibles. Lima (2018)
4. Instituto Nacional de Salud: Cerca del 70% de adultos peruanos padecen de obesidad y sobrepeso. <https://web.ins.gob.pe/es/prensa/noticia/cerca-del-70-de-adultos-peruanos-padecende-obesidad-y-sobrepeso>. Last accessed 07 Oct 2019 (2019)
5. Barrios, O., Alberto, D., Infantes, V., Raphael, E., Aguirre, A., Alexander, J.: Predictive modeling for presumptive diagnosis of type 2 diabetes mellitus based on symptomatic analysis. In: 2017 IEEE XXIV International Conference on Electronics, Electrical Engineering and Computing (INTERCON), pp. 1–4. IEEE (2017)
6. SAP: SAP Help Portal: R-CNR Tree. Retrieved from <https://help.sap.com/viewer/94dbf2ba9d4047618880187451c3b253/3.2/es-ES/e790ec0a80b7101487253286b0e91070.html>. Last accessed 06 Oct 2019
7. SAP: SAP Help Portal: R-Nnet Neural Network. Retrieved from <https://help.sap.com/viewer/94dbf2ba9d4047618880187451c3b253/3.2/es-ES/e7911c7b80b7101487253286b0e91070.html>. Last accessed 06 Oct 2019
8. SAP: SAP Help Portal: Auto Classification. <https://help.sap.com/viewer/94dbf2ba9d4047618880187451c3b253/3.3/en-US/38ad5a8b54e84f37a545a197f7af3adf.html>. Last accessed 06 Oct 2019
9. Ollila, M.-M. E., West, S., Keinänen-Kiukaanniemi, S., Jokelainen, J., Auvinen, J., Puukka, K., Järvelin, M.R., Tapanainen, J.S, Franks, S., Piltonen, T.T., Morin-Papunen, L.C.: Overweight and obese but not normal weight women with PCOS are at increased risk of Type 2 diabetes mellitus—a prospective, population-based cohort study. *Hum. Reprod.* **32**(2), 423–431 (2016)

# Mamey Apple Peel for Cr<sup>3+</sup> Removal from Contaminated Waters



Nathali Cotrina  and Ricardo Vejarano 

**Abstract** The aim of this study was to evaluate the capacity of an adsorbent based on mamey apple (*Mammea americana* L.) peel for Cr<sup>3+</sup> removal. Aqueous mediums based on distilled water and different initial concentrations of Cr<sup>3+</sup>, with a dose of 10 g of adsorbent per liter, were used. The residual concentrations of Cr<sup>3+</sup> were determined by atomic absorption spectrophotometry, obtaining optimum values of pH of 2.9, the adsorbent particle size of 300 μm, and stirring rate of 300 rpm, for Cr<sup>3+</sup> removal. Kinetic studies indicate a chemical adsorption process, with the best adjustment to pseudo-second-order models ( $R^2 \geq 0.9973$ ), a contact time of 120 min to reach the adsorbent-Cr<sup>3+</sup> equilibrium, and a good fit to the Freundlich model ( $R^2 = 0.9291$ ), with an adsorption intensity  $n$  of 1.5876. So, our results suggest that Cr<sup>3+</sup> ions can be efficiently removed by using mamey apple peel-adsorbent.

**Keywords** Chromium-contaminated waters · Adsorption · Mamey apple peel

## 1 Introduction

The leather tanning is an important industrial activity in Peru [1]. However, this industry generates considerable volumes of effluents with high contents of chromium (Cr), in many cases surpassing the maximum limits permitted by Peruvian legislation [2]. Chromium cannot be degraded or removed easily, affecting the biodiversity of soils, rivers, and lakes, killing living organisms present in those ecosystems [3]. Like most metals, it can be transported into bodies of water, filtered through the soil, reach drinking water sources or food crops, and ultimately be incorporated into the food

---

N. Cotrina

Ingeniería Ambiental, Universidad Privada del Norte, Trujillo, Peru

e-mail: [nathalicotrina@hotmail.com](mailto:nathalicotrina@hotmail.com)

R. Vejarano (✉)

Dirección de Investigación y Desarrollo, Universidad Privada del Norte, Trujillo, Peru

e-mail: [ricardo.vejarano@upn.edu.pe](mailto:ricardo.vejarano@upn.edu.pe)

© The Editor(s) (if applicable) and The Author(s), under exclusive license

to Springer Nature Switzerland AG 2021

Y. Iano et al. (eds.), *Proceedings of the 5th Brazilian Technology Symposium*,

Smart Innovation, Systems and Technologies 202,

[https://doi.org/10.1007/978-3-030-57566-3\\_18](https://doi.org/10.1007/978-3-030-57566-3_18)

chain and affect human beings with severe health consequences when is ingested at high levels [3, 4].

The leather tanning industry is considered the major source of Cr, due most of the tanneries adopt the Cr tanning process, where the leather takes up only 80% of added Cr, and the rest is usually discharged into the sewage system [5], representing a great environmental risk.

Chromium exists in several oxidation states. The tannery effluents mainly contain  $\text{Cr}^{3+}$ , which under aerobic conditions oxidizes to  $\text{Cr}^{6+}$  [6]. The  $\text{Cr}^{6+}$  specie is the most toxic, due to their higher solubility and mobility [5, 6]. In fact, previous studies report that high concentrations of  $\text{Cr}^{6+}$  cause skin rashes, nose bleeds, respiratory problems, suppressed immune system, liver and kidney diseases, diarrhea, cancer, among other diseases [3, 4]. Besides,  $\text{Cr}^{6+}$  can cross the cell membrane, and be converted to  $\text{Cr}^{3+}$  into the cells, where may lead to subsequent damage of lipids, proteins, DNA, and RNA molecules [7]. Therefore, it is needed to develop procedures focused on an efficient  $\text{Cr}^{3+}$  removal from these effluents, and thus mitigate its impact on affected ecosystems.

Treatments of industrial effluents with high levels of heavy metals based on chemical precipitation and coagulation, ion exchange chemical treatments, sorption using activated carbon, use of zeolites and organic resins, solvent extraction, or physical processes as filtration, reverse osmosis, among others, have been applied in the last years, which is evidenced by the studies published by different authors [3, 5, 6, 8]. However, these methods have shown some disadvantages, for example, the production of huge amounts of sludge that must also be treated before final disposal. Thus, these processes require a technological investment that, in many cases, make them economically unfeasible [3]. So, there has been increased interest in the last years in the use of low-cost technological alternatives.

The use of residual biomass as adsorbents, for example, the peel of some fruits [3, 9–11], is shown as a promising alternative due to its availability, low cost, and composition. Generally, these residues are underutilized and discarded. Previously we reported the feasibility of fruit peels as adsorbents to remove heavy metals [9–11]. The main reason for their high metal affinity is the presence of polymers, mainly pectin, in their cell walls.

Mamey Apple (*Mammea americana* L.) is a tropical fruit produced in Peru. Mostly, this fruit is consumed as fresh fruit, and its main residue is the peel, which contains pectin [12]. This polymer due to its content of hydroxyl (OH), carbonyl (CO), carboxyl (COOH) is capable of fixing metal ions through the chemical adsorption mechanism [11, 13]. The literature reports the use of mamey apple husks (chemically modified with formaldehyde) for  $\text{Cr}^{6+}$  removal [14]. Respect to  $\text{Cr}^{3+}$  removal, adsorbents based on algae biomass [4], and activated carbon from sugar cane waste, passion-fruit shell, and orange waste, have been used [5, 15, 16]. Likewise, we reported the feasibility of the passion-fruit shell as an efficient adsorbent for  $\text{Cr}^{3+}$  removal [9]. Nevertheless, the use of mamey apple peel-based adsorbents for  $\text{Cr}^{3+}$  removal has not been reported yet.

In this sense, the aim of the study was to evaluate the feasibility of mamey apple (*Mammea americana* L.) peel, as an adsorbent for  $\text{Cr}^{3+}$  removal from contaminated aqueous mediums through the mechanism of chemical adsorption, as a potential alternative to the treatments currently applied at industrial level.

## 2 Materials and Methods

### 2.1 Adsorbent Based on Mamey Apple Peel

Mamey Apple (*Mammea americana* L.) was purchased from the local market in the city of Trujillo, Peru. Peels were washed with distilled water and cut into pieces of 1.0 cm × 1.0 cm. Then, they were dried at 80 °C for 24 h in a UN55 PLUS oven (Memmert GmbH Co. KG, Germany) [17], and ground in a knife mill and sieved through different sieves (Tyler series, 75–1180 μm) to standardize the size of the particles. This material was stored and used directly without any later treatment.

The characteristics of this adsorbent were evaluated by measuring the point of zero charges (pH<sub>PZC</sub>), i.e., the pH in which the resultant net charge of the adsorbent surface is zero [18]. Distilled water was taken in 100 ml beakers, adjusting the pH between 2.0 and 6.0. These samples were added 0.5 g of adsorbent and after 12 h under stirring the final pH value was measured. The PZC corresponds to the value where the final net charge (ΔpH) curve cuts the X-axis (ΔpH = 0).

### 2.2 Adsorption Experiments

**Optimum Removal Conditions** Aqueous mediums based on distilled water and Cr(OH)SO<sub>4</sub> (commercial CUIREXTAN B33) were prepared. Three different sequential tests were performed in order to determine the optimum values of the parameters showed in Table 1. Parameters as Cr<sup>3+</sup> concentration 200 mg l<sup>-1</sup>, adsorbent dose 10 g l<sup>-1</sup>, temperature 25 °C, and stirring time 300 minutes, were fixed at constant values.

In all cases, after the stirring period, the samples were filtered with Whatman No. 42 filter paper, and the supernatant was mixed with 3 ml of HNO<sub>3</sub> and 1 ml of HCl. The mixture was heated at 140 °C in a DigiPREP Jr digester (SCP Science, Canada) [9, 10], and then, each digested sample was analyzed by Atomic Absorption Spectrophotometry (Agilent Technologies 200 Series AA, USA) [9]. All experiments were conducted in triplicate.

**Table 1** Assays performed in order to determine the optimum removal parameters

Test	Parameter	pH	Adsorbent particle size (μm)	Stirring rate (rpm)
		<b>2.0–6.0</b>	<b>75–1180</b>	<b>200–500</b>
1	pH	–	300	300
2	Adsorbent particle size (μm)	Optimum	–	300
3	Stirring rate (rpm)	Optimum	Optimum	–

**Adsorption Isotherms and Kinetics Study** Once the optimum values of pH, adsorbent particle size, and stirring rate were defined, the adsorption process was carried out using solutions of  $\text{Cr}^{3+}$  at 20, 50, 100, 250, and 400 ppm, with a fixed dose of 10 g of adsorbent per liter in 500 ml beaker at 25 °C. Aliquots of 15 ml were extracted at 5, 10, 15, 30, 60, 90, and 120 min, and filtered to separate the supernatant, following the same digestion procedure mentioned in the previous section. The amount of  $\text{Cr}^{3+}$  adsorbed per gram of adsorbent ( $q$ , mg/g) was calculated according to Eq. 1 [3]:

$$q = V \frac{(C_0 - C)}{m} \quad (1)$$

where  $V$  is the solution volume (l),  $m$  is the adsorbent dose (g), and  $C_0$  and  $C$  is the initial and final  $\text{Cr}^{3+}$  concentrations, respectively ( $\text{mg l}^{-1}$ ).

In order to study the system behavior, the isotherm models of Langmuir and Freundlich were fitted, judging the coefficients of determination ( $R^2$ ) in order to find the applicability of the developed models. The Langmuir model suggests monolayer adsorption on a homogenous surface. For its part, the Freundlich model explains the interaction adsorbate-adsorbent with multilayer adsorption on heterogeneous surfaces [19]. Additionally, in the case of the Langmuir model, the dimensionless parameter  $R'$  was calculated, which describes the type of isotherm, that according to Weber and Chakraborti [20] is defined by the equation:

$$R' = \frac{1}{1+b.C_0} \quad (2)$$

Where  $b$  is a Langmuir constant, which indicates the nature of adsorption and the shape of the isotherm.  $R'$ -values  $<1$  indicate that the adsorbent-adsorbate system shows a favorable adsorption process [5].

Finally, to evaluate the adsorption kinetics, the same results were evaluated by the mathematical models of pseudo-first and pseudo-second-order [21].

### 2.3 Statistical Analysis

Analysis of variance (ANOVA) and Fisher's LSD (Least Significant Difference) test at a 5% significance level ( $p < 0.05$ ) were performed using Statistica 7.0 software [9], in order to identify significant differences.

### 3 Results and Discussion

#### 3.1 Point of Zero Charge (pH<sub>PZC</sub>) and Effect of pH on Cr<sup>3+</sup> Removal

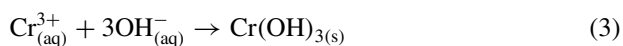
From the chemical point of view, when the aqueous medium has a higher pH than pH<sub>PZC</sub>, negative charges predominate on the adsorbent surface [22]. Figure 1 shows a pH<sub>PZC</sub> value of around 3.8 for adsorbent based on mamey apple peel.

In aqueous mediums, Cr<sup>3+</sup> exists in several states as a function of pH. The form Cr<sup>3+</sup> predominates at pH < 3.0, the forms Cr<sup>3+</sup> and Cr(OH)<sup>2+</sup> at pH 3.0–6.0, and the species Cr(OH)<sub>3</sub> at pH 6.5–10.0 [5]. Figure 1 indicates a good Cr<sup>3+</sup> removal process at pH values greater than 3.8 since no statistically significant differences (LSD Fisher, *p* < 0.05) were evidenced at higher pH values. In this region, Cr<sup>3+</sup> is adsorbed principally as Cr(OH)<sup>2+</sup>, since the adsorbent surface becomes negatively charged (carboxylic acids COOH of pectins in mamey apple peel) [12].

Previous studies reported a good removal process at pH values of 4.0, 5.0, 5.0, and 4.0, by using adsorbents based on algae biomass [4], and activated carbon from sugar industrial waste [5], passion-fruit shell [15], and orange waste [16], respectively.

Taking in account that most tannery effluents in Peru, and in other countries, are discharged at pH values between 3.0 and 4.0 into the sewage system [23–25], the obtained pH<sub>PZC</sub> value could be considered as an appropriate condition for the Cr<sup>3+</sup> removal treatment.

However, at an industrial level, chemical precipitation is the usual way for Cr<sup>3+</sup> removal, by using NaOH or Ca(OH)<sub>2</sub> as precipitating agents (Eq. 3), with greater efficiency as the pH value increases [26]. This phenomenon was verified in the present study by using different values of pH (NaOH addition), in mediums with an initial concentration of Cr<sup>3+</sup> of 275 mg l<sup>-1</sup>, in the absence of adsorbent (Fig. 2).



According to Fig. 2, at pH values greater than 2.9, Cr removal would be more related to the presence of NaOH. Since at industrial level, chemical precipitation is one of the most used methods, which has among its main disadvantages the high sludge generation [3], in the present study the pH value of 2.9 was chosen for the subsequent treatments, in order to evaluate the efficiency of the mamey apple peel-based adsorbent, without the interference of the basifying/precipitating agent.



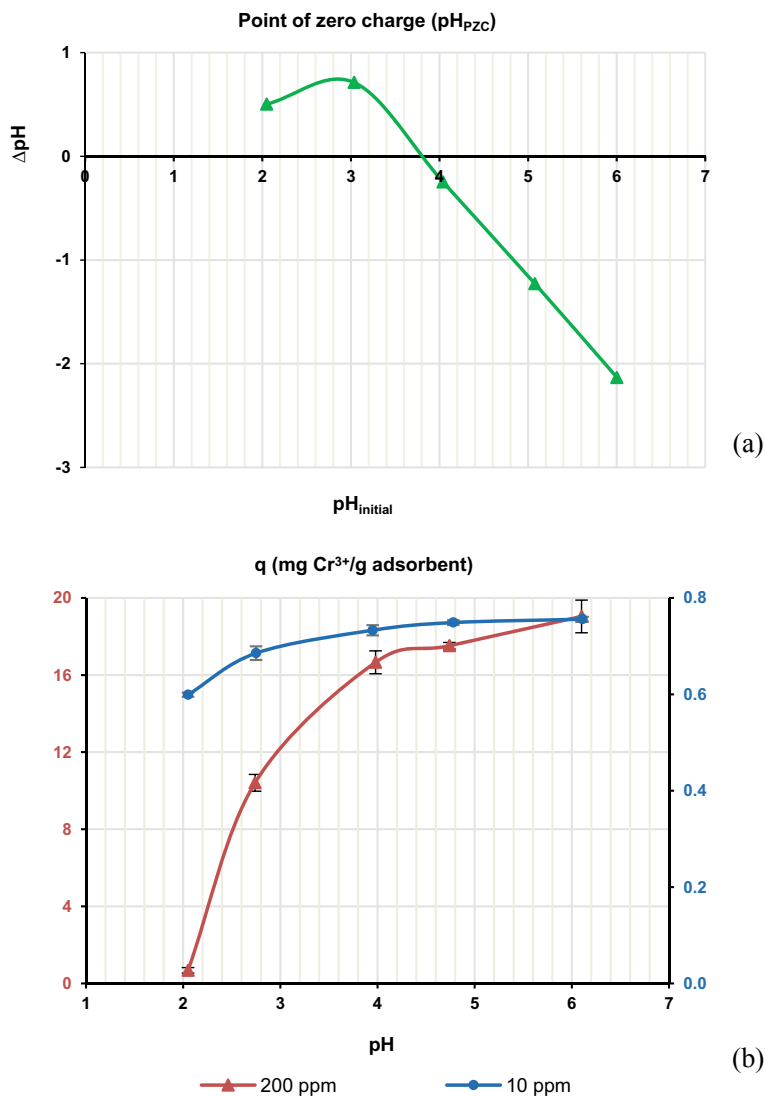


**Fig. 1** **a** pH<sub>PZC</sub> for the apple mamey peel-based adsorbent and **b** the effect of different pH values on Cr<sup>3+</sup> removal (agitation speed 300 rpm)

### 3.2 Effect of Adsorbent Particle Size and Stirring Rate on Cr<sup>3+</sup> Removal

Since the adsorption process occurs inside the particles (on the pore walls), the decrease in adsorbent particle size increases the internal surface area, and therefore, the number of available binding sites for the contact adsorbent-adsorbate [19].

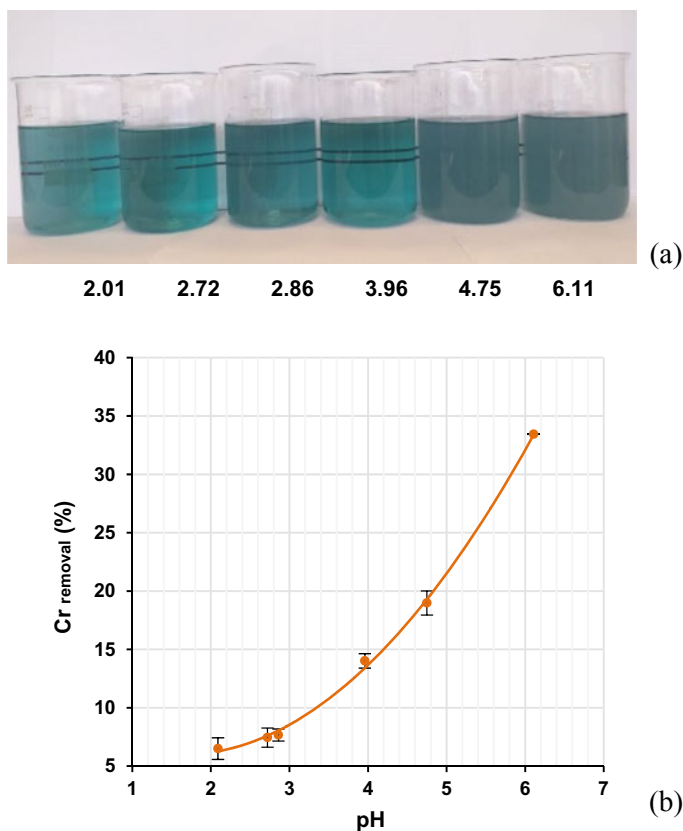


**Fig. 2** **a** Presence of  $\text{Cr}(\text{OH})_3$  and **b** the effect of different pH values on  $\text{Cr}^{3+}$  solubility in aqueous mediums at  $275 \text{ mg l}^{-1}$  of  $\text{Cr}^{3+}$ , in absence of adsorbent

According to Fig. 3, higher  $\text{Cr}^{3+}$  removal rates ( $q$ ) were evidenced at smaller particle sizes [27], with significant differences (LSD Fisher) between 75 and 425  $\mu\text{m}$ . However, the addition of adsorbent at particle sizes smaller than 300  $\mu\text{m}$  caused sludges-like suspensions, making difficult the stirring and the supernatant separation. Therefore, the 300  $\mu\text{m}$  adsorbent was chosen for further  $\text{Cr}^{3+}$  removal treatments.

For its part, the stirring rate helps the adsorbate overcome the boundary layer mass transfer resistance [28]. Figure 3 shows that agitation speeds of up to 300 rpm favor high  $\text{Cr}^{3+}$  adsorption, in accordance with Pathak et al. [28], who report efficient adsorption processes with agitation speeds between 200 and 300 rpm. Nevertheless, higher rpm values (>300), the observed decrease in adsorption could be due to the high mobility of  $\text{Cr}^{3+}$  ions in the solution, generating a weakening of the adsorptive forces, and therefore, greater  $\text{Cr}^{3+}$  desorption in relation to the adsorbed  $\text{Cr}^{3+}$ .

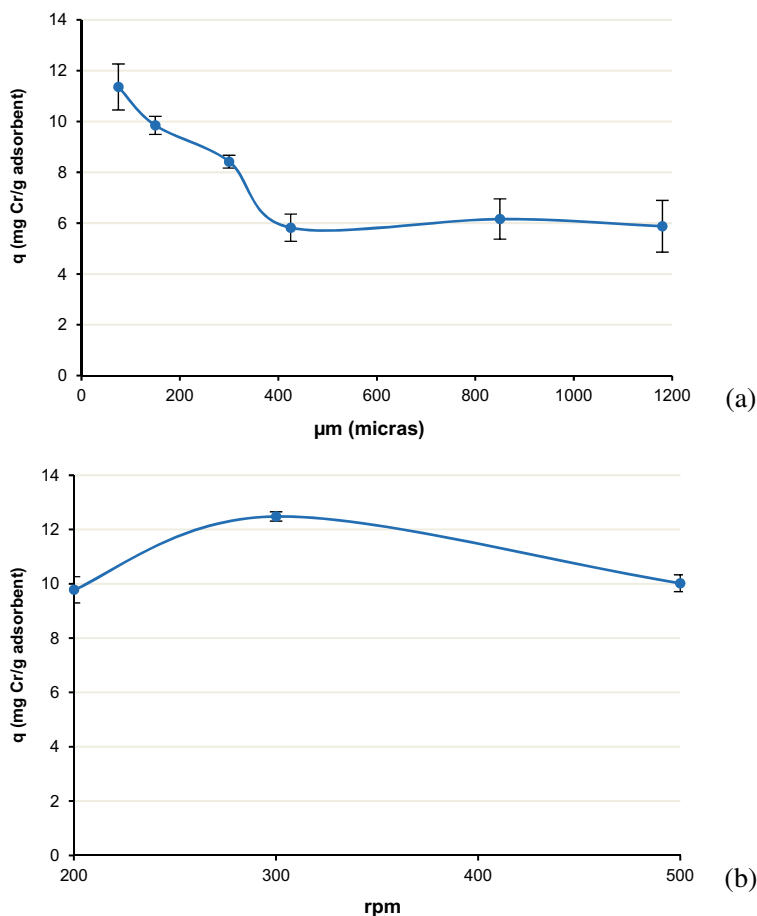


**Fig. 3** **a** Effect of different adsorbent particle sizes and **b** stirring rate, on  $\text{Cr}^{3+}$  removal from aqueous mediums ( $\text{Cr}^{3+}$ :  $200 \text{ mg l}^{-1}$ ) at  $25^\circ\text{C}$ , pH 2.9, and contact time 120 min

### 3.3 Kinetics Study and Adsorption Isotherms

Table 2 shows kinetic parameters for the removal of  $\text{Cr}^{3+}$ . The best values of  $R^2$  were obtained with the pseudo-second-order models. These results indicate a chemical adsorption process between mamey apple peel and the  $\text{Cr}^{3+}$  ions [21]. Besides, in this model,  $k_2$  is the pseudo-second-order rate constant, and  $h$  is the initial sorption rate.

The low values of  $k_2$  at high concentrations of  $\text{Cr}^{3+}$  indicate a low number of available sites for adsorption of  $\text{Cr}^{3+}$  ions, i.e., the surface of the mamey apple peel-based adsorbent begins to saturate [19].

**Table 2** Kinetics (pseudo-second-order models) for Cr<sup>3+</sup> removal by mamey apple peel

Solution (ppm)	Equation	R <sup>2</sup>	k <sub>2</sub> (g mg <sup>-1</sup> min <sup>-1</sup> )	h (mg g <sup>-1</sup> min <sup>-1</sup> )	q <sub>e_exp.</sub> (mg g <sup>-1</sup> )	q <sub>e_calc.</sub> (mg g <sup>-1</sup> )
20	$t/q = 0.6207t + 2.2002$	0.9973	0.1898	0.4545	1.6111	1.5476
50	$t/q = 0.2950t + 0.3919$	0.9999	0.1278	1.4453	3.3898	3.3633
100	$t/q = 0.1286t + 0.5115$	0.9987	0.0343	1.9550	7.7760	7.5530
250	$t/q = 0.0998t + 0.2779$	0.9998	0.0349	3.5984	10.0200	10.1546
400	$t/q = 0.0533t + 0.2139$	0.9994	0.0137	4.6751	18.7617	18.4720

q<sub>e\_exp.</sub>: q<sub>e\_experimental</sub>; q<sub>e\_calc.</sub>: q<sub>e\_calculated</sub>

Respect to equilibrium studies (Fig. 4), the capacity of adsorption of  $\text{Cr}^{3+}$  increases while the initial concentration of  $\text{Cr}^{3+}$  increases from 20 up to 400  $\text{mg l}^{-1}$ , a phenomenon attributed to the competition for the available binding sites, in concordance with kinetic parameter  $h$  (Table 2), as a consequence of the necessary strength to overcome the resistance in the mass transfer of the chromium ions between the medium and the adsorbent, provided by high metal concentrations [29].

Besides, a contact time of 120 min was necessary to reach the equilibrium adsorbent-adsorbate, i.e., the mamey apple peel-based adsorbent is no longer able to adsorb further  $\text{Cr}^{3+}$  from that moment, with  $q_e$  values of 1.5476, 3.3633, 7.5530, 10.1546, and 18.4720 for solutions of 20, 50, 100, 250, and 400  $\text{mg l}^{-1}$  of  $\text{Cr}^{3+}$  (Fig. 4).

Langmuir	
$R^2$	0.7978
$q_{max}$	21.7865
$b$	0.0117
<hr/>	
20 ppm	0.7942
50 ppm	0.6429
$R^*$	0.4419
100 ppm	0.4419
250 ppm	0.2599
400 ppm	0.1754
Freundlich	
$R^2$	0.9291
$k$	0.5866
$n$	1.5876

(a)

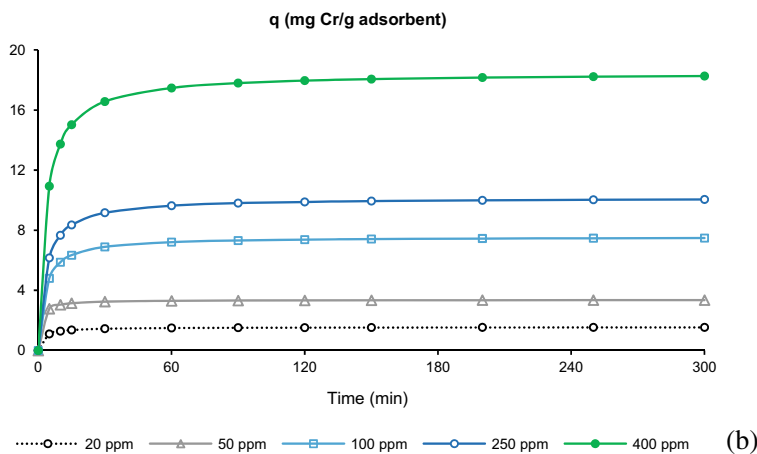


**Fig. 4** **a** Models for adsorption process of  $\text{Cr}^{3+}$  from aqueous mediums. Langmuir model:  $C_e/q_e = 0.0459 C_e + 3.9326$ ; Freundlich model:  $\text{Ln } q_e = 0.6299 \text{Ln } C_e - 0.5334$ . **b** Contact time to reach the equilibrium adsorbent-adsorbate at different concentrations of  $\text{Cr}^{3+}$

Based on the coefficient of determination ( $R^2 = 0.9291$ ), the Freundlich model was suitably fitted for Cr<sup>3+</sup> adsorption (Fig. 4). In this model  $k$  and  $n$  constants indicate the capacity and the intensity of adsorption, respectively [19]. The mamey apple peel-based adsorbent showed a capacity of adsorption  $k$  of 0.5866. A close value was obtained in a previous study for Cr<sup>3+</sup> removal by adsorbent based on passion-fruit shell [9]. Likewise, a good adsorption intensity ( $n = 1.5876$ ) was obtained, so it can be considered as a favorable adsorption process ( $n > 1$ , [30]).

Additionally, in the case of Langmuir model, the obtained values of the dimensionless parameter  $R'$  of 0.7942, 0.6429, 0.4419, 0.2599, and 0.1754 for solutions of 20, 50, 100, 250, and 400 mg l<sup>-1</sup> of Cr<sup>3+</sup> indicate a favorable adsorption process ( $R' < 1$  [5]).

These results indicate a high affinity between Cr<sup>3+</sup> ions and the polymers present in the mamey apple peel-based adsorbent, mainly pectin [12]. Pectin contains functional groups as COOH, OH, and CO, which would be the sites to Cr<sup>3+</sup> ions fixation [11, 13].

## 4 Conclusions

The adsorption capacity exhibited by the mamey apple peel-based adsorbent was very well obtaining optimum values of pH 2.9, adsorbent particle size 300  $\mu\text{m}$ , and stirring rate of 300 rpm, for Cr<sup>3+</sup> removal. Likewise, the results of kinetics studies showed the best adjustment to pseudo-second-order models ( $R^2 \geq 0.9973$ ), indicating a chemical adsorption process, and a contact time of 120 min would be enough to reach the adsorbent-Cr<sup>3+</sup> equilibrium, showing the best adjustment to the Freundlich model ( $R^2 = 0.9291$ ), with a favorable adsorption process, since the obtained value of adsorption intensity ( $n$ ), was 1.5876. So, our results suggest that Cr<sup>3+</sup> ions can be efficiently removed from contaminated waters by using mamey apple peel-based adsorbent, which with a minimum treatment could be used as a low-cost adsorbent, as a potential alternative to traditional methods nowadays used. Finally, further studies are needed to improve the adsorption capacity of the mamey apple peel, such as the evaluation of chemically modified mamey apple peel, in order to elucidate the efficacy of an activated adsorbent.

**Acknowledgements** This study was funded by “Project 20171002: Removal of heavy metals from contaminated waters by agroindustrial wastes” (Universidad Privada del Norte, Trujillo, Peru). The authors thank Yuliana Pairazaman and Julio Gurreonero (Instrumental Analysis Laboratory, UPN, Trujillo, Peru) for their technical assistance.

## References

1. Vilar, V.J.P., Botelho, C.M.S., Boaventura, R.A.R.: Influence of pH, ionic strength and temperature on lead biosorption by *Gelidium* and agar extraction algal waste. *Process. Biochem.* **40**(10), 3267–3275 (2005). <https://doi.org/10.1016/j.procbio.2005.03.023>
2. Ministerio del Ambiente: <http://www.minam.gob.pe/disposiciones/decreto-supremo-n-004-2017-minam/>. Last accessed 05 Jan 2020

3. Ali, A., Saeed, K., Mabood, F.: Removal of chromium (VI) from aqueous medium using chemically modified banana peels as efficient low-cost adsorbent. *Alex. Eng. J.* **55**, 2933–2942 (2016). <https://doi.org/10.1016/j.aej.2016.05.011>
4. Cazón, J., Benítez, L., Donati, E., Viera, M.: Biosorption of chromium(III) by two brown algae *Macrocystis pyrifera* and *Undaria pinnatifida*: Equilibrium and kinetic study. *Eng. Life Sci.* **12**(1), 95–103 (2012). <https://doi.org/10.1002/elsc.201100098>
5. Fahim, N., Barsoum, B., Eid, A., Khalil, M.: Removal of chromium(III) from tannery wastewater using activated carbon from sugar industrial waste. *J. Hazard. Mater.* **136**(2), 303–309 (2006). <https://doi.org/10.1016/j.jhazmat.2005.12.014>
6. Mohan, D., Pittman Jr., C.U.: Activated carbons and low cost adsorbents for remediation of tri- and hexavalent chromium from water. *J. Hazard. Mater.* **137**, 762–811 (2006). <https://doi.org/10.1016/j.jhazmat.2006.06.060>
7. Shrivastava, R., Upreti, R.K., Seth, P.K., Chaturvedi, U.C.: The effects of chromium on the immune system. *FEMS Immunol. Med. Microbiol.* **34**(1), 1–7 (2002). <https://doi.org/10.1111/j.1574-695X.2002.tb00596.x>
8. Gupta, V.K., Kumar, R., Nayak, A., Saleh, T.A., Barakat, M.A.: Adsorptive removal of dyes from aqueous solution onto carbon nanotubes: a review. *Adv. Colloid Interface Sci.* **193–194**, 24–34 (2013). <https://doi.org/10.1016/j.cis.2013.03.003>
9. Campos-Flores, G., Castillo-Herrera, A., Gurreonero-Fernández, J., Obeso-Obando, A., Díaz-Silva, V., Vejarano, R.: Adsorbent material based on passion-fruit wastes to remove lead (Pb), chromium (Cr) and copper (Cu) from metal-contaminated waters. In: *AIP Conference Proceedings*, pp. 020079-1–020079-4. AIP Publishing, Melville NY (2018). <https://doi.org/10.1063/1.5032041>
10. Vejarano, R., Gurreonero-Fernández, J., Castillo-Herrera, A.: Adsorption of lead (Pb) from contaminated aqueous mediums using banana (*Musa paradisiaca*) peel. In: *Proceedings of the LACCEI International Multi-conference for Engineering, Education and Technology*, p. 67. LACCEI Inc., Boca Raton (2018). <https://doi.org/10.18687/laccei2018.1.1.67>
11. Chao, H.P., Chang, C.C., Nieva, A.: Biosorption of heavy metals on *Citrus maxima* peel, passion fruit shell, and sugarcane bagasse in a fixed-bed column. *J. Ind. Eng. Chem.* **20**(5), 3408–3414 (2014). <https://doi.org/10.1016/j.jiec.2013.12.027>
12. Yahia, E., Guttierrez-Orozco, F.: Mamey apple (*Mammea americana* L.). In: *Postharvest Biology and Technology of Tropical and Subtropical Fruits*. Woodhead Publishing Limited, Cambridge, pp 474–482 (2011). <https://doi.org/10.1533/9780857092885.474>
13. Demirbas, A.: Heavy metal adsorption onto agro-based waste materials: a review. *J. Hazard. Mater.* **157**(2–3), 220–229 (2008). <https://doi.org/10.1016/j.jhazmat.2008.01.024>
14. Serrano-Gómez, J., Beltrán, C., Bonifacio-Martínez, J., Olguín, M.: Mamey (*Mammea americana* L.) husks for the removal of Cr(VI) from aqueous media. *Desalin. Water Treat.* **74**, 207–215 (2017). <https://doi.org/10.5004/dwt.2017.20574>
15. Jacques, R., Lima, E., Dias, S., Mazzocato, A., Pavan, F.: Yellow passion-fruit shell as biosorbent to remove Cr(III) and Pb(II) from aqueous solution. *Sep. Purif. Technol.* **57**(1), 193–198 (2007). <https://doi.org/10.1016/j.seppur.2007.01.018>
16. Marín, A., Ortuño, J., Aguilar, M., Meseguer, V., Sáez, J., Lloréns, M.: Use of chemical modification to determine the binding of Cd(II), Zn(II) and Cr(III) ions by orange waste. *Biochem. Eng. J.* **53**(1), 2–6 (2010). <https://doi.org/10.1016/j.bej.2008.12.010>
17. Cruz-Tirado, J.P., Vejarano, R., Tapia-Blácido, D., Barraza-Jáuregui, G., Siche, R.: Biodegradable foam tray based on starches isolated from different Peruvian species. *Int. J. Biol. Macromol.* **125**, 800–807 (2019). <https://doi.org/10.1016/j.ijbiomac.2018.12.111>
18. Mimura, A.M.S., Vieira, T.V.A., Martelli, P.B., Gorgulho, H.F.: Utilization of rice husk to remove Cu<sup>2+</sup>, Al<sup>3+</sup>, Ni<sup>2+</sup> and Zn<sup>2+</sup> from wastewater. *Quím. Nova* **33**(6), 1279–1284 (2010). <https://doi.org/10.1590/S0100-40422010000600012>
19. Tejada-Tovar, C., Villabona-Ortiz, A., Garcés-Jaraba, L.: Adsorption of heavy metals in waste water using biological materials. *Tecnol* **18**(34), 109–123 (2015)
20. Weber, T., Chakraborti, R.: Pore and solid diffusion models for fixed bed adsorbents. *AIChE J.* **20**(2), 228–238 (1974). <https://doi.org/10.1002/aic.690200204>

21. Ho, Y., McKay, G.: Pseudo-second order model for sorption processes. *Process. Biochem.* **34**(5), 451–465 (1999). [https://doi.org/10.1016/S0032-9592\(98\)00112-5](https://doi.org/10.1016/S0032-9592(98)00112-5)
22. Mohd Salleh, M., Mahmoud, D., Abdul Karim, W., Idris, A.: Cationic and anionic dye adsorption by agricultural solid wastes: a comprehensive review. *Desalination* **280**(1–3), 1–13 (2011). <https://doi.org/10.1016/j.desal.2011.07.019>
23. Cooman, K., Gajardo, M., Nieto, J., Bornhardt, C., Vida, G.: Tannery wastewater characterization and toxicity effects on *Daphnia* spp. *Environ. Toxicol.* **18**(1), 45–51 (2003). <https://doi.org/10.1002/tox.10094>
24. Lofrano, G., Meriç, S., Zengin, G., Orhon, D.: Chemical and biological treatment technologies for leather tannery chemicals and wastewaters: a review. *Sci. Total Environ.* **461–462**, 265–281 (2013). <https://doi.org/10.1016/j.scitotenv.2013.05.004>
25. Córdova, H., Vargas, R., Cesare, M., Flores, L., Visitación, L.: Tratamiento de las aguas residuales del proceso de curtido tradicional y alternativo que utiliza acomplejantes de cromo. *Rev. Soc. Quím. Perú* **80**(3), 183–191 (2014)
26. Esmaeili, A., Mesdaghinia, A., Vazirinejad, R.: Chromium (III) removal and recovery from tannery wastewater by precipitation process. *Am. J. Appl. Sci.* **2**(10), 1471–1473 (2005). <https://doi.org/10.3844/ajassp.2005.1471.1473>
27. Mishra, V., Balomajumder, C., Agarwal, V.: Biosorption of Zn (II) onto the surface of non-living biomasses: a comparative study of adsorbent particle size and removal capacity of three different biomasses. *Water Air Soil Pollut.* **211**(1–4), 489–500 (2010). <https://doi.org/10.1007/s11270-009-0317-0>
28. Pathak, D., Sachin, A., Bhaskar, D.: Fruit peel waste as a novel low-cost bio adsorbent. *Rev. Chem. Eng.* **31**(4), 361–381 (2015). <https://doi.org/10.1515/revce-2014-0041>
29. Lihan, M., Nourbakhsh, S., Kilicarslan, S., Ozdag, H.: Removal of chromium, lead and copper from industrial waste by *Staphylococcus saprophyticus*. *Turkish J. Biotechnol.* **2**, 50–57 (2004)
30. Masel, R.: Principles of Adsorption and Reaction on Solid Surfaces. Wiley, Hoboken, NY (1996)



# Method of Estimating River Levels with Reflective Tapes Using Artificial Vision Techniques



Lidia E. López Huamán , Marco Paul E. Apolinario Lainez ,  
and Samuel G. Huamán Bustamante 

**Abstract** Water level measurement in a river is a necessary step for flood prevention. Early recognition of this factor could reduce the vulnerability of the population in the surroundings. In this work, we use frames from videos as images to obtain water level measurement indirectly. We applied digital image processing techniques over these images to perform segmentation, edge detection, and we also applied multiple view geometry techniques as projective transformation in a plane. The proposed method estimates water level in specific locations where it is possible to install a reflective tape with a two-color pattern, used as an indicator of water level. We obtained the segmentation of the section out of the water of the reflective tape and so we get the estimation of water level. Through the relation of the real distances (in centimeters) that have four collinear points, seen from a perpendicular view, with the distances (in pixel unit) of those same points contained in an image, which has undergone a projective transformation. We made testing in a water tank built to this work and the tests produced a percentage error at the range of 0.01–2.06% to a distance of 1.5 m from a wall and 2 m high (location of camera).

**Keywords** Water level measurement · Image segmentation · Projective geometry

## 1 Introduction

Rivers are among the most important hydrographic reliefs present on the coast of Perú. In recent years, floods and river overflow, especially occurring in seasons

---

L. E. López Huamán (✉) · M. P. E. Apolinario Lainez · S. G. Huamán Bustamante  
Instituto Nacional de Investigación y Capacitación de Telecomunicaciones, Universidad Nacional de Ingeniería, Lima 15021, Peru  
e-mail: [lidiaelh@gmail.com](mailto:lidiaelh@gmail.com)

M. P. E. Apolinario Lainez  
e-mail: [mapolinariol@uni.pe](mailto:mapolinariol@uni.pe)

S. G. Huamán Bustamante  
e-mail: [shuaman@inictel-uni.edu.pe](mailto:shuaman@inictel-uni.edu.pe)

summer when the oceanic and climatic phenomenon “El Niño” manifest more strongly, have been increasing and causing more damage than expected in the surrounding areas, such as those caused by the Rímac River (see Fig. 1c). For this reason, the continuous monitoring of water level variation is essential.

Several techniques for measuring the level of water exist, but some are more accurate than others, in proportion to the investment of costs of equipment. Another important consideration is the selection of measurement points of a river basin. Normally, this task is in charge of the National Meteorological and Hydrological Service of Peru (SENAMHI) and the National Authority of Water (ANA). The automatic hydrological stations are used for measuring the level of rivers and rainfall, using pressure, bubble and radar meters (see Fig. 1a, b); the latter being the most popular [1, 2].

In this work, we focus on water level monitoring using artificial vision techniques, which are based on digital image processing for the acquisition of characteristics and interpretation of them, on the images acquired by an RGB video surveillance camera. The visual stability of the camera is essential for level measurement, so it is necessary to install it in a high area of the riverbank.

The objective of this work is to propose a method for the indirect measurement of the river level, using simple elements, such as a camera and a measurement indicator (see Fig. 1d) that has a color pattern for the differentiation of the variation of the water level. Then, we used computer vision techniques to perform a segmentation indicator as an object for the projection of its geometric characteristics and thus estimate the value of the water level.

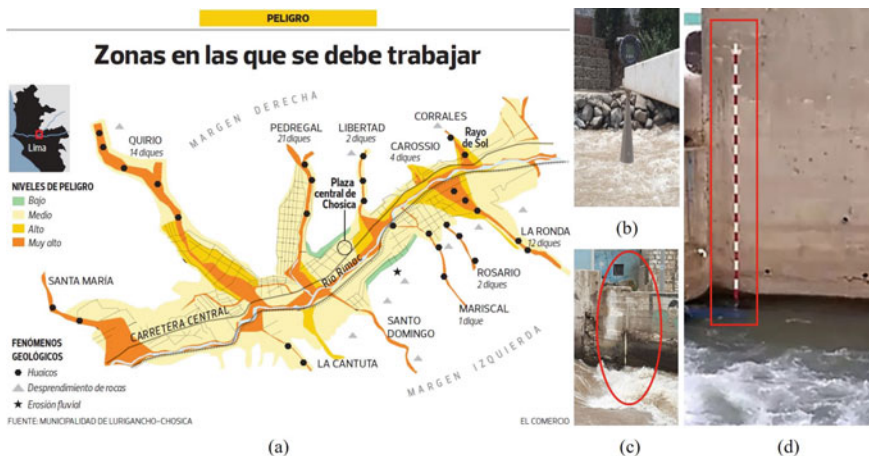


**Fig. 1** Area for which the study method is proposed. **a** Risk map of the sector in Chosica [11]. **b** Radar meter nearest and **c** limiter, in the area of the Rímac River in Chosica, San Juan de Lurigancho, Lima—Perú. **d** Proposal for the river level indicator based on reflective tape

## **2 Methodology**

### ***2.1 Water Level Estimation System Requirements***

As the main point, we have to consider the use of a water level indicator. In this study, we have chosen a reflective tape with a red and white color pattern as the indicator. This tape is commonly used to make objects or vehicles visible to reflections of low-intensity light sources, so its use is quite wide. In this case, the color and light refraction properties are critical because it can be easily seen at night, allow us continuous monitoring with the help of an external source of illumination; thus, reflective tapes become an alternative regarding the use of Near-Infrared (NIR) cameras [3].

On the other hand, the location of the acquisition system, especially the camera, must be installed in a high and fixed area [4] (in the study area of the Rimac River, a height of four meters must be exceeded in order to visualize the other bank). The camera view is in the direction of the other end of the riverbank, with a view capable of capturing from the deepest area of the river to the top of the level indicator. These conditions are taken into account when testing in a controlled environment as a water tank. If it is desired to have monitoring when the light is low, it will be necessary to implement a lighting system (flash or infrared) to take advantage of the reflective properties of the water level indicator.

### ***2.2 Processing Stages and Estimation of Water Level***

#### **2.2.1 Image Acquisition**

For this study, the acquisition of images was done previously using a digital camera NEX-7 SONY [5] with which video samples were taken during the time that the filling of the conditioned room for the sampling of the simulated water level variation took.

Subsequently, the processing of the videos obtained was analyzed to select the frames where the level variation was notable; the images are presented in the results stage. An algorithm was implemented to visualize the values obtained from measurement using the MATLAB software installed in a laptop that was used.

#### **2.2.2 Pre-processing and Segmentation for Water Level Measurement Indicator**

At this point, we followed the steps presented in the scheme of Fig. 2d. From the images obtained from a video, a cut of the area of interest [6, 7] will be made that contains the measurement indicator (reflective tape) located in the most uniform and stable area of the river. First, an analysis was made of the different color models that

can be obtained from an image, such as RGB, HSV, YCbCr,  $L * a * b$  and NTSC. The RGB model allows us to differentiate the colors of the tape, to highlight in one case the red color was raised by SR, see the Eq. (1), and in the white case SB, see the Eq. (2). It is necessary to determine the thresholds and the area of the submerged segments over the total of the analyzed area, [8].

$$SR = R1 - G1 \tag{1}$$

$$SB = R1 / (255 - B1 + 1) \tag{2}$$

The objects out of the water will be displayed later on the determination of the threshold. To reduce the number of pixels in resulting images, which form smaller objects and do not belong to the white and red objects of the indicator, is performing dilation, erosion, filling of internal pixels and deletion of unconnected objects. With this, we obtained better binary segmentation of the water level indicator. Then, we apply a technique for edge detection [9] and find the coordinates, on the new object detected, of its centroid and a point located on each side of the edge that is collinear with the centroids of the red and white segments. This procedure is applied to each of the objects with the highest number of pixels present in the masks of the red and white colors, obtained separately.

In total, four points are imported, among these are the centroid of the object of the largest white segment that is one closest to the chamber (point  $C'$ ), the centroid of the object of the red segment (point  $B'$ ), the points located on the lower ( $D'$ ) and upper ( $A'$ ) points of the river level indicator. The objects containing  $B'$  and  $C'$  points are imported because those have the least deformation of pixels in the image.

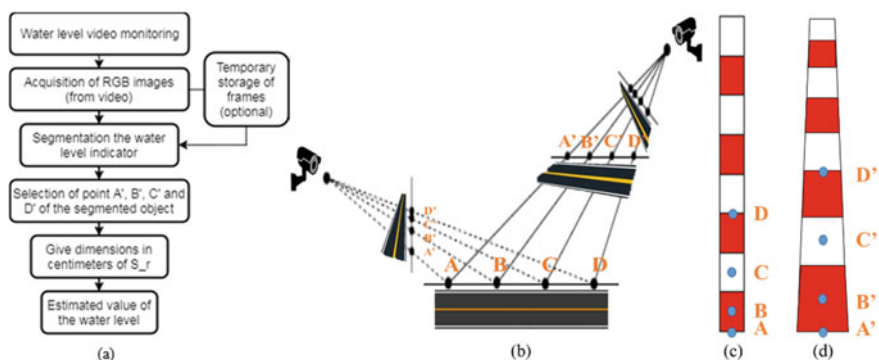


**Fig. 2** **a** Scheme of the proposed methodology. **b** Each set of points ( $ABCD$ ) is related to the others ( $A'B'C'D'$ ) by a line-to-line projectivity since the cross-ratio (CR) is an invariant under a projectivity. **c** Location of four points on the reflective tape and **d** in the projective transformation of its image

According to the concept of the cross-relationship invariance under projective transformation and single-view metrology [10]. The four points  $A, B, C,$  and  $D$  (see Fig. 2) remain invariant in an image and their distances have the relationship as shown in Eq. (3) which is the function CR (cross-radio).

$$\begin{aligned} CR(A, B, C, D) &= (AC/AD)/(BC/BD) \\ &= (A'C'/A'D')/(B'C'/B'D') \end{aligned} \tag{3}$$

From the above equation  $A, B, C$  and  $D$  are points located on the referenced object so  $AC, AD, BC,$  and  $BD$  would become the measured lengths in centimeters between those points. Likewise, the points defined as  $A', B', C'$  and  $D'$ , are the projections of  $A, B, C$  and  $D$ , which are found in the image and the lengths  $A'C', A'D', B'C', B'D'$  are in pixel unit.  $D'$  is a point on the surface of the water (which varies according to the water level). On the tape, the length of each segment, whether red or white, is equal and we define half of this value as the variable  $S_r$  and the length between the  $C$  and  $D$  points as the variable  $xx$  (in centimeters).

Then, considering that the water level will always be bellowing the first red–white segments,  $AC$  will be  $3 S_r$ ,  $AD$  will be equal to  $3 S_r + xx$ . The length of the  $AD$  segment (segment length not submerged) will vary inversely proportional to the water level and will depend on the values of  $xx$  and  $S_r$ .

Finally, replacing the known values in Eq. (3), where the values are in centimeters for the segments  $AC$  and  $AD$ . The  $BC$  segment is equal to  $2 S_r$ ,  $BD$  is equal to  $2 S_r + xx$ . For the second part of the Eq. (3), whose variables are in a pixel unit, we will call it  $Rel\_pixel$  as seen in the Eq. (4).

$$(3S_r/3S_r + xx)/(2S_r/2S_r + xx) = Rel\_pixel \tag{4}$$

We transform the Eq. (4) to solve for a variable  $xx$ , so we got the Eq. (5).

$$xx = 6S_r(1 - Rel\_pixel)/(2 Rel\_pixel - 3) \tag{5}$$

Once the value of  $xx$  has been calculated, we can determine the length of the segment  $AD$  in centimeters ( $Dt$ ) and, likewise, the height of the water level knowing the length of the belt ( $L$ ), as shown in Eqs. (6) and (7).

$$Dt = xx + 3 S_r \tag{6}$$

$$Water\_level = L - Dt \tag{7}$$

### 3 Results and Discussion

As mentioned previously, the measurements were obtained in a controlled enclosure or water tank (see Fig. 3), during the filling of the water tank. The water level fills out about 90 cm for a period of an hour where we tried to simulate the variation in the level of water that can happen in a river. The reflective tape was located on one of the tank walls and then a measuring tape was used to manually register the water level and its comparison with the estimated data obtained by the developed algorithm. After this, the camera was installed at a certain height and distance (it is important to consider the FOV and camera-resolution) where the length of the level indicator can be displayed almost entirely. All these considerations must be taken into account when acquiring the images and installing the system.

Once the images were obtained and saved in a computer, we continued with the digital processing, starting with cropping the area of interest at the length of the tape (with red-black pattern) as a resource to eliminate different objects that they do not matter in our analysis.

On the new image, the determination of the thresholds is to differentiate the red and white areas, with a threshold equal to 70, for segmentation on the red sections present on the surface of the water. In the case of white, there was a greater difficulty in determining the threshold, since the bottom used in the tank wall was also white. Given this, an analysis of the histogram more focused on the area when the water surface divides a segment level indicator, as shown in Fig. 4, obtaining a threshold equal to 2.54.

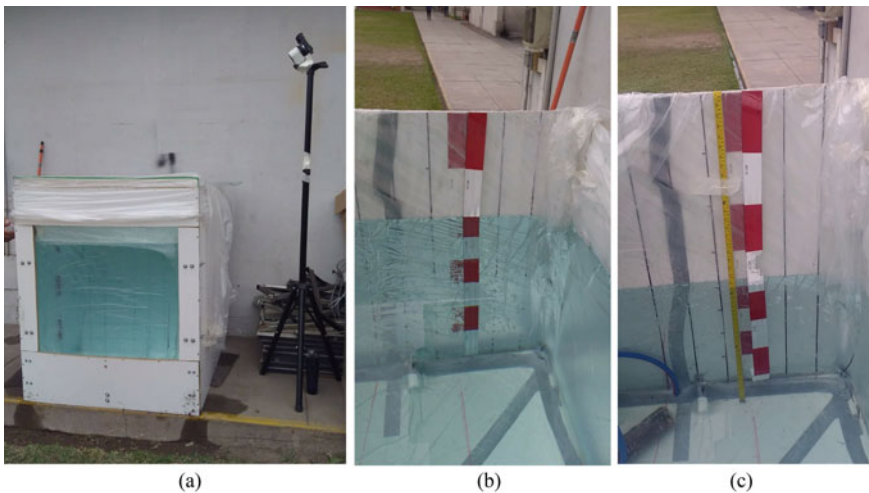


**Fig. 3** a Water tank for measurement level water by the NEX7 SONY camera (in INICTEL-UNI). b Camera view of reflective tape and c tape measure

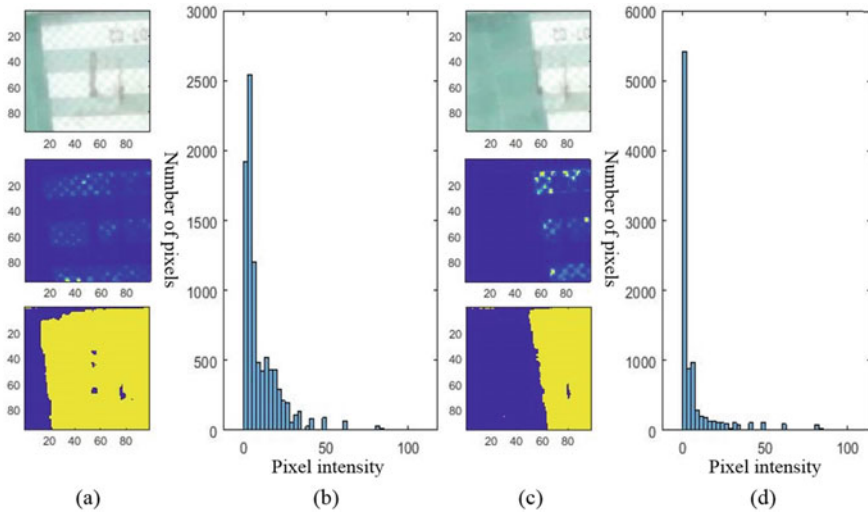


**Fig. 4** Segmentation **a, c** of the tape obtained after the histogram analysis **b, d** to obtain the threshold of white tape segment above the water surface, obtained at a different level of water

Better segmentation of both colors was obtained, using dilation and erosion techniques for the morphological treatment of their masks, which were then integrated to obtain a mask that contains the entire area of interest (region of the tape on the surface of the water), where point  $D'$  was obtained. For both the red and white masks, the centroids of the object with the highest number of pixels were extracted, these being pointed  $B'$  and  $C'$  respectively, present in the Eq. (3). Likewise, the coordinates of point  $A'$  are analyzed by analyzing the object with the greatest dimension on the mask obtained in the red color, and that is how it was possible to obtain the points of interest  $A'$ ,  $B'$ ,  $C'$  and  $D'$  necessary to estimate the distance in pixel unit at which the highest water level is.

It was necessary to know the real distance values between these four points; in our case, the measure of the length of each color segment was 15 cm. Some of the procedures described in the methodology to obtain a mask of the segment of the indicator that is located on the water surface of the acquired images are shown in Fig. 5a.

The accuracy of the water level measurement depends on the resolution of the image contained in the reference indicator and minimizing the deformation effect of the pixels present in the image.

The segmentation performance in this type of indicator was evaluated with the percentage of error presented with the measurement for 47 frames obtained from a video of the monitoring of the variation of the water level in the controlled enclosure. Some of the images and values are shown in Fig. 5.b. Figure 6 shows the experimental results compared with those obtained by us manually, the level of water compared to the estimated real value of different images taken at different times.

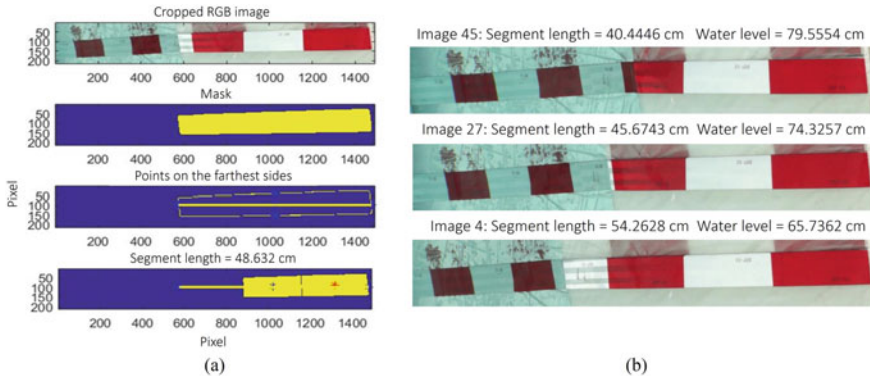


Fig. 5 Values obtained from different water levels

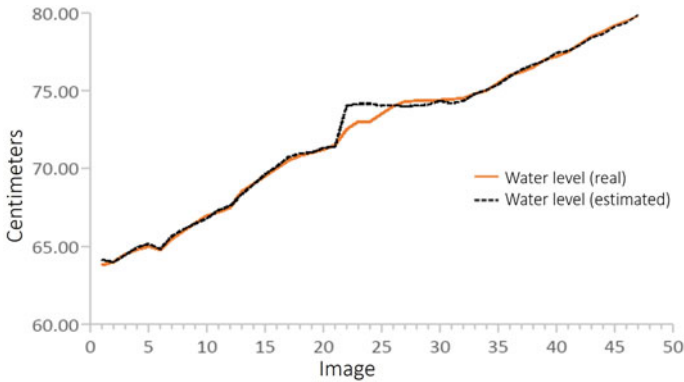
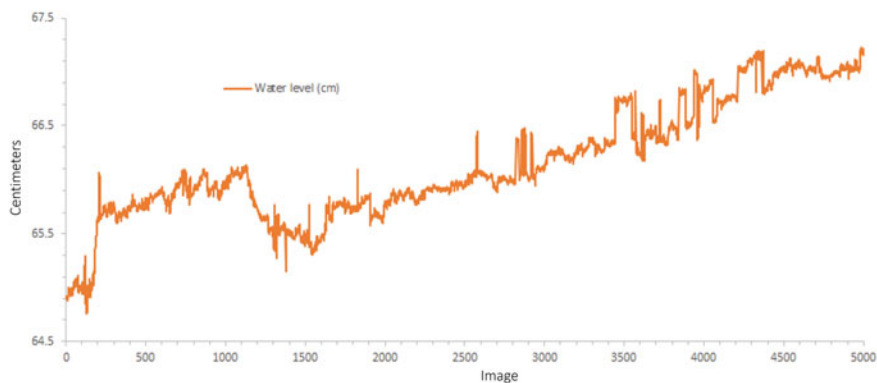


Fig. 6 Curves with values obtained water level when filling a water tank. Level estimation with the proposed method (dashed line), compared with the actual value and measured manually (orange line)

The average error rate of 0.13% was obtained, being the highest error value 2.06%, equivalent to 1.5 cm, and the lowest of 0.01%, equivalent to 0.01 cm, in 47 frames acquired 1.5 m away from the tape and 2 m high with respect to the background.

A video provides frames converted to images for processing by the method explained above. The values are shown in Fig. 7 were obtained with 5000 images that were processed in the MATLAB environment. The graph shows the increase in water level and some variations that are within the average error rate of the proposed method for estimating the water level.





**Fig. 7** Level water values obtained from 5000 images

## 4 Conclusion

In this work, it is demonstrated that a reference indicator with a red–white pattern of colors provides sufficient information to estimate the water level from the RGB images. It is worth saying that to find out a suitable threshold is necessary to properly differentiate the non-submerged area of the indicator.

Additionally, the proposed method is capable to estimate the water level in a water tank, with which a percentage error obtained is in the range of 0.01–2.06%, equivalent to the range of 0.01–1.5 cm, acquired at 2 m away from the belt and 2 m high from the bottom. That percentage of error is low; however, it increases with distance. This is mainly due to the decrease in the resolution of images contained in the reference tape.

**Acknowledgements** The primary support for this project was from INICTEL-UNI, which provided the necessary equipment to carry out this study. We would like especially to thank the team of Signal and Image Processing (G-PSI) of Research and Technological Development Department (DIDT) for their valuable suggestions during this process.

## References

1. Jia, L., Xue, B., Chen, S., et al.: A high-resolution ultrasonic ranging system using laser sensing and a cross-correlation method. *Appl. Sci.* **9**, 1483 (2019). <https://doi.org/10.3390/app9071483>
2. Kato, A., Sinde, R.S., Shubi, K.: Design of an automated river water level monitoring system by using global system for mobile communications. *Int. J. Comput. Sci. Syst. Anal.* **13**
3. Zhang, Z., Liu, Z., Wang, H.: Visual measurement of water level under complex illumination conditions. *Sensors* **19**(19), 4141 (2019). <https://doi.org/10.3390/s19194141>
4. Zhang, Zhen, Zhou, Yang, Liu, Haiyun, Gao, Hongmin: In-situ water level measurement using NIR-imaging video camera. *Flow Measur. Instrum.* **67**, 95–106 (2019)

5. SONY (2011) Equipment camera model Sony NEX-7 SEL-1855. <https://www.sony.es/electronics/support/e-mount-body-nex-7-series/nex-7/specifications>. Accessed 1 July 2019
6. Yu, J., Hahn, H.: Remote detection and monitoring of a water level using narrow band channel. *J. Inf. Sci. Eng.* **26**, 71–82 (2010)
7. Lin, Y.-T., Lin, Y.-C., Han, J.-Y.: Automatic water-level detection using single-camera images with varied poses. *Measurement* **127**, 167–174 (2018). <https://doi.org/10.1016/j.measurement.2018.05.100>
8. Hasan, I.: An effective camera based water level recording technology for flood monitoring. In: INTERPRAEVENT Conference Proceedings, pp. 290–295 (2016)
9. Solomon, C., Breckon, T.: *Fundamentals of Digital Image Processing a Practical approach with examples in Matlab*, pp. 63–76 (2011)
10. Hartley, R., Zisserman, A.: *Multiple View Geometry in Computer Vision*, 2nd edn, pp. 44–46. Cambridge University Press, Cambridge (2003)
11. El comercio (2015). Chosica: no existen estudios de las quebradas de riesgo. <https://elcomercio.pe/lima/chosica-existen-estudios-quebradas-riesgo-356568-noticia/?ref=ecr>. Accessed Nov 2019

# Design and Implementation of a Hydro-Energetic System in Water Distribution Networks



Lenin Jiménez , Cecilia Luna , Manuel Quiñones-Cuenca ,  
and Holger Benavides 

**Abstract** This thesis details the design and implementation of a prototype for hydro-energetic use in water distribution networks. The prototype is composed of two main systems. On one hand, the generation system, which is in charge of transforming the kinetic energy of water into electrical energy using microturbines, charge regulators and batteries. The second one is the drive and telemetry system. It controls whether the generation units turn on or off as well as allowing remote monitoring of electrical parameters such as power, voltage and current of each unit. The device that monitors the generation units is connected to the charge controller through an RS232 interface and enables acquiring the desired electrical parameters to later store them in an Internet of Things platform to visualize them through the Internet.

**Keywords** Drive and telemetry system · Electrical energy · IoT · Microturbines

## 1 Introduction

Nowadays, wireless sensor networks (WSNs) with a large number of sensor nodes allow interaction with the physical world, which is why they are widely used in industrial applications and also in monitoring physical and environmental variables

---

L. Jiménez (✉) · C. Luna · M. Quiñones-Cuenca  
Departamento de Ciencias de la Computación y Electrónica, San Cayetano Alto, Loja, Ecuador  
e-mail: [leninj\\_0995@hotmail.com](mailto:leninj_0995@hotmail.com)

C. Luna  
e-mail: [mcecil\\_1996@hotmail.com](mailto:mcecil_1996@hotmail.com)

M. Quiñones-Cuenca  
e-mail: [mfquinones@utpl.edu.ec](mailto:mfquinones@utpl.edu.ec)

H. Benavides  
Departamento de Geología y Minas e Ingeniería Civil, Universidad Técnica Particular de Loja,  
San Cayetano Alto, Loja, Ecuador  
e-mail: [hmbenavides@utpl.edu.ec](mailto:hmbenavides@utpl.edu.ec)

[1]. Like many technological advances, the WSNs had their origin in military applications. The Sound Surveillance System (SOSUS) was the first WSN application developed by the United States Militia in 1950 to detect and track Soviet submarines [2].

In the WSNs, the sensor nodes are responsible for capturing data and transmitting it over the network. A large amount of captured data and the process of transmission implies a continuous operation of each of the sensors [3]. These are powered by batteries that hardly provide long-term operation and need to be replaced periodically, making constant maintenance of the network nodes necessary [4].

Researchers have explored multiple alternative forms of energy acquisition to power wireless sensor networks such as solar panels, electromagnetic radiation, water or wind flows [5]. That is why the energy harvesting has emerged as a technique that allows extending the lifetime of the sensors by making use of the available energy in the environment to keep the nodes in constant operation within the network [1]. Among many sources of energy, water flow has been used to power WSN nodes [6] using small hydro-generators placed in irrigation systems or water pipes [7, 8].

The use of a TRD microturbine, whose operation depends on a control system, has been proposed to take advantage of water flow energy. The amount of energy that microturbines can contribute is directly related to the pressure of the circulating water [9].

The control system associated with the microturbine allows its continuous status observation, this being of great importance to determine if it is supplying enough energy and if its operation is optimal. So, it is convenient to store this information in an Internet of Things (IoT) platform to remotely monitor the system.

In this context, an energy generation system designed and built to power telemetry systems, as well as the control and monitoring system previously mentioned.

## 2 Methodology

This work aims to develop an autonomous system that uses TRD microturbines in hydraulic installations to power a node of a wireless sensor network that monitors water distribution network variables.

First, the TRD microturbine performance was characterized using a hydraulic bench and a pressure-break tank (generation system) to contrast with the parameters established in the manufacturer's datasheet. From this, it was determined what is the amount of energy generated by the microturbine as a function of the flow rate and the pressure that passes through the pipe.

Then, the energy consumption of the central node of the "SMART WATER NETWORK" project was obtained in each of the processes that it performs (active, reception and transmission of data) to determine the battery that will be used to keep the node active 24 h/day.

Next, the telemetry and drive system of the generation units was designed and built. This system obtains electrical parameters (voltage, current, power) of the microturbines and sends this information to an IoT platform. First, the design was carried out at hardware level, establishing the necessary components to obtain the electrical parameters of the generation units and then the algorithm to be used was developed.

Finally, the generation system and the telemetry and drive system were integrated into the UTPL Hydraulics Laboratory to observe the operation of these two systems as a whole.

### 3 The Electrical Energy Generation System

#### 3.1 TRD Microturbines Energy Efficiency

Table 1 shows the materials and equipment used in the project:

To characterize the microturbines, it was necessary to use a hydraulic bench. The hydraulic bench was built in the UTPL Hydraulics Laboratory. A diagram of the arrangement of the materials used for characterization within the hydraulic bench is shown in Fig. 1.

In Fig. 1, two instruments for measuring hydraulic parameters are identified: flow sensor and pressure gauge, which are used in order to know the pressure and flow that reaches the turbine. There is also a pump that is responsible for sucking the water located in a tank to push it toward the hydraulic circuit. In addition to this, a load is connected to the turbine generator’s output.

**Table 1** Equipment and materials

Detail	Quantity
TDR microturbine	5
Smart charger	5
Electrovalve	5
Phoenix inverter	5
12 V Bosch battery	5

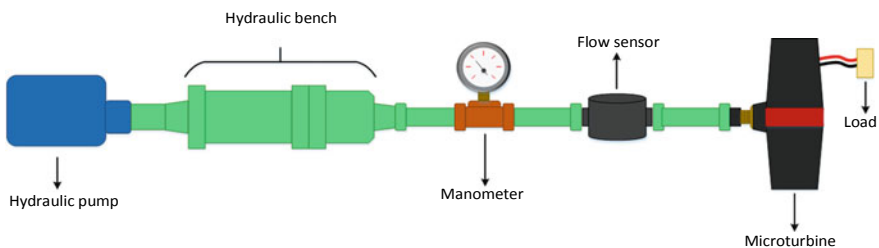


**Fig. 1** Microturbines characterization scheme

**Table 2** Obtained pressure and flow rate values

Pressure (bar)	Flow (l/min)	Hydraulic power (W)
1	6.98	11.63
1.5	8.23	20.49
2	9.3	30.88
2.5	10.26	42.58
3	11.11	55.33
3.5	12	69.72
4	12.72	84.46
4.5	13.38	99.95
5	14.08	116.86

Considering the characterization made by the manufacturer of microturbines, certain pressure values are taken as a reference to measure: voltage, current and flow rate. Tables 2 and 3 show the results obtained regarding the variables of pressure, flow rate, and power generated by each of the microturbines, respectively.

From the previous results, the performance curve of each microturbine is obtained. Now we contrast the performance curve of each microturbine with the information specified by the manufacturer in the datasheet. The performance curves obtained for the five turbines and the one specified in datasheets from the manufacturer are shown in Fig. 2.

The performance or efficiency of a turbine is defined by the relationship between the input power ( $P_{in}$ ) and the output power ( $P_{out}$ ). In this case, they are hydraulic power ( $P_{in}$ ) and electric power ( $P_{out}$ ). Knowing these values from previous results, we have the turbine efficiency at an average of 15.15%; although it exceeds what is specified by the manufacturer that is 10.41%, it is still low determined that the efficiency of a DC generator is between 45 and 50%.

**Table 3** Energy generated by the microturbines

Pressure (bar)	Electric Power (W)				
	Turbine #1	Turbine #2	Turbine #3	Turbine #4	Turbine #5
1	1.05	1.13	1.43	1.35	1.18
1.5	2.63	2.38	2.93	3.20	2.66
2	4.42	4.18	5.05	5.30	4.51
2.5	5.64	6.44	7.02	7.93	6.61
3	8.04	8.91	9.32	9.98	8.77
3.5	9.97	10.95	11.70	12.87	11.54
4	12.12	13.61	14.88	15.31	14.02
4.5	14.40	15.57	17.30	17.76	16.37
5	18.03	17.95	17.86	19.89	18.72

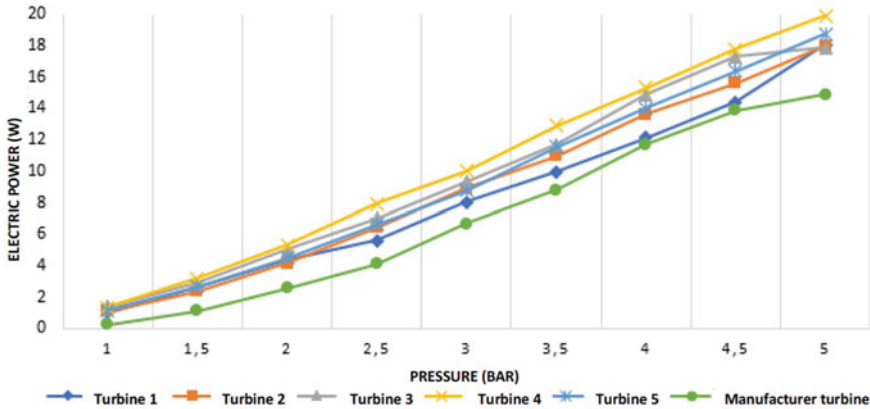


Fig. 2 Microturbines performance curve

### 3.2 Integration of Generation Units and Components in the Pressure-Break Tank

This section describes the implementation of the system, that is, each generation unit (microturbines) is installed, inside a pressure-breaking tank designed. This tank, like the hydraulic bench, is located in the UTPL Hydraulics Laboratory. The materials mentioned in Table 1 are used for the implementation.

The tank is built with galvanized iron sheets 0.9 mm thick. It has a layer of anticorrosive paint that helps it not rust and remain in good condition. The pressure-breaking tank is intended to dissipate energy and decrease hydrostatic pressure [10].

Figure 3 shows the energy generation system which consists of the following parts:

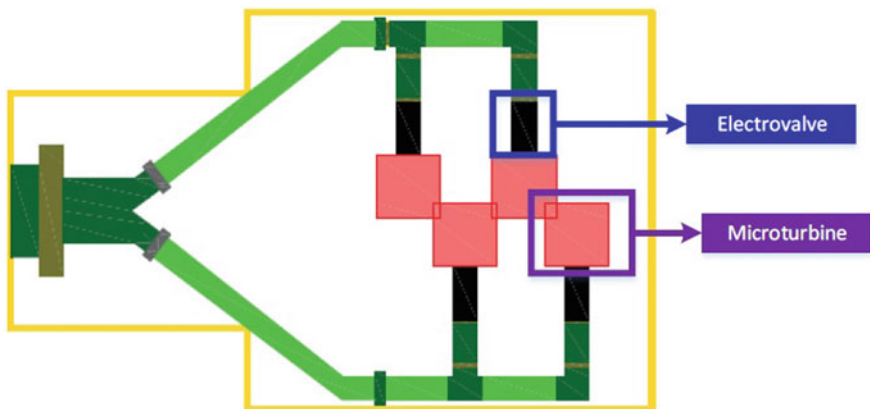


Fig. 3 Arrangement of turbines and components in the pressure-breaking tank

- 4 microturbines,
- 4 electro valves,
- 4 smart chargers,
- 4 batteries and,
- 4 inverters.

The smart chargers are located in a DIN rail that is attached to the side of the tank as well as the batteries. Each battery has an inverter connected to it. Additionally, the tank has iron hooks welded inside to support the weight of the turbines and keep the pipes fixed.

## 4 Drive and Telemetry System

This section shows the design and implementation of the drive and telemetry system of the generation units (GUs). This system must fulfill two objectives. First, to obtain electrical parameters such as voltage, current and power of each GU automatically and send this data to an IoT platform. And second is to guarantee a 24-hour functional generation system that maintains and adequate rest margin for the GUs.

The electrical parameters are provided by the smart charger through an RS-232 interface and to establish communication with it is necessary to login with user and password credentials. For the automatization, a relay board is used to activate and deactivate the GUs using a microcontroller. A general scheme of the whole system is shown in Fig. 4.

### 4.1 System Hardware and Connection

The drive and telemetry system is physically integrated by the following devices: Waspnote Pro V1.2 data acquisition board, Atlas Scientific 8:1 UART port multiplexer, RS-232 to TTL converter, a communication module, RJ11 connectors and a 4 relay board.

### 4.2 PCB Design

Figure 5 shows the PCB design composed on three MAX-232 integrated circuits, a 5 V regulation source, sockets for the connection between the MAX232 and the multiplexer and sockets for the connection between the Waspnote Pro card and the multiplexer.



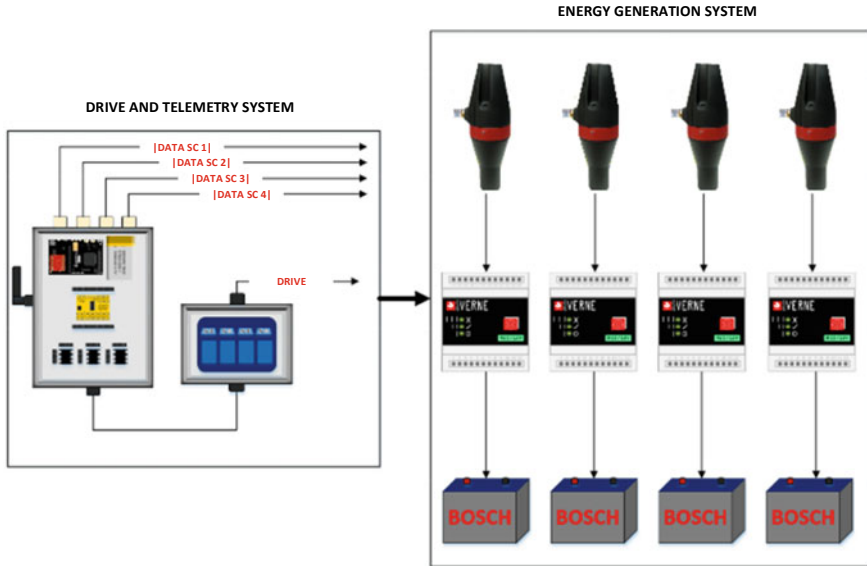


Fig. 4 Complete system general diagram

### 4.3 System Algorithm

Once the components have been established, an algorithm is developed to make use of this hardware. The proposed algorithm activates the GUs in pairs; this way the pressure in the hydraulic system remains almost constant and guarantees 24 h/day energy generation. Also, it makes the login in each smart charger in order to obtain the electrical parameters and sends this to the cloud.

As mentioned before, the GUs work in pairs, but the operation time is limited to 30 min for each pair. This allows a great rest margin for the GUs (required by the smart charger). When a transition is going to occur, the algorithm establishes a 15-second delay which is considered fundamental from the hydraulic point of view to avoid any damage to the turbines or pipeline. This means that the hydraulic system will not suffer pressure transients that at some point can lead to its collapse.

## 5 Results

### 5.1 Energy Generation System Implementation

Once the generation units are placed together with their components in the tank, the wiring is carried out, based on the user manual provided by the manufacturer [11]. As showed in Fig. 6 and 7, the microturbines are arranged inside the tank. PVC gutters

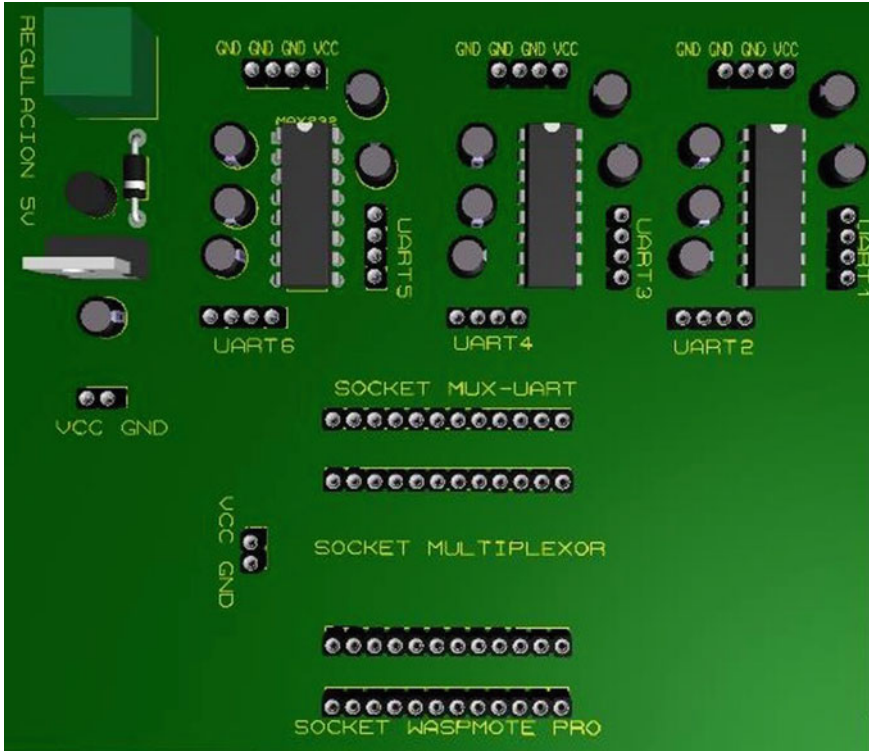


Fig. 5 PCB design for hardware connection

are used in order to properly organize wiring and improve aesthetics. Switches are also used to turn and off the smart chargers.

### 5.2 Power of the Installed System

For this analysis, the data obtained in Table 3 are used. It is worth mentioning that the data taken into consideration are those corresponding to 3 and 3.6 bar pressure has given that the smart charger works in that range. Table 4 shows the average power generated by the turbines that are part of the generation system.

The installed power of the system is obtained by adding the power generated by each of the turbines; therefore, an installed power of 42.51 W. is obtained. Each of the generation units operates 12 h a day and in groups of two, therefore, the entire system works 24 h a day. Taking this information into account, the energy generated by the entire system is 510.12 Wh/day.



**Fig. 6** Generation system installed in the pressure-breaking tank at UTPL Hydraulics Laboratory, top view

### ***5.3 Hardware Integration and Software Implementation***

Figure 8 shows the designed PCB, the multiplexer and the Waspnote Pro card together with its battery. These devices are grouped inside an airtight box protected from water and dust.

On the other hand, the algorithm was implemented through the Waspnote IDE version 06.04. It consists of several functions that allow fulfilling everything previously stated in the algorithm.

The main result of the implemented code is shown in Fig. 9. Parameters such as voltage, current, power, time of use are considered. All the data obtained is stored within a matrix and it is through the positions that these values occupy in the matrix that the value of each parameter can be obtained.

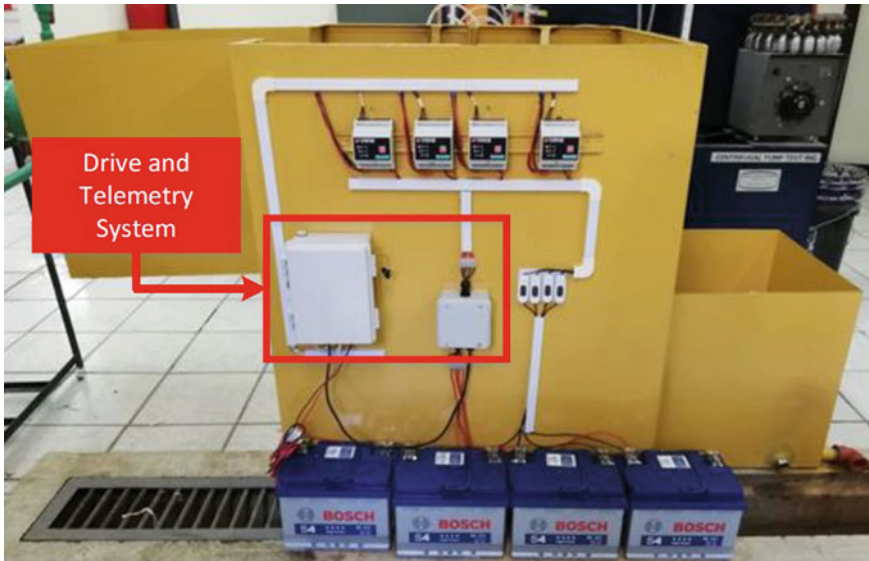


**Fig. 7** Generation system installed in the pressure-breaking tank at UTPL Hydraulics Laboratory, side view

**Table 4** The average power generated by each GU

Detail	Power (W)
GU #1	10.15
GU #2	10.51
GU #3	10.43
GU #4	11.42

### 5.4 Pressure Measurement in GU Transition

The generation system consists of 4 GU which work in pairs. That is, once the working units have reached 30 min of operation, they are turned off so that the other pair of GUs starts to work. When a UG is switched on and off, a pressure transient is produced in the hydraulic system. To avoid any damage to the system, the pressure variation in the on and off process must be as small as possible.

In order to quantify the pressure variation at the time one GU started the transition, the system was monitored with an MLH pressure sensor. The experiment consisted of measuring the instantaneous pressure of the system every 5 seconds to obtain the data while a GU was making a transition.

Figure 10 shows that the pressure ranges from 3 to 3.6 bars, with an average pressure of 3.3 bars, which is within the range allowed by the smart charger. As view in Fig. 10, there are two times when transitions occur (described as t1 and t2) where the pressure value decreases to 2.73 and 2.69 bar, resulting in variations of 0.57 and 0.61 bar of the average system pressure. The implemented algorithm forces these variations to be small in order to avoid any damage to the system.



Fig. 8 Hardware implementation

### 5.5 Data in an IoT Platform

In this work, the ThingSpeak platform is used. After the drive and telemetry systems obtain the electrical parameters, this is upload to the cloud. In the platform, four channels were created for each GU. In each channel, variables of voltage, current, power, time and state are stored. The write “APIKEYS” of each channel was added to the algorithm so the code knows where to send the data.

```
[2J

System Verne V1.0

Login: root
Password: ****

Command$
staus
Time:          00:23:56
Temp:          24,016 C
Vols:          12,628 V
Current:       0,914 A
Poewr:         11,5 W
Duty:          0,0 PWM
DutyPower:    0,0 W
Status: Run_Regulator_Current
Command$
```

Fig. 9 Smart charger login and electrical parameters

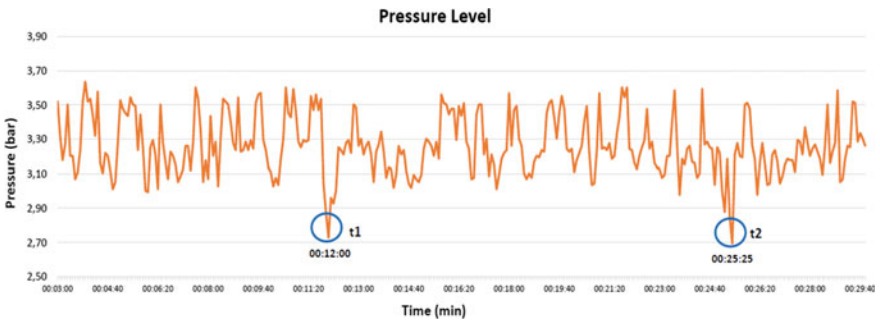


Fig. 10 Pressure variation in GU transitions

## 6 Conclusions

The implemented system uses the energy accumulated in water distribution lines to generate electricity. The system, which operates twenty-four hours a day, generates 510.12 Wh/day. In addition, the drive and telemetry system allows monitoring the status of the microturbines in real time as well as sending this data to an IoT platform.

In terms of electrical generation, the microturbines generate 10 to 11.5 W in the pressure ranges in which the smart charger works. Although they exceed the generation parameters established by the manufacturer, their energy efficiency, which is 15.15%, is low considering that the efficiency of a DC generator is between 45 and 50%.

The drive and telemetry system implemented allows for a 24-h functional generation system. In addition, thanks to this system, turning on and off the GUs does not produce large pressure variations, thus providing protection to the hydraulic system.

The use of other types of energy in sensor networks and IoT applications, apart from solar energy, makes these systems more robust and independent. For the specific case of the coordinating node, which cannot make use of rest functions due to the role it plays within the network, it is important to guarantee its energy autonomy by using energy generation systems such as the one developed in this paper.

## 7 Recommendations

VERNE, the manufacturer of the microturbines and smart chargers used in this work, is currently not operating, so there is little availability of information about the devices. It is recommended that for similar developments, the devices used should be from a manufacturer that is active in the market in case of requiring detailed information.

For the energy generation system, it is recommended for field applications to place a bypass to limit the fluid pressure at the system entrance. Also, this is necessary to carry out maintenance on the deployed electronic devices.

The pressure in the system must remain within a set range, and in a laboratory environment, it is easy to monitor and regulate this parameter. However, if deployed, it is recommended to implement an additional control system that constantly measures the pressure in the system to regulate it if necessary. The information obtained may also be available on an IoT platform.

Prior to the construction of the pressure-breaking tank, the design must consider the measures of all the elements to use in the energy generation system. These include microturbines, solenoid valves, pipes, elbows, joints, among others. Otherwise, space, where the generation units are located, will be limited resulting in additional adjustments to the tank.

In the case of deploying the system, protection for batteries and smart chargers must be considered. The batteries should be stored in a place where they are protected

from sudden changes in temperature. In addition, this place must have ventilation so that toxic gases are not stored. As for the chargers, they must be protected from rain as recommended by the manufacturer.

If the system is deployed and there is cellular coverage on the deployment area, it is recommended to use the mobile network to send data to the IoT platform. In addition, instead of HTTP, use the MQTT protocol in order to reduce costs.

## References

1. Kamruzzaman, S.M., Fernando, X., Jaseemuddin, M.: Energy Harvesting Wireless Sensors for Smart Cities, pp. 218–222 (2017)
2. Silicon Labs, The Evolution of Wireless Sensor Networks (2013)
3. K.Z. Panatik et al.: Energy Harvesting in Wireless Sensor Networks : A Survey, pp. 28–30 (2016). K. Elissa, Title of paper if known, unpublished
4. Azevedo, J.A.R., Santos, F.E.S.: Energy harvesting from wind and water for autonomous wireless sensor nodes. *IET Circ. Devices Syst.* **6**(6), 413–420 (2012)
5. Chaudhry, B.S.: Energy consumption and harvesting in WSNs: Challenges and solutions. In: 2017 International Conference on Innovations in Electrical Engineering and Computational Technologies (ICIEECT) (2017) pp. 1–2
6. Mecocci, A., Peruzzi, G., Pozzebon, A., Vaccarella, P.: Architecture of a hydroelectrically powered wireless sensor node for underground environmental monitoring. *IET Wirel. Sens. Syst.* **7**(5), 123–129 (2017)
7. Morais, R., et al.: Sun, wind and water flow as energy supply for small stationary data acquisition platforms. *Comput. Electron. Agric.* **64**(2), 120–132 (2008)
8. Mohamed, M.I., Wu, W.Y., Moniri, M.: Power harvesting for smart sensor networks in monitoring water distribution system. In: 2011 International Conference on Networking, Sensing and Control, 2011, pp. 393–398
9. Grupo Verne.: Microturbina TRD (2015). (Online). Available: <http://grupoverne.com/productos/microturbina-trd>. Accessed 01 Feb 2017
10. Vivanco, C., Comunicación oral: Tanque rompe-presión (2018)
11. Grupo Verne.: Microturbina TRD. Manual de Usuario (2015)



# Hydraulic Fill Assessment Model Using Weathered Granitoids Based on Analytical Solutions to Mitigate Rock Mass Instability in Conventional Underground Mining



Cristhian Portocarrero-Urdanivia , Angela Ochoa-Cuentas , Luis Arauzo-Gallardo , and Carlos Raymundo 

**Abstract** This study uses analytical solutions to assess a hydraulic fill model based on weathered granitoid to increase underground opening stability and mitigate rock bursts during mining operations in a conventional underground mining company located in the Coastal Batholiths of the Peruvian Andes. This study assesses the previous geological database provided by the mine, analyzes the on-site strengths produced by the exploitation works that will subsequently be filled, identifies the quality of the material used in the landfill (granitoids) through laboratory tests, and compares compressive strength at different depths, all contemplated within the landfill model used. This study focuses on the applicability of hydraulic fills in conventional underground mine using natural geological material such as granitoid.

**Keywords** Hydraulic fill · Granitoids · Conventional underground mining · Instability · Analytical solutions · Rock bursts

## 1 Introduction

The mining industry is one of the economic pillars that drive the development of several countries, such as Canada, Australia, and South Africa, relying on innovative

---

C. Portocarrero-Urdanivia · A. Ochoa-Cuentas · L. Arauzo-Gallardo · C. Raymundo (✉)  
Escuela de Ingeniería de Gestión Minera, Universidad Peruana de Ciencias Aplicadas (UPC),  
Lima 15023, Peru  
e-mail: [carlos.raymundo@upc.edu.pe](mailto:carlos.raymundo@upc.edu.pe)

C. Portocarrero-Urdanivia  
e-mail: [u201517258@upc.edu.pe](mailto:u201517258@upc.edu.pe)

A. Ochoa-Cuentas  
e-mail: [u201517180@upc.edu.pe](mailto:u201517180@upc.edu.pe)

L. Arauzo-Gallardo  
e-mail: [pccilara@upc.edu.pe](mailto:pccilara@upc.edu.pe)

technologies in open pit or underground mines [1]. In South America, countries such as Chile, Peru, and Brazil have exploited their mining resources for later commercialization. Although large, medium, and small mining operations are developed in some countries, accidents take place across all the mining operations. Some clear examples of these accidents are rock mass instability produced by the extraction of mineral ore, rockfalls, worker slips, trips, and falls, and poisoning–asphyxiation.

This study selected rock mass caused by mineral ore extraction as a key issue affecting conventional underground mining. Within this analyzed context and due to the different problems identified over time, this particular matter was deemed critical for the mining industry because exploited opening instability generates empty spaces subject to various stress and forces that increase with depth, thereby preventing resource exploitation operations. Hydraulic fill is currently used in Peru with several aggregates, such as cement, in large and medium mining operations. However, it is not yet used in conventional underground mining owing to its high cost and additives that must be added to the landfill to increase its resistance. Therefore, this study proposes adapting hydraulic fills with granitoid in a conventional underground mine. At the Marsa mining company located in the Pataz batholith, hydraulic fills were supplemented with granitoid and rock bursts were successfully controlled and safe operation was ensured [2].

This study aims to demonstrate the application of hydraulic fills with granitoid because it is more affordable and adaptable for conventional underground mining operations than other existing solutions, especially because of its short hardening times.

## 2 State of the Art

### 2.1 Hydraulic Fill Method in Underground Mining

Several types of research have investigated the hydraulic fill properties in underground mines and concluded that this type of landfill usually settles at a porosity of approximately 40% and its relative densities are in the range of 40–70% [3]. In addition, when settling as a suspension with 65–75% solid content, these landfills are deposited at a dry density of approximately 0.56 times the specific gravity. Furthermore, the permeability of pulp (10–30 mm/h) is much lower than that desired in the mining industry (100 mm/h) [4, 5].

As a part of their results, some authors agreed that hydraulic fills must ensure good drainage so that the excess water may drain quickly. For achieving a good drainage system, the effective size of the D10 grain must exceed 10  $\mu\text{m}$ . Finally, the literature has shown that when hydraulic fills are mixed as mud with 30% of water content, an extremely dense hydraulic fill is obtained [6, 7].

## ***2.2 Using Granitoids in Hydraulic Fill Models in Conventional Underground Mining***

Very few researches have investigated the application of granitoid to hydraulic fills; however, granite exhibits unique properties that provide better reinforcement to hydraulic fills. In previous research, granite rocks were used in landfills, and favorable results from the viewpoint of percolation, sedimentation, and permeability were obtained [8]. These characteristics help us better identify the properties exhibited by granites as an aggregate in hydraulic fills, thereby improving percolation, permeability, resistance, and hardness, among others. [9, 10].

## ***2.3 Using Analytical Solutions in Hydraulic Fills in Conventional Underground Mining***

Researchers have considered rock bursts as dynamic disasters that take place when the energy accumulated in the rock mass of the mine is released suddenly, abruptly, and violently. Therefore, these studies used analytical solutions to assess the quality of the rock mass to be filled [10, 11].

Researchers have also claimed that the results obtained using analytical solutions in the landfill, such as the constraining strength and pressures developing in the landfill mass, must be determined according to the geometry of the exploded pits and initial stress conditions [12].

# **3 Contribution**

This hydraulic fill assessment model is based on two concepts: granitoid, i.e., the material used as input, and analytical solutions, which will be a determining factor in terms of design and implementation. The proposed model displays the developed methodological approach and different steps used for predicting hydraulic fill performance properties and streamline its mixing. The methodology includes three main phases: experimental, modeling, and optimization, as presented in Fig. 1.

## ***3.1 Model Components***

**Phase 1** This phase includes the experimental process of the pulp formed by water and granitoid in laboratory tests based on the main parameters and analysis that may affect its strength and consistency. This phase aims to generate inputs, such as granulometry and percolation, through experimental and analytical assessments aligned with the theoretical model.

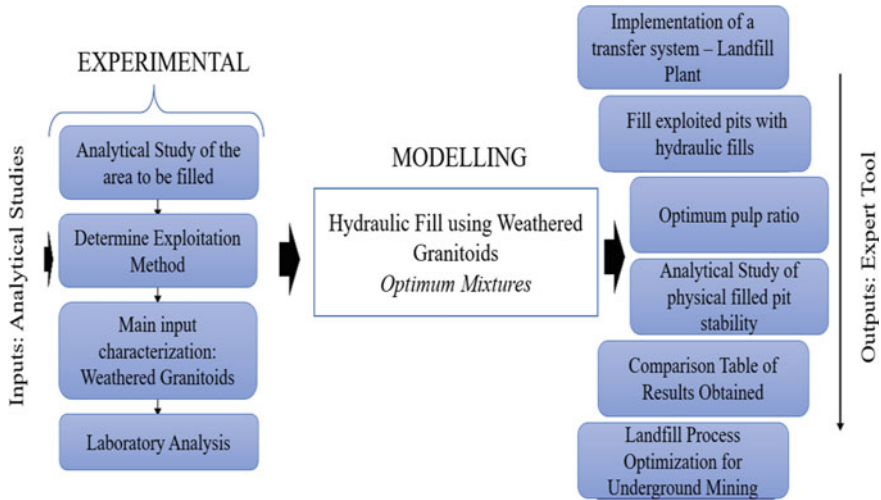


Fig. 1 Applied methodology

**Phase 2** This phase includes simulation of the hydraulic fill model based on analytical solutions and laboratory tests in the established domains and parameters.

**Phase 3** Proposed model validation process: For this purpose, the results obtained are assessed in terms of the following three basic factors: uniaxial compressive strength, slump test, and the costs incurred for its subsequent application. The aim is to optimize landfill improvements by creating optimum mixtures, thereby providing a tool focused on landfills.

### 3.2 Process View

As a first step in the implementation of this type of landfill, the current situation must be analyzed to gather information on the mining site conditions through studies focusing on the rock mass and exploited area that will subsequently be filled. Gathering information regarding the exploitation method and rock mass parameters will provide the basic knowledge related to the compressive strength for which the hydraulic fill is subjected.

The geometric dimensions of the pits to be filled must be established according to theoretical values of the arc, whose width can determine as follows:

$$Wt = (0.15D + 18.3)^{3/4} \tag{1}$$

where:  $Wt$  =Pit width,  $D$  =Pit depth from the surface.

Any value between these parameters will allow the internal pit to withstand a load equivalent to half the width of the pit. However, if the operational requirements are exceeded, the safety factor of 2.5 will have to be used instead of 2.

If the room and pillar mining method are considered, the hydraulic fill using granitoid will recover the alternate pillars by acting as ultimate active support that facilitates the exploitation of the adjacent pit. For structures exceeding 4 meters, mining operations must be performed by level or using another mining method, such as a sublevel stopping method. To determine the volume to be filled, determining the dimensions of an exploded and empty front would be ideal (Fig. 2).

$$F(x) = -\frac{x^2}{1.30} \tag{2}$$

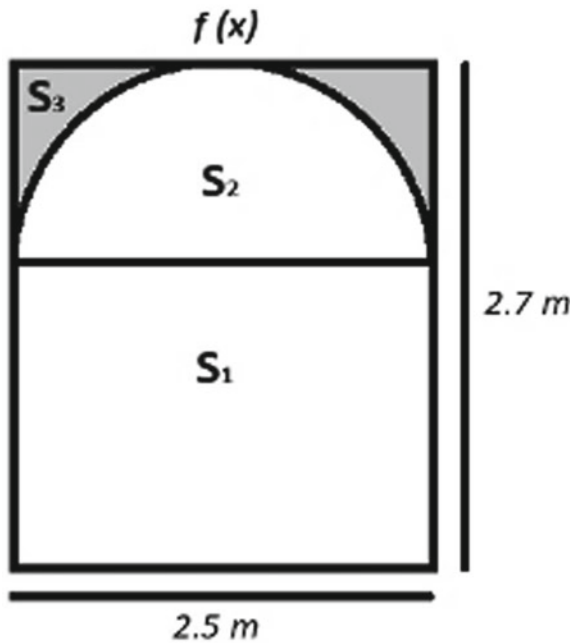
$$S_3 = \int_{-1.25}^{1.25} \frac{x^2}{1.30} dx$$

$$S_3 = 1 \text{ m}^2 \tag{3}$$

$$S_2 = 2.5 \times 1.20 - S_3$$

$$S_2 = 2 \text{ m}^2 \tag{4}$$

Fig. 2 Section pending of filling



Item	BASIC CLASSIFICATION PARAMETERS	Vein		Roof Cavity		Floor Cavity	
		DESCRIPTION	VALUE	DESCRIPTION	VALUE	DESCRIPTION	VALUE
1	Undisturbed Rock Strength	0.33	7	100-250 Mpa	12	100-250 Mpa	12
2	Rock Quality Designation	50-75%	13	50-75%	13	75-90%	17
3	Fracture Span	Under 60 mm	4	Under 60 mm	20	Over 2 m	20
4	Fracture Status	Hard Surface Under 5 mm	4	None	6	Soft Surface Over 5 mm	0
5	Underground Water Conditions	Dry	15	Dry	15	Dry	15
6	Effect from Crack Direction and Dip	Regular	-5	Favorable	-2	Favorable	-2
	Rock Mass Rating	RMR(Vein)	38	RMR(Roof)	64	RMR(Floor)	62
Correlation with Q	Bieniaswki RMR=9lnQ+44	Q(Vein)	0.51	Q(Roof)	9.23	Q(Floor)	7.39
	Barton RMR=15logQ+50	Q(Vein)	0.16	Q(Roof)	8.58	Q(Floor)	6.31
	Unsupported Roof Span (m)		0.3		0.9		0.9

Fig. 3 Rock mass assessment

$$S_1 = 2.5 \times 1.5$$

$$S_1 = 3.75 \text{ m}^2 \tag{5}$$

In addition, a detailed geomechanical assessment was conducted. All the relevant parameters for a conventional underground mine are listed in Fig. 3.

The optimum particle size distribution for the landfill to reach a maximum on-site density that may guarantee the design uniaxial compressive strength value is determined by the Talbot curve because it provides the maximum density required for landfill optimization.

Furthermore, other laboratory calculations were also made, as shown below:

- Specific gravity: To calculate the specific gravity or bulk density, two samples of previously standardized and quartered weatherized granodiorite was extracted. After assessing both samples, an average specific gravity of 2.58 was obtained.
- Material hardness: According to the MOHS scale of mineral hardness, the hardness of weathered granitoid is 4.0. The critical speed of the pulp was 2.59 m/s.
- Pore ratio: It is defined as the ratio between the volume occupied by pores ( $V_p$ ) and that occupied by solids ( $V_s$ ). In a granular mass, the pore ratio is generally 30%.
- Porosity: It was calculated as 64.89%, revealing an excellent porosity rate, which is positive for hydraulic fills since water is quickly percolated. This means that water will flow out of the landfill in less time; therefore, the pulp will also dry faster.
- Solid percentage: The number of solids present in the landfill was 75% of the total weight.
- Sedimentation rate (slump test): First, the granodiorite and water must be mixed in a ratio of 3:1 to form the pulp. Then, the pulp will be gradually filled in the slump at a height of 19 cm, as per the requirements for the slump test. After standing for 3 min, the final height was 18 cm.

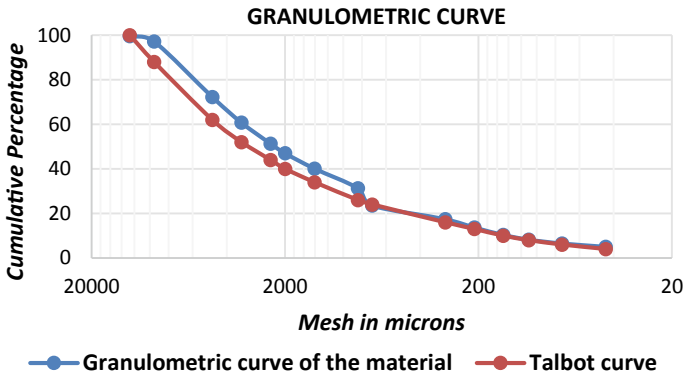


Fig. 4 Comparison against the talbot curve

### 3.3 Indicator View

The function that indicates the amount of strength exhibited by the landfill with granitoid for each meter of the height of the self-established slope was obtained (Fig. 4).

Since the excellent quality of the granitoid exceeds in the Talbot curve, the strength of the proposed models exceeds the required strength, thereby validating the proposed model.

## 4 Validation

### 4.1 Scenario Description

The hydraulic fill system model supplemented by granitoid will be implemented at the San Marcelo Mining project geographically located in the Paucartambo batholith in the Eastern Andes. The study area covers an approximate area of 600 hectares of weathered granitoid from the Quaternary age.

**Current conditions of the San Marcelo Mining Landfill** The required landfill volume is determined based on the current production volume reported by the company, listed as (Table 1).

Based on these results, an approximate landfill volume was determined for a production level of 24,000 t/month with a specific gravity of 3 t/m<sup>3</sup>.

We also identified the volume of the different landfill types currently used, listed as (Table 2).

**Table 1** Monthly production

Method	T.C.S.	Percentage
Overhand cut and fill	16,468.00	76.26
Shrinkage	3154.00	14.61
Advances	1973.00	9.14
Monthly production	21,595.00	100

**Table 2** Landfill progress in meters

Landfill type	m <sup>3</sup>	Percentage
Hydraulic fill	5745.00	77.65
Conventional fill	1654.00	22.35
Total	7399.00	100

## 5 Discussions

The main contribution of this study is that we are using a material that is not common for use in hydraulic fillings, however, its use would bring operational benefits. A detritic filling and a hydraulic filling with granitoid, the difference is that the detritic filling is a mechanical filling, while the hydraulic filling with granitoid is a pulp that will be transported by pipes providing more consistency in the empty spaces (interstium) of the exploited pits. The hydraulic filling with granitoid is a filler specifically suitable for the method of exploitation cut and ascending filler where it will not be necessary to use a lot of cement (cemented hydraulic filler), since the weathering granodiorite in contact with water has a welding effect (clay repellent, plagioclase), which after 5 h percolates all the water creating a consistent platform that allows entering the next guard to continue the programmed exploitation, bringing productivity improvements, reducing operational times and costs. This type of hydraulic filling can be implemented in other types of deposits located exclusively in batoliths (precambrian rocks) since it is a place where granitoid can be found. This type of hydraulic filling is beneficial in gold deposits since many gold companies started with the recovery of the ore (gold) that goes to the tailings, and it would not be feasible to use that same tailing for their mine filling, so they use the hydraulic filling with granitoid, because even this filling allows the recovery of pillars.

## 6 Conclusions

The applicability of hydraulic fill conditions using weathered granitoid is governed by the physical characteristics of the rock mass and exploitation method. Some of the variables applied in this model are the presence of an incompetent roof cavity, subhorizontal veins, variable vein shoot, continuous mineralized structures, and mineral recovery close to 100%. The recovery exhibited by this hydraulic fill model exceeds



95%. Results obtained for this type of landfill using granitoid were the exposure of filled pits exceeding 5 m without requiring cement because a uniaxial compressive strength close to  $0.8 \text{ kg/cm}^2$  was achieved. The proposed hydraulic fill with granitoid would eventually reach the pit; however, considering a case in which the work conducted at a level higher than that at the plant, we hereby propose a pumping system. Different scenarios can be identified to assimilate the on-site stress that the hydraulic fill may withstand. At the depth of 740 m, the horizontal stress considered is at 19.98 and vertical stress is at 28.02 MPa.

We propose the expansion of this research as a contribution to the study of hydraulic fillings in underground mining since its application would imply the improvement of the company as an organization compared to the competition.

## References

1. Dietz, M., Oremek, G.M., Groneberg, D.A., Bendels, M.H.K.: Was ist ein Gebirgsschlag? Zentralblatt Für Arbeitsmedizin, Arbeitsschutz Und Ergonomie **68**(1), 45–49 (2018). <https://doi.org/10.1007/s40664-017-0215-z>
2. Farhad Howladar, M., Mostafijul Karim, M.: The selection of backfill materials for Barapukuria underground coal mine, Dinajpur, Bangladesh: insight from the assessments of engineering properties of some selective materials. Environ. Earth Sci. **73**(10), 6153–6165 (2015). <https://doi.org/10.1007/s12665-014-3841-1>
3. Köken, E., Özarslan, A., Bacak, G.. Weathering effects on physical properties and material behaviour of granodiorite rocks. In: ISRM International Symposium - EUROCK 2016, pp. 331–336 (2016). Retrieved from <https://www.scopus.com/inward/record.uri?eid=2-s2.0-85061015692&partnerID=40&md5=959e2c56486f0ebf5f3ddc715f387a67>
4. Momeni, A., Karakus, M., Khanlari, G.R., Heidari, M.: Effects of cyclic loading on the mechanical properties of a granite. Int. J. Rock Mech. Min. Sci. **77**, 89–96 (2015). <https://doi.org/10.1016/j.ijrmm.2015.03.029>
5. Strozik, G.: Design of underground mine voids filling operations in difficult flow conditions of fly ash—water mixtures. In: IOP Conference Series: Earth and Environmental Science, vol. 174, p. 012014 (2018). <https://doi.org/10.1088/1755-1315/174/1/012014>
6. Yang, H., Liu, J., Zhou, X.: Effects of the loading and unloading conditions on the stress relaxation behavior of pre-cracked granite. Rock Mech. Rock Eng. **50**(5), 1157–1169 (2017). <https://doi.org/10.1007/s00603-016-1161-3>
7. Zhao, K., Li, Q., Yan, Y., Zhou, K., Gu, S., Zhu, S.: Numerical calculation analysis of the structural stability of cemented fill under different cement-sand ratios and concentration conditions. Adv. Civil Eng. **2018**, 1–9 (2018). <https://doi.org/10.1155/2018/1260787>
8. Gupta, A.K., Paul, B.: Comparative analysis of different materials to be used for backfilling in underground mine voids with a reference to hydraulic stowing. Int. J. Oil Gas Coal Technol. **15**(4), 425 (2017). <https://doi.org/10.1504/IJOGCT.2017.084830>
9. Stone, D.: The evolution of paste for backfill. In: Proceedings of the 11th International Symposium on Mining with Backfill: Mine Fill 2014, Australia, pp. 31–38 (2014)
10. Sivakugan, N., Rankine, K.J., Rankine, R.M.: Permeability of hydraulic fills and barricade bricks. Geotech. Geol. Eng. **24**, 661–673 (2006)
11. Beltran, W.: Estudio Experimental de relleno hidráulico en mina Atacocha (2014)
12. Webb, P.: Hydrated lime vs hydraulic lime (2018); Rankine, K.J., Sivakugan, N., Cowling, R.: Emplaced geotechnical characteristics of hydraulic fills in a number of Australian mines. Geotech. Geol. Eng. **24**, 1–14 (2006)

# A Study on Investigations Carried Out in Dams from the Perspective of Risk Analysis



Gabriel Gomes de Oliveira , Yuzo Iano ,  
Ana Carolina Borges Monteiro , Reinaldo Padilha França ,  
Diego Pajuelo , and Pablo David Minango Negrete 

**Abstract** With the population growth, the Petrobras modernization REPLAN (Paulinia Refinery), the progressive region development and the shortage of resources from new wellsprings, there was a need to increase the water availability of the region of Campinas—SP and with that will be implanted two dams, one in the municipality of Quarry—SP and another in the district of Two Bridges in the municipality of Amparo—SP. The construction of the dams occurred for many reasons, one of which is to benefit many cities through water reserves serves to about 5.5 million inhabitants are that downstream of the reservoirs. These concepts, the present work AIMS to present all the criteria and principles that are related to the construction of the dams. Through research and consultations will be all the characteristics presented, direct and indirect information,

**Keywords** Dam · Case study · Environmental impact · Water availability

---

G. G. de Oliveira (✉) · Y. Iano · A. C. B. Monteiro · R. P. França · D. Pajuelo · P. D. M. Negrete  
School of Electrical and Computer Engineering (FEEC), University of Campinas, UNICAMP, Av.  
Albert Einstein-400, Barão Geraldo, Campinas, SP, Brazil  
e-mail: [oliveiragomesgabriel@ieec.org](mailto:oliveiragomesgabriel@ieec.org)

Y. Iano  
e-mail: [yuzo@decom.fee.unicamp.br](mailto:yuzo@decom.fee.unicamp.br)

A. C. B. Monteiro  
e-mail: [monteiro@decom.fee.unicamp.br](mailto:monteiro@decom.fee.unicamp.br)

R. P. França  
e-mail: [padilha@decom.fee.unicamp.br](mailto:padilha@decom.fee.unicamp.br)

D. Pajuelo  
e-mail: [diego.pajuelo.castro@gmail.com](mailto:diego.pajuelo.castro@gmail.com)

P. D. M. Negrete  
e-mail: [pablodavid218@gmail.com](mailto:pablodavid218@gmail.com)

## 1 Introduction

The construction of dams has always been paramount to the growth and development of mankind, from the oldest to which it is registered, such as Egypt, the Middle East, and India. Currently, concern about water resources involving quantity and quality has been accentuated due to drastic population growth and high pollution index, so the water has become a precious commodity and the construction of dams is a way to save her in order to have adequate human consumption without scarcity and quality [1–4].

The implementation of dams directly affects areas of major proportions, and thus end up being great potential works negative impact on the environment (flora, relief, and fauna), to the cultural environment (historical, artistic, archeological, architectural, heritage and people celebrations), artificial (towns, urban areas, villages) and labor (and material and immaterial that are necessary for the performance of labor exercises for humans) [5, 6].

These types of reservoirs are artificially made obstacles able to retain water for the purpose of industrial or domestic supply, navigation, irrigation, recreation, sedimentation control, and flood and are also intended for the production of electricity. For water supply dams it is a necessary follow-up, monitoring, and also its maintenance, it is one way to avoid any kind of accident that can occur and thereby ensure the proper functioning of these reservoirs. Such containers are made with different constructive techniques and varied sizes and this is set as required for the use, in the case of farms are generally used small clumps of earth and often large structures used for hydroelectric power supply and water supply, and between various other purposes are constructed from landfills or concrete [7, 8].

The amount of water that is stored in the reservoir will depend on the needs to be met. It should be set immediately after getting the planialtimetric survey of where they will be flooded by the dam. The main dam construction means are concrete arch, riprap, concrete, fill and gravity. These structures have further included the houses of power, spillways, discharge structures, and control units.

Brazil is the largest country in Latin America (in territorial extension), having approximately 209.3 million inhabitants, who live in 26 Brazilian states and the Federal District. Its states are divided into five regions (North, Northeast, Midwest, Southeast, and South), is the most populous southeast region, with approximately 80 million inhabitants, distributed among the states of Rio de Janeiro, Espirito Santo, Minas Gerais, and São Paulo. The state of Sao Paulo has about 12 million individuals. This high population concentration is due to large industrial and technological investments in these areas, thus generating greater financial circulation and consequently more chances of employment [9–12].

Located in the state of Sao Paulo, the Campinas region is made up of 22 cities (Americana, Artur Nogueira, Campinas, Cosmópolis, Engenheiro Coelho, Holambra, Hortolândia, Indaiatuba, Itatiba, Jaguariuna, Monte Mor, Morungada, Nova Odessa, Paulínia, Pedreira, Santa Barbara d ‘Oeste, Santo Antonio de Posse, Sumaré, Valinhos, and Vinhedo), 3,224,443 inhabitants, and total GDP (Gross

Domestic Product) of R \$ 142,301 million. This scenario has attracted more and more people to live and work in this region. However, with warming and public misconduct, many Brazilian cities have been suffering from water shortages at certain times of the year, especially when temperatures can reach 37 degrees Celsius. Based on this, there is a need to create dams to supply the entire population. Thus, in 2014 the process was started for the construction of the dams of the cities of Pedreira, Duas Pontes and Amparo, which when completed will be dependent on the Jaguari and Camanducaia rivers, which are located in the cities of Pedreira and Amparo, respectively [9–12].

With the construction of dams stands out as a major benefit, increased water availability for the population of the municipalities to be covered, which will require well in water security, since studies show that if you do not adopt such measures in 2025 about 7 cities entered for water resource vulnerability list [8].

Environmental and socio-cultural impacts of water projects of this size require a great preventive assessment, influencing the idea of design, formulation, and alternatives to the system, as well as in the design and detailed design. This assessment is extremely important both for environmental and social viability as economic, highlighting the impact studies, expropriation, flooding so that future problems directly related spending can be avoided. This assessment helps minimize problems, but not extinguished, it is inevitable that some of the forests are devastated for project implementation causing the loss of biodiversity, degradation of upstream areas caused by the flooding of the reservoir area, among other problems [13, 14].

Investigations based on geological studies are primary tools for dam analysis, mainly as a form of prophylaxis for future human, environmental, financial and health problems. However, due to the high costs resulting from this study often generates the negligence of large companies in the supervision of their dams. Based on this, the present study aims to perform an analysis of works related to the construction of these dams in order to detect possible failures during the process as well as to expose the possible damages and risks that populations face when there is negligence on the part of companies.

## 2 Methodology

This study was conducted by gathering bibliographic data in the literature on dams in Brazil, focusing on the water dam under construction in the Campinas region and the two largest Brazilian environmental disasters involving ore tailings dams. The results found are confronted with environmental, social and health issues.

### 3 Results and Discuss

The dam at the Two Bridges dominates site and reservoir are characterized by elongated mirrors, medium to high slopes (>15%) and local amplitudes below 100 m. The hills have rounded tops and straight slopes, south relief mountains, known as Serra dos Feixos. The well where the future dam will be installed cuts the Camanducaia River, characterized by stretches of rocks inserted in sandy soil, providing rapids in the east-west direction. Drilling tests were performed at the locations on the edge of the right SMDP probe 01, at a level of 1.60 m of residual soil followed by a change in the soil rock composite by micaceous clayey sludge that overcame resistance 40 strokes in the test SPT after 15.00 m deep [15, 16].

In the left margin, it was necessary to carry out three points polls for more precise information because there is greater instability in the soil. The 02-SMDP probe, located near the river, pierced a layer of 4.00 m landfill, followed by a 1.00-m alluvial layer comprising silt, sandy loam, with rock elements grayish-yellow in pigment. Further down, at approximately 22.00 m deep, there is a change in rock with silty-sandy texture micaceous. Continuing were performed on the left edge 03 and the SMDP-SMDP-04 polls, which is characterized in general by having layer of 1.00 m thick composed of colluvium bit sandy silt clay having small gravel; layer 5.60–6.00 m mature little residual soil sandy silt clay consistency and depth resistant 03–10 strokes; a ground-level shift of rock with silty-sandy texture micaceous found some rock fragments. The SMDP-03 and-04 SMDP found groundwater surveys the depth of 7.50 m and 20.00 m, respectively [15, 16].

In the report of the study pointed out that the quarry reservoir is inserted in a mountainous relief Elongated hills, and its average slope characteristics and high (>15%) and areas with ranges greater than 300 m. And it has shaped angular tops with ravines and slopes with rectilinear shapes. The axis is intercepted by sharp bends river Jaguari with portions of the bedrock originating tubing [15, 16].

During the surveys were carried out on the banks, both right and left, on the right edge was performed SMPE-01 and found layers of rock changes, micaceous clay and sandy silt clay micaceous. And by the results, it has resistance at SPT 40 strokes starting at 12.00 m deep. In the left margin, analyzes were performed 4, 02-SMPE polls the SMPE-05. The SMPE-02 probe was implemented on top of the rocky bed of the water body and provided with mylonite gneiss depth of 15.90 m. Since the SMPE-03 polls the SMPE-05, identified rock material layers (thickness varying from 1.00 to 4.50 m), silty clay-bit sandy soil, silt, clay and sandy micaceous the mylonite gneiss. The resistance values presented a gradual penetration to the depth reaching 40 blows to 15 m. In the investigation pointed rock masses that show medians and consistent changes at the top, passing the bedrock little changed in the final meters [15, 16].

## 4 Physical Impacts Analysis of Two Bridges and Reservoirs Quarry

With the introduction of Quarry and Two Bridges dam, according to Article 2 of CONAMA Resolution 349 (1986) to Directly Area Affected (DAA) is the place where will be implemented the project with its settled structures, access roads that may be increased produced or changed, with its unit procedures related to his work infrastructure. Therefore the Direct Area of Influence (DAI) is the region which will be reached directly from the impacts on the development coinciding with the (DAA) may have positive or negative interference. The quarry dam, in turn, affects the EPA (Environmental Protection Area) of Piracicaba/Juqueri-Mirim, the city of Campinas also has an affected area and the same is located on the left edge of the reservoir deployment. The APA of Piracicaba/Juqueri-Mirim, in turn, covers part of the left edge of the tank and all directly affected and influenced area [17, 18].

With the implementation of the quarry dam, Annex K will be flooded about 105 ha APA corresponding part of Campinas being flooded. Thus all the DAI, which corresponds to the left corner of the reservoir presented zoning in the management scheme, the Hydro Conservation area Jaguari, which its procedures is to ensure the preservation of sources and water, the Just as the recovery and protection of riparian vegetation, and permanent banning of pesticides and chemical fertilizers [17].

This application boundaries EPA and DAI, follows the same design of the study units for sub-basins and may require adjustments, it helps the planned environmental programs Pedreira dam act in proportion to the guidelines and the EPA region of objectives belonging to the Basin Jaguari. The introduction of the quarry will have a dam reservoir with an area of approximately 2.02 km<sup>2</sup> to about 82 ha overflow of the storage units. In this case, the conservation area of Campinas will have about 33 ha and the Piracicaba/Juqueri-Mirim have lost 97 ha. It tends to be noted that this total is added to a flood area of approximately 72 ha area corresponding to the overlapping of the two affected areas [18].

The EPA in Campinas will be affected by more than 105 ha which represent the sum of the areas of 33 ha reservoir and the area lost with limits applied to 72 ha. When added to the array of the tank, that area will have a total of 232 ha affected. In turn, EPA Piracicaba/Juqueri Mirim 169 ha has affected areas occupied by the quarry and reservoir 97 ha area is lost with overlapping boundaries 72 ha. When added to the array of quarry dam the entire length will have a total of 370 ha affected. In Table 1 is showed the affected storage units [17, 18].

The Two Bridges and quarry reservoir will occupy areas that are material goods, residential and agricultural activities that are called a small scale, mainly for self-consumption. In the case of the dam of Two Bridges, besides the presence of a small proportion of activity, there is also the presence of large areas where there is major business uses. In this case, there is the Farm Jaborandi industrial group Ypê which carries out large-scale poultry farming jobs. There is also the Agriculture Tuiuti (Shefa), which is a dairy, which will not be fully impaired. Since the establishment

**Table 1** Protected areas affected by quarry dam

Conservation Unit	Total area	Flooded area	DAA occupation	Total	Total with overlapping
Campinas	22.278	33	53	86	232
Overlapping area between conservation units	2966	72	74	146	–
Piracicaba/Juqueri-Mirim	287.000	97	127	224	370

Resorts, 4 Angels who works as a research laboratory and studies of animal vaccines and is a Research Center for Animals of Brazil will be completely flooded [18].

Regarding the commercial activities can point to the known “Ecological Reserve Mundão of Trails,” which develops tourism activities, relying primarily on the area and structure to track and camping near the river Camanducaia, the District of Arcadas, Amparo. Although titled “Ecological Reserve” is not protected conservation unit or established by law, unless that focus on permanent preservation areas and reserves. On the left edge of the river is located Jaguari the “Aunt Bar,” downstream from the dam quarry, which is likely to suffer interference by dam construction [17, 18].

There are also two small main dams that will be flooded. The river Jaguari is located the PCH White Monkey, with 2.36 MW of installed capacity owned by Electricity company and should be affected by the formation of the quarry dam and river Camanducaia, SHP Feixos, with 1.15 MW installed capacity of the Company Energy Wolf Jump Ltda, which will be hindered by the Two Bridges bus. In population surveys in areas to be occupied by the dam quarry and two bridges a total of 82 families were identified, of these 27 families are located in the area to be flooded quarry and 55 families in the dam Amparo [17, 18]. Table 2 shows the families living in the area that will be compromised by construction.

The compensation for expropriation can be performed in two ways: through payment in cash or government bonds (in urban environments or in the case of land reform). The impacts in rural areas with productive activity, considering the loss of areas dedicated to agriculture and forestry, will be enormous because these areas are in the direction of the dam spillway. The quarry dams and bridges two reservoirs should form with total area respectively of 202 and 486 ha<sup>2</sup>, the areas to be flooded effectively correspond to 181 ha and 463 ha and other areas are occupied by the river.

**Table 2** Families living in the area directly affected (DAA)

Families	Two bridges	Quarry	Total
Families interviewed	44	25	69
Family no information (*)	11	2	13
Total families	55	27	82

\* indicates without information about these families

In recent years the region near these rivers is increasing its population rate significantly, so has increased pressure on water demand, finally, states have adopted measures to be no lack of water at the time and in the future for the population and aimed at development of the region, thereby improving the quality of life of the population. The quarry reservoir is located near Highway John Beira, known as SP-095 and the town road Basil Vieira de Godoi, already the Two Bridges is close to the highway John Beira, also known as SP-095 and the highway Aziz Lian, also known as SP-107 [17].

The quarry dam is 3 km from the urban center of the city of Pereira and will be installed in the river Jaguar, located in the municipalities of Pedreira and Campinas, such reservoir will have an area of 2.02 km<sup>2</sup> and can store about 32 billion liters of water. Already the dam of Two Bridges is 8 km from the city of Amparo, and will be introduced in the river Camanducaia and will run until Ribeirão Pantaleon such a reservoir will have an area of 4.86 km<sup>2</sup> and can store about 53 billion liters of water [18].

Both dams are in regions with rapid economic development and population, and that was by agribusiness enterprises and large national and multinational companies in the region, so it has been the need to increase the water demand in the region.

## **5 Environmental Disasters in Brazil: The Mariana and Brumadinho Dams**

Actually in Brazil, when the word “dam” is said, it is associated with the word catastrophes, deaths, environmental crime, ecological disaster. This is because, on November 5, 2015, there was a breakdown of an ore tailings dam in the city of Mariana, Minas Gerais (Southeast Brazil). The Mariana tailings dam is owned by Samarco, which is managed by Vale S. A. and BHP Billiton. The disruption resulted in 43.7 million cubic meters of tailings dumped and a total of 19 deaths. The mud-covered a total of 663 km until it reached the sea in the state of Espírito Santo. In addition, the mud has reached the Doce River, which covers 230 municipalities that have their bed as a subsistence tool. According to environmentalists, the effects of tailings at sea will be felt for at least 100 years. One month after this catastrophe occurred, 11 tons of dead fish were removed in both Minas Gerais and Espírito Santo. Lives were taken, districts were destroyed and thousands of residents were left without water, homeless and without work. The rupture of the tailings dam (Fundão) in Mariana is considered the biggest environmental disaster in the country's history. Until the moment the region remains uninhabited and covered with mud. Many residents still receive government assistance. The feasibility of building a new district for the relocation of these families is studied [19–22].

However, isolation from communities and loss of access to health services can aggravate existing chronic diseases in the affected population (hypertension, diabetes,



kidney failure, tuberculosis, etc.), as well as triggering new deleterious health situations such as mental illness (depression). and anxiety), hypertensive crises, respiratory diseases, domestic accidents and outbreaks of infectious diseases. The increased incidence of pre-existing diseases in the region, such as yellow fever, diarrhea, and schistosomiasis may be a consequence of the medium-term disaster. In addition, contact with mud and water may lead to cases of leptospirosis [23].

On January 29, another tragedy struck the city of Brumadinho, Minas Gerais. This dam belongs to the Brazilian multinational mining company Vale S.A. As much as this breach has dumped a smaller amount of waste compared to Mariana, its social and environmental impacts have been as great. According to the National Mining Agency, the dam had no documentary backlogs, and was considered inactive, meaning it was not receiving any new tailings. The volume of excrement manure was about 12 million m<sup>3</sup> (1 m<sup>3</sup> equals 1000 L) and the speed of the mud reached 80 km per hour. At the time of the tragedy, security sirens should have been sounded to alert Vale workers and local residents. This, however, did not happen [19–22].

The mud, which contained iron, silica, and water, reached the Paraopeba River, which in turn negatively affected water quality, as this water present in the river presented risks. By the end of August 2019 (about 7 months later), 241 deaths and 21 people still missing are counted [19–22].

It is necessary to examine the presence of heavy metals in the tailings and their monitoring along these rivers to avoid the consumption and use of contaminated waters in the coming years. Heavy metal-enriched sediment can be remobilized to rivers with heavy rainfall, dredging and hydroelectric dam operation over the next few years [23].

It is important to point out that both environmental disasters were due to human failures, one of them based on a communication failure between the responsible companies, employees and city dwellers. Therefore, it is necessary to implement more modern communication systems that present low abstraction level, speed and low computational memory consumption [23–26], regardless of the operating system used by the company [27]. Moreover, it is important to invest in low cost, high accuracy medical methodologies that do not depend on specific equipment, so that the exams can be performed through a simple computer [28, 29].

## 6 Conclusions

By analyzing all the necessary procedures for the implementation of these dams, it was found that the project will benefit several cities in the region with the supply of water, which is recurrent shortages in drought times, and also will bring, all matters involving environmental impacts in the area, and the physical impacts that are associated with the expropriation of the owners of homes and loss of heritage sites to be flooded.

With work and the technical site, visit can understand the size and grandeur of the buses that aims to help society as a whole, and also comprehend and understand

the frustration of residents who are expropriating their homes because their lands were some generations of family heritage and for the construction of dams, but cannot observe reality broadly and understand that this project will benefit millions of people.

Since it is extremely important to build these dams even if it works with considerable environmental impacts in the affected area and physical impact on people's lifestyle directly injured with expropriations, but that in the future will benefit because there are no setbacks with the lack of d ' water, it will be one of the viable alternatives to the water crisis that is regular and that affects most municipalities that are downstream of future works, and as this will minimize the dependence of water coming from the Cantareira System to supply the region.

## References

1. Kutzner, C.: *Earth and Rockfill Dams: Principles for Design and Construction*. Routledge (2018)
2. Reynolds, N.Y.: *City of the high dam: Aswan and the promise of postcolonialism in Egypt*. *City Soc.* **29**(1), 213–235 (2017)
3. De Chatel, F.: *Water Sheikhs and Dam Builders: Stories of People and Water in the Middle East*. Routledge (2017)
4. Bidoglio, G., Berger, M., Finkbeiner, M.: An environmental assessment of small hydropower in India: the real costs of dams' construction under a life cycle perspective. *Int. J. Life Cycle Assess.* **24**(3), 419–440 (2019)
5. England, M.I.: India's water policy response to climate change. *Water Int.* **43**(4), 512–530 (2018)
6. Garchitorena, A., Sokolow, S.H., Roche, B., Ngonghala, C.N., Jocque, M., Lund, A., Andrews, J.R.: Disease ecology, health and the environment: a framework to account for ecological and socio-economic drivers in the control of neglected tropical diseases. *Philos. Trans. Roy. Soc. B Biol. Sci.* **372**(1722), 20160128 (2017)
7. Zhang, L.M., Xu, Y., Jia, J.S.: Analysis of earth dam failures: a database approach. *Georisk* **3**(3), 184–189 (2009)
8. Junior, A.M.L.: *Environmental licensing and cultural heritage: the licensing aspects of Serro Azul dam in Pernambuco*. 68 2016. f. Dissertation (Training Course of Cultural Managers of the Northeastern States)—Federal University of Bahia, Recife (2016)
9. Salgado, A.A.R., Santos, L.J.C., Paisani, J.C. (eds.): *The Physical Geography of Brazil: Environment, Vegetation and Landscape*. Springer (2019)
10. Dantas, E.W.C., Silva, J.B.D.: Brazilian urban geography: from a diachronic analysis to the most cited works in the last decade. *Confins. Revue franco-brésilienne de géographie/Revista franco-brasilera de geografia* **38** (2018)
11. Cano, W., Brandão, C.A.: *A Região metropolitana de Campinas. Urbanização, Economia, Finanças e Meio Ambiente*. Campinas: Editora da Unicamp (2002)
12. Minuzzi, R.B., Sediyaama, G.C., Barbosa, E.D.M., Melo Júnior, J.C.F.: Climatologia do comportamento do período chuvoso da região sudeste do Brasil. *Revista Brasileira de Meteorologia* **22**(3), 338–344 (2007)
13. Durst, J., Neumann, L., Smith A.: *Contested development: the Belo Monte Dam, Brazil*. In: *Water, Climate Change and the Boomerang Effect*, pp. 84–99. Routledge (2018)
14. Poff, N.L., Olden, J.D.: Can dams be designed for sustainability? *Science* **358**(6368), 1252–1253 (2017)

15. Cancellara, M.A.: Two Bridges basic dam project: Final report. Paulinia: Projectus (2013). 184 f
16. Cancellara, M.A.: Final report: Basic quarry dam project. Paulinia: Projectus (2013). 190 f
17. EIA—Pedreira Two Dams and Bridges. Volume V—impacts and environmental pro-grams take 1—text. Department of Sanitation and Water Resources Department of Water and Power (2015)
18. EIA—Study Quarry dams and Two Bridges environmental impact. Volume III—diagnosis of biotic take 1—text (part 1). Department of Sanitation and Water Resources Department of Water and Power (2015)
19. Sousa, V.S., de Freitas, V.M.: Revisão Teórica Sobre os Desastres Da Mineração Brasileira Incididos em Mariana-Mg (2015) E Brumadinho-Mg (2019). In: Anais Colóquio Estadual de Pesquisa Multidisciplinar (ISSN-2527-2500) & Congresso Nacional de Pesquisa Multidisciplinar (2019)
20. Freitas, C.M.D., Barcellos, C., Asmus, C.I.R.F., Silva, M.A.D., Da Xavier, D.R.: Samarco em Mariana à Vale em Brumadinho: desastres em barragens de mineração e Saúde Coletiva. *Cadernos de Saúde Pública* **35**, e00052519 (2019)
21. Almeida, I.M.D., Jackson Filho, J.M., Vilela, R.A.D.G.: Razões para investigar a dimensão organizacional nas origens da catástrofe industrial da Vale em Brumadinho, Minas Gerais. Brasil. *Cadernos de Saúde Pública* **35**, e00027319 (2019)
22. dos Santos, D.A., Martins, J.E.R., Rodrigues, M.R.: Breve ensaio sobre a responsabilidade civil do Estado no contexto dos desastres ambientais em Mariana e Brumadinho. *Revista do Curso de Direito da Uniabeu* **12**(1), 158–161 (2019)
23. Padilha, R., Iano, Y., Monteiro, A.C.B., Arthur, R., Estrela, V.V.: Betterment proposal to multipath fading channels potential to MIMO systems. In: *Brazilian Technology Symposium*, pp. 115–130. Springer, Cham (2018)
24. França, R.P., Iano, Y., Monteiro, A.C.B., Arthur, R.: Improvement for channels with multipath fading (MF) through the methodology CBEDE. In: *Fundamental and Supportive Technologies for 5G Mobile Networks*, pp. 25–43. IGI Global (2020)
25. França, R.P., Iano, Y., Monteiro, A.C.B., Arthur, R.: A proposal of improvement for transmission channels in cloud environments using the CBEDE methodology. In: *Modern Principles, Practices, and Algorithms for Cloud Security*, pp. 184–202. IGI Global (2020)
26. França, R.P., Iano, Y., Monteiro, A.C.B., Arthur, R.: Improvement of the transmission of information for ICT techniques through CBEDE methodology. In: *Utilizing Educational Data Mining Techniques for Improved Learning: Emerging Research and Opportunities*, pp. 13–34. IGI Global (2020)
27. França, R.P., Peluso, M., Monteiro, A.C.B., Iano, Y., Arthur, R., Estrela, V.V.: Development of a kernel: a deeper look at the architecture of an operating system. In: *Brazilian Technology Symposium*, pp. 103–114. Springer, Cham (2018)
28. Monteiro, A.C.B., Iano, Y., França, R.P., Arthur, R., Estrela, V.V.: A comparative study between methodologies based on the hough transform and watershed transform on the blood cell count. In: *Brazilian Technology Symposium*, pp. 65–78. Springer, Cham (2018)
29. Monteiro, A.C.B., Iano, Y., França, R.P., Arthur, R.: Methodology of high accuracy, sensitivity and specificity in the counts of erythrocytes and leukocytes in blood smear images. In: *Brazilian Technology Symposium*, pp. 79–90. Springer, Cham (2018)

# Numerical Simulation of Hydrodynamic Conditions in Rivers Facing Extreme Events Due to the “El Niño” Phenomenon



Gabriela Alvarez , Alvaro Moreno , Emanuel Guzmán ,  
and Sissi Santos 

**Abstract** Disasters caused by floods are increasingly common around the world, such as the case in the western part of North and South America, due to the presence of the “El Niño” phenomenon, which causes an increase in rainfall and flow rates of the rivers causing floods. For this reason, this present work has carried a numerical simulation of flooding in the face of extreme events such as “El Niño,” with the purpose of validating a hydrodynamic model that subsequently allows to predict the magnitude of a future event, for this, hydrological data of average flows and instantaneous maximums over a period of 40 years has been used. The hydrological information was processed using the Gumbel method to obtain simulation flows for return periods of 2, 5, 10, 50, 100 and 500 years. As a result, an approximation of 75% of the model was obtained in comparison with the historical event. Additionally, an increase of 103% in water elevation was found for discharge with a return period of 500 years, compared with the event of March 27, 2017, which represents a discharge with a return period of 36 years.

**Keywords** Flood · Hydraulics · “el niño” phenomenon

---

G. Alvarez · A. Moreno (✉) · E. Guzmán · S. Santos  
Universidad Peruana de Ciencias Aplicadas, Av. Prolongación Primavera 2390, Santiago de Surco, Lima, Peru  
e-mail: [u201422958@upc.edu.pe](mailto:u201422958@upc.edu.pe)

G. Alvarez  
e-mail: [u201623464@upc.edu.pe](mailto:u201623464@upc.edu.pe)

E. Guzmán  
e-mail: [pcipeguz@upc.edu.pe](mailto:pcipeguz@upc.edu.pe)

S. Santos  
e-mail: [sissi.santos@upc.pe](mailto:sissi.santos@upc.pe)

## 1 Introduction

Floods caused by river overflows are recurring problems worldwide and are related to increased rainfall, structural failures in dams or protection structures, as well as the occurrence of extreme phenomena such as the “El Niño” phenomenon (FEN). It affects the western part of North and South America, causing large economic and human losses. Facing this situation, the authorities carry out contingency plans to mitigate the negative impacts caused by these phenomena.

Several studies and investigations have been carried out in order to study the floods and prevent the disasters they cause [1–13], one of the techniques used for this is hydraulic modeling where programs such as IBER [5], HEC-RAS [13], FLO2D [11], among others are used.

In order to develop the modeling, it is common to use digital terrain elevation models (DEM) to characterize the topographic configuration of the study area. The DEM is a computational representation of the triangular irregular networks (TIN) of the surface that can be obtained from satellites that take images obtaining from horizontal ( $x$ ,  $y$ ) and vertical ( $z$ ) vectors in such a way that it generates the digital terrain models with different resolutions [14, 15]. From the DEM obtained, TINs are created, which are a necessary requirement for hydraulic simulation, since from this it is possible to generate the mesh that covers the study area, the river cross-sections, among others [6]. A joint work of data collected in the field and a digital model facilitates and enriches the information extracted from the satellite at the time of the extraction of cross-sectional sections of the river for 1D or 1D/2D modeling [16–18]. The hydrological data (rain, river or both) implemented in the models help determine flood plains that occur around the river or within the study basin. For the calibration of the generated model, it is possible to make use of statistical parameters that start from physical properties of the place or the digital calibration is carried out, which consists in the comparison of models of different satellites to obtain the best available model with the least possible error and closely related [10, 16]. On the other hand, to carry out the validation of the model there are different studies that compare the numerical models obtained in a combination of the digital elevation models and the hydraulic information of historically observed events, comparing mainly their physical differences. Maswood & Hossan [14] use the comparison of the bathymetry water levels of the flooded days and the numeric values obtained, while Abdul Kadir [1] compares the longitudinal profiles observed with the numerical ones, and in the key points are compared to verify if they have a significant difference. In addition, Surwase [17] compares flood plains by changing roughness parameters, proving that for a higher Manning  $n$  value, an increase in the flood area will be generated.

Therefore, the use of numerical modeling is an important tool since it allows evaluating real and hypothetical scenarios, considering return periods of up to 500 years, which allow obtaining extreme events and assessing and identifying the most vulnerable areas to flood risks, which allows competent authorities to prepare management plans for these risks. The present investigation provides a hydrodynamic model in

HEC-RAS applied in Peru, to simulate possible future extreme events caused by “El Niño” phenomenon.

## 2 Area of Interest

The study area is located in the northern part of Perú, in the department of Piura and includes the section between the Los Ejidos dam to the Bolognesi Bridge (Fig. 1). Likewise, other bridges are shown within the study area, such as the Andrés Avelino Cáceres Bridge, Eguiguren Bridge, Sánchez Cerro Bridge, and San Miguel Suspension Bridge, being its distribution with downstream direction.



Fig. 1 Study section from Los Ejidos dam to Bolognesi Bridge

The district of Castilla and the district of Piura represent a part of the urban area of Piura. In these areas, there are homes, schools, parks, etc. Points of importance due to flooding are places such as the main square of Piura and the open plaza of Piura due to its proximity to the river.

The Sánchez Cerro Bridge hydrometric station is administered by the National Water Authority (ANA) [4] and is in the district of Miraflores, at a height of 34 m.a.s.l. in the coordinates of latitude =  $05^{\circ} 11' 37.15''$ , longitude =  $80^{\circ} 37' 24.39''$ . The station records average normal flow conditions of  $752.6 \text{ m}^3/\text{s}$ , while in extreme events it reaches  $4424.0 \text{ m}^3/\text{s}$ . In the structure of the Sánchez Cerro Bridge, its cross-section supports a maximum avenue of  $2000 \text{ m}^3$  before overflowing; this flow is recorded and usually exceeded when natural phenomena such as the “El Niño” phenomenon occur.

### 3 Methodology

The work began with the collection of data from different official institutions such ANA [4], Regional Emergency Operations Center of Piura (COER-PIURA) [3] and the Special Project Chira-Piura (PECHP) [12], from where the information of maximum daily, daily average and hourly discharged was obtained. For the morphological characterization of the area, information has been used on a digital terrain elevation model (DEM), obtained from the SPOT-7 satellite, with a resolution of  $6 \times 6 \text{ m}$ , which was collected from National Aerospace Research and Development Commission (CONIDA) [2]. DEM has been processed, the land data and the corresponding cross-sections of the river were obtained and exported to HEC-RAS for simulation.

For the generation of the model, after adding the input data in the HEC-RAS, in the geometry section, the mesh was defined according to the DEM resolution. Also, the upstream edge conditions were defined, where the hydrograph corresponding to the date and time of the event was entered, while the average slope of the river in the study area was placed downstream.

Subsequently, the values of Manning  $n$  were chosen according to the river's characteristics as observed in the study area, since it is a coefficient that represents the roughness of the riverbed and was used to calibrate the model, also, when modifying that parameter, it will change substantially the results of the model. To have a better fit, the calculation intervals of the model were determined according to the Courant stability criterion, which is indicated in the HEC -RAS 5.0.7 manual. The hydrodynamic simulation was visualized in RAS Mapper, and the validation was carried out by means of a comparison of the flood area with the high-resolution digital image of the same date and time selected. Finally, an extreme flood event was modeled with the data obtained of discharge for 500 years of the return period, where the flooded area is visualized, and this allowed to generate control and prevention plans in the vulnerability area to these disasters. This methodology was adapted according to Surwase for the respective purposes [17]. The extremes discharge values were

obtained using Gumbel Distribution, which passed the Kolmogorov-Smirnov test to verify that it has a normal distribution, and the flows for the return periods of 10, 20, 50, 100 and 500 years.

## 4 Simulations

The DEM for the required study area was adjusted and modified since it has elevation data. For the study, the contour lines were extracted at an interval of every 3 m to provide the necessary precision for the model. The contours achieved to consider the topography of the terrain, from them a tin (irregular triangulation networks) was created, showing the different elevations in the area. Then, the cross-sections were created, following the axis alignment and the defined river limits. The terrain geometry was entered in the HEC-RAS in the “RAS Mapper” window to display the respective elevations. In the “Geometric Data” window, the calculation mesh within the flood area was defined, which must contain a cell size that conforms to the DEM resolution for best results. Different boundary conditions were considered for the calculation mesh, for example, for the upstream the respective input hydrograph was entered and for the downstream, the slope of the land was entered, which was 1.2%. Finally, for the calculations of computation interval, the cell parameters and speed of the unsteady flow for different levels of river water with a Courant coefficient equal to 1 were considered, according to the equations defined in the HEC-RAS Manual 5.0.7.

Simulations were developed for the event of March 27, 2017, date that a flood event was reported due to the FEN, in this stage, it was proceeded to calibrate the model and validate with a satellite image. In the second stage, an extreme event was modeled for the discharge rate obtained for a return period of 500 years, so the flood hazard area was obtained.

### 4.1 Event Simulation: FEN March 27th, 2017

For the simulation, a Manning roughness coefficient of 0.035 was considered as roughness for dredged material with short grass and some weeds [7] and the hydrogram of March 27th from 00:00 h until 21:00 h taken from the Ejidos dam (Table 1; Fig. 2).

The modeling result for March 27th, 2017 (Fig. 3b) shows a flooded area of 3.18 km<sup>2</sup>, where two mainly affected areas such as the main square and the Open Plaza Shopping Center are observed due to its large audience attendance.

Figure 2 shows the difference between (a) the observed flood, by calculating the Normal Differential of Water Index NDWI index, obtained from the Sentinel-2 satellite, image from April 4th, 2017 and (b) the modeled flood of the DEM obtained from CONIDA. For the main square, the observed event and the modeling have



an area of 0.98 km<sup>2</sup> and 0.74 km<sup>2</sup>, respectively, this represents an approximation of 75.5%. Also, for the Open Plaza, the observed event and the modeling have an area of 0.30 km<sup>2</sup> and 0.23 km<sup>2</sup>, respectively, this represents an approximation of 79.31%. In addition, results were obtained from the depths and average speeds in areas such as the open plaza Piura, the main square, Sánchez Cero Bridge and Bolognesi Bridge, which are consistent with the historical information of the “Niño Costero” phenomenon of the year 2017 (FEN Costero 2017) (Table 2).

**Table 1** Hourly discharge of March 27th, 2017 at the Ejido dam station. *Source* COER [8]

Ejidos dam					
Time	Flow m <sup>3</sup> /s	Time	Flow m <sup>3</sup> /s	Time	Flow m <sup>3</sup> /s
00:00	2270	08:00	3095	16:00	3133
01:00	2325	09:00	3095	17:00	3076
02:00	2396	10:00	3264	18:00	3035
03:00	2501	11:00	3378	19:00	3005
04:00	2574	12:00	3468	20:00	2923
05:00	2864	13:00	3264	21:00	2850
06:00	2895	14:00	3216		
07:00	3016	15:00	3174		

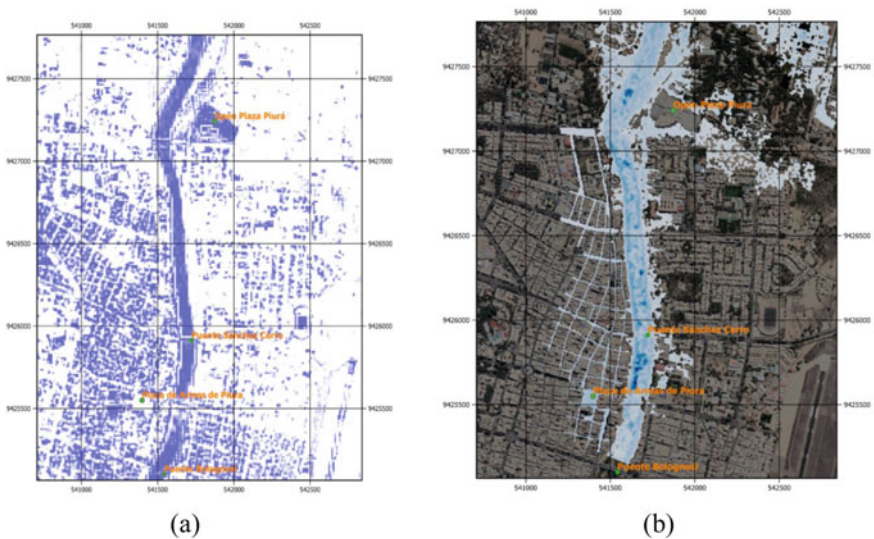


**Fig. 2** a Flood observed by the SENTINEL-2 satellite for April 4th, 2017 [9]. b The simulated flood of March 27th, 2017

For calibration, adjustments were made to both the digital elevation model and the roughness coefficients, so that the results of the flood are more in line with reality, for the calibration of our model. For this, several simulations of the scenario of March 27th, 2017 (FEN Costero 2017) are carried out, verifying that the information about water levels is consistent with what happened historically.

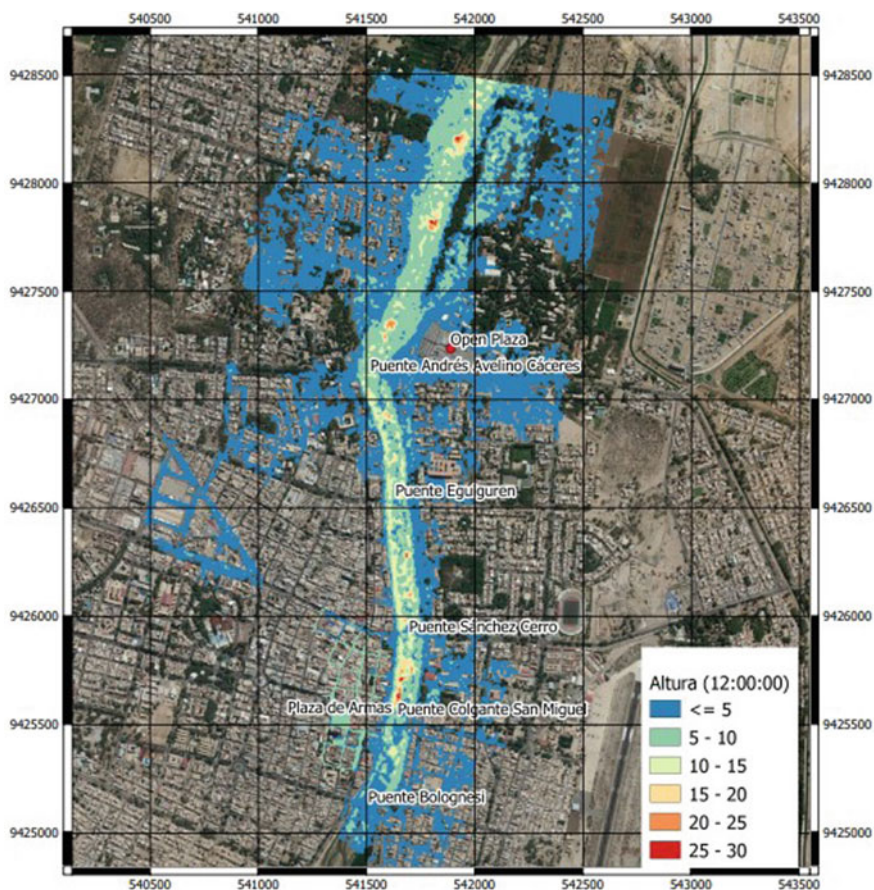


**Fig. 3** Flood simulation of the city of Piura for discharge with a return period of 500 years

**Table 2** Results of depth and speed obtained from modeling in HEC-RAS

Location	Depth (m)	Speed (m/s)
Open Plaza Piura	2.57	1.26
Main square	1.80	0.099
Sánchez Cerro bridge	3.10	4.25
Bolognesi bridge	2.18	9.90

**Table 3** Extremes discharge obtained for different return periods

$T$ (years)	$Q$ (m <sup>3</sup> /s)
10	2335.29
20	2950.13
50	3745.97
100	4342.34
500	5720.47

**Table 4** Depth and speed for discharge for the return period of 500 years

Location	Depth (m)	Speed (m/s)
Open Plaza Piura	3.55	2.42
Main square	4.72	1.54
Sánchez Cerro bridge	7.37	10.20
Bolognesi bridge	3.80	11.75

## 4.2 *Extreme Event Simulation with a 500 Year of the Return Period*

To achieve the extreme event with a return period of 500 years, the distribution of Extreme Values Type I of the maximum instantaneous discharge of the Chira-Piura project was made from 1971 until 2017 when the last El Niño phenomenon occurred. Once the probability of exceedance for this distribution was realized, the flows were calculated for the return periods of 10, 20, 50, 100 and 500 years. To do this, the flows were obtained as shown in Table 3.

Then, the modeling of the extreme event was performed for a 500-year return period, where an increase in the extent of the flood could be seen (Fig. 3). The results of the depths and speeds with a flow rate for the return period of 500 years are presented in Table 4.

## 5 Results

The simulation performed with HEC-RAS shows an accuracy between 75.5 and 76.67% respect Sentinel Satellite image for April 4th, 2017. For 500 years of the return period, water levels show a significant increase of 103% respect the last FEN 2017, it will generate a greater impact on vulnerable areas and the population.

The simulation carried out for the extreme event provides data on the most affected areas to be damaged by flooding, thus to mitigate the impact of this situation is necessary to develop a contingency, that involves building hydraulic protection structures, dredging plans for water depth that can control these effects.

Water surface elevation (WSE) vary along the stretch of the Piura River, obtaining values between 55 and 63 m.a.s.l (0–15 m water depth), due to the geometry of its channel and the discharge obtained and simulated for a return period of 500 years. The highest WSE found were located by the Open Plaza Piura, being an average of 61 m.a.s.l, since it is upstream and the riverbed was narrower and while going downstream the channel decreases.

The velocity found for a 500-year return period event would vary between 0 and 4 m/s in public places such as sidewalks, streets, the main square, open plaza, etc., and the velocity would increase in the riverbed becoming values between 10 and 17 m/s as in the Sanchez Cerro Bridge and Bolognesi Bridge which predicted speeds of 10.2 and 11.75 m/s, respectively.

## 6 Conclusions

The main contribution of the work is to make a model as close as possible to the events that occurred historically. As a result of the investigation, a model with a 75% approximation to the facts was obtained, in this way, simulations can be carried out for possible future extreme events of different return periods, as can be done in the simulation for 500 years, where an increase of the flood area of 80% was obtained in comparison with a simulation for 10 years, which represents a normal condition of the river. Also, based on the results of this study, once the most vulnerable areas are found, risk maps and contingency plans will be developed, such as the implementation of riverine defense structures to mitigate the economic and human impact caused by floods.

## References

1. Abdul Kadir M.A., Abustan I., Abdul Razak M.F.: 2D flood inundation simulation based on a large scale physical model using course numerical grid method. *Int. J. GEOMATE* **17**, 230–236 (2019). <https://doi.org/10.21660/2019.59.icee17>
2. Agencia Espacial del Perú. (n.d.). Comisión Nacional de Investigación y Desarrollo Aeroespacial. Lima: CONIDA. Available in: <http://www.conida.gob.pe/>
3. Agencia Peruana de Noticias. (2014). Inauguran en Piura Centro de Operaciones de Emergencia Regional. Piura. Available in: <https://andina.pe/agencia/noticia-inauguran-piura-centro-operaciones-emergencia-regional-499055.aspx>
4. Autoridad Nacional del Agua (ANA). (n.d.). Autoridad Nacional del Agua. Lima: ANA. Available in: <https://www.ana.gob.pe/>
5. Blade, E., et al.: Iber: herramienta de simulación numérica del flujo en ríos. *Revista internacional de métodos numéricos para cálculo y diseño en ingeniería* **30**(1), 1–10 (2014). <https://doi.org/10.1016/j.rimni.2012.07.004>
6. Chakraborty, S., Biswas, S.: Application of geographic information system and HEC-RAS in flood risk mapping of a catchment. **33**, 215–224 (2020). [https://doi.org/10.1007/978-981-13-7067-0\\_17](https://doi.org/10.1007/978-981-13-7067-0_17) (unpublished)
7. Chow, V.T.: *Hidráulica de Canales Abiertos*. McGraw-Hill, Bogotá, Colombia (2004)

8. COER.: Reporte de caudales del Río Piura para el 27/03/2017”, Centro de Operaciones de Emergencia Regional—Piura. Marzo (2017)
9. COPERNICUS (n.d). Copernicus Open Access Hub.: Copernicus, Europe’s eyes on Earth. Available in: <https://scihub.copernicus.eu/dhus/#/home>
10. Farooq, M., Shafique, M., Shahzard Khattak, M.: Flood hazard assessment and mapping of River Swat using HEC-RAS 2D model and high-resolution 12-m TanDEM-X DEM (WorldDEM). *Nat. Hazards* **97**, 477–492 (2019). <https://doi.org/10.1007/s11069-019-03638-9>
11. FLO-2D Software, INC. (n.d.). FLO-2D. Florida: FLO-2D Software, INC. Available in: <https://www.flo-2d.com/>
12. Gobierno Regional de Piura.: Proyecto Especial Chira Piura. Piura (2019). Available in: <http://www.chirapiura.gob.pe/>
13. Hydrologic Engineering Center (HEC). (n.d.). HEC-RAS. Washington: HEC. Available in: <https://www.hec.usace.army.mil/software/hec-ras/>
14. Maswood, M., Hossain, F.: Advancing river modelling in ungauged basins using satel-lite remote sensing: the case of the Ganges-Brahmaputra-Meghna basin. *Int. J. River Basin Manage.* **14**, 103–117 (2016). <https://doi.org/10.1080/15715124.2015.1089250>
15. Mohamad Faudzi, S.M., Abustan, I., Abdul Kadir M.A., Wahab, M.K., Abdul Razak M.F.: Two-dimensional simulation of Sultan Abu Bakar Dam release using hec-ras. *Int. J. GEOMATE* **16**, 124–131 (2019). <https://doi.org/10.21660/2019.58.icee18>
16. Patel, D.P., Ramirez, J.A., Srivastava, P.K., Bray, M., Han, D.: Assessment of flood inun-dation mapping of Surat city by couple 1D/2D hydrodynamic modeling: a case application of the new HEC-RAS 5. *Nat. Hazards* **89**, 93–130 (2017). <https://doi.org/10.1007/s11069-017-2956-6>
17. Surwase, T., SrinivasaRao, G., Manjusree, P., Begum, A., Nagamani, P.V., JaiSankar, G.: Flood inundation of Mahanadi River, Odisha during September 2008 by using HEC-RAS 2D Model, pp. 851–863 (2018). [https://doi.org/10.1007/978-3-319-77276-9\\_77](https://doi.org/10.1007/978-3-319-77276-9_77)
18. Vozinaki, A.K., Morianou, G.G., Alexakis, D.D., Tsanis, I.K.: Comparing 1D-and com-bined 1D/2D hydraulic simulations using high resolution topographic data, the case study of the Koiliaris basin, Greece. *Hydrol. Sci. J.* **7**, 642–656 (2016). <https://doi.org/10.1080/02626667.2016.1255746>

# Dynamic Amplification Factor Proposal for Seismic Resistant Design of Tall Buildings with Rigid Core Structural System



Eder Quezada , Yaneth Serrano , and Guillermo Huaco 

**Abstract** Currently, there is an increase in the demand for tall buildings in the city of Lima. This research proposes to reduce the dynamic amplification factor through the seismic design of tall buildings based on the requirements of Peruvian code considering that they are regular in plan and height. Minimum base shear values according to the comparison of static seismic shear and dynamic shear from the spectral modal analysis were reviewed for cases of buildings larger than 120 m. The study of 28 reinforced concrete buildings was proposed, with different heights - varying from 24 to 36 floors, with different floor configurations, as well as the arrangement of the walls considering as a rigid core structural system. Additionally, the characteristics of the materials, the loads and combinations were defined. The responses of these buildings were determined by the response spectrum analysis (RSA) and then compared with those obtained by the lineal response history analysis (LRHA), for the last analysis, five Peruvian seismic records were used and scaled to 0.45 g. The seismic responses of the LRHA procedure were taken as a benchmark. The result of this study is the analysis and proposal of the  $C/R$  factor for high-rise buildings, as well as obtaining the base shear and drift verification. Minimum base shear values can be reduced for high or long-term buildings, being regular in plan and height.

**Keywords** High-Rise buildings · Long natural period · Minimum seismic base shear force · Rigid core

---

E. Quezada · Y. Serrano · G. Huaco (✉)  
Peruvian University of Applied Sciences UPC, Av. Prolongación Primavera 2390, Santiago de Surco, Lima, Peru  
e-mail: [pccighua@upc.edu.pe](mailto:pccighua@upc.edu.pe)

E. Quezada  
e-mail: [u201610055@upc.edu.pe](mailto:u201610055@upc.edu.pe)

Y. Serrano  
e-mail: [u201423812@upc.edu.pe](mailto:u201423812@upc.edu.pe)

## 1 Introduction

A study by the United Nations estimates that by the end of 2050, approximately 64% of developing countries and 86% of the population of developed countries will live in cities. To solve the increase in population density in urban areas, these must be expanded, or high-rise buildings built [1]. For this reason, in the last decade, Lima has experienced an increase in the verticality of its buildings. Therefore, it is necessary to use a structural system resistant to wind and earthquake forces. Based on this, several structural systems have been developed for high-rise buildings. The rigid core structural system constitutes such a solution and offers the advantage of faster construction, flexible architecture and open space availability [1–8]. To design these structures that resist earthquake loads, there are several numerical methods [2]. One of them is the response spectrum analysis (RSA) which is widely used in various seismic codes such as ASCE 7, UBC-97, FEMA-356 and ATC-40 to determine design forces and displacement demands [3]. In addition, must be taken into consideration that tall buildings are complex due to the numerous structural components and several vibration modes [4]. In the case of the Peruvian Code, this method is related to the Equivalent Lateral Force (EFL) by means of the dynamic amplification factor, which guarantees that the current base is not less than 80% of the value calculated by EFL for regular structures. To determine the shear force by means of the EFL, the Standard establishes a minimum  $C/R$  factor. The subject of this analysis is to corroborate this parameter in the case of tall buildings by comparing inelastic responses with the LRHA. In addition, few studies prove that the RSA established by the standard is adequate for high-rise buildings. The advantage of using an adequate value for this factor will avoid the design of the building with unnecessary robust elements that meet the seismic requirements, which would significantly increase the cost of such infrastructure since it would cause a lack of investment due to the cost overrun.

The methodology adopted in this work is proposed by our authorship and is described as follows:

1. The case studies are defined taking into consideration the following criteria: use of the building, dimensions, predominant material, mezzanine height, slab thickness and variation in compressive strength.
2. Selection of five seismic acceleration records according to soil type and moment magnitude range.
3. Proceed with the EFL and RSA, as established by the Seismic Resistant Design Code E.030.
4. The inelastic responses of the spectral modal dynamic analysis are compared with the linear time-history analysis to determine the adjustment of the  $C/R$  factor.
5. The results analysis is carried out and an adjusted  $C/R$  value is proposed for high-rise reinforced concrete building.

## 2 Methodology

### 2.1 Description of the Buildings

Twenty-eight tall buildings located in Lima, Peru, are considered in this study (Fig. 1). The number of floors of the cases analyzed is 24, 26, 28, 30, 32, 34 and 36 floors. Fourteen of these buildings correspond to a square plan and the other fourteen to a rectangular plan. Likewise, the structural configuration was modified considering frames and post-tensioned slabs.

Each beam and column was modeled as an elastic frame element. The slabs and the cutting walls are modeled with a thin shell elastic element and the foundation was idealized as recessed base support. For all buildings, the columns on each floor resist less than 30% of the total lateral force; therefore, the structural system is considered as structural walls in accordance with Code E.030. The  $P - \Delta$  effects are included in all the methods [5] (Table 1).

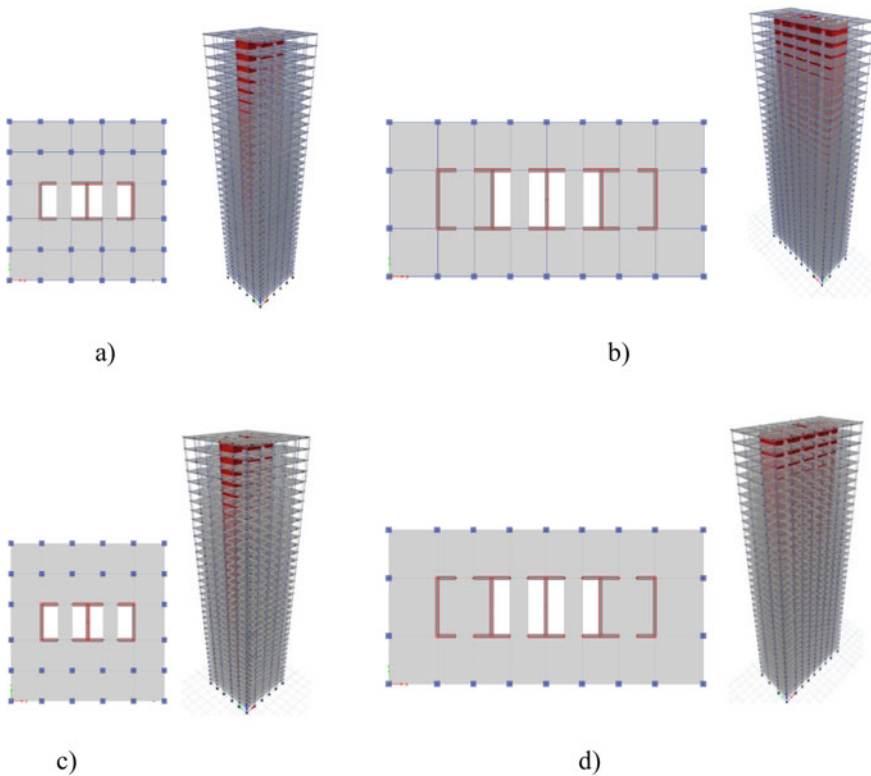


**Fig. 1** Floor plans and 3D models. **a** PC-POR, **b** PR-POR, **c** PC-POS y **d** PR-POS



**Table 1** Coding of the square and rectangular floor model

Number of stories	Walls and Columns		Post-tensioned slab	
	PC-POR	PR-POR	PC-POS	PR-POS
	Square	Rectangular	Square	Rectangular
24	N24-PC-POR	N24-PR-POR	N24-PC-POS	N24-PR-POS
26	N26-PC-POR	N26-PR-POR	N26-PC-POS	N26-PR-POS
28	N28-PC-POR	N28-PR-POR	N28-PC-POS	N28-PR-POS
30	N30-PC-POR	N30-PR-POR	N30-PC-POS	N30-PR-POS
32	N32-PC-POR	N32-PR-POR	N32-PC-POS	N32-PR-POS
34	N34-PC-POR	N34-PR-POR	N34-PC-POS	N34-PR-POS
36	N36-PC-POR	N36-PR-POR	N36-PC-POS	N36-PR-POS

## 2.2 Selected Seismic Records

In this study, a set of five seismic records was selected and the information was obtained from the Japanese Peruvian Center for Seismic Research and Disaster Mitigation (CISMID) [7]. The selection of these registers took into consideration the type of soil where the building is to be cemented (Very rigid soil) and with magnitude in the range of 6–8.5-moment magnitude. In addition, these were scaled to  $0.45 \text{ g cm/s}^2$  (Fig. 2).

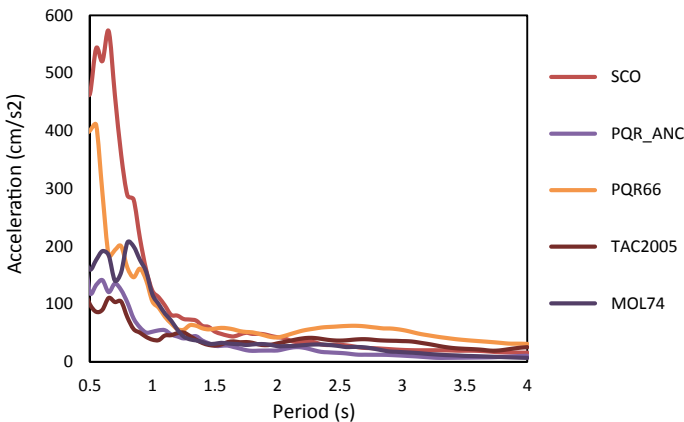


**Fig. 2** The response spectrum of selected earthquakes with a damping of 5%

## 2.3 *Methods of Analysis for Earthquake Resistant Design*

### 2.3.1 **Equivalent Lateral Force Procedure (ELF)**

The ELF procedure in Code E.030 is adopted in this study [6]. This method represents the seismic solicitations as a set of lateral forces that act in the center of mass of each level of the building. It consists of determining five seismic parameters that are: zone factor ( $Z$ ), soil factor ( $S$ ), use factor ( $U$ ), seismic amplification factor ( $C$ ), seismic force reduction coefficient ( $R$ ). The determination of the shear force at the base of the structure for each direction considered is calculated as follows:

$$V = \frac{ZUCS}{R} \cdot P; \frac{C}{R} \geq 0.11 \quad (1)$$

This methodology cannot be applied to structures of reinforced concrete bearing walls for buildings with a height greater than 30 m. However, it is necessary to carry out this analysis in the design of reinforced concrete elements by what establishes the norm as a minimum base shear force.

### 2.3.2 **Response Spectrum Analysis (RSA)**

The RSA method in Code E.030 is adopted in this study [6], where the elastic response is combined for several vibration modes to obtain the total elastic response, using the complete quadratic combination (CQC), which is then reduced by a force reduction factor ( $R$ ) to obtain the design forces of the structure.

## 3 **Results**

### 3.1 *Comparison of Design Demands Between RSA and LRHA*

The following graphs represent the base shear through different types of analysis in both directions. The first bar represents the RSA analysis with the  $C/R$  factor calculated, while the second bar depicts the base shear obtained with the RSA analysis with the minimum  $C/R$  factor proposed by the Peruvian Code. Additionally, the other bars represent the base shear calculated from LRHA analysis with the seismic records mentioned above (Figs. 3, 4, 5, 6, 7, 8, 9 and 10).

The shear forces calculated from the LRHA are significantly lower than those calculated from RSA established by the Peruvian Standard of Seismic-Resistant Design E.030, only a few exceptions for the seismic record of Surco1974 for the N34PC\_POR model. Therefore, it can be deduced that the  $C/R$  value is lower than what is established in the regulations. The results of the LRHA were reduced by a factor  $R$ . There are greater requests in terms of cut in square and rectangular plants of 36 levels.

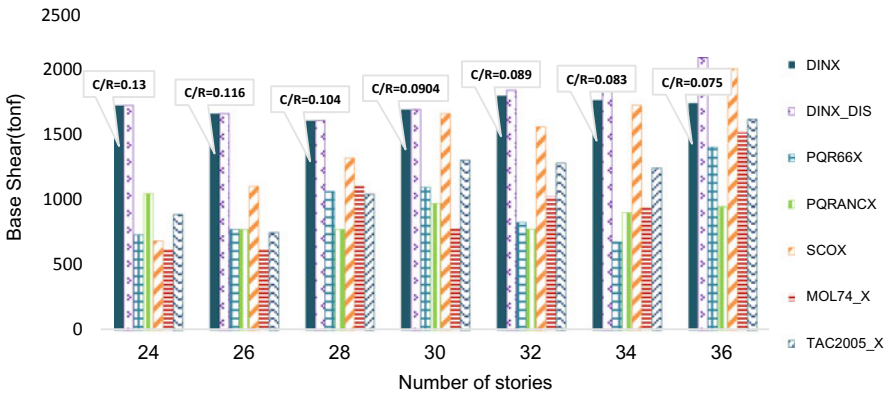


Fig. 3 Base Shear for PC-POR in the X-direction

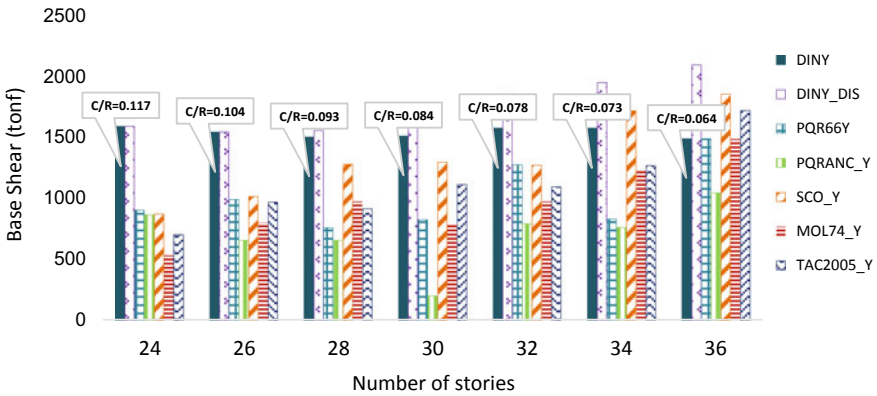


Fig. 4 Base Shear for PC-POR in the Y-direction

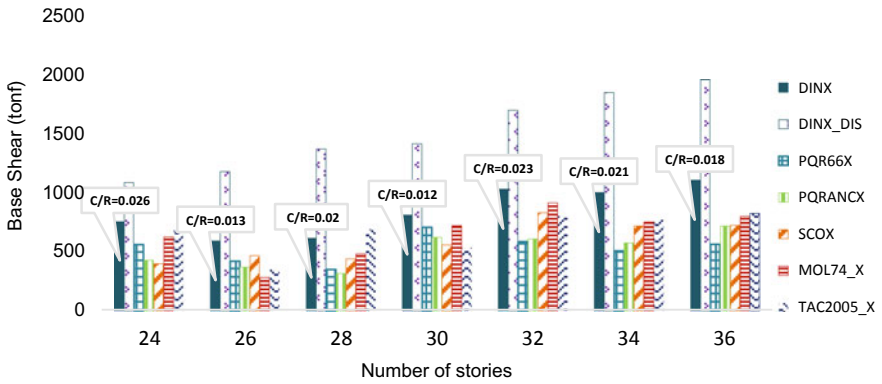


Fig. 5 Base Shear for PC-POS in the X-direction

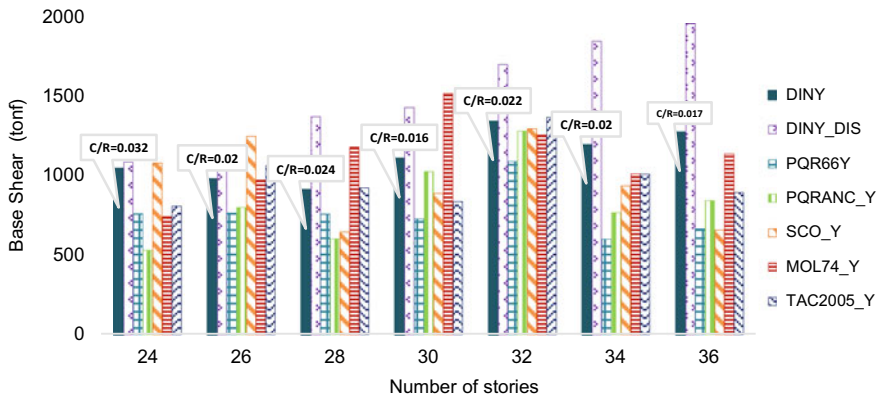


Fig. 6 Base Shear for PC-POS in the Y-direction

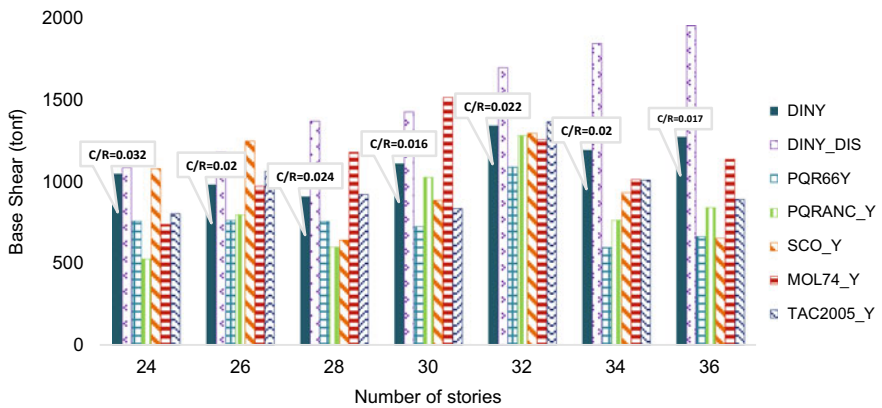


Fig. 7 Base Shear for PR-POR in the X-direction

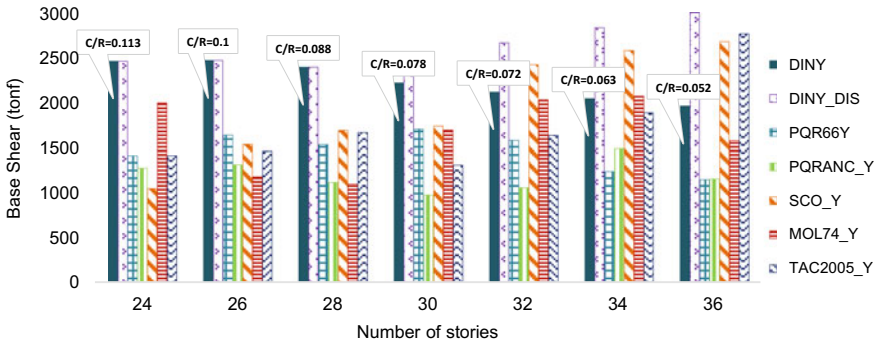


Fig. 8 Base Shear for PR-POR in the Y-direction

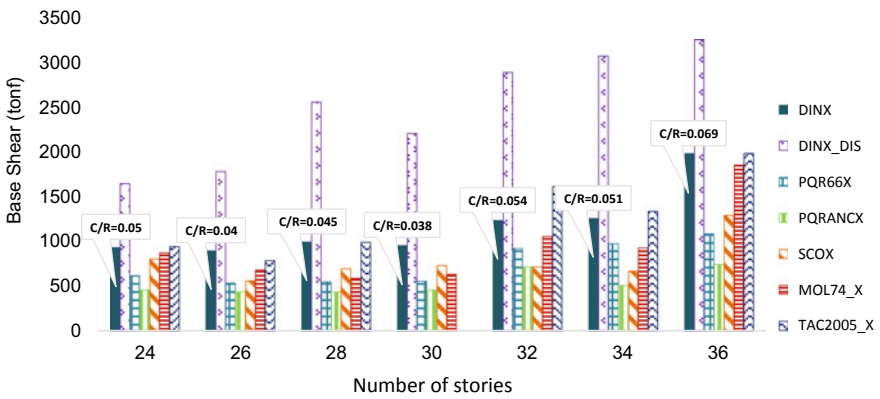


Fig. 9 Base Shear for PR-POS in the X-direction

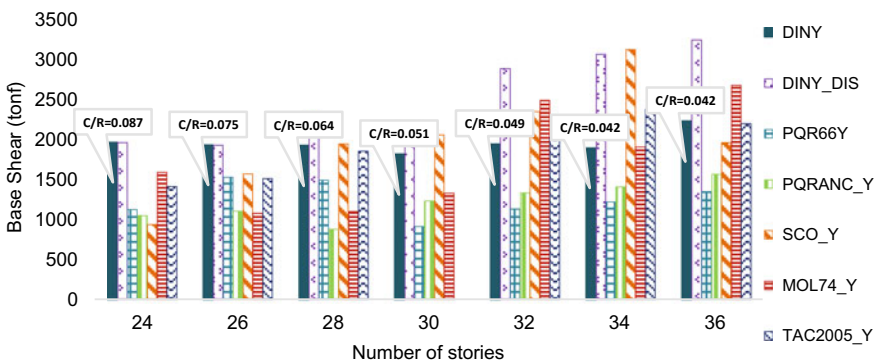


Fig. 10 Base Shear for PR-POS in the Y-direction

The general procedure to determine the value of  $C/R$  for high-rise buildings consists of computing ratios that are based on the base shear obtained by the RSA and the LRHA. Then the ratios are multiplied by the  $C/R$  values obtained from the LRHA. Finally, the most critical values were chosen as the final value (Tables 2 and 3).

**Table 2** Summary of proposed  $C/R$  values in the  $X$ -direction

	Level	Tx	$C/R$ calc.	$C/R$ proposed				
				PQR 66	PQR70	SCO74	MOL74	TACNA
PC-POR	24	1.284	0.13	0.055	0.079	0.052	0.047	0.067
	26	1.441	0.116	0.054	0.054	0.077	0.044	0.052
	28	1.602	0.104	0.069	0.050	0.085	0.072	0.067
	30	1.779	0.094	0.061	0.054	0.092	0.044	0.072
	32	1.873	0.089	0.041	0.039	0.077	0.051	0.063
	34	2.01	0.083	0.032	0.043	0.081	0.045	0.058
	36	2.23	0.075	0.060	0.041	0.086	0.065	0.070
PC-POS	24	2.666	0.059	0.044	0.033	0.031	0.049	0.054
	26	3.848	0.028	0.020	0.017	0.022	0.013	0.017
	28	3.074	0.044	0.025	0.023	0.031	0.034	0.049
	30	3.91	0.027	0.024	0.021	0.019	0.024	0.018
	32	2.863	0.051	0.029	0.030	0.041	0.045	0.040
	34	2.96	0.048	0.024	0.027	0.034	0.036	0.037
	36	3.229	0.04	0.020	0.026	0.026	0.029	0.030
PR-POR	24	1.111	0.15	0.059	0.097	0.069	0.100	0.097
	26	1.229	0.136	0.055	0.064	0.054	0.063	0.071
	28	1.353	0.123	0.060	0.072	0.085	0.047	0.052
	30	1.542	0.108	0.058	0.042	0.066	0.053	0.052
	32	1.557	0.107	0.070	0.053	0.079	0.064	0.063
	34	1.696	0.098	0.066	0.040	0.097	0.069	0.072
	36	1.835	0.091	0.045	0.045	0.084	0.052	0.073
PR-POS	24	2.901	0.05	0.033	0.025	0.043	0.047	0.050
	26	3.227	0.04	0.024	0.020	0.025	0.030	0.035
	28	3.045	0.045	0.025	0.020	0.032	0.027	0.045
	30	3.317	0.038	0.022	0.018	0.029	0.025	0.038
	32	2.789	0.054	0.040	0.031	0.031	0.046	0.071
	34	2.853	0.051	0.040	0.021	0.027	0.038	0.054
	36	2.401	0.069	0.038	0.026	0.045	0.064	0.069

**Table 3** Summary of *C/R* proposed values in the *Y*-direction

	Level	Ty	<i>C/R</i> calc.	<i>C/R</i> proposed				
				PQR 66	PQR70	SCO74	MOL74	TACNA
PC-POR	24	1.426	0.117	0.066	0.064	0.064	0.039	0.052
	26	1.605	0.104	0.067	0.044	0.068	0.054	0.065
	28	1.786	0.093	0.047	0.041	0.079	0.060	0.057
	30	1.975	0.084	0.046	0.047	0.072	0.044	0.062
	32	2.152	0.078	0.063	0.039	0.063	0.048	0.054
	34	2.298	0.073	0.038	0.035	0.080	0.057	0.059
	36	2.55	0.064	0.064	0.045	0.080	0.064	0.074
PC-POS	24	2.32	0.072	0.052	0.036	0.074	0.051	0.056
	26	3.04	0.045	0.035	0.037	0.057	0.045	0.049
	28	2.78	0.054	0.045	0.036	0.038	0.070	0.055
	30	3.446	0.035	0.023	0.032	0.028	0.048	0.026
	32	2.904	0.049	0.040	0.047	0.047	0.046	0.050
	34	3.04	0.045	0.023	0.029	0.035	0.038	0.038
	36	3.349	0.037	0.019	0.025	0.019	0.033	0.026
PR-POR	24	1.472	0.113	0.065	0.058	0.048	0.092	0.065
	26	1.672	0.1	0.066	0.053	0.062	0.048	0.059
	28	1.886	0.088	0.056	0.041	0.062	0.040	0.061
	30	2.149	0.078	0.060	0.034	0.061	0.060	0.046
	32	2.321	0.072	0.054	0.036	0.082	0.069	0.056
	34	2.58	0.063	0.038	0.046	0.080	0.064	0.058
	36	2.843	0.052	0.030	0.031	0.071	0.042	0.073
PR-POS	24	1.928	0.087	0.050	0.046	0.041	0.071	0.063
	26	2.235	0.075	0.059	0.043	0.061	0.042	0.059
	28	2.549	0.064	0.049	0.029	0.065	0.036	0.062
	30	2.872	0.051	0.025	0.035	0.058	0.037	0.042
	32	2.906	0.049	0.029	0.034	0.059	0.063	0.051
	34	3.162	0.042	0.027	0.031	0.070	0.042	0.053
	36	3.146	0.042	0.025	0.029	0.037	0.050	0.041

## 4 Discussions

This work incentive the design of buildings that meet the seismic requirements and is economically feasible, besides that it was resolved the lack of information regarding high-rise reinforced concrete buildings in Peru and investigates the advantages of regular seismic buildings as seen in other international buildings such as the case of Burj Khalifa.

The range of periods found for the PC-POR and PR-POR buildings is between 1.5 and 3 s, while for the PC-POS and PR-POS structures their range corresponds to 2.5–4 s, being the largest period, the cross-section that is slenderer.

## 5 Conclusions

The value of  $C/R$  is analyzed in the case of tall reinforced concrete buildings by comparing the design shears indicated by Peruvian seismic regulations with the base shear obtained from an LRHA, which have been scaled to 0.45 g.

It was found lower drifts of the LRHA smaller than what is indicated in Code E.030, except for specific cases, but all are less than 0.7%, which establishes said norm. The dynamic amplification factor is sensitive to the  $C/R$  value. It was noticed that for PC-POR and PR-POR buildings, considering the minimum  $C/R$  equal to 0.11, the shear does not need to be amplified for buildings smaller than 30 floors, however, for larger buildings the factor of amplification would be in the order of 150%. On the other hand, for PC-POS buildings, it is not necessary to amplify the shear, and for PR-POS it is amplified from the 32-story buildings, in the order of 250%.

The main finding of this paper proposes a minimum value of  $C/R$  less than 0.11 for each of the 4 studied cases of the high-rise building. It was obtained due to the regularity in the plan and height of the building and the use of a rigid core structural system. As for PC-POR buildings, it is established that  $C/R$  values are much lower than 0.08 for buildings with up to 32 levels, for buildings with a higher number of levels this value is close to 0.08; something similar happens for structures type PR-POR. In addition, for PC-POS and PR-POS buildings, the value of  $C/R$  is less than 0.08 at all levels. Two  $C/R$  values differentiated by the structural system are proposed,  $C/R$  equal to 0.075 for PC-POS and PR-POS and for 0.10 for PC-POR and PR-POR.

There is a pressing need to extend the research to study the implications of the wind force due to the predominant effect for high-rise buildings such as this one because of its high natural period. It is suggested to study it. Furthermore, the value of  $R$  must be improved or studied, being able to be less than 6, for this, it is suggested to perform a nonlinear response history analysis (NLRHA).

## References

1. Rahman, A., Zaman, Q., Irshad, M.: Evaluation of Simplified Analysis Procedures for a High-Rise Reinforced concrete core wall structure. *Adv. Civil Eng.* **16**, 599–614 (2019)
2. Khy, K., Chintanapakdee, C., Wijeyewickrema, A.: Modified response spectrum analysis to compute shear force in tall RC shear wall buildings. *Eng. Struct.* **180**, 295–309 (2019)



3. Najam, F, Warnitchai, P.: A modified response spectrum analysis procedure to determine nonlinear seismic demands of high-rise buildings with shear walls. *Struct. Des. Tall Special Build.* **27** (2017)
4. Mehmood, T., Warnitchai, P., Suwansaya, P.: Seismic evaluation of tall buildings using a simplified but accurate analysis procedure. *J. Earthq. Eng.* **22**(3), 356–381 (2017)
5. Liu, Y., Kuang, J.: Spectrum-based pushover analysis for estimating seismic demand of tall buildings. *Bull. Earthq. Eng.* **15**, 4193–4214 (2017)
6. Peru Seismic Code E.030.: Seismic Design Requirements for Buildings, SENCICO, Peru (2018)
7. Accelerometers Network Database, Center for Earthquake Engineering Research and Disaster Mitigation, CISMID, Lima Peru (2019)
8. Ali, M., Moon, K.: Advances in structural systems for tall buildings: emerging developments for contemporary urban giants. *Buildings* **8**, 104 (2018)

# A Mechanical Development of a Dry Cell to Obtain HHO from Water Electrolysis



Gustavo Salazar , Wilmer Solis , and Leonardo Vincés 

**Abstract** This article proposes a mechanical development of a dry cell in order to obtain HHO through water electrolysis. Calculations and technical specifications of the materials used for implementation are supported by mathematical, physical and chemical formulas and theories (Faraday's Law, electrolysis process and mechanical design). The importance of mechanical design is focused on achieving efficient use of the energy provided to the cell that allows the H<sub>2</sub> and O<sub>2</sub> molecules to be separated without overheating the cell, evaporating the water, loss of current due to the geometry of the electrodes (Foucault Current). Moreover, choosing materials for proper implementation and physical robustness is mandatory. In addition, the mechanical design is not justified in different articles. Nevertheless, the mechanical design of the cell and the efficiency in the production of HHO are related. Therefore, the mechanical design and the calculations were performed, as well as the construction of the dry cell to obtain HHO. The results of the implementation and production were placed and compared with what theoretically the dry cell should produce from the law of Faraday. Finally, the volumetric flow of HHO obtained was 2.70 L per minute. It means a production efficiency of 98.68%. It is higher than the majority of the dry cells.

**Keywords** HHO generation · Electrolysis · Dry cell · Faraday · Mechanical design

---

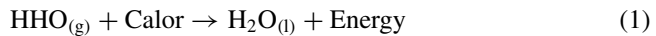
G. Salazar · W. Solis · L. Vincés (✉)  
Universidad Peruana de Ciencias Aplicadas, Av. Prolongación Primavera 2390, Santiago de Surco, Lima, Peru  
e-mail: [nikolai.vinces@upc.edu.pe](mailto:nikolai.vinces@upc.edu.pe)

G. Salazar  
e-mail: [u201510860@upc.edu.pe](mailto:u201510860@upc.edu.pe)

W. Solis  
e-mail: [u201519263@upc.edu.pe](mailto:u201519263@upc.edu.pe)

# 1 Introduction

Currently, global energy demand has increased and will continue for 25% more by 2040, according to the International Energy Agency [1]. In many countries, most of the energy comes from fossil sources like energy generated by coal, oil or its derivatives. An example of this is the energy balance carried out in Peru by the Ministry of Energy and Mines in 2016 recovered by the Latin American Energy Organization [2]. The results of this study show that the main source of energy is natural gas and oil (47% and 30%, respectively), both non-renewable and polluting energy sources. Because of this, there is a need to use a renewable and less polluting alternative fuel. Hydroxy gas or brown gas (HHO) is a clean and renewable source of energy due to the absence of hydrocarbon compounds; therefore, carbon dioxide or other potentially dangerous gases are not released after combustion, it only produces water vapor [3], as shown in (1).



HHO is produced by dividing water into hydrogen and oxygen molecules through electrolysis. An electrolyzer, also called a hydrogen generator, is necessary for this process. Some works on this field have been developed, the ones mentioned below are the most important.

Rusdianasari et al. [4] used a software capable of calculating the production of HHO gas and the power consumed of a wet cell according to the number, dimensions of the electrodes, the voltage and current provided. In addition, the authors arrived and compared the value of the HHO flow produced with the value calculated by the software. However, the authors did not justify the characteristics chosen for the design of the wet cell test resulting in an efficiency of 89.13%.

Shah et al. [5] compare the energy efficiency, production of HHO, the maintenance and safety considerations of the dry and wet cell. As a result, they conclude the dry cell being better in all the fields described above with the same input conditions as the cell wet. The authors described the components of the dry cell and the physical characteristics of the mechanical system that influenced the production of HHO. In addition, they present a detailed design of the dry cell. However, the design presented, and the components used for implementation don't present technical specifications or mathematical calculations that justify them.

Nabil et al. designed in [6] several cells with different numbers of electrodes and configurations. In addition, the authors show a table with all the designs made and they compare the energy consumption, the production of HHO gas, the molarity used and the temperature of each one. However, despite using Faraday's first law in their article, the authors do not compare the production flow of each mechanical design with what the cell should theoretically produce. Moreover, they don't demonstrate the efficiency of each configuration. In addition, the measurements and the shape of the electrodes are not justified.

Because of the cases seen before, it is proposed to make a design based on mathematical calculations, physical and chemical formulas (Faraday's Law, electrolysis process and mechanical design). Furthermore, the implementation of a correct selection of dry cell components. Finally, the production of HHO of the designed cell will be compared with what should theoretically be produced from Faraday's law.

## 2 Description of the Proposed Method

To have an overview of the dry hydrogen cell that was designed, the P&ID diagram of the electrolysis process can be seen in Fig. 1.

The diagram shows the instrumentation to be used in the process and the parts that comprise it. In the dry cell is where the separation of water molecules occurs. Moreover, it is where the research will focus on. In order to obtain an efficient mechanical design, the following phases shown in Fig. 2 must be followed.

### 2.1 *Calculations of Preliminary Cell Dimensions*

For the design of the dry cell, calculations had to be made based on the power available for the process. In this case, we have a 12 V battery and the current will be regulated at 20 A. From this data, we can configure the cell plates. In the same way that series circuits can be created by connecting various chained elements to each other and connecting the power supply only at the ends, it is also possible to do the same with the electrodes. Nevertheless, with the difference that the connection between them occurs through the electrolyte. The plates that remain unconnected are called neutral or bipolar, these plates are not connected to any source of electricity and are placed between two plates connected to different polarities. In this way, it is achieved that in each separation created between the connected plates there is a voltage equal to the total divided by the number of spaces, without the need to adjust the voltage output of the source or use cables.

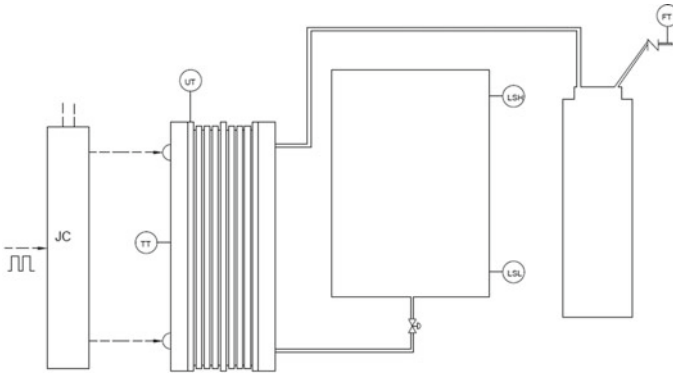


**Fig. 1** P&ID diagram of the electrolysis process

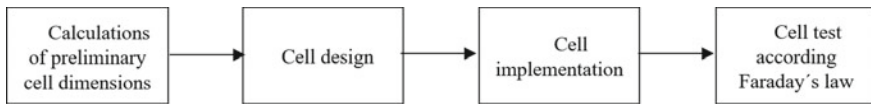


**Fig. 2** Block diagram of the proposed method

According to Gamez [7], to calculate the number of plates, the voltage between electrodes and the total source voltage must be considered. The number of plates is obtained by applying Eq. (2):

$$V_C = \frac{V_T}{n - 1} \tag{2}$$

The  $n$  is the number of plates per group,  $V_T$  the total cell voltage and  $V_C$  the calculated voltage between electrodes. The result of  $n$  will be 7, two of which will be polarized (cation and anion) and the other five will be neutral. For greater production, the following configuration will be chosen:

$$-NNNNN + NNNNN-$$

The  $N$ 's are the neutral plates between the polarizing plates (+ -). In addition, it must be considered that the current delivered by the source will be divided into two groups. However, having two negatively polarized plates, hydrogen production will be higher because it has a positive ion.

The geometry chosen for the plates is circular since there will be no electrical losses due to vertices of the electrode. These currents are called Foucault currents. In certain cases, these currents can produce undesirable effects. For example, they increase internal energy and temperature. A conductive material with angular edges and corners has electrical losses (corner effects) as a result of the accumulation of electromagnetic fields in said vertices caused by a non-uniform current density [8].

Moreover, the current that will give energy to the cell will be regulated with a PWM wave, the current will be variable, and the current density will be non-uniform.

Gómez defines the current density as the amount of current that circulates per unit area of an electrode, and is calculated using (3):

$$d_C = \frac{I_E}{S_E} = \frac{I_E}{N_A \times S_E} \quad (3)$$

where  $d_C$  is the current density ( $A/m^2$ ),  $I_E$  the intensity of the current flowing through the electrode (A),  $S_E$  the surface of the electrode ( $m^2$ ) and  $N_A$  the number of cell groups.

Assuming the same electrode surface, by increasing the current flowing through the cell the production of gas will be increased, but also the voltage necessary to circulate this current, so that the efficiency of the cell will decrease. To avoid this, Gómez mentions that the idea is to maintain a flow of  $1000 A/m^2$ , since, at a smaller area, a higher voltage will be needed to circulate the same amperage, which will generate more heat.

Having an electrode surface (SE) of  $0.01 m^2$  and a circular geometry of the electrode, an electrode radius equal to 56 mm is obtained. That is the theoretical radius that the cell's circular plate should have. However, for experimentation and ease of machining, a plate with a radius of 75 mm will be implemented. In addition, the excess area can serve as a heat sink for the cell.

## 2.2 Cell Design

The software called Inventor [9] was used to design the plates. Two types of plates will be designed: neutral and polarized. The polarizing plates will have an extension in one corner, as seen in Fig. 3 so that it is attached to the stud that will pass through the cell to assemble it. This stud will be connected to a pole of the power supply. However, the extension made on the plate will be with a rounded corner to avoid the phenomenon of stray currents. The neutral plate will not be connected to any pole of the power supply and will be fully circular as seen in Fig. 3.

For the separation between electrodes and to ensure the sealing of the same, nitrile O-ring will be used. Due to the current that will pass through the cell, a separation of 4–8 mm is recommended. Because of the current that will pass through the cell and the high gas productions, the electrolyte will bubble and foam, appearing spaces without liquid between the electrodes that will reduce the efficiency of the cell. Consequently, 6.99 mm thick O-rings were chosen, standardized measurement of this material [10]. To give greater physical strength to the cell, 18 mm thick acrylic will be used. The design of these acrylic plates is seen in Fig. 4.

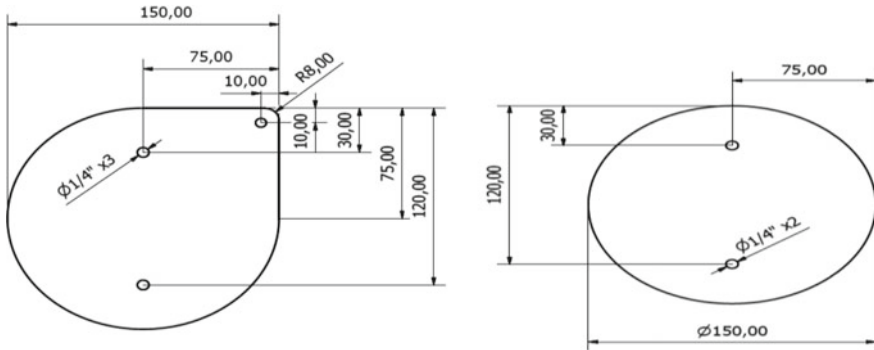


**Fig. 3** Detailed plane of the polarized and neutral plate

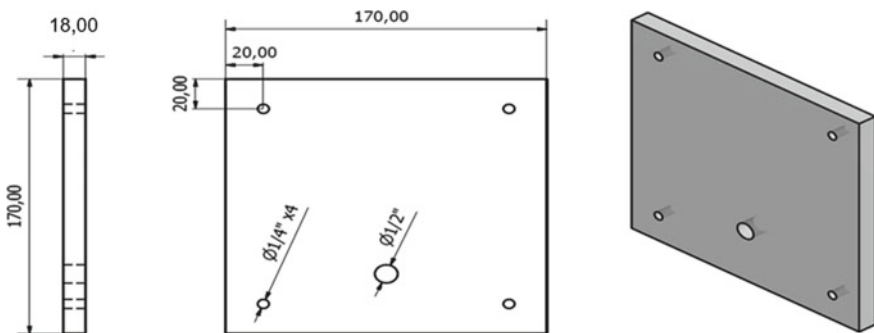


**Fig. 4** Detailed plane of acrylic plate

### 2.3 Cell Implementation

To carry out the implementation of the cell it was necessary to make a previous study of the materials to be used. The 316 L stainless steel was used in the plates since the dry hydrogen cell will be in constant contact with salts and water and this material offers a high electrical conductivity for electrolysis (electrical resistivity:  $70\text{--}78 \times 10^{-8} \Omega \times \text{m}$ ). In addition, it has a high resistance to corrosion due to its chemical composition [11]. In the case of the O-rings, nitrile was used, since it is not high priced, its working temperature is adequate ( $-20$  to  $90$  °C) and it is very durable [12]. For the electrolyte, KOH was chosen with a concentration of 10%, since it is the best electrolyte for any application and at this concentration, the best results are obtained. This is because it supports more varied conditions and leaves no residue. Sodium hydroxide, on the other hand, generates a brown residue that clouds the solution and soils the cell, progressively reducing its efficiency if it is not cleaned periodically [13, 14]. Finally, to seal the cell, 18 mm thick transparent acrylic and Teflon couplings were used to enter the solution and exit hydrogen. After choosing

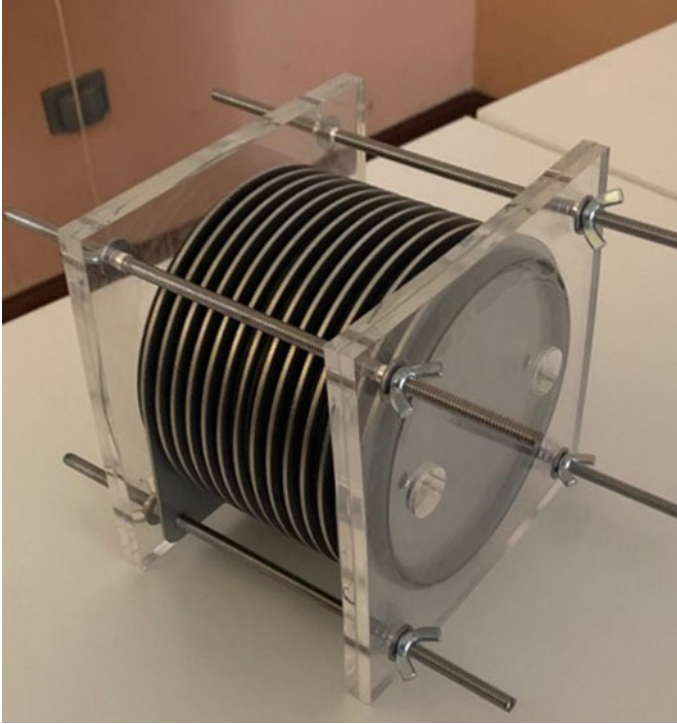


**Fig. 5** HHO dry cell assembled

all the materials, the cell assembly is carried out. Subsequently, tightness tests were performed to avoid leaks. In Fig. 5, the fully assembled cell can be seen.

#### ***2.4 Cell Test According to Faraday's Law***

The electrolysis process is basically based on Faraday's laws for electrolysis, thus having both the first (4) and the second law that refers to the fact that the amount of altered substance in an electrode directly depends on the electric current in Coulombs. In addition, the mass deposited in an electrode is proportional to its molecular weight or chemical equivalent.

$$Q = I \times t \tag{4}$$

where  $Q$  is the necessary energy (C),  $I$  the current intensity supplied (A) and  $t$  the time (s). Then, we proceed to calculate the number of chemical equivalents of a substance deposited in an electrode with (5):



$$n^{\circ}\text{eqq} = \frac{Q}{F} \quad (5)$$

In this equation, “ $n^{\circ}\text{eqq}$ ” is the number of chemical equivalents of a substance deposited in an electrode, which is directly proportional to “ $Q$ ” (1200 C). The necessary energy calculated with Faraday’s first law (4), divided between Faraday’s constant, “ $F$ ”. The chemical equivalent found with (5) must be transformed to mass of  $\text{H}_2$ , considering the molecular weight of  $\text{H}_2$  (2 g/mol) and its valence electrons (+2) we can obtain that its “ $\text{eqq}$ ” is 1. With this calculation, the mass of  $\text{H}_2$  ( $m_{\text{H}_2}$ ) can be transformed using the following relation (6):

$$n^{\circ}\text{eqq} \times \frac{1\text{g}}{1\text{eqq}} = m_{\text{H}_2} \quad (6)$$

Knowing the mass of hydrogen to be obtained per minute, 0.0124 g  $\text{H}_2$ , now it is desired to pass this mass to volume, specifically to liters, for this the ideal gas equation is used, replacing the values at normal conditions resulting in 152 mL per minute to calculate the production of  $\text{O}_2$  we can use the proportionalities of the volume of  $\text{H}_2$  ( $\dot{V}_{\text{H}_2}$ ) and  $\text{O}_2$  ( $\dot{V}_{\text{O}_2}$ ) that have a ratio of 2: 1. Therefore, the volume of HHO ( $\dot{V}_{\text{HHO}}$ ) produced per compartment can be obtained. Since there are 12 compartments, the equation is obtained in (7):

$$\dot{V}_{\text{HHO}} = (\dot{V}_{\text{H}_2} + \dot{V}_{\text{O}_2}) \times 12 \quad (7)$$

Assuming 100% efficiency, this value found in (7) is approximately 2.73 L/min.

### 3 Results

In order to obtain the production efficiency of the dry cell, we implemented the P&ID shown in Fig. 1, using a rotameter as a flow meter. In the test, the rotameter indicated an HHO flow rate of 2.7 L/min with a peak current of 20 A. This result gives us an efficiency of 98.68% as shown in Table 1.

**Table 1** Production comparison

	Rusdianasari [4]	Our work
HHO production (L/min)	0.1028	2.73
Efficiency	89.13%	98.68%

## 4 Conclusion and Future Work

Our development can increase efficiency by 9.55% compared to the cell of Rusdianasari. Moreover, the mechanical design is just the beginning of this work. The purpose of developing this dry cell is to generate electricity by using an engine without any kind of gasoline.

## References

1. International Energy Agency. <https://www.iea.org/newsroom/news/2018/november/world-energy-outlook-2018-examines-future-patterns-of-global-energy-system-at-a-t.html>. Last Accessed 21 Aug 2019
2. Ministerio de Energía y minas. [http://www.minem.gob.pe/minem/archivos/BNE\\_2016.pdf](http://www.minem.gob.pe/minem/archivos/BNE_2016.pdf). Last Accessed 10 Act 2019
3. Choodum, N., Sangwichien, C., Yamsaengsung, R.: Optimization of a closed-loop HHO production system for vehicles and houses. *Environ. Progress Sustain. Energy* **38**(1), 268–277 (2019)
4. Rusdianasari, R., Bow, Y., Dewi, Y.: HHO gas generation in hydrogen generator using electrolysis. *Earth Environ. Sci.* 258 (2019)
5. Shah, S., Ali, Z., Larik, J., Kaimkhani, A.: Comparative study of dry and wet cell for HHO gas generation as a supplement fuel for I.C. Engine. *Int. Conf. Comput. Math. Eng. Technol.* (2018)
6. Nabil, T., Mohamed, M., Dawood, K.: Enabling efficient use of oxy-hydrogen gas (HHO) in selected engineering applications; transportation and sustainable power generation. *J. Clean. Prod.* 237 (2019)
7. Gámez, D.: El hidrógeno y sus aplicaciones energéticas. INS La Ferrería, España (2010)
8. Montrose, M.: Time and frequency domain analysis for right angle corners on printed circuit board traces, 551–556 (1998)
9. Autodesk Homepage. <https://www.autodesk.com/products/inventor/overview>. Last Accessed 28 Nov 2019
10. Parker Homepage. [https://www.parker.com/literature/o\\_ring.pdf](https://www.parker.com/literature/o_ring.pdf). Last Accessed 20 May 2019
11. King, M.: Water electrolyzers and the zero-point energy. *Phys. Procedia* **20**, 435–445 (2011)
12. Komariah, L., Arita, S., Aprianjaya, F., Novaldi, M., Fathullah M.: O-rings material deterioration due to contact with biodiesel blends in a dynamic fuel flow. *J. Phys. Conf. Serie* (2019)
13. Streblau, M., Mihail, S., Aprahamian, B., Dimova, T.: The influence of the electrolyte parameters on the efficiency of the oxyhydrogen (HHO) generator. *IEEE Electr. Apparatus Technol. (SIELA)*, 31–39 (2014)
14. Fiala, J., Kuracina, M., Hrusovsky, I., Soldan, M.: Study of basic characteristics of hydrogen generator. *Appl. Mech. Mater.* **10**, 3078–3081 (2013)

# An Automated System for the Stage of Hydrolysis and Filtration in the Extraction of Pectin from the Cocoa Shell



Maritza Ccencho , Valeria Quijada , and Leonardo Vinces 

**Abstract** Pectin obtained from cocoa husks has recently been investigated because of its gelling and stabilizing properties that have great potential for the food, cosmetic and pharmaceutical industries. However, its production at the industrial level has not been studied or developed in Peru. A fundamental part of the extraction process is the stage of hydrolysis and filtering of the cocoa shell. Because of this, an automated system for acid-thermal hydrolysis and shell filtration is proposed. The control of both processes is of great importance because the quality and efficiency of the extracted pectin will depend on it. The tests will be carried out in a cylindrical taper with a 100 L capacity which is adapted to contain a 20 L cylindrical filter, both made of AISI 304 stainless steel. The filter has a motor to homogenize the temperature and pH of the mix. The pH of the process is 2 and the temperature is  $90 \pm 2$  °C, since in these ranges the pectin is released more easily from the cocoa shell. The method consists of the structural design of the tank and the filter, and in the design of the pH regulator and the heating system. The yield of the extraction process was achieved by 10%.

**Keywords** Hydrolysis · Shell filtering · Pectin extraction · Cocoa shell

---

M. Ccencho · V. Quijada · L. Vinces (✉)  
Universidad Peruana de Ciencias Aplicadas, Av. Prolongación Primavera 2390, Santiago de Surco, Lima, Peru  
e-mail: [leonardo.vinces@upc.pe](mailto:leonardo.vinces@upc.pe)

M. Ccencho  
e-mail: [u201517106@upc.edu.pe](mailto:u201517106@upc.edu.pe)

V. Quijada  
e-mail: [u201511543@upc.edu.pe](mailto:u201511543@upc.edu.pe)

## 1 Introduction

Pectin is made up of complex molecules formed by polysaccharides, mainly by galacturonic acid units, esterified or by groups of methoxyl. These molecules are classified as high methoxyl and low methoxyl according to their degree of esterification, providing different properties and gelation power to each of them [1]. These characteristics have allowed it to be used primarily as a gelling and stabilizing agent in the food and cosmetic industries, and it can also be used in the pharmaceutical industry for its hydrocolloid, therapeutic and increased properties of the active ingredients. New uses have also been investigated in the plastics industry and in the manufacture of foaming products, such as clarifying agents and binders [2]. The global pectin market has grown at a compound annual rate of around 6% during 2011–2018 [3] and is estimated to reach USD 1.87 billion by 2026 [4]. At present, this product is not produced in Peru, and demand is fully covered with imports from Mexico and China. Currently, 365 t of pectin are imported into the country per year [5].

Likewise, it was decided to extract pectin from the cocoa shell to use this product that is wasted nowadays. In Peru, 134,676 tons of cocoa are produced per year [6]. Of that amount, only 10% represents the fruit and the rest to the shell that is later discarded.

Finally, the main objective of the project is to extract pectin from the cocoa shell automatically and effectively. For this, a tank is designed where the hydrolysis stage is allowed to be carried out at 90 °C and with a pH of 2. Also, a filter containing the cocoa shell is designed to prevent contamination of the pectin when the extraction is finished.

## 2 Literature Review

Previously, works on the subject have been developed. And now, the most important ones are mentioned:

Andersen et al. have identified in [7] the variation of the properties and chemical composition of the peels of different citrus fruits that are used to make pectin. The dynamic model of the pectin extraction process was developed by determining the main phenomena involved in a batch extraction reactor to predict the effect on the performance and properties of the pectin in the key process conditions: temperature and pH. Pectin was extracted from 0.5 kg of dried lime peel at different temperatures (60, 70, 80 °C) and pH (1.5, 2.3, 3.1). However, this work only focuses on the stage of acid hydrolysis. Likewise, the regulation of pH and filtering is done manually. In addition, the proposed method is performed in two tanks, which has a greater investment.

Casas-Orozco, Villa, Bustamante, and González propose in [8] the dimensioning and programming of a semi-continuous plant for the production of 348 t/year of pectin from Valencia orange peels in optimal experimental extraction conditions (90 °C,

75 min,  $\text{pH} = 1.5$ ). The designed plant includes the acid hydrolysis, the filtration of the hydrolyzed suspension, the precipitation of pectin, the gel pressing, the gel drying and the reduction of pectin size. Total production of 337.610 kg/year of pectin is achieved in the designed facility, with a lot size of 3383 kg of shell and a cycle time (3.61 h) determined by the hydrolysis stage. However, this work only focused on the simulation of the process and the implementation stage was not carried out.

Marsiglia et al. provide [9] information on the extraction and characterization of the pectin from the cocoa shell. The cleaning, drying, grinding and sieving of the shell were performed. For the extraction, dried and ground cocoa husk was used. Each sample was mixed with acidified water to reach pH levels (2, 2.5 and 3). For hydrolysis, the sample was placed in a three-necked flask with a mechanical stirrer, a thermometer, and a heating mantle. Then, the mixture was cooled, centrifuged, precipitated with 96% ethanol and dried at 40 °C. The highest yield was 15.97% and it was obtained with citric acid at a pH of 2. However, this work is carried out at a laboratory in small quantities and manually. Also, pretreatment of the cocoa shell is needed.

Torres and Gonzales [10] developed a stainless steel agitator type tank with a volume of 4.2 L was designed to carry out thermal, enzymatic and thermal-acidic hydrolysis. The tank has a heating system through a 2000 W immersion resistance to achieve constant temperatures of 50, 80 and 95 °C with a control system that includes a thermostat, voltmeter, and autotransformer also has a Rushton agitator connected to a reduction motor with frequency converter. The price of the equipment was \$15,000. However, this work only focused on the theoretical design of the tank but not on its implementation.

In the absence of the implementation, automation and economic viability of the other projects in the extraction of pectin, we propose to make an automatic system that meets the appropriate characteristics for the realization of acid hydrolysis and filtering of the cocoa shell. These stages are important in the extraction of pectin since they determine the yield and quality of it.

### 3 Description of the Proposed Method

Figure 1 shows the block diagram of the development of the proposed method.

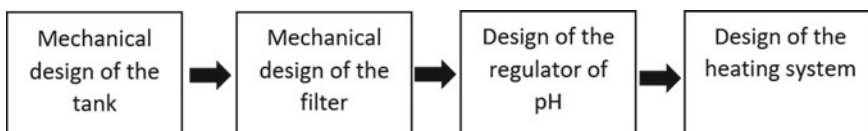


**Fig. 1** Block diagram of the process

### 3.1 Mechanical Design of the Tank

The tank size is calculated taking into account the volume that the filter would occupy and the 50 L of water that will enter the tank. Therefore, a 100-L tank will be used. Also, so that the container is resistant to corrosion, high temperatures and is sanitary, stainless steel of 2 mm thick will be used in manufacturing.

The bottom of the tank is shaped like a cone trunk with a volume of 7 L. Therefore, the cone trunk apothem is found with the following relationship.

$$Ap = \sqrt{\left(\frac{V_1}{\frac{\pi}{4} \times \left(\frac{D+d_t}{2}\right)^2}\right)^2 + \left(\frac{D-d_t}{2}\right)^2} \quad (1)$$

where  $V_1$  is the volume of the cone trunk,  $D$  is the diameter of the tank,  $d_t$  the lower diameter of the cone trunk and  $Ap$  is the cone trunk apothem.

Knowing that the diameter of the tank is 0.5 m, the bottom diameter is for a 1" tube and the volume is 0.007 m<sup>3</sup>. The data is replaced in (1) and obtained  $Ap = 0.270$  m.

The volume of the cylindrical part of the tank is expressed in (2).

$$V_2 = \pi \times \left(\frac{D}{2}\right)^2 \times h_2 \quad (2)$$

where  $V_2$  is the volume of the cylinder part and  $h_2$  is the height of the cylinder.

Knowing what is determined in (2) and that  $V_1$  is 0.007 m<sup>3</sup>, the expressions (3), (4) and (5) are found.

$$V_T = V_1 + V_2 \quad (3)$$

$$V_T = 0.007 + \pi \times \left(\frac{D}{2}\right)^2 \times h_2 \quad (4)$$

$$h_2 = \frac{V_T - 0.007}{\pi \times \left(\frac{D}{2}\right)^2} \quad (5)$$

where  $V_T$  is the total volume of the tank.

Knowing that the total volume of the tank is 0.1 m<sup>3</sup> and the diameter of the tank is 0.5 m, it is replaced in (5) and obtained  $h_2 = 0.474$  m.

Once the measurements are obtained, the tank is shown in Fig. 2.

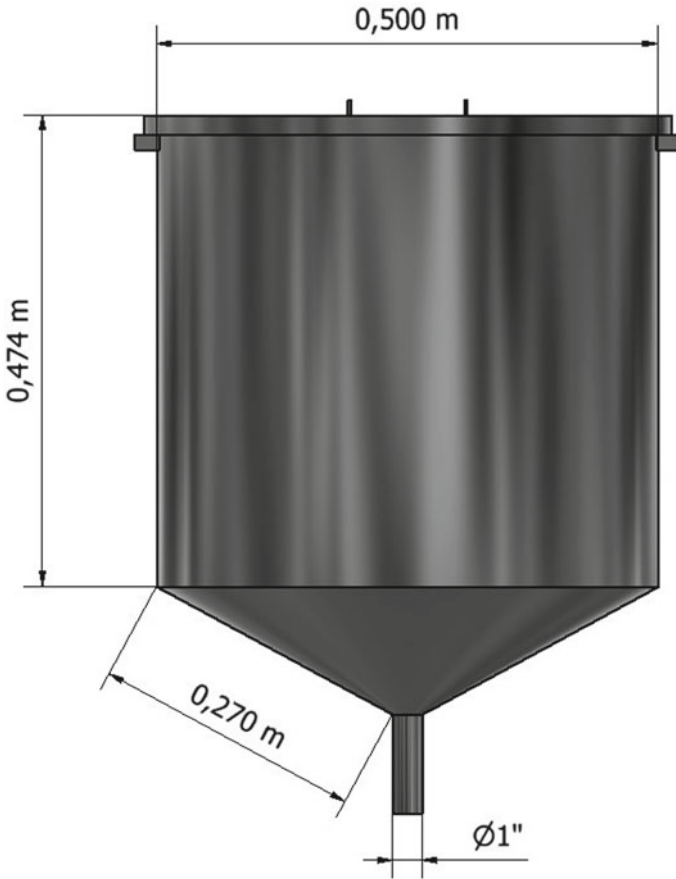


Fig. 2 Hydrolysis tank

### 3.2 Mechanical Design of the Filter

The filter size for 5 kg of the cocoa shell is calculated. The reference is that the density of the cocoa shell is 0.3 kg/L. Therefore, the filter would have a capacity of 20 L. Also, the same tank material will be used. As the filter vessel is a cylinder, the following relationship is obtained.

$$V = \pi \times \left(\frac{d_f}{2}\right)^2 \times h \tag{6}$$

where  $V$  is the volume of the cylinder,  $d_f$  is the diameter and  $h$  is the height.

Knowing that the volume is  $0.020 \text{ m}^3$  and the diameter is 0.4 m, this data is replaced in (6) and obtained  $h = 0.160 \text{ m}$ .

Once the measurements are obtained, the filter is shown in Fig. 3.

Also, the filter has holes of 1 mm in all its cylindrical structure.

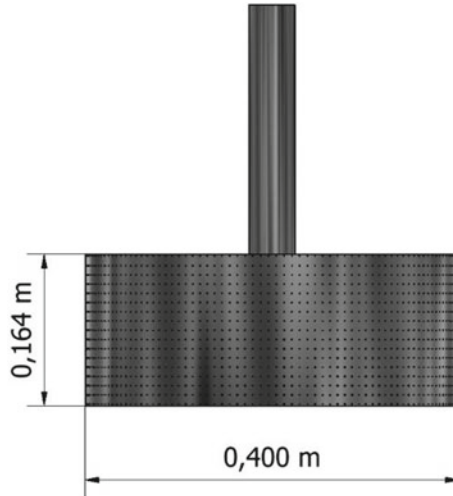


**Fig. 3** Hydrolysis tank filter

### ***3.3 Design of the Regulator of PH***

A certain pH is required in the acid hydrolysis stage. This variable is controlled with the amount of citric acid dosed in the tank and with the electrode that measures the pH in the mixture. For this process, an electric valve is used that drops citric acid into the tank.

In the laboratory tests with 500 ml of water, approximately 40 g of citric acid were needed. With these data, the ratio of water and acid is 25:2 (volume/mass). Therefore, approximately 50 kg of citric acid is needed with the 50 L of process water.

First, the citric acid is dropped in portions of 500 g and then the response of the pH electrode is expected. Once a pH of 2.2 or less is reached, the dosage portion is reduced to 100 g.

A pH of 2 is set as a setpoint. Once the desired pH is reached, the dosing system stops completely.

### ***3.4 Design of the Heating System***

In the hydrolysis stage, a heating system is required, which has a temperature transmitter that measures the temperature variables throughout the process. Also, there is an electrical resistance of the band type around the tank. This will be the actuator that will be used to generate the temperature change, which will vary with the power



given to the resistor by means of a PID control. Accuracy of  $\pm 2^\circ\text{C}$  is necessary for this heating system.

To obtain the necessary power for a transfer of energy in a certain time, the following relation (based on the law of Fourier for conduction) is used [11].

$$P = \frac{m \times C_e \times (T_f - T_i)}{t} \times 4.184 \quad (7)$$

where  $P$  is the power,  $m$  is the mass,  $C_e$  is the specific heat,  $T_i$  is the initial temperature,  $T_f$  is the finale temperature and  $t$  is the time.

A mixture of 50 kg of water at a pH of 2 with 5 kg of cocoa was used for the pectin extraction process. The mixture was heated from 20 to 90 °C and kept constant for 90 min. The specific heat of the water is 1 kcal/kg°C and of the cocoa shell is 0.4 kcal/kg°C. Also, the heat that the filter will remove inside the tank is taken into consideration. Therefore, the specific heat of stainless steel that is 0.12 kcal/kg°C is taken into account. Replacing the data in (7), the expressions (8), (9) and (10) are obtained.

For the water:

$$P_{\text{Water}} = \frac{50 \times 1 \times (90 - 20)}{3600} \times 4.184 = 4.067 \text{ kW} \quad (8)$$

For the cocoa shell:

$$P_{\text{cocoa}} = \frac{5 \times 0.4 \times (90 - 20)}{3600} \times 4.184 = 0.163 \text{ kW} \quad (9)$$

For the filter:

$$P_{\text{Filter}} = \frac{10 \times 0.12 \times (90 - 20)}{3600} \times 4.184 = 0.098 \text{ kW} \quad (10)$$

Knowing what is determined in (8), (9) and (10), the sum of the powers is obtained in (11).

$$P_{\text{Total}} = 4.067 + 0.163 + 0.098 = 4.328 \text{ kW} \quad (11)$$

A total power of 4.328 kW is obtained. Therefore, a 5 kW commercial value resistor is used.

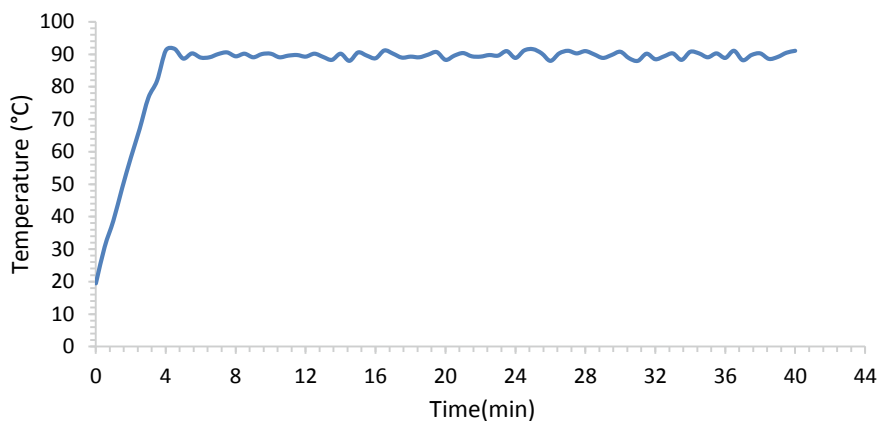


Fig. 4 Temperature variation during extraction time

## 4 Results

The tests were carried out in a place without air current, so as not to affect or impair the process of hydrolysis of the cocoa shell. For the tests, 500 ml of water with 36 g of critical acid was used to obtain acidified water with a pH of 2. Then, it was mixed with 50 g of dried cocoa husk. The temperature was checked to be at 90 °C for 40 min (Fig. 4). During all the time, the mixture was in constant agitation.

50 ml of liquid pectin with a weight of 50 g was obtained from 50 g of the cocoa shell.

To obtain the dry pectin mass for yield, 96% ethanol was added and dried to obtain 5 g of dry pectin.

To obtain the yield the following relationship was used.

$$\% \text{Yield} = \frac{\text{mass of dry pectin}}{\text{mass of dry cocoa shell}} \times 100 \quad (12)$$

Knowing that the mass of dry pectin is 5 g and that the mass of dried cocoa shell is 50 g, it was obtained that the yield was 10%.

## 5 Conclusions

According to the analysis performed for the hydrolysis and filtration stage in the pectin production process from the cocoa shell, it was determined that is feasible the implementation of an automatic system that allows the pectin extraction from the cocoa shell. In this way, due to the high demand for this input, this market could begin to be covered with a natural product. Also, it would be of great importance

that future studies automate the remaining stages of the process of obtaining pectin powder.

## References

1. Canteri, M., Moreno, L., Wosiacki, G.: Pectina; da matéria-prima aoproducto final. *Polímeros* **22**(2), 149–157 (2012)
2. Bazarte, H., Sangronis, E., Unai, E.: La cáscara de cacao (*Theobroma Cacao L.*): una posible fuente comercial de pectinas. *Archivos Latinoamericanos de nutrición* **58**(1), 64 (2008)
3. IMARC Services Private Limited Report List: Pectin Market: Global Industry Trends, Share, Size, Growth, Opportunity and Forecast 2019–2024 (2019)
4. Polaris Market Research: Pectin Market Size, Share, Trends, & Industry Analysis Report, (By Sources (Thickener, Stabilizer, Gelling Agent, Fat Replacer), By Application (Food & Beverage, Pharmaceuticals, Bakery, Dairy Products), By Regions: Segment Forecast, 2017–2026 (2018)
5. Comercio exterior para el agro V.1.1. <http://sistemas.minagri.gov.pe/siscec/usuarios/home>. Last Accessed 10 Sep 2019
6. Andina.: <https://www.andina.pe/agencia/noticia-minagri-proyecta-una-produccion-cacao-149000-toneladas-2019-753060.aspx>. Last Accessed 9 Sep 2019
7. Andersen, N., Cognet, T., Santacolma, P., Larsen, J., Armagan, I., Larsen, F., Gernaey, K., Abildskov, J., Huusom, J.: Dynamic modelling of pectin extraction describing yield and functional characteristics. *J. Food Eng.* **192**, 61–71 (2017)
8. Casa-Orozco, D., Villa, A., Bustamante, F., González, L.: Process development and simulation of pectin extraction from orange peels. *Food Bioprod. Process.* **96**, 86–98 (2015)
9. Marsiglia, D., Ojeda, K., Ramírez, M., Sánchez, E.: Pectin extraction from cocoa pod husk (*Theobroma cacao L.*) by hydrolysis with citric and acetic acid. *Int. J. ChemTech Res.* **9**(7), 497–507 (2016)
10. Torres, K., Gonzales, M.: Diseño de un tanque agitado para la etapa de hidrólisis en la producción de miel de agave. *Jóvenes en la ciencia* **1**(3), 22–26 (2015)
11. Çengel, Y.: *Transferencia de calor y masa*, 3rd edn. McGraw-Hill/interamericana editores, S.A. de C.V., Mexico (2007)

# Automatic Leaf Segmentation from Images Taken Under Uncontrolled Conditions Using Convolutional Neural Networks



Itamar Franco Salazar-Reque   
and Samuel Gustavo Huamán Bustamante 

**Abstract** Automatic leaf segmentation from images taken in-field in uncontrolled conditions is a very important problem that has not been properly reviewed and that is crucial due to its possible use as a previous step in classification algorithms that can be used in agriculture applications. In this work, a CNN architecture (LinkNet) was trained to solve the isolated leaf segmentation problem under natural conditions. To do so, an open dataset has been modified and augmented, using rotations, shearing, and artificial illumination changes, in order to have a proper amount of imagery for training and validation. We have tested the CNN in two different datasets: The first belongs to the original open dataset that shares some visual characteristics with training and validation dataset. The second one contained its own imagery from a different set (images from different plants and with different illumination conditions) in order to evaluate the CNN model generalization. We obtained a mean Intersection Over Union (IoU) value of 0.90 for the first test and a 0.92 for the second one. An analysis of these results has been made and some problems regarding classification applications were commented.

**Keywords** Leaf segmentation · CNN · In-field acquisition

## 1 Introduction

Leaves are biological structures that play a crucial role in trees life due to the photosynthesis process they are in charge of, a process which is necessary to produce energy. Most of the year leaves are present on trees, even more than fruits or flowers. For this reason, farmers often use them to inspect the development of their crops.

---

I. F. Salazar-Reque (✉) · S. G. Huamán Bustamante  
Instituto Nacional de Investigación y Capacitación de Telecomunicaciones, Universidad Nacional de Ingeniería, Lima 15021, Peru  
e-mail: [isalazarr@uni.pe](mailto:isalazarr@uni.pe)

S. G. Huamán Bustamante  
e-mail: [shuaman@inictel-uni.edu.pe](mailto:shuaman@inictel-uni.edu.pe)

In fact, it is possible to observe over leaves visual manifestations triggered by nutritional deficiencies, diseases, or pests attacking the tree. However, the process to identify these visual manifestations tend to be highly subjective and time-consuming. Computer vision techniques applied to leaves digital images have been developed to tackle this problem, some of those use classical techniques like color components ratios [1], histogram over new color models [2] or multilayer perceptron (MLP) trained with superpixels [3] to classify or to segment visible diseases manifestations over the leaves. Recently, convolutional neural networks (CNN) have shown great performance in classification problems, for this reason, in [4], the authors used that approach to tackle the plant disease detection problem. Nevertheless, some works have reported that CNN's are using image background information to perform their identifications (i.e., parts of the image different than the leaf of interest) [4, 5]. For example, in [5], the author found that removing image background (uniform or complex background) alters classifier performance, that is, CNN's found spurious correlations [6] in data and used those to classify between classes. This motivates the need for a previous step to eliminate image background information. By doing this, we ensure that CNN is focusing only on characteristics from the leaf of interest. A review of leaf segmentation in the uniform background can be found in [7], in that research authors also proposed a method that used Expectation-Maximization (EM) clustering in saturation-value space to provide priors that serve as energies used in a graph cut step to perform the task. In [8], a modification of that technique, which used superpixels and k-means clustering, was proposed achieving similar results over images taken in-field with a white sheet of paper under the leaf of interest. Even though, capturing pictures under this type of semi-controlled conditions is a laborious and unpractical procedure. Other works, focused on the segmentation of all individual leaves present in an image, this is a challenging task due to the presence of occlusions and shape variability. In [9] a review of techniques to segment all individual leaves in images of rosette plants taken under lab conditions was made. However, for practical applications to be made, image segmentation should be performed under natural conditions, exposed to illumination changes, variety of shapes, occlusion among others. With this in view, in [10] the authors presented Dense-Leaves, a dataset of images captured in dense foliage with a ground-truth segmentation label. They also proposed a CNN architecture to automatically discriminate leaf boundaries that were used in a watershed-based algorithm to perform segmentation of all leaves. In this work, we have used the same dataset to train a CNN to directly segment the leaf of interest, which we assumed is always centered in the image.

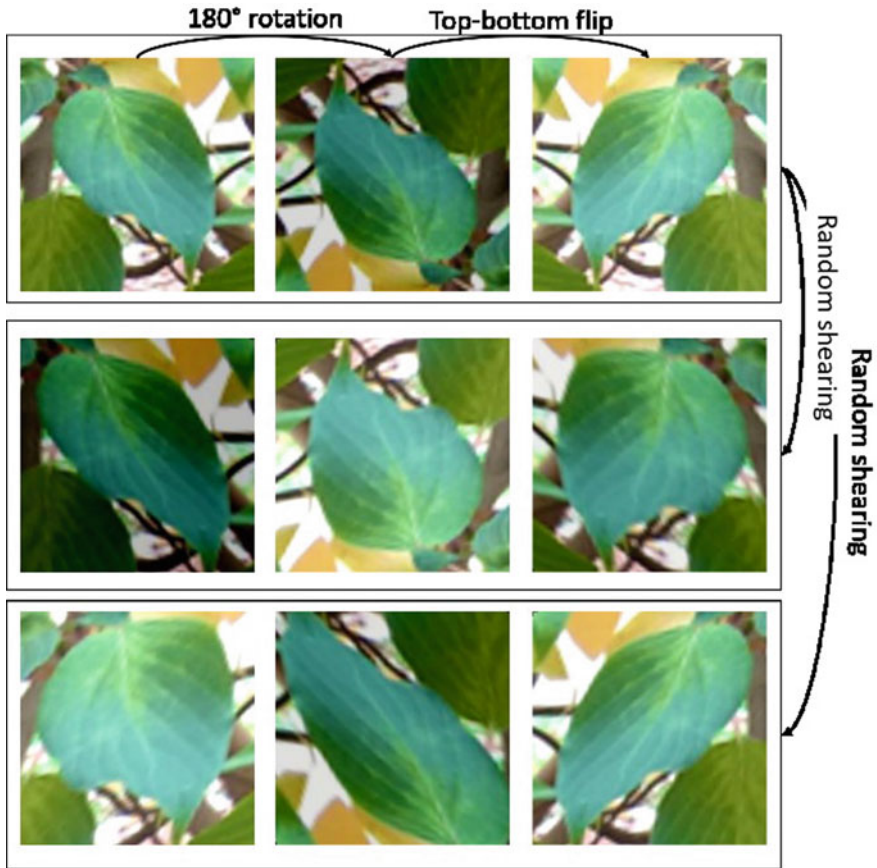


**Fig. 1** A sample of augmented images using the procedure described. The first row, from left to right: original, rotated, and flipped image. Second and third-row show images with random shearings. Each transformation was followed by a random illumination change

## 2 Method

### 2.1 Image Datasets

Our dataset is a modification of the one provided in [10]. The original dataset is composed of 146 foliage images, each one with labels from leaves present in the image, although, no all leaves were labeled. We used labels provided to generate new images by isolating and centering leaf of interest. After that, we manually selected best-isolated images, this was a necessary step due to the fact that some leaves were highly occluded so the resulting isolated image was incomplete. Thus, we obtained 910 images for training, 187 for validation, and 412 for the test, each of

those with respective masks. We performed data augmentation techniques in order to have a proper amount of data to train a CNN. Data augmentation was made by rotating images  $90^\circ$ ,  $180^\circ$ , and  $270^\circ$  degrees, images were horizontally and vertically flipped, we applied random shearing transformations over the leaves and finally, we performed illumination changes in every image (excepting the original) by modifying luma component by a maximum value of 0.3. Thus, we obtained 32,670 images for training, 6732 for validation, and 14,832 for testing, all of them with a spatial resolution of  $224 \times 224$  pixels. A sample of this procedure is shown in Fig. 1, in which we performed one rotation ( $180^\circ$ ), one flipping (vertical), two shearings, and illumination changes to one centered leaf.

## 2.2 CNN Architecture and Training Procedure

Some architectures have been proposed to solve the leaf segmentation problem [11–13], all of them with images captured in lab conditions as the techniques reviewed in [9]. In this work we used LinkNet [14], a CNN architecture developed to perform segmentation in complex scenes that reuses CNN parameters efficiently so that the total number of parameters is small. This architecture has four residual encoding blocks and four decoding blocks using full-convolutions. Due to spatial information loss caused by subsampling in encoding blocks this architecture links each encoding block input to corresponding decoding block output. In Fig. 2, we show encoding blocks in blue and decoding blocks in green, see how encoding blocks have residual units and green blocks have full-convolutional steps. The kernel size ( $k$ ), the stride ( $s$ ), and the up-sampling ( $up = 2$ ) hyperparameters are also indicated. Gray boxes correspond to pre-processing and post-processing blocks described in [14]. We have used augmented RGB images (see Sect. 2.1) with corresponding binary masks to train and validate (test images are defined in the next section) the CNN architecture by 100 epochs.

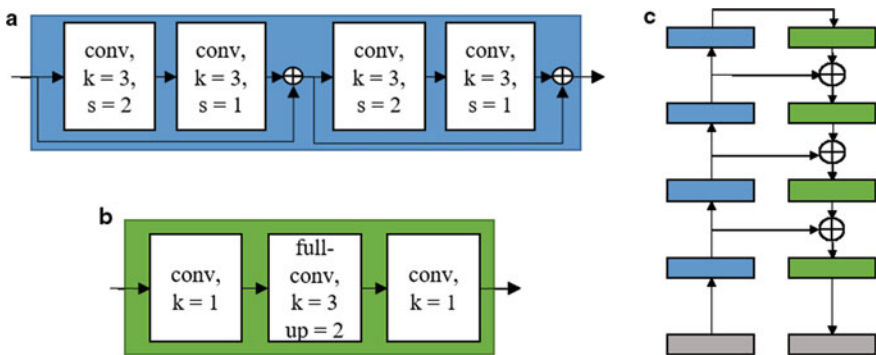


**Fig. 2** a Residual encoding block b Decoding block c Convolutional neural network architecture based on residual encoding and decoding blocks

Adam [15] and AMSGrad [16] were used as optimizer techniques, both with learning rate of 0.0005,  $\beta_1$  coefficient of 0.9 and  $\beta_2$  coefficient of 0.999; parameters updating was made every 16 images ( $N = 16$ ) and, as loss function, we have used binary cross-entropy (BCE) whose formulation is defined in Eq. (1). Additionally, we have monitored mean intersection over union ( $\overline{\text{IoU}}$ ) metric defined in Eqs. (2) and (3).

$$BCE = -\frac{1}{N} \sum_{i=1}^N \frac{1}{P} \left( \sum_{j=1}^P (T_i(j) \log(Y_i(j)) + (1 - T_i(j)) \log(1 - Y_i(j))) \right) \quad (1)$$

$$\overline{\text{IoU}} = \frac{1}{K} \sum_{\gamma \in \Gamma} \text{IoU}(\gamma) \quad (2)$$

$$\text{IoU}(\gamma) = \frac{(Y_i \geq \gamma) \cap T_i}{(Y_i \geq \gamma) \cup T_i} \quad (3)$$

where  $N$  is the batch size,  $P$  is the number of pixels of the target binary mask (in our case  $P = 50,176$  since binary masks dimension is  $224 \times 224$ ),  $T_i(j)$  is the value of pixel “ $j$ ” from target binary mask “ $i$ ” ( $T_i$ ).  $Y_i(j)$  is the value of pixel  $j$  from CNN output image ( $Y_i$ ),  $Y_i$  is the CNN result, the parameter  $\gamma$  is a threshold value used to binarize  $Y$  and  $\Gamma$  is the set of  $K$  discrete values that  $\gamma$  can take, in our case  $\Gamma = \{0.5, 0.55, 0.60, \dots, 0.95\}$ .

### 2.3 Test Datasets

We used two image datasets to test CNN efficiency. Test dataset 1: Images with similar characteristics that training and validation sets, i.e., they were obtained from the original Dense-Leaves dataset. Test dataset 2: Images with different characteristics that training and validation datasets. They were captured in-field under uncontrolled conditions from avocado trees having different nutrient deficiencies and plagues. We used them to assess whether the trained CNN maintained its performance with images other than those used for training and validation.

## 3 Results

The BCE and  $\overline{\text{IoU}}$  training values per epoch are shown in Fig. 3. In general, a lower BCE value implies less difference between values from target binary masks ( $T_i$ ) and outputs ( $Y_i$ ). A higher IoU value implies a greater similarity between  $T_i$  and binarized output ( $Y_i \geq \gamma$ ).



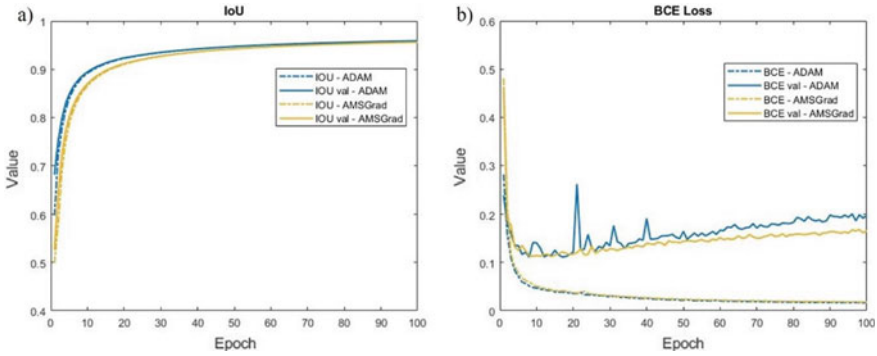


**Fig. 3** a IoU metrics and b BCE loss during training

**Table 1** Average IoU( $\gamma = 0.5$ ) for training, validation, test 1 and test 2 datasets

	Train	Val	Test 1	Test 2
ADAM—best	0.953	0.906	0.897	0.909
AMSGrad—best	0.962	0.911	0.903	0.913
ADAM—100	0.976	0.910	0.902	0.921
AMSGrad—100	0.975	0.907	0.899	0.915

In general, AMSGrad made BCE values lower than those obtained with ADAM. It can be seen how, independently of the optimization technique, BCE loss tends to increase around the 20th epoch. This would imply a decrease in performance, however, this trend contrasts with  $\overline{\text{IoU}}$  the metric tendency which, instead of decreasing, increases for both optimization techniques (a discussion of this is made in Sect. 4). Table 1 shows average IoU values for  $\gamma = 0.5$  for training, validation, tests 1 and 2 datasets using best CNNs, which are the ones with the lowest BCE, and CNNs of the 100th epoch. We contrasted these results to verify whether there was indeed a decrease in CNN performance by letting BCE continue to increase. A sample of the segmentation visual results is shown in Fig. 4. This figure is divided into eight groups. Groups A, B, C and D have images from test data 1 and groups E, F, G and H have images from test data 2. Each group has an RGB image that is accompanied by five binary images. The corresponding ground-truth image ( $T_i$ ) is shown just below the RGB image. The remaining four binary images correspond to binarized results ( $Y_i \geq 0.5$ ) for ADAM and AMSGRAD and for best CNN or 100th epoch CNN.

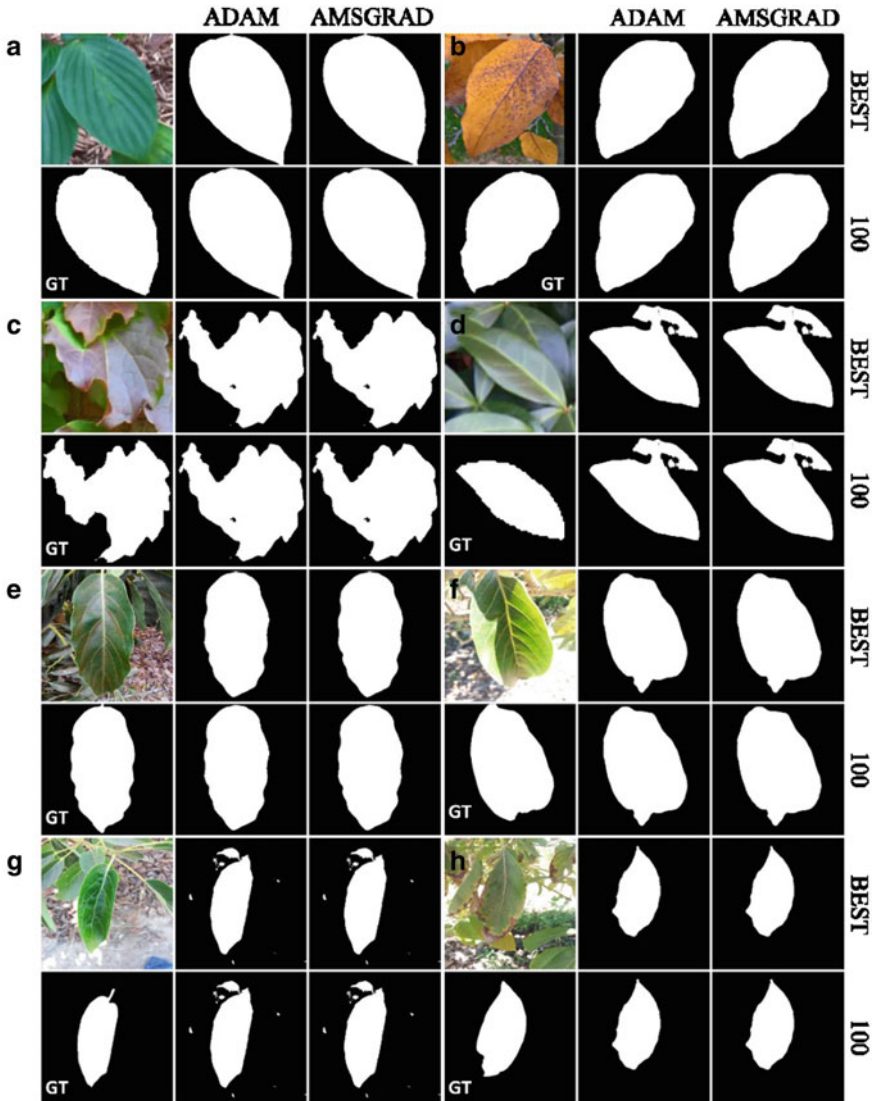


Fig. 4 Sample of the segmentation visual results

## 4 Discussion

From Fig. 4 and Table 1, we noted that masks obtained from CNN's optimized using ADAM and AMSGRAD do not differ considerably. In addition, we do not observe substantial differences between “best” CNNs and “100th” CNNs, even though the latter had a higher BCE (see Fig. 3). This can be explained by Eqs. (1), (2), and (3).

The IoU metric is formulated so that a binarized output ( $Y_i \geq \gamma$ ) is necessary, while BCE equation uses directly CNN's output ( $Y_i$ ). Therefore, for IoU computation there is no need for  $Y_i$  and its corresponding  $T_i$  to be close. This would explain why  $\overline{\text{IoU}}$  continues to improve while BCE loss function worsens (see Fig. 3). Images from test 2 have different characteristics than ones used in training and validation. This was made to assess CNN's ability to generalize. We found that results in test 2 datasets were similar to those in validation and test 1. That is, it maintained a similar behavior even with different images, this contrasts with the behavior that CNNs trained for classification tasks have shown [4, 5]. We argue that this happens because leaf segmentation is a more complex problem than enforces CNN to include context information which makes generalization easier. However, CNN segmentations are not perfect, it should be studied if these imperfections impair the performance in classification tasks. There are two main imperfections. First, sometimes CNN masks included elements outside the leaf. For example, in Fig. 4, masks from groups D, F, and G add some elements to the output mask that differ from GT. If we use these masks to segment RGB images and use those as inputs to a CNN trained for classification this could lead to uncontrolled errors. Even when some floating elements can be handled with morphological transformations, these transformations will be image-dependent. A second problem is that in some cases CNN eliminates damaged areas from the leaf. Take the example of the image in group H in Fig. 4, in which brown areas from leaf apex were confused with an image background and therefore were not included in the final mask. Usually, diseased regions in a leaf represent a small area, thus, segmentation performance metrics are not very affected. However, in classification tasks, the no inclusion of these areas could seriously affect the expected results.

## 5 Conclusions

In this work, we have trained a CNN to segment leaves images acquired in-field under uncontrolled conditions with complex backgrounds. CNN generalization was evaluated using two test sets: the first belongs to the original Dense-Leaves dataset that shares some visual characteristics with training and validation sets and the second one, containing own imagery from different plants and with different illumination conditions. We found that, despite having some overfitting, the CNN kept its validation results constant for the two test sets, indicating good generalization. This was true for the two optimization techniques used (ADAM and AMSGRAD) and for CNN at two different states of training. Also, it has been reported that an increase in the loss function does not necessarily imply a decrease in  $\overline{\text{IoU}}$ . Additionally, we have observed that, in some cases, the resulting mask has floating elements; in others, it eliminates part of the leaf, especially injured parts. These problems can generate errors if resulting masks are used for classification purposes.

**Acknowledgements** The authors thank FONDECYT PERU for the funds allocated to the project 97-2018-FONDECYT-BM-IADT-AV.

## References

1. Barbedo, J.G.A.: A new automatic method for disease symptom segmentation in digital photographs of plant leaves. *Eur. J. Plant. Pathol.* **147**, 349–264 (2017)
2. Camargo, A., Smith, J.S.: An image-processing based algorithm to automatically identify plant disease visual symptoms. *Biosyst. Eng.* **102**, 9–21 (2009)
3. Salazar-Reque, I.F., Huamán, S.G., Kemper, G., Telles, J., Diaz, D.: An algorithm for plant disease visual symptom detection in digital images based on superpixels. *Int. J. Adv. Sci. Eng. Inf. Technol.* **9**, 194–203 (2019)
4. Mohanty, S.P., Hughes, D.P., Salathé, M.: Using deep learning for image-based plant disease detection. *Frontiers Plant Sci.* **7**, 1–10 (2016)
5. Barbedo, J.G.A.: Impact of dataset size and variety on the effectiveness of deep learning and transfer learning for plant disease classification. *Comput. Electron. Agricul.* **153**, 46–53 (2018)
6. Arjovsky, M., Bottou, L., López-Paz, D.: Invariant risk minimization. arXiv preprint [arXiv:1907.02893](https://arxiv.org/abs/1907.02893) (2019)
7. Soares, J.V.B., Jacobs, D.W.: Efficient segmentation of leaves in semi-controlled conditions. *Mach. Vis. Appl.* **24**, 1623–1643 (2013)
8. Salazar-Reque, I.F., Pacheco A.G., Rodríguez, R.Y., Lezama, J.G., Huamán, S.G.: An image processing method to automatically identify Avocado leaf state. In: 22nd Symposium on Image, Signal Processing and Artificial Vision (STSIVA). pp. 1–5. IEEE Press, Bucaramanga, Colombia (2019)
9. Scharr, H., Minervini, M., French, A.P., et al.: Leaf segmentation in plant phenotyping: a collation study. *Mach. Vis. Appl.* **27**, 585–606 (2016)
10. Morris, D.: A pyramid CNN for dense-leaves segmentation. In: 15th Conference on Computer and Robot Vision (CRV). pp. 238–245. IEEE Press, Toronto, Canada (2018)
11. Aich, S., Stavness, I.: Leaf counting with deep convolutional and deconvolutional networks. In: Proceedings of the IEEE International Conference on Computer Vision. pp. 2080–2089. IEEE Press, Venice, Italy (2017)
12. Romera-Paredes, B., Torr, P.H.S.: Recurrent instance segmentation. In: European Conference on Computer Vision. pp. 312–329. Springer, Cham, (2016)
13. Ren, M., Zemel, R.S.: End-to-end instance segmentation with recurrent attention. In: Proceedings of the IEEE Conference on Computer Vision and Pattern Recognition. pp. 6656–6664. IEEE Press, Honolulu, Hawaii (2017)
14. Chaurasia, A., Culurciello, E.: Linknet: Exploiting encoder representations for efficient semantic segmentation. In: 2017 IEEE Visual Communications and Image Processing (VCIP). pp. 1–4. IEEE Press, St. Petersburg, FL, USA (2017)
15. Kingma, D.P., Ba, J.: Adam: A method for stochastic optimization. arXiv preprint [arXiv:1412.6980](https://arxiv.org/abs/1412.6980) (2014)
16. Reddi, S.J., Kale, S., Kumar, S.: On the convergence of adam and beyond. arXiv preprint [arXiv:1904.09237](https://arxiv.org/abs/1904.09237) (2019)

# Method of Anomalies Detection in *Persea Americana* Leaves with Thermal and NGRDI Imagery



Bruno D. Rivadeneyra Bustamante   
and Samuel G. Huamán Bustamante 

**Abstract** Among the main agricultural export products of Perú is the *Persea Americana* (Hass avocado). However, pests and deficiencies cause a decrease in avocado crop yield. For that reason, anomalous visual characteristics detection of a leaf has been studied for thermal and multispectral images. In this study, we propose a procedure for imagery acquisition and evaluate factors that can affect the acquisition of thermal imagery; furthermore, we propose a method for the extraction of characteristics to classify between a healthy leaf and a leaf with some visible anomalies that indicate some deficiency or pest. This method consists of the following stages: segmentation of thermal and NGRDI images, resampling, clustering with *k-means* algorithm and classification with SVM. Likewise, we test three cases of image acquisition to analyze the effects on statistical descriptors. Finally, the classification stage was tested with leaves processed; as a result, we got out an average accuracy of 82.67%, from ten experiments with the same set of images.

**Keywords** Thermal imagery · NGRDI · K-means · SVM

## 1 Introduction

Peru is one of the countries with the highest export of *Persea Americana* (avocado) in the world, as well as in its production [1]. The most common avocado varieties in Peru are Hass and “Fuerte” [2]. However, 95% of avocados exported by Peru are of the Hass variety.

---

B. D. Rivadeneyra Bustamante (✉) · S. G. Huamán Bustamante  
Instituto Nacional de Investigación y Capacitación de Telecomunicaciones, Universidad Nacional de Ingeniería, Lima 15021, Peru  
e-mail: [bruno.rivadeneyra.b@gmail.com](mailto:bruno.rivadeneyra.b@gmail.com)

S. G. Huamán Bustamante  
e-mail: [shuaman@inictel-uni.edu.pe](mailto:shuaman@inictel-uni.edu.pe)

The growing demand for both the production and export of this fruit is reflected in the consolidation of trade with the USA and the European Union and with the opening of new markets such as Chinese since 2015 [1].

However, the yield of avocado tree crops is not as expected. Peru produced an average of  $11.8 \text{ t ha}^{-1}$  in 2017, which places it out of the top ten countries in avocado yield [1]. One of the causes of low agricultural yield was the poor control and care of the vegetation. For this reason, hard work is necessary to achieve the reduction of pests and deficiencies in avocado crops.

The vegetation type detection or classification in multispectral images using artificial neural networks has been studied in recent years. For instance, the images have been segmented to restrict the area where a leaf or tree is located and, from this result, the color characteristics are extracted in order to train a classifier [3–7]. In that sense, the addition of thermal images into training has improved the accuracy of those classifiers [7].

Thermal images in crops have been studied [8, 9], demonstrating that, in general, any leaf increases the temperature in the diseased areas of its beam surface [8] and, in addition, the average of the temperature over a tree canopy varies depending on the hour of acquisition [7].

For this work, the acquisition and processing of thermal and RGB images is performed to detect anomalies in Hass avocado leaves, using a proposed method that considers the temperature distribution in the beam of the leaves, as a descriptor of the anomalous characteristics that may occur on a leaf, and color characteristics, through the Normalized Green-Red Difference Index (NGRDI).

Section 2 details the procedure for acquiring images using an infrared camera. In Sect. 3, the method used in extracting information from images, using the  $k$ -means algorithm, and the classification stage, with a Support Vector Machine (SVM), is explained.

Section 4 has the results and discussions of experiments related to the average surface temperature variation of the Hass avocado leaf beam at different times of the day and the resultant performance of the proposed method for the classification of healthy leaves and leaves with anomalies.

## 2 Image Acquisition

### 2.1 Instruments and Environmental Considerations

Image acquisition was carried out in the avocado cultivation area of the National Institute of Agrarian Innovation (INIA), located in Lima (Peru), during this time, 499 thermal images and 499 RGB images of Hass avocado leaves were acquired, of which 100 of each type were selected, according to the visible and thermal characteristics useful for anomalies detection. These images were acquired with the FLUKE TiS 45 9 Hz infrared camera [10], of which 20 correspond to healthy leaves and 80 to

diseased leaves or with visible anomalies. Thermal images have a size of  $320 \times 240$  pixels and RGB images have a size of  $640 \times 480$  pixels.

Regarding the configuration of the infrared camera, this was adjusted to an emissivity of 0.95, as an average of the accepted values for the surface of a leaf [9]. In addition, the specific background temperature is considered for each of the acquisitions. This temperature was measured with a FLUKE 80bk-a thermocouple.

## ***2.2 Image Acquisition Procedure***

The proposed procedure for image acquisition is the result of various field tests and consists of the following steps:

1. Locate a leaf, which must not be directly exposed to the Solar light but has adequate lighting.
2. Gently wipe the surface of the leaf with a cloth until dust and dirt are removed, then wait a few minutes until the leaf surface again acquires thermal equilibrium with the environment.
3. Insert the background temperature in the infrared camera. This will be the temperature measurement that thermocouple marks at leaf position. For this, the measurement is made by placing the thermocouple as close to the leaf beam surface as possible.
4. Position the camera so that the leaf extension is located vertically inside the camera's viewfinder. Then, focus, capture and finally, store.
5. Repeat the acquisition procedure for all the chosen leaves.

In conditions of high air temperatures, it will be necessary not to keep the camera on for more than an hour to avoid electronic system overheating. In these cases, it is recommended, after one hour of activity, turn it off for 15 min and then continue with the acquisition.

The thermographic camera configuration only allows manual focus adjustment. Then, a leaf will be correctly focused as soon as the RGB and thermal images fit as well as possible. Likewise, it is recommended that the camera position does not obstruct direct radiation that is toward the leaf surface.

The hands and, in general, the human body emits thermal radiation that can alter the surface measurement of the leaf in the infrared camera. Therefore, it is recommended to be placed at one meter away from the leaf at the acquisition time.

## **3 Proposed Image Processing and Acquisition Method**

The thermal images acquired with the thermographic camera are exported as a text file, which contains a matrix of representative temperature values for each acquisition.

Within the mentioned matrix, the leaf is segmented, selecting four points (on a displayed image) that determine a rectangle of minimum dimensions but that encloses the leaf. Then, the  $k$ -means technique [11] is used in order to divide the leaf into  $k = 15$  clusters. From each of these clusters, the statistical descriptors, mean and standard deviation, are extracted to obtain a total of 30 descriptors of the thermal image of the avocado leaf.

On the other hand, RGB images acquired by the infrared camera are also exported, but in jpg format. As in thermal imaging, these are segmented in each of their bands, following the same procedure.

Once a leaf is cut, it is resized to the size of the corresponding thermal image, then, Normalized Difference Green-Red Index (NGRDI) [12], is calculated in each pixel and It is defined by the following expression:

$$\text{NGRDI} = \frac{\text{ND}_G - \text{ND}_R}{\text{ND}_G + \text{ND}_R} \quad (1)$$

where  $\text{ND}_G$  is the digital value of each pixel in the green band and  $\text{ND}_R$  is the digital value of each pixel in the red band. While the resulting image of a single color band whose pixel values correspond to the respective NGRDI value will be called the NGRDI image.

Similar to the thermal image processing, the  $K$ -means algorithm is used to divide the NGRDI image into 15 clusters and for each one, the mean and standard deviation is calculated. These values add a total of 30 descriptors.

Finally, the number of pixels of each cluster is calculated, both in the thermal image and in the NGRDI image, adding 15 descriptors. In total, there is a set of 90 descriptors for each leaf, they are inserted into an SVM network [13], which uses a linear Kernel transformation function. Likewise, the images were distributed in training, validation and test groups (70%, 15%, and 15% respectively).

In Fig. 1, the diagram of the stages of the proposed method is shown.

## 4 Results and Discussions

The experiments carried out and shown below are proposed to analyze the characteristics of descriptors and the effects of environmental conditions on these and, consequently, on the detection of the anomalous and non-anomalous condition of a tree leaf.

These experiments were carried out in the experimental station of the National Institute of Agrarian Innovation (INIA), in Lima. Thus, in the proposed first experiment to verify the effects due to direct solar radiation, images were acquired of two healthy Hass avocado leaves, one under the shade and another exposed to direct solar radiation, both belonging to different trees. The results are shown in Fig. 2.



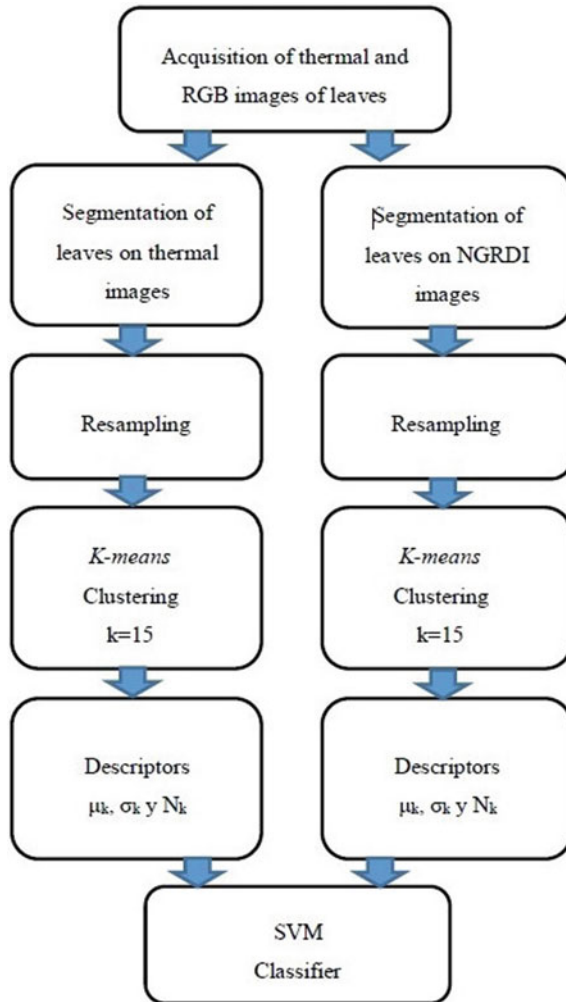
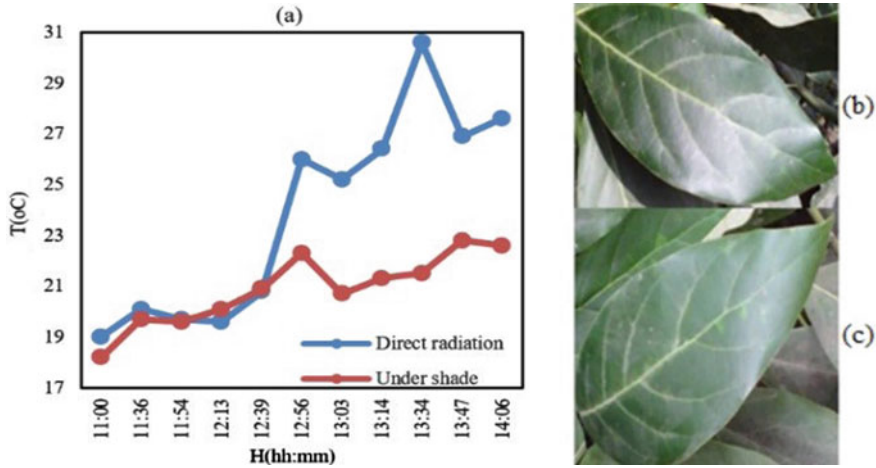


Fig. 1 Diagram with the processing steps of the proposed method

During this experiment, the sky remained cloudy during the first five acquisitions, in which, there was a minimum temperature difference over time between both leaves. However, from the following acquisitions, the solar radiation modified the temperature of the exposed leaf significantly. In Fig. 2, the hourly temperature is shown where there was an incidence of direct solar radiation on the leaf, as well as the temperature of a leaf under the shade, called an unexposed leaf. To quantify the relationship between these temperatures, the Spearman correlation coefficient [14] was used, whose value is 0.4857; this represents a moderate correlation. In addition, temperature differences between both measurements are of 4–10 °C.



**Fig. 2** a Variations in the average surface temperature of b a healthy leaf exposed to direct solar radiation and c a healthy leaf under the shade and in different Hass avocado trees

The results are shown in Fig. 2, require caution to avoid direct solar radiation in the beam of Hass avocado leaves during acquisition procedure in the following experiments. The second experiment consisted of acquiring images from healthy leaves and leaves with anomalies. Thus, the acquisition of 22 thermal images and 22 RGB images of the Hass avocado leaf was carried out, in the range from 11 h to 15 h on May 31, 2019, at INIA. Each acquisition was simultaneously carried out for a healthy leaf and an anomalous leaf, both were under shade. The resulting temperature curves, shown in Fig. 3a, represent the variation of the average surface temperature of the healthy and the anomalous leaf beam. The temperature of the curve that represents the healthy leaf is below the temperature of the curve that represents the leaf with an anomaly, for each acquisition. Both leaves, of the same tree and very close to each other, always remained in the shade. In addition, the curves show a similar trend over time. Spearman's correlation for this case has a value of 0.9018, with significance value  $p = 0.0001$ ; this result indicates a high correlation.

On the other hand, Fig. 3b shows the comparison of the same leaf with an anomaly, this time with a healthy leaf belonging to another tree also under shade. In this case, Spearman's correlation of 0.8064, with significance value  $p = 0.0027$ , is still high. In spite of a reduction in the correlation, a significant difference was maintained between the healthy leaf temperatures and the leaf anomalous temperatures, which allows those to be differentiated.

Consequently, a third experiment was carried out to analyze the variation of the temperature distribution in three different acquisition positions on the Hass avocado leaf beam. In this experiment, three thermal images were acquired by rotating on the azimuth: front and two lateral sides, all of them correspond to a healthy leaf under a shade, but with sufficient illumination. The acquired thermal images were preprocessed, cropping the region bounded by the leaf, then, they were divided into  $k = 15$  significant clusters, following the method mentioned in Sect. 3. Next, an analysis of the regions of the leaf that belong to clusters with the highest number of pixels, as well as a surface distribution of clearly identifiable temperatures.

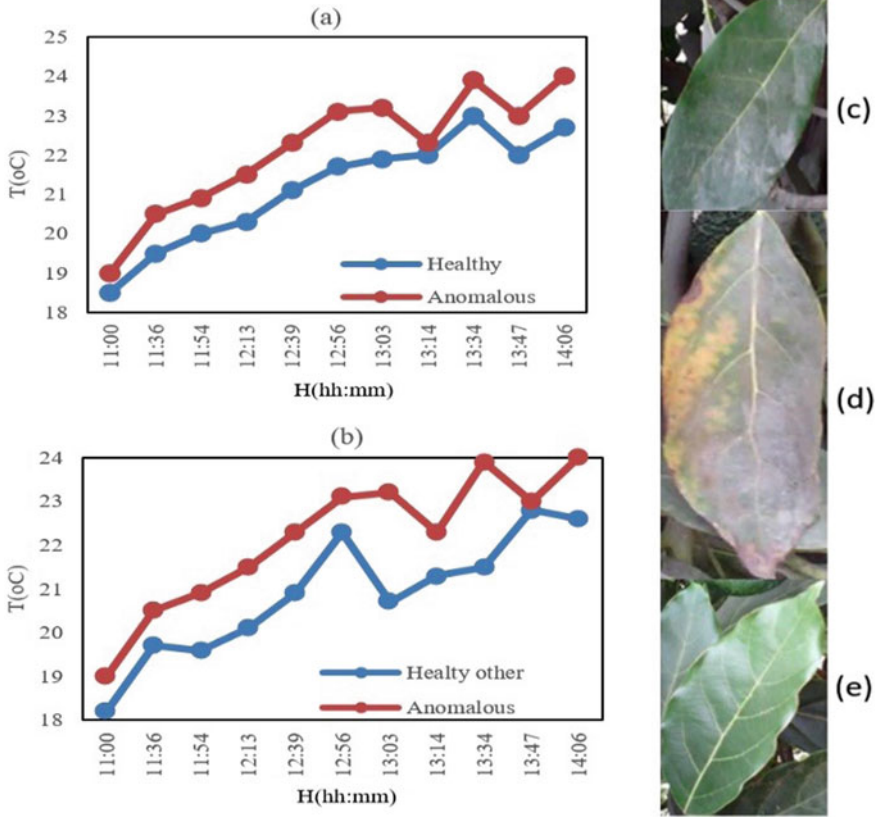


**Fig. 3** a Average surface temperature variation of c a healthy leaf and d an anomalous leaf of the same avocado tree and, b the average surface temperature variation of e a healthy leaf of different avocado tree and the same anomalous leaf in 11 different hours of the day

Figure 4 shows the temperature distribution of three clusters on the two healthy leaves for the three views (one front and two sides), where one is under a shade and the other exposed to direct solar radiation.

Table 1 shows that there is a variation of pixels between the different views, which varies from 26 to 28% for cluster 1 and 33–35% for cluster 2; Despite this, the average temperature does not vary. While the number of pixels for cluster 3, for all three views, varies from 35 to 62%, in addition to the temperature variation up to 0.3 °C. This means that different views have an effect on temperature for clusters with the least number of pixels; consequently, this variation may have an effect on the performance of the classification algorithm.

In the case of Table 2, in cluster 1 it is observed that the average temperature varies from 0.1 to 1.4 °C, in cluster 2 from 0.5 to 1.7 °C and in cluster 3 from 0.5 to 1.4 °C. In this case, when acquisition in any different view is carried out, the variations in average temperature are significant, so that it is necessary to perform the acquisition under shade.

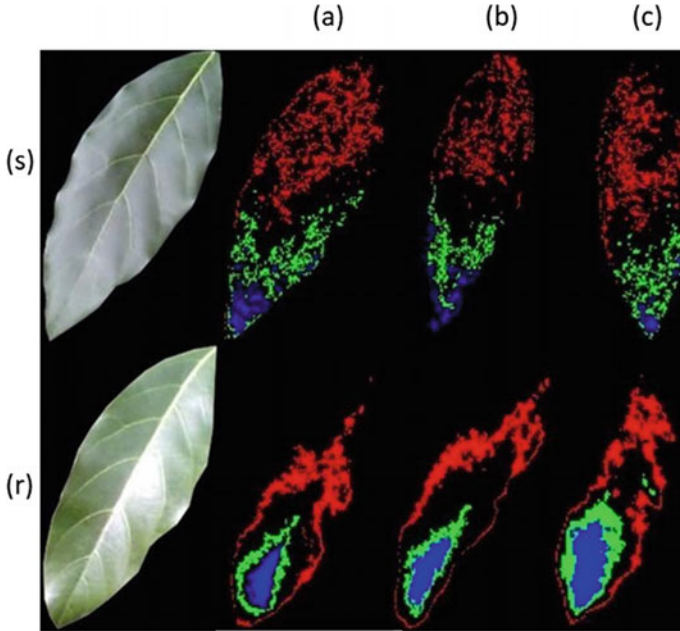


**Fig. 4** Images of two healthy leaves in three views. From left to right, the RGB image and three views (front, side 1 and side 2, respectively) are shown. In (s) the top row, (s, a) a leaf under a shade and their respective clusters for (s, b) the front view, (s, c) side 1 and (s, d) side 2. In (r) the bottom row, (r, a) a leaf exposed to solar radiation and their respective cluster for (r, b) the front view, (r, c) side 1 and (r, d) side 2. Clusters 1, 2 and 3 can be observed in green, red and blue respectively

**Table 1** Effects of the infrared camera rotation on three clusters that belong to a healthy leaf under the shade and obtained with the K-means algorithm. In the upper region of the avocado leaf cluster 1 and in the lower region cluster 2. In addition, cluster 3 with a variation of the average temperature

Leaf under shade	View	Number of pixels	Mean (°C)	Standard deviation (°C)
Cluster 1	Front	1464	19.10	0
	Side 1	1122	19.10	0
	Side 2	1082	19.10	0
Cluster 2	Front	747	19.70	0
	Side 1	500	19.70	0
	Side 2	484	19.70	0
Cluster 3	Front	258	20.00	0
	Side 1	165	20.26	0.06
	Side 2	98	20.02	0.06

**Table 2** Effects of the infrared camera rotation on three clusters that belong to a healthy leaf exposed to direct solar radiation and obtained with the *K*-means algorithm

Leaf exposed to solar radiation	View	Number of pixels	Mean (°C)	Standard deviation (°C)
Cluster 1	Front	1290	23.70	0.06
	Side 1	493	25.03	0.09
	Side 2	749	24.90	0.06
Cluster 2	Front	690	24.64	0.09
	Side 1	605	26.38	0.06
	Side 2	509	25.85	0.09
Cluster 3	Front	345	25.42	0.12
	Side 1	299	26.85	0.09
	Side 2	508	26.31	0.17

In both Tables 1 and 2, uniform temperature distributions are assumed on the leaf and, consequently, standard deviations of uniform distribution. For the analysis of the three experiments described above, only the region bounded by the leaf is considered, where temperatures have a distribution similar to a uniform distribution. However, for the method proposed in Chap. 3, the rectangular re-cutting of the leaf justifies the use of a standard deviation for a normal distribution, due to the variability of the environment surrounding the leaf.

It should be noted that the standard deviation of cluster 3 increase in a leaf under a shade, for a smaller number of pixels. While its behavior is erratic in a leaf exposed to solar radiation.

The SVM classifier to healthy leaves and anomalous leaves was trained and tested with 100 thermal and NGRDI images, which are images that correspond to leaves not exposed to solar radiation, each of which was processed following the method proposed in Sect. 3. This classifier uses a linear Kernel transformation function, as well as a distribution of seventy-five training images, fifteen for validation and fifteen for the test. The result of an average of 10 experiments for the same set of 100 images shows an accuracy of 82.67%.

## 5 Conclusions

In this work, we propose a new method to process, cluster and classify Hass avocado leaves condition using thermal and NGRDI images and a procedure to acquire thermal and RGB images of leaves in the field, using a handheld infrared camera.

The four experimental results about the effects of solar radiation on avocado leaves show alteration in the temperature measurements and, consequently, to clustering of healthy or dead zones of a leaf.

In future works, the accuracy of the classification stage can be improved with a greater variety and quantity of images obtained by the image acquisition process and processed by the method proposed in this work.

**Acknowledgements** The authors thank Innóvate Peru and the Ministry of Production of Peru for financing with contract No. 119-INNOVATEPERÚ-IDIBIO-2018 and the National Institute of Agrarian Innovation (INIA) for access to their experimental stations.

## References

1. MINAGRI Dirección General de Políticas Agrarias: La Situación del Mercado Internacional de la Palta. Boletín técnico, 8–35 (2019)
2. Huaman, N.L., Zapana, V., Granados, C.E.: Aislamiento e identificación de *Phytophthora cinnamomi* Rands en el cultivo de palto variedades Hass y Fuerte. *Journal de Ciencia y Tecnología Agraria* **1**, 57 (2015)
3. Blanco, J.A.U.M.E.: Desarrollo de una aplicación móvil para la detección y clasificación de hojas de árboles. Dissertation, Universitat Politècnica de València (2015)
4. Galárraga, J.L.: Clasificador de hojas mediante Deep Learning. Dissertation, Universidad Politécnica de Madrid (2017)
5. Garnique, L.A.V., Cabrera, H.I.M., Chavarry, K.L.V., Barco, M.J.V.: Visión artificial: Aplicación de filtros y segmentación en imágenes de hojas de café. *Ingeniería: Ciencia, Tecnología e Innovación*. **1**(2), 71–81 (2014)
6. Salazar-Reque, I. F., Pacheco, A. G., Rodríguez, R. Y., Lezama, J. G., Huamán, S. G.: An image processing method to automatically identify Avocado leaf state. Paper presented at the 2019 XXII Symposium on Image, Signal Processing and Artificial Vision (STSIVA), Universidad Industrial de Santander, Bucaramanga, 24–26 Apr 2019
7. Calderón, R., Zarco, P., Navas, J., Blanca, M.: Detección de enfermedades de cultivos mediante imágenes hiperespectrales y térmicas de alta resolución espacial. *Grandes cultivos*, **18** (2018)
8. Granum, E., Pérez, M., Calderón, C., Ramos, C., de Vicente, A., Cazorla, F., Barón, M.: Metabolic responses of avocado plants to stress induced by *Rosellinia necatrix* analysed by fluorescence and thermal imaging. *Eur. J. Plant Pathol.* **142**(3), 625–632 (2015)
9. Jones, H.: Application of thermal imaging and infrared sensing in plant physiology and eco-physiology. In: *Advances in botanical Research*, pp. 107–163. Academic Press (2004)
10. FLUKE Corporation. FLUKE TiS45 Infrared Camera. <https://www.fluke.com/en-us/product/thermal-cameras/tis45>. (2019). Accessed 1 Dec 2019
11. Jain, A.K.: Data clustering: 50 years beyond K-means. *Pattern Recogn. Lett.* **31**(8), 651–666 (2010)
12. Hunt, E.R., Doraiswamy, P., McMurtrey, J.E., Daughtry, C.S., Perry, E.M., Akhmedov, B.: A visible band index for remote sensing leaf chlorophyll content at the canopy scale. *Int. J. Appl. Earth Obs. Geoinf.* **21**, 103–112 (2013)
13. Vapnik, V.: *The nature of statistical learning theory*. Springer Science and business media (2013)
14. Zhang, W.Y., Wei, Z.W., Wang, B.H., Han, X.P.: Measuring mixing patterns in complex networks by Spearman rank correlation coefficient. *Physica A* **451**, 440–450 (2016)

# Development of a Machine to Control the Level of Washing in Panca Chili Seeds



Anthony De La Cruz , Jaime Cardenas , and Leonardo Vinces 

**Abstract** The washing of Panca chili seeds requires innovative solutions that allow controlling this process. It is necessary to handle variables (conductivity, pH, colorimetry) in the face of the challenge of working with small seeds. At present, there are no machines that are dedicated to the washing of this type of seeds, since in many companies this work is done manually, which is not the one indicated because this technique cannot guarantee homogeneity in the seed washing. In addition, direct handling of this type of seeds can cause irritation to the eyes and skin of the person who maintains contact with the seeds. That is why, it is proposed to make a machine to scale by means of a motorized rotary agitator inside a tank, in order to guarantee the homogeneity of the mixture when washing seeds. The present work will allow to determine, among two different types of agitators (axial and radial), which type of agitator is the most efficient in the washing of seeds of Panca chili, to achieve this objective the measurement of pH and electrical conductivity to the water will be carried after the mixture, after stirring. Finally, the analysis of the tests performed on the mixture obtained and washed by each type of agitator allowed to identify the turbine-type radial agitator, like the one that obtained greater efficiency in the washing of seeds, with respect to the helical agitator and pallets, designed for development of this work, in turn, could also confirm that this type of palette with the conductivity control allows to guarantee the homogeneity of the mixture during washing.

**Keywords** Stirring · Mixing · Washing seeds · Capsaicin · pH measurement · Electrical conductivity measurement

---

A. De La Cruz · J. Cardenas · L. Vinces (✉)  
Universidad Peruana de Ciencias Aplicadas, Av. Prolongación Primavera 2390, Santiago de Surco, Lima, Peru  
e-mail: [leonardo.vinces@upc.pe](mailto:leonardo.vinces@upc.pe)

A. De La Cruz  
e-mail: [u201517116@upc.edu.pe](mailto:u201517116@upc.edu.pe)

J. Cardenas  
e-mail: [u201320596@upc.edu.pe](mailto:u201320596@upc.edu.pe)

# 1 Introduction

Currently, chili pepper is the sixth most exported product in the non-traditional agricultural sector. In 2017, Peru exported Capsicum for more than 238 million soles, according to the Association of Exporters (ADEX). In addition, it is estimated that the per capita consumption of chili peppers and peppers in Peru is 3.9 kilos per year, the most prominent categories were canned chili peppers (57.4%) and dried chili peppers (38.4%) [1]. Peru has a wide variety of chili peppers, as this is valued from pre-Hispanic cultures for its high nutritional value, exquisite taste, and exotic aroma, native peppers descend from common ancestors that originated in South America, in heights of Bolivia and Peru or in southern Brazil, Peru being the country that has the greatest diversity of this product in the world, among which is the Panca pepper [2].

Seed oil production occurs from dried peppers such as the Panca pepper. This type of pepper is grown in all regions of Peru, especially on the north coast, this product is a food with low caloric intake since it is formed in almost 90% by water. In addition, it has largely capsaicin. This component is what gives it the spicy flavor and serves as an analgesic and anticoagulant, ideal for people at risk of cardiovascular diseases. Likewise, its consumption helps to combat the pain generated by arthritis, stimulates the nervous system, because it causes the body to produce endorphins, regulates blood sugar levels, generates a bactericidal effect, eliminating stomach bacteria, which helps decrease the possibility of stomach diseases [3].

It is thanks to these positive health effects that many products are made from chili peppers, such as oil production, which uses the seeds of the Panca pepper as raw material, which is carefully processed to get to the final product. Thus, to produce chili seed oil it is necessary to perform the washing of the seeds, then the drying and finally the dehydration of the seed. The great challenge within this whole process is to perform the washing, this procedure should be the most appropriate so that at the end of the process a clean seed is obtained and that it always loses a constant amount of itching (capsaicin). Capsaicin is a compound that is found naturally in fruits, although in different proportions. In chili, it usually varies between 0.1 and 1% by weight, although it seems small, that amount is enough to produce the typical sensation of itching [4]. This compound is not uniformly distributed in the fruit; It usually concentrates on the seeds and on the cover that surrounds them (pericarp), these are the hottest areas of chili pepper [5].

The application of capsaicin on the skin or mucous membranes causes burning and hyperalgesia, but repeated application leads to loss of sensitivity to capsaicin; the application of higher doses causes a blockage of the C fibers that lead to a long-term sensory deficit. This property has been used therapeutically in neuropathic pain as an option when the other drugs are ineffective. Thus, capsaicin has demonstrated its efficacy after repeated administration in postmastectomy pain, stump pain, reflex sympathetic dystrophy, oral neuropathic pain, fibromyalgia, and especially in diabetic neuropathy and postherpetic neuralgia. Consequently, there is a high interest in finding new drugs analogous to capsaicin [6].



While some studies have been developed, such as the one carried out in 1912, by chemist Wilbur Scoville, who developed a scale with his surname, which measures the degree of itch of a pepper. Scoville assigned the value of zero to sweet peppers, which do not bite [6]. At the other end of the scale, he placed capsaicin to which he gave a value of sixteen million, as the spiciest substance. At the time of washing the seeds, the capsaicin molecules are mixed with the water reducing the concentration of capsaicin in the seeds, therefore, the oil itching (final product) should decrease.

On the other hand, the continuous development of automatic and semi-automatic machines has allowed the performance in the production, operational, and quality control areas to be improved [7]. However, in the processing of seeds, to obtain derivative products (oils, resins, etc.), great advances in automatic machines have not been achieved. This is mainly due to the limitation of the sensors when controlling variables [8]. For example, in Ecuador, the washing of sesame seeds is generally also done manually, due to the complexity of handling the small size of the seed and the little use of sesame seeds in this part. of the world. Given this, projects are also being carried out that allow the washing of this type of seeds and in turn allow the production needs to be met [9].

In the absence of a specific sensor intended to measure the concentration of capsaicin in a mixture, it will be necessary to indirectly measure the amount of capsaicin that is removed in the water during each wash. For this purpose, it has been considered to measure the level of pH and electrical conductivity (Ppm) of the water that has been mixed with the seeds, in this way it is expected to be able to control the level of washing in the seeds, without affecting the organoleptic properties of this. Additionally, it is guaranteed that the experiment will always keep the proportions constant throughout the test (Rpm, exposure time, etc.), all with the intention of guaranteeing the result of the tests performed.

The main objective of this study is to identify the design, process, and control of variables that allow obtaining an efficient machine to wash the seeds of the pepper. To achieve this objective, the washing tank and two types of agitators (axial and radial flow) have been designed, the appropriate water temperature has also been identified, the control of a variable that allows me to know the level of washing and the time of agitation necessary for washing. With each of the agitators, a process of washing pepper seeds will be carried out in a machine made to scale that allows controlling the speed of rotation of the agitator, as well as the washing time for a mixture of two hundred grams of seeds for a liter of water.

## **2 Description of the Design of the Machine for Washing Chili Seeds**

Figure 1 shows the block diagram of the design of the chili seed washing machine. The details of each of the process steps will be described in the following sections.

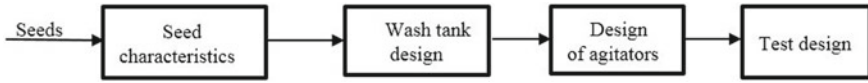


Fig. 1 Block diagram of the machine design for chili seed washing

### 2.1 Characteristics of the Seeds

Figure 2 shows the diameter and thickness measurements of the chili seed.

In order to find the density of the seeds, we perform the corresponding division. We divide the measured mass of 50 ml of test tube seeds over 50 ml. In order to perform the following calculation, it is necessary to use the data in Fig. 3, which represents the weight of 50 ml of chili seeds.

$$\rho_{\text{semillas}} = \frac{m_{\text{Seeds}}}{50\text{ml}} \tag{1}$$

Fig. 2 Dimensions of diameter and thickness of chili seeds



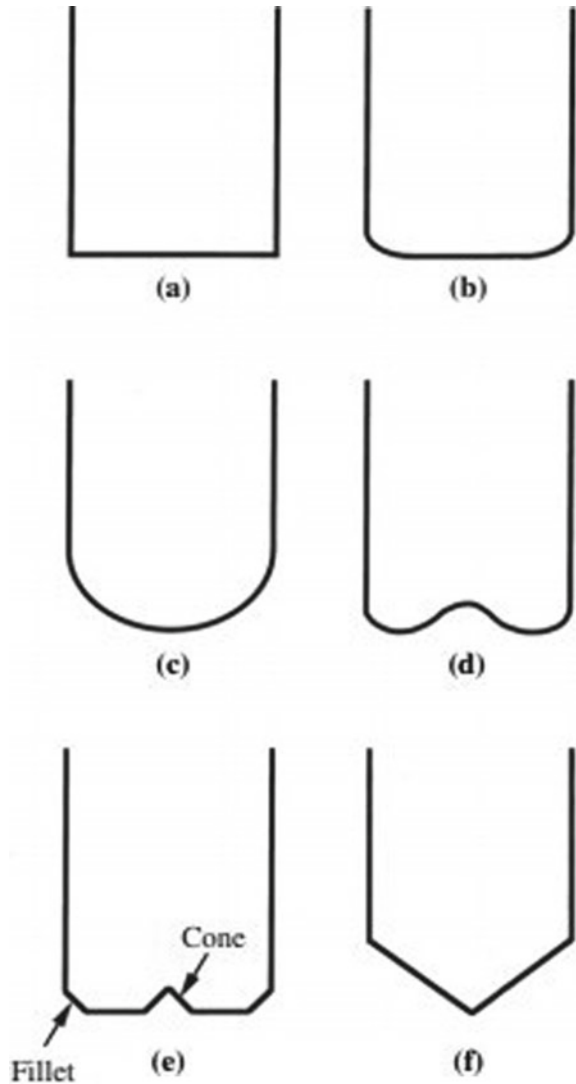
Fig. 3 Weight of 50 ml of seed



## 2.2 Design of Agitators

The base of the agitated tanks affects the efficiency of the mixture. Several base forms are shown in Fig. 4. The base should be rounded at the edges instead of the flat; This eliminates sharp corners and bags in which fluid flows may not penetrate, reducing the formation of stagnant areas. The energy required to suspend solids in agitated tanks is sensitive to the shape of the vessel base: according to the type of impeller and the generated flow pattern, the modified geometries are shown in Fig. 4b through

**Fig. 4** Different profiles for the base of agitated vessels. Extracted from [10]



(e) are can be used to improve particle suspension compared to the flat bottom tank of Fig. 4a. In contrast, sloping sides or a conical base like the one shown in Fig. 4f promote sedimentation of solids and should be avoided if a suspension of solids is required [8].

To perform the sizing of the tank, it is necessary to know the total volume that the tank must contain. To carry out the design of the washing tank, the use of two hundred grams of seeds will be considered. The ratio between the mass of seeds and water will be 1–5. Therefore, the mass of water needed to wash 200 g of seeds will be 1000 g of water. Finally, the machine must be sized correctly considering the appropriate volume of the container for raw material to be processed in addition to assigning an additional percentage of volume for safety. The water ratio for washing is as follows:

$$m_{\text{Seeds}} = 5 \times m_{\text{Seeds}} \quad (\text{g}) \quad (2)$$

Volume calculation:

Step 1: Calculation of the volume of 200 g of seeds.

$$v_{\text{Seeds}} = m_{\text{Seeds}} \times \rho_{\text{Seeds}} \quad (3)$$

Step 2: Calculation of the volume of tolerance for washing.

$$V_{\text{tolerance}} = v_{\text{Seeds}} \times 0.25 \quad (4)$$

Step 3: Calculation of the total volume.

$$V_{\text{total cylinder}} = V_{\text{tolerance}} + V_{\text{Seeds}} + V_{\text{washed water}} \quad (5)$$

### 2.3 Design of Agitators

At this stage of the process, three types of agitators were designed, which are; straight pallet agitator (Rushton), helical type agitator, and inclined pallet type agitator, which are shown in Fig. 5a–c, respectively.

Table 1 presents the equations for the design of the three wash pallets. These three palettes will be designed in Autodesk Inventor [9] and subsequently manufactured in 3D printers, as shown in Fig. 6. The design and manufacturing process was carried out with the aim of testing in the next stage and thus being able to determine which of them are the most suitable for washing chili seeds.

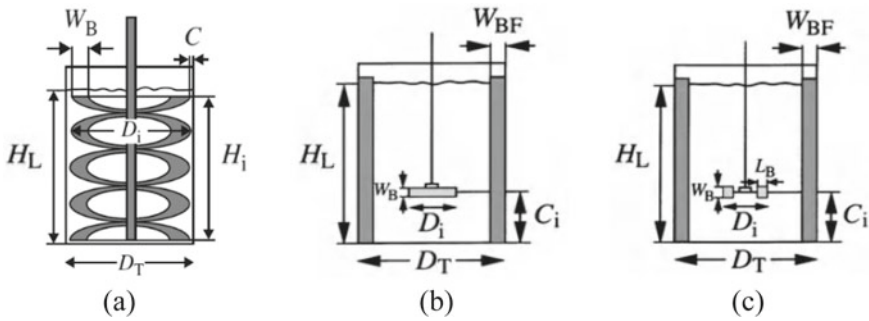


**Fig. 5** Types of agitators used in the project

**Table 1** Patterns for agitator design

Agitator	$D_i/D_T$	$H_L/D_T$	$C_i/D_T$	$W_{BF}/D_T$	Number
Turbine Rushton $W_B/D_i = 0.2, L_B/D_i = 0.25$	0.33	1	0.33	0.1	6
Inclined turbine $W_B/D_i = 0.2, L_B/D_i = 0.125$ 6 blades, 45°	0.33	1	0.33	0.1	6
	$D_T/D_i$	$C/D_i$	$H_i/D_i$	$W_B/D_i$	
Helical	1.02	0.01	1	0.1	

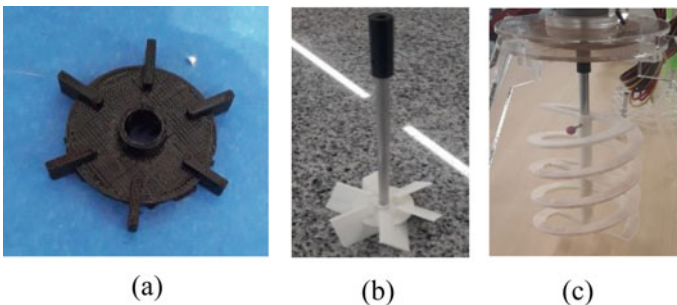


**Fig. 6** Agitators designed in the project

### 2.4 Test Design

In order to establish the level of washing of the seeds, it is necessary to define some measurement variables. For this, the seeds will not be directly analyzed, the water in the mixture will be analyzed at the time of washing. The level of pH and the level of electrical conductivity in the water will be measured after each wash. It is considered that, by washing the seeds, the water can become more acidic. This is mainly due to the substances that expel the seeds. Seed washing is a cyclic process, which is repeated approximately every 15 min. This process is detailed below with the following steps described.

**Table 2** Washing process specification

Washed	Washed 1	Washed 2	Washed 3
Sample	Sample 1	Sample 4	Sample 7
	Sample 2	Sample 5	Sample 8
	Sample 3	Sample 6	Sample 9
Time	15 min		
RPM	400		
Temperature	25 °C		

- Step 1. Income of raw material selected and weighed previously (200 g of seeds and 1000 ml of water).
- Step 2. Start of washing for a time interval of 15 min.
- Step 3. After 15 min of washing, proceed to remove a sample of 50 ml where pH and Electrical conductivity should be measured.
- Step 4. Start of the second washing period for 15 min.
- Step 5. After 15 min of washing, proceed to remove a sample of 50 ml where it is necessary to measure pH and Electrical conductivity.
- Step 6. The water in the mixture is changed to new (clean) water. With this change, we will proceed to what we will call “Second Wash” and stages 2, 3, 4, 5, and 6 should be repeated until the appropriate wash number is found, this will be achieved with the precise measurement of the variables described above. Table 2 shows the specifications of the washing process.

### 3 Results

The following graphs show the measured values of conductivity and pH obtained in each sample during the washing tests, the behavior of the three pallets is also observed at the time of washing (agitating) the seeds. Figure 7 shows that the level of pH between the samples of different pallets is very similar, that is, there is no significant change in the tests, despite the change of pallets. However, there is a significant increase in pH every three samples, that is, after changing the water. This allows us to know the number of washes in which our process is located.

In Fig. 8, it is observed that the conductivity measurement in each sample, of different agitator, has a significant change, that the change of pallet allows obtaining a higher conductivity value. The straight pallet is the one that allows obtaining a higher conductivity value in the samples. Secondly, there is the inclined pallet and thirdly the helical pallet. For the final design of the washing machine, it is recommended to use a straight pallet agitator because it allows for greater agitation and the construction is much simpler than the other two designs.

Additionally, it was observed that the color of the water changes during washing, as the agitation of the seeds increases, and the color decreases each time the water

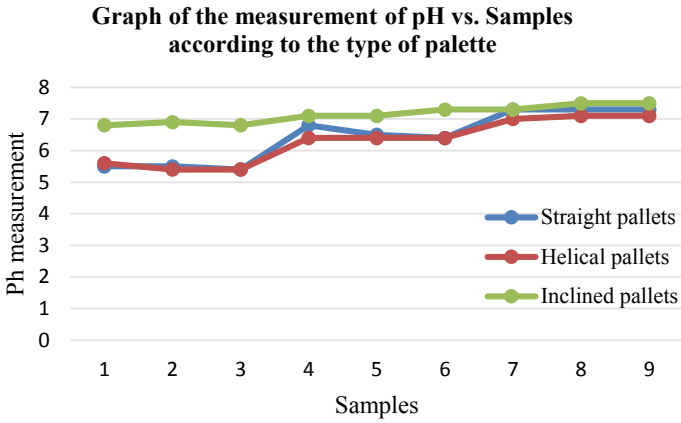


Fig. 7 Graph of the measurement of pH versus Samples according to the type of palette

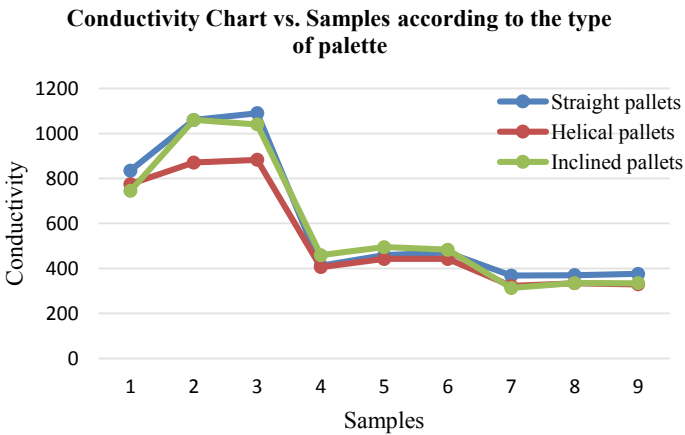
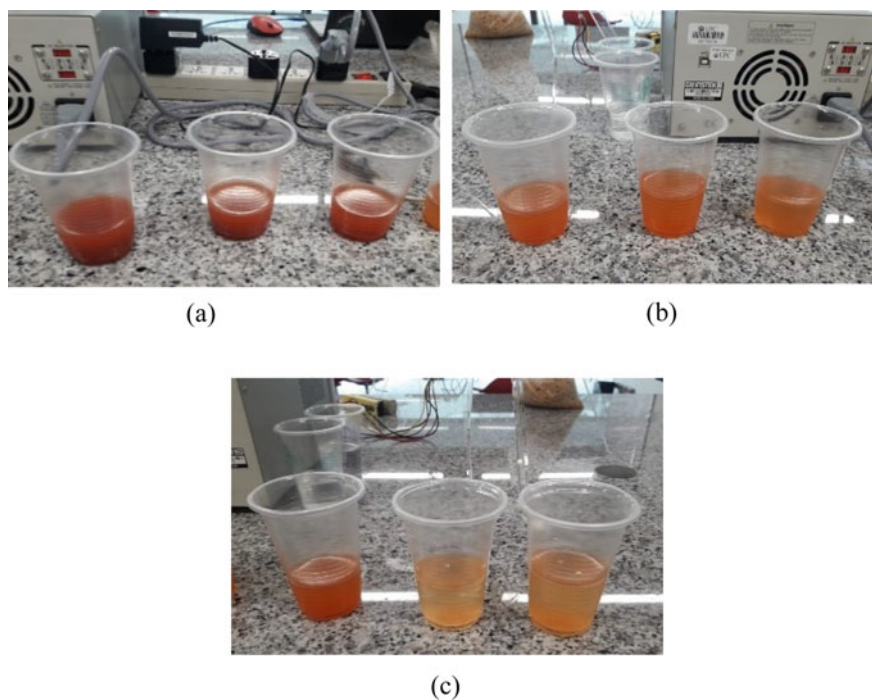


Fig. 8 Conductivity chart versus Samples according to the type of palette

change is made. The control of the level of color in the water could help us to control the level of agitation of the seeds, in this way we could know when to stop stirring the seeds. This can be determined in Fig. 9, since the samples obtained during the washing process, can be observed.

## 4 Conclusions

The tests carried out determined that the best agitator to wash seeds is that of straight blades, the performance of the blades is shown in Fig. 8. For this test, the time



**Fig. 9** Images of the samples obtained in the washing process

established to agitate the seeds was 15 min, after this time a variation (increase) of conductivity in the water is obtained. This increase was observed each time the mixture was stirred more. However, the second variable we control (pH) does not provide much information, since it only varies each time the water is changed. An additional test was performed where hot water (40 °C) was used, as a result, the number of washes decreased. This is mainly since the conductivity in the water reaches, in less time of agitation, the values obtained in the first test. It is important to mention that the water obtained during each wash had a reddish color and this increased every time the mixture was stirred; in this way, the water could be analyzed by image processing in order to detect the level of washing.

## References

1. A. de E. ADEX: Perú puede mejorar su posicionamiento como proveedor mundial de pimientos y ajíes. *Asociación de exportadores*. IOP Web. <http://www.adexperu.org.pe/notadeprensa/peru-puede-mejorar-su-posicionamiento-como-proveedor-mundial-de-pimientos-y-ajies/>. (2017) Accessed on 9 May 2019
2. Amazon Andes: Ají panca. *Amazon Andes*. IOP Web. <https://peruvianchili.com/es/product-item/aji-panca/>. (2017). Accessed on 9 June 2019



3. Comisión de Promoción del Perú para la Exportación y el Turismo: Súper ajíes nativos. *Super Foods Peru*. IOP Web. <https://peru.info/es-pe/superfoods/detalle/super-ajies-nativos>. Accessed on 17 June 2019
4. Cedrón, J.C.: La Capsaicina la molécula destacada. *Revista de Química Pontificia Universidad Católica del Perú* **27**, 816–824 (2013)
5. Yañez, P., Balseca, D., Rivadeneyra, L., Larenas, C.: Características morfológicas y de concentración de capsaicina en cinco especies nativas del género *Capsicum* cultivadas en Ecuador. *La Granja: Revista de Ciencias de La Vida. Universidad Politécnica Salesiana*, (2015)
6. Peralta, G.: Determinación del nivel de pungencia en unidades Scoville para *Capsicum annum* var. *aviculare* procedente de regiones productoras de Guatemala. *Informe de tesis, Universidad de San Carlos de Guatemala*, (2007)
7. Medina, R., Atencio, B., Romero, M., Castro, R.: Análisis estratégico del proceso productivo en el sector industrial. *Rev. Ciencias Sociales* **8**(1), 135–156 (2002)
8. Suntaxi, J.: Diseño y construcción de una máquina lavadora de ajonjolí para la empresa productos Schullo con una capacidad de procesamiento de 100 Kg/h. Informe de Tesis Universidad Politécnica Salesiana de Quito (2016)
9. Sørstad, S., Imenes, K., Johannessen, E.: Hybrid electrochemical sensor platform for capsaicin determination using coarsely stepped cyclic squarewave voltammetry. *Biosens. Bioelectron.* **130**, 374–381 (2019)
10. Doran, P.: *Bioprocess Engineering Principles*. Academic Press, (2013)

# Bacteriological Contaminants Detection in Some Consumed Raw Vegetables Based on Spectrometry in Ayacucho Town, Peru



José Yauri , Manuel Lagos , Rousell Vidalón , Julio Cárdenas , Kay Jeri , Lisber Arana , and Yuzo Iano 

**Abstract** Humans need to eat foods for growing and getting energy to carry out your daily activities. However, to find quality foods have become difficult because most of them have been cultivated in contaminated environments. So, to detect contaminated foods is a critical issue to care the human health. Being microorganisms the most frequent sour of contamination, it is desirable to have a detector tool for discarding unsanitary foods. In opposite to the traditional, expensive, slow, and invasive microbiological analysis, approaches to quickly detect microorganisms have been proposed. This work presents an approach to use spectrophotometry to detect bacteria in three consumed raw vegetables and expended in Ayacucho tow, Peru. Cultures of lettuce, peppermint, and cilantro irrigated with water with a high presence of *Escherichia coli* and *Thermotolerant coliforms* were successfully detected using the measured

---

J. Yauri (✉) · J. Cárdenas · K. Jeri  
School of Technological Sciences and Engineering, University of Ayacucho Federico Froebel,  
Ayacucho, Peru  
e-mail: [jyauri@udaff.edu.pe](mailto:jyauri@udaff.edu.pe)

J. Cárdenas  
e-mail: [jcardenas@udaff.edu.pe](mailto:jcardenas@udaff.edu.pe)

K. Jeri  
e-mail: [kjeri@udaff.edu.pe](mailto:kjeri@udaff.edu.pe)

M. Lagos  
Department of Mathematics and Physics, National University of San Cristobal de Huamanga,  
Ayacucho, Peru  
e-mail: [manuel.lagos@unsch.edu.pe](mailto:manuel.lagos@unsch.edu.pe)

R. Vidalón  
Technical-Productive Education Center, Polytechnic of Ayacucho, Ayacucho, Peru  
e-mail: [ruzvidalon@gmail.com](mailto:ruzvidalon@gmail.com)

J. Yauri · L. Arana · Y. Iano  
School of Electrical and Computer Engineering, University of Campinas, Campinas, Brazil  
e-mail: [lisberarana@gmail.com](mailto:lisberarana@gmail.com)

Y. Iano  
e-mail: [yuzo@decom.fee.unicamp.br](mailto:yuzo@decom.fee.unicamp.br)

© The Editor(s) (if applicable) and The Author(s), under exclusive license  
to Springer Nature Switzerland AG 2021

Y. Iano et al. (eds.), *Proceedings of the 5th Brazilian Technology Symposium*,  
Smart Innovation, Systems and Technologies 202,  
[https://doi.org/10.1007/978-3-030-57566-3\\_30](https://doi.org/10.1007/978-3-030-57566-3_30)

spectrum from only their stem. Using an SVM classifier, we achieved a detection accuracy rate of 91.89% and Kappa 89.87%, which demonstrates the feasibility of our approach.

**Keywords** Bacteriological contaminants · Spectrometry · Consumed raw vegetables · *Escherichia coli* · *Thermotolerant coliforms*

## 1 Introduction

Daily, humans need to eat food to obtain nutrients, proteins, and vitamins that allows to have a healthy life and get the energy required to develop their activities [1]. But having poor nutrition increases vulnerability to diseases alters the normal physical and mental development, and diminishes productivity. Therefore, people need to eat nutrient-rich foods, aiming to cover their dietary requirements [2].

Today, getting clean and healthy food is becoming hard –healthy foods are varied in nutrient-rich foods such as fruits, vegetables, cereals, etc. which have been grown preferably naturally, in accordance with the environment [3]. Because of the pollution and bad agricultural practices, more crops are contaminated by pathogens [4], and organic and inorganic residuals [5, 6]. Usually, farms are cultivated with contaminated soil and streams, which contain residual waters from the population and livestock [7–9], rest of chemical fertilizers [10] and pesticides [11]. The consumption of such foods can cause health problems, usually infectious diseases of the stomach, which are commonly observed in children and elderly people [12, 13].

In order to mitigate the action of pathogens, it is recommended a good hygiene and washing practices for consumed raw fruits and vegetables, since recent studies have concluded that the pathogen immigration on the leaf surface or pathogen internalization within the plant augment their environment survival [14]. Thus, many studies have been conducted in favor to identify the type of contamination in soils [9], water [6–8], fruits and leafy vegetables [11, 12, 14]. Identification and measure of bacterial contamination are carried out by microbiological analysis. In such a process, bacteria are identified, cultured and counted in a laboratory [15]. However, the analysis for detecting pathogenic microorganisms of a single product is complex, time-consuming and expensive. So, it is desirable to obtain a general contamination profile, since some vegetables are more contaminated than others, depending on its origin.

Recently, powered by new sensing technologies, novel methods for rapid detection of bacteriological contamination in vegetables were presented [16]. A rapid detection method has to be simple, rapid, and sensitive. Lately, rapid non-destructive detection methods are based on bio-sensors and spectroscopy. The work [17] reported the use of bio-sensors to detect effectively *Pseudomonas aeruginosa* and *Salmonella typhimurium*, [18] use a laser ray to detect microorganisms, and in [19] used the near-infrared (NIR) spectral as an indicator of contamination livestock products.

This paper presents a method to detect the presence of bacteriological contaminants in three consumed raw vegetables (lettuce, cilantro, peppermint). To learn a discriminative model, the vegetables come from two different places: the first, a field irrigated with the river water that exceeds the permissible limits of biological organisms for irrigation [20]; the second, a home garden irrigated with drinking water. No fertilizer and no pesticides were applied. In harvest time, vegetables were collected and measured their reflectance spectrum using a spectrophotometer [21]. By using both of the visible and NIR measured wavelength as feature descriptors, trained a linear Support Vector Machine (SVM), we achieved encouraging results as a fast bacteriological contamination detector.

The remainder of this paper is organized as follows. Section 2 presents related work. Section 3 explains the proposed method. Section 4 details the experimental results and discussions. Finally, Sect. 5 exposes conclusions and future work.

## 2 Related Work

Humans need to eat foods to satisfy the nutritional requirements that allow them to make activities. Among foods, vegetables and fruits are the most recommended, because they content-rich carbohydrates, vitamins, and minerals [3]. However, usually consumed raw vegetables or fruits can cause infectious diseases since they were contaminated or handled hygienically [14]. The presence and degree of contaminants usually depend on the environmental conditions where the growth of the food [22]. The contamination could come from the used water, soil, and fertilization type employed during farming. Therefore, vegetables cultivated with the residual stream are more contaminated than vegetables irrigated using water compliant with irrigation water quality.

Because eating contaminated foods can produce undesirable diseases, the detection and discarding of contaminated foods can avoid them. Usually, bacteriological contamination such as *Escherichia coli* is among the most common cause of stomach and intestinal infections, recently even antibiotic-resistant [23]. Therefore, people require methods to detect contaminated food.

In opposite to traditional detection methods based on biochemical analysis which is lagging and costly, recent methods are faster and credible at low cost to detect bacteriological contaminants [16–18]. In this sense, spectrometry seems a promising method to detect microorganisms [19] and other properties of the object of interest. Spectroscopy is concerned about the interaction between the light and the object of interest and the spectrometry measures the electromagnetic radiation to obtain information about the object [24]. Normally, a spectrometer provides a measurement of the reflection of electromagnetic radiation, named reflectance [21], usually from the visible and near-infrared spectrum–NIR (between 350 and 2500 nm).

Spectrometry has many applications. For instance in agriculture, instead of a soil chemical test, the measurements of a spectrometer can provide data to determine

the contamination level and type of particles in the soil [25]; can be detected microbial contamination in water [26] and pesticide residues in lettuces [27]; also plant diseases can be detected as the yellowing leaves caused by the *rhizospheric* bacteria in chrysanthemum [28], the leaf miner damage on tomato leaf [29], and fungal pathogens on sugar beet leaves [30]. All these presented diseases are produced by some microbiological pathogen, so is feasible to use a spectrometer to detect it.

Taking advantage of the spectrometry, in this work, we present an automatic recognizer to detect bacteriological contaminants in three consumed raw vegetables in Ayacucho town, Peru. Lettuces, cilantro, and peppermints were cultivated using highly contaminated water with microbiological pathogens, such as *Escherichia coli* and *thermotolerant coliforms*. According to the official report [20], the irrigation water of the field contains  $2.2E + 5$  CFU/100 of *Escherichia coli* and  $1.7E + 6$  NMP/100 mL of *thermotolerant coliforms*, which is above the permissible 1000 CFUs for irrigation water.

### 3 Our Proposal

Ayacucho is a town located in the central part of Peru. There, it is common to eat raw vegetables as an accompaniment to typical dishes. However, to eat that food is becoming a health problem for citizens: most fruits and vegetables are irrigated with wastewater of Ayacucho city. The residual treatment plant flows its residual waters into the Alameda river, without proper treatment to make it suitable for irrigation, so the river and the basin are contaminated.

Among contaminants, we highlight *Escherichia coli* and *thermotolerant coliforms* reported in [20], because they cause digestive intoxication, and in a long term cancer (recently, the Healthy Ministry of Peru communicated a high incidence of stomach cancer in Ayacucho [31]). In the market, to detect and distinguish a vegetable from a contaminated or non-contaminated field is hard, since microorganisms are imperceptible to the human eye and because the sellers usually do not say the origin of the product. Therefore, people are at risk of getting sick. For instance, Fig. 1 shows two lettuce samples: one is from a field irrigated with contaminated water (Fig. 1a) and then another one, from a field, irrigated with potable water (Fig. 1b), however, they seem healthy.

To build an automatic detector, to discriminate between contaminated and non-contaminated vegetables, the proposed framework is shown in Fig. 2. It works as follows:

**Vegetable dataset.** The collected dataset consists of wavelengths of the electromagnetic spectrum measured with a spectrometer [21] for each vegetable sample.

The used sensor provides measurements of the reflectance of the sunlight between 350–2500 nm, e.g., the visible and the near-infrared spectrum. Therefore, measures were performed at 12 m–01 p.m., on different sunny days outdoor.

Vegetables consist of lettuce, cilantro, and peppermint and form two groups:

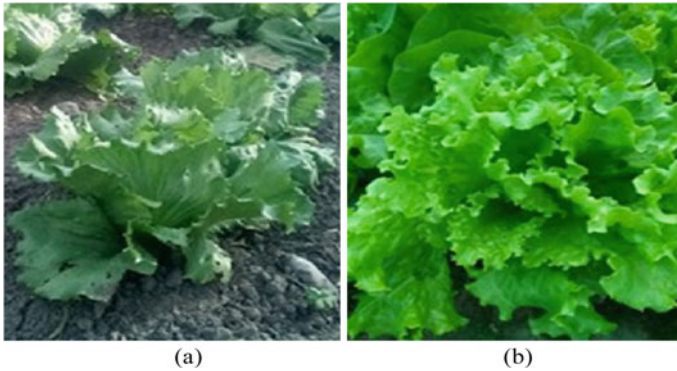


**Fig. 1** Lettuce samples. **a** From a contaminated field, **b** From a non-contaminated field

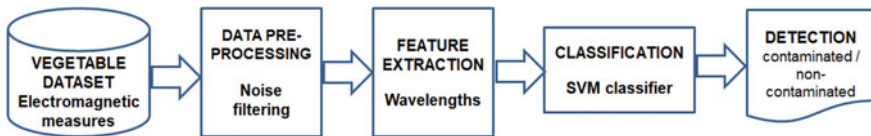


**Fig. 2** The proposed detection framework

- The first group was cultivated in a field at the Latitude = - 13.136103 and Longitude = - 74.193728, irrigated using residual water coming from the wastewater treatment plant of Ayacucho city, located at the Latitude = - 13.140945, Longitude = - 74.206654. Samples were labeled as contaminated.
- The second group was cultivated in a field at the Latitude = - 13.164441 and Longitude = - 74.248020, irrigated using potable water. Samples were labeled as non-contaminated.

**Data pre-processing** For this stage, each electromagnetic spectral measurement can be thought of as a row vector. Because of the sun intensity, the moisture and the wind at the time of measurement can produce noise, we applied two pre-processing steps:

- To remove that noisy water band, approximately 1800–2000 nm [21], so the vector length is 1753–dim.
- To normalize the measurement according to Eq. 1, since the spectrum wavelengths could have variations in their intensity, but nothing in their shape.

$$x_n = \frac{x - x_{\min}}{x_{\max} - x_{\min}} \tag{1}$$

**Feature extraction** Since the sensor provides a single row data for each spectral measurement, each of one is treated as a row feature vector.

**Classification** To perform detection tasks, we trained an SVM classifier in one-against-one fashion [32]. For classification, we have six classes lettuce-co, lettuce-nc, cilantro-co, cilantro-nc, peppermint-co, and peppermint-nc, where co means contaminated and nc, non-contaminated.

**Detection** This stage recognizes the given unknown vegetable and labels it as contaminated or non-contaminated.

## 4 Results and Discussions

### 4.1 Spectral Wavelengths Dataset

We collected a dataset which contains spectral wavelengths from 20 samples of lettuce, 10 of cilantro, and 10 of peppermint, both from contaminated and non-contaminated fields, and both from the leaves and the stems. An illustration of the measurement process to collect data is shown in Fig. 3.

Next, in order to remove noisy data, we discarded three segments from the collected raw data: 1340–1350 nm, 1800–2000, and 2400–2500 nm. They are produced by uncontrolled changes in moisture and wind during measurements. Next, the data is normalized. Figure 4 illustrates the pre-processing step: the raw data Fig. 4a, the raw data is cropped Fig. 4b and the raw data is normalized Fig. 4c.

We collected data from both the leaves and the stems of the vegetables. Figure 5 shows the plotted data as 1D signals for both the leaves and stem of lettuce, peppermint, and cilantro.

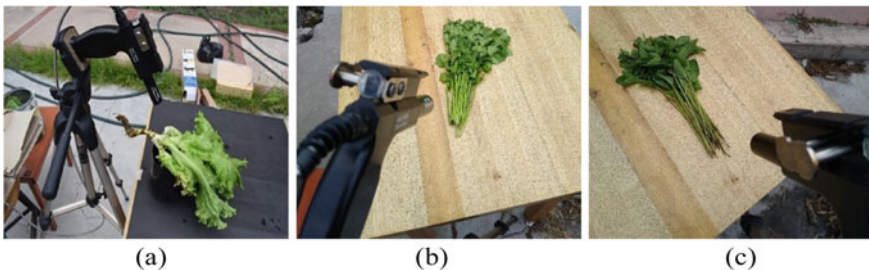


**Fig. 3** Electromagnetic spectrum measurement: **a** Lettuce, **b** Cilantro, and **c** peppermint

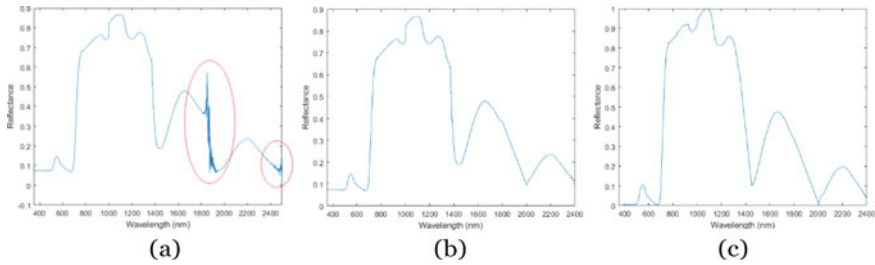


**Fig. 4** Pre-processing of the data: **a** Raw data signal, **b** Raw data after removing some useless bands, and **c** Normalized data

## 4.2 Experiments

In order to assess the discriminative power of the measured electromagnetic spectral data (both the visible and the near-infrared data), the classification was performed changing the features in three ways: (I) Only measurements from the leaves, (II) Only measurements from the stem, and (III) Concatenating of I and II. To reduce the effect of a small dataset, experiments were conducted using the Leave-One-Out Cross-Validation (LOOCV) scheme [32].

## 4.3 Results

Table 1 shows the obtained results using the Linear SVM (Cost = 1) under the LOOCV experimental setup.

According to Table 1, the experimental setup II outperforms the other approaches, achieving a detection accuracy rate of 91.89% and a Kappa statistic measure rate of 89.87%. Using only leaf features leads to lower performance, and even contrary to be expected, combined features get the worst performance.

These results suggest that the classifier has detected microorganisms on the stem of these vegetables but no on their leaf. It is reasonable since, during the irrigation the residual water covers up to the stem of the plant, microorganisms remain on the stem and over other parts that got wet. And few bacteria live on the leaves because the water does not contact them and because of the bactericidal effect of the light [33].

## 5 Conclusions and Future Work

This paper presented an approach to detect bacteriological contaminants in three consumed raw vegetables, named lettuce, peppermint, and cilantro, in Ayacucho



tow, Peru. The proposal resides on the use of spectroscopy to measure the reflected light spectrum of the object and since spectrophotometry is a low cost, fast, and non-invasive tool of analysis. By measuring only the reflectance on the stem, the detector achieved a recognition rate of 91.89% in a collected dataset from a highly contaminated basin with bacteriological pathogens. It demonstrates his feasibility in favor of food safety and people’s health in Peru.

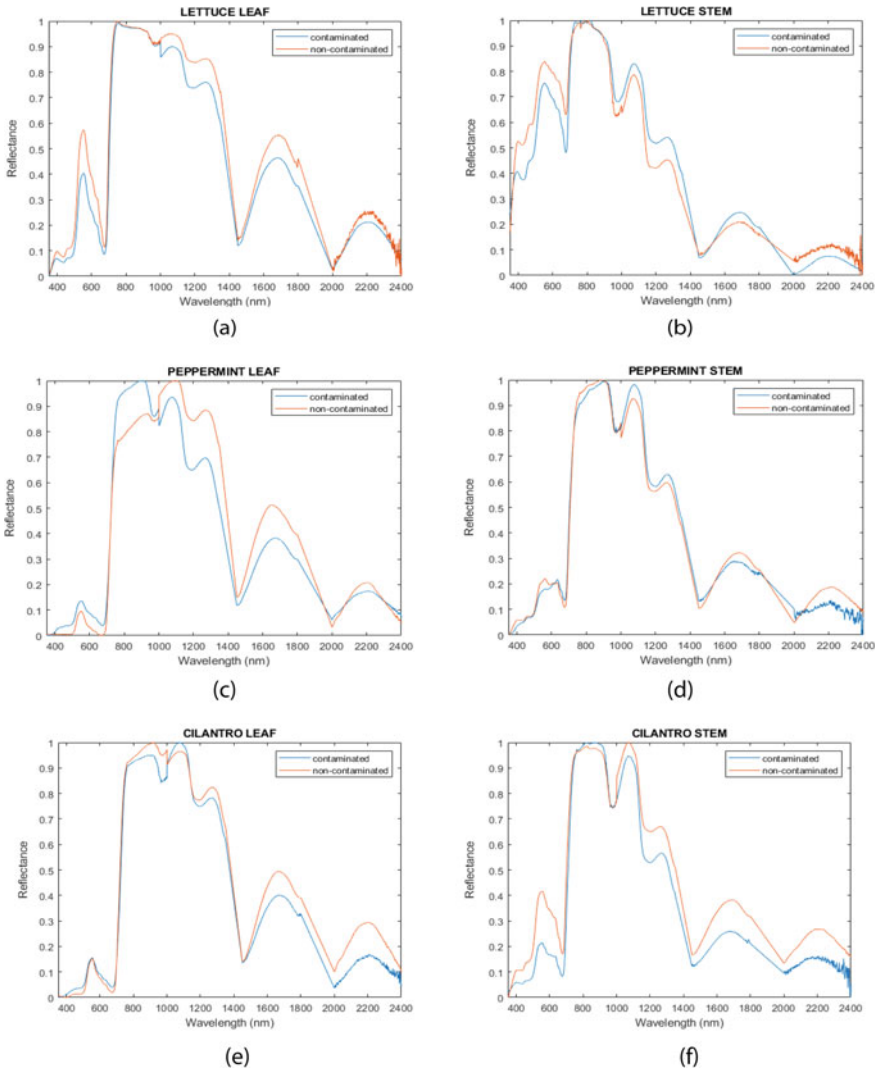


**Fig. 5** Illustration fo the spectral data both from the leaf and stem from a sample: **a** Lettuce leaf, **b** Lettuce stem, **c** Peppermint leaf, **d** Peppermint stem, **e** Cilantro leaf, and **f** Cilantro stem. The blue signal represents the contaminated data, while the red signal shows the non-contaminated one

**Table 1** Experimental results according to their accuracy and Kappa metrics

Protocol	Accuracy (%)	Kappa (%)
(I) Only leaf features	84.00	80.19
(II) Only stem features	91.89	89.87
(III) Both I and II	83.56	79.57

As future work, we intend to extend this study to other vegetables and to establish the degree of contamination.

**Acknowledgements** This research was partially supported by the University of Ayacucho Federico Froebel. The authors would like to thank Walter Solano, Renato Soca, and Noel Torres from the Laboratory of Remote Sensing of the National University of San Cristobal de Huamanga, and the anonymous reviewers for their valuable suggestions and helpful feedback.

## References





1. World Health Organization: Health Topics: Nutrition (2014). <https://www.who.int/topics/nutrition>. Accessed on 09 Sep 2019
2. Hernández Rodríguez, M., Sastre Gallego, A.: Tratado de Nutrición. Ediciones Díaz de Santos (2000)
3. Mañas Almendros, M., Martínez de Victoria Muñoz, E., Yago Torregrosa, M.D.: Principios Generales de Nutrición. Ediciones Díaz de Santos (2000)
4. Steele, M., Odumeru, J.: Irrigation water as source of foodborne pathogens on fruit and vegetables. *J. Food Protect.* **67**(12), 2839–2849 (2004). <http://jfoodprotection.org/doi/abs/10.4315/0362-028X-67.12.2839>
5. Kumar, V., Thakur, R.K., Kumar, P.: Assessment of heavy metals uptake by cauliflower (*Brassica oleracea* var. botrytis) grown in integrated industrial effluent irrigated soils: a prediction modeling study. *Sci. Horticul.* **257**, 108682 (2019). <https://www.sciencedirect.com/science/article/pii/S0304423819305680>
6. Weldegebriel, Y., Chandravanshi, B.S., Wondimu, T.: Concentration levels of metals in vegetables grown in soils irrigated with river water in Addis Ababa, Ethiopia. *Ecotoxicol. Environ. Safe.* **77**, 57–63 (2012). <https://www.sciencedirect.com/science/article/pii/S0147651311003368>
7. Okafo, C.N., Umoh, V.J., Galadima, M.: Occurrence of pathogens on vegetables harvested from soils irrigated with contaminated streams. *Science Total Environ.* **311**(1–3), 49–56 (2003). <https://www.sciencedirect.com/science/article/pii/S0048969703000573>
8. Ensink, J.H.J., Mahmood, T., Dalsgaard, A.: Wastewater-irrigated vegetables: market handling versus irrigation water quality. *Trop. Med. Int. Health* **12**, 2–7 (2007). <http://doi.wiley.com/10.1111/j.1365-3156.2007.01935.x>
9. Rostami, A., Ebrahimi, M., Mehravar, S., Fallah Omrani, V., Fallahi, S., Behniafar, H.: Contamination of commonly consumed raw vegetables with soil transmitted helminth eggs in Mazandaran province, northern Iran. *Int. J. Food Microbiol.* **225**, 54–58 (2016). <https://www.sciencedirect.com/science/article/pii/S0168160516301180>
10. Sultana, Z., Sultana, R., Rokonujjaman, M., Simol, H.A., Sultan, M.Z., Salam, M.A.: Impact of gypsum and potash fertilizers on heavy metals and nutrients levels in some selected leafy vegetables and assessment of potential health risk. *Bangladesh Pharm. J.* **22**(1), 56–67 (2019). <https://www.banglajol.info/index.php/BPJ/article/view/40074>

11. Ng, P.J., Fleet, G.H., Heard, G.M.: Pesticides as a source of microbial contamination of salad vegetables. *Int. J. Food Microbiol.* **101**(2), 237–250 (2005). <https://www.sciencedirect.com/science/article/pii/S0168160505000097>
12. Mercanoglu Taban, B., Halkman, A.K.: Do leafy green vegetables and their ready-to-eat [RTE] salads carry a risk of foodborne pathogens?. *Anaerobe* **17**(6), 286–287 (2011). <https://www.sciencedirect.com/science/article/pii/S1075996411000552>
13. American Academy of Pediatrics: Food Poisoning and Food Contamination (2014). <https://www.healthychildren.org/english/health-issues/conditions/abdominal/pages/food-poisoning-and-food-contamination.aspx>. Accessed on 09 Sep 2019
14. Heaton, J., Jones, K.: Microbial contamination of fruit and vegetables and the behavior of enteropathogens in the phyllosphere: a review. *J. Appl. Microbiol.* **104**(3), 613–626 (2008). <http://doi.wiley.com/10.1111/j.1365-2672.2007.03587.x>
15. Lightfoot, N.F., Maier, E.A.: *Microbiological Analysis of Food and Water: Guidelines for Quality Assurance*. Elsevier (1999)
16. Law, J.W.F., Ab Mutalib, N.S., Chan, K.G., Lee, L.H.: Rapid methods for the detection of foodborne bacterial pathogens: principles, applications, advantages and limitations. *Front. Microbiol.* **5**, 770 (2014). <http://www.pubmedcentral.nih.gov/articlerender.fcgi?artid=PMC4290631> <http://www.pubmedcentral.nih.gov/articlerender.fcgi?artid=PMC4290631>
17. Starodub, N.F., Novgorodova, O., Ogorodnijchuk, Y.: Biosensors and express control of bacterial contamination of different environmental objects. *Microbial Contam. Food Degradation*, 367–394 (2018). <https://www.sciencedirect.com/science/article/pii/B9780128115152000123>
18. Yoon, J., Lee, K., Park, Y.: A simple and rapid method for detecting living microorganisms in food using laser speckle decorrelation. <https://arxiv.org/abs/1603.07343> (2016). <http://arxiv.org/abs/1603.07343>
19. Atanassova, S., Veleva, P., Stoyanchev, T.: Near-infrared spectral informative indicators for meat and dairy products, bacterial contamination, and freshness evaluation. *Microbial Contam. Food Degradation*, 315–340 (2018). <https://www.sciencedirect.com/science/article/pii/B978012811515200010X>
20. ALA Ayacucho: Results of Participatory Monitoring of Surface Water Quality in the Mantaro Basin—2017, Local Water Administration of Ayacucho, (2017). <https://www.ana.gob.pe/org/anos-desconcentrados/aaa-mantaro/ala-ayacucho>
21. ASD Inc.: ASD Technical Guide, Analytical Spectral Devices Inc., (1999)
22. Alemu, G., Mama, M., Siraj, M.: Bacterial contamination of vegetables sold in Arba Minch town, Southern Ethiopia. *BMC Res. Notes* **11**(1), 775 (2018). <https://bmresnotes.biomedcentral.com/articles/10.1186/s13104-018-3889-1>
23. Lillie, P., Johnson, G., Ivan, M., Barlow, G., Moss, P.: Escherichia coli bloodstream infection outcomes and preventability: a six-month prospective observational study. *J. Hosp. Infect.* **103**(2), 128–133 (2019). <https://www.sciencedirect.com/science/article/pii/S0195670119302208>
24. Ozaki, Y., McClure, W.F., Christy, A.A.: *Near-Infrared Spectroscopy in Food Science and Technology*. Wiley, Hoboken, NJ, USA (2006). <http://doi.wiley.com/10.1002/0470047704>
25. Schwartz, G., Eshel, G., Ben-Dor, E.: Reflectance spectroscopy as a tool for monitoring contaminated soils (Chap. 4). In: Pascucci, S. (ed.) *Soil Contamination*. InTech (2011). <http://www.intechopen.com/books/soil-contamination/reflectance-spectroscopy-as-a-tool-for-monitoring-contaminated-soils>
26. Jung, A.V., Le Cann, P., Roig, B., Thomas, O., Baur'es, E., Thomas, M.F.: Microbial contamination detection in water resources: interest of current optical methods, trends and needs in the context of climate change. *Int. J. Environ. Res. Public Health* **11**(4), 4292–4310 (2014). <http://www.mdpi.com/1660-4601/11/4/4292>
27. Sun, J., Ge, X., Wu, X., Dai, C., Yang, N.: Identification of pesticide residues in lettuce leaves based on near-infrared transmission spectroscopy. *J. Food Process Eng.* **41**(6), e12816 (2018). <http://doi.wiley.com/10.1111/jfpe.12816>
28. Pérez Naranjo, J.C., Soler Arango, J., Arango Pulgarín, G., Meneses Ospina, E., Ruiz Villadiego, O.S., Villadiego, O.S.R.: Espectroscopia NIR como Técnica Exploratoria Rápida

- para Detección de Amarillamiento de Hojas Crisantemo (*Dendranthema grandiflora* var. Zembra). *Revista Facultad Nacional de Agronomía Medellín* **67**(1), 7163–7168 (2014). <https://revistas.unal.edu.co/index.php/refame/article/view/42629>
29. Xu, H., Ying, Y., Fu, X., Zhu, S.: Near-infrared spectroscopy in detecting leaf miner damage on tomato leaf. *Biosyst. Eng.* **96**(4), 447–454 (2007). <https://www.sciencedirect.com/science/article/pii/S1537511007000268>
  30. Mahlein, A.K., Steiner, U., Dehne, H.W., Oerke, E.C.: Spectral signatures of sugar beet leaves for the detection and differentiation of diseases. *Precis. Agricult.* **11**(4), 413–431 (2010). <http://link.springer.com/10.1007/s11119-010-9180-7>
  31. MINSA Peru: Analysis of the Cancer Situation in Peru 2013. Technical Report, Ministry of Health of Peru—General Direction of Epidemiology, Lima (2013). <http://www.dge.gob.pe>
  32. Murphy, K.P.: *Machine Learning: A Probabilistic Perspective*. The MIT Press, Cambridge, MA (2012)
  33. Lubart, R., Lipovski, A., Nitzan, Y., Friedmann, H.: A possible mechanism for the bactericidal effect of visible light. *Laser Ther.* **20**(1), 17 (2011). <http://www.pubmedcentral.nih.gov/articlerender.fcgi?artid=PMC3806074>

# Feasibility in Using Banana Flour in Bread Production: Centesimal and Sensory Analysis



Nathália Rafaela Santos de Carvalho ,  
Maria Thereza de Moraes Gomes Rosa ,  
Isabela Francabandiera Torniziolo ,  
and Daniela Helena Pelegrine Guimarães 

**Abstract** Brazil produces about six million tonnes per year of banana (*Musa spp*), with 35 kg/inhabitant/year average consumption. Banana peel represents about 47–50% (w/w) of ripe fruit but it doesn't have industrial applications; sometimes it is used in animal feed but in small-scale. On the other hand, banana flour already has proved to be a very promising ingredient, is used in baking, diet products, children's food, and animal feed. Based on these benefits and considering the great banana productivity in Brazil, the present work proposes the development of formulations of bread from banana flour, as well as analyze the sensory parameters, where acceptance tests were carried out, with a hedonic scale of 9 points; the attributes evaluated: flavor, appearance, texture, aroma, and overall impression. The results showed that the formulations, in general, have been accepted, except that produced by a mixture composed of 70% banana flour and 30% wheat flour, which presented a significant difference in relations with the other, for all attributes analyzed.

**Keywords** Banana · Flour · Baking · Sensorial analysis · Centesimal analysis · Acceptance

---

N. R. S. de Carvalho · D. H. P. Guimarães (✉)  
Lorena Engineering School (EEL-USP), São Paulo University, Campinas Highway, 12602-810  
Lorena, SP, Brazil  
e-mail: [dhguima@usp.br](mailto:dhguima@usp.br)

M. T. de Moraes Gomes Rosa · I. F. Torniziolo  
Center of Science and Technology, Mackenzie Presbyterian University, Brazil Avenue 1220,  
Campinas, SP 13073-148, Brazil

N. R. S. de Carvalho · M. T. de Moraes Gomes Rosa · D. H. P. Guimarães  
The University of Taubaté (UNITAU), Taubaté, SP, Brazil

## 1 Introduction

Banana (*Musa spp*) is one of the most consumed fruits in the world, whose consumption is increased every year, due to its high energy content (about 100 kcal per 100 g of pulp), for presenting easily assimilable carbohydrates, and also for being rich in vitamins, potassium, phosphorus, calcium, and iron, when compared to apples or oranges [1].

In green bananas, the main component is the starch (55–93% of the total solids content), and as the fruit matures, the starch is converted to sugars (glucose, fructose, and sucrose), reducing the acidity and, consequently, increasing sweetness [2].

The concentration of starch in the green banana makes it of great industrial interest, and beside the fact that its shell surpasses the pulp content of some nutrients, this organic residue became an inexpensive source of carbohydrates and minerals [3]. In this context, the flour of the green banana peel appears in the bakery industry, which can be used as supplementation or in partial substitution of wheat flour. Moreover, the fact that banana flour is not digested by the small intestine makes it very efficient in diets to eliminate weight [4].

Bread is one of the most popular foods and one of the main caloric sources of diet in many countries and it is, therefore, the subject of many types of research, in order to add nutritional value to the product, either by enhancing the nutrient content or by correcting its deficiencies [5].

The consumer market for bread has grown, varying from region to region. The Southeast and South Regions of Brazil consume around 35 kg/inhabitant/year, while the Northeast reaches only 10 kg/inhabitant/year. The consumption of bread in Brazil is 27 kg per year per person, which represents half of the proportion recommended by world organizations such as the WHO—60 kg/inhabitant/year—, and the FAO—50 kg/inhabitant/year. Baked goods occupy third place in the Brazilian shopping list, representing, on average, 12% of the family budget for food [6].

Considering the great interest in the industrialization of green banana peel, together with the great popularity of bakery products, the present work<sup>1</sup> aims to analyze the viability of the use of banana flour in the development of form loaves formulations, alternative nutritional enrichment of the product, as regards the fiber content. The different formulations were tested by means of sensorial acceptance tests.

## 2 Materials and Methods

In order to obtain banana flour, bananas of the variety nanica (*Musa acuminata* 'Dwarf Cavendish') were used in the  $\frac{3}{4}$  fat development stage, that is, still green. First, the fruits were dehydrated in tray drier (Macanuda, MS-P), and then crushed in the industrial crusher (Metvisa, LQ-25). The obtained flour was evaluated for moisture,

---

<sup>1</sup>This research was carried out by the author at the University of Taubaté.

protein content, ashes, and fat. The bread loaf was prepared by adding the banana flour, partially replacing the wheat flour, following different formulations, in relation to the proportions of brown flour/flour.

The sensorial attributes of the different bread formulations (flavor, appearance, texture, aroma and overall impression) were analyzed by means of acceptance tests with a hedonic scale of 9 points of conducting a survey are the agility and economy in obtaining data, as well as obtaining data grouped in tables, which allow a rich statistical analysis.

## ***2.1 Characterization of the Banana Flour***

The processed banana flour was initially characterized, and physicochemical analyses were performed to determine its centesimal composition, and the following physicochemical analyses were performed:

Moisture [7—Method 16192];

Ashes [7—Method 16196];

Total Lipids [8];

Proteins [7—Method 38012].

The analyses concerning the characterization of the banana flour were carried out in triplicate, to verify if there is a divergence of results in the repetitions.

## ***2.2 Processing of Loaves***

The preparation of this type of bread followed the basic formulation composed of flour, biological yeast, eggs, salt, sugar, and milk. Instead of wheat flour, it was used a mixture composed of BANANA FLOUR + WHEAT FLOUR in different proportions, as follows:

*F1*: 100% wheat flour

*F2*: 50% wheat flour + 50% banana flour

*F3*: 70% wheat flour + 30% banana flour

*F4*: 30% wheat flour + 70% banana flour.

The flour, together with the biological yeast, was sieved to be added in a spiral kneader (Paniz, AE-25) and homogenized to the mixture composed of eggs, sugar salt, and milk. Thereafter, the dough was shaped and baked at 180 °C for 30 min.

## ***2.3 Sensory Evaluation***

In the present work, the different formulations for bread loaf were subjected to sensory analysis for appearance, flavor, and aroma, with reference to the product

prepared in a conventional manner (i.e., from wheat flour), the samples served in single portions, in white disposable plates and coded with three figures.

In the sensory analysis, the evaluations were made using 40 testers, as indicated by Stone and Sidel [9]. Prior to sensory testing, each tester signed the free and closed consent term. Because it was a work involving human beings, it had to be submitted to the evaluation of the Research Ethics Committee of the University of Taubaté, according to protocol n° 603/11. Along with the bread loaves samples, each taster received a score sheet containing 9 faces corresponding, respectively to 9 (extremely enjoyed), 8 (liked very much), 7 (liked moderately), 6 (liked slightly), 5 (displeased slightly), 3 (displeased moderately), 2 (disliked a lot) and 1 (disgusted extremely). For the intent to buy the test, it contained 5 faces, corresponding to 5 (would certainly buy), 4 (possibly buy), 3 (maybe buy/not buy), 2 (possibly not buy), and 1 (certainly would not buy).

In order to verify significant differences between the different product formulations, Variance Analysis (ANOVA) was necessary, in relation to the attributes analyzed.

### 3 Results and Discussion

#### 3.1 Characterization of Products

Table 1 presents the results concerning the characterization of banana flour, where each value represents the average of the three, and the values in parentheses, the respective standard deviations.

In relation to the results expressed in Table 1, it can be verified that the batches of the products that were used in the elaboration of the different bread formulations presented centesimal composition characteristics of each product, according to results obtained by Neto et al. [10].

**Table 1** Physical and chemical properties of banana flour

Analysis (%)	Content (standard deviation)
Moisture	6.63 (0.03)
Ash	0.048 (0.007)
Lipid	0.0071 (0.0002)
Protein	4.534 (0.080)



**Table 2** Sensory analysis of the bread enriched with banana flour

Attribute	<i>F.1</i>	<i>F.2</i>	<i>F.3</i>	<i>F.4</i>
Texture	6.90 <sup>a</sup>	5.35 <sup>b</sup>	5.13 <sup>b</sup>	4.45 <sup>b</sup>
Flavor	7.03 <sup>a</sup>	5.16 <sup>b</sup>	5.16 <sup>b</sup>	3.81 <sup>c</sup>
Appearance	7.19 <sup>a</sup>	5.55 <sup>b</sup>	5.23 <sup>b</sup>	5.35 <sup>c</sup>
Global impression	6.94 <sup>a</sup>	5.03 <sup>b</sup>	5.09 <sup>b</sup>	4.13 <sup>c</sup>

<sup>a</sup> and <sup>b</sup> correspond to statistical parameters; the same item, along the same line, means that there is no significant difference with respect to a certain sensory parameter

### 3.2 Sensory Analysis

The results of the sensory analysis, referring to the four different formulations of bread enriched with banana flour, are shown in Table 2.

The results presented in Table 2 showed that the formulations, in general, presented a great acceptance, except that elaborated from a mixture composed of 70% of banana flour and 30% of wheat flour, which presented significant difference before the others, with respect to all attributes analyzed.

From the results of Table 2, it can be observed that banana flour-enriched bread presented satisfactory acceptability since, except for the *F4* formulation, the others presented scores above 5 for all attributes, indicating good acceptance. Still, in relation to the results of Table 2, it can be observed that the different formulations of bread form presented significant differences in relation to all the attributes.

For all the sensorial attributes analyzed, it was observed that the greatest rejection, by the tasters, was for the formulation 4, which proves the impossibility of replacing the wheat flour for banana flour by more than 50%, in the production of bread. The satisfactory acceptability of formulations 2 and 3 demonstrate viability in the nutritional enrichment of loaves, partially replacing wheat flour with banana flour to a certain extent (50% banana flour and 50% wheat flour), although preference, by the tasters, was by formulation 1, that elaborated with 100% of wheat flour.

## 4 Conclusion

From the results presented in the previous item, it can be concluded that, except for the formulation *F.4*, the others presented good acceptance, being that they differed significantly from the one elaborated with 100% of wheat flour, in relation to all the sensory attributes. In this way, it can be affirmed that the addition of the banana flour interferes in the organoleptic qualities of the bread of form. The formulations, in general, presented satisfactory acceptability, except that elaborated from a mixture composed of 70% of banana flour, which proves the viability in the nutritional enrichment of bread loaves with banana flour to some extent.

## References

1. Castelo-Branco, V.N., Guimarães, J.N., Souza, L., Guedes, M.R., Borges, A.M., Pereira, J., Lucena, E.M.P.: Green banana flour characterization. *Food Sci. Technol. Cambridge* **2**, 333–339 (2009)
2. Melo, M. T. P., Rocha Júnior, V. R., Caldeira, L. A., Pimentel, P. R. S., Reis, S. T., Jesus, D. L. S.: Cheese and milk quality of F1 Holstein x Zebu cows fed different levels of banana peel. *Acta Scientiarum. Anim. Sci.* **32**(2), 181187 (2017)
3. Agama-Acevedo, E., Islas-Hernández, J.J., Pacheco-Vargas, G., Osorio-Díaz, P., Bello-Pérez, L.A.: Starch digestibility and glycemic index of cookies partially substituted with unripe banana flour. *LWT—Food Sci. Technol. Amsterdam* **46**, 177–182 (2012)
4. Almeida, E. L.: Efeito da adição de fibra alimentar sobre a qualidade de pão préassado congelado, 328f. Dissertação (Mestre em Tecnologia de Alimentos). Universidade Estadual de Campinas (UNICAMP), Campinas (2006)
5. Tavares, T.S., Bastos, S.C., Sousa, M.E., Pimenta, G., Pinheiro, A.C.G., Fabrício, L.F.F., Leal, L.S.: Perfil sensorial de pão de forma enriquecido com farinha de Matrinxã (*brycon lundii*). *Anais do XIX Congresso de Pós-Graduação da UFLA. UFLA, Lavras* (2010)
6. Castelo-Branco, V.N., Guimarães, J.N., Souza, L., Guedes, M.R., Silva, P.M., Ferrão, L.L., Miyahira, R.F., Guimarães, R.R., Freitas, S.M.L., Reis, M.C., Zago, L.: Uso da farinha de polpa e de casca de banana verde (*Musa balbisiana*) como ingrediente para a elaboração de massa tipo talharim. *Braz. J. Food Technol.* **20**, e20161119 (2017)
7. AOAC.: Official Methods of Analysis of the of AOAC International (1<sup>a</sup> edn.) 17th edn. Gaythersburg, MD. Adolfo Lutz, p. 1020 (2000/2008)
8. Bligh, E.G., Dyer, W.J.: A rapid method of total lipid extraction and purification. *Canad. J. Biochem. Physiol.* **37**, 911–917 (1959)
9. Stone, H., Sidel, J. L.: Sensory evaluation practices, p. 308. Elsevier Academic Press, San Diego (1993)
10. Neto, J. M. M., Cirne, L. M. E. R., Pedroza, J. P. P., Silva, M. G.: Componentes químicos da farinha de banana (*Musa ssp.*) obtida por meio de secagem natural. *Revista Brasileira de Engenharia Agrícola e Ambiental* **2**(3), 316–318 (1998)

# Spectral Behavior of Maize, Rice, Soy, and Oat Crops Using Multi-spectral Images from Sentinel-2



Lady Angulo  and Sergio Pamboukian 

**Abstract** Monitoring the status of crops at regional, local and smallholder farming levels is essential in the search for sustainable agricultural management. One of the methodologies applied for this purpose is precision agriculture, which, together with the technological tools and equipment (Global Navigation Satellite Systems, Remote Sensing, Geographic Information Systems and drones), form an integrated agricultural system based on information of crop production and evolution. Measures of the interaction response from electromagnetic radiation (ER) with soil and vegetation are a basis for the development of agricultural yields and harvest index predictors. In this research, spectral signatures and the Normalized Difference Vegetation Index (NDVI) were analyzed for maize, soybean, rice and oat crops in a growing area of 320 ha, located in the city of Tremembé (São Paulo-Brazil) for the summer harvest period from November to March of the crop cycles of 2017/2018 and 2018/2019, through the use of multi-spectral images of Sentinel-2 satellite platform (and one image from Landsat-8 to cover the missing image for December 2017). The results showed a higher spectral response (especially in the RedEdge and Near-InfraRed) for soybean crops, followed by rice and corn around the 60–90 days of sowing, and a decrease with the approach to the harvest. In addition, were found higher NDVI values to the crop cycle 2017/2018 (0.962), around 55–80 days of sowing for the soybean and rice crops. However, the development of crop cycle 2018/2019 shows more homogeneous spectral results.

**Keywords** NDVI · Precision agriculture · Spectral signatures · Sentinel-2

---

L. Angulo (✉) · S. Pamboukian  
Center of Radio Astronomy and Astrophysics at Mackenzie (CRAAM), Mackenzie Presbyterian University, São Paulo, SP 01302-907, Brazil  
e-mail: [victoria.angulo.valencia@gmail.com](mailto:victoria.angulo.valencia@gmail.com)

S. Pamboukian  
e-mail: [sergio.pamboukian@mackenzie.br](mailto:sergio.pamboukian@mackenzie.br)

# 1 Introduction

Digital geographic information is now considered a basis for acquiring essential environmental and crop monitoring information, adding the availability of acquiring data from different times and places. The increase in the availability of digital geographic information data sources, as well as satellite platforms with a free and unrestricted imagery access policy and improvements in spatial, spectral, and radiometric resolutions, have made the multi-spectral imagery very useful for detecting crop and vegetation changes [1]. One of the methods for obtaining information from different objects through instruments that are not in physical contact with those objects is remote sensing, broadly known as the science that studied the responses of ER interactions with terrestrial materials by developing ground surface imaging [2]. To increase Earth monitoring possibilities, space agencies have created initiatives such as the Copernicus Sentinel-2 (S2), and Landsat-8 satellite missions, to guarantee a permanent supply of satellite images of mid-spatial resolution (with 10 and 30 m, respectively) and a great potential for generating vegetation coverage information.

The European's Space Agency (ESA) Copernicus mission Sentinel-2 is a polar-orbiting, multi-spectral mid-resolution imaging (10 m pixel size and 10–5 days of temporal resolution) with twin polar-orbiting satellites, Sentinel-2A (launched 23 June 2015) and 2B (launched 7 March 2017) [3]. In addition, other of the satellite programs widely used for Earth observation applications is the joint NASA/U.S. Geological Survey (USGS) Landsat series; this program is the longest-operating Earth observation satellite enterprise providing imagery of the Earth from space. The USGS opened the access of the Landsat satellite data since 2008, with the last satellite launched in February 2013 (Landsat-8) [4].

Remote sensing technology applications on satellite platforms, aerial unmanned vehicles, and portable radiometers together with the use of Global Navigation Satellite System (GNSS), Geographic Information System (GIS), and farm equipment form an integrated system based on information of crop production and evolution known as precision agriculture. This system has as a principal goal the practice of sustainable agriculture and seeks to improve the management of agricultural inputs (fertilizers, herbicides, seeds, and fuel) by increasing crop productivity and reducing adverse impacts on the environment. Remote sensors capture the interaction response of ER with soil and vegetation as a measure of the ratio of reflected radiance flux to incident radiance flux at a specific wavelength (spectral reflectance of the surface) [5]. Analyzing the spectral signature response of different crop types and vegetation index values as the NDVI during the development of the crop can provide technical support in farming practices such as fertilizer application, water management, and a tool to estimates the crop health and growth status [3].

In this respect, we aim to obtain the spectral signatures (spectral reflectance values) for maize, soybean, rice and oat crops in a growing area of 320 ha, located in the city of Tremembé (São Paulo-Brazil) for summer sowing cycles (November to March) 2017/2018 and 2018/2019 (oat culture is studied from April to June 2018), with the purpose of analyzing the signature behavior in the different phases of the crops. In

addition, we seek to employ the NDVI index to determine the behavior of the crops in each cycle, showing the advantage, usefulness, and utility of Sentinel-2 images in precision agriculture.

## 2 Materials and Methods

### 2.1 Data

There are some differences in the image characteristics from satellite platforms, given in the spatial, spectral, radiometric, and temporal resolutions. The Multi-Spectral Imager (MSI) sensor of Sentinel-2 and the Operational Land Imager (OLI) sensor of Landsat-8 are similar but have a different spectral and spatial resolution, and their data have different levels of radiometric and atmospheric correction.

Landsat 8 bands have wavelengths analogous to Sentinel-2 bands [6], as Table 1 shows.

The MSI Sentinel-2 sensor covers 13 spectral bands (443–2190 nm), but only 10 are useful for agricultural monitoring, involving the regions of visible (B2–B4), vegetation redEdge (B5–B7 and B8A), NIR (Near infra-red B8) and the SWIR (Short wave infra-red B11 and B12). About the OLI sensor of Landsat-8, it covers 8 spectral bands (443–2200 nm), capturing also image data in the regions of visible (B2–B4), NIR (B5), SWIR 1 (B6) and SWIR 2 (B7), adding the panchromatic region band (B8), being only 6 of this bands useful in vegetation studies.

**Table 1** The Landsat-8 OLI and Sentinel-2 MSI equivalent spectral bands considered in this study

Landsat-8 OLI	Sentinel-2 MSI
<sup>a</sup> B2 (Blue)-30-(452–512)	B2-10-(458–523)
B3 (Green)-30-(533–590)	B3-10-(543–578)
B4 (Red)-30-(636–673)	B4-10-(650–680)
	B5 (RedEdge 1)-20-(689.1–719.1)
	B6 (RedEdge 2)-20-(725.5–755.5)
	B7 (RedEdge 3)-20-(762.8–802.8)
B5 (NIR)-30-(851–879)	B8-10-(785–900)
	B8A (RedEdge 4)-20-(843.7–885.7)
	B9 (WaterVapor)-60-(843.7–885.7)
B6 (SWIR1)-30-(1566–1651)	B11-20-(1565–1655)
B7 (SWIR2)-30-(2107–2294)	B12-20-(2100–2280)
B8 (PAN)-15-(500–680)	
B9 (CIRRUS)-30-(1360–1390)	B10-60-(1342,5–1404,5)

<sup>a</sup>Band number (name)-spatial resolution (m)-spectral band range (nm)

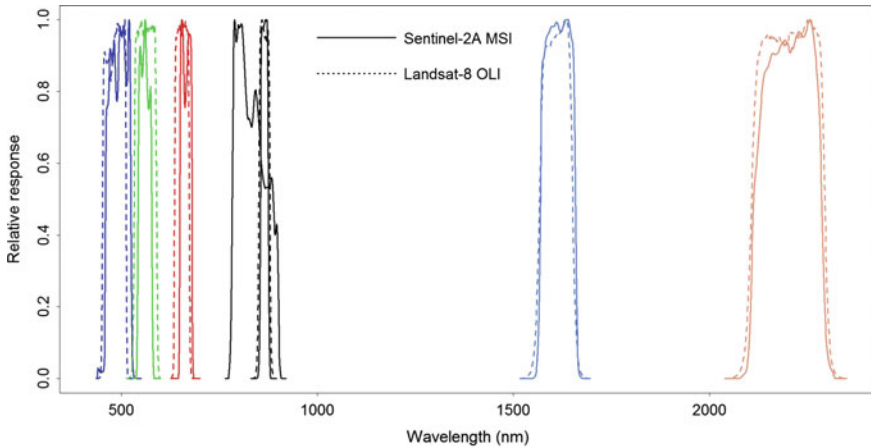


**Fig. 1** Spectral response for the approximately equivalent Sentinel-2 MSI (solid lines) and Landsat-8 OLI (dashed lines) [6]

The revisit time of Landsat-8 satellite and Sentinel-2 platforms are 16 and 5 days, respectively, availing observations spread over time; different Sentinel-2 image data were used to this study, involving one image per month to the summer sowing period (November to March) for the crop cycles of 2017/2018 and 2018/2019, which allowed to include five images for each of the cycles under study, except for the Sentinel-2 image of December 2017 that showed dense cloud cover over the area of interest, and was replaced for a Landsat-8 image for this research, given the equivalent spectral band characteristics (see Fig. 1) and the available tools for their corrections.

## 2.2 Study Area

The study area is a plantation (maize, rice, soybean and oat crops) of approximately 320 ha located in the city of Tremembé (São Paulo-Brazil) (see Fig. 2) at the Universal Transversal Mercator (UTM) coordinates of 438,814.90 m E, 7,461,118.52 m N for the reference system SIRGAS 2000 zone 23 S. Local measures in the nearest weather station identify as the driest month to July, with precipitation about 21 mm, in contrast to the highest precipitation in January with an average precipitation of 238 mm [7].

## 2.3 Image Processing

Sentinel-2 (Level-1C) products were downloaded from OpenHub, an ESA's web platform for the publicly available download of Copernicus mission products (available at <https://scihub.copernicus.eu/>), those are delivered directly at top of atmosphere

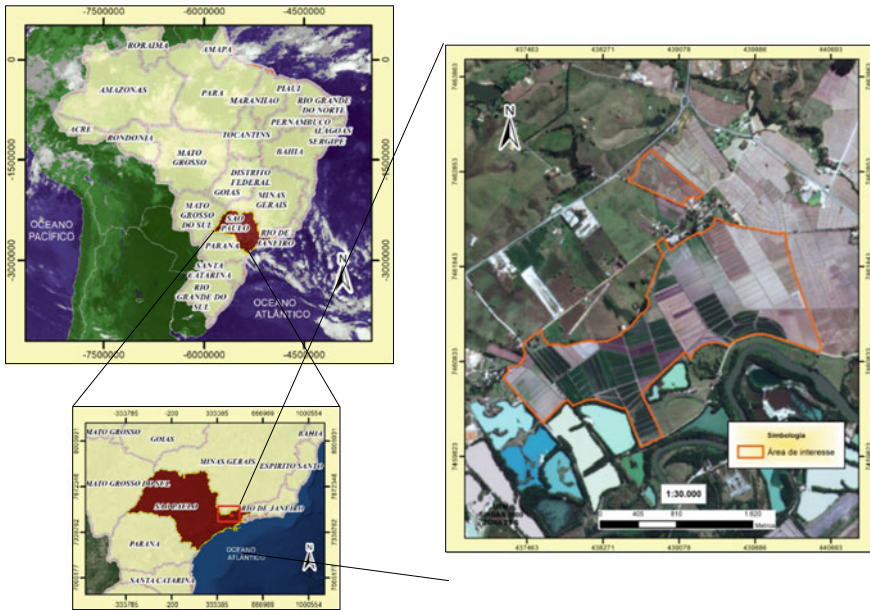


**Fig. 2** The study area (delimiting boundary in the orange right region) in the city of Tremembé (São Paulo)

reflectance values (feature a TOA—top of atmosphere geometric and radiometric correction), and using Qgis 3.2 version software semiautomatic classification (SCP) plugin for atmospheric correction to obtain the reflectance values at the base of atmosphere (BOA) applying the dark object subtraction (DOS1) correction method. One of the sources of error that can completely alter the image radiometrically is the atmosphere, it affects the radiance measured in the image in two ways: as a reflector, by adding extra radiance to the signal and as an absorber, attenuating the intensity of energy illuminating the target on the surface. DOS1 atmospheric correction method uses (1), (2) and (3) for an image-based technique which uses a metadata file that contains the information required to transfer the digital counts (DC) of the image into physical reflectance values [8].

$$LDO1\% = \frac{0.01 ESUN\lambda * COS\theta_s * T_z + E_{down} * T_v}{\pi * d^2} \tag{1}$$

$$L_p = L_{min} - LDO1\% \tag{2}$$

$$\rho = [\pi * (L\lambda - L_p) * d^2] / ESUN\lambda * cos\theta_s \tag{3}$$

where:  $L\lambda$  = Spectral radiation in the sensor (Radiance in the satellite),  $L_p$  = Path radiance,  $L_{min}$  = Radiance obtained with the digital count value ( $DN_{min}$ ),  $LDO1\%$

= radiance of Dark Object, assumed to have a reflectance value of 0.01,  $d$  = Earth-Sun Distance in Astronomical Units (AU),  $T_v$  = Transmittance of the atmosphere in the direction of vision,  $T_z$  = Atmospheric transmittance in the lighting direction,  $ESUN_\lambda$  = Mean solar exo-atmospheric irradiances ( $W/(m^2 \mu m)$ ),  $\theta_s$  = Solar zenithal angle in degrees,  $E_{down}$  = Diffuse irradiance descending,  $\rho$  = surface reflectance.

Several DOS techniques consider different values about  $T_v$ ,  $T_z$ , and  $E_{down}$ . The DOS1 technique gives for  $T_v$  and  $T_z$  the value of 1, and for  $E_{down}$  the value of 0 [9]. After applying the atmospheric correction, the digital counts of Sentinel-2 images resulting are measures of land surface reflectance.

In the case of the Landsat-8 image, the Earth Explorer website provides free access to level L2A processed products, which have geometric, radiometric, and atmospheric correction by applying the Landsat Surface Reflectance Code (LaSRC) physical correction method. This method uses OLI sensor information for capture values and optical properties of the atmosphere to correct the images and present digital image counts in reflectance values of the surface (BOA) [10].

The physical reflectance values for each of the cultures were obtained after the atmospheric correction of the images, and the graphics of the spectral signatures were made using python 3. Considering the date of every image and the records of field books obtained from the farmers (separate zoning areas were considered to identify crop differences), different spectral firms were obtained, corresponding to the development of the crops.

## 2.4 Normalized Difference Vegetation Index (NDVI)

NDVI is the most commonly used vegetation index when analyzing vegetation vigor, it is one of the oldest, best known and most frequently used vegetation index [11]. The NDVI approach is based on the fact that healthy vegetation has low reflectance in the visible portion of the spectrum due to chlorophyll and absorption of other pigments, and has high reflectance in NIR due to internal reflectance by the green leaf tissue, the values of NDVI calculations for a given pixel always result in a number ranging from  $-1$  to  $+1$ , where, only positive values correspond to vegetation areas, values close to zero do not mean vegetation, and negative values belong to clouds, snow, water, uncovered soil areas and rocks. In the formula for NDVI (4), NIR is the near-infrared range band and R is the red range band [11].

$$NDVI = \frac{NIR - R}{NIR + R} \quad (4)$$



### 3 Results and Discussion

#### 3.1 Spectral Signatures Analysis

Comparative experimental analysis of the spectral behavior graphs (spectral signatures) of the corn, rice, and soybean crops for the 2017/2018 and 2018/2019 sowing cycles present the following observation results:

- In general, there is a similarity to the specific assumptions of all the cultures studied (oat, rice, soybeans, maize), with marked differences in the spectral response by presenting inflection points of values at bands 3 (0.560  $\mu\text{m}$ ), 4 (0.665  $\mu\text{m}$ ), 5 (0.705  $\mu\text{m}$ ), 7 (0.783  $\mu\text{m}$ ), 8 (0.842  $\mu\text{m}$ ) and 8A (0.865  $\mu\text{m}$ ) of Sentinel-2.
- In crop zone, 10b (rice), Fig. 3a, b, showed a higher reflectance response for the spectral signatures in the 2017/2018 cycle, with a peak value (circled in red) around of 48% (0.865  $\mu\text{m}$ ) for 60 days of sowing in equivalent to the 32% peak value (circled in red) for the 2018/2019 cycle for 85 days of sowing.
- Similarly, in crop zone 10d (rice) (Fig. 3c, d), the maximum peak of reflectance value is 57% (pointed out in red), given in band 8A (0.865  $\mu\text{m}$ ) at 50 days of sowing, for crop cycle 2018/2019, different from the spectral response in the 2017/2018 of 47% at 45 days of sowing (circled in red), which gives the idea that there is a better development of this culture in the second cycle, being that the common behavior in all cultivation areas.

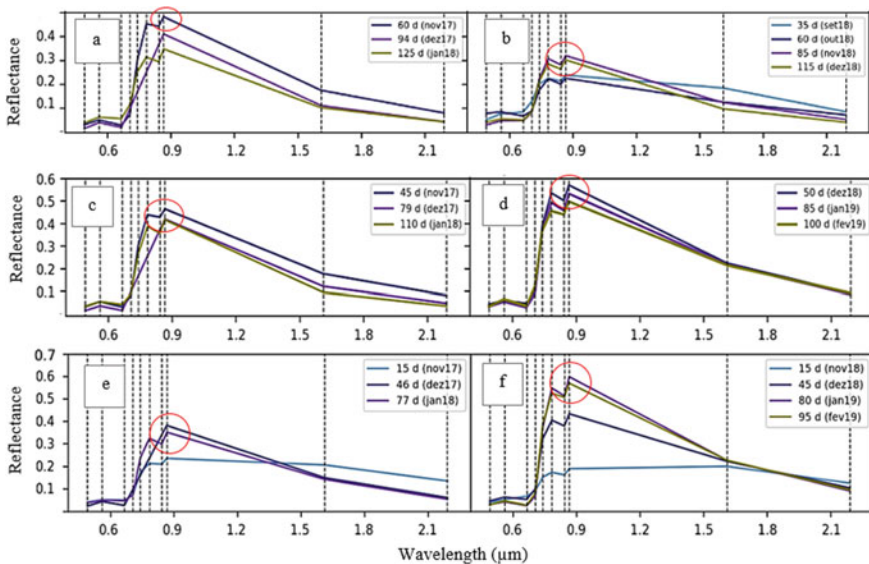


**Fig. 3** Spectral behavior results of cycles 2017/2018 (left) and 2018/2019 (right) for growing zones 10b-rice (a and b), 10d-rice (c and d), 6-maize (e and f)

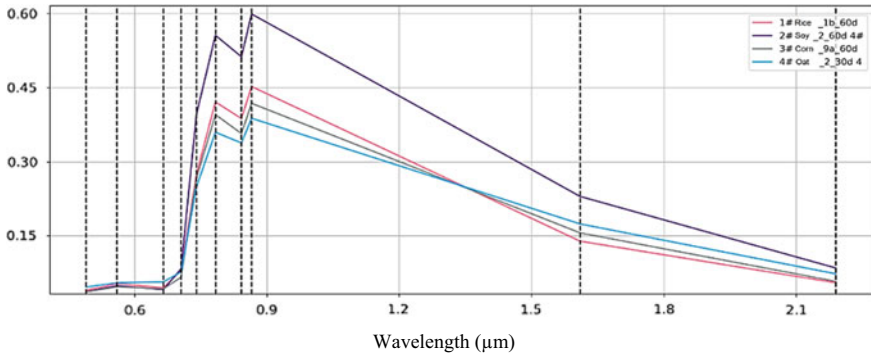


**Fig. 4** Spectral behavior of corn, rice, soybean and oat crops for around 60 days of sowing

- For the sowing area, 10a (maize), Fig. 3e, f shows a spectral response peak in the band 8A in the 2017/2018 cycle at 40% with 46 days of sowing and a spectral peak in the same band of 60% for 80 days of sowing in the 2018/2019 cycle. It is also noted that the duration of the first cycle was shorter (77 days) than the 95 days of the second cycle, assuming a problem (a nutrient deficiency, for example) in this parcel for the 2017/2018 cycle.
- The soybean crop has higher reflectance values compared to other crops (rice, corn, oats) (Fig. 4), with the highest response values in the NIR region and the lowest in the green region, which would be related to the good percentage absorption for the soybean of nitrogen in the visible range (focused on green 0.560  $\mu\text{m}$ ).

According to [12] the values of reflectance in the visible range (0.490–0.665  $\mu\text{m}$ ) are related to the content of chlorophyll (carotenes and anthocyanins) and nitrogen in crops. Thus, it can be identified, as in [13], that nitrogen content (also associated with better crop yields) is related to lower visible reflectance and higher redEdge reflectance (0.705–0.783  $\mu\text{m}$ ). As is shown in [1], the spectrum intervals where peaks occur may have the potential to generate information related to some plant characteristics. In the case of nitrogen (*N*) content in leaves, it presents a highly significant coefficient with reflectance values in the wavelength range of 450 and 780 nm. This may be related to the higher reflectance values found in soybean crops, given the increased consumption of nitrogen fertilizers over the period of the sowing.

### 3.2 NDVI Analysis

The calculation of the normalized vegetation index (NDVI) revealed the relationship of the spectral response of the crops with the NDVI values, that is an index that measures the vigor of the crops, begins to decrease with get close to the harvest season, given the variation of the pigment in the leaves that tend to yellow in the crops studied.

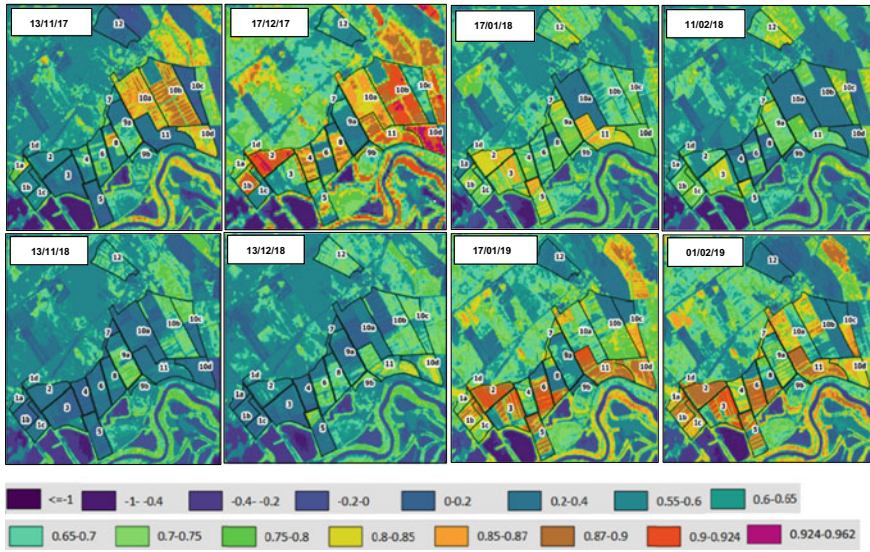


**Fig. 5** NDVI variations obtained for the 2017/2018 and 2018/2019 sowing cycles (November–March)

The maximum value obtained for NDVI as seen in Fig. 5 was in the 2017/2018 cycle (0.962) for the December 2017 image, with sowing zones 10d (rice 79 days) and 2 (soybeans 54 days) showing the largest area with the maximum value.

In the 2018/2019 cycle, the maximum value obtained for NDVI was 0.924 for the January 2019 image, with the sowing zones 2 (soybeans 55 days), 3 (soybeans 65 days), and 11 (Soybeans 80 days) showing the largest area with the maximum value. For the growing zones 6, 8, and 10 a (sown with maize) also showed a better response in the 2018/2019 cycle with larger areas of 0.86 NDVI values.

### 4 Conclusion

There is a marked tendency in the curvature of a signature; generally, the reflectance curves showed their highest responses around 60–90 days of sowing. The spectral responses decrease with the approach to harvest, which is given by nutrient loss and leaf chlorosis.

Thus it was also found that according to what was manifested in [12] the spectral responses decrease with the approach to harvest, which is given by the senescent dry vegetation, nutrient loss, and leaf chlorosis (yellowing).

In addition, it was observed in most cases that the soybean crop has higher reflectance values compared to other crops (corn, rice, oats), this can be related to the nitrogen content in the sowing and during the development of the crop. It

can be seen that apparently there is better crop development in the second cycle (2018/2019).

In general, spectral signatures can be influenced by various external factors, such as sowing time, nutrient content, soil moisture, leaf density, and others. Therefore, spectral response analysis is considered as a baseline for area discrimination of interest in field campaigns. It is also evidenced that vegetation indices can be used as a tool in the detection of possible affected areas.

Results can only be verified by joining field analyzes of crop nutrient content (nitrogen, potassium, phosphorus, and others), which are usually obtained using spectroradiometers or chemical methods by taking soil and leaf samples.

## References

1. Martinez, L.J.: Relationship between crop nutritional status, spectral measurements and Sentinel 2 images. *Agron. C.* **35**(2), 205–215 (2017). <https://doi.org/10.15446/gron.colomb.v35n2.62875>
2. Tanriverdi, C.: A Review of remote sensing and vegetation indices in precision farming. *KSU, J. Sci. Eng.* **9**(1), 69–76 (2006)
3. Pasqualotto, N., Delegido, J., Van Wittenberghe, S., Rinaldi, M., Moreno, J: Multi-crop green LAI estimation with a new simple sentinel-2 LAI index (SeLI). *Sensors (Basel, Switzerland)* **19**(4), 904 (2019). <https://doi.org/10.3390/s19040904>
4. Costa, S., Santos, V., Melo, D., Santos, P.: Evaluation of Landsat 8 and Sentinel-2A data on the correlation between geological mapping and NDVI, pp. 1–4 (2017). <https://doi.org/10.1109/grss-chile.2017.7996006>
5. Nicodemus, F., Richmond, J., Hsia, J.: Geometrical Considerations and Nomenclature for Reflectance. National Bureau of Standards, US Department of Commerce: Washington, DC, USA, (1977). URL: <http://physics.nist.gov/Divisions/Div844/facilities/specphoto/pdf/geoCon sid.pdf>
6. Hankui, K., David, P., Lin Yan, P., Zhongbin Li, Haiyan Huang, Vermote, E., Skakun, S., Roger, J.: Characterization of Sentinel-2A and Landsat-8 top of atmosphere, surface, and nadir BRDF adjusted reflectance and NDVI differences. *Remote Sensing Environ.* **215**, 482–494 (2018). <https://doi.org/10.1016/j.rse.2018.04.031>
7. Matarazzo, A.: The Tremembé Green Areas, p. 3. São Paulo, Economic Brazil (2012)
8. Moran, M., Jackson, R., Slater, P., Teillet, P.: Evaluation of simplified procedures for retrieval of land surface reflectance factors from satellite sensor output. *Remote Sensing Environ.* **41**, 169–184 (1992)
9. Sobrino, J., Jiménez-Muñoz, J., Paolini, L.: Land surface temperature retrieval from LANDSAT TM 5. *Remote Sensing Environ.* (Elsevier) **90**, 434–440 (2004)
10. U. S. Geological Survey: Landsat 8 Surface Reflectance Code (LaSRC) Product Guide (2009). URL: [https://prd-wret.s3-us-west-2.amazonaws.com/assets/palladium/production/atoms/files/LSDS-1368\\_L8\\_Surface\\_Reflectance\\_Code\\_LASRC\\_Product\\_Guide-v2.0.pdf](https://prd-wret.s3-us-west-2.amazonaws.com/assets/palladium/production/atoms/files/LSDS-1368_L8_Surface_Reflectance_Code_LASRC_Product_Guide-v2.0.pdf)
11. Pinter, P., Hatfield, J., Schepers, J., Barnes, M., Moran, C., Daughtry, et al.: Remote sensing for crop management. *Photogramm. Eng. Remote Sensing* **69**, 647e–664 (2003)
12. Blackburn, G.: Hyperspectral remote sensing of plant pigments. *J. Exp. Bot.* **58**, 855e–867 (2007). URL: [http://www.scielo.br/scielo.php?script=sci\\_arttext&pid=S1516-35982009000900001](http://www.scielo.br/scielo.php?script=sci_arttext&pid=S1516-35982009000900001)
13. Schlemmer, M., Francis, D., Shanahan, J., Schepers, J.: Remotely measuring chlorophyll content in corn leaves with differing nitrogen levels and relative water content. *Agron. J.* **97**(1), 106–112 (2005)

# **Emerging Trends in Humans and Urban Sciences**

# Production Process of Bioethanol Fuel Using Supported *Saccharomyces Cerevisiae* Cells



L. C. Fardelone , T. S. Bella de Jesus , G. P. Valença , J. R. Nunhez , J. A. R. Rodrigues , and P. J. S. Moran 

**Abstract** A new immobilization process of *Saccharomyces cerevisiae* cells with calcium alginate and coating with solubilized chitosan in citric acid solution was developed. The biocatalyst is used in fermentation processes to produce bioethanol fuel through the use of carbon sources such as glucose, sugarcane juice, and corn hydrolysate, which provided very good yields of productivity (71.3–88.7%) and shows excellent biocatalyst stability during all production processes.

**Keywords** Bioethanol fuel · Calcium alginate beads · Fermentation process

---

Author Contributions: Fardelone, L. C. and Bella de Jesus, T. S. contributed equally

---

L. C. Fardelone (✉) · T. S. B. de Jesus · G. P. Valença · J. R. Nunhez  
School of Chemical Engineering, University of Campinas - Unicamp, Campinas, Brazil  
e-mail: [lucfardelone@gmail.com](mailto:lucfardelone@gmail.com)

T. S. B. de Jesus  
e-mail: [taciani\\_bella@hotmail.com](mailto:taciani_bella@hotmail.com)

G. P. Valença  
e-mail: [gustavo@feq.unicamp.br](mailto:gustavo@feq.unicamp.br)

J. R. Nunhez  
e-mail: [nunhez@feq.unicamp.br](mailto:nunhez@feq.unicamp.br)

J. A. R. Rodrigues · P. J. S. Moran  
Chemistry Institute, University of Campinas - Unicamp, Campinas, Brazil  
e-mail: [jagusto@iqm.unicamp.br](mailto:jagusto@iqm.unicamp.br)

P. J. S. Moran  
e-mail: [moran@iqm.unicamp.br](mailto:moran@iqm.unicamp.br)

## 1 Introduction

The research for more efficient biofuel processes is strategic for Brazil, due to climate change, world economic policies and the growing demand for sustainability regarding the issue of energy generation [1–6]. Thus, bioethanol fuel has gained worldwide prominence because it is biodegradable, has clean combustion due to the presence of oxygen in its composition, and reduces the emission of nitrogen oxides and particulate matter, as well as reducing CO<sub>2</sub> and SO<sub>2</sub> emissions into the atmosphere [5].

The process of alcoholic fermentation using sugarcane juice *S. cerevisiae* cells is a process well established in the Brazilian mills [1, 4], however, the search for cost reduction, unit operations and process time, as well as productivity increase is a big challenge, which motivates us in this development of bioethanol fuel production. Also, the production of bioethanol fuel from corn has numerous advantages, such as logistics and storage, shorter plant cultivation cycle time and depending on the variety 3–4 annual harvests, can also be obtained during the sugar cane off-season, and if planted in the same area can bring improvements to the soil, decreased fertilization and correction of it [7, 8]. Corn also has lower production costs and its planting is established in different regions of the country [8].

Our research group has been working on fermentative processes for bioethanol fuel production using cellular supports such as calcium alginate [9], Montmorillonite K-10 [10], and other clays. The literature also describes supported processes that can promote longer process time and consequently higher productivity, as they simplify product separation and purification, and biocatalysts are reused in consecutive production recycles [9–16].

However, the biggest problem is still the stabilization of the biocatalyst-support and its reuse, as well as the costs, which hinder its implementation in certain industrial processes [17, 18]. The use of sodium alginate is extremely important because of its compatibility and non-toxicity [13–21], but this type of matrix support is generally used in only one process cycle, as during this process the spheres rupture due to calcium leaching, agitation and the formation of gases that cause the deterioration of the support, thus requiring further technical development.

We are developing a new cell support processes, to overcome the alginate bead disruption problem, that provided greater mechanical resistance strength and non-leaching of calcium when used citric acid instead of acetic acid to recover the spheres of alginates. The bioethanol fuel production process used glucose in a batch reactor for 24 h with yields of 89–95% [18].

In this work, we report the bioethanol fuel production using this cell support in a more complex media as sugarcane juice and corn hydrolysate as carbon sources, which provide us with greater robustness to the process enabling technology to be transferred to industry.

## 2 Methodology

### 2.1 General Process

Fermentations were conducted in the fed-batch regime, replacing the regular time intervals of two-thirds of the reactor volume. This avoids product inhibition and allows the beads to be kept in action for long periods of time. Regardless of the medium used, 3 g/L  $\text{CaCl}_2$  was added, as it is used for avoiding the leaching  $\text{Ca}^{2+}$  ions, responsible for the rigidity of the alginate matrix. The fermentations were conducted using 75 g of alginate beads and 0.150 L of media (which was replaced in periods of 24 h) in 0.5 L lightly stirred bioreactor for 168 h.

Ethanol and glucose concentrations were determined by HPLC with refractive index detector, coupled to an Aminex HPX-87H column (300 mm  $\times$  7.8 mm, Bio-Rad) and using 5 mmol/l mobile phase  $\text{H}_2\text{SO}_4$ , with flow 0.6 mL/min at 50 °C. Quantifications of products and sugars were performed from calibration curves using an external standard.

**Microorganism** *S. cerevisiae* JAY270 is being used for this process, which has high-temperature resistance and high substrate concentration, pH variation, oxidative stress, high cell mass production, and bioethanol fuel [22]. This strain of *S. cerevisiae* JAY270 is found in our laboratory and is stored in the form of BCM (Master Cell Bank) and BCT (Master Cell Bank) and WCB (Working Cell Bank), respectively and were prepared in accordance with international precepts for good production and laboratory practices [23–25].

**Preparation of culture media** For cell expansion (inoculums and pre-inoculums) of *S. cerevisiae* yeast the culture medium with industrial components previously established with a composition of 3.0 g/L malt extract, 3.0 g/L of yeast extract, 5.0 g/L peptone and 10 g/L glucose at pH 6.0. To obtain a high cell density (OD) baffled flask is being used, which promotes a better shaker mix for 18 h at 120 rpm.

**Cell Immobilization** After cell mass growth, the cells are centrifuged at 1844 g for 20 min, and under aseptic conditions, the obtained cells undergo immobilization in calcium alginate, followed by chitosan coating [9, 18, 26].

The cell immobilization technique is porous matrix entrapment using a 3% sodium alginate suspension and *S. cerevisiae* cells. The mixture is then dripped and remains for one hour in 0.3 M calcium chloride solution to obtain spheres with a diameter of approximately 3–4 mm. To have a better calcium distribution in the cell support matrix gel, the beads are kept in 0.3 M  $\text{CaCl}_2$  solution for one hour, followed by coating with 0.25% chitosan solubilized in 5% citric acid for 30 min, with recalcification for another hour in 0.3 M  $\text{CaCl}_2$  solution.

The coating of spheres containing *S. cerevisiae* in calcium alginate is performed with the use of citric acid, an unprecedented technique developed in our laboratory, in such a way as to promote greater mechanical resistance against the fermentation



process time, as well as to maintain homogeneity the possibility of calcium leaching present in the polymeric network of the spheres. The use of citric acid used in the coating also decreases the lag phase from 24 to 8 h of bioethanol fuel production due to its toxicity to *S. cerevisiae* cells.

**Analytical Methodology** The final concentration of ethanol and residual glucose is determined by High-Performance Liquid Chromatography (HPLC) with refractive index detector coupled to an Aminex HPX-87H column (300 mm × 7.8 mm, Bio-Rad) and uses 5 mmol/L mobile phase H<sub>2</sub>SO<sub>4</sub>, with 0.6 mL/min flow at 50 °C. Product and residual carbohydrate quantifications are performed from calibration curves using external standards for ethanol and sucrose, glucose, fructose, and other carbohydrates.

### 3 Results and Discussion

Fermented batch processes were carried out for bioethanol fuel production using *S. cerevisiae* JAY270 cells immobilized in calcium alginate and coated with chitosan. This process requires the addition of a small amount of calcium in the medium (0.03 g/1.0 g of beads) to recalcify the beads, allowing for greater durability and efficiency of the bioethanol fuel production process as shown in Table 1. It is important to emphasize that the final yield was defined through the ethanol produced in relation to the maximum conversion of carbon source to ethanol.

Coating the spheres with chitosan using citric acid and adding calcium to the fermentation broth provided a highly stable process with a small lag (8 h) phase and high productivity, 81.0, 88.7, and 71.3% yield in bioethanol fuel for glucose, sugarcane, and corn hydrolysate, respectively. It also promoted greater mechanical resistance of the spheres, as no support rupture was observed, nor free *S. cerevisiae* cells were detected in the fermentation broth. Thus, the developed methodology is stable and robust for supported bioethanol fuel production processes and can be extended to other processes, when compared to other processes that provide low yields and beads disruptions [9, 27] (Fig. 1).

**Table 1** Bioethanol fuel production using *S. cerevisiae* JAY270 cells immobilized in calcium alginate and coated with chitosan and glucose, sugarcane and corn hydrolysate aqueous solutions

Process using	Consumption (g)				Bioethanol fuel (g)	Productivity (g/(Lh))	Yield (%)
	Glucose	Fructose	Sucrose	Maltose			
Glucose <sup>a</sup>	185.64	–	–	–	56.91	1.21	60.0
Glucose	256.26	–	–	–	106.10	4.21	81.0
Sugarcane	71.34	20.94	11.06	–	48.50	1.92	88.7
Corn hydrolysate	78.29	–	–	48.37	47.10	2.06	71.3

<sup>a</sup>Process using acetic acid in chitosan coating of cell support up to 94 h of bioethanol fuel production process, with 60% of broken spheres

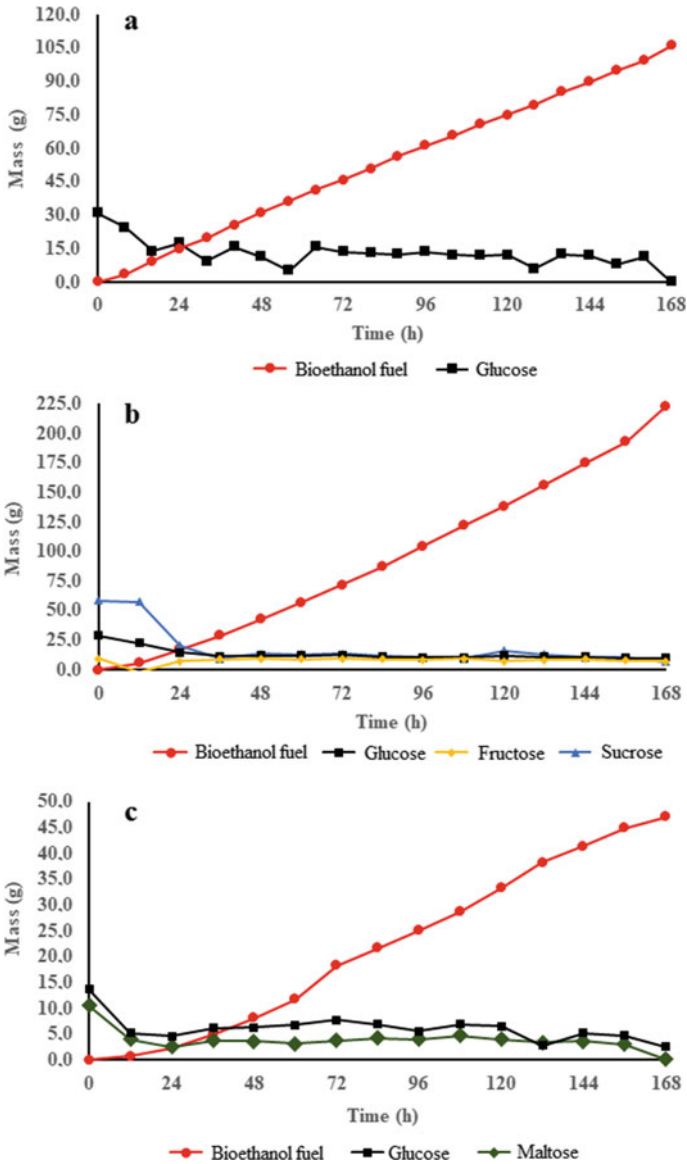


**Fig. 1** Carbohydrate mass profiles and bioethanol fuel production in batch fed reactors provided with immobilized cells of *S. cerevisiae* in calcium alginate spheres coated with solubilized chitosan in citric acid solution **a** glucose; **b** sugar cane juice; **c** corn hydrolysate

In these fermentation processes, 75 g of beads were used, 150 ml of medium containing ~200 g/L of carbon source (glucose, sugar cane or corn hydrolysate), 2 g/L of ammonium phosphate and 8 g of  $\text{CaCl}_2$ . During the fermentation process, 2/3 of the medium volume was exchanged by a new medium every 8 h to maintain bioethanol fuel production by a total period of 168 h. The medium exchange was made by simple suction of the fermented liquid and replaced by the same volume of new medium.

The biocatalyst supported on calcium alginate beads coated with citric acid-soluble chitosan after 21 cycles in a total period of 168 h of fermentation shows any disruption of the cell support spheres as shown in Fig. 2c in contrast to Fig. 2a, where the calcium alginate beads were coated with acetic acid solubilized chitosan.

During the production process, it is also possible to visually monitor the production of bioethanol fuel by observing the spheres of biocatalyst, in the process the spheres of biocatalyst are floating due to the presence of  $\text{CO}_2$  inside and when all carbon source is consumed the spheres decant for the absence of  $\text{CO}_2$  within the spheres, Fig. 3.

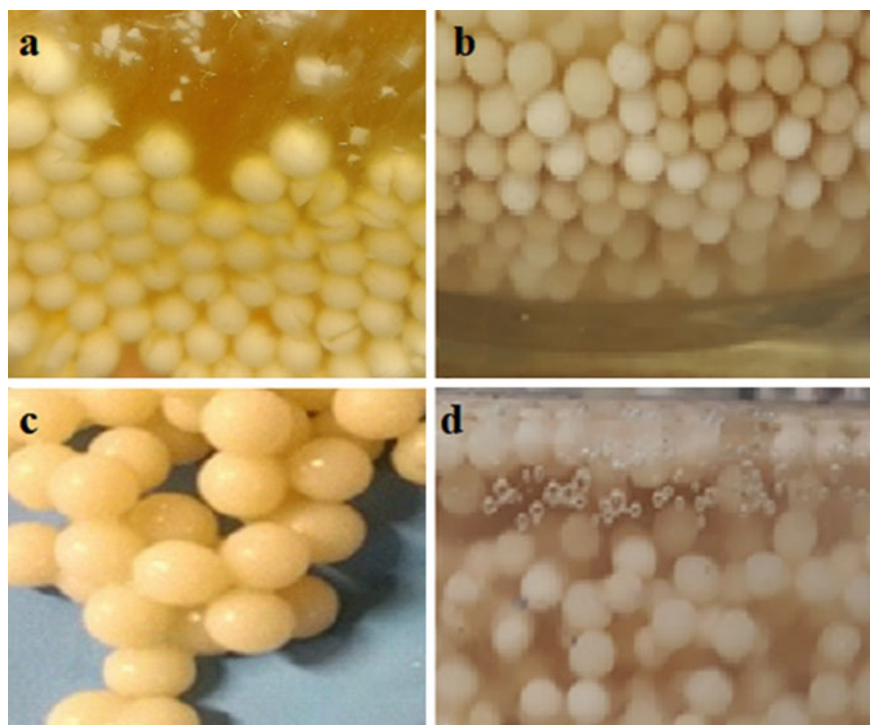


**Fig. 2** **a** Biocatalyst supported on calcium alginate beads coated with acetic acid solubilized chitosan after 94 h of fermentation process; **b** Biocatalyst supported on calcium alginate beads coated with citric acid-soluble chitosan before use in fermentation process; **c** Biocatalyst supported on calcium alginate beads coated with citric acid-soluble chitosan after 21 cycles in a total period of time of 168 h of fermentation; **d** typical process fermentation

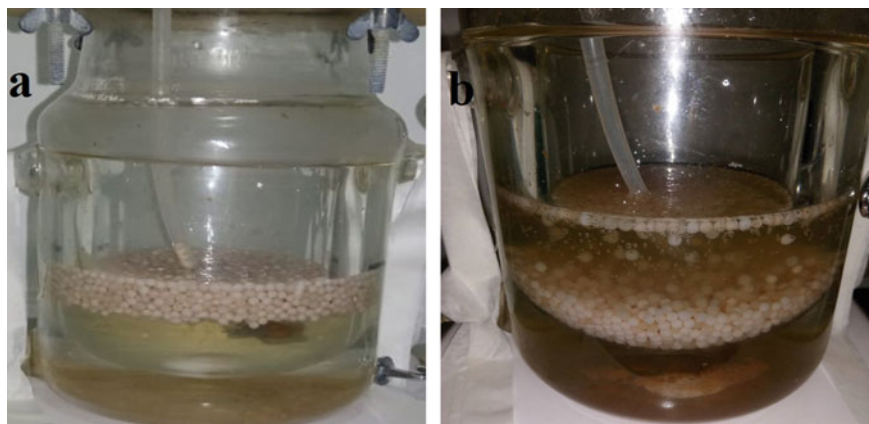


**Fig. 3** **a** Biocatalyst in bioethanol fuel production process, with carbon source present in a bioreactor; **b** Biocatalyst at the end of the presence of carbon source

The conversion of the used carbohydrates to combustible bioethanol was achieved excellently (>88%) after 21 cycles, demonstrating that the process developed using *S. cerevisiae* cells supported on solubilized chitosan-coated calcium alginate beads in citric acid is extremely efficient and robust, since the supports are intact and reusable, and fermentation processes can be used for extended periods.

Another extremely important fact is that we can use more complex substrates, such as sugarcane juice, corn hydrolysate, among others, with great possibilities for technology transfer for application of this process to an industrial scale. The production of bioethanol fuel with corn hydrolysate requires gelatinization and starch hydrolysis steps, followed by fermentation [28, 29]. Generally, industrial processes with corn hydrolysate take a very long time, over 48 h, and we intend to reduce this time and increase productivity. This same technology can be extended to support other microorganisms (engineered or not), enzymes, and various production processes.

## 4 Conclusions

The developed immobilization process gave excellent mechanical resistance of the cell support, is possibly more than 21 consecutive reuse cycles in longer processes, providing high productivity of bioethanol fuel using glucose, sugarcane juice, and corn hydrolysate as carbon sources. Also, the easy of the beads separation from the fermentative medium shows the possibility of process optimization to a larger scale. Scaling up study is being developed and the results will be reported in the future.

**Acknowledgements** The authors thank São Paulo State Research Support Foundation (FAPESP, 2016/12074-7), Higher Education Personnel Improvement Coordination (CAPES,

88,882.329694/2019-01), and National Council for Scientific and Technological Development (CNPq) for financial support.

## References

1. Amorim, H.V., Lopes, M.L., Oliveira, J.V.C., Buckeridge, M.S., Goldman, G.H.: Scientific challenges of bioethanol production in Brazil. *Appl. Microbiol. Biotechnol.* **92**, 1267–1275 (2011)
2. Kang, A., Lee, T.S.: Converting sugars to biofuels: ethanol and beyond. *Bioengineering* **2**, 184–203 (2015)
3. Breisha, G.Z.: Production of 16% ethanol from 35% of sucrose. *Biomass Bioenerg.* **34**, 1243–1249 (2010)
4. Miranda, M., Batistote, M., Cilli Jr., E.M., Ernandes, J.R.: Sucrose fermentation by Brazilian ethanol production yeasts in media containing structurally complex nitrogen sources. *J. Inst. Brewing* **115**(3), 191–197 (2009)
5. Gonçalves, F.A., Ruiz, H.A., dos Santos, E.S., Teixeira, J.A., de Macedo, G.R.: Bioethanol production by *Saccharomyces cerevisiae*, *Pichia stipitis* and *Zymomonas mobilis* from delignified coconut fiber mature and lignin extraction according to biorefinery concept. *Renew. Energy* **94**, 353–365 (2016)
6. Rosales-Calderon, R., Arantes, V.: A review on commercial-scale high-value products that can be produced alongside cellulosic ethanol. *Biotechnol. Biofuel* **12**, 240 (2019)
7. Mohanaty, S.K., Swain, M.R.: Bioethanol production from corn and wheat: food, fuel and future (Chapter 3). In: Ramesh, R.C., Ramachandran, S. (eds.) *Bioethanol Production from Food Crops*, pp. 45–59 (2019)
8. Marques, S.J.P., da Cunha, M.E.L.: Production of fuel alcohol using corn. *Unopar Científica Ciências Exatas e Tecnológicas* **7**, 45–51 (2008)
9. Duarte, J.C., Rodrigues, J.A.R., Moran, P.J.S., Valença, G.P., Nunhez, J.R.: Effect of immobilized cells in calcium alginate beads in alcoholic fermentation. *ABM Express* **31**, 1–8 (2013)
10. Wendhausen, R., Fregonesi, A., Moran, P.J.S., Joekes, I., Rodrigues, J.A.R., Tonella, E., Althoff, K.: Continuous fermentation of sugar cane syrup using immobilized yeast cells. *J. Biosci. Bioeng.* **91**, 48–52 (2000)
11. Karagoz, P., Ozkan, M.: Ethanol production from wheat straw by *Saccharomyces cerevisiae* and *Scheffersomyces stipitis* co-culture in batch and continuous system. *Biores. Technol.* **158**, 286–293 (2014)
12. Singh, A., Sharma, P., Saran, A.K., Singh, N., Bishnoi, N.R.: Comparative study on ethanol production from pretreated sugarcane bagasse using immobilized *Saccharomyces cerevisiae* on various matrices. *Renew. Energy* **50**, 488–493 (2013)
13. Lee, H., Kim, S., Yoon, J., Kim, K.H., Seo, J., Park, Y.: Evolutionary engineering of *Saccharomyces cerevisiae* for efficient conversion of red algal biosugars to bioethanol. *Biores. Technol.* **191**, 445–451 (2015)
14. Duarte, J., Lourenço, V., Ribeiro, B., Saagua, M.C., Pereira, J., Baeta-Hall, L.: Ethanol production from different substrates by a flocculent *Saccharomyces cerevisiae* strain. *Int. J. Chem. Reactor Eng.* **7**, Article A58 (2009)
15. Sebayang, F., Bulan, R., Hartanto, A., Huda, A.: Enhancing the efficiency of ethanol production from molasses using immobilized commercial *Saccharomyces cerevisiae* in two-layer alginate-chitosan beads. *IOP Conf. Ser. Earth Environ. Sci.* **305**, 012014 (2019)
16. Ivanova, V., Petrova, P., Hristov, J.: Application in the ethanol fermentation of immobilized yeast cells in matrix of alginate/magnetic nanoparticles, on chitosan-magnetite microparticles and cellulose-coated magnetic nanoparticles. *Int. Rev. Chem. Eng. (I.R.E.C.H.E.)*, **3**(2), 289–299 (2011)

17. Ghorbani, F., Younesi, H., Sari, A.E., Najafpour, G.: Cane molasses fermentation for continuous ethanol production in an immobilized cells reactor by *Saccharomyces cerevisiae*. *Renew. Energy* **36**, 503–509 (2011)
18. Fardelone, L.C., Bella de Jesus, T.S., Oura, L.A.K., Valença, G.P., Nunhez, J.R., Rodrigues, J.A.R., Moran, P.J.S.: Produção de bioetanol utilizando células de *Saccharomyces cerevisiae* imobilizadas em esferas de alginato de cálcio recobertas com quitosana. Editora Atena, Impactos das Tecnologias na Engenharia Química (2019)
19. Călinescu, I., Chipurici, P., Trifan, A., Bădoiu, C.: Immobilization of *Saccharomyces cerevisiae* for the production of bioethanol. *U.P.B. Scientific Bulletin, Series B* **74**, 33–40 (2012)
20. Najafpour, G., Younesi, H., Ismail, K.S.K.: Ethanol fermentation in an immobilized cell reactor using *Saccharomyces cerevisiae*. *Biores. Technol.* **92**, 251–260 (2004)
21. Kubota, N., Tatsumoto, N., Sano, T., Toya, K.A.: Simple preparation of half N-acetylated chitosan highly soluble in water and aqueous organic solvent. *Carbohydr. Res.* **324**(4), 268–274 (2000)
22. Argueso, J.L., Carazzolle, M.F., Mieczkowski, P.A., Duarte, F.M., Netto, O.V.C., Missawa, S.K., Galzerani, F., Costa, G.G.L., Vidal, R.O., Noronha, M.F., Dominska, M., Andrietta, M.G.S., Andrietta, S.R., Cunha, A.F., Gomes, L.H., Tavares, F.C.A., Alcarde, A.R., Dietrich, F.S., McCusker, J.H., Pereira, G.A.G.: Genome structure of a *Saccharomyces cerevisiae* strain widely used in bioethanol production. *Genome Res.* **19**, 2258–2270 (2009)
23. Stacey, G.: Fundamental issues for cell-line banks in biotechnology and regulatory affairs. In: Fuller, B.J., Lane, N., Benson, E.E. (eds.) *Life in the Frozen State*, pp. 437–452. CRC Press LLC, Boca Raton, Florida (2004)
24. Health products and food branch inspectorate—Annex 2 to the current edition of the good manufacturing practices guidelines schedule drugs (biological drugs)—GUI-0027 (2002)
25. Coecke, S., Balls, M., Bowe, G., Davis, J., Gstraunthaler, G., Hartung, T., Hay, R., Merten, O.-W., Price, A., Schechtman, L., Stacey, G., Stokes, W.: Guidance on good cell culture practice. *ATLA* **33**, 261–287 (2005)
26. Nagashima, M., Azuma, M., Nogucid, S., Inuzuka, K., Samejima, H.: Continuous fermentation using immobilized yeast cells. *Biotechnol. Bioeng.* **26**, 992–997 (1984)
27. Bellido, J.D., Lemos, F.R., de Oliveira, M.C.A., Prota, M., Magalhães, J.S.F.: Immobilization study of *saccharomyces cerevisiae* on polyurethane foam for ethanol production. *Int. J. Sci. Eng. Invest.* **7**, 83 (2018)
28. Thiruvengadathan, T.N.: Bioethanol Production Using *Saccharomyces cerevisiae* Cultivated in Sugarcorne Juice. Master of Engineering Science. Western University Ontario, Canada (2017)
29. Bharti, B., Chauhan, M.: Bioethanol production using *Saccharomyces cerevisiae* with different perspectives: substrates, growth variables, inhibitor reduction and immobilization. *Ferment. Technol.* **5**(2), 1000131 (2016)

# An Automatic Biodiesel Decanting System for the Optimization of Glycerin Separation Time by Applying Electric Field and Temperature



Kevin Bulnes , Diego Paredes , and Leonardo Vincés 

**Abstract** During biodiesel production, crude biodiesel and glycerin are separated in resting tanks due to gravity and differences in density, glycerin accumulates at the base of the contender; such operation is called decantation. The decantation stage, within the production of biodiesel based on recycled oil, takes from 8 to 24 h to complete. Therefore, the development of an automatic biodiesel decanting system is presented in order to optimize the production time in the line of this bio-fuel. The process consists of applying an electric field through two electrodes at 9 kV and simultaneously applying temperature. The results of the implementation showed that the production time was reduced by up to 99% without affecting the quality of biodiesel, according to the parameters of the American Society for Testing and Materials (ASTM).

**Keywords** Biodiesel · Purification · Electrocoagulation · Electric field · Decantation stage

## 1 Introduction

Currently, there are several types of processes for obtaining biodiesel from recycled cooking oils. However, the transesterification process is the most researched and used in recent years [1]. This process consists of the chemical reaction of vegetable or animal oils and alcohol (methanol or ethanol), through a homogeneous or heterogeneous catalyst. This reaction generates fatty acid methyl esters (Biodiesel) and

---

K. Bulnes · D. Paredes · L. Vincés (✉)

Universidad Peruana de Ciencias Aplicadas, Av. Prolongación Primavera 2390, Santiago de Surco, Lima, Peru

e-mail: [nikolai.vinces@upc.edu.pe](mailto:nikolai.vinces@upc.edu.pe)

K. Bulnes

e-mail: [u201312745@upc.edu.pe](mailto:u201312745@upc.edu.pe)

D. Paredes

e-mail: [u201410146@upc.edu.pe](mailto:u201410146@upc.edu.pe)

© The Editor(s) (if applicable) and The Author(s), under exclusive license to Springer Nature Switzerland AG 2021

Y. Iano et al. (eds.), *Proceedings of the 5th Brazilian Technology Symposium*, Smart Innovation, Systems and Technologies 202, [https://doi.org/10.1007/978-3-030-57566-3\\_34](https://doi.org/10.1007/978-3-030-57566-3_34)

glycerin, as the main product and by-product, respectively [2, 3]. Once said the process is finished, due to the difference in densities between biodiesel and glycerin ( $880 \text{ kg/m}^3$  and  $1050 \text{ kg/m}^3$ , respectively), the latter sits at the bottom of the transesterification reactor in a time of 8 to 24 h [4, 5]. The subsequent stage of transesterification, within the production process, is refining. Biodiesel refining is a process that is responsible for purifying biodiesel to bring it to the quality necessary for its consumption, impurities such as loose glycerin particles, soaps, and water [2, 6]. Among the most common refining strategies are water washing and spinning [7, 8]. As can be evidenced, the process for the production of biodiesel has a demand for resources and time. This could have a negative impact on production at all biodiesel scales.

The application of the electric field has been proposed by the scientific literature with the aim of overcoming these limitations. Z. E. Ismail et al. [4] and Ratanabuntha et al. [9] have proposed the immersion of an electric field in the biphasic mixture of biodiesel and glycerin to accelerate the decantation. This theory has served as the initial framework for the present investigation due to the scientific explanation and laboratory experimentation that was carried out in both studies.

However, in the research of Ratanabuntha et al., the type of electrode they applied has a very complex geometry, which complicates the acquisition or manufacture, while Z. E. Ismail et al. did not carry out a study of optimal materials for the tank and electrodes during the decanting stage.

On the other hand, Ahmad et al. [10] studied the extent to which the shape and distance of electrode separation are involved. This proposal finds another way to reduce the time it takes to decant the mixture of biodiesel and glycerin. However, this study specifies that it was expected 24 h for the mixture to decant.

Noureddin et al. [11] studied the effect of temperature at the stage of decanting where it was found that increasing this parameter above  $30^\circ\text{C}$  accelerates the decantation. Despite the aforementioned, this study only focused on varying said parameters and not the effect that it could have on the application of the electric field. On the other hand, Moncada et al. [12] make an analysis of time, economy, and technologies when the entire process for the production of biodiesel is automated. However, the biodiesel obtained is based on seaweed and marine microalgae, not with recycled cooking oil.

The present study proposes to accelerate the process in the decanting stage and thus optimize the production of biodiesel. At the same time, it is sought that such a proposal does not affect the quality of the product. The final results showed that the production time was reduced by up to 99% and the quality of biodiesel meets the parameters according to the ASTM [13].

## 2 Development of the Proposed System

Figure 1 shows a block diagram of the proposed system. The details are shown in the following sections according to the order specified in this diagram.



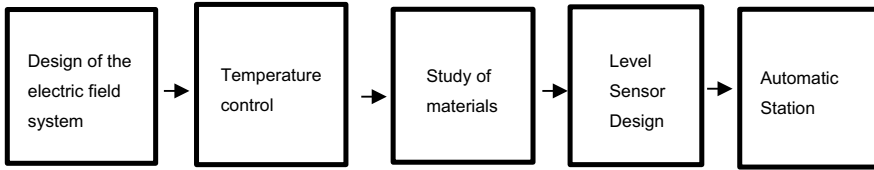


**Fig. 1** Block diagram of the proposed system

## 2.1 Design of the Electric Field System

The objective of this stage is to accelerate the decantation of glycerin. For this, an electric field is applied through two electrodes charged with 9 kV in the biodiesel-glycerin mixture. The magnitude of the said electric field is directly proportional to the speed of separation of the mixture [9]. Therefore, according to

$$E = \frac{V}{d} \quad (1)$$

where  $V$  is the voltage in volts;  $d$  is the distance between electrodes in meters and  $E$  is the magnitude of the electric field in volts per meter. It is convenient to place the electrodes as close as possible.

The shape of the electrodes also influences the speed of separation of the glycine from biodiesel. According to [10], the second most effective type of electrode is flat geometry.

The electric field lines, following the path of an elliptical cylinder, which perform the coagulation effect of glycerin [4], must be distributed vertically to achieve maximum contact volume with the mixture. For the present design, the distance between the electrodes is 6 cm, whereby a magnitude of 150 k V/m of the electric field is obtained. The average field application time is 1.50 min.

## 2.2 Temperature Control

For temperatures above 55°C, glycerin keeps its viscosity low, and therefore it is easier to decant [11]. With a resistance of 1.5 kW and PID control, it is controlled that the temperature does not fall below the optimum. In control, the temperature is carried out according to

$$Q = m \times cp \times \Delta T \quad (2)$$

where  $Q$  is the heat delivered to the mixture in Joules,  $m$  is the mass of the mixture in kilos,  $cp$  in Joules over kilos by degrees Celsius and  $\Delta T$  the variation of the temperature of the mixture in degrees Celsius. The power delivered by the electric resistor is recalculated in real-time according to the variation of the temperature within the mixture.



**Fig. 2** Two stainless steel electrodes 51 cm long and 1-inch width each with thickness 3 mm

The temperature control prevents the temperature from exceeding 70 degrees, thus preventing the biodiesel from degrading to modify the acids by less than 0.5 mg KOH/g, also preventing the temperature from falling below 50 for the displacement of glycerin in the mixture.

### **2.3 Study of Materials**

This stage served to select the appropriate materials to be used for the decanting station. Due to its high corrosivity, biodiesel tends to be corrosive to some materials. The material used for the tank designed at the station was fiberglass. This material, in addition to supporting liquids with high corrosion rates, functions as an insulator against the high electrical voltage used in the station.

On the other hand, stainless steel was used for the electrodes (Fig. 2). Stainless steel has the property of supporting liquids with high corrosivity but also being a good current conductor. This property is important to reduce energy losses and the magnitude of the electric field.

Devices in contact with the mixture must be kept isolated from the electric field. The Pt100 [14], the temperature sensor used in this project, has a ceramic sleeve in the thermowell. The calorifier is made of stainless steel but is connected at the ends to the pump and water storage with polymer hoses.

### **2.4 Level Census Design**

Figure 3 shows the interface that forms between glycerin and biodiesel when the decanting stage, with the proposed methodology, has ended. Through the control of the level variable, at this stage, the state of separation of the mixture is monitored in real-time. Thus, when the decantation has been completed, the application of the electric field must also end.



**Fig. 3** Interface line between Biodiesel and Glycerol when the mixture finishes settling

An 8 MP CMOS camera is used together with a Raspberry Compute Module 3 + device capable of processing images. The algorithm is based on a basic segmentation of the “CV2” library based on the Python language. The color range of the segmentation according to the Hue, Saturation, and Value (HSV) color model is between [358 78 39.2] and [355 89.9 62.4], with the maximum-minimum glycerin shades, respectively.

## 2.5 Station Automation

Using a Raspberry Compute Module 3 + computer, complete control of the decanting station is taken. The sensors and actuators that are immersed in the development of this project are connected to the computer to be monitored in real-time and in this way, the decanting station works continuously. The P&ID diagram of this work is shown in Fig. 4.

## 3 Results

For the evaluation of the settling station proposed in this document, 5L of the biodiesel-glycerin mixture was fed to the settling tank. Table 1 shows the results of the six tests performed. From this table, we show that the time, taken for the glycerin to decant, can be reduced by up to 99% using the proposed settling station.

Table 2 compares the quality of biodiesel obtained with the parameters established by the ASTM according to the Glycerol (Total) and Glycerol (Free) analyzes. These analyses were performed on the biodiesel obtained in test one that was applied electric field (Table 1). The results showed that the parameters analyzed are within the standard set by ASTM. This allows the proposed decanting station to be considered a satisfactory solution.

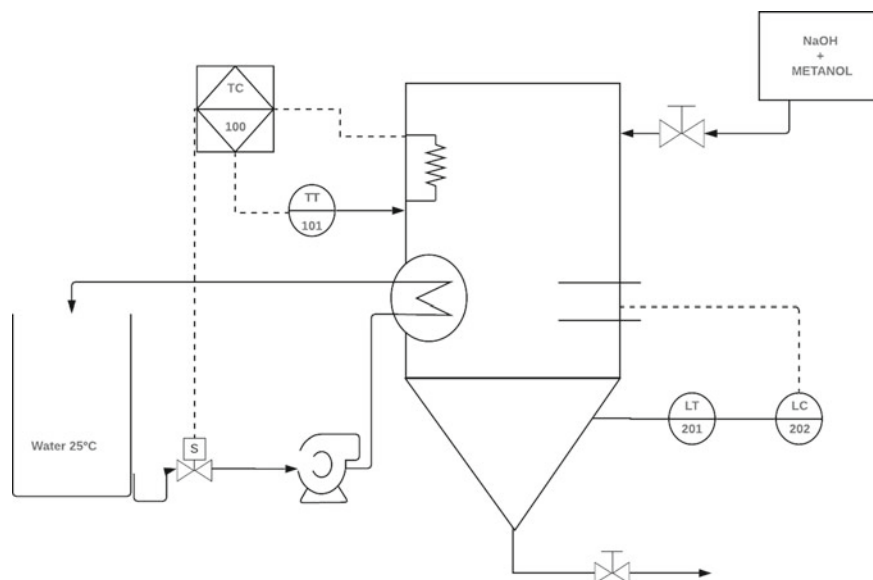


**Fig. 4** P&ID diagram of the proposed system

**Table 1** Results of 5L of the mixture at 9 kV of the applied voltage

Test Number	Electric Field Application Time (min)	Decantation Time by Gravity (hours)	Percent of glycerin (%)
1	2.00	6.00	23
2	1.32	6.30	25
3	1.54	6.50	25
4	2.10	7.20	20
5	1.44	5.50	28
6	0.30	2.00	15

**Table 2** Results of the Biodiesel analysis of test number 1 of Table 1

Analysis Type	Norm/Method	Limits Min. value	Limits Max. value	Results
Glycerol (Total)	AOCS Ca 14-15	–	0.240	0.182
Glycerol (free)	AOCS Ca 14-15	–	0.020	0.002

## 4 Conclusion

In conclusion, the results in this investigation showed that the glycerin-biodiesel decanting-time was reduced by up to 99% and the glycerin percentage in the biodiesel

produced. This result regards the parameters proposed by the American Society for Testing and Materials (ASTM). As future work, the level of impact and the affection to the biodiesel decantation process will be studied when higher or lower voltages frequencies are considered.

## References

1. Verma P., Sharma M.P.: Review of process parameters for biodiesel production from different feedstocks. *Renew Sustain Energy Rev* 62:1063–71. doi: <https://doi.org/10.1016/j.rser.2016.04.054> (2016)
2. Shirazi M.M.A., Kargari A., Tabatabaei M. et al.: Acceleration of biodiesel–glycerol decantation through NaCl assisted gravitational settling: a strategy to economize biodiesel production. *Bioresour Technol.* 134:401–406. <https://doi.org/10.1016/j.biortech.2013.02.026> (2013)
3. Chouhan A., Sarma A.: Modern heterogeneous catalysts for biodiesel production: a comprehensive review. *Renew Sustain Energy Rev* 15(9):4378–99. <https://doi.org/10.1016/j.rser.2011.07.112> (2011)
4. Ismail Z.E., Moussa A.I., Deff M.M.: Utilization of High Voltage to Separate Glycerol during Producing Biodiesel. *J.Soil Sci. and Agric. Eng. Mansoura Univ.* 9:329–332. <https://doi.org/10.21608/jssae.2018.35867> (2018)
5. Barbosa C., Ramírez L.N., Morales N.: Obtein of Biodiesel (ethyl-ester) by Basic Catalysis to Level Pilot Plant Oils Derived Food Industry. *Revista Especializada en Ingeniería* 8:99–116. <https://doi.org/10.22490/25394088.1293> (2014)
6. Ma, F., Hanna, M.A.: Biodiesel production: a review. *Biores. Technol.* **70**, 1–15 (1999)
7. Sdrula N.: A study using classical or membrane separation in the biodiesel process. *Desalination* 250:1070–1072. <https://doi.org/10.1016/j.desal.2009.09.110> (2010)
8. Atadashi I.M., Aroua M.K., Abdul A.: Biodiesel separation and purification: a review. *Renew Sustain Energy Rev* 36:437–443. <https://doi.org/10.1016/j.renene.2010.07.019> (2011)
9. Ratanabuntha T., Tonmitr K., Suksri A.: Acceleration in biodiesel production from palm oil process by high voltage electric field. *International Journal of Smart Grid and Clean Energy* 7:225–230. <https://doi.org/10.12720/sgce.7.3.225-230> (2018)
10. Abbaszadeh, A., Ghobadian, B., Najafi, G.: Electrostatic Coagulation for Separation of Crude Glycerin from Biodiesel. *Advances in Environmental Biology* **8**(1), 321–324 (2014)
11. Nouredin A., Shirazi M.M.A., Tofeily J., Kazemi P et al.: Accelerated decantation of biodiesel–glycerol mixtures: Optimization of a critical stage in biodiesel biorefinery. *Separation and Purification Technology* 132:272–280. <https://doi.org/10.1016/j.seppur.2014.05.011> (2014)
12. Naranjo, S.: Automation Of A Biodiesel Production Plant From Algae And Marine Microalgae. *Telematique* **16**, 81–105 (2017)
13. Knothe, G.: Biodiesel Fuel Quality And The Astm Standard. *Palmas* **31**, 162–171 (2010)
14. JM Industrial Technology SA.: PT100. Iztapalapa, MX.: JM Industrial Technology SA de CV. Retrieved from <https://www.jmi.com.mx/> (2020)

# Prototype Proposal for Control and Inspection of Gas Stations



Lucas Eder de Araújo Sousa , Felipe Silveira Stopiglia ,  
Luiz Vicente Figueira de Mello Filho ,  
Daniela Helena Pelegrine Guimarães ,  
and Maria Thereza de Moraes Gomes Rosa 

**Abstract** The current fuel market in Brazil has high rates of the so-called “white flag” posts, increasing the difficulty of enforcement due to the numerous types of fraud present in this market. About 19% of the prohibitions made by the National Agency of Petroleum, natural gas and biofuels (ANP) in 2017, relating to the scams of minor bombs, which is applied to gas stations whose marketing is currently addicted to quantity. Regarding inspection, the problem exposed here is that most posts that practice this type of fraud use the technology to make it difficult to identify, either by the user or by the inspection agency. The prototype developed in this work can support the user complaint by allowing the monitoring of his vehicle supply from a mobile application, connected to a flow meter, which is activated at the time of supply, in case of disagreement between pump and application the user gives access to the ANP complaints form, aiming at further investigation and records linked to this type of fraud. This study shows that over 80% of surveyed consumers do not feel safe about refueling your vehicle, and they are interested in the proposed device. This device does not identify fuel chemical tampering.

**Keywords** Fraud · Gas station · Fuel · Control · Prototype

---

L. E. de Araújo Sousa (✉) · F. S. Stopiglia · L. V. F. de Mello Filho ·  
M. T. de Moraes Gomes Rosa  
Center of Science and Technology, Mackenzie Presbyterian University, Brazil Avenue, 1220,  
13073-148 Campinas, SP, Brazil  
e-mail: [sousale74@gmail.com](mailto:sousale74@gmail.com)

D. H. P. Guimarães  
Lorena Engineering School (EEL-USP), São Paulo University, Campinho Highwat, 12602-810  
Lorena, SP, Brazil

## 1 Introduction

According to data from EPE [1], liquid fuels, from renewable sources or not, represent 40% of the Brazilian energy matrix, and the major consumers of this energy processed in Brazil are the transportation and industry sectors, demanding 61% and 6,90% respectively.

The oil industry generates goods that are hard substitute inputs in the production matrix of any country, which are of paramount importance for production and consumption in modern society. This importance can be evidenced mainly in petroleum derivatives used with liquid fuels for combustion engines (e.g. gasoline, diesel). Without it, the productive and modern industry would not function [2].

In this energy industry of great importance to the national economy, there are also fuel stations and distributors responsible for directing fuel to the final consumer. Data from the 2017 National Petroleum, Natural Gas and Biofuels Agency (ANP) show that there are currently 41,829 regulated gas stations in Brazil, which about 40% are white flag gas stations, that is, they buy fuels freely without compulsory binding a specific distributor [3].

The existence gas stations, despite contributing to increase competition and lower prices, makes checks more difficult, since adultery can come not only from clandestine distributors but from the establishments themselves that, by not following the regulations required by the supervisory bodies, can bring economic and environmental impacts, given that their activity influences a whole supply chain and it is, of course, extremely polluting [4–6].

Given the scenario above, it is possible to notice the difficulty that the ANP has when it comes to inspecting and noting mainly the irregular gas stations. In 2017, out of the 22,134 complaints received by the agency, only 67% were answered and of these 12,910 were inspection actions performed at fuel dealers, where only 4064 were fined in some way. So, there is a large deficit between the complaints and gas stations effectively fined, and this is due not only to the difficulty ANP has in carrying out the inspections, but also to the doubt of the consumers, who make the complaint without being sure if they are really being injured.

Enforcement action has a cost, and there are a lot of actions taken that did not reach the assessments and enforcement measures, this waste of resources is immense. This is mainly because the current system is flawed and it lacks technology that could identify and highlight sectors that really need to be scrutinized on the spot, saving resources and protecting the market from the economic inefficiency.

Understanding the importance of the fuel sector to the national economic scenario and the problem exposed here with the difficulty of enforcement and regulatory standards, this paper aims to develop a device that facilitates the identification of minor pump fraud and mediate the way ANP receives the complaints too.

## 2 Methodology

Ethical approval for the experiment in this study was deemed unnecessary by the Ethics Committee. As also the activities in the experiment do not pose risks greater than those ordinarily encountered in daily life and all the subjects remained anonymous. As well as all participants were given consent and were also informed about the academic objective of the research as well as the guarantee of anonymity giving the choice of participation or not. Still considering that as it is an opinion poll, according to Resolutions 466 and 510 of the National Health Council, there is no need to go through the University's Ethics Committee. This is following CNS Resolution 466/12 of the National Health Council, of December 12, 2012, (available at <https://conselho.saude.gov.br/resolucoes/2012/Reso466.pdf>). Idem with Article 1 of Resolution 510, of 7 April 2016, of Brazil's National Health Council (available at <http://www.conselho.saude.gov.br/resolucoes/2016/Reso510.pdf>) and also with item 8.0.5 of the Ethical Principles of Psychologists and Code of Conduct of the American Psychological Association (available at <https://www.apa.org/ethics/code/principles.pdf>).

In order to ascertain the real need for this control device and the gas stations enforcement, and to support its development, the current study was elaborated in a quantitative model that, according to Fonseca [7], can be characterized as an objective study, which considers that reality can be understood based on the analysis of raw data and through the aid of standardized and neutral instruments. A survey was conducted, elaborated with closed questions in order to check the consumer's confidence in gas stations where they are consumers, and to measure the level of interest in the device developed. The research was conducted in a structured questionnaire model, developed in Google Forms. The model with the questions was disseminated through e-mail and social media, being used for convenience by selecting individuals who are available to participate in the study. According to Fonseca [7], among the benefits of conducting a survey are the agility and economy in obtaining data, as well as obtaining data grouped in tables, which allow a rich statistical analysis.

From the extraction of data through the tools available in the Google Forms and Google Sheets platforms, it was found that from the sample of 30 responses collected, about 88% of respondents have already questioned the amount supplied and the amount that was presented by the pump and, of these, 86% are interested in buying of the product. With this scenario established, the experimental procedures were started, which, according to Gil [8], consists in determining the study object and the variables capable of influencing it, defining the forms of control and observation of the effects that the variable produces on the object. For this, it was proposed a new product concept, which aims to detect the frauds in gas stations and make accessible the submission of complaints by the user.



## 2.1 *Materials for Product Composition*

According to Morrison [9], the low acceptance rate of new products is directly related to the 21st-century consumer's profile, which is richer, more demanding and with high expectations of quality, service, and design, all offered at a low price.

Based on this precept, the activity of defining and selecting materials for the composition of a product has a strong influence on its functional and/or marketing success, since it is subject to aspects such as respect for the environment, usability, and even economic viability. Because these are many variables to be considered, measuring the efficiency of material selection and subsequent product development becomes a difficult task, in which there are even divergences within the literature [10].

After the devices available research for the construction of the project, it was possible to obtain a list of materials with sufficient characteristics to compose it. In view of the literature and the available materials found, the criterion for selecting those that were used in this project was the cost/benefit. The components listed here are presented in the functional prototype.

- DN20 pipe 3/4" water flow hall sensor Hall Flowmeter: consists of a plastic fairing, coupled blade rotor, and Hall effect sensor. When the fluid begins to flow inside, the paddles coupled to the rotor move, and when the paddles pass through the sensor, the device sends a 5 V pulse through the communication cable. The sensor can operate at a flow rate of up to 30 L per minute, pressure below 1.75 MPa, and has 3% accuracy in its results as indicated by the manufacturer. The Reading of the input pulses will be converted to absolute values by the coupled microprocessor, the Arduino.
- Arduino Board UNO R3: Arduino can be described basically like an opensource single-board microcontroller that allows data input and output configurations and is easily programmed using the C/C++ language. Widely used in academia, it is possible to combine this tool with other devices, establishing communication, reading and sending data through them. In the project, Arduino was crucial for reading the data emitted by the flow sensor and sending it to the mobile application through the Bluetooth module attached to the board. Receiving, sending and processing the data were developed through a "Sketch" code that will be approached later.
- Bluetooth Module—HC05: This module was coupled to the Arduino for the purpose of sending information (output) from it. It was possible to establish communication between the microprocessor and the mobile application responsible for displaying the data.
- Android App(MIT App Inventor): This is a visual and intuitive programming environment capable of creating functional applications for smartphones and tablets. The tool treats programming as blocks and facilitates the creation of complex applications for users unfamiliar with the common software language.

Within the platform was developed an application capable of reading the data emitted by the Arduino, controlling the devices attached to it, as well as facilitating access to the ANP’s complaint panel.

### 3 Results and Discussion

After selecting the materials to compose the device, it was necessary to establish a connection between them. The electrical scheme used is shown in Fig. 1.

The Arduino microprocessor board, after programming input, only needs a 12 V power connection. If it is properly configured, it will operate constantly, and does not require external interference. The flowmeter is connected to port 2, a digital pin that allows it to work as an interrupt, thereby detecting the number of pulses emitted by the Hall sensor in a given time frame. The sensor was also connected to power ports 5 (V) and GND, responsible for power and grounding, respectively.

The Bluetooth was connected to Arduino’s digital ports 0 (RX) and 1 (TX). Also known as SERIAL, these ports are responsible for communication, and in this case, outputting information from the Arduino. The Bluetooth module was also connected to the power supply port 5 (V) and the grounding GND port.

The mobile application has in its own layout an option to connect to a tablet. After pairing with Bluetooth and connecting to the same device, it is ready for use.

#### 3.1 Sketch Code Used for Microprocessor Programming

The language used is suitable for Arduino programming and closely resembles C++ programming (Fig. 2). To establish the connection between the three components, some researches were conducted on similar projects that used the device as a whole for other purposes, such as water flow reading or irrigation control.

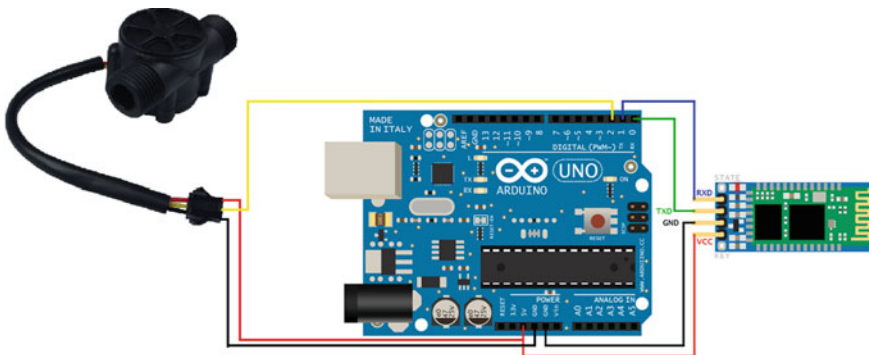


Fig. 1 Device electrical diagram

```

float vzo;
int contPlo;
int i=0;
int contpls;
double ltros;
double cont;

void setup()
{
  Serial.begin(9600);

  pinMode(2, INPUT);
  attachInterrupt(0, incpls, RISING);
  Serial.println("t");
}

void loop ()
{
  contPlo = 0;
  sei();
  delay (1000);
  cli();
  cont= contpls;
  ltros = (cont)/390;
  i++;

  Serial.println(ltros);

  if(Serial.available())
  {
    if (Serial.read()=='a'){
      contpls=0;
    }
  }
}

void incpulso ()
{
  contPlo++;
  contpls++;
}

```

**Fig. 2** Programming codes

### 3.2 Data Read Code

With the correct functioning of the device, it was necessary to find ways to constitute the communication app. With the platform defined, all the code was written in blocks, with the aid of research and studies in the sources mentioned below (Fig. 3).

Within the software, besides creating a box for automatic display of how much was filled, four buttons have been configured with distinct functions that aim to make the user's life easier, according to Fig. 3. These buttons are: Connect/Disconnect buttons to Bluetooth; button to reset the liters display after measurement; button to direct the user to the ANP's report page. Because it is a relatively simple platform, the model contains some layout and operation constraints, but fully meets the proposal (Fig. 4).

### 3.3 Device Calibration

After the communication between device and application was occurring without fail and with the assembly of the device properly completed (Fig. 5), it was necessary to calibrate the device so that the displayed numbers corresponded to the value supplied with the lowest possible error coefficient.

Calibration was performed using a 0.02 (g) precision scale, a 500 ml water measurement and the device powered by a 3/4 hose. Through this procedure it was

```
when ListPicker1 BeforePicking
do
  set ListPicker1 Elements to BluetoothClient1 AddressesAndNames

when Button1 Click
do
  if BluetoothClient1 IsConnected
  then
    call BluetoothClient1 Disconnect

initialize global receive to ""

when Clock1 Timer
do
  if BluetoothClient1 IsConnected
  then
    if BluetoothClient1 BytesAvailableToReceive > 0
    then
      set global receive to call BluetoothClient1 ReceiveText
      numberOfBytes call BluetoothClient1 BytesAvailableToReceive
    else

when Botão1 Click
do
  set ActivityStarter1 DataUrl to http://www.anp.gov.br/
  call ActivityStarter1 StartActivity

when Botão2 Click
do
  call BluetoothClient1 SendText
  text ""

when ListPicker1 AfterPicking
do
  if call BluetoothClient1 Connect
  address ListPicker1 Selection
  then
    call Notifier1 ShowAlert
    notice "Bluetooth successfully connected"
  else
    call Notifier1 ShowAlert
    notice "Couldn't connect to Bluetooth"
```

Fig. 3 Application code in blocks

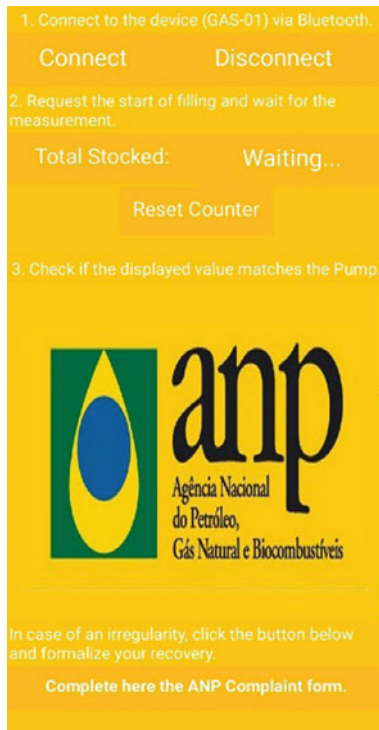
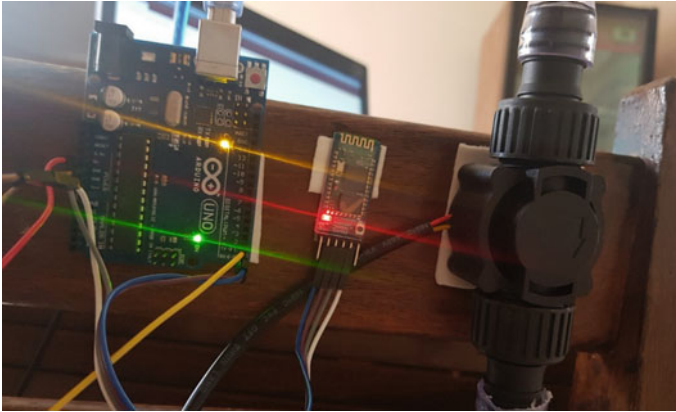


Fig. 4 Application layout



**Fig. 5** Device connected and turned on

**Table 1** Experimental testing for vendor reported error

Measurements	Observed value (ml)	Error percentage
1	530	6
2	510	2
3	540	8
4	520	4
5	510	2
6	520	4
7	510	2
8	530	6
9	540	8
10	530	6
Average	524	5

possible to convert the pulses to liters, described in item 3.2 of this article, the observed value corresponds to the hall effect meter manufacturer, where each liter is equivalent to 390 pulses. The error aggregated to the device is 5%, information also provided by the manufacturer and observed in tests presented in Table 1.

### **3.4** *Improvements*

Nevertheless, the prototype has points to be worked on and developed in further research, such as the device's adaptation to the vehicle and its accuracy when using variable flow rates. Regarding these points, difficulties were found due to the need for

the adaptation to the tank to be universal and versatile, aiming to maintain the device's low cost and accessibility. Proposals that can be considered for this adaptation would be to use a rubber hose fitted to the gas tank inlet and connected to the flow sensor at the end of it. The other device components could be allocated externally, near the tank or even under the passenger seat, as these are relatively small materials and it would not be a problem. Another proposal that could be considered for this problem would be the use of the sensor in the external region of the tank, being adapted with a screw nozzle and manually coupled directly to the supply nozzle during the process and removed later. But in this case, the use of the device would be dependent on the attendant's allocation at the time of fueling.

## 4 Conclusion

This study showed consumer insecurity regarding current supply control methods. This insecurity becomes even greater when considering the evolution of fraudulent bombs and the stagnation of supply detection methods of fraud, resulting in the conversion of only 30% of complaints into cases. This research has brought to the fuel market a new concept of a product to be worked on, which can help consumers and the law enforcement agencies to detect and report bomb fraud at gas stations. The device developed is functional, captures the actual volume supplied by the pump and give to consumers the basis for formalizing his complaint to the ANP, by completing the agency complaint form, which can be accessed through the application presented here, developed throughout the project.

## References

1. EPE.: Política Nacional de Biocombustíveis. Empresa de Pesquisa Energética, Rio de Janeiro, RJ (2006)
2. Canelas, A.L.S.: Evolução da importância econômica da indústria de petróleo e gás natural no Brasil: contribuição a variáveis macroeconômicas. Mestrado em Engenharia Ciências do planejamento energético, COPPE/UFRJ (2007)
3. ANP—Agência nacional do petróleo, gás natural E Biocombustíveis.: Anuário estatístico brasileiro do petróleo, gás natural e biocombustíveis. Rio de Janeiro: ANP (2017)
4. Rocha, J.A.: Padrões de concorrência e estratégias empresariais no setor de distribuição de derivados de petróleo no Brasil. Instituto de Economia. Universidade Federal do Rio de Janeiro, Rio de Janeiro, Rio de Janeiro (2002)
5. Dalmonech, L.F., Sant'anna, J.M.B., Teixeira, A.C.C.: Análise dos fatores intervenientes nas quebras de contrato no setor de combustíveis brasileiro, RAE eletrônica, Escola de administração de empresas, São Paulo (2010)
6. Machado, F.H., Ferreira, O.M.: Postos de combustíveis: quantificação e qualificação da atividade no município de Goiânia. Universidade Católica de Goiás, Goiás (2007)
7. Fonseca, J.J.S.: Metodologia da pesquisa científica. UEC, Fortaleza (2002)
8. Gil, A.C.: Como elaborar projetos de pesquisa, 4th edn. Atlas, São Paulo (2007)
9. Morrison, I.A.: Segunda Curva. Campus, Rio de Janeiro (1997)

10. Ferroli, P.C.M.: MAEM-6F (Método auxiliar para escolha de materiais em seis fatores): suporte ao design de produtos, industriais. Doutorado em Engenharia de Produção. Universidade Santa Catarina, Florianópolis (2004)

# Modeling of Solid-Liquid Equilibrium in Nitrobenzene and Para-Xylene Mixtures



Michelli Fontana , Caroline dos Santos Ribas , Paulo Henrique Schuck , Rafael Lopes Turino , and André Zuber 

**Abstract** Solid-liquid mixtures are very important for the study of molecular interactions that describe the thermodynamic properties of the components. The objective of this work was to determine the behavior of the nitrobenzene and para-xylene mixtures by means of two excess energy models, Margules and Non-Random Two-Liquid (NRTL), comparing the calculated results with experimental data from the literature. The Margules model, whose parameters varied with temperature, was more accurate than the model that did not consider the temperature variation. The NRTL model was also accurate, presenting only a small deviation in the lower para-xylene compositions, while the ideal case and Margules model with temperature independence presented a large imprecision. Therefore, the two-parameter Margules model with temperature dependence presented the best approximation of the equilibrium system.

**Keywords** Nitrobenzene · Para-xylene · Solid-liquid · NRTL · Margules · Equilibrium

---

M. Fontana · C. dos Santos Ribas · P. H. Schuck · R. L. Turino · A. Zuber (✉)  
Academic Department of Engineering, Federal University of Technology—Paraná (UTFPR),  
Francisco Beltrão, Brazil  
e-mail: [andrez@utfpr.edu.br](mailto:andrez@utfpr.edu.br)

M. Fontana  
e-mail: [fontana.michelli@gmail.com](mailto:fontana.michelli@gmail.com)

C. dos Santos Ribas  
e-mail: [carolineribas.cr@gmail.com](mailto:carolineribas.cr@gmail.com)

P. H. Schuck  
e-mail: [paulohschuck@gmail.com](mailto:paulohschuck@gmail.com)

R. L. Turino  
e-mail: [raturino@gmail.com](mailto:raturino@gmail.com)



## 1 Introduction

In solid-liquid mixtures, crystallization is a process where thermodynamic conditions lead the molecules to approach and group in highly organized structures, reaching a state of solid-liquid equilibrium. Among many ways to describe the solid-liquid equilibrium of a binary system, establishing the parameters of an excess energy model may be satisfactory to represent the behavior of the substances in the mixture.

In the phase equilibrium calculations, one of the most important steps is fitting adjustable parameters of activity coefficient models to experimental data [1]. Each model has a certain number of parameters, and their estimation is a common challenging problem. Considering the importance of the study of solid-liquid equilibria, the mixture of xylene and nitrobenzene emerges as an interesting case.

Xylenes are light aromatic hydrocarbons derived from petroleum and processed in petrochemical industries. Para-xylene is part of BTXs (benzene, toluene, and xylene), which may be used to react to producing compounds as nitrobenzene [2]. The study of the equilibrium of nitrobenzene and para-xylene may contribute to describing its synthesis [3]. To the best of our knowledge, the solid-liquid equilibrium modeling of nitrobenzene and para-xylene mixtures using the two-suffix Margules and the Non-Random Two-Liquid (NRTL) models was not investigated in literature before.

Thus, the aim of this study was to determine the behavior of nitrobenzene and para-xylene mixtures by means of two excess energy models, the two-suffix Margules with dependence and independence of temperature and the NRTL, identifying the eutectic point of the mixture and comparing the calculated results with those obtained experimentally by Proust and Fernandez [4].

## 2 Methods

From the Gibbs excess energy definition of the two-suffix Margules model ( $G^e$ ) (1), using the definition of Eq. (2), we obtained the equations that determine the activity coefficients ( $\gamma$ ) (3 and 4).

$$G^e = x_1 \cdot x_2 \cdot [A + B \cdot (x_1 - x_2)] \quad (1)$$

$$R \cdot T \cdot \ln[\gamma_1] = [\partial(n \cdot G^e)/\partial n_1]_{P,T,n^2} \quad (2)$$

$$\ln[\gamma_1] = [(A + 3 \cdot B) \cdot x_2^2 - 4 \cdot B \cdot x_2^3]/(R \cdot T) \quad (3)$$

$$\ln[\gamma_2] = [(A - 3 \cdot B) \cdot x_1^2 + 4 \cdot B \cdot x_1^3]/(R \cdot T) \quad (4)$$

The activity coefficients were fitted using compositions obtained experimentally by Proust and Fernandez [4] for different temperatures, considering molar fractions in the liquid phase for para-xylene ( $x_1$ ) and for nitrobenzene ( $x_2$ ), and using an initial

estimation for parameters  $A$  and  $B$ . The calculation of the activity coefficients was repeated considering parameters  $A$  and  $B$  temperature-dependent.

Theoretical compositions were calculated by means of the equilibrium condition with the variation of activity coefficients for each temperature. Solid and liquid heat capacity were considered the equal and the theoretical composition of the liquid phase in equilibrium was calculated for each experimental temperature (5).

$$\ln[x_i \cdot \gamma_i] = [\Delta h_{f,T}/R] \cdot [1/T - 1/T_m] \quad (5)$$

The deviation between theoretical and experimental compositions (6) of the calculated liquid phase (ARD %) was minimized by varying the parameters ( $A$  and  $B$ ) of activity coefficients (3 and 4). The deviations were evaluated neglecting experimental or calculated values for molar fractions equal to zero or one (pure substances).

$$\text{ARD}(\%) = \Sigma 100 \cdot |[(x_1^{\text{calc}} - x_1^{\text{exp}})/(x_1^{\text{exp}})]/(\text{total points})| \quad (6)$$

The second model used was NRTL (7).

$$\begin{aligned} G^e/(x_1 \cdot x_2 \cdot R \cdot T) = & G_{21} \cdot \tau_{21}/(x_1 + x_2 \cdot G_{21}) \\ & + G_{12} \cdot \tau_{12}/(x_2 + x_1 \cdot G_{12}) \end{aligned} \quad (7)$$

Taking the definition presented by Eq. (2), we obtain (8 and 9).

$$\begin{aligned} \ln[\gamma_1] = & x_2^2 [\tau_{21} \cdot (G_{21}/(x_1 + x_2 \cdot G_{21}))^2 \\ & + (G_{12} \cdot \tau_{12}/(x_2 + x_1 \cdot G_{12}))^2] \end{aligned} \quad (8)$$

$$\begin{aligned} \ln[\gamma_2] = & x_1^2 [\tau_{12} \cdot (G_{12}/(x_2 + x_1 \cdot G_{12}))^2 \\ & + (G_{21} \cdot \tau_{21}/(x_1 + x_2 \cdot G_{21}))^2] \end{aligned} \quad (9)$$

With the parameters defined as (10, 11, 12 and 13).

$$G_{12} = \exp(-\alpha \cdot \tau_{12}) \quad (10)$$

$$\tau_{12} = b_{12}/(R \cdot T) \quad (11)$$

$$G_{21} = \exp(-\alpha \cdot \tau_{21}) \quad (12)$$

$$\tau_{21} = b_{21}/(R \cdot T) \quad (13)$$

The same procedure used to obtain theoretical compositions in Margule's excess energy model was used to obtain the theoretical compositions of the mixture for the NRTL model. Subsequently, the theoretical composition of the liquid phase of the mixture was calculated for the ideal case. Table 1 shows the properties of the pure components used in this study.

**Table 1** Properties of nitrobenzene and para-xylene

Parameter	Para-xylene	Nitrobenzene
Melting point (K)	286.29	278.79
$\Delta h_{\text{fus}}^{273,15\text{ K}}$ (J/mol)	16,810	11,590
Molecular mass (g/mol)	106.16	123.06

### 3 Results and Discussion

Both Figs. 1 and 2 show that different regions can be identified in the phase diagram of the models. These regions separate the zones of the existence of different phases. Eutectic line defines two regions: under it, there is a solid phase composed of para-xylene and nitrobenzene, and over it, there are three other regions. The left region is composed of a nitrobenzene solid phase and a liquid mixture of both compounds. The right region is composed of para-xylene in the solid phase and a liquid mixture. And the central upside region is composed of a liquid mixture of both compounds.

NRTL usually leads to reasonable phase equilibria predictions [5, 6]. NRTL model (Fig. 1) provided eutectic point compatible with experimental data, both in temperature (259.22 K) and composition ( $[x_1 = 0.38]$  and  $[x_2 = 0.62]$ ). However, it was evidenced that along the curve for low para-xylene molar fraction, there was a deviation when compared to the experimental one (ARD = 3.56%). The parameters of this model were:  $\alpha$  equal to 0.015,  $b_{12}$  equal to 9.896 and  $b_{21}$  equal to 10.437. Also, in order to define the behavior of all parameters, some correlations were obtained as

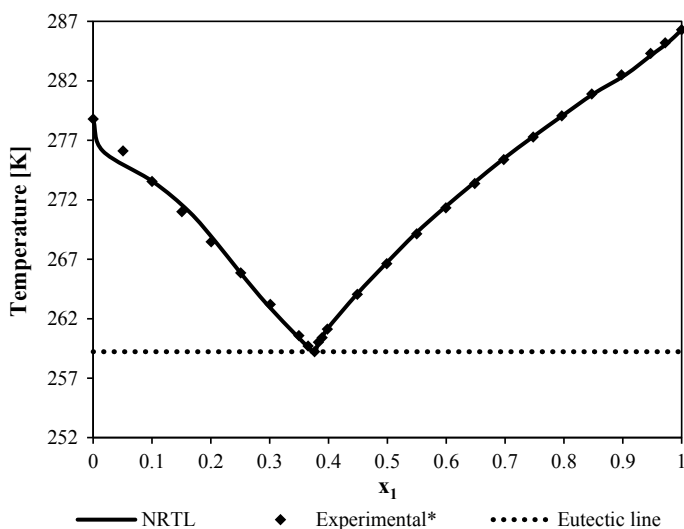


**Fig. 1** Phase diagram of the NRTL model to para-xylene ( $x_1$ ) and nitrobenzene mixture  
 \*Experimental data from Proust and Fernandez [4]

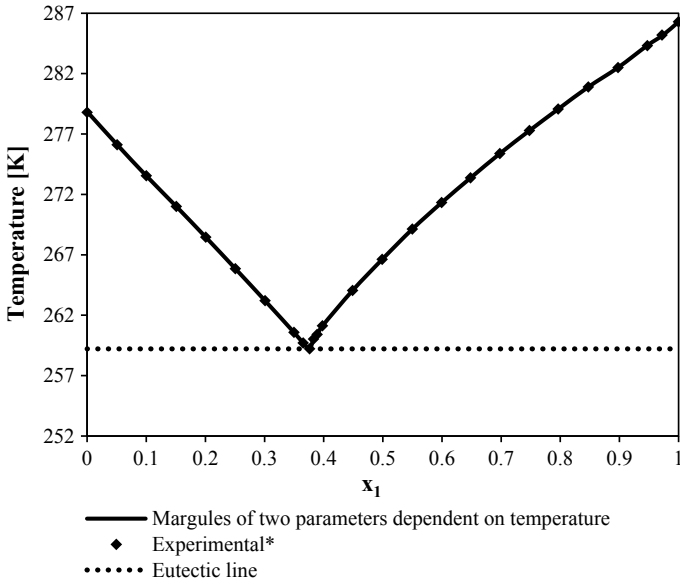


**Fig. 2** Phase diagram of the Margules model of two parameters dependent on temperature to para-xylene ( $x_1$ ) and nitrobenzene mixture \*Experimental data from Proust and Fernandez [4]

follows:

$$G_{12} = -0.1691 \cdot x_1^5 + 0.4482 \cdot x_1^4 - 0.407 \cdot x_1^3 + 0.1348 \cdot x_1^2 - 0.008 \cdot x_1 + 0.0063; (R^2 = 0.977).$$

$$G_{21} = -0.1372 \cdot x_1^5 + 0.3635 \cdot x_1^4 - 0.3301 \cdot x_1^3 + 0.1094 \cdot x_1^2 - 0.0065 \cdot x_1 + 0.0048; (R^2 = 0.9766).$$

$$\tau_{12} = 1341.1 \cdot x_1^5 - 3554.1 \cdot x_1^4 + 3221.7 \cdot x_1^3 - 1046.4 \cdot x_1^2 + 49.27 \cdot x_1 + 330.03; (R^2 = 0.984).$$

$$\tau_{12} = 1414.4 \cdot x_1^5 - 3748.4 \cdot x_1^4 + 3397.8 \cdot x_1^3 - 1103.6 \cdot x_1^2 + 51.962 \cdot x_1 + 348.06; (R^2 = 0.984).$$

In the two-suffix Margules model of Gibbs excess energy with temperature dependence (Fig. 2), there was a better estimation of the composition as a function of temperature. Thus, the calculated eutectic point was compatible with the experimental one, both in temperature (259.22 K) and in molar composition ( $[x_1 = 0.38]$  and  $[x_2 = 0.62]$ ). The correlations of the molar fraction of nitrobenzene with both parameters A and B are presented below. These correlations do not consider the points  $x_1 = 0$  and  $x_1 = 1$ , because these points did not adapt to any model proposed.

$$A = -2^7 \cdot x_1^6 + 4^7 \cdot x_1^5 - 5^7 \cdot x_1^4 + 3^7 \cdot x_1^3 - 8^6 \cdot x_1^2$$

$$\begin{aligned}
 &+ 1^6 \cdot x_1 - 70450; (R^2 = 0.983). \\
 B = &7^6 \cdot x_1^6 - 2^7 \cdot x_1^5 + 1^7 \cdot x_1^4 - 3^6 \cdot x_1^3 - 712407 \cdot x_1^2 \\
 &+ 468146 \cdot x_1 - 60596; (R^2 = 0.984).
 \end{aligned}$$

Despite its simplicity, the Margules equations showed a reasonable quality (ARD = 0.01%) for the description of eutectic solid-liquid equilibrium profiles [7].

In the two-suffix Margules model of Gibbs excess energy with temperature independence (Fig. 3), (ARD = 27.15%) the eutectic point was also at the same temperature (259.22 K) of that obtained with experimental data. However, the composition of molar fraction in the liquid phase was different (experimental  $[x_1 = 0.38]$  and  $[x_2 = 0.62]$ , model  $[x_1 = 0.27]$ , and  $[x_2 = 0.73]$ ). The parameter A of this model was equal to 10,833.546 and B were equal to 185.106.

In the ideal case (Fig. 4), both the range of the para-xylene composition from 0.2–0.8 as the eutectic point was different from experimental data (ARD = 7.93%). This can be justified by the fact that in the ideal case, the interactions between distinct molecules are disregarded.

Margules model, whose parameters varied with temperature, was more accurate than the one without considering temperature changes. In fact, this result is in good agreement with the observations presented by Rocha and Guirardello [8] that also used the two-parameter Margules equation, with temperature dependence, to model the liquid phase in solid-liquid equilibria for many other binary systems.

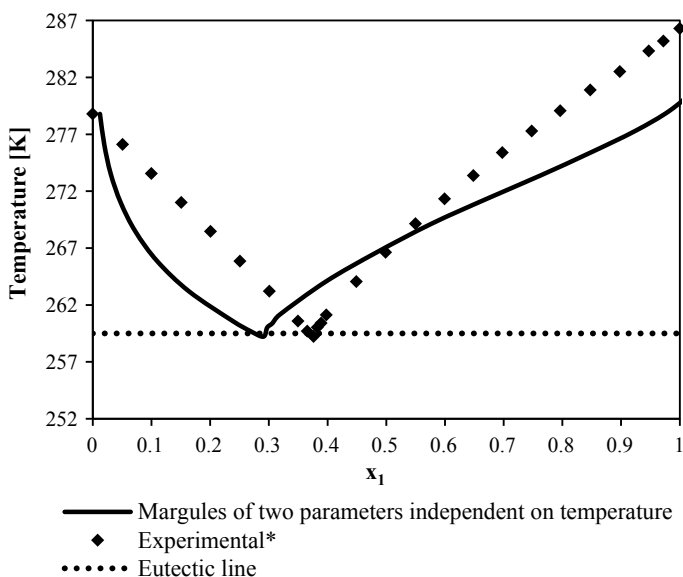


**Fig. 3** Phase diagram of the Margules model of two parameters independent on temperature to para-xylene ( $x_1$ ) and nitrobenzene mixture \*Experimental data from Proust and Fernandez [4]

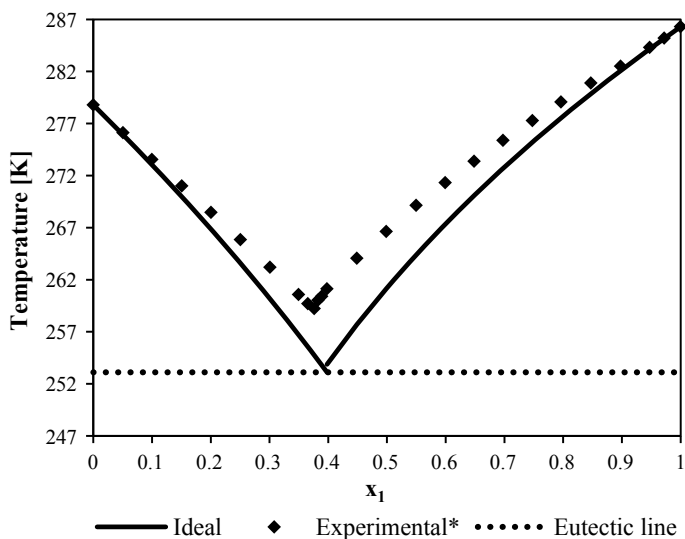


**Fig. 4** Phase diagram of the ideal case to para-xylene ( $x_1$ ) and nitrobenzene mixture \*Experimental data from Proust and Fernandez [4]

Furthermore, NRTL was also accurate, showing a small deviation in the lower molar composition of para-xylene. NRTL model is also efficient to provide a great approximation of solid-liquid equilibrium to other systems [9]. Literature also brings the use of Margules and NRTL models to represent other solid-liquid equilibrium systems. Pelaquim et al. [10] used NRTL and three-suffix Margules models to describe the properties of the liquid of many solid-liquid mixtures of fatty acids. Likewise, Matos et al. [11] evaluated binary solid-liquid equilibrium of fatty acids, fatty alcohols, and triolein, in which the liquid lines of these systems were adequately described. Three-suffix Margules and NRTL models were also accurate in representing the solid-liquid equilibrium of octacosanol in three pure solvents 1-pentanol, 1-hexanol, and toluene [12].

Margules model with temperature independence, however, showed great deviation when compared to experimental data, even bigger than the ideal case deviation. This is justified by the lack of information that the absence of temperature dependence causes. This mixture shows an increase in the intensity of attractive molecular interactions with increasing system temperature [3]. The literature also highlights the need to develop unified interaction parameters to represent all possible phase equilibria [5].

## 4 Conclusion

This study presented an analysis of Gibbs's excess energy models to describe the equilibrium system of the solid-liquid mixture of para-xylene and nitrobenzene. It was found that the Margules model of two parameters with temperature dependence was the best to represent the equilibrium of the system. NRTL model also provided a good prediction of the experimental data. However, Margule's model of two parameters independent of temperature did not represent the mixture effectively. The representation of the ideal case was also not accurate.

Although some models are known to represent well mixtures, there are some cases that they can diverge, so it is very important to compare experimental data with the modeling results. The agreement between the predicted results by means of Margules and NRTL models with the experimental phase equilibrium data contributes to the modeling of solid-liquid mixtures with nitrobenzene and para-xylene.

**Acknowledgements** To the Federal University of Technology—Paraná (UTFPR).

## References

1. Vatani, M., Asghari, M., Vakili-Nezhaad, G.: Application of Genetic Algorithm to the calculation of parameters for NRTL and Two-Suffix Margules models in ternary extraction ionic liquid systems. *J. Indus. Eng. Chem.* **18**, 1715–1720 (2012). <https://doi.org/10.1016/j.jiec.2012.03.008>
2. Franck, H.G., Stadelhofer, J.W.: Production of benzene, toluene and xylenes. In: *Industrial Aromatic Chemistry*. Springer, Berlin, Heidelberg, pp. 99–131 (1988). doi: 10.1007/978-3-642-73432-8\_4
3. Rafiee, H.R., Frouzesh, F.: The study of partial and excess molar volumes for binary mixtures of nitrobenzene and bensenaldehyde with xylene isomers from  $T = (298.15 \text{ to } 318.15) \text{ K}$  and  $P = 0.087 \text{ MPa}$ . *J. Adv. Res.* **7**(5), 769–780 (2016). <https://doi.org/10.1016/j.jare.2015.11.003>
4. Proust, P.C., Fernandez, J.C.: Experimental solid-liquid equilibria of binary mixtures of organic compounds. *Fluid Phase Equilib.* **29**, 265–272 (1986)
5. Moudjari, Y., Louaer, W., Meniai, A.: Modeling of solid-liquid equilibrium using a modified group contribution based NRTL model. *Fluid Phase Equilib.* **492**, 118–136 (2019). <https://doi.org/10.1016/j.fluid.2019.03.021>
6. Zhang, X., Zhao, Y., Liu, Y., Tang, W.: The effects of solvent properties on solid-liquid phase equilibrium of ethylene thiourea. *J. Mol. Liq.* **285**, 459–467 (2019). <https://doi.org/10.1016/j.molliq.2019.03.178>
7. Maximo, G.J., Carareto, N.D.D., Costa, M.: Chapter 8—Solid-liquid equilibrium in food processes. In: *Thermodynamics of Phase Equilibria in Food Engineering*, pp. 335–384 (2019). <https://doi.org/10.1016/b978-0-12-811556-5.00008-9>
8. Rocha, S.A., Guirardello, R.: An approach to calculate solid-liquid phase equilibrium for binary mixtures. *Fluid Phase Equilib.* **281**, 12–21 (2009). <https://doi.org/10.1016/j.fluid.2009.03.020>
9. Tan, Q., Leng, Y., Wang, J., Huang, C., Yuan, Y.: Correlation and prediction of the solubility of the racemic tartaric acid–ethanol–water system with the NRTL model. *J. Mol. Liq.* **216**, 476–483 (2016). <https://doi.org/10.1016/j.molliq.2016.01.080>
10. Pelaquim, F.P., Matos, F.C., Cardoso, L.P., Batista, E.A.C., Meirelles, A.J.A., Costa, M.C.: Solid-liquid phase equilibrium diagrams of binary mixtures containing fatty acids, fatty alcohol

- compounds and tripalmitin using differential scanning calorimetry. *Fluid Phase Equilib.* **497**, 19–32 (2019). <https://doi.org/10.1016/j.fluid.2019.05.020>
11. Matos, F.C., Costa, M.C., Meirelles, A.J.A., Batista, E.A.C.: 12. Binary solid-liquid equilibrium systems containing fatty acids, fatty alcohols and triolein by differential scanning calorimetry. *Fluid Phase Equilib.* **404**, 1–8 (2015). <https://doi.org/10.1016/j.fluid.2015.06.015>
  12. Cuevas, M.S., Crevelin, E.J., Moraes, L.A.B., Oliveira, A.L., Rodrigues, C.E.C., Meirelles, A.J.A.: Solubility of commercial octacosanol in organic solvents and their correlation by thermodynamic models at different temperatures. *J. Chem. Thermodynamics* **110**, 186–192 (2017). <https://doi.org/10.1016/j.jct.2017.02.025>



# X-Ray Characterization of TiO<sub>2</sub> Obtained by Chemical Route for Photocatalysis



Tiago Siqueira Lima , Wesley Rafael Penteadó ,  
André Luis de Castro Peixoto ,  
and Ademir Geraldo Cavallari Costalonga 

**Abstract** The need for freshwater in our time has become a problem of important concern. Recovered water for new uses makes purification an essential process to achieve a desired degree of quality. This need depends on each different purpose, such as purification of drinking water or reuse water for industrial needs. Due to the toxic characteristics of non-biodegradable organic pollutants, new treatment technologies must be studied and advanced oxidation processes (AOPs) come up as suitable for degradation of a wide range of organic contaminants in polluted water. For catalyst effectiveness, the crystalline phase of TiO<sub>2</sub> present contributes to photocatalytic activity in the material. This work involved the synthesis of titanium dioxide from Pechini's method using citric acid, titanium isopropoxide, and ethylene glycol, obtaining samples of titanium dioxide in calcination temperatures from 500, 600, and 700 °C. From the X-ray diffraction results, it is possible to check the TiO<sub>2</sub> crystalline phases present in the samples synthesized at different temperatures and identified as T500, T600, and T700. For sample T500, there was a mixture of phases between anatase and rutile, and for samples T600 and T700, the predominant phase was rutile. With this, we can say that the calcination process influenced the polymorphic composition of the material, increasing the rutile phase with increasing temperature, which brings undesirable characteristics for application in photocatalytic processes.

**Keywords** Photocatalysis · Titanium dioxide · Rietveld's method

## 1 Introduction

The need for freshwater in our time has become a problem of important concern. The water is not only for industrial purposes but also for domestic uses, and many sources of freshwater have been polluted due to industrial activity. Many different chemicals

---

T. S. Lima · W. R. Penteadó · A. L. de Castro Peixoto · A. G. C. Costalonga (✉)  
IFSP—Instituto Federal de Educação Ciência e Tecnologia de São Paulo Câmpus Capivari,  
Avenida Doutor Ênio Pires de Camargo, 2971, Capivari, SP-CEP 13360-000, Brazil  
e-mail: [ademirgcc@ifsp.edu.br](mailto:ademirgcc@ifsp.edu.br)

© The Editor(s) (if applicable) and The Author(s), under exclusive license  
to Springer Nature Switzerland AG 2021

Y. Iano et al. (eds.), *Proceedings of the 5th Brazilian Technology Symposium*,  
Smart Innovation, Systems and Technologies 202,  
[https://doi.org/10.1007/978-3-030-57566-3\\_37](https://doi.org/10.1007/978-3-030-57566-3_37)

are discharged into the aquatic environment. Some of them are biodegradable and nontoxic, however, others not are.

Due to the toxic characteristics of non-biodegradable organic pollutants, new treatment technologies must be studied and advanced oxidation processes (AOPs) come up as suitable for degradation of a wide range of organic contaminants in polluted water.

In the previous work,<sup>1</sup> we have focused on optimizing photocatalysis, as many factors interfere with photocatalytic activity, finding the best conditions for the degradation of methyl orange [1], working on a variation of the amount of TiO<sub>2</sub> and the temperature of the solution. We also focus on optimizing photocatalysis as an important issue to make the process viable and present experimental results using a mixture of HNO<sub>3</sub> and NaNO<sub>3</sub> in aqueous solutions to optimize photocatalytic activity [2].

Heterogeneous photocatalysis is an example of AOP that is showing good results for the oxidation of these pollutants. TiO<sub>2</sub> is potentially the best catalyst that researchers chose for this reaction, due to its high efficiency, physical and chemical stability, low cost, and low toxicity [3].

For this catalyst, the crystalline phase of TiO<sub>2</sub> present in the material contributes to the efficiency of photocatalytic activity in the material, P<sub>25</sub> Degussa is the one that presents the best results, one of the aspects that contributes to its efficiency is the phase mixture (75% anatase and 25% rutile) [4]. The photocatalyst can be synthesized when one wants to evaluate some variables in the synthesis process and effect on photocatalytic activity.

The most commonly used TiO<sub>2</sub> synthesis routes [5–8] can be classified according to the reaction medium (liquid or gas). In the gas phase, the most commonly used methods are chemical vapor deposition (CVD) and liquid phase flame oxidation, and the most reported methods are sol–gel, microemulsion, polymeric precursors, and homogeneous precipitation. Synthetic routes performed in the liquid phase are preferable when obtaining powders and films, as they allow greater stoichiometric control of reagents which gives greater morphological control [6].

Work is developed [5, 6] in the synthesis of titanium dioxide from the Pechini method (1967) using citric acid, titanium isopropoxide, and ethylene glycol, obtaining five samples of titanium dioxide in 1:1, 2:1 stoichiometric proportion, 3:1, 4:1, and 5:1. First, a titanium citrate solution was prepared, and then, polyesterification reaction with ethylene glycol was added until the resin was formed which was calcined at 400 °C for 1 h. This resin was macerated and sieved for 1 h calcination at a temperature of 500 °C, and later, the compound was characterized by X-ray diffraction. In diffraction, it was possible to determine that according to the variations of citric acid concentrations, 78.99–94.70% were obtained in the anatase crystalline phase.

Synthesis and crystallization methods that offer the best cost-effectiveness and speed in terms of improving the properties that qualify these materials for technological applications are of interest. Some parameters such as the crystalline phase,

---

<sup>1</sup>Note of transparency that indicates that it was based on earlier work by one of the co-authors, according to Refs. [1, 2].

surface area, morphology, crystallinity, particle size, and porosity are influenced by the heat treatment employed in TiO<sub>2</sub> synthesis [4].

## 2 Materials and Methods

### 2.1 Synthesis and Characterization of TiO<sub>2</sub>

To perform the synthesis, the adapted Pechini (1967) method was used. Initially, a citric acid solution was prepared by dissolving 21 g of the reagent in approximately 30 mL of distilled water. The addition of isopropanol (20 mL) was continued under heating to 60 °C. For the formation of titanium citrate, it was necessary to prepare a 30 mL 1:2 ratio of titanium isopropoxide: isopropanol, which was slowly poured into the citric acid solution while stirring until slightly liquid formed yellowish and clear.

The solution was boiled, and upon reaching approximately 50, 10 mL of glycerin was added. The mixture was stirred and heated until a clear, viscous gel formed. Subsequently, 4 mL of concentrated H<sub>2</sub>O<sub>2</sub> was poured, thereby developing an intense orange tinge. The gel was muffled and pyrolyzed at 300 °C. Finally, the synthesis product was fractionated in three to study the effect of calcination temperature on the photochemical properties of the material. The calcination temperatures adopted were 500, 600, and 700 °C, and the obtained materials were coded as T500, T600, and T700, respectively, besides the commercial one, coded as TC.

The materials were characterized to identify the crystalline phases of the compound, applying the X-ray diffraction (XRD) technique by the powder method. Using Panalytical diffractometer and Empyrean model, in which the samples were scanned in the range of 2θ from 15° to 85°, with copper anode tube, applying electromagnetic waves wavelength,  $\lambda = 1.5418 \text{ \AA}$ , with a voltage of 45 kV acceleration and 40 mA applied current.

## 3 Results

### 3.1 Characterization by X-Ray Diffraction

All TiO<sub>2</sub> samples obtained with different heat treatments at different temperatures were characterized by X-ray powder diffraction to identify and quantify the possible phases present in the obtained material. For TiO<sub>2</sub>, the possible phases present are the rutile and anatase in the sample; using the X-ray diffraction technique, it was possible to identify the crystalline phases present.

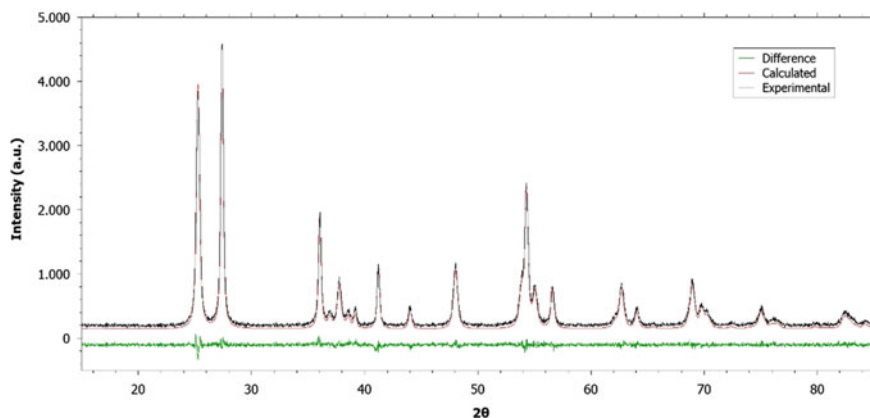


**Fig. 1** X-ray diffractogram of  $\text{TiO}_2$  synthesized by the Pechini method with heat treatment at 500 °C. Analysis performed with scanning range between 15° and 85°, with copper anode tube, applying electromagnetic waves wavelength,  $\lambda = 154.18$  pm. Diffractogram calculated by the Rietveld method, experimental diffractogram and the difference between calculated and experimental diffractograms

**Table 1** Quantitative results from characterization by X-ray diffraction

Phase	TC	T500	T600	T700
Anatase	99.42	42.43	0.56	0.04
Rutile	0.58	57.57	99.44	99.96

To identify and quantify these phases, the Rietveld method was applied, which uses the result of X-ray diffraction to quantify each phase. Figure 1 shows the result of applying the method with the X-ray diffractogram calculated by the Rietveld method, the experimental diffractogram and the calculated and experimental difference for the treated sample at a temperature of 500 °C. In Fig. 1, we can observe an excellent agreement between the calculated result and the experimental result, with all the diffractions, identified, indicating the presence of only the two phases before proposed.

Using the same methodology for analyzing diffractograms, the sample TC presents the crystalline anatase phase in greater quantity, for the T500 sample there was a mixture of phases between anatase and rutile, and for the samples, T600 and T700 were observed to be the rutile phase and predominant as shown in Table 1.

## 4 Conclusion

From the X-ray diffraction analysis, it is possible to evaluate the  $\text{TiO}_2$  crystalline phases present in the samples synthesized at different temperatures and identified

as T500, T600, and T700. For the T500 sample, there is a mixture of anatase and rutile phases, and for the T600 and T700 samples, it was observed that the rutile phase and the predominant phase. With this, we can say that the calcination process influenced the polymorphic composition of the material, increasing the rutile phase with increasing temperature, which brings undesirable characteristics for application in photocatalytic processes.

**Acknowledgements** This work was partly supported by Grants 2018/17913-2 and 2018/05698-0, São Paulo Research Foundation (FAPESP).

## References

1. Iga, G. D., de Castro Peixoto, A. L., Costalonga, A. G. C.: Optimization of photocatalytic degradation of methyl orange using TiO<sub>2</sub>. In: Iano, Y., Arthur, R., Saotome, O., Vieira Estrela, V., Loschi, H. (eds.) Proceedings of the 3rd Brazilian Technology Symposium. BTSym 2017. Springer, Cham (2019)
2. Iga, G. D., de Castro Peixoto, A. L., Costalonga, A. G. C. (2019) Efficient optimization of photocatalytic process for Azo Dyes. In: Iano, Y., Arthur, R., Saotome, O., Vieira Estrela, V., Loschi, H. (eds.) Proceedings of the 4th Brazilian Technology Symposium (BTSym'18). BTSym 2018. Smart Innovation, Systems and Technologies, vol. 140. Springer, Cham (2018)
3. Kanakaraju, D., Glass, B., Oelgemöller, M.: Titanium dioxide photocatalysis for pharmaceutical wastewater treatment. *Environ. Chem. Lett.* **12**(1), 27–47 (2014)
4. SANTOS: Lidiaine Maria dos. Síntese e caracterização de TiO<sub>2</sub> com modificações superficiais para aplicação em fotocatalise heterogênea. 2017. 135 f. Tese (Doutorado em Química) - Universidade Federal de Uberlândia, Uberlândia, Disponível em (2017). <http://dx.doi.org/10.14393/ufu.te.2017.48>
5. Araujo, dos Santos, D., et al.: Avaliação gap óptico do TiO<sub>2</sub> obtido pelo método Pechini: influência da variação das fases anatásio-rutilo. *Matéria (Rio J.)*, Rio de Janeiro **23**(1), e-11949 (2018)
6. Brito, S. L. M.: Síntese, caracterização e modificação superficial de nano partículas de titanato de bário produzidas pelo método Pechini. Tese de Doutorado, Escola Politécnica. Universidade de São Paulo, São Paulo (2009). <https://doi.org/10.11606/t.3.2009.tde-28052009-141416>
7. Costa, A.C.F.M., et al.: Síntese e caracterização de nanopartículas de TiO<sub>2</sub>. *Cerâmica*, São Paulo **52**(324), 255–259 (2006)
8. Mutuma, B.K., Shao, G.N., Kim, W.D., Kim, H.T.: Sol-gel synthesis of mesoporous anatase-brookite and anatase-brookite-rutile TiO<sub>2</sub> nanoparticles and their photocatalytic properties. *J. Colloid Interface Sci.* **442**, 1–7 (2015)

# Co-authors Networks in Adsorption Refrigeration and Air-Conditioning with Solar Energy



Carla Abregú Marcos , Abraham Sopla Maslucán ,  
Miguel Cano Lengua , and José C. Alvarez 

**Abstract** The refrigeration and air conditioning systems by adsorption with solar energy are a very interesting option to replace the conventional compression systems because they save energy, are noiseless and use non-aggressive ozone layer refrigerants; however, there are scarcities of studies at this topic. The acquisition of knowledge and positioning in research on this topic by new research groups could be facilitated by knowing the context, trends, and collaborations that emerge in the subject. A map of collaborative co-authors between the greatest authors on the subject was drawn up, the same one that is done using Gephi software. From the analysis of these maps, the centrality degree and collaboration between the authors were determined.

**Keywords** Refrigeration · Air-conditioning · Adsorption · Solar energy · Co-authoring

## 1 Introduction

Adsorption cooling systems, which use a refrigerant/adsorbent pair, are an ecological alternative to conventional refrigeration systems because they do not use refrigerants that damage the ozone layer and use recovered heat or solar thermal energy. Dieng and Wang [1], through a literature review, pointed out the importance of the applicability

---

C. A. Marcos · A. S. Maslucán · M. C. Lengua  
Universidad Nacional Mayor de San Marcos, Lima, Peru  
e-mail: [carla.abregu@unmsm.edu.pe](mailto:carla.abregu@unmsm.edu.pe)

A. S. Maslucán  
e-mail: [abraham.sopla@unmsm.edu.pe](mailto:abraham.sopla@unmsm.edu.pe)

M. C. Lengua  
e-mail: [miguelangel.cano@unmsm.edu.pe](mailto:miguelangel.cano@unmsm.edu.pe)

J. C. Alvarez (✉)  
Universidad Peruana de Ciencias Aplicadas, Lima, Peru  
e-mail: [pcijalv@upc.edu.pe](mailto:pcijalv@upc.edu.pe)

of solar energy in both air conditioning and refrigeration by adsorption, for the reason of performance coefficient improvement, air conditioning and ice making are quiet, non-corrosive and environmentally friendly.

According to Hassan and Mohamad [2], refrigeration and air conditioning processes are considered essential needs for all human beings in today's world, but it is necessary providing refrigeration using green energy such as solar energy as the key solution to electricity and pollution problems that traditional refrigeration systems present.

Therefore, new research is necessary to improve efficiency, through development, test and simulate working prototypes. In this sense, using technology surveillance, business intelligence, and data mining, particularly co-authorship it is possible to search and identify new research topics.

Wang et al. [3] performed a co-authorship analysis among Chinese researchers in the field of management, in the period 2006–2015, finding a low network density that means a weak collaboration between authors on this topic, and the opportunity for new collaborations. These authors [4] also encountered that: similar work, academic authority, and geographical closeness, helping to increase the collaboration network. Yeo and Lewis [4], through a qualitative case study of the process, the benefits, the motivations, and the difficulties of co-authorship in the field of linguistics, these authors [4] concluded that the co-authorship generates benefits for both co-authors and it is a trend.

Zang [5] makes a quantitative analysis of the network of 511 co-authors of Paul Erdős, using Grey relationship analysis, for which previously, based on the UCINET software analysis network, this author [5] evaluate five measures of the significant influence of co-authors: degree, betweenness, closeness, eigenvector, and publications.

Thus, there is a great possibility, applying co-authorship qualitative or quantitative analysis, to determinate relations between authors and until the form that the knowledge is constructed by the researchers. The contribution of this work is the determination of the research co-authors groups around the topic adsorption refrigeration and air-conditioning with solar energy, and the measure of the centrality degree.

## 2 Methodology

Firstly, the keywords are defined: “refrigeration” and “air conditioning” and “adsorption” and “solar energy”. After that, a search was made in the Science Direct database [6] using search strings. Identifying the authors with more publications in the period 2000–2019.

### 2.1 Search for Co-authors and Publications

Technological surveillance was carried out based on authors and journals for the following chain: “refrigeration” and “air conditioning” and “adsorption” and “solar energy”, for this purpose we searched the Science Direct Database, obtained 17 papers from 2001 to 2019, as appear in Table 1.

Table 2 was also implemented with co-authors who had more publications from 2000 to 2019.

**Table 1** Co-authors of the papers

Keywords	Papers	Main co-authors
“Refrigeration” and “air conditioning” and “adsorption” and “solar energy	17	[1, 2, 7–21]

**Table 2** Authors with more publications in that period

Keywords	Papers	Main authors	Source title	No
“Refrigeration” and “air conditioning” and “adsorption” and “solar energy	17	R. Z. Wang	Renewable and sustainable energy reviews	2
			Energy conversion and management	2
			Applied energy	1
			Progress in energy and combustion science	1
			Energy and buildings	1
			Applied thermal engineering	1
			Renewable and sustainable energy reviews	1
		T. S. Ge	Energy conversion and management	1
		Energy	2	
		Y. J. Dai	Renewable and sustainable energy reviews	1
			Energy conversion and management	1
			Applied energy	1



**Table 3** A representative part of the co-authoring matrix

	F. Xu	Z. F. Bian	T. S. Ge	Y. J. Dai
F. Xu	0	1	1	1
Z. F. Bian	0	0	0	0
T. S. Ge	0	0	0	1
Y. J. Dai	0	0	0	0

## 2.2 Construction of Author-Networks

The networks between the authors are mapped using Gephi software to determine the groups of authors that have generated the greatest collaboration in the study of the subject. The nodes of each group are analyzed separately looking for determining the co-authorly inside each group.

## 3 Results

### 3.1 Relations Between Authors

Firstly, the collaboration network between authors was determined using the Gephi network analysis tool. For this, the co-authoring matrix was generated (Table 3); in that matrix, the names of the authors are written in a column, these same authors are written in a header row, then for 17 articles is identified the co-authoring “1” or not co-authoring “0”. The network allows determining which authors have more co-authoring, as well as the authors who have less co-authoring. This determination is through the observation of links quantity. In Fig. 1, the results obtained were evidenced.

In Fig. 1 the most prominent authors through the size of the tags represent greater co-authorship. Next, the modularity of the graph is established by means of the Gephi modularity command, obtaining Fig. 2.

The modularity of the networks is a measure of the structure of the networks or graphs, so high-modularity networks have strong connections inside the groups but weak between nodes of different groups.

In Fig. 2 the labels are removed, and a 90° rotation is made, thus obtaining a new distribution of the nodes in the network. In Fig. 3 the subgraph with the largest number of nodes is separated, that is, the subgroup with the highest number of authors.

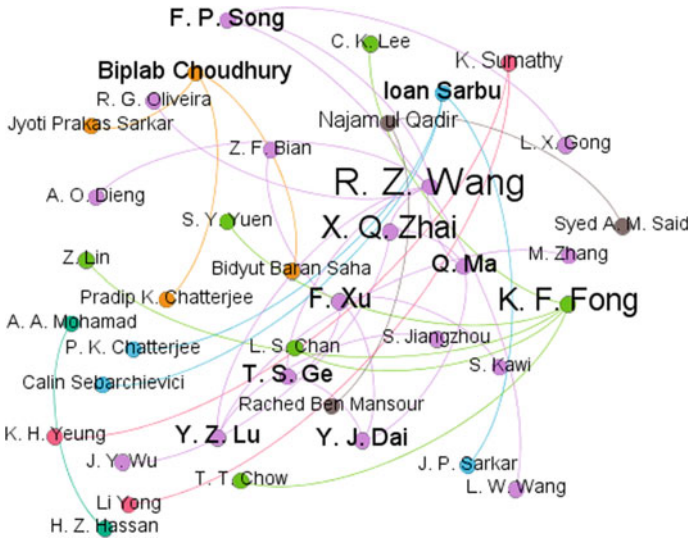


Fig. 1 Network of authors

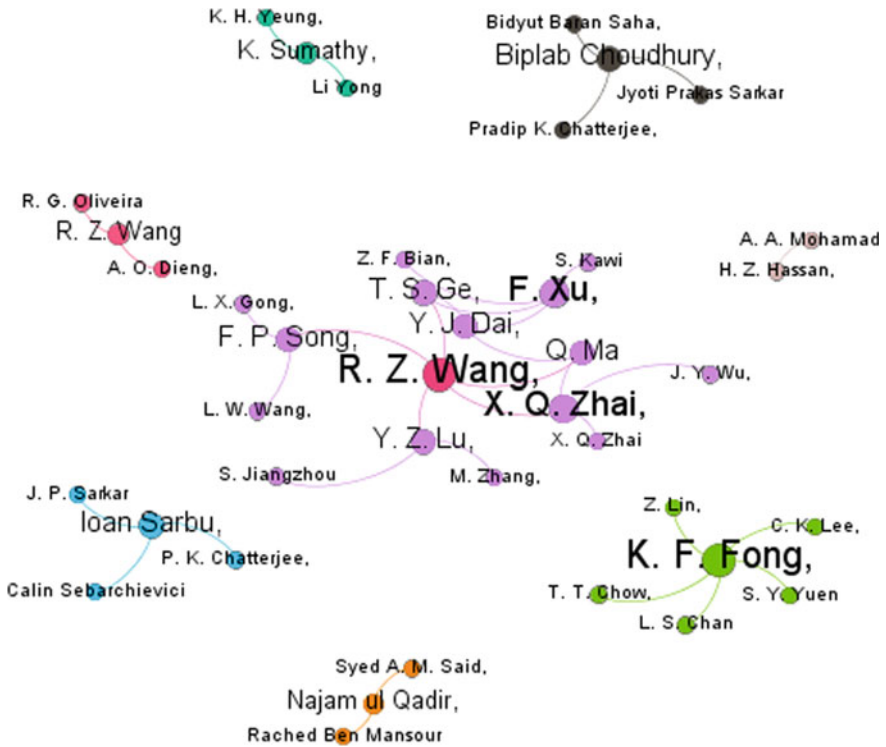
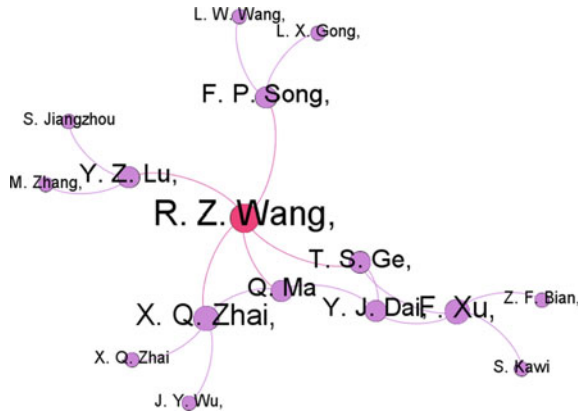


Fig. 2 Group of authors

**Fig. 3** Extraction of the main node



### 4 Analysis of the Results

According to Fig. 1, the font size of the author’s name indicates that the author has more co-authorship. In this case R. Z. Wang has most co-authors, followed by Zhai, Fong, Choudhury, Sarbu, Ma, Xu, Ge, Lu and Day.

In Fig. 2, eight nodes are identified (R. Z. Wang, I. Sarbu, R. Z. Wang, K. F. Fong, K. Sumathy, H. Z. Hassan, B. Choudhury, and N. Qadir as main authors), of which the nodes of R. Z. Wang are almost at center the image and are more scattered than the authors of the other node of this same author on the left of Fig. 2, which means that these authors are conducting further research.

It is also evident that four nodes (K. F. Fong, K. Sumathy, N. Qadir and H. Z. Hassan) haven’t bridge with any another group, indicating that no author of these sub-groups collaborates outside their group; however, a bridge is observed in common with two nodes (both of R. Z. Wang). In the largest node of R. Z. Wang, it’s also seen that five main authors are Song, Lu, Zhai, Ge, and Xu, having all of them as the principal author of R. Z. Wang. Also is observed that the nodes of Choudhury and Sarbu have a tenuous connection by Chatterjee author.

By the dispersion of nodes in the network of Fig. 2, it is evidenced that it is a multigraph with eight groups, which also is visualized that in the central part the nodes are more connected these are two groups (both of R. Z. Wang, one minor and one major). In Fig. 3, the connectivity inside the major group of R. Z. Wang, which is linked to the minor group of R. Z. Wang evidenced the preponderance of this author.

The centrality degree, that is measured by the number of connections of each node with another node, was determined as 7 for R. Z. Wang, 5 for K. F. Fong, 4 for X. Q. Zhai and 3 for B. Choudhry and I. Sarbu.

## 5 Conclusions

In the matter of refrigeration and air conditioning by adsorption with solar energy, it is found that the research from 2001 to 2019 did not provide many bibliographical references, but it was possible to identify seventeen documents that were analyzed by Gephi software, the result was that the main author of this topic is R. Z. Wang, who is referenced as the main author in two nodes, having as major co-authors Song, Lu, Zhai, Ge, and Xu. However, there are other authors such as Fong, Qadir, Sumathy, and Hassan who do not have any bridge in common but are still investigating.

Inside these identified research nodes and their respective links, knowledge is codified participatory and the understanding of this construction results important to enter and participate in these knowledge spaces.

The challenge is to continue with these measurements of software tools in much more numerous environments and in contexts in which social networks are part of the daily life of each author, comparing performance and results according to the case study proposed.

New researches about the publication's contents of determined groups (node and links) with tools as *Lingua Kit*, for a revision and classification of contents without a previously reading, will be the continuity of this research.

## References

1. Dieng, A.O., Wang, R.Z.: Literature review on solar adsorption technologies for ice-making and air-conditioning purposes and recent developments in solar technology. *Renew. Sustain. Energy Rev.* **5**(4), 313–342 (2001). [https://doi.org/10.1016/S1364-0321\(01\)00004-1](https://doi.org/10.1016/S1364-0321(01)00004-1)
2. Hassan, H.Z., Mohamad, A.A.: A review on solar-powered closed physisorption cooling systems. *Renew. Sustain. Energy Rev.* **16**(5), 2516–2538 (2012). <https://doi.org/10.1016/j.rser.2012.02.068>
3. Wang, C., Cheng, Z., Huang, Z.: Analysis on the co-authoring in the field of management in china: based on social network analysis. *Int. J. Emerg. Technol. Learn.* **12**(6) (2017). <https://doi.org/10.3991/ijet.v12i06.7091>
4. Yeo, M., Lewis, M.: Co-Authoring in action: practice, problems and possibilities. *Iran. J. Lang. Teach. Res.* **7**(3), 109–123 (2019)
5. Zang, X.L.: The data mining based on the co-author network. *Adv. Mater. Res.* **926–930**, 3402–3405 (2014). <https://doi.org/10.4028/www.scientific.net/AMR.926-930.3402>
6. Science Direct Database. <https://www.sciencedirect.com/>
7. Choudhury, B., Chatterjee, P.K., Sarkar, J.P.: Review paper on solar-powered air-conditioning through adsorption route. *Renew. Sustain. Energy Rev.* **14**(8), 2189–2195 (2010). <https://doi.org/10.1016/j.rser.2010.03.025>
8. Xu, F., Bian, Z.F., Ge, T.S., Daia, Y.J., Wang, C.H., Kawi, S.: Analysis on solar energy powered cooling system based on desiccant coated heat exchanger using metal-organic framework. *Energy* **177**, 211–221 (2019). <https://doi.org/10.1016/j.energy.2019.04.090>
9. Sarbu, I., Sebarchievici, C.: General review of solar-powered closed sorption refrigeration systems. *Energy Convers. Manag.* **105**, 403–422 (2015). <https://doi.org/10.1016/j.enconman.2015.07.084>

10. Fong, K.F., Lee, C.K., Chow, T.T., Lin, Z., Chan, L.S.: Solar hybrid air-conditioning system for high temperature cooling in subtropical city. *Renew. Energy* **35**(11), 2439–2451 (2010). <https://doi.org/10.1016/j.renene.2010.02.024>
11. Fong, K.F., Lee, C.K., Chow, T.T., Lin, Z., Chan, L.S.: Simulation-optimization of solar—thermal refrigeration systems for office use in subtropical Hong Kong. *Energy* **36**(11), 6298–6307 (2011). <https://doi.org/10.1016/j.energy.2011.10.002>
12. Zhai, X.Q., Wang, R.Z., Wu, J.Y., Dai, Y.J., Ma, Q.: Design and performance of a solar-powered air-conditioning system in a green building. *Appl. Energy* **85**(5), 297–311 (2008). <https://doi.org/10.1016/j.apenergy.2007.07.016>
13. Ul Qadir, N., Said, S. A. M., Ben Mansour, R.: Modeling the performance of a two-bed solar adsorption chiller using a multi-walled carbon nanotube/MIL-100 (Fe) composite adsorbent. *Renew. Energy* **109**(C), 602–612 (2017). <https://doi.org/10.1016/j.renene.2017.03.077>
14. Choudhury, B., Saha, B.B., Chatterjee, P.K., Sarkar, J.P.: An overview of developments in adsorption refrigeration systems towards a sustainable way of cooling. *Appl. Energy* **104**, 554–567 (2013). <https://doi.org/10.1016/j.apenergy.2012.11.042>
15. Sumathy, K., Yeung, K.H., Yong, L.: Technology development in the solar adsorption refrigeration systems. *Prog. Energy Combust. Sci.* **29**(4), 301–327 (2003). [https://doi.org/10.1016/S0360-1285\(03\)00028-5](https://doi.org/10.1016/S0360-1285(03)00028-5)
16. Lu, Y.Z., Wang, R.Z., Zhang, M., Jiangzhou, S.: Adsorption cold storage system with zeolite–water working pair used for locomotive air conditioning. *Energy Convers. Manag.* **44**(10), 1733–1743 (2003). [https://doi.org/10.1016/S0196-8904\(02\)00169-3](https://doi.org/10.1016/S0196-8904(02)00169-3)
17. Ma, Q., Wang, R.Z., Dai, Y.J., Zhai, X.Q.: Performance analysis on an air-conditioning system of a green building. *Energy Build.* **38**(5), 447–453 (2006). <https://doi.org/10.1016/j.enbuild.2005.08.004>
18. Ge, T.S., Day, Y.J., Wang, R.Z.: Review on powered rotary desiccant cooling system. *Renew. Sustain. Energy Rev.* **39**, 476–497 (2014). <https://doi.org/10.1016/j.rser.2014.07.121>
19. Song, F.P., Gong, L.X., Wang, L.W., Wang, R.Z.: Study on gradient thermal driven adsorption cycle with freezing and cooling output for food storage. *Appl. Therm. Eng.* **70**(1), 231–239 (2014). <https://doi.org/10.1016/j.applthermaleng.2014.04.066>
20. Wang, R.Z., Oliveira, R.G.: Adsorption refrigeration - An efficient way to make good use of waste heat and solar energy. *Prog. Energy Combust. Sci.* **32**(4), 424–458 (2006). <https://doi.org/10.1016/j.pecs.2006.01.002>
21. Ge, T.S., Dai, Y.J., Wang, R.Z.: Performance study of silica gel coated fin-tube heat exchanger cooling system based on a developed mathematical model. *Energy Convers. Manag.* **52**(6), 2329–2338 (2011). <https://doi.org/10.1016/j.enconman.2010.12.047>

# Microsimulation of Public Transport Stops for the Optimization of Waiting Times for Users Using the Social Force Model



Francis Mendoza , Mayling Tong , Manuel Silvera ,  
and Fernando Campos 

**Abstract** Cities in the world aim to ensure the mobility of people, through the implementation of efficient Integrated Transportation Systems (ITS). This aims to improve the transport of people, which guarantees that they can be mobilized safely and without delays in the terminals and bus stops of the public transport system. The present article proposes a design of public transport stops aimed at optimizing the waiting time of users when transferring from one bus to another. For the validity of the proposal, the social force model of the Vissim program was used, where the behavior of the users within the bus stops was reflected. The results showed that the waiting times in the calibrated and validated microsimulation model were optimized by approximately 20%, which generates an improvement in the efficiency of the public transport system.

**Keywords** Bus stops · Transshipment · Public transport · Social force model

## 1 Introduction

Lima is a city composed of 43 districts and a population of approximately 9.32 million inhabitants, most of which are mobilized through the public transport system. Within this large number of users who have multiple trips, there are those who travel for work

---

F. Mendoza (✉) · M. Tong · M. Silvera · F. Campos  
Universidad Peruana de Ciencias Aplicadas, Av. Prolongación Primavera 2390, Santiago de Surco, Lima, Peru  
e-mail: [u201319942@upc.edu.pe](mailto:u201319942@upc.edu.pe)

M. Tong  
e-mail: [u201517371@upc.edu.pe](mailto:u201517371@upc.edu.pe)

M. Silvera  
e-mail: [manuel.silvera@upc.edu.pe](mailto:manuel.silvera@upc.edu.pe)

F. Campos  
e-mail: [pccifcam@upc.edu.pe](mailto:pccifcam@upc.edu.pe)

and study reasons. These represent the largest number of trips in the public transport system, especially during peak hours [1]. The municipality of Lima, in an attempt to provide a service that facilitates interurban transport, has implemented an Integrated Transportation System (ITS) which has failed to meet the needs of intermodal users. Taking these limitations into account, people have spontaneously identified, between the different public transport lines, interconnections where transshipment is made for the purpose of reducing travel time. These intersections can be identified within the city of Lima as specific points where a large number of these intermodal operations are carried out. An example where this type of activity is presented is the intersections located on main avenues. However, in general, these intersections present problems in the geometric design that prevent detecting the transshipment of people in an optimal and safe way, thus denying conflicts in the vehicle–turbo interaction and increases in the waiting time in the users. Considering that this problem is common in the entire public transport system of the city of Lima, the present research selects as an area of study an intersection located in a commercial area that has bus stops where this type of interconnections is located. This intersection will be simulated in the program Vissim<sup>1</sup> that uses the social force model<sup>2</sup> with the aim to optimize the current transshipment times seeking the efficiency of the public transport system.

## 2 State of the Art

The study of “urban transshipment” derived from the term “modal exchange,” has been successfully developed in several cities of the world such as Melbourne, Toronto, London, Sao Paulo, New Jersey, among others, as a clear concept used for the transport system management [2]. The main objective of these studies is to design an intermodal bus stop that guarantees the integrated and efficient transfer of passengers between routes and different modes of transport [3]. In this sense, the bus stops infrastructure must be designed taking into account the distribution of spaces to facilitate the route of the pedestrians, thus providing easy access to two or more modes of transport at the same time [4].

On the other hand, the safety of people during transshipment is one of the main elements in the design of an efficient intermodal bus stop. The security takes into account the protection of passengers against climatic conditions, the analysis of passenger travel paths, and the operating conditions of different modes of transport [5]. In addition, the waiting time and the user spacing when walking are considered when assessing the comfort level of a modal interchange stop [6]. In this way, the satisfaction and stress levels of the users are measured.

There is little research related to the use of microsimulation models to measure the residence time of buses at a bus stop. This is due to a large amount of data to be collected and the high costs that are generated in this kind of study. It is for this reason

---

<sup>1</sup>PTV Vissim—Viswalk.

<sup>2</sup>Helbing and Molnár [9].

that existing investigations take into account for the calculation of transshipment time only small field samples where a single route is analyzed, in order to identify the reasons for delays in the arrival of buses [7].

With regard to the Social Force Model<sup>3</sup> (SFM), there are several studies that apply it from different points of view. For example, extensions of the model have been made to analyze how the increase in the walking speed of some pedestrians generates an aggressive interaction in pedestrian behavior [8]. On the other hand, SFM allows the modeling of attractive and repulsive forces, to simulate the concentration and dispersion of pedestrians in specific places within the environment, such as artistic attractions and places where people who share social bonds gather [9]. In addition, SFM is also used to simulate people waiting for the arrival of a vehicle or bus. These waiting times influence the level of service of intermodal stations because they generate various paths that represent the pedestrian flow. Thus, Johansson et al. [10]. conclude that the analysis of people in the intermodal bus stop waiting for a vehicle, interacting with pedestrians walking through the same area, has a significant impact on the predictions provided by pedestrian microsimulation models.

### 3 Methodology

For the development of the new design of the intersection looking for the optimization of the waiting times of the buses, first, the information survey of the study area was carried out. Here, data related to intersection geometry, vehicular and pedestrian volumes, and pedestrian travel times were collected. Then, the different trajectories and maneuvers of public and private transport vehicles were identified.

Taking into account the scope of the investigation, four main vehicular interconnection patterns present at the intersection were considered within the analysis. With this information, the different routes and trajectories described by the users of the public transport system were plotted as shown in Fig. 1. In this way, it can be seen that each transshipment pattern has two different routes at most. These are the most used by the people present in the study area.

One of the particular problems of the study area was the identification of two transshipment routes described in unofficial pedestrian crossings, which puts the safety of pedestrians at risk. Another of the difficulties encountered in the transshipment is in the pedestrian–pedestrian interaction due to their density in zebra-type pedestrian cruises.



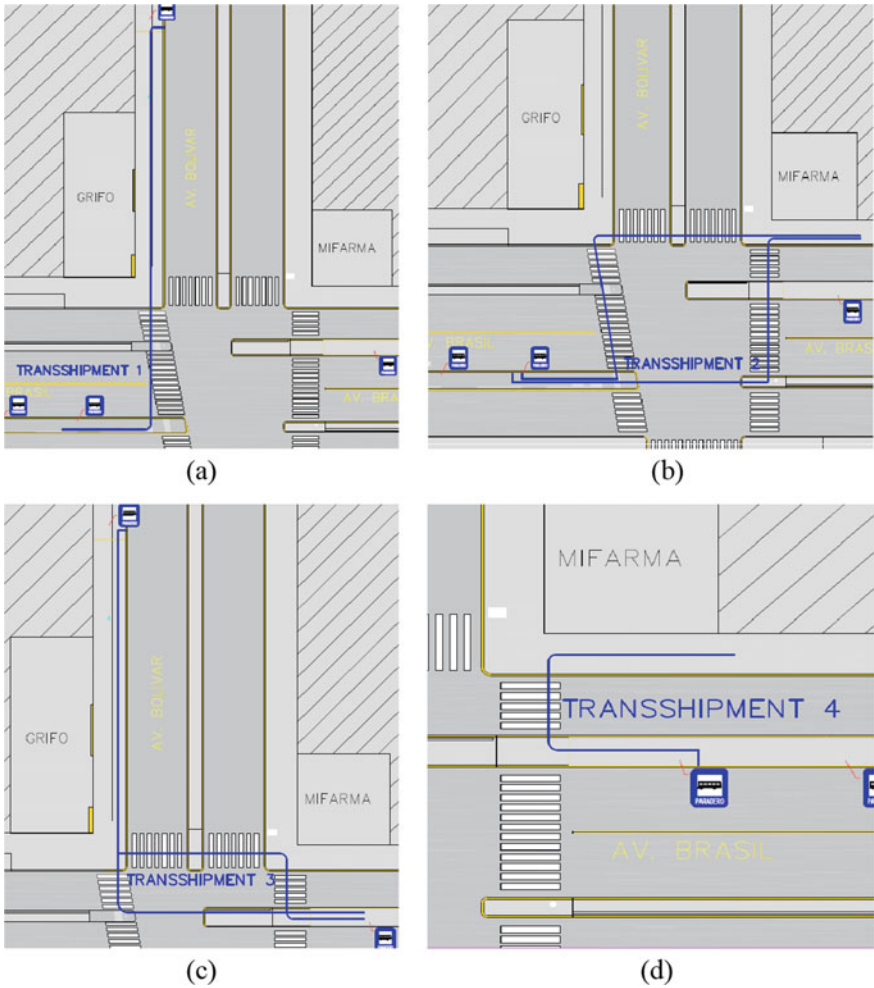


Fig. 1 Routes used by people for transshipment at the intersection studied

### 3.1 Technical Considerations

More than two transshipment paths within the study area overlap each other and, as a consequence, conflicts between pedestrians paths are generated. Moreover, the current state of the study area exposes the users to danger while they make an unofficial crossing between refuges islands. In order to increase the safety of the users and to reduce the necessary time to make a complete transshipment, some modifications aimed to facilitate the flow of pedestrians were proposed:

<sup>3</sup>Helbing and Molnár [9].

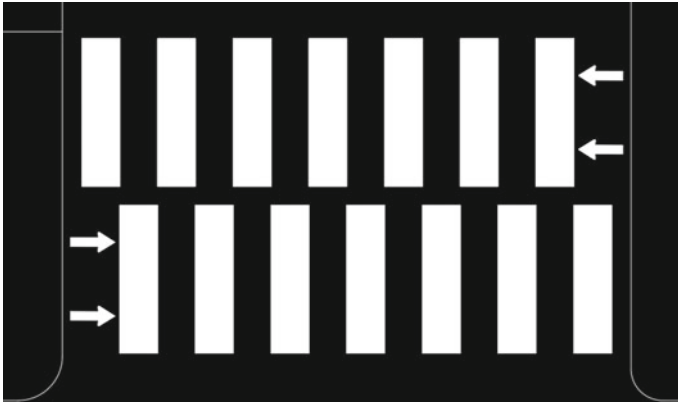


Fig. 2 Pedestrian crossing design proposed in the National Roads Authority (NRA)

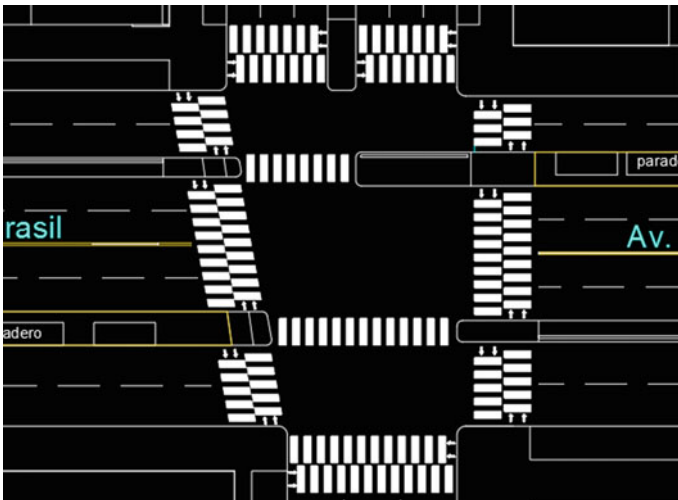


Fig. 3 Design proposal for pedestrian cruises within the intersection studied

1. Two-way pedestrian cruises to facilitate the flow of pedestrians by normalizing the direction of the crossings and channeling the flows as shown in Fig. 2. In order to perform the simulation of this new pedestrian behavior, it was necessary to iterate the social force parameters (Tau, Lambda, and Noise);
2. Considering the different transshipment routes generated by pedestrians, new pedestrian crossings were generated as shown in Fig. 3, which are made between the four refuge islands within the intersection. This facilitated the implementation of two transshipment routes (transshipment 2 and 3);
3. The Tau parameter was iteratively decreased until it reached a value that guarantees the optimum use of the spaces designated for pedestrians. Particularly

the calibration of this parameter in the corners of the intersection was considered, where the turning radius of the vehicles had to be reduced to increase the acceleration of the pedestrians.

4. The Lambda parameter was reduced due to the volume of pedestrians that make the transshipment. As this number of users is high, they are not very influenced by the people present in their environment; therefore, they can move together optimizing the space designated for pedestrians within the intersection.
5. The noise parameter of randomness was modified to ensure the optimum speed of pedestrians at the intersection. In this way, an efficient walking path of the pedestrian flow is guaranteed when the transshipment is made.

## 4 Results

When evaluating the behavior of the system with the modifications proposed at the intersection, reductions were obtained in the four transshipment times.

In the current configuration, the average time for transshipment 1 ranges between 90.92 and 99.53 s. However, when our proposal was implemented regards the simulation scenario, this average time decays to a range of 72.81–80.25 s as shown in Fig. 4.

In the case of transshipment 2, it can be seen that for the current state, the waiting times range between 120.12 and 142.23 s. This particular transshipment shows quite large data ranges compared to the other three transshipments, reaching up to 22.11 s in amplitude. However, through implementation, the average time could be reduced by 21.1% as shown in Fig. 5.

In the case of transshipment 3, the average times range between 134.56 and 147.82 s. These values were reduced to a new range of 107.61 and 116.54 s. In this case, the difference in amplitudes is 4.33 s and the average transshipment time for the 30 runs was reduced by 20.3% as shown in Fig. 6.

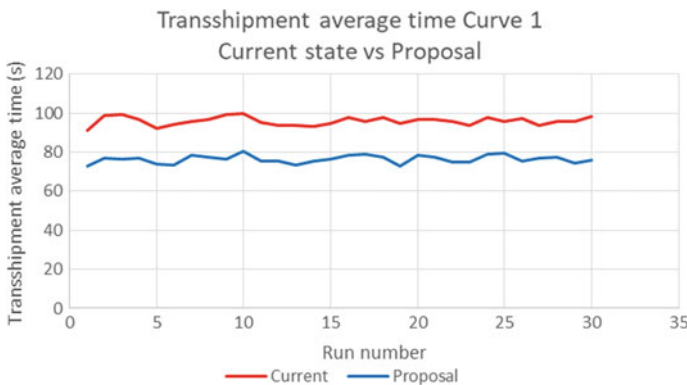


**Fig. 4** Comparative chart of current delays versus delays generated with the proposal for transshipment 1



Fig. 5 Comparative chart of current delays versus delays generated with the proposal for transshipment 2

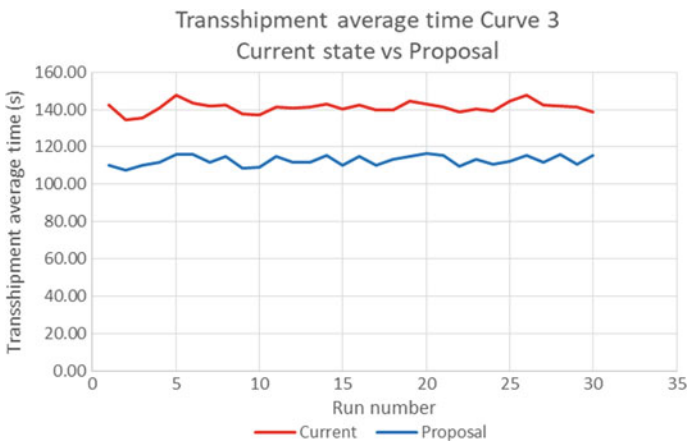


Fig. 6 Comparative chart of current delays versus delays generated with the proposal for transshipment 3

In the case of transshipment 4 shows average time values between 46.35 and 49.35 s, which were optimized to achieve a new range with limits of 35.47 and 41.05 s. In this transshipment, the amplitude of the results of the proposal is greater than those of the current state, however, a decrease in the average transshipment time of 20.2% was obtained, as shown in Fig. 7.

Finally, Table 1 summarized the results obtained in this research highlighting the difference regards the average time for each transshipment.



**Fig. 7** Comparative chart of current delays versus delays generated with the proposal for transshipment 4

**Table 1** Evaluation of maximum, minimum, and average transshipment times between the current situation (field data) of the intersection and our proposal

	Transshipment 1		Transshipment 2		Transshipment 3		Transshipment 4	
	Current	Proposal	Current	Proposal	Current	Proposal	Current	Proposal
Min (s)	90.92	72.78	120.12	96.07	134.56	107.61	46.35	35.47
Max (s)	99.53	80.25	142.23	112.61	147.82	116.54	49.35	41.05
Average (s)	95.91	76.32	131.84	104.00	141.19	112.57	48.34	38.56
Dif % average	20.42		21.09		20.26		20.24	

## 5 Conclusions

It is of high importance the preferences that pedestrians on some routes for transshipment. This helped our research to optimize the transshipment time and to facilitate decision making from the pedestrians. With the new design and redistribution of the spaces designated for pedestrians and vehicles, the time of each transshipment was approximately reduced by 20% compared to the times measured in the field. This result shows that studies involved in the optimal use of the current infrastructure are desired. As future work, the existing circumstances created by the users will be studied in order to enhance the current system considering other scenarios.

## References

1. Vamos, L.C.: IX Informe de percepción sobre calidad de vida en Lima y Callao. PUCP, Lima (2018)
2. Durán Bernal, L.M.: Basic parameters for the design of intermodal public. Transport. Res. Procedia **14**, 499–508 (2016)
3. Pitsiava-Latinopoulou, M., Iordanopoulos, P.: Intermodal passengers terminals: design standards for better level of service. Procedia Soc. Behav. Sci. **48**, 3297–3306 (2012)
4. Steinsiek, D.: On the Way to an Intermodal Transportation System-Improving the Cooperation in the Public Transport Sector of the Stadsregio, Utrecht (2014)
5. Litman, T.: Introduction of Multi-Modal Transportation Planning. Victoria Transport Policy Institute, Victoria (2009)
6. Oostendorp, R., Gebhardt, L.: Combining means of transport as a users' strategy to optimize traveling in an urban context: empirical results on intermodal travel behavior from a survey in Berlin. J. Transp. Geogr. **71**, 72–83 (2018)
7. Milkovits, M.N.: Modeling the factors affecting bus stop dwell time: use of automatic passenger counting, automatic fare counting, and automatic vehicle location data. Transp. Res. Rec. **2072**, 125–130 (2008)
8. Parisi, D., Dorso, C.: Microscopic dynamics of pedestrian evacuation. Phys. A **354**, 606–618 (2005)
9. Helbing, D., Molnár, P.: Social force model for pedestrian dynamics. Phys. Rev. **51**, 4282–4286 (1995)
10. Johansson, F.: Pedestrian Traffic Simulation Platform. Swedish National Road and Transport Research Institute (2013)

# Mathematical Model for the Improvement of Vertical Traffic at Universities



Julio C. Lazo Lozano  and Grimaldo Wilfredo Quispe Santivañez 

**Abstract** This article seeks to develop a methodology to reduce the travel time of the elevators and also to increase the number of users served by the elevators of the university, according to the schedule, said time saved achieves an improvement of the elevator service. The methodology based on a mathematical algorithm will determine that by changing the configuration of the elevators in attention capacity per floor and the round and attention times they establish a better travel time of the elevators. It is concluded that by applying the methodology developed in this article, a reduction of up to 37.5% of the travel time of the elevators is achieved, as well as an increase of the users attended by the elevators, being the increase of 10.66%.

**Keywords** Elevators · Mathematical model UpPeak · Vertical transport · Timing

## 1 Introduction

Multistory buildings have faced vertical elevator traffic problems during the past few years. Even though elevators solve transportation issues in high-rise buildings, they can also cause problems. For example, if an elevator is not correctly programmed for a building several stories high and with many different types of inhabitants (workers, students, etc.), it will probably experience an excess of demand and therefore fail to properly accomplish its task.

---

J. C. Lazo Lozano  
Universidad Tecnológica del Perú, Lima, Peru  
e-mail: [1410982@utp.edu.pe](mailto:1410982@utp.edu.pe)

G. W. Quispe Santivañez (✉)  
Universidad Nacional San Marcos, Lima, Peru  
e-mail: [gquispes@unmsm.edu.pe](mailto:gquispes@unmsm.edu.pe)

Vertical elevator traffic is not properly managed at universities. Although there have been several changes to the existing elevator stopping points at the university, these changes only provide a temporary solution to the problem. Assessments such as the waiting time approach allow recording the times and rhythms of the work corresponding to the elements of a given activity, either a specific or a general task, with the aim to measure exactly the entire workflow [1]. The queues that are formed in a vertical traffic system have irregular sizes [2] because many times this type of system is designed according to the criteria and experience of the designer without objective parameters [3], and cannot be maximized the service provided [4]. The problem of vertical traffic is centered on buildings for work purposes, which have a large number of floors. Traffic patterns can be divided into five different traffic patterns, which are: maximum ascending traffic, maximum descending traffic, noon traffic, traffic with balanced plans, and traffic between unbalanced plans [5]. To carry out an adequate study [6], the simulation will compare different designs [7], which will be analyzed in discrete events [8], which are generated in the vertical upward traffic pattern, because preliminary evidence shows that demand of the users comes mainly from the main floor to the other floors of the building and are the busiest hours of traffic. In this context, this study assesses the possibility of an optimal selection of the elevator stop points to avoid vertical traffic. Consequently, an UpPeak mathematical model and a study of times in the elevators of the Technological University of Peru (UTP) were developed and validated.

## 2 Mathematical Model for Upward Traffic (UpPeak)

The items below are the most relevant for the mathematical vertical traffic model. They will be listed with their corresponding mathematical formulas:

1. The average number of passengers departing from the main floor:

$$P = \frac{80}{100}CC \quad (1)$$

CC maximum capacity of each car,

P average number of passengers per second departing from the main floor.

2. The average number of stops for a single elevator in each trip:

$$S = N \left( 1 - \left( \frac{N-1}{N} \right)^P \right) \quad (2)$$

N total number of floors served by the elevator without counting the main floor.



3. The average number of floors served at higher altitude:

$$H = N - \sum_{i=1}^{N-1} \left( \frac{i}{N} \right) P \quad (3)$$

4. The Average time per cycle, RTT :

$$\text{RTT} = T_r + T_d + T_p + T_l \quad (4)$$

$$T_l = 0.1 * T_d * T_p \quad (5)$$

$$T_d = t_d * S \quad (6)$$

$$T_p = T_{po} + T_{pi} \quad (7)$$

$$T_{pi} = P \quad (8)$$

$$T_{po} = k * P * f^{\frac{1}{3}} \quad (9)$$

- $T_l$  Calculation of time lost while the elevator is stopped  
 $T_d$  Calculation of time when the door opens until it closes.  
 $T_r = t_{\text{Lighth}}$  Time taken by a stopped elevator to reach the next adjacent floor at nominal speed.  
 $T_p$  Calculation of passenger loading and unloading times.

5. Meantime of arrival at the ground floor for each elevator:

$$\text{INT} = \frac{\text{RTT}}{L} \quad (10)$$

$L$  The total number of elevators in the group was considered.

6. System solvency capacity: It is defined as the number of passengers, measured as a percentage of the total population of the building, that the system is capable of transporting to its destination in 5 min (300 s) at maximum demand

$$\text{INT} = \frac{300}{\text{RTT}} \text{PL} \quad (11)$$

PL Number of people measured as a percentage of the total population of the building in 300 s.

7. Average waiting time per passenger:

$$AWT = \left( 0.4 + \left( 1.8 \frac{P}{CC} 0.77 \right)^2 \right) INT \quad (12)$$

8. Average elevator trip time:

$$ATT = 0.5 INT + 0.5 RTT \quad (13)$$

9. Average journey time:

$$AJT = AWT + ATT. \quad (14)$$

### 3 Methodology

First, we assessed the current UTP elevator service by conducting a user survey to better understand the degree of user dissatisfaction. Once the current service was assessed, a time study was performed to measure the time the elevator takes to travel to each floor, the time the elevator takes to go from the main floor to the last floor, the time the elevator takes to respond to a call from the main floor (Floor No. 01), and passenger waiting times from the moment they call the elevator to their arrival at their destination.

After the necessary information was gathered, an analysis is carried out [9], for the introduction of data to the software (Arena), once the current situation was simulated to observe the number of users served in more detail. Finally, we proposed a new distribution of the elevator stop point to increase the number of users served while traveling times are reduced, and the speed of service provided is increased [10].

### 4 Design

For the purposes hereof, the population is represented by the total number of users, approximately 15,160, during the night shift elevator service from 18:30 until

20:00 pm). The sample will be determined by a statistical calculation with a 95% confidence interval and an estimated error of 5%, which gives us 375 users.

#### **4.1 Time Study**

A time study was performed for all elevators, with the exception of the elevator that must stop on all floors according to regulation A.120, Sec.4 of the Accessibility for Disabled and Elderly People Act, which establishes that elevators must be set up to allow disabled people to move freely throughout the building. Therefore, this elevator, which is required by law to make a stop at every floor, was not taken into consideration.

The study began by taking the travel time from the main floor (Floor 1) to different floors and the number of users exiting the elevator on these floors.

#### **4.2 Simulations**

The following data were required to prepare the simulation [11].

- Passenger arrival time: 6 s
- Travel time to each floor
- Number of passengers that fit inside the elevator
- Number of passengers exiting the elevator on each floor.

The simulation timeframe was from 6:30 to 7:00 pm (30 min), as the highest demand occurs within this period. Passengers arrive every 6 s, pass through a counter, and then make a queue to use the elevator. The elevator departs once it is loaded with 17 passengers, which represents the mean capacity of the elevator. Two passengers exit on the 4th floor, six passengers exit on the 8th floor, eight passengers exit on the 12th floor, and one passenger exits on the 15th floor. Similarly, the time taken by the elevator to go up to the fourth floor and unload passengers is 12.91 s, from the 4th to the 8th floor is 24.64 s, from the 8th to the 12th floor is 29.14 s, from the 12th to the 15th floor is 26.48 s, from the 1st to the 15th floor is 88.97 s, from the 1st to the 12th floor is 60 s, and from the 1st to the 8th floor is 38.81 s. Therefore, current traffic flow at the Arequipa tower elevator service is as follows:

In the first simulation performed in Hall A, a total of 229 passengers were served from 6:30 to 7:00 pm. As two elevators are being used, we may consider 458 passengers served in total.

In the second simulation conducted in Hall B, a total of 169 passengers were served from 6:30 to 7:00 pm. As two elevators are being used, the total would be 338 considering both.

### 4.3 Mathematical Model Application

The mathematical model was applied for data validation. A small margin of error can be found between the field study and the mathematical model.

Table 1 presents the data obtained by applying the mathematical model, it can be concluded that current elevator passenger travel times can be reduced.

Regarding the time summary table for elevators in Halls A and B, there is a 4% difference between the mathematical model and the field study as presented in Table 2.

### 4.4 New Floor Selection

Considering the results from the simulation above, the new stopping points proposed are as follows:

- Tower A:
  - S2-1-4-8-12
  - 1-8.
- Tower B:
  - S2-1-4-8-12-15
  - 1-12.

The stopping floor assignment will be changed only for two elevators, one for each tower, choosing the 8th and 12th floors as stopping points because there are many classrooms on them. Therefore, by applying the new stopping points, we obtain the following flow:

**Table 1** Arequipa tower summary (UpPeak Math.Mod.)

	RTT (seg.)	AWT (seg.)	ATT (seg.)	AJTT (seg.)
1.2	100.61	83.45	75.45	158.90
3.4	107.07	88.81	80.31	169.12

**Table 2** Time summary—arequipa tower

	Field study (seg.)	M. M. UpPeak (seg.)	Delta (seg.)
A	133	158.90	25.90
B	182.14	169.12	13
Average	315.14	328.02	12.88 <> 4%

**Table 3** Journey times

Current		Proposed		Improvement (seg.)
Assignment	Journey time (seg.)	Assignment	Journey time (seg.)	
s2-1-4-8-12	133	1-8	77.62	55.38
s2-1-4-8-12-15	182.14	1-12	120	62.14
Total	315	Total	197	117.52 <> 37.5%.

- In the simulation of the new floor proposal for the tower A elevator, a total of 255 users were served from 6:30 to 7:00 pm.
- In the simulation of the new floor proposal for the tower B elevator, a total of 238 users were served from 6:30 to 7:00 pm.

## 5 Results and Discussion

A time study was performed for all elevators, with the exception of elevators that are required to stop at all floors according to government regulation [12], which establishes that elevators must be set up to allow disabled people to move freely throughout the building.

Based on the results obtained, the stop points defined for the elevator represent the main factor increasing journey times; the more the number of stop points, the longer the trip will take. Hence, a new stop point distribution was realized to reduce the number of elevator stops.

After acquiring the journey times, it was concluded that the elevator does not need to stop at the 4th and 15th floors because their passenger flow was between 1 and 2 people, which does not compensate for the time this journey lasts (Table 3).

As a result, the floors were only redistributed for two elevators, one from each tower. Comparing the current design with the new proposed design, total journey times could be reduced by 117.52 s, which translates into a 37.5% reduction.

## 6 Conclusion

This works found that reducing the points of stops of the elevators allows improving the efficiency and effectiveness of their service by 37.5%. In addition, the number of passengers served increased by 10.66%, thus reducing the waiting time. The main factor that generates an increase in travel time, are the stop points, the more stop points, the longer the trip will take.

As future work, a study of route frequencies may be carried out in order to calculate performance measures and propose improvements in the vertical traffic.

## References

1. Wong, P.: Propuesta de mejora del proceso de admisión en una empresa privada que brinda servicios de salud ambulatorios (2009)
2. Singer, M.: Una introducción a la teoría de colas aplicada a la gestión de servicios. En revista Abante (2008). <http://www.abante.cl/files/ABT/Contenidos/Vol-11-N2/Singer.pdf>. Last accessed 29 Apr 2019
3. Al-Sharif, L., Al Sukkar, G., Hakouz, A., Al-Shamayleh, N.A.: Rule-based calculation and simulation design of elevator traffic systems for high-rise office buildings. *Build. Serv. Eng. Res. Technol.* **38**(5), 536–562 (2017). <https://doi.org/10.1177/0143624417705070>
4. Ruiz, C.: Análisis de mejora de eficiencia energética en ascensores (2017). <https://dialnet.unirioja.es/servlet/tesis?codigo=122704>. Last accessed 07 Apr 2019
5. Iglesias, G.: Diseño y simulación de un algoritmo basado en lógica difusa para el despacho de ascensores en un edificio (2013). <http://docplayer.es/41380371-Disenyo-y-simulacion-de-un-algoritmo-basado-en-logica-difusa-para-el-despacho-de-ascensores-en-un-edificio.html>. Last accessed 27 Apr 2019
6. Fernández, F.: El análisis de contenido como ayuda metodológica para la investigación (2002). <https://www.revistacienciasociales.ucr.ac.cr/images/revistas/RCS96/03.pdf>. Last accessed 07 May 2019
7. Urquía, A.: Modelo orientado a objetos y simulación de sistemas híbridos en el ámbito del control de procesos químicos (2000) (Consulted on April 29, 2019)
8. Silva, C. A., Oliveira, M. N., Calixto, W. P., Santos, L. E. B., Barbosa, J. L. F., Silva, D. F. A.: Simulation and minimization of waiting time in rows of elevators of public buildings. In: 2017 CHILEAN Conference on Electrical, Electronics Engineering, Information and Communication Technologies (CHILECON), Pucon, pp. 1–6 (2017)
9. Suntaxi, C.: Diseño e implementación de un sistema de control y monitoreo para ascensores residenciales (2009). <http://dspace.ups.edu.ec/handle/123456789/6734>. Last accessed 29 Apr 2019
10. Hurtado, D.: Eficiencia en el proceso de instalación de ascensores en edificios residenciales para lograr un servicio de calidad (2016). <http://repositorio.usil.edu.pe/handle/USIL/2584>. Last accessed 29 Apr 2019
11. Systems Modeling: Arena (software) (2000). <https://www.arenasimulation.com>
12. Norma A.120 Accesibilidad para personas con discapacidad (2 de marzo de 2019) diario oficial del bicentenario el peruano

# A Novel Dataset for the Transport Sector in a Province of Peru



Miguel Arango Guerrero  and Pedro Shiguihara Juárez 

**Abstract** Problems related to public transport and private transport in Peru are persistent. New proposals to solve them arise, currently the world of data analysis is starting in Peru, there are not many open datasets useful that allow proposing solutions in each environment. In this paper, we will collect relevant data of the transport located in a province of Peru with more than 1000 users involved, restricted by a delimited geographic area and with 2 years of operations and more than 3000 transport services tracked. In this way, we highlight the importance of the data, the possible potential uses within the transport, and a case of use of the collected dataset.

**Keywords** Transport planning · Transport dataset · Public and private transport

## 1 Introduction

In this paper, we study a forecast model simulation for dropoff locations of the users in transport, using the concept of collaborative filtering and knowledge-based approaches. We construct a dataset from information provided by an urban transport system. The dataset contains records of completed transport services covering one year from December 2016 until October 2018 restricted by the geographic location in the province of Pisco, Perú. The generated data is quite faithful about the current behavior of users in that location. In Peru, urban transport systems are evolving at the digital level, regarding both public and private transports for different segments of socioeconomic groups, with the sole objective of improving the service provided to their customers. The advantage of digitizing transport systems is the ability to improve management, operations, reduce response times in processes, and especially

---

M. A. Guerrero (✉) · P. S. Juárez  
Universidad Peruana de Ciencias Aplicadas, Av. Prolongación Primavera 2390, Santiago de Surco, Lima, Peru  
e-mail: [u201211759@upc.edu.pe](mailto:u201211759@upc.edu.pe)

P. S. Juárez  
e-mail: [pedro.shiguihara@upc.pe](mailto:pedro.shiguihara@upc.pe)

the new way of storing and managing the data that is recorded through interactions with users [1]. Due to the interactions of users and operators of urban transport systems, it is possible to record all operations performed, regarding a request for a service to a rating based on the performance of the service provided. This data can be used to process them and get valuable information for the business in transport. The obtained dataset can be used to predict the destination location of a user. To do that, it is necessary to use algorithms that can detect patterns of behavior counting the variables that we provide and that have determined your destination location within a service.

To carry out this project, a prediction model of the user's destination location was built and allows to forecast a model for dropoff locations of users.

In Sect. 2, the related work is described. In Sect. 3, a brief theoretical foundation is depicted. In Sect. 4, the process for the generation of the dataset is detailed. In Sect. 5, the conclusions of this work are described.

## 2 Related Work

In [2], the destination or next pickup location prediction problem was explored and the authors proposed four new incremental learning methods. They found that multivariate multiple regression (MMR) is the best method in terms of accuracy when the training data sizes are large. When the training data sizes are small or moderate, then both the random forest (RF) and support vector regression (SVR) methods are good choices considering prediction accuracy and computational time.

Also, when the next pickup prediction problem is considered, the MMR method and the ensemble method are good performers in terms of prediction accuracy. Finally, in [2], the MMR method is seen to be generally better than the incremental artificial neural network (ANN) method in terms of prediction accuracy.

In [3], the authors used neural networks, obtaining a range of possible outputs for any given instance. Also, their work is focused on the personalized driving experience, helping to prevent accidents by reducing driver distraction. It can be trained to recognize who is in the car, learning their specific preferences and driving style and then apply this learning by using a range of variables, event history in the neighborhood can be added.

In [4], the authors experimented with models for predicting taxi pickups in New York City, observing the decision tree regression model performed best, likely due to its unique ability to capture complex feature dependencies. The decision tree regression model achieved a value of 33.47 for root-mean-square deviation (RMSD) and 0.9858 for R2—a significant improvement upon the baseline values of 145.78 for RMSD and 0.7318 for R2. The model proposed in [4] could be useful to city planners and taxi dispatchers in determining where to position taxicabs and studying patterns in ridership.

In [5], the authors proposed  $k$ -means clustering in order to estimate the most likely pickup points at any given hour and also predict the top nightlife hotspots by



learning trends from past pickups. In [6], the authors highlighted special events with peak travel times such as holidays, concerts, inclement weather, and sporting events. In this sense, the authors asseverate that to calculate demand time series forecasting during extreme events is a critical component of anomaly detection, optimal resource allocation, and budgeting that need to be covered.

In [7], it is specified that the travel demand can be measured and analyzed by different ways depending on the metrics like the entire trip route, the area of the end trip, traffic volume, person trip and vehicle trip, passenger vehicle and freight vehicle, person-mile traveled and vehicle-mile traveled. On the other hand, the travel demand can be measured and analyzed by different ways depending on metrics such as the entire trip route, the area of the end trip, traffic volume, person trip and vehicle trip, passenger vehicle and freight vehicle, person-mile traveled, and vehicle-mile traveled [8].

### 3 Theoretical Foundation

A forecast model allows us to estimate predictions from historical data and live data. It can be used regularly for the trending analysis. The prediction of time series or predictions of time series are a research area of great interest that has been in development for several decades.

In particular, in the last three decades, the interest in this area has increased especially because of the highest processing capacities by the computers, which allows realizing complex calculations in a few minutes or even in a few seconds. This increase in interrelation is reflected in the diversity of its applications in different disciplines, ranging from economics to engineering, where the prediction of time series is a currently active field of research.

With the information collected by urban transport systems, a dataset can be made available sequentially through time with the use of Bayesian networks and automatic learning is possible to find patterns or abstract behaviors that allow us to make predictions and make decisions based on the results.

The collaborative filtering approach uses the identities of users and items. Implicit descriptions of the user and items are obtained from a sparse matrix of ratings of items by users [9]. It is possible to learn about a user by the items they have previously rated and the users who have rated items in common with them by using cutting-edge technologies related to the machine learning modules provided by different software frameworks [10].

### 4 Datasets

In this paper, we provide two datasets, one for users and other for trips. Dataset related to users contains 1383 user records, collected from December 1, 2016, to October

1, 2018. The quality of the user dataset is consistent because they were recorded by real people located in the area delimited by the project and were manually verified by the data entered through the mobile application.

Between the months of August and September of 2017, greater user activity is seen within the application, since marketing strategies were applied in order to attract more users and promote the use of the application as shown in Fig. 1.

In Fig. 2, we can observe a heatmap of the final locations of all trips made by users, the green areas represent the locations geographically and the green areas represent locations in high attendance. A heatmap was made of the routes taken by each driver to complete the trips assigned to the dataset. The place that has been taken by more drivers is ‘Abraham Valdelomar’ Avenue, which is one of the most transited because connects almost the entire city.

Figure 3 shows the heat map of all the routes of the trips made by the drivers, the colors represent the number of times a driver has passed through that area, where then the green color represents a frequency of few times, and the red color represents a frequency of many times. For the elapsed time in the trips, we have categorized the time of all registered trips, in such a way:

1. High time trips: trips that last from 301 up to the maximum allowed number of seconds elapsed.
2. Medium time trips: trips that last from 121 to 300 s of duration.
3. Low time trips: trips that last from 0 to 120 s of duration.

The largest number of trips has been recorded with a lapse of time between 121 and 300 s. For the distances traveled in the trips, we have categorized the distance of all the records such as long-distance: trips that locomote from 2.51 km to the maximum allowed amount of distance traveled, medium-distance: trips that locomote from 0.51 to 2.5 km of travel and low-distance: trips that locomote from 0 to 0.5 km away. Further analysis corroborates that the largest number of registered trips is represented by low-distance trips.

As a compilation, Fig. 4 shows the categories of the trips by time and the quantity



**Fig. 1** User activity—from December 1, 2016, to October 1, 2018

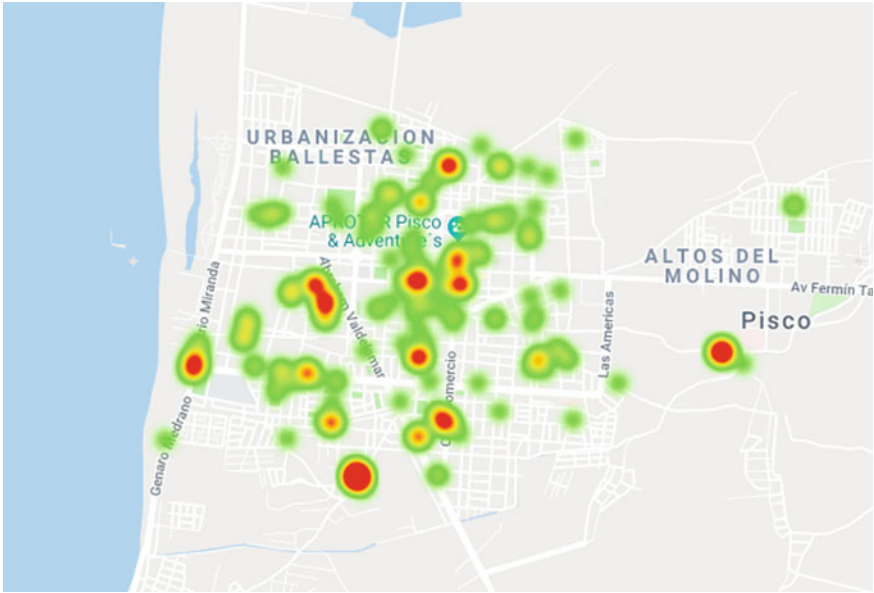


Fig. 2 Heatmap of dropoff locations for users

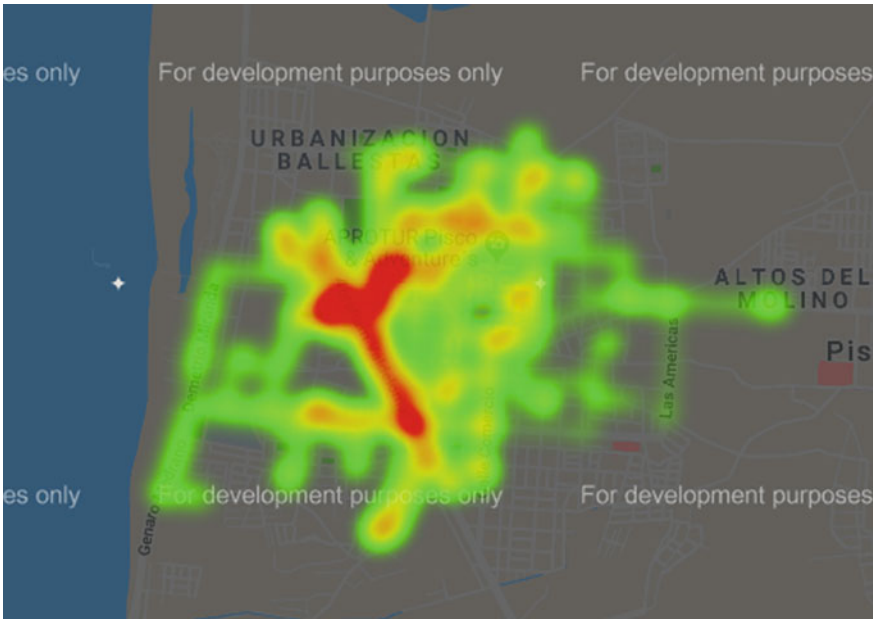


Fig. 3 Heatmap of drivers routes for trips

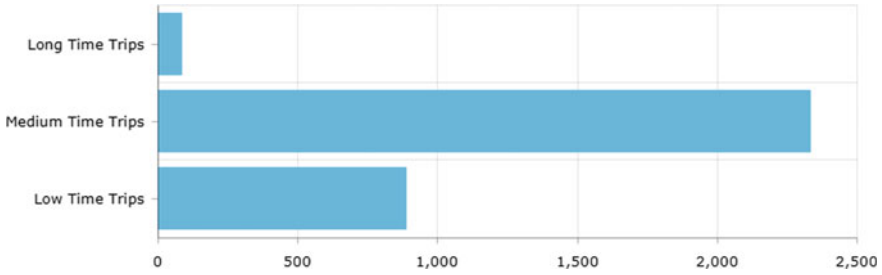


Fig. 4 Frequency of validated trips according to time

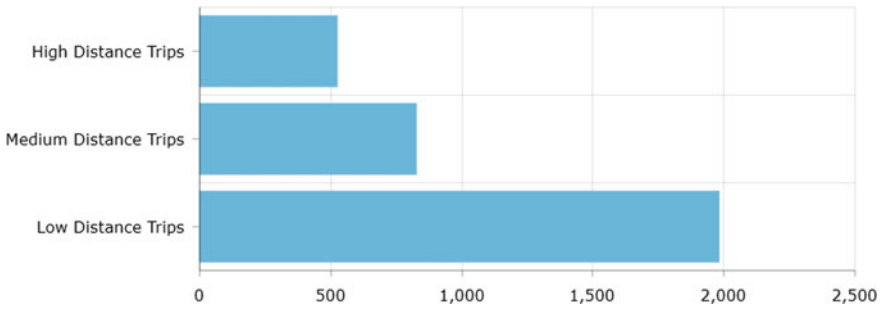


Fig. 5 Frequency of validated trips according to distance

of validated trips and Fig. 5 shows the categories of the trips by distance and quantity of validated trips.

These preliminary results indicate all the potentials this database might be able to have. Potential uses of the dataset could be (1) forecasting of service demand: get to predict the demand of trips within a certain period, (2) forecasting of the shortest route to complete a trip: get to choose the shortest route to get as quickly as possible to the user’s destination location, (3) forecasting of the estimated time for the journey of the trip: get to predict the time it will take the trip to be completed, (4) forecasting of the estimated distance for the journey of the trip: get to predict the distance that the driver will travel on the trip to be completed, (5) recommendation system for dropoff locations oriented to drivers: recommend dropoff locations to the driver, after having accepted a trip without a defined destination.

## 5 Conclusions

This work obtains information from a transportation business with a moderate effort. As a result, heat maps characterizing the behavior of users from private transport regards dropoff location in the city of Pisco, Perú, was successfully unveiled and

with more than three thousand records, it is possible to predictive models with an acceptable likelihood for final destinations from users.

As future work, there are some issues that can be approached such as forecasting of service demand, forecasting of the shortest route to complete a trip and forecasting of the estimated time for the journey.

## References

1. Westerman, G., Tannou, M., Bonnet, D., Ferraris, P., McAfee, A.: The Digital Advantage: How Digital Leaders Outperform Their Peers in Every Industry (1 June, 2019). <https://www.capgemini.com/resources/the-digital-advantage-how-digital-leaders-outperform-their-peers-in-every-industry/>
2. Laha, A. K., Putatunda, S.: Real Time Location Prediction with Taxi-GPS Data Streams. India (2017)
3. Gandhi, S.: Analysing and Predicting Driver's Next Location (2015)
4. Grinberg, J., Jain, A., Choksi, V.: Predicting Taxi Pickups in New York City. Autunmn (2014)
5. Kumar, J., Surana, J. Kapoor, M., Nahar, P. A.: Perfecting Passenger Pickups: An Uber Case Study
6. Nikolay, L.: Engineering Uncertainty Estimation in Neural Networks for Time Series Prediction at Uber (1 June, 2019). <https://eng.uber.com/neural-networks-uncertainty-estimation/>
7. Chatterjee, A., Venigalla, M.: Travel Demand Forecasting for Urban Transportation Planning (2004)
8. Studio 3T, GUI for MongoDB. Available in: <https://studio3t.com/>
9. Ben, J., Dan Frankowski, S., Jon, H., Shilad, S.: Collaborative Filtering Recommender Systems
10. Machine Learning Studio. Available in: <https://azure.microsoft.com/es-es/services/machine-learning-studio/>

# Development of a Mobile Application for English Language Learning Through Corrective Feedback



Adriana Guanuche , Gustavo Caiza , Osana Eiriz , and Roberto Espí 

**Abstract** Learning English as a foreign language is committed to using learning models that are linked to error correction by analyzing comments provided through corrective feedback to correct the error or to confirm the correct response. Having the chance to receive immediate corrective feedback allows students to be in contact directly with their learning process. This article implements an augmented reality application for learning English as a foreign language using corrective feedback and thus creating an accessible teaching tool that allows students to have additional teaching material to interact with the real world with virtual objects and animations. The application was designed by using Vuforia, Unity, Visual and Android Studio software. The objective of this article is to teach the student in an interactive way and consequently create a user-friendly link. The results show a great application in functionality using augmented reality for English language learning.

**Keywords** Corrective feedback · Augmented reality · Vuforia · Mobile application

## 1 Introduction

Knowledge and proficiency in the English language have become a fundamental necessity to meet the challenges of the twenty-first century. 1.5 billion people out of

---

A. Guanuche · G. Caiza (✉)  
Universidad Politécnica Salesiana, UPS, 170146 Quito, Ecuador  
e-mail: [gcaiza@ups.edu.ec](mailto:gcaiza@ups.edu.ec)

A. Guanuche  
e-mail: [aguanuche@ups.edu.ec](mailto:aguanuche@ups.edu.ec)

A. Guanuche · O. Eiriz · R. Espí  
Universidad de La Habana, 10200 La Habana, Cuba  
e-mail: [osanaeg@gmail.com](mailto:osanaeg@gmail.com)

R. Espí  
e-mail: [respi@flex.uh.cu](mailto:respi@flex.uh.cu)

7.53 billion people who exist in the world speak English, according to [1], that is, approximately one in five people are dominant by English, and so if English is their second language, any professional will be given better opportunities in the personal and professional world.

Due to the above and with the advance in Information and Communication Technologies (ICT), new techniques and applications for learning English have been developed. As for the techniques [2], mentions four models for language improvement which focus on learning-acquisition, self-monitoring, entry and affective filter. The first model focuses on language learning in a similar way to language maternal naturally and unconsciously, the second one has to do with conscious learning which is exposed to the correction of errors, the third model connects the student with their next level of language proficiency and the fourth takes into account the motivation of the student. In relation to the second and fourth models both take into account corrective feedback and motivation through apps. Corrective feedback consists of making known the errors present in evaluation so that the student does not feel dissatisfaction or annoyance with the mistake made, on the contrary, this serves to motivate him or her not to commit it again [3]. The main advantages of corrective feedback are: It provides comments on the wrong answers. It keeps students informed about their academic performance. It fosters in students the interest in self-correction. It is timely because it intervenes at the right time. It is flexible since it is adapted to the level of the student. It uses technological resources to speed up their intervention and, above all, it contributes to the improvement of learning [4–8]. The Augmented Reality (AR) aims to combine images generated by electronic devices, on the real-world vision captured by one or several cameras of that device [9, 10].

In several educational and design applications, information that is associated with the real world is generated; it can be mentioned the 4D Anatomy application, which allows visualizing on a class book the anatomical parts of the human body with their names and main characteristics in a three-dimensional way [11], a design application that has been very popular in North America is IKEA Place, which allows placing furniture from your catalog in the different home spaces having a three-dimensional idea of the appearance of this furniture before being placed [12].

This article implements an application of augmented reality for learning the English language using corrective feedback, the application was designed with vuforia, unity, visual studio, and android studio software. The objective is to reach the student in an interactive way and thus to create a friendly link with the user, leaving aside the traditionalism of education. The article is organized as follows: Sect. 2 describes the materials and methods used, Sect. 3 shows the design and implementation, Sect. 4 shows the results and finally Sect. 5 provides the conclusions.

## 2 Materials and Methods

### 2.1 *Augmented Reality*

Augmented reality increases the images of reality, from its capture by the camera of computer equipment or mobile device that adds virtual elements for the creation of a mixed reality to which computer data has been added. There are four levels at which levels can be understood as a way of measuring the complexity of the technologies involved in the development of RA systems [13, 14].

### 2.2 *Vuforia and Unity*

Vuforia is an application for the development of augmented reality applications, it is a web environment where the users can create and administrate their markers. This app is the leader thanks to its exceptional technology of artificial vision, efficient tracking benefits and its compatibility with multiple platforms. It is the most used software for digital devices and sunglasses currently available in the market [15].

Unity is a 3D figure reader that uses C, C++ and C Sharp languages. In order to execute the projects from Unity to mobile devices, it is indispensable to have the appropriate software development kits (SDK) that enable their reading [15].

### 2.3 *English Language Learning with M-Learning*

Mobile learning can be defined as the educational modality that facilitates knowledge construction, learning problem solving and the development of different skills in an autonomous way through the interaction with portable mobile devices. The development of M-learning has resulted in the creation of multiple applications for English language learning, being the most important ones: Duolingo, Wibbu English, uSpeak.

### 2.4 *Corrective Feedback*

It is defined as the information given to the students about their academic performance, it can be used to correct errors or congratulate on a correct answer [16]. The corrective feedback should be coherent, dynamic, clear, frequent and proactive [17–19]. The corrective feedback is classified as follows.

**Positive and negative:** Named positive to comments based on the correct answers, and the negative is granted to the wrong answers [8].



**Oral, written and mixed:** The corrective feedback could be through the oral or written word, and the mixed one with the combined use of the previous two [20].

**Explicit and implicit:** The first occurs when the teacher identifies the error and directly provides the correct answer, and the second occurs when the teacher invites the student to find the correct answer [21].

**Self-correction and peer correction:** The self-correction provides the opportunity for students to address the correct answer for themselves [22].

### 3 Development of the Mobile Application

The following tools were used to perform the English test application with AR: vuforia analyzes the recognition of images, unity allows to develop the graphic environment, and android installs the application previously generated in visual as shown in Fig. 1.

#### 3.1 Images Selection

For image recognition, the vuforia target image tool was implemented, this tool recognizes full detail images. The selected numbers obtained a result of 4 stars so, they will have easy recognition when executing the augmented reality application. The numbers selected to perform the application are those shown in Fig. 2.

Once the images are selected, each of the numbers is imported into vuforia, to generate the points that allow recognizing the characteristic patterns of the image, this analysis is carried out in grayscale, in this instance the image qualification is generated obtaining 4 stars as shown in Fig. 3.



Fig. 1 Implementation of the application

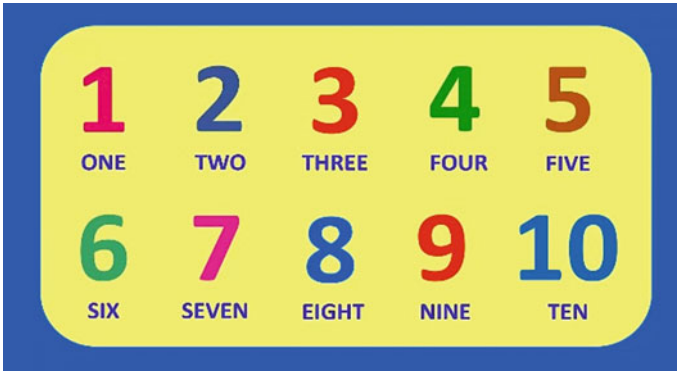


Fig. 2 Numbers selected for the augmented reality application



Fig. 3 Image recognition points

### 3.2 Application Development

The images must be imported to Unity where the application screen is configured with a resolution of  $2200 \times 1400$  pixels because it is the standard size of the screens, in addition, this measure allows us to run the application on higher resolution screens. Each image was assigned a scene of its own, each question has its own interface, where the texts of the application, theme, question number, answers, option buttons for correct or incorrect answers and feedback animations are generated as shown in Fig. 4.

Through Visual Studio, the feedback animations for correct or incorrect responses were programmed, this algorithm remains active for 2 s and then becomes invisible so that the user can practice several times until the topic is understood.

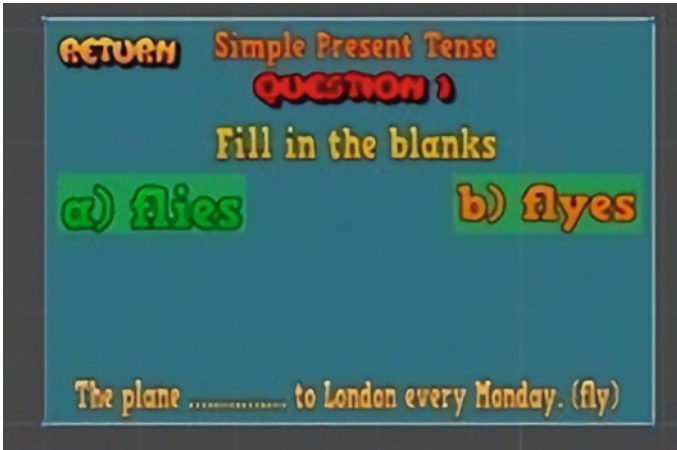


Fig. 4 Development in the unity program

### 3.3 Simulation of the Application

Before installing the app on the Smartphone, simulation in Unity is performed. Once the correct answer is chosen the app displays the message “Correct” within the check icon and a happy face as shown in Fig. 5.



Fig. 5 Correct answer feedback

### 4 Results

Next, the apk file, English Test.apk, is generated. Finally, the application is built through the Android Studio platform and now is ready to be installed in a Smartphone. The application contains 4 types of questions: Fill in the blanks, Multiple Choice, Structure Sentences and True or False. The type of questions used on the application responds to the advantage of using accurate content on learning, an appropriate technological medium, and proper monitoring of the academic progress. Figure 6 shows how the application works for Multiple Choice questions. The first step is to run the application on the smartphone, the next step is to focus on any number belonging to the database. Finally, the question is shown.

In the last figure the option “ANSWER ME” is displayed, in which you click on and the different options appear depending on the type of question. Then the student chooses whatever option and up to his answer a message is showed if the choice was correct or incorrect with the corresponding feedback as it is seen in (Fig. 7).

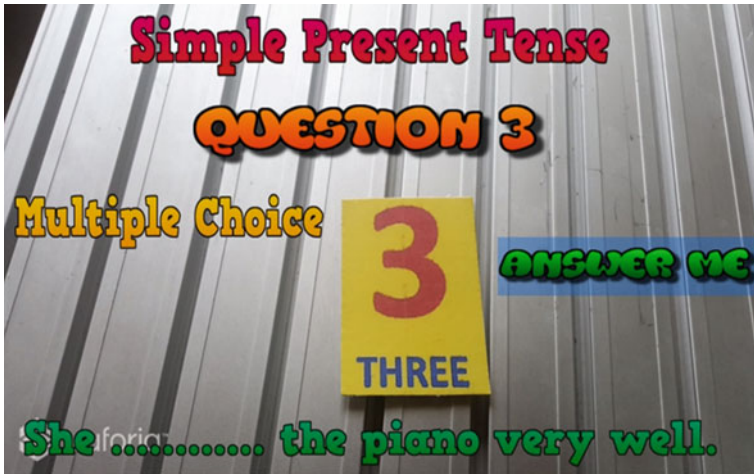


Fig. 6 Development of the unity program application

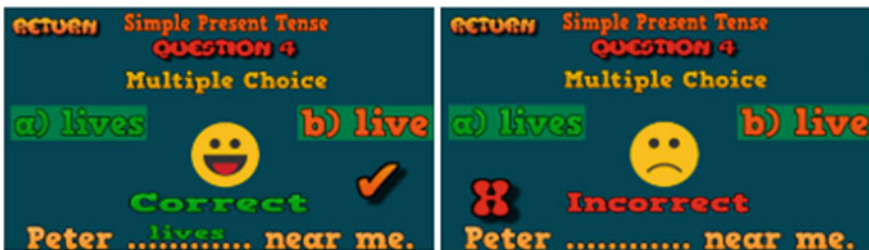


Fig. 7 Feedback for answers

The functioning application results show that it is very friendly with the user and considers advantages of corrective feedback for learning of the English language.

## 5 Conclusions

The English learning application as a foreign language using augmented reality is an approachable and didactic tool that allows students to have extra didactic material in order to interact with the real world through virtual objects and animations. An important fact of the application is that it can be installed in whatever mobile phone without being limited to the operative system so it can be set up for multiplatform systems.

The corrective feedback represents support for the English learning process since it allows students and teachers to have the possibility of being informed about the academic advance as well as it encourages students to be more participative through the error correction or the verification of the correct answer. If the answer is correct feedback allows students to confirm their response or if it is incorrect error correction motivates students to look for the right response.

## References

1. Robin, L.: ¿Podrá el inglés seguir siendo el 'idioma favorito' del mundo? (2018). Available: <https://www.bbc.com/mundo/noticias-44232687>. Accessed: 22 July, 2019
2. Cerdas, G., Ramírez, J.: La enseñanza de lenguas extranjeras: historia, teoría y práctica. *Rev. las Lenguas Mod.* 297–316 (2015)
3. Aumentada, R.: Aplicaciones De Los Dispositivos Móviles Augmented Reality, an Evolution of Theapplication. *Rev. Medios Y Educ.* **41**, 197–210 (2012)
4. Daneshvar, E., Rahimi, A.: Written corrective feedback and teaching grammar. *Procedia Soc. Behav. Sci.* **136**, 217–221 (2014)
5. Aranguiz, M. F., Espinoza, A. Q.: Estudios de lingüística inglesa aplicada, 103–131 (2016)
6. Chen, S., Nassaji, H., Liu, Q.: EFL learners' perceptions and preferences of written corrective feedback: a case study of university students from Mainland China. *Asian-Pacific J. Second Foreign Lang. Educ.* 1–17 (2016)
7. Lima, S.: Enriquecer la realimentación para consolidar aprendizajes **14**, 9–26 (2017)
8. Ene, E., Upton, T.A.: Journal of second language writing synchronous and asynchronous teacher electronic feedback and learner uptake in ESL composition. *J. Second Lang. Writ.* **41**(May), 1–13 (2018)
9. Prendes Espinosa, C.: Realidad aumentada y educación: análisis de experiencias prácticas. *Píxel-Bit, Rev. Medios y Educ.* (46), 187–203 (2014)
10. Basogain, X., Olabe, M., Espinosa, K., Rouèche, C., Olabe, J. C.: Realidad Aumentada en la Educación: una tecnología emergente (2012)
11. Interactive Anatomy Zrt: 4D Anatomy (2018). Available: <https://www.4danatomy.com/>. Accessed: 23 July, 2019
12. Inter IKEA Systems: IKEA Mobile App (2019). Available: <https://www.ikea.com/gb/en/customer-service/mobile-apps/>. Accessed: 23 July, 2019
13. Fombona Cadavieco, J., Vázquez-Cano, E.: Posibilidades de utilización de la geolocalización y realidad aumentada en el ámbito educativo 319–342 (2017)

14. Méndez, M., Carracedo, J. P.: Realidad Aumentada: Una Alternativa Metodológica en la Educación Primaria Nicaragüense. *IEEE Rita* **7**, 102–108 (2012)
15. Estefanía, Paspuel, T.: Estudio del motor de videojuego unity con sdk vuforia para el desarrollo de aplicaciones móviles de realidad aumentada, aplicación de tarjetas ilustradas en pares para niños (2014)
16. Kerr, P.: Giving feedback on speaking. *Giv. Feed. Speak. Part Cambridge* **92**, (December, 2017)
17. Sánchez, S.: retroalimentación oral en la adquisición de segundas lenguas, 283–311 (2014)
18. Hernández-Islas, M.: La retroalimentación automatizada en la enseñanza del inglés como segunda lengua. *Rev. Iberoam. Ciencias* **3**, 156 (2016)
19. Núñez, L. M.: La retroalimentación en la enseñanza de la expresión escrita en inglés: un proyecto de desarrollo profesional *Feedback on teaching writing in English* (2016)
20. Ortiz, M.: Uso de la retroalimentación correctiva focalizada indirecta con claves metalingüísticas en la adquisición del sufijo -s en la tercera persona del singular en inglés, en estudiantes de un programa de formación pedagógica en efl de una universidad chilena. *Folios* **44**, 127–136 (2016)
21. Hernández, M.: La retroalimentación automatizada en la enseñanza del inglés como segunda lengua. *Rev. Iberoam. Ciencias* **3** (2016)
22. Silva, M.: La retroalimentación en la corrección de la escritura. *Rev. Lingüística* **15** (2015)

# Influence of the Chinese Culture on the Negotiation Process Peru-China



Nicole Alexandra Acevedo Cueva 

**Abstract** This research is an intercultural study conducted with a deductive approach by generating theory-based questions derived from the socio-cultural framework of the Chinese business negotiation process, to be proved by the application of a self-managed open questionnaire on a sample of seven experienced Peruvian negotiators in negotiating with Chinese in order to determine how the Chinese negotiating culture influences the negotiation process. The results proved that the Chinese negotiating culture does influence the negotiating process according to the perception of 100% of the participating Peruvian negotiators and derives the following characteristics that a Peruvian negotiator could visualize and for which should be prepared during negotiations with Chinese to achieve success: the importance of knowing about the negotiating culture of the Chinese counterpart, the relevance of presenting exact information, the presence of an intermediary or mediator, the significance of socializing with the Chinese, the difficulty of negotiating the price, the slow and hierarchical Chinese decision-making process, the reluctant Chinese attitude to make concessions, the importance of signing a legal contract, and the Chinese tendency to renegotiate.

**Keywords** Chinese negotiating culture · Negotiation process · Peruvian negotiator

## 1 Introduction

China has held a position of being an economic power worldwide that made Chinese culture and its negotiation process the focus of attention for western countries [1] interested in establishing agreements to access the desired Chinese market. However, the negotiation with a Chinese counterpart is complicated [2], since foreign and Chinese negotiation process often seems incompatible because of their differences

---

N. A. Acevedo Cueva (✉)  
Universidad Privada del Norte, Trujillo 13006, Peru  
e-mail: [acevedoc.nicole@gmail.com](mailto:acevedoc.nicole@gmail.com)

with deep cultural origins [3], which indicates that the way people negotiate is influenced by culture. At the same time, culture is defined as a framework in which international negotiators adjust their strategies, tactics, and styles in order to obtain success in negotiations; because when intercultural negotiations fail, the common reason is related to cultural misunderstandings. So, this fact determines that a Peruvian negotiator will have to adapt to the culture and, especially, to the negotiation process of the Chinese counterpart in order to achieve success [4].

### ***1.1 The Influence of Chinese Negotiating Culture on the Negotiation Process***

Ghuri and Fang [2] designed a framework that lends a way of studying the influence of Chinese negotiating culture in three interlinked dimensions such as Confucianism, Sun Tzu's stratagems, and sociopolitical and cultural condition; on the stages of negotiation process: pre-negotiation (search for influence, presentation, informal discussion, and trust-building), formal negotiation (task-related exchange of information, persuasion, concession, and agreement), and post-negotiation (new rounds of negotiation). Therefore, the Chinese cultural bases are determining factors in the negotiation process with a Chinese counterpart, because the success or failure will depend on the adaptation and comprehension that the negotiator has about Chinese culture and its way of doing business [5].

### ***1.2 The Motivation of the Work***

China has positioned for four consecutive years as Peru's first strategic business partner with almost 170 Chinese companies operating in Peru's territory with an investment of more than 18 billion dollars [6]. A reality that proves the existence of efficiently developed negotiations.

The purpose of this investigation was to benefit the negotiations between Chinese and Peruvian parties by providing a number of characteristics derive from the influence of Chinese negotiating culture on the negotiation process that a Peruvian negotiator could face and therefore adapt in order to establish agreements, which is highly feasible due to the Peruvian tendency to accommodate their negotiation process according to the counterpart's culture in order to avoid conflicts and obtain success [7]. Despite being able to collect numerous documents about the commercial trajectory between Peru and China, almost none of them describes the actual negotiation; and regardless the numerous theory about Chinese negotiation or culture that describes how the Chinese act during international negotiations, there is a possibility that could be certain variations while negotiating with Peruvians. Because of this,



the importance of this exploratory investigation is to be an initial point for further investigations about the intercultural negotiations.

This research sought to determine how the Chinese negotiating culture influences the negotiation process according to the perception of a Peruvian negotiator. Therefore, the first objective is to determine the manifestation of the Chinese negotiating culture regarding the dimensions of Confucianism, Sun Tzu's stratagems, and sociopolitical and cultural condition, according to the perception of a Peruvian negotiator. The second objective is to determine the existence of influence of the Chinese negotiating culture's dimensions on the stages of the negotiation process according to the perception of a Peruvian negotiator. The third objective is to determine the characteristics of the negotiation process influenced by the Chinese negotiating culture's dimensions regarding to the stages of pre-negotiation, formal negotiation, and post-negotiation according to the perception of a Peruvian negotiator.

## 2 Methodology

This research is based on a qualitative methodology, a triangulation technique of three types: data triangulation, methodological triangulation, and theoretical triangulation [8] was applied to derive a procedure of three phases: (1) applying data triangulation by designing the self-administered open questionnaire in line with the indicators of each of the dimensions of the respective study variables; (2) applying the methodological triangulation by executing the questionnaire; and (3) applying theoretical triangulation by compiled the participants responses and classifying the qualitative data, involved that the data collected had to be read and reread, where codes were assigned to the participants to identify their responses in each category and how often they alluded to the same topic or word—to finally be contrasted with previous research, theories, or findings.

The study was carried out considering a type of non-probability sampling for convenience, obtaining a sample of seven Peruvian international negotiators with experience in the role of negotiator with a counterpart of Chinese nationality. The self-managed open questionnaire data collection method was applied and declared qualified with a corrected range validity coefficient of 1.00. As a qualitative research that required consent by implying the identification, dissemination, and interpretation of the participants judgments and perceptions, this research was conducted in an ethical manner by delivering to the participants an informed consent letter that detailed the reasons and conditions of the investigation, while recognizing the commitment to ensure the integrity and confidentiality of the information provided during the completion of questionnaire, and certified the consent of the participants through their personal data and digital signature.

The investigation was conducted and took place on 2019, where all the participants signed an Act of Informed Recognition. At this act, they acknowledge the objective of the study and that all the information provided would be only used for this research

as well as the guarantee of anonymity giving the choice of participation or not, with no need for appreciation by ethics committee.

### 3 Results

#### 3.1 Chinese Negotiating Culture’s Manifestation During the Negotiation

Figure 1 shows the results of the questionnaire about the Confucianism dimension. The 100% of Peruvian negotiators determined the importance for Chinese to build relationships and trust to access to concessions, the relevance of understanding non-verbal communication, and the tendency of showing off power to be more demanding. The 85.7% pointed out that Chinese delegations are numerous, while 14.3% alluded that depends on the extent of the topic and could be taken as a signal of inexperience. Another 85.7% mentioned the relevance for Chinese to have a formal behavior; however, 14.3% declared that it depends on the context because there is not formalism while negotiating with Chinese merchants or in the public sector. The 74.4% classified Chinese communication as direct.

Figure 2 shows the results of the questionnaire about Sun Tzu’s stratagems dimension. The 100% of Peruvian negotiators declared the use of tactics from the Chinese as manipulating the counterpart by pointing out weakness, intimidating by being aggressive or mocking, and showing off power to make the others give in and the 71.4% of them cataloged the Chinese way of doing business as mixed (cooperative and competitive).

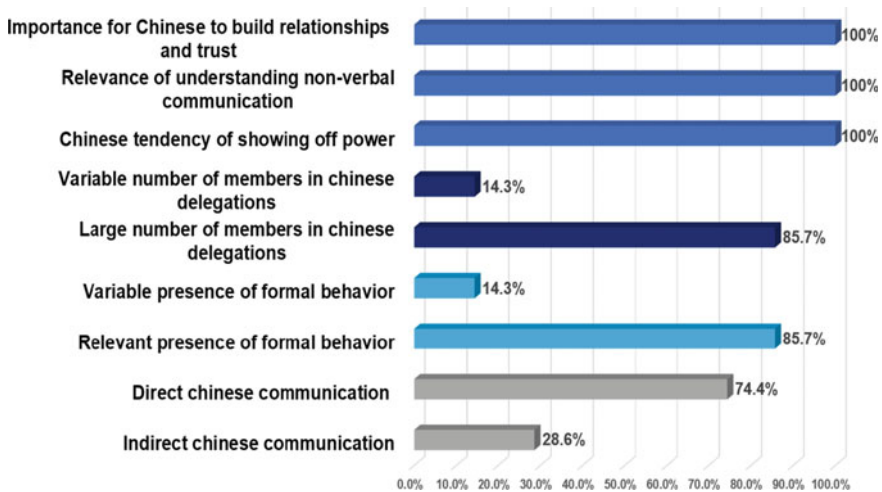


Fig. 1 Chinese confucianism dimension manifestation during a negotiation

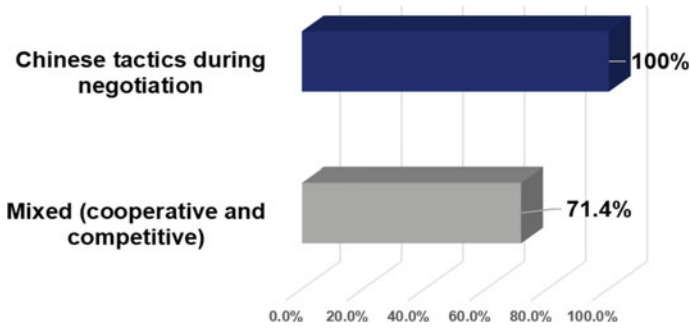


Fig. 2 Chinese Sun Tzu's stratagems dimension manifestation during a negotiation

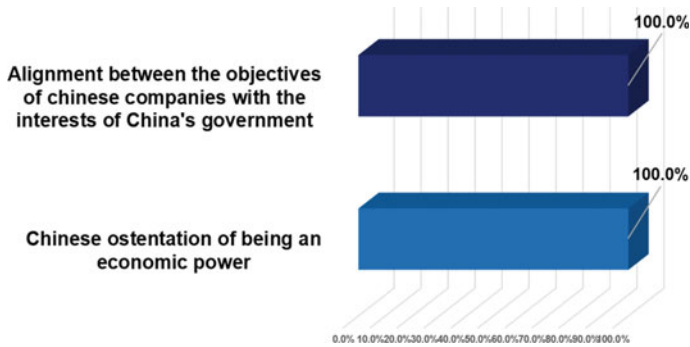


Fig. 3 Chinese sociopolitical and cultural dimension manifestation during a negotiation

Figure 3 shows the results of the questionnaire about the sociopolitical and cultural condition dimension. The 100% of Peruvian negotiators declared that the Chinese ostentation of being an economic power is used as a negotiation mechanism and the alignment between the plans of Chinese companies with the interests of their government since this is the major shareholder of most of the companies.

### 3.2 Chinese Negotiating Culture's Influence on the Negotiation Process

Figure 4 shows the results of the questionnaire about the influence of Chinese culture when negotiating. The 100% of Peruvian negotiators affirmed that the Chinese negotiating culture does influence the negotiation process. The 57.14% of them considered that this derived the need of adaptation that should be only in a cultural way to gain more receptiveness from the Chinese part to ensure a good negotiation.

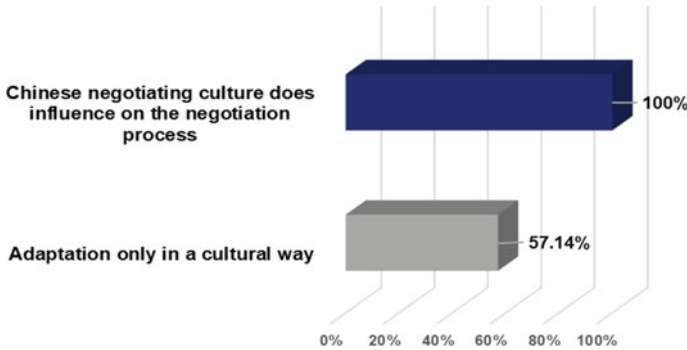


Fig. 4 Influence of the Chinese negotiating culture on the negotiation process

### 3.3 Stages of the Negotiation Process Influenced by the Chinese Negotiating Culture

Figure 5 shows the results of the questionnaire about the pre-negotiation stage. The 100% of Peruvian negotiators described the importance of knowing about the Chinese negotiating culture to identify Chinese strategies and the relevance of presenting exact information to ensure credibility. The 71.4% described the significance of socializing with Chinese to gain more fluidity of the negotiation even when 28.6% cataloged it as not mandatory until the negotiations have significant advances. The 57.1% considered relevant the presence of an intermediary or mediator with experience or member of Chinese culture to help in building trust; however, 42.9% described it as unnecessary when both parties are officials or representatives in international organizations.

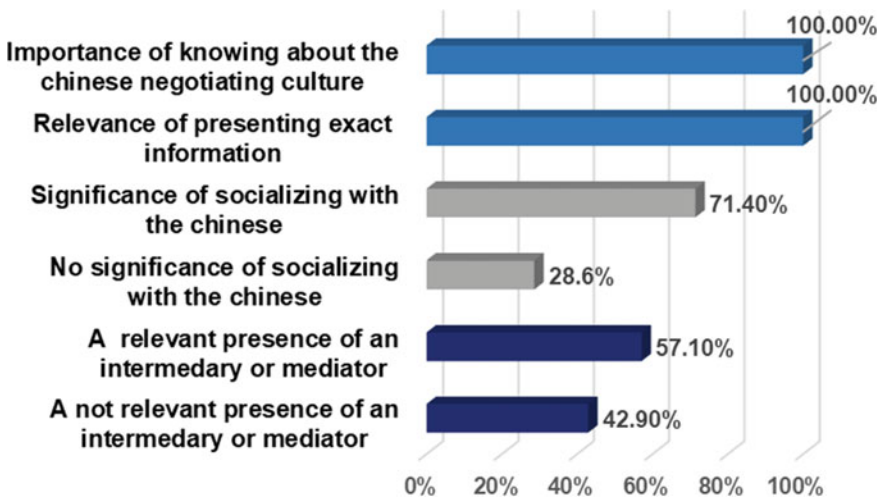


Fig. 5 Characteristics of the pre-negotiation stage influenced by the Chinese negotiating culture

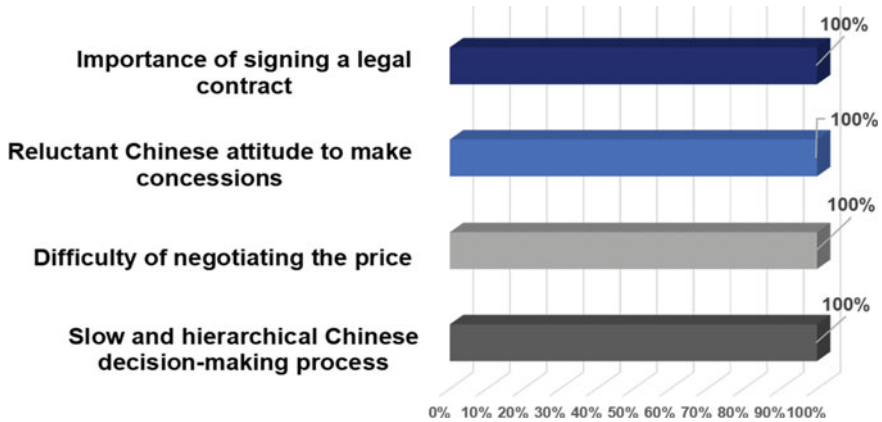


Fig. 6 Characteristics of the formal negotiation stage influenced by the Chinese negotiating culture

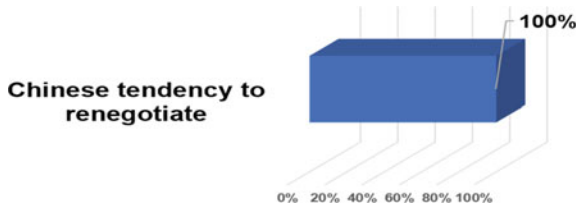


Fig. 7 Characteristics of the post-negotiation stage influenced by the Chinese negotiating culture

Figure 6 shows the results of the questionnaire about the formal negotiation stage. The 100% of Peruvian negotiators described the existence of slow and hierarchical Chinese decision-making process, the difficulty of negotiating the price due to the Chinese custom of bargaining, the reluctant Chinese attitude to make concessions, and the importance of signing a legal contract where the Chinese expect that any formal verbal declaration during the negotiation will be considered in the contract.

Figure 7 shows the results of the questionnaire about the post-negotiation stage. The 100% of Peruvian negotiators described the Chinese tendency to renegotiate where the Chinese consider feasible to change or adapt some terms on the already signed contract that could bring them complications.

## 4 Discussion

Considering the accomplish of the objectives, there are main differences and similarities between the recollected theory about Chinese negotiating culture that describes how the Chinese act during international negotiations, and the actual findings of this paper about the Chinese-Peruvian negotiation's reality.

About the main similarities, the first and most important is when 100% of Peruvian negotiators affirmed that the Chinese negotiating culture does influence in the negotiating process and leads to the need of adaptation; something aligned to the findings of Rodriguez [5] that declared that Chinese cultural bases are decisive during negotiation because the success or failure depends on the negotiator's adaptation to Chinese culture and its way of doing business, which is highly feasible due to the fact explained by Ogliastri and Salcedo [7] that a peruvian negotiator tends to adapt or accommodate the negotiating process according to the counterpart's culture as much as possible by the negative conception of conflicts and by the continuous search for success. The second is when 74.4% of Peruvian negotiators described that Chinese negotiation style as cooperative and competitive, agreeing with Torres [4] that considered that the Chinese negotiation style is nurtured by stratagems of Sun Tzu, and that a "seeming" cooperative Chinese attitude during negotiation could also be stratagems of Sun Tzu, as stratagem number 17 which consists in "giving the adversary something to obtain greater benefit," or stratagem number 11 which refers to "making concessions to achieve the main objective."

About the main differences, the first lies in the explanation of Rodriguez [5] that described that Chinese prioritize formalism or etiquette in all negotiations due to the Confucianist value of respect, while 14.3% of Peruvian negotiators declared that a formal behavior during negotiation actually depends of the context—especially while negotiating with Chinese merchants and at the public sector where there is not formalism at all. The second resides in the declaration of Torres [4] that explained that a large number of Chinese delegations derives from Chinese position of feeling more confidence negotiating in group; however, 14.3% of Peruvian negotiators alluded that the number of members on Chinese delegations actually depends on the extent of the topic and could be also taken as a signal of inexperience from the Chinese counterpart. The third is when Hall and Reed Hall [9] classified Chinese communication as indirect due to the definition of high context culture. Nevertheless, this is at the same time a similarity, because 74.4% of Peruvian negotiators cataloged Chinese communication as direct, matching the declarations of McColl et al. [1] that Chinese have adapted western forms of negotiation and communication. The fourth is found on the statement of Miles [10] that proposed socializing with the Chinese counterpart as mechanism to gain more fluidity at the beginning of the negotiation, a fact world-wide endorsed by other authors, while 25.6% of Peruvian negotiators cataloged it as "not mandatory" and declared it as something that can be postponed until negotiations have advance between parties. The fifth lies in the declaration of Graham and Lam [11] that highlighted the need of a permanent intermediary or mediator during negotiations with a Chinese counterpart as a way of building relationships and trust; however, 42.9% of Peruvian negotiators cataloged as "unnecessary" when both parties are officials or representatives in international organizations, or in other words, share groups or affiliation in common.

## 5 Conclusions

This paper aimed to determine how the Chinese negotiating culture influence the negotiation process according to the perception of the Peruvian negotiator, by providing a list of characteristics derive from this influence, that a Peruvian negotiator could face and therefore adapt in order to establish agreements.

The main findings were the importance of knowing about the negotiating culture of the chinese counterpart; the relevance of presenting exact information; the presence of an intermediary or mediator that 42.9% of peruvian negotiators cataloged as “unnecessary” when both parties are officials or representatives in international organizations, or in other words, share groups or affiliation in common; the significance of socializing with the chinese that according 25.6% of peruvian negotiators is “not mandatory” and declared it as something that can be postpone until negotiations have advance between the parties; the difficulty of negotiating the price due to the chinese custom of bargaining; the slow and hierarchical chinese decision-making process; the reluctant chinese attitude to make concessions derived from the chinese disgust of yielding that implies having to show them the mutual benefit of a concession; the importance of signing a legal contract where the chinese counterpart expect that any formal verbal declaration during the negotiation will be considered; and the chinese tendency to renegotiate where the chinese counterpart consider feasible to change or adapt some terms on the already signed contract that could bring them complications.

## References

1. McColl, R., Descubes, I., Elahee, M.: How the Chinese really negotiate: observations from an Australian-Chinese trade negotiation. *J. Bus. Strateg.* **38**(6), 38–46 (2017)
2. Ghauri, P., Fang, T.: Negotiating with the Chinese: a socio-cultural analysis. *J. World Bus.* **36**(3), 303–325 (2001)
3. Messmann, S.: Management by Sun Zu and confucius—doing business with Chinese partners. In: 2nd International OFEL Conference on Governance, Management and Entrepreneurship, pp. 44–45. Ciru, Dubrovnik (2014)
4. Torres, J.: Chinese Negotiation Styles in International Business Negotiation, pp. 9–65, Argosy University, Sarasota (2011)
5. Rodriguez, C.: Key Aspects of the Current Business Negotiations in China. Universitat Oberta de Catalunya, Catalunya (2013)
6. UDEP Homepage. <http://udep.edu.pe/hoy/2018/relaciones-entre-china-y-peru-estan-en-su-mejor-momento/>. Last accessed 21 November 2019
7. Ogliastri, E., Salcedo, G.: Peruvian negotiating culture: a exploratory study. *J. Econ. Finance Adm. Sci.* **13**(25), 9–33 (2008)
8. Russeft, D., Preskill, D.: Evaluation in Organizations: A Systematic Approach to Enhancing Learning, Performance and Change, 1st edn. Perseus, Cambridge
9. Hall, T., Reed Hall, M.: Hidden Differences, 2nd edn. Anchor, New York (1990)
10. Miles, M.: Negotiating with the chinese: lessons from field. *J. Appl. Behav. Sci.* **39**(4), 453–472 (2003)
11. Graham, J., Lam, M.: The Chinese Negotiation. Harvard Business Review Press, Boston (2003)

# Phone Calls Speech-to-Text: A Comparison Between APIs for the Portuguese Language



Nilton M. Iinuma  and Massaki de O. Igarashi 

**Abstract** Automation and artificial intelligence technologies are bringing improvements in efficiency and cost savings to companies in different areas. These technological developments and software use, platforms and infrastructure as a service have grown significantly in recent years, especially in the field of speech-to-text conversion. The rapid scalability and abstraction associated with the democratization of technology may be the cause of this growth. Developers often make the latest technologies and solutions available through routines and programming standards, the Application Programming Interface—API. Therefore, this paper aims to compare the effectiveness of speech-to-speech conversion tools available by cloud solution providers based on Portuguese telephone call recordings. For the development of this paper, some audio recordings and text conversion were made in order to compare the efficiency of the conversion. The test shows that Word Error Rate (WER) has a direct impact on conversion quality.

**Keywords** Speech to text · API · Phone calls · Comparative

## 1 Introduction

The customer relationship sector of various companies has been seeking greater efficiency and lower cost driven by technologies, for example, the use of “platform as a service” (*platform as a service—PaaS*), infrastructure as a service (IaaS) and even artificial intelligence. These technologies have changed the landscape of call centers. They are replacing people with smart systems that aggregate these technologies.

---

N. M. Iinuma · M. de O. Igarashi (✉)  
Mackenzie Presbyterian University, Campinas, Brazil  
e-mail: [massaki.igarashi@mackenzie.br](mailto:massaki.igarashi@mackenzie.br)

N. M. Iinuma  
e-mail: [nilton.iinuma@gmail.com](mailto:nilton.iinuma@gmail.com)



More drastic cases have already been reported, such as the complete closure of a call center. It was replaced by a debt renegotiation startup that uses software and technological solutions [1].

This demand has driven the PaaS market, which has grown by almost 20% per year [2], probably due to its scalability and abstraction capability. This growth also seems to have been favored by the “democratization of technology” through the free access to these advanced technologies made available by any developer.

This access is available through routines and programming standards, popularly called API (Application Programming Interface—API). According to [3], the use of PaaS, IaaS and SaaS (software as a service) brings some advantages such as: not going through the company’s firewall, elasticity (rapid scalability), cost optimization (due to resource sharing), available for all, virtualization (easy resource allocation), operation and management functionality, different levels of hiring, IP address provided via DHCP per VM (IP Static/global are also available but at additional cost), private VLANs, IP addresses, VPN, round-robin DNS for load balancing, content compression, geographic load distribution (example: Big-IP global traffic manager).

The technology-minded companies such as IBM, Google, Microsoft, and Amazon already offer services that use artificial intelligence; for example, in the speech-to-text converters, artificial intelligence is used to combine language and grammar structures with speech signal processing, in order to get more accurate identification of the words.

Therefore, this research, which aimed to test and compare the efficiency of some voice-to-text conversion APIs from leading cloud solution providers, can be used for future implementations in further researches in this area.

## 2 Theoretical Reference

Artificial intelligence, more specifically neural networks, as reported by [4], can be used to automatically build a training dataset used for speech recognition from YouTube videos. Several filters and post-processing steps were used in this work and the amount of noise and the Word Error Rate (WER) were evaluated (in this study the data sets presented results ranging from 15.8 to 36.6%) after transcription.

Another subarea of artificial intelligence reported in the bibliography is natural language processing (NLP), a core of cognitive computing that enables the processing of natural language diction. NLP is a very extensive topic and includes many subdivisions (of which: natural language understanding, natural language generation, knowledge base building, dialog management systems, intelligent tutor system, speech processing, data mining—text mining—text analytics) [5].

Among the technologies available and necessary for speech transcription, the speech-to-text tool plays an important role in this regard. However, it is important to note that the telephone system may have additional difficulties, such as distortion.

Voice digitization in a telephone system is performed by sampling the voice signal. In this process, it is common to limit the frequency range of the optimization system.

It is important to remember that humans can hear frequencies in the range of 20 Hz–20 kHz. However, studies state that the range between 200 Hz and 3.2 kHz is sufficient for a minimum understanding of speech. [6].

According to the Shannon–Nyquist sampling theorem [7], the sampling rate must be at least twice the highest frequency so the sampling rate in telecommunications systems is usually 8 kHz. But this reduction, despite understanding, still causes some distortions in the digitized signal. Therefore, the necessity to analyze the performance of speech-to-text systems in the context of telephone calls is justified by comparing the conversion error rates of different API.

### 3 Methodology

Ethical approval for the experiment in this study was deemed unnecessary by the Ethics Committee. As also the activities in the experiment do not pose risks greater than those ordinarily encountered in daily life and all the subjects remained anonymous. As well as all participants were given consent and were also informed about the academic objective of the research as well as the guarantee of anonymity giving the choice of participation or not. Still considering that as it is an opinion poll, according to Resolutions 466 and 510 of the National Health Council, there is no need to go through the University's Ethics Committee. This is following CNS Resolution 466/12 of the National Health Council, of December 12, 2012, (available at <https://conselho.saude.gov.br/resolucoes/2012/Reso466.pdf>). Idem with Article 1 of Resolution 510, of 7 April 2016, of Brazil's National Health Council (available at <http://www.conselho.saude.gov.br/resolucoes/2016/Reso510.pdf>) and also with item 8.0.5 of the Ethical Principles of Psychologists and Code of Conduct of the American Psychological Association (available at <https://www.apa.org/ethics/code/principles.pdf>).

It is a descriptive study of exploratory research. Because it sought a better understanding of the topic of voice-to-text conversion in order to provide a better overview and guide research delimitation and objectives. This is a descriptive study because a systematic data collection was performed, recording, analyzing, classifying and interpreting the observed phenomena without, however, at any time, any interference from the researcher.

The audio recordings were performed from six different Brazilian speakers (three females and three males) with a “divine comedy” standard text. The speakers have a postgraduate degree and age between 40 and 50 years. The call recordings were performed using some APIs for telephony and text messaging services that enable the recording of the telephone conversation between a VoIP client (an acronym for Voice over IP) and the destine telephone. After finalized calling, the audio was downloaded through the link provided by the web service accessed via the call token + id [8]. Then the recorded audios were treated and converted using three different APIs for voice-to-text conversion: AWS, Google, and IBM.

It is important to observe that the recordings were made using the same equipment and the same telecommunications provider so that the results of the experiments could be comparable.

## 4 Results and Discussion

### 4.1 Record Preparation

Initially, it is necessary to configure recorder software (Fig. 1).

To configure, it is important to insert the caller and the destination numbers, the date and consecutively activate the start of recording.

### 4.2 Treatment of Recordings

Consequently, the recording audio process has some steps for a correct voice-to-text conversion.

Figure 2 shows the workflow required to handle the audio signal before its conversion:

**Chamada** : Realiza uma chamada telefonica entre dois números

POST /chamada Realiza uma chamada telefônica entre dois números: A e B

Respostas (Status 200)  
Mensagem encaminhada para envio

Modelo Modelo esquema

```
{
  "status": 200,
  "sucesso": true,
  "motivo": 0,
  "mensagem": "chamada criada com sucesso",
  "dados": {
    "id": 4921
  }
}
```

Tipo de conteúdo da resposta application/json

Parâmetros

Parâmetro	Valor	Descrição	Tipo de parâmetro	Tipo de dados
ChamadaParam	-		body	Modelo Modelo esquema

\*numero\_origem (obrigatório)  
Número de A, formato DDD + Número  
exemplo: 4832830151

\*numero\_destino (obrigatório)

```
{
  "numero_origem": "4832830151",
  "numero_destino": "4832830151",
  "data_criacao": "2017-03-30T17:14:03:00",
  "gravar_audio": true,
  "bina_origem": "4832830151",
  "bina_destino": "4832830151",
  "..."
}
```

Fig. 1 API documentation

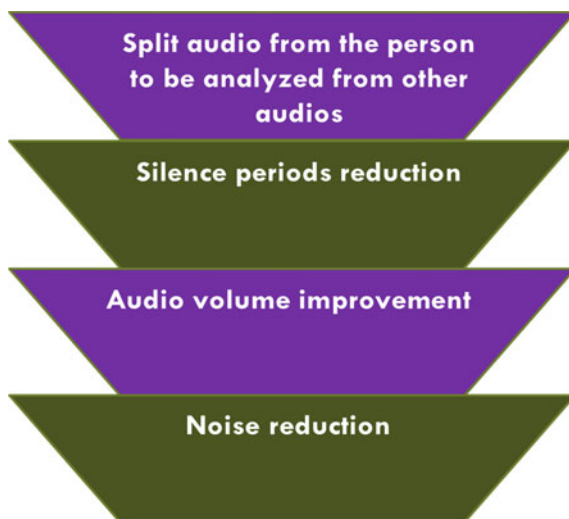


**Fig. 2** Workflow for audio processing and conversion

All steps described in Fig. 2 are performed through the Audacity® software [9].

Each party's voice is separated by simply copying and pasting the recorded audio signal.

Then, the elimination of speechless periods was performed by clicking on the “effects” menu > ”lock silence” option (Fig. 3). The program detects as “silence” the configured thresholds. In this case, it was configured a  $-20$  dB threshold with 0.2 s duration for silent parameters and 0.2 for discard section parameters.

The callers can have different tones and voice volumes. Thus, it is important to introduce a gain in the signal to equalizes the audio quality and ensures good conversion. In the “effects” menu the “amplify” option was used. In this option, the software already provides a dB gain suggestion that best applies to audio.

Finally, noise must be removed using the same software. By clicking on the “effects” > ”noise reduction” menu, it is possible to detect the “noise profile” and reduce it in the entire audio signal.

### **4.3 Voice-to-Text Conversion API**

The experiments were performed by using the following APIs:

- Google Cloud Speech to Text [10]
- IBM Watson Speech to Text [11]
- Amazon Transcribe [12].

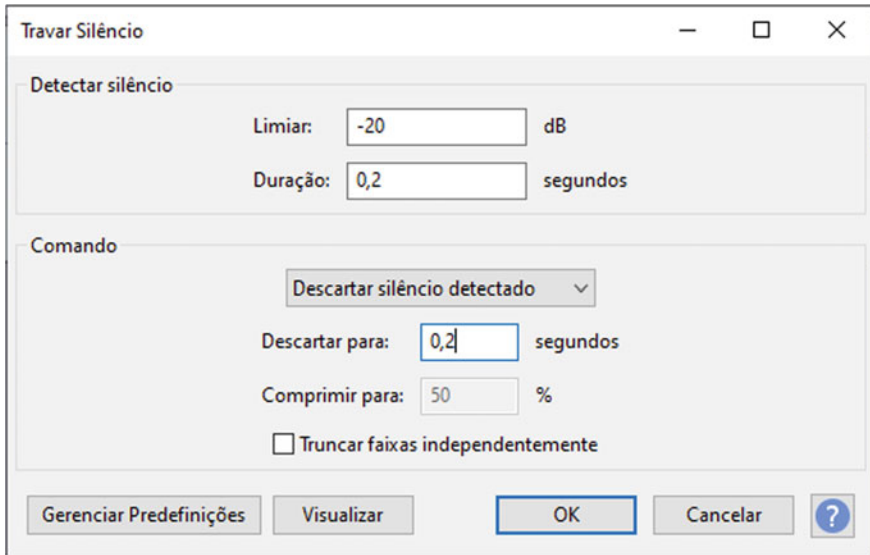


Fig. 3 Filters applied in the lock silence option

#### 4.4 Word Error Rates

Word Error Rate (WER) was used to compare the efficiency of speech-to-text API algorithms. WER is a value that indicates the transcription error rate. Thus, the lowest value means a better quality conversion [13].

WER is calculated based on the formula (1) described by Koo Alison [14]:

$$\text{WER} = \frac{S + I + D}{\text{NWS}} \quad (1)$$

- *S = Substitutions*. These are errors which some word is exchanged to another;
- *I = Insertions*. These are unspoken words that are added. It may, for example, be a single word that has been described as more than one word;
- *D = Deletions*. These are missing words in the transcript.
- *NWS = Number of Words Spoken*. The number of pronounced words.

#### 4.5 Analysis of Voice-to-Text Conversion Results

Figure 4 presents the WER relationship separating the conversion results by interlocutor and the types of APIs used.

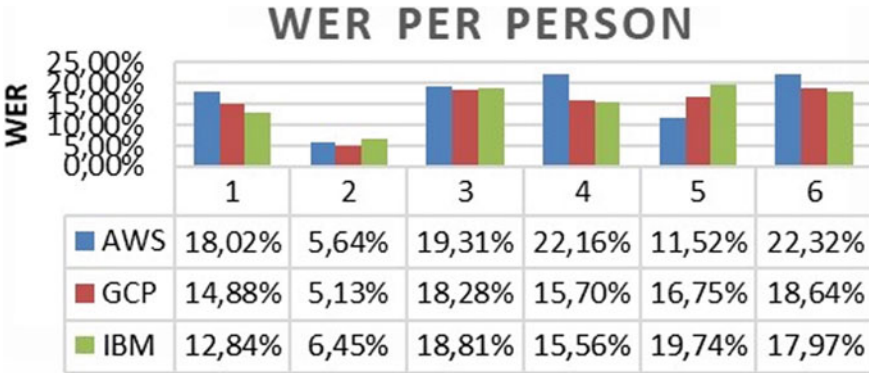


Fig. 4 WER values relating the caller and the API used

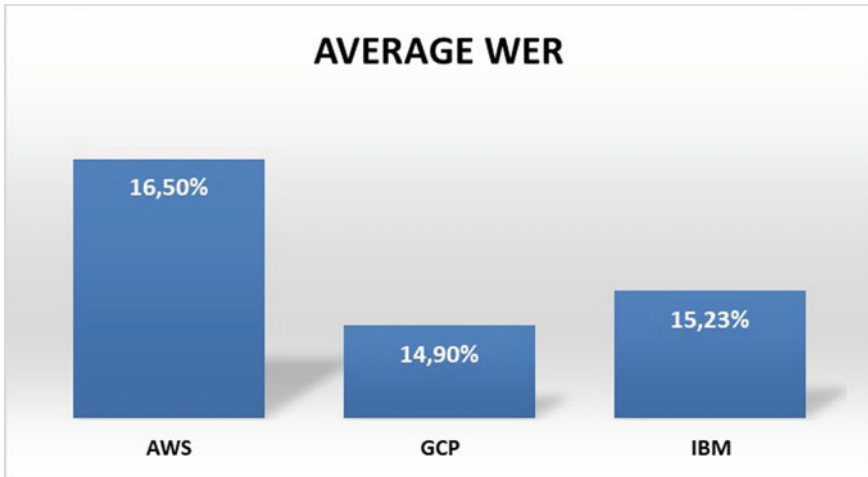
Figure 4 shows that person 2 presented the lowest WER value in all APIs while the other persons presented a variation of WER value in all experiments in a uniform way. Therefore, person 2 has a positive influence on the efficiency of voice-to-text conversion. It is also noteworthy that person 2 is a university teacher, so this fact may also have possibly influenced the result due to their greater care with pronunciation.

Figure 5 presents the same WER results, but now filtered by API type, where the WER was listed for each party.

Regarding the conversion using the AWS API, WER ranged from 11.52 to 22.32% for people 1, 3, 4, 5 and 6 (Fig. 5); and between 5.13 and 6.45% for person 2.



Fig. 5 WER values relating to API and interlocutors



**Fig. 6** WER médiums for APIs tested

Figure 6 shows the average WER values calculated based on the APIS conversion results used.

From the average WER values obtained in Fig. 7, it can be seen that the Google API presented the lowest average WER value (14.90%), thus, the highest efficiency of all APIs. However, the value is very close to the value obtained by the IBM API (15.23%) and slightly less than the value of the AWS API (16.50%); it demonstrates that despite differences at values, APIs have close conversion errors and thus similar efficiencies. Noteworthy in this case is the average WER value obtained by the AWS API (16.50%), which was approximately 10.7% higher than Google’s average WER, i.e., it was virtually 10.7% less efficient than Google’s and 7.69% less efficient than IBM.

## 5 Conclusions and Future Works

The WER analysis considering different persons in the experiments shows a higher conversion efficiency of the Google API, followed by the IBM API and lastly the AWS API. However, it is important to highlight that these conclusions refer to 18 recordings samples in total and a small sample of people (just 6 interlocutors). Therefore, it is recommended a larger number of experiments and people samples for future experiments and more assertive conclusions.

It follows that the transcript was closer to the original text in the transcript using the Google API (GCP), which had the lowest Word Error Rate—WER. However, the WER difference in error rate was not very significant (10.7% between AWS and GCP and 2.21% between IBM and GCP).

## References

1. Scheller, F., Capelas, B.: Inteligência Artificial toma conta de call centers (2019). <https://link.estadao.com.br/noticias/inovacao,inteligencia-artificial-toma-conta-de-call-centers,70003023316>
2. Krancher, O., et al.: Key affordances of platform-as-a-service: self-organization and continuous feedback. *J. Manage. Inf. Sys. (Bern–Switzerland)* (2018). <https://doi.org/10.1080/07421222.2018.1481636>
3. Rhoton, J.: *Cloud Computing Explained: Implementation Handbook for Enterprises*. Recursive Press (2009)
4. Lakomkin, E., et al.: *KT-Speech-Crawler: Automatic Dataset Construction for Speech Recognition from YouTube Videos*. University of Hamburg, Hamburg, Germany (2019)
5. Moreno, A., Redondo, T.: *Text Analytics: the Convergence of Big Data and Artificial Intelligence*. Universidad Autónoma de Madrid and Instituto de Ingeniería del Conocimiento, Madrid Espanha (2016)
6. Pinheiro, P.: *Tutoriais Telefonia Fixa - Ciclos Evolutivos: O Início da Digitalização* (2004). [https://www.teleco.com.br/tutoriais/tutorialciclos/pagina\\_4.asp](https://www.teleco.com.br/tutoriais/tutorialciclos/pagina_4.asp)
7. Haykin, S.S., et al.: *Sinais e sistemas*. Bookman, Porto Alegre (2001)
8. Total Voice: A startup que se reinventou para crescer seis vezes em um ano (2019). <https://scinova.com.br/total-voice-startup-que-se-reinventou-para-crescer-seis-vezes-em-um-ano/>
9. AUDACITY: Audacity (2019). <https://www.audacityteam.org>
10. GCP: Google Cloud Speech to Text (2019). <https://cloud.google.com/speech-to-text>
11. IBM. Watson Speech to Text (2019). <https://speech-to-text-demo.ng.bluemix.net>
12. AWS: Amazon Transcribe (2019). [https://docs.aws.amazon.com/pt\\_br/transcribe/latest/dg/how-it-works.html](https://docs.aws.amazon.com/pt_br/transcribe/latest/dg/how-it-works.html)
13. Popovic, M., Hremann, N.: *Word Error Rates: Decomposition over POS Classes and Applications for Error Analysis*. University Aachen, Germany (2002). <http://citeseerx.ist.psu.edu/viewdoc/download?doi=10.1.1.310.4832&rep=rep1&type=pdf>
14. Koo, A.: How to Calculate Word Error Rate. *rev.ai* (2019). <https://www.rev.ai/blog/how-to-calculate-word-error-rate/>



# Production of Cantonese Lexical Tones by Native Speakers of Brazilian Portuguese: A Comparative Analysis



João Vítor Possamai de Menezes and Adriano Vilela Barbosa

**Abstract** This study presents a quantitative analysis of the production of lexical tone by speakers of a non-tonal language. More specifically, we look at how well native speakers of Brazilian Portuguese are able to produce the six tones of Cantonese. An experiment was conducted where six subjects listened to a number of tone words previously produced by a native speaker of Cantonese. For each word they heard, the subjects were asked to try to reproduce it as best as they could. No further instructions were provided. A total of 150 tokens per subject were produced (5 phonetic strings  $\times$  6 tones  $\times$  5 repetitions). The quality of the non-native productions was assessed by comparing them to the productions of the native speaker. This was done by extracting the F0 contours from all recorded tokens (both native and non-native), approximating them by polynomials (first, second, and third order) and then using the polynomial parameters to group the tokens into six classes corresponding to the six lexical tones of Cantonese. The analysis was performed in two ways: (1) by using an F0 onset  $\times$  offset graph already proposed in the literature and (2) through a classification task using a Linear Discriminant Analysis (LDA). In both cases, each subject was analyzed separately. The F0 onset  $\times$  offset graphs presented differences between native and non-native data; the non-native productions showed great variability while the native productions were better defined, presenting less variability. Classifiers trained on the Cantonese native speaker's data resulted in accuracies above 90%, whereas those trained on the Brazilian Portuguese speakers' data resulted in accuracies between 40 and 60%.

---

J. V. P. de Menezes · A. V. Barbosa (✉)

Graduate Program in Electrical Engineering, Universidade Federal de Minas Gerais, Av. Antônio Carlos 6627, Belo Horizonte, MG 31270-901, Brazil

e-mail: [adrianovilela@ufmg.br](mailto:adrianovilela@ufmg.br)

J. V. P. de Menezes

e-mail: [joaovmenezes@ufmg.br](mailto:joaovmenezes@ufmg.br)

A. V. Barbosa

Department of Electronic Engineering, Universidade Federal de Minas Gerais, Av. Antônio Carlos 6627, Belo Horizonte, MG 31270-901, Brazil

© The Editor(s) (if applicable) and The Author(s), under exclusive license

to Springer Nature Switzerland AG 2021

Y. Iano et al. (eds.), *Proceedings of the 5th Brazilian Technology Symposium*,

Smart Innovation, Systems and Technologies 202,

[https://doi.org/10.1007/978-3-030-57566-3\\_45](https://doi.org/10.1007/978-3-030-57566-3_45)

**Keywords** Lexical tone · Non-native production · Discriminant analysis · Cantonese · Brazilian Portuguese

## 1 Introduction

About 70% of all known languages are tonal [1]. These languages are characterized by the use of lexical tones, which is the use of pitch to distinguish lexical or grammatical meaning [1]. Tonal languages are spread over East Asia [2], Africa [3], the Americas [4], and other regions [5].

The differences in meaning between fundamental frequency (F0), pitch, and tone are important in this work. F0 is an acoustic term defined as the physiological frequency of vibration of the vocal folds. Pitch is a psychoacoustic term related to the perception of F0. Thus, F0 and pitch are terms associated with the production and the perception of speech, respectively. Although high F0 values are associated with a high pitch, and low F0 values are associated with a low pitch, the relation between them is not linear. In turn, a tone is a linguistic unit, expressed in terms of F0 and perceived in terms of pitch that manifests itself as lexical tone within words and as intonation within sentences. In intonation, tones are responsible for associating different meanings to sentences, whereas lexical tones, in tone languages, are responsible for contrasting different words [1]. As an example, the syllable [yau] in Cantonese means “worry” when uttered with a high-level tone, and it means “paint” when uttered with a high-rising tone [1].

Tone language learning and perception are recurrent research subjects [6, 7], mainly due to the significant number of speakers and learners of these languages. Many of these learners are speakers of non-tonal languages who have to familiarize themselves with the structure of the new language and learn how to produce and perceive lexical tones. Since the ability to produce sounds on a target language is crucial to enable communication between native and non-native speakers, non-native lexical tone production is being researched in several tone languages, such as Thai [8] and Mandarin [9], and also in pitch-accent languages such as Norwegian [10] and Swedish [11].

This work focuses on Cantonese, a tonal language with six lexical tones that are generally described by their corresponding F0 contours. Figure 1 shows a simple representation of these contours as straight lines [12], whereas Fig. 2 shows a more accurate representation based on F0 tracking of recorded data [13]. Based on these figures, the six lexical tones can be classified as level, if the F0 remains practically constant throughout its production, or contour, if the F0 changes as the tones are being produced. In Cantonese, tones 1, 3, 6 (T1, T3, and T6) are level tones whereas tones 2, 4, 5 (T2, T4, and T5) are contour tones.

Previous studies about non-native production of lexical tone and pitch accent have focused on different aspects of production, such as accentedness ratings [8], the improvement in production after perception training [9], and the ability to produce sounds distinguishable by native speakers [10]. General results suggest that non-native speakers have more difficulty in producing level tones than contour tones [8], that the perception affects the production of lexical tones [9], and that the ability to

produce F0 contours and levels are not mastered in parallel, with the level tones being more challenging than the contour tones [10]. From these results, we hypothesize that non-native speakers in our experiment will (1) encounter difficulties in producing native-like lexical tones, because they will not benefit from any previous perceptual training and (2) encounter more difficulty in the production of Cantonese level tones (T1, T3, and T6) than in the production of contour tones (T2, T4, and T5).

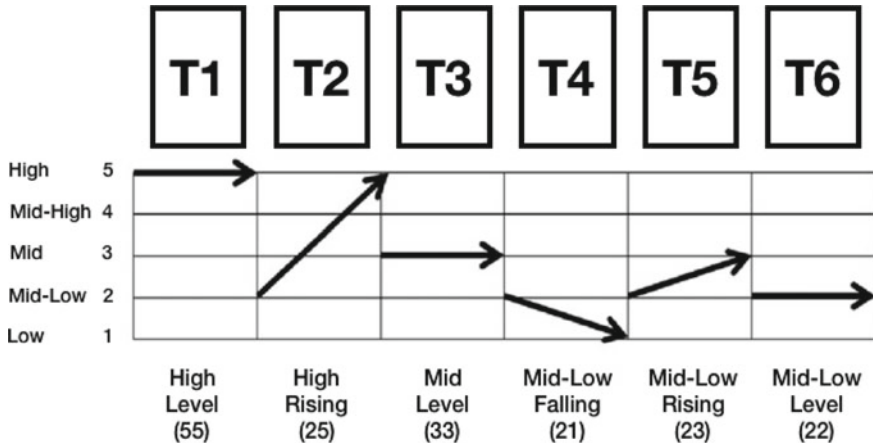


Fig. 1 F0 contours of the six lexical tones of Cantonese. They are here drawn didactically, focusing on the initial and end frequencies of each tone. Adapted from [12]

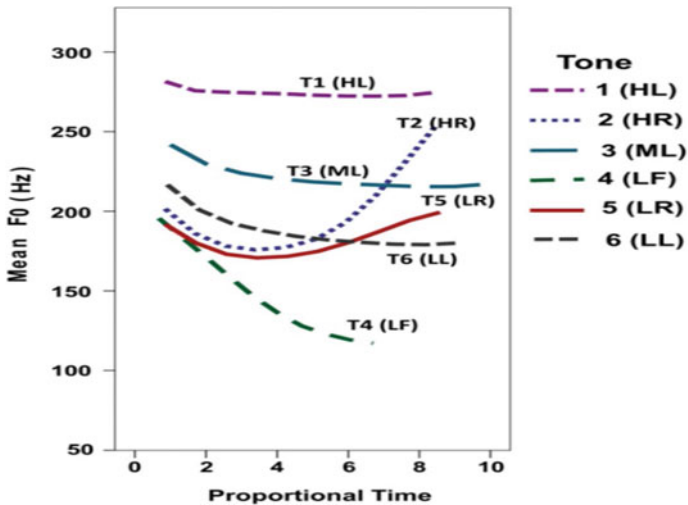


Fig. 2 F0 contours of the six lexical tones of Cantonese. They are here the mean contours of 198 native productions [13]

This work presents two main contributions: (1) the use of Brazilian Portuguese speakers, with no familiarity with Cantonese, as subjects and (2) the use of discriminant analysis [14] in order to assess the ability of these speakers to produce the six lexical tones of Cantonese. We also look to reproduce the F0 onset  $\times$  offset graphs proposed by Barry and Blamey [15] with the Brazilian Portuguese speakers.

The objective of this work is to compare native and non-native production of Cantonese lexical tones. More specifically, we compare the production of a native speaker of Cantonese (henceforth CN speaker) to those of six native speakers of Brazilian Portuguese (henceforth BP speakers). Some of the questions we try to address in this work are: (1) How do BP speakers perceive and produce Cantonese tone words? (2) Do these speakers have more difficulty in the production of level tones or of contour tones? (3) Are they able to produce all the six tones equally well? If not, which tones are more challenging to them?

The rest of this paper is organized as follows. Section 2 describes the data acquisition process for the CN speaker and the BP speakers. Section 3 presents the techniques used in the analysis. Section 4 presents and discusses our results, and Sect. 5 presents the conclusions.

## 2 Materials

The Cantonese data was provided by collaborators (see the acknowledgment section) and only used as a stimulus in this study. The data consists of 30 tone words (five phonetic strings bearing each of the six lexical tones) produced by a female, 24-year-old CN speaker. The phonetic strings used were: “fan,” “fu,” “hau,” “soej,” and “wai.” Each tone word was repeated five times, resulting in 150 tokens.

The Brazilian Portuguese data was recorded in a speech production experiment. Before the experiment,<sup>1</sup> the subjects were given an information sheet explaining them, among other things, the objectives of the study and also informing them about the voluntary and anonymous nature of their participation. The subjects then signed a consent form agreeing with the experiment terms and proceeded to the actual data collection. All subjects were native speakers of Brazilian Portuguese (three females, three males) ranging from 20 to 37 years. Some of them showed a background in music (2) and knowledge of foreign languages (6) such as English, Spanish, French, or Italian. None of them had any previous knowledge of Cantonese or any other tone language. The recording took place in an acoustically treated sound booth, using a MacBook Pro (Mid 2014). The 150 original Cantonese stimuli (tone words) were

---

<sup>1</sup>ethical approval for the experiment in this study was deemed unnecessary by the Ethics Committee of the Federal University of Minas Gerais, since the activities in the experiment do not pose risks greater than those ordinarily encountered in daily life and all the subjects remained anonymous. This is in accordance with Article 1 of Resolution 510, of April 7th 2016, of Brazil’s National Health Council (available at <http://www.conselho.saude.gov.br/resolucoes/2016/Reso510.pdf>) and also with item 8.0.5 of the Ethical Principles of Psychologists and Code of Conduct of the American Psychological Association (available at <https://www.apa.org/ethics/code/principles.pdf>).

randomly presented to each subject, one stimulus at a time. For each word they heard, the subjects were asked to try to reproduce it as best as they could. No further instructions were provided; the subjects did not even know that what they were listening to were Cantonese words. One recording was made for each subject and for each Cantonese audio token, resulting in 150 tokens produced by each subject ( $150 \times 6 = 900$  non-native tokens in total). The subjects were allowed to pause at any time.

### 3 Methods

F0 contours were extracted from each token using Praat [16]. The rest of the analysis was performed in R [17]. Initially, the F0 contours exported by Praat were imported into R by means of the rPraat library [18]. The imported F0 contours were then approximated by polynomials of different orders (first, second, and third).

The polynomial orders were chosen based on the F0 contours shown in Figs. 1 and 2. A first-order polynomial would be sufficient to characterize Cantonese lexical tones as displayed in Fig. 1, but not the lexical tones as displayed in Fig. 2. Given that the data used here consists of natural recordings, its F0 contours should be more similar to those in Fig. 2, which would be better approximated by higher-order polynomials, such as second and third order. Figures 3 and 4 show the F0 contours for the CN speaker and for the BP speaker six upon which our analysis was based. In this paper, we also compare results obtained with each polynomial approximation order, possibly suggesting an optimal polynomial order for Cantonese F0 contour approximations.

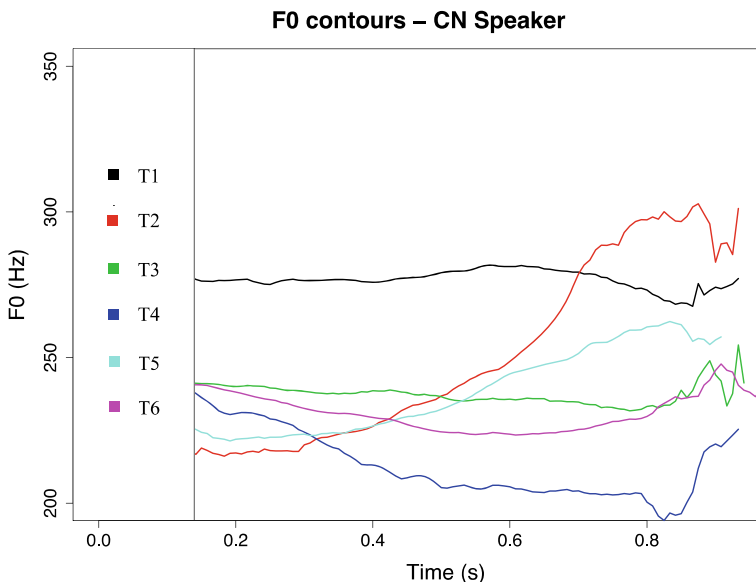


**Fig. 3** F0 contours produced by the CN speaker for the word [fu] with all of the six lexical tones

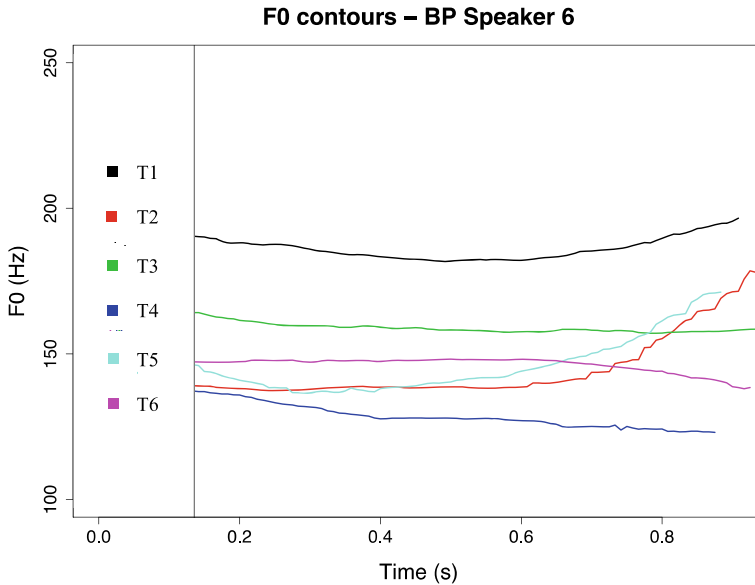


**Fig. 4** F0 contours produced by the BP speaker 6 for the word [fu] with all of the six lexical tones

Finally, each F0 contour was represented by 2, 3, or 4 polynomial coefficients. Based on these coefficients, a linear classification task was carried out using Linear Discriminant Analysis (LDA).

### 3.1 F0 Onset $\times$ Offset Graph

As a theoretical basis for their proposal of a F0 onset  $\times$  offset graph, Barry and Blamey [15] cite the five acoustic dimensions that define tone differences from a listener's perspective: (a) average pitch, (b) direction, (c) length, (d) extreme endpoint, and (e) slope [19]. All of those dimensions, except for length, can be captured by such a graph. The onset was defined as the first point of the F0 contour and the offset as the endpoint, so they are able to define the frequency at which the contour starts the frequency at which it ends.

In the F0 onset  $\times$  offset graph, each repetition is a point, generating a cloud of points. To measure how clear the speaker acoustically differentiates each lexical tone, Barry and Blamey [15] proposed two indices ( $I_1$  and  $I_2$ ) that can be calculated based on ellipses centered at each tone's mean value and with axes as wide as the standard deviation of each tone repetitions. The area of each ellipse illustrates how consistent the speaker is for each tone: The smaller the ellipse, the more consistent is the speaker.

The first index ( $I_1$ ) is based on the three more distinguishable tones, T1 (high level), T2 (high rise), and T4 (low falling), and on the concept of tonal space. Being T1, T2, and T4 normally at the outer boundaries of the graph, the tonal space is defined as the area of the triangle whose vertices are the mean values of T1, T2, and T4. Index 1, described in (1), is then calculated as the reason between the area of the tonal space triangle ( $A_t$ ) and the area of T1, T2, and T4 ellipses ( $A_{1,2,4}$ ). The higher its value, the greater the chance of overlapping between tones.

$$I_1 = A_t/A_{1,2,4} \quad (1)$$

The second index ( $I_2$ ) is based on all of the six tone ellipses, giving it an advantage over Index 1. It measures how separate they are from one another and how homogeneous they are among themselves. This index, described in (2), is calculated as a reason between the average distance between the center of every ellipse to each other ( $D_{avg}$ ) and the average of the sum of the radius of every ellipse ( $S_{avg}$ ).

$$I_2 = D_{avg}/S_{avg} \quad (2)$$

### 3.2 Classification Task

The classification task consists of a Linear Discriminant Analysis, which is a method used both for dimensionality reduction and classification. As a classifier, the LDA tries to define linear separators between classes, whose distributions are estimated as normal and is popular when the classification task consists of more than two classes [14].

Some of our previous studies with the same native Cantonese lexical tone data showed that native-produced lexical tones can be classified based on their F0 contour almost error-free (95% of accuracy for third-order polynomial approximation). In this direction, each subject (one native CN speaker and six non-native BP speakers) will have its own samples classified separately to verify how accurate the classification is. The benchmark is the classification accuracy achieved for the CN speaker, and the closer to it the BP speaker's classification accuracy is, the better their lexical tone production is.

Firstly, a baseline accuracy value was obtained for each subject using a single LDA. After that, more meaningful values were obtained by performing twelve five-fold cross-validation runs and taking the mean and standard deviation of the 60 (12 runs  $\times$  5 folds) accuracy values.

## 4 Results

The results come from the F0 onset  $\times$  offset analysis and the classification task. For each of them, results for every approximation are presented (first, second, and third order).

### 4.1 F0 Onset $\times$ Offset Graph

Figures 5, 6, and 7 show the F0 onset  $\times$  offset graph for the CN speaker with polynomial approximations of third, second, and first order, respectively. The figures show similar separation between, and variation within, tones. According to Barry and Blamey's results [15], T1, T2, and T4 should lie at the outer edges of the graph, defining the tonal space, whereas T3, T5, and T6 should lie within this space, tending to overlap with each other. This was also observed in the graphs for the CN speaker, in Figs. 5, 6, and 7.

Figures 8 and 9 show the F0 onset  $\times$  offset graphs for two BP speakers using the third-order polynomial approximations. Figure 8 (BP speaker 6) shows a graph similar to the CN speaker's, with a large and well-defined tonal space with differences within tones smaller than differences across tones. On the other hand, the graph shown in Fig. 9 (BP speaker 5) is an example of poorly defined tones with large overlaps between the ellipses. Some instances of T1, T2, and T4 are well separated from the others, but the ellipses associated with T3, T5, and T6 significantly overlap. Figures 8 and 9 highlight how different the ability of BP speakers to produce Cantonese lexical tones may be.

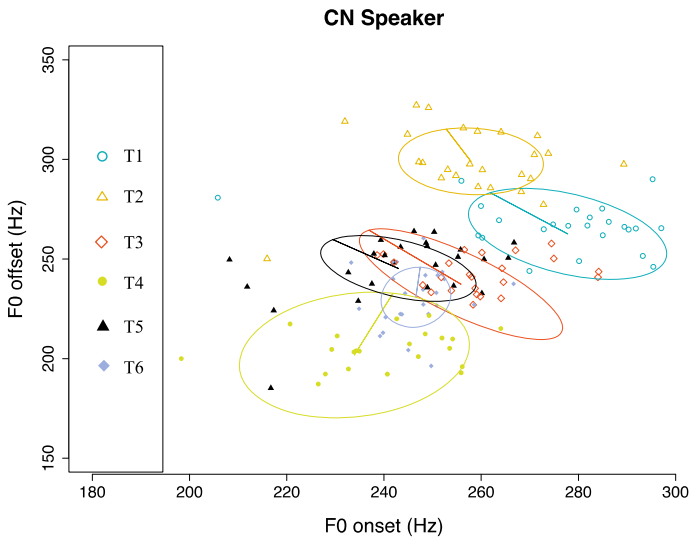


**Fig. 5** F0 onset  $\times$  offset graph based on the F0 contour approximated by a third-order polynomial. Subject: CN speaker



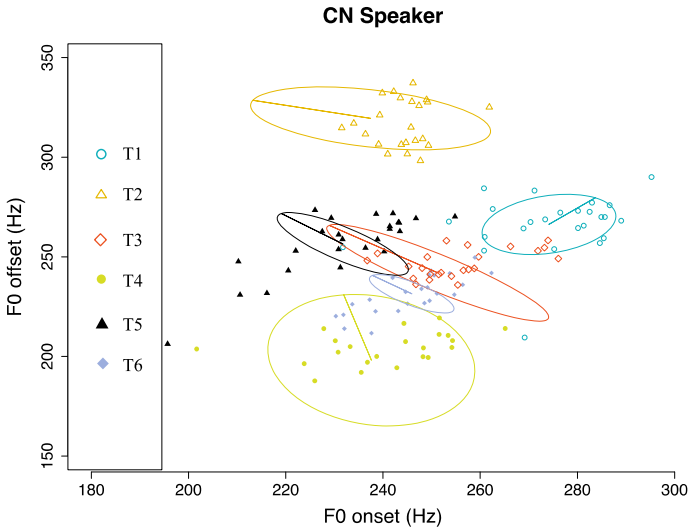


**Fig. 6** F0 onset  $\times$  offset graph based on the F0 contour approximated by a second-order polynomial. Subject: CN speaker

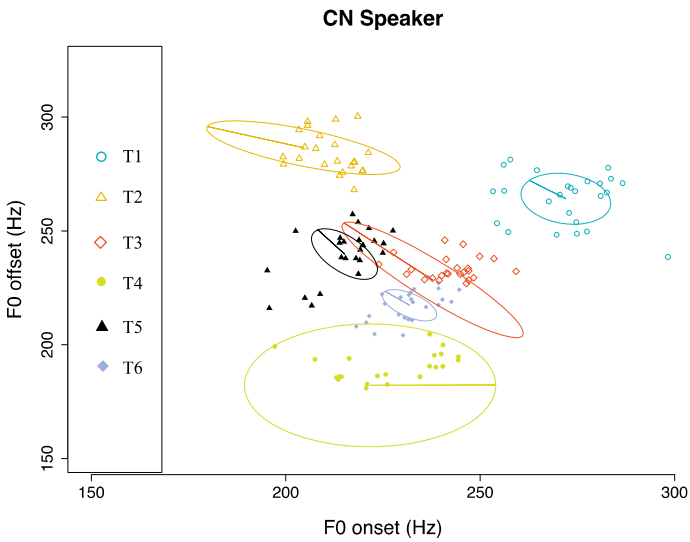


**Fig. 7** F0 onset  $\times$  offset graph based on the F0 contour approximated by a first-order polynomial. Subject: CN speaker

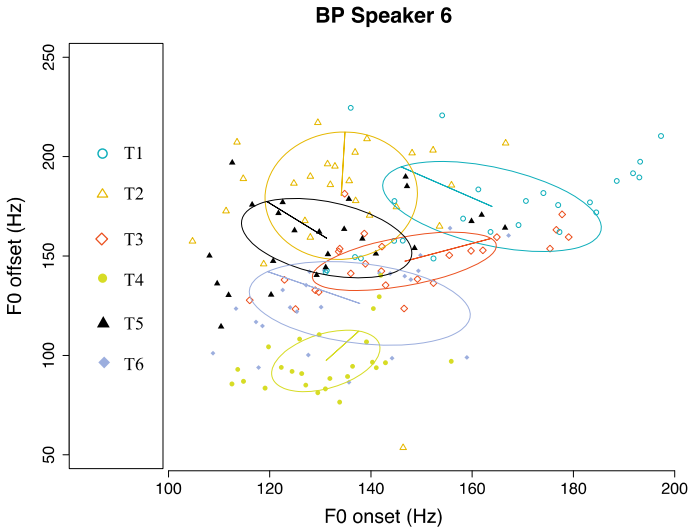


**Fig. 8** F0 onset  $\times$  offset graph based on the F0 contour approximated by a third-order polynomial. Subject: BP speaker 6

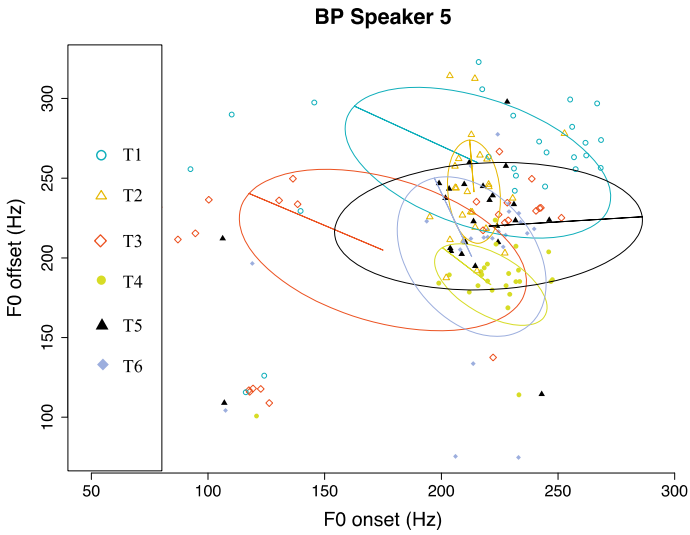


**Fig. 9** F0 onset  $\times$  offset graph based on the F0 contour approximated by a third-order polynomial. Subject: BP speaker 5

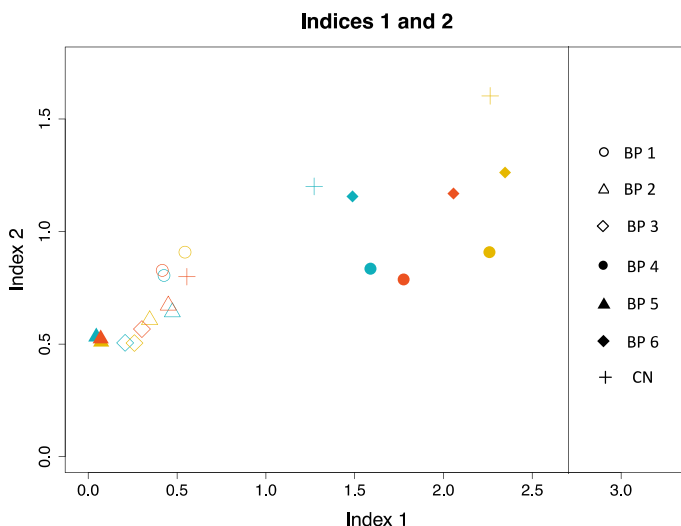


**Fig. 10** Index 1  $\times$  Index 2 graph. The results from the first-order approximation are in red, from the second-order approximation are in yellow, and from the third-order approximation are in blue

An  $I_1 \times I_2$  plot is shown in Fig. 10. The subjects in this figure may be divided into two groups based on index  $I_1$ : those with values smaller than 1 and those with values larger than 1. Separability based on  $I_2$  is not as clear. From the definition of the indices, a well-defined tonal space means a higher value for  $I_1$  and good separation between tones means a higher value for  $I_2$ . These characteristics can, however, have effects on both indices. Apart from the CN speaker, BP speakers 4 and 6 showed higher values for  $I_1$ , whereas BP speakers 1, 4, and 6 showed higher values for  $I_2$ . This suggests that their productions of Cantonese lexical tones are more similar to a native's than the production of the other subjects.

One effect that stands out in Fig. 10 is the difference in the indices between the different order polynomial approximations from the CN speaker. They form almost a straight line, with the first-order approximation at the bottom end and the second-order approximation at the upper end. This may suggest that a second-order polynomial approximation is more appropriate for the F0 onset  $\times$  offset graph.

## 4.2 Classification Task

The classification analysis attempted to measure the similarity of non-native and native productions of Cantonese lexical tone. The benchmark is the linear classification result of native production, which resulted in accuracy above 90% in some of our previous studies with the same data.

**Table 1** Baseline accuracies for each subject

Single LDA			
Subject	First order	Second order	Third order
	Accuracy	Accuracy	Accuracy
BP 1	0.53	0.67	0.47
BP 2	0.47	0.43	0.50
BP 3	0.43	0.53	0.33
BP 4	0.63	0.67	0.60
BP 5	0.43	0.50	0.43
BP 6	0.50	0.50	0.47
CN	0.83	0.90	0.83

The baseline accuracy values obtained with single LDA for the three polynomial approximations are shown in Table 1. Aside from the CN speaker, with accuracies near 90%, BP speakers 1, 4, and 6 achieved the best overall classification accuracies, with accuracies ranging from 47 to 67%.

In order to obtain a more robust measure of how good the lexical tone production of each BP speaker is, we performed twelve fivefold cross-validation runs using the same LDA classifier. The results are shown in Table 2. According to the baseline results from a single LDA, the CN speaker had the best results, around 90%, and the BP speakers 1, 4, and 6 performed better than BP speakers 2, 3, and 5. All of the subjects, however, showed above chance (16.67%) accuracy rates. The CN speaker also showed the lowest Standard Deviation (SD) value of all, suggesting productions with smaller variability.

**Table 2** Accuracies for each subject using 12 trials of fivefold cross-validation

LDA with 12 trials of fivefold cross-validation						
Subject	First order		Second order		Third order	
	Accuracy	SD	Accuracy	SD	Accuracy	SD
BP 1	0.51	0.094	0.57	0.092	0.55	0.084
BP 2	0.45	0.059	0.43	0.075	0.43	0.075
BP 3	0.39	0.075	0.40	0.074	0.40	0.083
BP 4	0.66	0.070	0.66	0.083	0.66	0.070
BP 5	0.42	0.087	0.43	0.071	0.45	0.090
BP 6	0.53	0.082	0.53	0.096	0.54	0.083
CN	0.91	0.051	0.90	0.050	0.89	0.053

**Table 3** Confusion matrix for all of the subjects using third-order polynomial approximation

All subjects		Reference					
Third order		1	2	3	4	5	6
Prediction	1	<b>27</b>	4	9	0	3	3
	2	1	<b>22</b>	1	0	5	2
	3	4	1	<b>12</b>	1	7	8
	4	1	0	2	<b>25</b>	2	6
	5	0	8	3	1	<b>15</b>	5
	6	2	0	8	8	3	<b>11</b>

Bold values represent correct predictions

To also measure how well each of the tones was classified, confusion matrices for all of the productions of each subject, as well as for all of them together, were created. The general confusion matrix, shown in Table 3, presents the predictions made for the 210 test samples (20% of the total samples) using a third-order polynomial approximation. The tones more accurately predicted were T1, T2, and T4, the tones which delimit the tonal space [12]. That can be explained by the relative proximity between T3, T5, and T6 and the fact that T1, T2, and T4 stand commonly apart from each other, with no big superposition with any other tone, as shown by the graphs in Figs. 1, 2, 3, 4, and 5.

Since, from the results in Table 2, BP speaker 3 achieved the lowest and BP speaker 4 achieved the highest accuracy among non-native speakers, we will present their confusion matrices, as well as the confusion matrix for the CN speaker. The trend shown in Table 3 that T1, T2, and T4 are better classified than the other tones can also be observed for the BP speakers in Tables 4 and 5. The CN speaker, on the other hand, achieved an almost perfect classification, as shown in Table 6.

According to Table 2, the classification task did not present significantly different results when the polynomial order changed. This suggests that the classification of F0 contours have similar accuracies in 2, 3, and 4 dimensions.

**Table 4** Confusion matrix for BP speaker 3 using third-order polynomial approximation

BP speaker 3		Reference					
Third order		1	2	3	4	5	6
Prediction	1	<b>2</b>	1	2	0	0	0
	2	0	<b>3</b>	0	0	1	0
	3	1	0	<b>1</b>	0	2	0
	4	1	0	0	<b>2</b>	0	1
	5	0	0	2	0	<b>2</b>	4
	6	1	0	0	0	3	<b>0</b>

Bold values represent correct predictions

**Table 5** Confusion matrix for BP speaker 4 using third-order polynomial approximation

BP speaker 4		Reference					
Third order		1	2	3	4	5	6
Prediction	1	<b>5</b>	0	0	0	0	0
	2	0	<b>5</b>	1	0	1	1
	3	0	0	<b>0</b>	0	0	3
	4	0	0	1	<b>4</b>	1	0
	5	0	0	0	0	<b>2</b>	0
	6	0	0	3	1	1	<b>1</b>

Bold values represent correct predictions

**Table 6** Confusion matrix for the Cantonese native subject using third-order polynomial approximation

CN speaker		Reference					
Third order		1	2	3	4	5	6
Prediction	1	<b>5</b>	0	0	0	0	0
	2	0	<b>4</b>	0	0	0	0
	3	0	0	<b>5</b>	0	0	2
	4	0	0	0	<b>5</b>	0	0
	5	0	1	0	0	<b>5</b>	0
	6	0	0	0	0	0	<b>3</b>

Bold values represent correct predictions

## 5 Conclusion

The goal of this work was to compare the production of Cantonese lexical tones by speakers unfamiliar with that language with those produced by a native speaker of the language. The BP speakers had no knowledge of tonal language structure, a condition meant to prevent speakers from making any conscious effort to produce specific lexical tones, for they faced each Cantonese tone word as unknown audio.

The reproduction of the F0 onset  $\times$  offset graphs proposed in [15] with the data we collected showed that BP speaker's productions presented high variability within and across subjects when compared to the CN speaker's productions. This means (1) that some BP speakers' F0 contours produced graphs quite different from other BP speakers and (2) that the F0 contours produced by some BP speakers were not like the graphs expected by Barry and Blamey [15], showing significant overlap between all of the tones.

Results from the classification task showed that the BP speakers' accuracy was in the range between 39 and 66%, much below the accuracy of the native CN speaker (between 89 and 91%). The accuracy was interpreted here as a measure of how good

a non-native speaker could produce lexical tones: the closer they were to the native's accuracy, the better.

Comparisons between the classification task results and the F0 onset  $\times$  offset graph (and its related  $I_1$  and  $I_2$  indices) showed that the subjects with best results were BP speakers 1, 4, and 6, the same subjects with higher values of  $I_2$ . Also, the tones which were more accurately classified were T1, T2, and T4, which are the boundaries for the tonal space defined in the F0 onset  $\times$  offset graph.

Our results point, therefore, in the direction that BP speakers can produce some lexical tones better than others (namely T1, T2, and T4). This may, however, be biased by our method, which was a linear classifier. A perception task could be used to determine how good the BP speakers' productions are based on the native listener's perspectives.

Regarding the effect of polynomial order on the analysis, the F0 onset  $\times$  offset related indices produced similar results across orders, except for the CN speaker, which showed different index values for different polynomial orders. An effect of the polynomial order on the classification task could not be perceived.

An additional result is that the male BP speakers (1, 4, and 6) performed better than the female BP speakers (2, 3, and 5) both in the F0 onset  $\times$  offset indices and in the classification task. However, further tests with a larger number of subjects should be carried out in order to establish a significant relationship between the gender of the subjects and of the native speaker.

Next steps in the analysis of BP speakers' production of Cantonese lexical tones can be (1) the recording of more native data (only a female speaker was used in this experiment); (2) the recording of more non-native speakers; (3) the execution of a perception stage, which would require native Cantonese listeners to judge the non-native lexical tone productions and (4) the usage of more methods, such as non-linear classifiers.

**Acknowledgements** Support for this work was provided by CAPES (Coordination for the Improvement of Higher Education Personnel, Brazil) to João Vítor Possamai de Menezes and by FAPEMIG (Fundação de Amparo à Pesquisa do Estado de Minas Gerais, Brazil) to Adriano Vilela Barbosa (process APQ-03701-16). The Cantonese data was kindly provided by Dr. Denis Burnham (the MARCS Institute at the Western Sydney University, Australia).

## References

1. Yip, M.: *Tone*, 1st edn. Cambridge University Press, Cambridge (2002)
2. Yip, M.: *The tonal phonology of Chinese*. Ph.D. Dissertation, MIT (1980)
3. Odden, D.: Tone shift and spread in Taita I. *Stud. Afr. Linguist.* **30**(1), 75–110 (2001)
4. Soares, M.F.: Traços acústicos das vogais em Tükuna. *Cadernos de Estudos Linguísticos* **7**, 137–175 (1984)
5. Maddieson, I.: *Tone*. In: Dryer, M.S., Haspelmath, M. (eds.) *The World Atlas of Language Structures Online*. Max Planck Institute for Evolutionary Anthropology, Leipzig (2013)

6. Burnham, D., Ciocca, V., Stokes, S.: Auditory-visual perception of lexical tone. In: EUROSPEECH 2001 Scandinavia, 7th European Conference on Speech Communication and Technology, 2nd INTERSPEECH Event, Aalborg, Denmark, 3–7 September (2001)
7. Lee, K.Y.S., Chan, K.T.Y., Lam, J.H.S., van Hasselt, C.A., Tong, M.C.F.: Lexical tone perception in native speakers of Cantonese. *Int. J. Speech-Lang. Pathol.* **17**(1), 53–62 (2015)
8. Wayland, R.: Non-native production of Thai: acoustic measurements and accentedness, ratings. *Appl. Linguist.* **18**(3), 345–373 (1997)
9. Wang, Y., Jongman, A., Sereno, J.A.: Acoustic and perceptual evaluation of Mandarin tone productions before and after perceptual training. *J. Acoust. Soc. Am.* **113**(2), 1033–1043 (2003)
10. Steien, G.B., van Dommelen, W.A.: The production of Norwegian tones by multilingual non-native speakers. *Int. J. Bilingualism* **22**(3), 316–329 (2016)
11. Kaiser, R.: Do Germans produce and perceive the Swedish word accent contrast? A cross-language analysis. *TMH-QPSR* **51**(1), 93–96 (2011)
12. Cheng, S.T.T., Lam, G.Y.H., To, C.K.S.: Pitch perception in tone language-speaking adults with and without autism spectrum disorders. *I-Perception* **8**(3), 1–15 (2017)
13. Wong, P., Leung, C.T.: Suprasegmental features are not acquired early: perception and production of monosyllabic cantonese lexical tones in 4- to 6-year-old preschool children. *J. Speech Lang. Hearing Res.* **61**(5), 1070–1085 (2018)
14. James, G., Witten, D., Hastie, T., Tishirani, R.: An introduction to statistical learning: with applications in R, 1st edn. Springer, New York (2013)
15. Barry, J.G., Blamey, P.J.: The acoustical analysis of tone differentiation as a means for assessing tone production in speakers of Cantonese. *J. Acoust. Soc. Am.* **116**(3), 1739–1748 (2004)
16. Boersma, P., Weenink, D.: Praat: doing phonetics by computer [Computer Program]. Version 6.1.03. Retrieved 1 Sept 2019 from <http://www.praat.org/> (2019)
17. R Core Team: A Language and Environment for Statistical Computing. R Foundation for Statistical Computing, Vienna, Austria (2019)
18. Bořil, T., Skarnitzl, R.: Tools rPraat and mPraat. In: Sojka, P., Horák, A., Kopeček, I., Pala, K. (eds.) *Text, Speech and Dialogue*. Springer (2016)
19. Gandour, J.T.: The perception of tone. In: Fromkin, V.A. (ed.) *Tone: A Linguistics Survey*, 1st edn. Academic Press, New York (1978)



# Smart Campus IoT Guidance System for Visitors Based on Bayesian Filters



Alvaro Aspilcueta Narvaez , Dennis Núñez Fernández , Segundo Gamarra Quispe , and Domingo Lazo Ochoa 

**Abstract** In this work, we proposed an indoor location system that makes use of a Raspberry Pi embedded computer and WiFi signals to guide a person inside a region of the faculty of Electrical and Electronic at Universidad Nacional de Ingeniería, Peru. The main advantage with similar indoor location systems like beacons or RFID technology is that the presented system does not require additional hardware since it makes use of the pre-installed WiFi routers. The experimental tests show promising results, achieving a location accuracy of 92.31%.

**Keywords** Indoor location · WiFi · Bayes filter · Embedded computer

## 1 Introduction

The existing navigation systems like Global Positioning System (GPS) offer a precise location in outside environments but an inaccurate location inside common buildings [1]. This problem of localization has attracted the interest of researchers and developers due to the high demand for such systems for indoor navigation, immersive experiences, asset tracking, augmented reality, and more.

During the last decade, several approaches for indoor location systems [2] such as radio frequency identification (RFID), wireless local area networks (WLAN), and Bluetooth among others have been proposed [3]. In [4, 5], an indoor positioning

---

A. Aspilcueta Narvaez · D. Núñez Fernández (✉) · S. Gamarra Quispe · D. Lazo Ochoa  
Universidad Nacional de Ingeniería, Lima 15333, Peru  
e-mail: [dnunezf@uni.pe](mailto:dnunezf@uni.pe)

A. Aspilcueta Narvaez  
e-mail: [alvaro.aspilcueta.n@uni.pe](mailto:alvaro.aspilcueta.n@uni.pe)

S. Gamarra Quispe  
e-mail: [sgamarraq@uni.edu.pe](mailto:sgamarraq@uni.edu.pe)

D. Lazo Ochoa  
e-mail: [dlazo@uni.edu.pe](mailto:dlazo@uni.edu.pe)

system for smart buildings was used to obtain relatively good results; however, the system makes use of RFID technology, which produces an additional cost for hardware implementation. Regarding indoor location using WiFi signals, [4] makes use of Monte Carlo (MC) filter for a precise WiFi-based indoor localization, but the system is intended for tracking objects with a high precision employing relative high computing processing, which is not suitable for real-time applications since it demands high computing resources and a small division of the regions. In recent work, [6, 7] proposes a novel, incremental approach that reduces the energy consumption of WiFi localization by scanning just a few selected channels. The results are remarkable and provide a way for the implementation of indoor location on embedded systems. In addition, Indoor Google [8] provides guidance; however, its accuracy is not enough (5–15 m).

In this paper, we propose an indoor location system for a region of the faculty of Electrical and Electronic of Universidad Nacional de Ingeniería, Peru. Unlike the indoor location systems presented before, which rely on external devices like RFID hardware or Bluetooth beacons, the proposed system does not demand external equipment or additional costs. Therefore, employing an embedded computer and pre-installed access points, our indoor location system is able to provide a good position accuracy and the guidance to the destination region.

## 2 Proposed Method

### 2.1 Overview

Our system performs indoor localization and guidance on an embedded computer using WiFi signal levels. In this way, the system works on small embedded devices with low computational resources. With the aim to achieve response time and power computational constraints, a simple and effective Bayes recursive estimator was used in this work.

The methodology used for this work has two phases: offline and online phase. At the offline phase, the WiFi levels were captured several times in every region, thus obtaining a received signal strength indicator (RSSI) table per region. Later, the RSSI data were divided into training and testing datasets in order to perform the evaluation. Then, the normalized histograms are cleaned using the Gaussian distribution. Finally, the localization system is evaluated offline using average accuracy and confusion matrix. At the online phase, the Bayesian filter was implemented in a Raspberry Pi embedded computer. This filter uses the captured WiFi signal levels and the cleaned RSSI database to predict the most likely region. Figure 1 shows the diagram of the proposed methodology.

### 2.2 Data Recollection

First, the principal regions of the faculty of Electrical and Electronic of Universidad Nacional de Ingeniería are identified and divided into several areas. Figure 2 shows

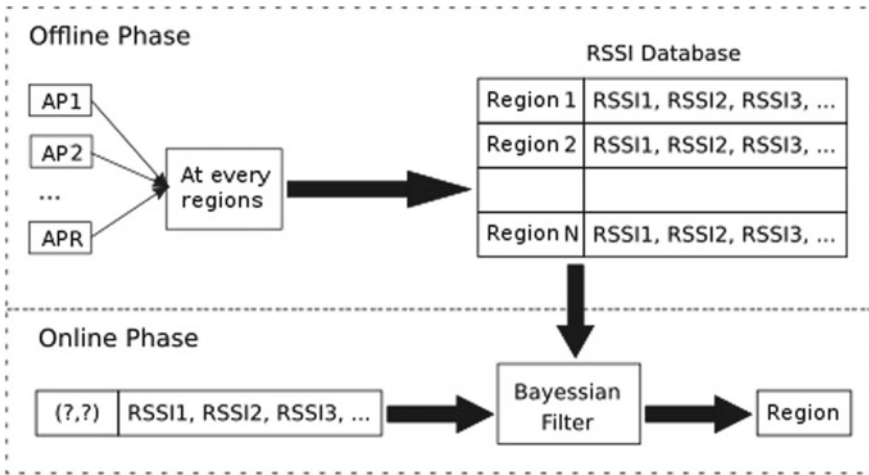


Fig. 1 Scheme of the proposed interior locating system

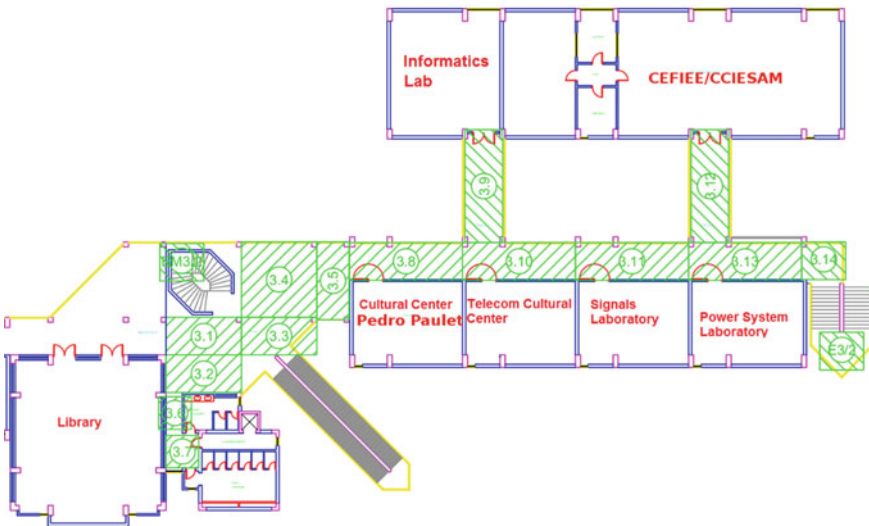


Fig. 2 Sampling points and destination in the third-floor scheme

such a distribution of regions. After division, the main WiFi information like service set identifier (SSID), media access control (MAC) and RSSI is recollected via a custom application in for the Raspberry Pi. Thereby, 150 samples in each region at different times during three non-consecutive days/nights were captured. Finally, filtering processing for non-stable access points (APs) was carried out, so the final dataset was constructed using only the best APs in order to have the best results.

### 2.3 Bayesian Filter

Several relevant papers about RSSI-based indoor location systems assume Gaussian probability density function (PDF) [9, 10]. It is justified by the relation of the noise of the radio receiver together to the influence of average white Gaussian radio channel noise, which is modeled by a Gaussian PDF. Therefore, original histograms could be cleaned by approaching each histogram to a Gaussian PDF. In Eq. (1), the formulation of a Gaussian PDF is presented. It is described by two parameters:  $\mu$  (mean) and  $\sigma$  (standard deviation).

$$f(x|\mu, \sigma^2) = \frac{1}{\sqrt{2\pi}\sigma} e^{-\frac{(x-\mu)^2}{2\sigma^2}} \quad (1)$$

In order to achieve response time and computational requirements, a straightforward and effective estimator is used, and it is based on the Bayes recursive estimator. This is able to infer the posterior using sensed and prior knowledge (see Eq. (2)). Being  $A$  the event we want the probability, and  $B$  the new evidence that is related to  $A$ . Therefore, the posterior  $P(A|B)$  is calculated by the likelihood  $P(B|A)$  (probability of observing the new evidence) and the prior  $P(A)$  (probability of our hypothesis without any additional prior information).  $P(B)$  is the marginal likelihood, which is the total evidence probability.

$$P(A|B) = \frac{P(B|A)P(A)}{P(B)} \quad (2)$$

The algorithm presented below corresponds to the implementation of the Bayes-based estimator. This takes the AP tables and current WiFi measurement as inputs and returns the estimated region and its probability. Thereby, the algorithm recursively calculates the probability of the posterior region (line 11), and then, the probability (line 12) and predicted region (line 13) are calculated. Algorithm 1 was implemented in Python for evaluation of the performance of the Bayes estimator and for inference on the Raspberry Pi platform.

**Algorithm 1** Bayes Estimator Algorithm

---

```

1:  $N$  = number of regions;  $R$  = number of routers
2:  $W_r$  = AP table for router  $r$ 
3: procedure BAYESESTIMATOR( $w_1, w_2, \dots, w_R$ )
4:   # Start with uniform distribution
5:    $priorW_{1,2,\dots,R} = [1/N; 1/N; \dots; 1/N]_{N \times 1}$ 
6:    $probability = (100/N)\%$ 
7:   while  $probability < 95\%$  do
8:     # Perform Bayes
9:     for  $r$  from 1 to  $R$  do
10:        $posteriorW_r = norm(priorW_r \times W_r[:, w_r])$ 
11:        $prob_r = max(posteriorW_r)$ 
12:        $pred_r = where(posteriorW_r == prob_r)$ 
13:     end for
14:     # Find the highest probability
15:      $probability = max(prob_{1,2,\dots,R})$ 
16:      $r\_best = where(prob_{1,2,\dots,R} == probability)$ 
17:      $prediction = pred_{r\_best}$ 
18:     # Update the new prior
19:     for  $r$  from 1 to  $R$  do
20:        $priorW_r = posteriorW_{r\_best}$ 
21:     end for
22:   end while
23:   Return  $prediction, probability$ 
24: end procedure

```

---

## 2.4 Guidance System

The flowchart of the operation of our guidance system is shown in Fig. 3. The start screen allows the manual entry of the destination point through a drop-down menu, based on the plane of sampling points shown in Fig. 2. Once selected, the user pushes the central button in order to start the guidance system. The destination region is displayed on the screen.

Then, the system calculates the current node where the user is located, which is the returned result of the indoor location algorithm based on the Bayes filter, see Fig. 3. Based on the current node and the destination node initially entered, the graph of the nodes is expressed in an adjacency matrix of the distances and angles between the nodes (based on the plane of the faculty facilities). Then, the algorithm of Dijkstra calculates the shortest route and returns the next node to go, which is based on the minimum route.

From the provided map of the facilities, the orientation with respect to the magnetic north is also shown, and the use of a magnetometer was added to indicate the orientation in degrees from the magnetic north; so, it works like a compass, no matter the direction of the user it will always orient to the north direction. In order to have the same direction, it was previously calibrated. Some considerations were taken such as a small variation because the screen generates a magnetic field, see Fig. 4.

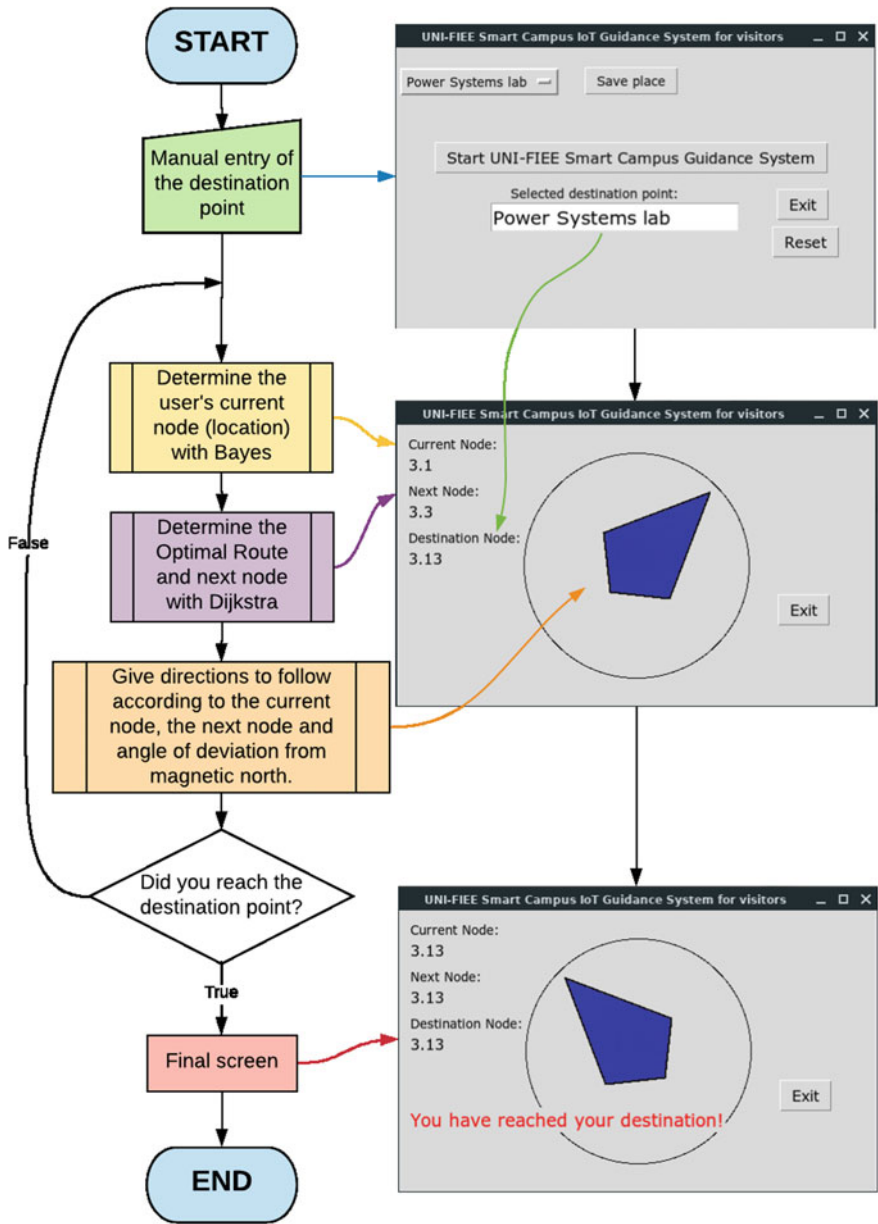


Fig. 3 Flowchart of the smart campus guidance system program

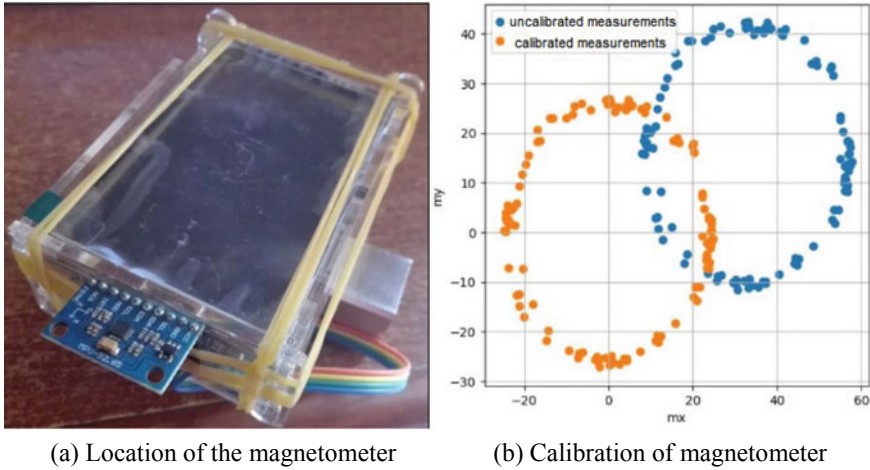


Fig. 4 Hardware and calibration related to the magnetometer

Using the angle with respect to the magnetic north, and the angle between the current node and the next node, which was determined by the Dijkstra algorithm, the direction of the guiding compass is independent of the direction of the user to the next node, which follows the minimum route to reach its destination.

When the user arrives at their final destination, the system finishes working and the next short message will appear on the screen of the Raspberry Pi board: “*You have arrived at your destination!!!*”.

### 3 Experimental Results

In order to obtain the performance and other metrics for the indoor localization system, we evaluated it on the testing dataset. The overall accuracy and the confusion matrix (see Fig. 5) define the results. This matrix for the proposed system shows high accuracy for the diagonal values and low accuracy for the others, and it means that the system has a high accuracy per class/region. In addition, the accuracy of the indoor location system is about 92.31%.

For the evaluation of the system, we use a Raspberry Pi model 3B+ , an LCD 3.5” screen, an MPU9250 sensor, and an external battery. It was conducted in different regions and several positions. As expected, the system correctly predicted the locations in all regions. Figure 6 shows some results of the test. As we can see, our system correctly predicts the location.

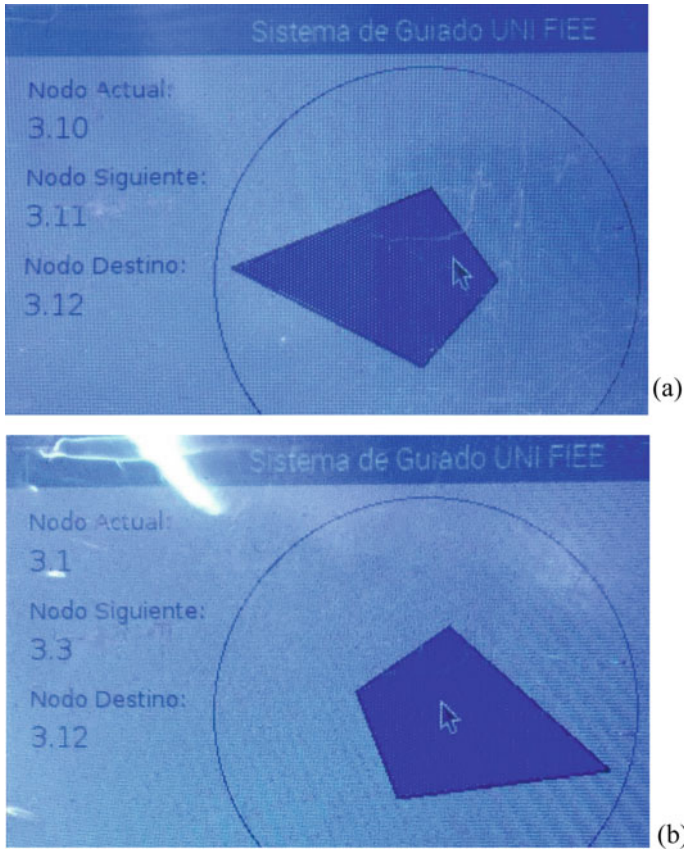
	R01	R02	R03	R04	R05	R06	R07	R08	R09	R10
R01	0.97	0	0	0	0	0.01	0.01	0	0	0.01
R02	0	0.97	0	0	0	0.01	0	0.02	0	0
R03	0.01	0	0.95	0	0.01	0	0	0.01	0.02	0
R04	0	0	0	0.93	0	0.04	0	0	0.02	0.01
R05	0	0.04	0	0.03	0.9	0	0	0.02	0	0.01
R06	0	0	0.05	0	0	0.92	0	0.01	0	0.02
R07	0	0	0	0.02	0	0	0.93	0	0	0.05
R08	0.01	0.01	0	0	0	0	0	0.96	0	0.02
R09	0	0	0.04	0	0	0	0.02	0	0.94	0
R10	0	0.02	0	0	0.01	0	0	0	0	0.97

Fig. 5 Confusion matrix for the proposed system

### 4 Conclusions

This paper introduced the implementation of a Smart Campus WiFi-based indoor location system to guide visitors in a region of the faculty of Electrical and Electronic of Universidad Nacional de Ingeniería, Peru. With the aim to accomplish a high positioning accuracy and a low computational power consumption, the proposed system makes use of Bayes recursive estimator. Experiments show promising results, obtaining an accuracy of 92.31%. As further work, the processing could be performed in remote servers in order to have a better response time. Thus, the proposed methodology is not limited to this work, but can also be applied to similar localization tasks such as immersive experiences, augmented reality, and asset tracking, among others.





**Fig. 6** Online results on the Raspberry Pi. **a** Result in region 3.10. **b** Result at region 3.1

**Acknowledgements** We thank Ph.D. Marco Zúñiga Zamalloa for their time and inspiring teaching. This work was funded by the Research Institute of the Faculty of Electrical and Electronic Engineering (IIFIEE UNI).

## References

1. Motte, H., Wyffels, J., De Strycker, L., Goemaere, J.-P.: Evaluating GPS data in indoor environments. *Adv. Electr. Comput. Eng.* **11**(3), 25–28 (2011). <https://doi.org/10.4316/AECE.2011.03004>
2. Sakpere, W., Adeyeye Oshin, M., Mlitwa, N. B.: A state-of-the-art survey of indoor positioning and navigation systems and technologies. *S. Afr. Comput. J.* **29**(3), 145–197 (2017)
3. Brena, R. F., García-Vázquez, J. P., et al.: Evolution of indoor positioning technologies: a survey. *J. Sensors* **2017**, 21 (2017)

4. Dhital, A., Closas, P., Fernández-Prades, C.: Bayesian filters for indoor localization using wireless sensor networks. In: 2010 5th ESA Workshop on Satellite Navigation Technologies and European Workshop on GNSS Signals and Signal Processing (NAVITEC), pp. 1–7. Noordwijk (2010)
5. Moreno-Cano, M. V., Zamora-Izquierdo, M. A., Santa, J., Skarmeta, A. F.: An indoor localization system based on artificial neural networks and particle filters applied to intelligent buildings. *Neurocomputing* **122**, 116–125 (December 2013)
6. Brouwers, N., Zuniga, M., Langendoen, K.: Incremental Wi-Fi scanning for energy-efficient localization. In: 2014 IEEE International Conference on Pervasive Computing and Communications (PerCom), pp. 156–162. Budapest (2014)
7. Lin, K., Chen, M., Deng, J., Hassan, M. M., Fortino, G.: Enhanced fingerprinting and trajectory prediction for IoT localization in smart buildings. *IEEE Transact. Autom. Sci. Eng.* **13**(3), 1294–1307
8. Indoor Google Maps. (Online Web, accessed on January 2014). Available: <http://maps.google.com/help/maps/indoormaps/>
9. Chruszczyk, L.: Statistical Analysis of Indoor RSSI Read-outs for 433 MHz, 868 MHz, 2.4 GHz and 5 GHz ISM Bands. *Int. J. Electr. Telecommun.* **63**(1), 33–38 (2017)
10. Kaji, K., Kawaguchi, N.: Design and implementation of WiFi indoor localization based on Gaussian mixture model and particle filter. In: 2012 International Conference on Indoor Positioning and Indoor Navigation (IPIN), pp. 1–9. Sydney, NSW (2012)

# Research of the Academic Performance of University Students Through Statistical Models



Olga Solano Dávila , Luis Nuñez Lira , Olga Bolaños Solano ,  
and Néstor Mamani-Macedo 

**Abstract** In this work, there were analyzed some factors, such as demographic variables, study habits, and academic stress, which influence academic performance, especially in students of the faculty of mathematical sciences of a public university. A cross-sectional, descriptive, and explanatory study was used from a statistical approach, which was made up of 311 students. The data were collected during the first semester of 2019 using the academic stress inventory, the vicuna study habits inventory, and the demographic variables, age, gender, professional school, and socioeconomic level; subsequently, the weighted average of the students was obtained. The results show that variables that influence academic performance are: age, professional school, study habits, and the dimension reactions to academic stress and the variables that do not influence performance are: gender, socioeconomic level, level of stress, stressors, and coping strategies for academic stress.

**Keywords** Academic performance · Demographic variables · Study habits · Academic stress

---

O. Solano Dávila (✉) · N. Mamani-Macedo  
Facultad de Ciencias Matemáticas, Universidad Nacional Mayor de San Marcos, Lima, Peru  
e-mail: [osolanod@unmsm.edu.pe](mailto:osolanod@unmsm.edu.pe)

N. Mamani-Macedo  
e-mail: [nmamanim@unmsm.edu.pe](mailto:nmamanim@unmsm.edu.pe)

L. Nuñez Lira  
Facultad de Educación, Universidad Nacional Mayor de San Marcos, Lima, Peru  
e-mail: [lnunezl@unmsm.edu.pe](mailto:lnunezl@unmsm.edu.pe)

O. Bolaños Solano  
Facultad de Psicología, Universidad Nacional Mayor de San Marcos, Lima, Peru  
e-mail: [obolanoss@unmsm.edu.pe](mailto:obolanoss@unmsm.edu.pe)

## 1 Introduction

Over the years, experts warn that education in Latin America has the worst academic performance. The statistical data of the countries state that the region is below the general patterns of academic achievement. Countries like Peru, Colombia, Brazil, and Argentina are among the lowest 10th percentile whose students have a lower performance in the disciplines of math, science, and reading [1].

A study habit is a researched behavioral standard that is automatically observed in the face of frequently determined circumstances on a regular basis, where the subject does not have to meditate on how to proceed. Vicuña proposes as fundamental aspects of learning habits, method, ordering, time, and distractibility [2]. According to academic stress, it is considered a methodical procedure, of an adaptive nature, mainly psychological, which is observed (a) at the time the student is in academic settings and has to make a list of requirements to be evaluated, and these are considered stressors (entrance); (b) when these produce methodical disorder (overwhelming state) it reveals a list of signals (signs of instability); and (c) when this instability pressures the student to do coping activities (exit) to renew systemic stabilization [3]. The aim of this paper is to show a statistical model to explain academic performance based on academic stress, study habits, and sociodemographic variables.

## 2 State of the Art

Several researchers have found that there is an association between study habits and university achievement [4, 5]. This means that the more convenient the habits of learning, the better the academic achievement. However, students do not have study habits, a plan to study, and certain care has their scope of study and the motivation with their studies not to disapprove of the enrolled courses. These results should be applied a program of improvement of the habit of learning, taking into account the organization of tests, work, planning of your time, attitude, physical condition, and the issues associated with the place of study.

From other points of view, there are findings that indicate that there is no association between the habit of studying with academic achievement and moral values among students. This means that students have good learning habits and more moral values; and that the influence of academic achievement is due to factors such as the community, family, economic environment, the cognitive-affective and sensitive structures of each student [6]. However, in the process of training students, not only the cost of studying and their techniques support an appropriate development of study, but other causes of the particular individual such as dignity, self-representation, self-judgment, own capacity, incentives, social capacities, balance and management of the sensitive universe, as well as parental, governmental or physiological causes (student health) can have a positive or negative impact on the task of learning [7]. Related references on academic stress indicate that this affects the academic achievement of

students [8] and is strongly associated with the perceived physical and mental health dimensions [9].

Other stress-related researches have not been able to verify associations with other variables, in addition to academic performance [10]. The main stressors in students are the excess of homework and university work, as well as the short time to perform them [10]; other investigations have found that stressors are considered most relevant examinations, contradictory approach work by teachers, inconsistent approach work by teachers, and lack of practical to theoretical classes [11]. For [12], the most affecting stressors in students are teacher methodological deficiencies, examinations, and interventions in public. In [13], the author concluded that students are stressed by the fact of competing with classmates, academic overload, teacher character, exams, the tasks requested by teachers, limited time to do homework and not understand well the topics analyzed in class. On the other hand, most students suffer stress during the academic year, and academic, psychosocial, and environmental stressors are associated with perceived stress [14].

### 3 Methodology

The quantitative, descriptive, and explanatory approach was used because this design intends to explain academic performance based on study habits, academic stress, and sociodemographic variables in students of the Faculty of Mathematical Sciences (FMS) of a higher university center [15].

The authorization of the director of the Administrative Direction of the FMS of a public university was obtained to carry out the research. The students signed an informed consent before applying the instruments used in the research, the Vice-Dean's Office was also asked to list of enrolled students from the third cycle to the tenth cycle, and the head of enrollment provided this information in a Microsoft Excel file.

#### 3.1 Population Sampling

The universe in this study is constituted by students from the third to the tenth cycle enrolled in the FMS of a public university on semester 2019-I, and the unit of analysis is each student with the characteristics mentioned above. Random probabilistic sampling was used, separated by groups according to the characteristic of the professional school, proportional to the percentage of students in four schools [16]. Each professional school was used as a stratum, in total four, which are: mathematics, operation research, statistics, and computing science. The selection of students for the study was random in each school. According to this sampling scheme, the sample size was calculated, with a significance level of 5%, a margin of error of 4.47%, the proportion of students with moderate academic stress level in each of the professional

school and historical information is provided by the registration office of the FMS [16], and the sample size was 311 students.

### ***3.2 Data Collection Techniques and Instruments, Validity, and Reliability***

The general characteristics were considered as age, gender, professional school, socioeconomic level, then the inventory of study habits was considered, whose purpose is to recognize in the student the appropriate and inappropriate habits expressed at the time of studying and, finally, the academic stress inventory that aims to identify the stress attributes that undergraduate and graduate students experienced during their university education.

The instrument that was used was divided into three parts: (1) general characteristics of the student; (2) inventory of study habits [2]; and (3) inventory of academic stress [17]. The length of the application of the instruments was from 15 to 20 min, which was carried out during the month of June of this year. To perform the internal consistency reliability analysis for this inventory of academic stress, Cronbach's Alpha was used. It was found that the value of this coefficient for the full scale was 0.89. For the validity of the instrument construct, the confirmatory factor analysis (CFA) was used [18], and the goodness-of-fit indexes were: goodness-of-fit index (GFI) = 0.964, adjusted goodness-of-fit index (AGFI) = 0.958, normed fit index (NFI) = 0.946, and relative of fit index (RFI) = 0.942 superiors to 0.90, so it is confirmed that the proposed model is adequate, with the three dimensions of the inventory of academic stress: symptoms, stressors, and coping strategies. Regarding the reliability of the study habits scale, it was considered KR-20 reliability, reliability of the entire scale was 0.74, which means that reliability is acceptable [19, 20].

## **4 Results**

For the logistic regression analysis [21], we use the academic performance variables, 0: approved and 1: disapproved, as a dependent variable and the explanatory variables are study habits, academic stress, stress level, and sociodemographic variables: age, gender, professional school, and socioeconomic level. The explanatory variable  $\beta$  is the logistic regression model parameter, Wald is the test statistic, which evaluates the significance of each parameter,  $Df$  degrees of freedom, the  $p$  - value is the probability associated with the test statistic which also evaluates the significance of each one of the parameters,  $\exp(\beta)$  is the exponentiation of the  $\beta$  coefficient, and (IC) at 95%  $\exp(\beta)$  is the interval confidence for  $\exp(\beta)$  at 95% confidence.

When analyzing the study habits variable, which was considered as categorical, the category (positive level) was taken as a reference and we can observe that the

positive value of  $\beta$  for the first category (trend level(-)) indicates that in students who had this type of study habits increases the possibility of disapproving courses in relation to those who had positive study habits. Students who have very negative or negative study habits are 4.477 times more likely to disapprove courses (Exp ( $\beta = 4.477$ )).

For the variable ‘professional school,’ four professional schools were considered: computer science, statistics, operations research, and mathematics. Mathematics school was used as a reference in order to calculate the odds ratio with respect to the other professional schools. In an attempt to reflect certain patterns, it is verified that students of the professional school of statistics are 8.40 times more likely to disapprove courses compared to students from other professional schools (Exp ( $\beta = 8.4$ )).

As a result, Table 1 shows the variables that influence academic performance and these are: age, professional school, study habits, and the dimension of reactions to academic stress, at a 5% level of significance. On the other hand, Table 2 shows the variables that do not influence performance that are gender, socioeconomic level, stress level (mild, moderate, deep), stressors, and coping strategies for academic stress, at a 5% level of significance ( $p - \text{value}$  greater than 0.05 level of significance).

**Table 1** An estimated logistic regression model with the significant variables of the academic performance of FMS students of a public university—Semester 2019-I

Variable	B	$\beta$ (odds) <sup>a</sup>	Wald	Df	p – value	exp( $\beta$ )	IC 95% exp( $\beta$ )	
							Lower	Higher
Age	-0.055		8.200	1	0.004	0.946	0.911	0.983
Professional school <sup>b</sup>			39.715	3	0.000			
Professional school (1)		0.899	6.553	1	0.010	2.458	1.235	4.892
Professional school (2)		2.128	27.835	1	0.000	8.400	3.810	18.520
Professional school (3)		1.627	25.452	1	0.000	5.087	2.704	9.569
Study habits <sup>c</sup>			10.825	3	0.013			
Study habits (1)	1.499		5.363	1	0.021	4.477	1.259	15.917
Study habits (2)	0.379		0.658	1	0.417	1.461	0.584	3.651
Study habits (3)	-0.189		0.128	1	0.721	0.828	0.294	2.330
Reactions to stress	0.026		4.542	1	0.033	1.026	1.002	1.050

<sup>a</sup>Odds value regards mathematics school

<sup>b</sup>Professional school (1): computing science, professional school (2): statistics, and professional school (3): operations research

<sup>c</sup>Study habits (1): Very negative or negative. Study habits (2): trend (-). Study habits (3): trend (+)

**Table 2** An estimated logistic regression model with the non-significant variables of the academic performance of FMS students of a public university—Semester 2019-I

Variable	Wald	Df	p – value
Sex	0.184	1	0.668
Socioeconomic level <sup>a</sup>	3.147	3	0.370
Socioeconomic level (1)	1.258	1	0.262
Socioeconomic level (2)	0.718	1	0.397
socioeconomic level (3)	1.903	1	0.168
Stressors	1.916	1	0.166
Coping strategies	0.001	1	0.976
Stress level <sup>b</sup>	0.819	2	0.664
Stress level (1)	0.212	1	0.645
Stress level (2)	0.777	1	0.378

<sup>a</sup>Socioeconomic level (1): high, socioeconomic level (2): medium and socioeconomic level (3): low

<sup>b</sup>Stress level (1): mild and stress level (2): moderate

The logistic regression model to predict the probability if a student is approved in its weighted average the Semester 2019-I is the following:

$$\hat{\pi} = \frac{1}{1 + e^{-z}}, \quad 0 \leq \hat{\pi} \leq 1 \tag{1}$$

where

$$\begin{aligned} z = & -0.055 \text{ Age} + 0.899 \text{ School}(1) + 2.128 \text{ School}(2) \\ & + 1.627 \text{ School}(3) + 1.499 \text{ Study Habits}(1) + 0.379 \text{ Study Habits}(2) \\ & - 0.189 \text{ Study Habits}(3) + 0.026 \text{ Reactions} \end{aligned}$$

The probability of a student approved is when  $\hat{\pi}$  is greater than 0.5 and less than one and the probability of a student disapproved is when  $\hat{\pi}$  is greater than zero and less to 0.5.

## 5 Discussion

The results show that age, professional school, study habits, and reactions to academic stress influence academic performance. This is consistent with other researchers whose findings indicate associations, but lack study habits, a study plan, implying the necessity to apply improvement plans in attitudes-time planning-physical development-motivation [22–24].



It is important to note that students having study habits generate greater academic performance because they generally manage their time well because they have attitudes and aptitudes for cognitive development and the desire to excel. On the other hand, stress generates the stimulation of stressors, generating physiological and psychological responses, and diseases can be generated. Other studies also agree that study habits and university achievement are associated, where students obtained good academic performance [23, 24].

Training processes in education not only consist of having study habits but also, it is important to have knowledge of the development of techniques and technologies that require the development of skills in students. The statement by [8] is also true that academic stress causes poor performance. And this stress is generated not only by the excess of tasks but the evaluations, incoherent works, or lack of theoretical–practical classes. On the other hand, in the study of [25], it refers to multiple causes of academic performance, and it indicates that it is caused by the interaction of multiple social, personal, institutional-academic factors that differ from a group of subjects. In addition, the author also believes that there are significant differences between university satisfaction, the index of study habits, levels of support in university students, satisfaction with teachers, and the socioeconomic level. Likewise, according to [26], the self-esteem variable influences academic performance. In our study, stress reactions or symptoms influence academic performance, and this is due to the fact that 77.2% of students have moderate to deep stress, also, in physical reactions, students state that they are drowsy or greater need to sleep, with respect to psychological reactions they express that they have restlessness (inability to relax and be calm), they also affirm that they have concentration problems, in light of these results, academic stress is present in the student.

## 6 Conclusions and Recommendations

In this work, we present a statistical model that explains the academic performance according to the variables' study habits, academic stress, and demographic variables, in this sense, we conclude that the variables that influence academic performance are: age, professional school, study habits, and reactions to academic stress, and the variables that do not influence performance are: gender, socioeconomic level, stress level, stressors, and coping strategies for academic stress ( $p$  – value greater than 0.05 level of significance). It is recommended that the FMS authorities design appropriate policies to help students who experience academic stress so that they can receive adequate treatment at the university clinic and improve their mental health. Also, the authorities may develop programs for students who have low academic performance so that they are taught the management and practice of study habits.

## References

1. OCDE, Pisa 2015: Resultados Clave (2016). <https://www.oecd.org/pisa/pisa-2015-results-in-focus-ESP.pdf>. Last accessed 14 Oct 2019
2. Vicuña, L.: Inventario de hábitos de estudio. CEDES, Lima (1998)
3. Barraza, A.: Un modelo conceptual para el estudio del estrés académico. *Revista Electrónica de Psicología Iztacala* **9**(3), 110–129 (2006). <http://www.psicologiacientifica.com>. Last accessed 11 Oct 2019
4. Atsiaya, E., Maiyo, J.K.: Study of the relationship between study habits and academic achievement of students: a case of Spicer Higher Secondary School, India. *Int. J. Educ. Adm. Policy Stud.* **7**(7), 134–141 (2015). <https://doi.org/10.5897/IJEAPS2015.0404>
5. Garbanzo, G.: Factores asociados al rendimiento académico en estudiantes universitarios, una reflexión desde la calidad de la educación superior pública. *Educación* **31**(1), 43–63 (2007). <https://www.redalyc.org/pdf/440/44031103.pdf>. último acceso 15 Oct 2019
6. Mondragón, C. M., Cardoso, D., Bobadilla, S.: Hábitos de estudio y rendimiento académico. Caso estudiantes de la licenciatura en Administración de la Unidad Académica Profesional Tejupilco, 2017. *Revista Iberoamericana para la Investigación y el Desarrollo Educativo.* **8**(15), 1–25 (2018). <http://dx.doi.org/10.23913/ride.v8i15.315>
7. Enriquez, M. F., Fajardo, M., Garzón, F.: Una revisión general a los hábitos y técnicas de estudio en el ámbito universitario. *Psicogente* **18**(33), 166–187 (2015). <http://doi.org/10.17081/psico.18.33.64>
8. Alfonso, B., Calcines, M., Monteagudo, R., Nieves, Z.: Estrés académico. *Edumecentro* **7**(2): 163–178 (2015). <http://scielo.sld.cu/pdf/edu/v7n2/edu13215.pdf>. Last accessed 15 Oct 2019
9. Chau, C., Vilela, P.: Variables asociadas a la salud física y mental percibida en estudiantes universitarios de Lima. *Liberabit* **23**(1), 89–102 (2017). <https://doi.org/10.24265/liberabit.2017.v23n1.06>
10. García, A., Del Toro, A. Y., Cisneros, E., Querts, O., Cascaret, X.: Algunas variables psicosociales asociadas al bajo rendimiento académico en estudiantes de primer año de medicina. *Medisan* **21**(4), 433–439 (2017). [http://scielo.sld.cu/scielo.php?script=sci\\_arttext&pid=S1029-30192017000400007](http://scielo.sld.cu/scielo.php?script=sci_arttext&pid=S1029-30192017000400007). Last accessed 15 Oct 2019
11. Cano, S. T., Ramos, J. A., Medina, M. G.: Análisis del estrés académico en estudiantes de ingeniería como estrategia para el aprendizaje significativo. *ANFEI Digital* **2**(5), 1–8 (2016). <http://www.anfei.org.mx/revista/index.php/revista/article/view/280/921>. Last accessed 15 Oct 2019
12. Zárate, N. E.: Estrés académico en estudiantes universitarios: medidas preventivas. *Revista de la Alta tecnología y la Sociedad* **9**(4), 92–8 (2017). <http://www.academiajournals.com/revista-alta-tec-y-sociedad>. Last accessed 15 Oct 2019
13. Rodríguez, B., González, M. D. P., Blanco, L. E.: Estresores académicos percibidos por estudiantes pertenecientes a la escuela de enfermería de Ávila, centro adscrita la Universidad de Salamanca. *Revista Enfermería C y L.* **6**(2), 98–105 (2014). <http://www.revistaenfermeriacyl.com/index.php/revistaenfermeriacyl/article/view/131/104>. Last accessed 15 Oct 2019
14. Zárate-Depraect, N. E., Soto-Decuir, M. G., Martínez-Aguirre, E. G., Castro-Castro, M. L., García-Jau, R. A., López-Leyva, N. M.: Hábitos de estudio y estrés en estudiantes del área de la salud. *FEM: Revista de la Fundación Educación Médica* **21**(3), 153–57 (2018). [http://scielo.isciii.es/scielo.php?script=sci\\_arttext&pid=S2014-98322018000300007](http://scielo.isciii.es/scielo.php?script=sci_arttext&pid=S2014-98322018000300007). Last accessed 15 Oct 2019
15. Khaleef, F. F., Saud, H., Nasser, M. F., Saliman, R. T., Elhaj, A.: Stress and its impact among medical students in Hail University, KSA. *Int. J. Adv. Res.* **6**(4), 1381–1387 (2018). <http://dx.doi.org/10.21474/IJAR01/6999>
16. Hernández, T., Mendoza, C.P.: *Metodología de la Investigación*, 6a edn. McGraw Hill, México (2018)
17. Scheaffer, R., Mendenhall, W., Ott, L.: *Elementos de muestreo*, 6ª edn. Paraninfo Cengage Learning, Madrid (2007)

18. Barraza, A.: Propiedades psicométricas del Inventario SISCO del estrés académico. *Psicología Científica.com.* **9**(10) (2007). <http://www.psicologiacientifica.com/sisco-propiedades-psicometricas/>. Last accessed 15 Oct 2019
19. Aldas, J., Uriel, E.: *Análisis multivariante aplicado con R*, 2ª edn. Editorial Paraninfo, Madrid (2017)
20. Kuder, G.F., Richardson, M.W.: The theory of the estimation of test reliability. *Psychometrika* **2**(1), 151–160 (1937)
21. Hosmer, D. W., Lemeshow, S., Sturdivant, R. X.: *Applied Logistic Regression*. New Jersey, Wiley (2013)
22. Chilca, L.: Autoestima, hábitos de estudio y rendimiento académico en estudiantes universitarios. *Propósitos y Representaciones* **1**(5), 71–127. (2017). <http://dx.doi.org/10.20511/pyr2017.v5n1.145>
23. Espinoza, J. L.: Relación entre los hábitos de estudio y el rendimiento Académico de los alumnos de escuelas profesionales acreditadas. *Revista Científica Tzhoecon* **9**(4), 29–40. (2017). <https://doi.org/10.26495/rtzh179.423933>
24. Gilavand, A.: Investigating the study habits among students of iranian medical sciences universities: a review. *Indo Am. J. Pharm. Sci.* **4**(12), 4734–4738 (2017). <https://doi.org/10.5281/zenodo.1133164>
25. Sreelekha, V., Indla, Y. R., Reddy, R., Rameswarudu, M., Swathi, A., Yamini, D., et al.: Study habits and academic performance of first year MBBS students. *Int. J. Med. Sci. Public Health* **5**(9), 1831–1835 (2016). <https://go.galegroup.com/ps/anonymou?id=GALE%7CA466520071&sid=googleScholar&v=2.1&it=r&linkaccess=abs&issn=23204664&p=HRCA&sw=w>. Last accessed 15 Oct 2019
26. Nicho J.: Relación entre la autoestima y el rendimiento académico de los estudiantes de la e.b.c. Tecnológica de la Facultad de Educación de la Universidad Nacional José Faustino Sánchez Carrión. *Universidad Nacional, Perú* **2**(5), 606–615 (2013)

# Model of Sustainable Digital Transformation Focused on Organizational and Technological Culture for Academic Management in Public Higher Education



Jessie Bravo , Janet Aquino , Roger Alarcón , and Nilton Germán 

**Abstract** Currently, public universities in Peru are undergoing changes due to new market requirements, aspects that regulatory entities took into account to rethink their operational requirements, therefore, it is necessary that their processes are adapted and comply with these new characteristics regulated according to law, especially academics who relate directly to teachers and students, these processes must be transformed taking into account emerging technologies. To solve this problem, a sustainable digital transformation model was developed, consisting of four dimensions: infrastructure, business architecture, digitalization, and people. In each dimension, indicators were used to assess at what stage of maturity it is found, which by integrating them allowed us to know the level of general maturity of the digital transformation of the institution in which our case study was applied to the effects of knowing the digital divide. This model was validated in a national university of Peru, specifically in the process of managing the digital teaching portfolio.

**Keywords** Digital transformation · Academic management · Maturity level

---

J. Bravo (✉) · J. Aquino · R. Alarcón · N. Germán  
School of Computer and Informatics Engineering, Pedro Ruiz Gallo National University,  
Lambayeque, Peru  
e-mail: [jbravo@unprg.edu.pe](mailto:jbravo@unprg.edu.pe)

J. Aquino  
e-mail: [jaquino@unprg.edu.pe](mailto:jaquino@unprg.edu.pe)

R. Alarcón  
e-mail: [ralarcong@unprg.edu.pe](mailto:ralarcong@unprg.edu.pe)

N. Germán  
e-mail: [ngerman@unprg.edu.pe](mailto:ngerman@unprg.edu.pe)

## 1 Introduction

At present, public universities in Peru under the licensing context have led them to adapt to the new requirements of both infrastructure and technology, so they are looking for ways to improve their academic services, reduce costs and achieve the basic quality conditions. These conditions, in addition to being an indispensable requirement for the functioning of universities, will allow students to receive an educational service according to the needs and expectations of the student population and society in general. On the other hand, with the information and communications technologies present in the market, which provide tools to be competitive, it is necessary to create new scenarios adapted to the measures and needs of public universities. The purpose of this study is to provide a model of sustainable digital transformation in order to solve the needs of public universities in Peru with the main axis, the person, through the measurement of their digital and organizational maturity, allowing digitalization processes streamline management and improve the quality of the educational service.

## 2 State of the Art

It can be stated that according to [1] digital transformation in the public sector means new ways of working with stakeholders, building new service delivery frameworks and creating forms of relationships. Digital transformation is mainly associated with the need to use new technologies to remain competitive in the Internet era, where services and products are delivered both online and offline. Others define digital transformation as a way to rebuild business models following the needs of customers through the use of new technologies [2].

In the research conducted by Bernhard [3] on the current state of digitalization of adult, continuing education in Switzerland and Germany identifies that information technology infrastructure, staff development, and management/leadership are the most relevant challenges to implement digital media in continuing education organizations for adults. According to [4], digital transformation processes must have an innovative model for how to work with students with the aim of improving the scope of teaching. Similarly, [5] consider that digital transformation introduces a new business model through the implementation of new business logic to create and capture value, it affects the entire company and its ways of doing business. Jackson [6] examines problems that have always needed ambidexterity, also of innovation and considering the past trajectories that had caused problems in education. For Aguiar et al. [7] the multidimensional environment of the modern university must be considered as something fundamental to address the innovation needs demanded by society, the bearer of the largest commission. Without a doubt, the progress made by the Internet makes it the main protagonist of the great technological revolution of the twenty-first century. Its inescapable presence has constituted it as a great scenario in which new ways of learning, thinking, communicating, doing and acting take place.

According to [8] digital transformation in higher education was referenced in seven dimensions, governance dimension was included in the process on its own, differing in that our proposal is based only on four dimensions and a transversal activity that allows the monitoring and tracking of this entire transformation process.

In [9] a conducted research on cultural diversity and new communication ecosystem of the emerging digital culture are analyzed in the discourses that guide the Information and Communication Technologies (ICT) policies in education in the cities of Brazil, Argentina and Chile.

### 3 Proposal

Based on a review of the literature, a sustainable digital transformation model for academic management in public universities is proposed, where, according to the exploratory analysis performed, it is evident that the personal factor is relevant to the success of the digital transformation required in the university. Our model integrates aspects of organizational culture and digital culture. The proposed model focuses on four dimensions: person, business architecture, digitalization, supported in the infrastructure dimension as shown in Fig. 1.

- **Person Dimension (*P*):** It is one of the most important dimensions public higher education, it is observed that the main limiting factor of an adequate digital transformation is the person, so it is necessary to measure the digital culture (DC) and organizational culture (OC) of the people involved, thus referring to teachers, as the main agent of change. Regarding organizational maturity, key aspects such as institutional identification, soft skills and organizational climate have been considered, since this will allow recognizing limitations and defining organizational change strategies. The maturity model of digital culture takes into account three dimensions: the use of technology, digital skills and communication, and the Internet. Within this digital ecosystem, different profiles of users have been found, which present totally different habits.
- **Infrastructure Dimension (*I*):** Every public university must have the physical infrastructure, which includes classrooms, laboratories, workshops, administrative offices, leisure spaces, and sports fields. The technological infrastructure such as the Internet connection, cloud computing, servers, multimedia projectors, smart boards and a security system which includes aspects such as surveillance, safe areas, gauging, drills, use of fire extinguishers and security protocols are considered.
- **Business Architecture Dimension (BA):** This dimension has been divided into two levels: user and manager. The user-level includes the processes that interact directly with students, teachers, and graduates. At the manager level, it has been subdivided into directive processes and academic management processes.
- **Digitalization Dimension (*D*):** Based on the business model dimension, it has been divided into three levels: service platform digitalization, the directive digitalization level and the academic digitalization.

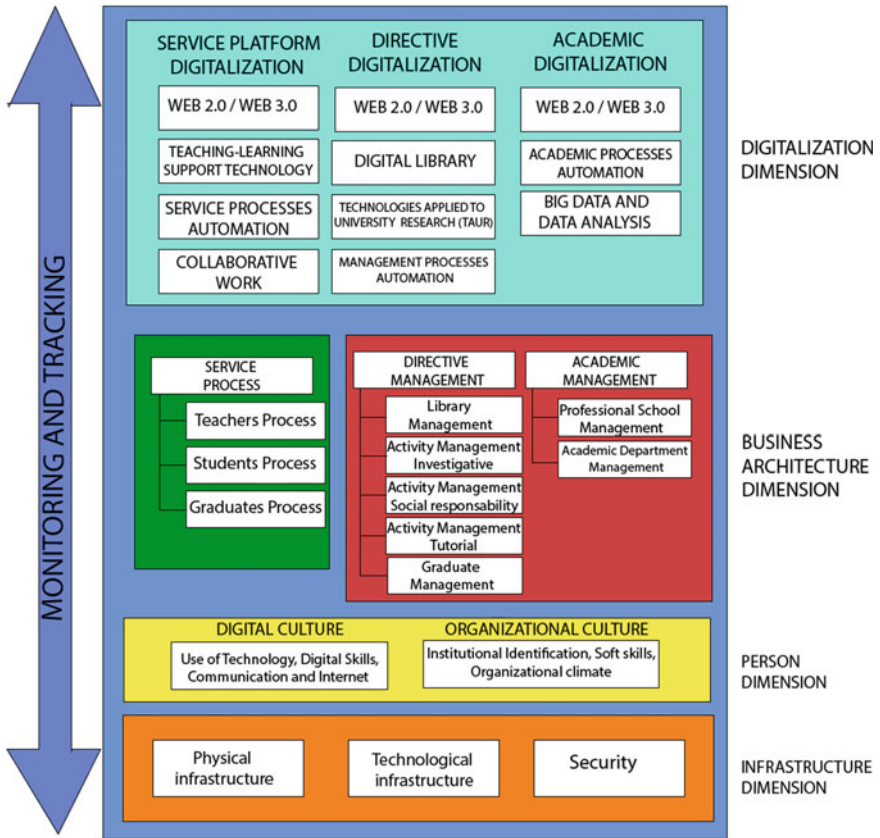


Fig. 1 Model of sustainable digital transformation

For the calculation of the score in each dimension:

$$Score_{Dimension} = \frac{\sum_{i=1}^n Score_{criteria}}{n} \tag{1}$$

For the calculation of the model score:

$$Score_{Model} = \frac{\sum_{j=1}^{nd} Score_{Dimension}}{nd} \tag{2}$$

Tables 1 and 2 describe the proposed maturity levels for the person dimension.

For the remaining dimensions (infrastructure, business architecture, and digitalization) the maturity levels are defined according to Table 3.

**Table 1** Maturity levels regard organizational culture

The maturity level of organizational culture	General score	Average score
Indifferent	0–15	0–5
Interested	16–29	6–9
Involved	30–44	10–15
Committed	45–60	16–20

**Table 2** Maturity level regards digital culture

The maturity level of digital culture	General score	Average score
Primitive	0–17	0–5
Basic	18–34	6–11
Intermediate	35–51	12–17
Advanced	52–68	18–23

**Table 3** Maturity levels by infrastructure, business architecture, and digitalization

Dimension	Infrastructure	Business architecture	Digitalization
General score by maturity levels			
Incipient	0–8	0–8	0–8
Basic	9–16	9–16	9–16
Managed	17–25	17–25	17–25
Optimized	26–34	26–34	26–34

Finally, the level of maturity (LM) of the institution’s digital transformation model was evaluated by separately first the dimensions of the person and second the three remaining dimensions, infrastructure, business architecture, and digitalization. The formulas to apply for our digital transformation model are the following:

$$LM_{TD} = Index_I + Index_{BA} + Index_D \tag{3}$$

$$LM_P = Index_{OC} + Index_{DC} \tag{4}$$

## 4 Validation

To validate the sustainable digital transformation model presented, we applied a case study to show that the proposal successfully resolves the application of ICT in the academic management of university higher education. Figure 2 shows the methodologies chosen for each dimension in the process of digitalization of the teaching portfolio of a national university.



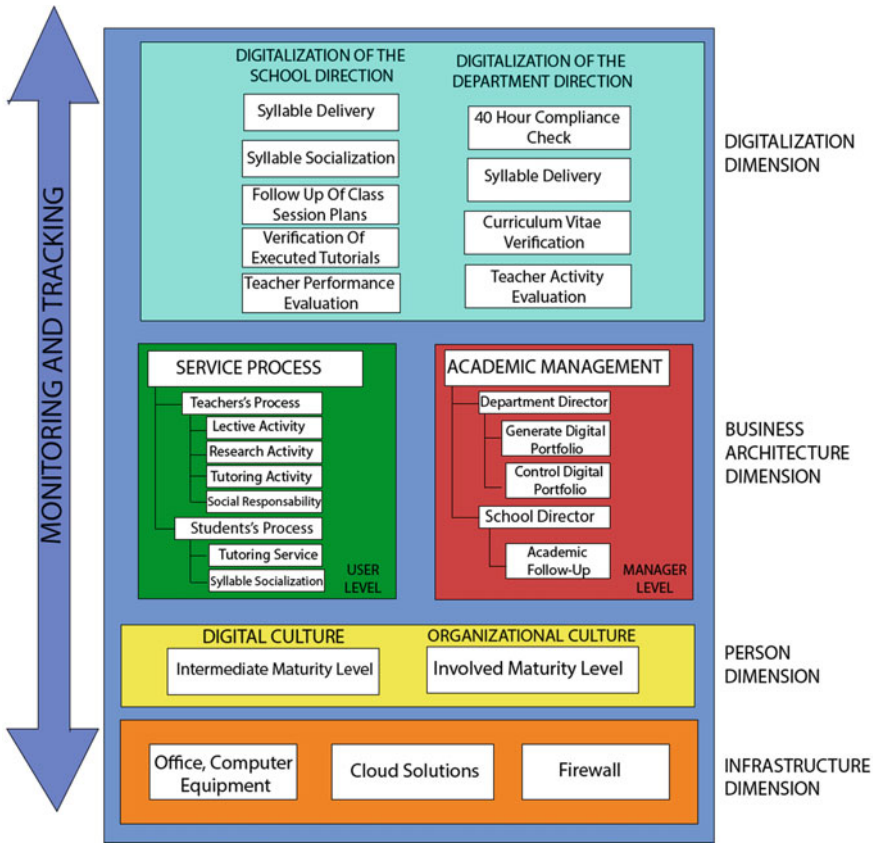


Fig. 2 Result of the application of the model of sustainable digital transformation

- Person dimension: For this dimension, two surveys were applied, one to measure the organizational culture and the other the digital culture. Regarding the organizational culture, 216 surveys were applied, this was validated regarding its content and reliability using the Cronbach Alpha obtaining a good result (0.812). It was observed that for 35 people its level is interested, which represents 43.52%, in terms of institutional identification, instead, 190 people are committed, it represents 87.96% in the management of soft skills and 130 people are at the level involved (60.19%) in relation to the organizational climate. For the digital culture, 228 surveys were applied, this was validated regarding its content and reliability using the Cronbach Alpha obtaining an acceptable result (0.799), from these results it can be observed that referring to the digital culture in the university 153 people (67.11%) have an intermediate maturity level and 46 people (20.18%) have an advanced maturity level that will allow us to successfully face the proposed technological changes.

- **Business architecture dimension:** This dimension includes two levels, for the student user, their relationship is indirect through the tutoring service provided by teachers and socialization of the syllabus. The teaching user is the main entity that will allow him to manage his academic activity related to the activities: teaching, research, tutoring and social responsibility. Regarding the second level: manager, it will be the responsibility of the director of the department and part of the director of the school. The department director is responsible for generating and controlling the digital teaching portfolio every academic year. The school directors are responsible for the academic follow-up, the teaching portfolio being an important tool for such activity.
- **Digitalization dimension:** For this case study, academic digitalization has been implemented through mandatory use of institutional mail, digital portfolio digitalization using the institutional virtual platform such as the classroom tool. The activities carried out by the school director and department director that are currently digitized, related to the teaching digital portfolio process, represent 66.7%.

To determine the level of maturity based on the three dimensions of infrastructure, business architecture and digitalization, based on the indicators expressed in Table 3, the following was obtained:

$$LM_{TD} = 18.22 + 25.0 + 22.23 = 65.46 \quad (5)$$

It can be seen that the university maturity level of digital transformation in the teaching digital portfolio process is at the managed-level, but there are still improvements to be made that will be achieved thanks to the monitoring and tracking based on the strategies mentioned in the following section to achieve the optimized level.

Regarding the person dimension, the organizational and digital culture was evaluated, obtaining the following results, organizationally the teachers are involved and in terms of the digital aspect, their level is intermediate.

$$LM_{OC} = 74.07 \quad (6)$$

$$LM_{DC} = 67.11 \quad (7)$$

#### ***4.1 Tracking and Monitoring***

The purpose we propose is that our model allows for sustainability, this means that the University has the capacity to ensure its continuity and long-term positioning, as well as contributing to the continuous improvement of the basic conditions of academic quality, to we have considered the following strategies:

- The people dimension: improvement of the organizational climate, permanent training of teachers in terms of management and digital skills, awareness campaigns.
- The infrastructure dimension: implementation of the school management offices and academic departments with technological equipment, improvement of Internet bandwidth, adequately define the policies for access to information and technological equipment.
- The business architecture dimension: elaborate the procedure for executing the tutorials performed on the students, continue with the follow-up of the teaching digital portfolio.
- The digitalization dimension: follow up the class session plans, verify the tutorials executed, and determine indicators to evaluate the teacher's teaching activity.

## 5 Conclusions

The result of the proposed model demonstrates that the initial level of digital maturity in teachers was basic and it was possible to reach the intermediate level. The initial level of organizational maturity is pondered as interested, reaching the level involved. The initial level of infrastructure, digitalization and architecture of the business were pondered as basic, reaching the level managed. Also, the organizational culture is essential to achieve the strategic objectives, since the mastery of the technological tools is not enough if the teacher does not commit to his institution. As future work, a much more exhaustive analysis of the teacher's characterization should be made to identify which criteria are relevant and determine a profile of the university teacher for its digital transformation.

## References

1. Mergel, I., Edelman, N., Nathalie, H.: Defining digital transformation: results from expert interviews. *Gov. Inf. Q.* **36**, 1–16 (2019)
2. Berman, S.: Digital transformation: opportunities to create new business models. *Strat. Leader.* **40**(2), 16–24 (2012)
3. Bernhard-Skala, C.: Organisational perspectives on the digital transformation of adult and continuing education: a literature review from a German-speaking perspective. *J. Adult Contin. Educ.* **25**, 20 (2019)
4. Ariño Martín, L. A.: Digital transformation: key points and considerations for reflection of the digital transformation in the university. *RUIDERAE: Revista de Unidades de Información*, pp. 1–20 (2018)
5. Verhoef, P. C., Broekhuizen, T., Bart, Y., Bhattacharya, A., Qi Dong, J., Fabian, N., Haenlein, M.: Digital transformation: a multidisciplinary reflection and research agenda. *J. Bus. Res. Paris* 1–13 (2019)
6. Jackson, N.C.: Managing for competency with innovation change in higher education: examining the pitfalls and pivots of digital transformation. *Bus. Horiz.* **62**, 761–772 (2019)

7. Aguiar, B., Velásquez, R., Aguiar, J.: Innovación docente y empleo de las TIC en la Educación Superior. *Espacios* **40**(2), 8–19 (2018)
8. Almarz Menéndez, F., Maz Machado, A., López Esteban, C.: Analysis of the digital transformation of Higher Education Institutions. A theoretical framework, *Revista de educación mediática y TIC, España* 181–202 (2016)
9. Vivanco, G., Gorostiaga, J.: Cultura digital y diversidad: perspectivas de discursos de políticas TIC-Educación. *Cadernos de Pesquisa* **47**(165), 1016–1043 (2017). <https://doi.org/10.1590/198053144261>

# University of Brasilia's Potential for Bioeconomy Services and Innovation



Flávio Duque Estrada Soares Pereira  and Wagner Augusto Fischer 

**Abstract** Bioeconomy is an emerging concept that has been more and more integrated into discussions concerning sustainable development. Such a theme became one of Brazil's main strategies for science, technology and innovation, spurring several initiatives seeking to better understand the country's bioeconomic capacity. The present study was one of several conducted in Distrito Federal attempting to assess the state and its surrounding region's economic strengths and weaknesses, part of Projeto Brasília 2060. The aim of this study was to perform a descriptive analysis of the University of Brasília's potential in the field of Bioeconomy. We conducted semi-structured interviews with respondents from 74 laboratories from four different institutes/faculties of the Darcy Ribeiro Campus. Our results showed that 48 laboratories had the latent capacity to start/expand activities related to technological innovation or service provision to firms, government or society. Most laboratories seemed more inclined to provide services than technological innovation. Using the content analysis methodology, we were able to detect six categories of obstacles that hinder UnB's potential to Bioeconomy.

**Keywords** Innovation policy · Technology transfer · Content analysis · Research management

## 1 Introduction

Bioeconomy is an emerging concept that has been progressively more integrated into the global agenda concerning sustainable development. Such term came into the spotlight due to the climate change scenario and the perspective of several non-renewable resources being depleted in the near future. The European Union, for

---

F. D. E. S. Pereira (✉) · W. A. Fischer  
Instituto Brasileiro de Informação em Ciência e Tecnologia—IBICT, Brasília, DF 70070-912,  
Brazil  
e-mail: [fdquexiv@gmail.com](mailto:fdquexiv@gmail.com)

example, is structuring policies towards a more resource-efficient and sustainable economy, promoting innovation, food security and environmental protection [1].

Similarly, Bioeconomy became part of Brazil's main strategies for science, technology and innovation [2, 3]. A few reasons for this theme's inclusion in the national strategy are the country's commitments in the Paris Agreement to reduce emissions of greenhouse gases, as well as Brazil's potential in this field thanks to its biodiversity. Ever since it gained a strategic status, several Brazilian initiatives have aimed to better understanding and developing of the country's bioeconomic capacity.

One of the projects that dealt with this subject was Projeto Brasília 2060, carried out by the Brazilian Institute for Information in Science and Technology (IBICT). Its goal was to develop studies to better comprehend the potentials for sustainable development in Brasília's Metropolitan Area. Bioeconomy was, among other thematic axes, considered one of the most promising fields for this economic region. The present study was part of such project and its objective was to analyse the University of Brasília's (UnB) capacity in Bioeconomy. UnB was chosen for this study because it is Distrito Federal's oldest and largest University.

Although there is more than one definition to Bioeconomy in official strategic documents from the Brazilian Government [2, 3], we opted to use the one from the Organization for Economic Cooperation and Development (OECD): economic activities that come from innovation in fields related to biological sciences, culminating on the development of sustainable products, processes and services [4].

## 2 Methods

### 2.1 *Defining the Sample*

Ethical approval for the experiment in this study was deemed unnecessary, as the research was designed to investigate laboratories, not human individuals. Our questions were aimed at evaluating the laboratory itself as part of a public university. Also, the activities in the survey do not pose risks greater than those ordinarily encountered in daily life, and all the interviewed subjects remained anonymous. All participants that opted to participate were also informed about the academic objective of the research, as well as ensured preservation of their anonymity. This is in accordance with Article 1 of Resolution 510, of 7 April 2016, of Brazil's National Health Council (available at <http://www.conselho.saude.gov.br/resolucoes/2016/Reso510.pdf>) and also with item 8.0.5 of the Ethical Principles of Psychologists and Code of Conduct of the American Psychological Association (available at <https://www.apa.org/ethics/code/principles.pdf>). Furthermore, Brazilian Law no. 12.527, of 8 November 2011 states that public universities (and therefore its workers—see Art. 7; III) have the obligation to provide any information requested related to its resources (Art. 7; VI), organization, activities, projects, goals and indicators (Art. 7; VII).

UnB is a federal university comprised of five different campi, including the Fazenda Água Limpa (FAL), an open campus/laboratory (a farm) destined to conduct experiments in Biology, Veterinary, Agronomy and other research fields. According to their respective websites, there are 14 different laboratories on the Ceilândia Campus (CC), most of them carrying out health sciences research. Ten research laboratories are located on the Planaltina Campus (PC), most of which are dedicated to Bioeconomy and Biotechnology studies. All of the five laboratories on the Gama Campus (GC) perform engineering research. The Darcy Ribeiro Campus (DRC), on the other hand, was the first one created for UnB, accommodating over 400 laboratories from several academic fields.

Because Darcy Ribeiro Campus (DRC) is the largest and oldest of the campi, we chose to restrict our research to this site, since it is expected that its researchers would be more familiar with the university's mechanisms for technology transfer and innovation. The next step of our study was to identify which institutes or faculties in DRC congregate most of the laboratories that perform (or have the potential to perform) research and services in the field of Bioeconomy. Therefore, we analysed all information from laboratories and research groups available on UnB's website. Our analysis indicated that most laboratories with research and activities related to Bioeconomy on DRC were located on the Institute of Biology (IB), the Faculty of Health Sciences (FHS), the Institute of Chemistry (IC), the Faculty of Agronomy and Veterinary (FAV) and the Faculty of Technology (FT), specifically on the Department of Environmental Engineering.

## 2.2 Survey Design

Once our sample universe was defined, we developed and applied our survey consisting of seven questions, two of which aimed to identify the respondent (*Q1*, *Q2*), four were to delineate the activities, infrastructure, collaborations and funding of the laboratory (*Q3*, *Q4*, *Q6*, *Q7*), and one question was to obtain information about the laboratory's current situation when it comes to innovation and technological transfers (*Q5*). The survey is detailed below:

- *Q1*. Name of the interviewed researcher
- *Q2*. Researcher's contact
- *Q3*. Research themes under way at the laboratory
- *Q4*. Main equipment in use at the laboratory
- *Q5*. Laboratory's capacity (latent or consolidated) to provide services to the society or either the private or public sector, and its capacity (latent or consolidated) for technological production/innovation. Here, we specifically asked the researchers to:
  - cite the main services and technologies that could be provided/developed by the laboratory.

- talk about the barriers that hindered the laboratory’s potential to develop new services and technologies.
- report what would be necessary to expand the provision of services/technological innovations that already existed in the laboratory.
- Q6. Research collaboration (I) within the same institute/faculty, (II) with different institutes/faculties within the same university, (III) with other Brazilian universities and (IV) with other countries.
- Q7. Is the laboratory being funded?

### 2.3 Survey Application

All interviews were conducted in loco, along three months (from July to September 2018), with whichever researchers (researcher-professors or either Ph.D. or post-doctorate students when the professors were not available) were present in the laboratories during the visitation period. The interviews were conducted in a semi-structured manner, and the respondents’ answers were written on a printed form containing the seven questions, being posteriorly transcribed to a Microsoft Excel table. All respondents agreed to participate in the study and were informed of its objectives. In order to acquire a representative description of what factors possibly hindered DRC’s laboratories capacity in the field of Bioeconomy, we used content analysis to identify recurring topics in the respondent’s answers [5, 6]. Francis and collaborators [7] recommend establishing a sample size for the first round of analysis (referred to as initial analysis sample), then performing a certain number of interviews to confirm if the data is saturated (i.e. no new topics appearing). The authors recommend at least three interviews following the initial analysis sample to confirm saturation.

Therefore, our visits to the laboratories/correspondent researchers started on the Faculty of Agronomy and Veterinary (FAV), followed by the Institute of Biology (IB), Institute of Chemistry (IC) and Faculty of Technology (FT). The answers obtained were analysed (as detailed in our Sect. 2.4: content analysis), and the initial categories of topics were proposed.

Afterwards, we conducted five interviews in the Faculty of Health Sciences (FHS) to test the hypothesis of data saturation. Indeed, no new topics emerged during this process. The FHS was chosen for this purpose because its laboratories acting in the Bioeconomy field only represent a small percentage of its total laboratories. Even though there were new mentions of topics already presented, data from FHS was excluded entirely, since only five interviews would not constitute a representative sample from the faculty. We consider this was not harmful to our analysis, since there were evidences that responses obtained from the other institutes were enough to reach saturation (i.e. an optimal sample size [6]).

In total, we visited 74 laboratories on the DRC: FAV (16 laboratories), IB (38), IC (12) and FT (8), accumulating over 100 respondents. Laboratories on Darcy Ribeiro Campus frequently have more than one researcher-professor responsible for carrying



out different lines of research. In order to avoid overstatement of the answers provided in our survey, we grouped the answers of all researchers from the same laboratory.

## **2.4 Content Analysis**

Once the answers from the 74 laboratories were tabulated, we proceeded to the pre-analysis of their content. The organization of the material is followed by its “floating reading” [8], with the objective of impregnating the researcher with its content [9]. After reading the entire material, we proposed six categories, or topics, related to the capacities for technological innovation and service provision, as well as two binary variables for the presence/absence of innovation or service provision and the possibility for expanding current activities. Each category was associated with certain terms and themes which appeared in the sample of interviews [10].

The next step encompassed counting which categories were represented in each of the answers, being assigned the value 1 (one) if terms or themes related to that topic were present and 0 (zero) if none were present. We aggregated all data from each institute before presenting it in order to preserve the identity of the respondents. Furthermore, a topic was considered relevant to our study only if it reached a minimum of five occurrences in the sample. Other topics that appeared more than once but failed to meet this criterion will also be addressed in our next section.

## **3 Results and Discussion**

Our results and discussion will be divided into three sections. The “Findings from the survey” section will focus on the answers obtained from questions Q5–Q7, presenting an overview of the results. The following “Barriers for innovation and services related to Bioeconomy” will detail the findings presented in the preceding section. Finally, “Limitations of the study” will discuss the methodological limitations in this research as well as recommendations for future studies.

### **3.1 Findings from the Survey**

The main themes/categories detected during the floating reading of question Q5's answers were “need for physical space”, “need for equipment maintenance”, “lack of equipment”, “need for laboratory technicians”, “need for laboratory consumables and reagents” and “bureaucratic problems”. A brief summary of the categories with examples of answers that fit in each of them is presented in Fig. 1, including statements that indicate if the laboratory had an established capacity in technological production or service provision, as well as the latent capacity to start or expand such activities.

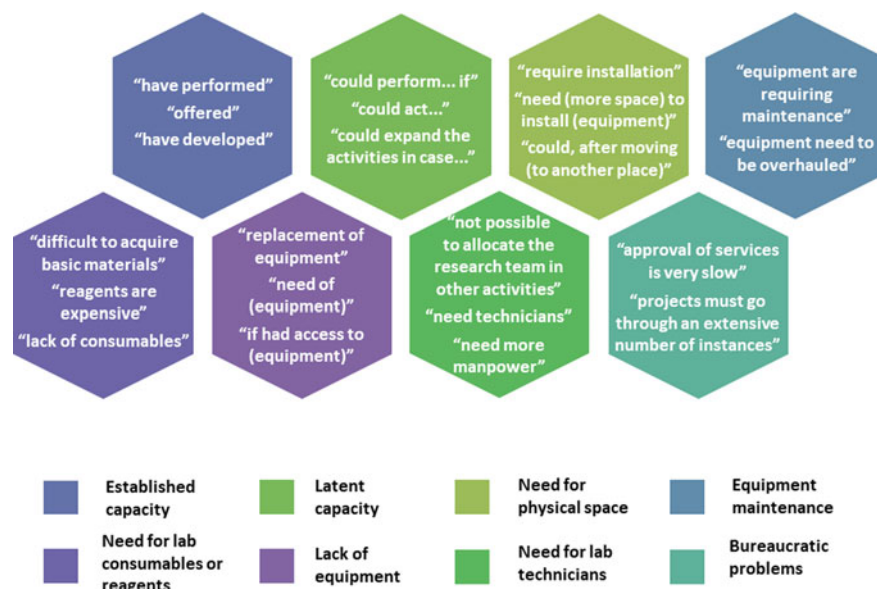


**Fig. 1** Categories/dimensions with examples of answers that fit in each of them

The absolute frequency of answers per laboratory that fits into each category can be seen in Table 1. On the same table is the number of laboratories that declared having provided services to the society or either the private/public sector or had developed technology (established capacity) or had the capacity to start/expand such activities (latent capacity).

The topics are shown in Fig. 1 and Table 1 were not the only ones that appeared during the interviews. Others, such as difficulty to conform to standards required

**Table 1** Absolute frequency of answers per institute that fit into each topic/category, including declared established and latent capacity

Topic	Institute (or faculty)				
	FT	IC	FAV	IB	Total
Established capacity	4	9	6	9	28
Latent capacity	6	9	7	26	48
Need for physical space	2	3	0	0	5
Equipment maintenance	3	0	0	2	5
Lack of equipment	2	7	3	5	17
Need for laboratory technicians	3	3	4	10	20
Need for laboratory consumables or reagents	1	1	1	4	7
Bureaucratic problems	0	3	1	5	9
Interviewed laboratories	8	12	16	38	74

for laboratory certification (such as INMETRO or ANVISA) and need for funding showed up in the answers with a total absolute frequency of 2 and 4, respectively. The topics related to certification could either be a specific scenario to the laboratories that reported them or even another type of problem associated with the “bureaucratic problems” dimension. The need for funding, on the other hand, was most likely linked to a specific need of the laboratory related to other topics (such as equipment maintenance or acquisition) that was not properly disclosed by the interviewees.

It is also important to highlight that none of the presented categories/themes were mutually exclusive. For example, researchers could declare to have an established capacity to provide services or produce technologies, and also believe their laboratory could expand such activities.

When it comes to resources, 44 of the laboratories declared being funded at the moment, and the most frequent source cited was the Research Support Foundation of Distrito Federal (FAPDF). Most of the other funding sources cited were also from the public sector. The question Q6 of the form (about research collaboration) showed that DRC laboratories in the field of Bioeconomy have a high amount of cooperation within institutes/faculties, with other Universities and research centres of Distrito Federal (especially EMBRAPA) and Universities from other Brazilian states or countries. Interestingly, the cooperation among institutes from the same campus was relatively small.

Our results show that 28 of the 74 interviewed laboratories (37.8%) had an established capacity to perform technological production/innovation or services (Table 1). In this group, 13 (46.4%) also declared they could expand such activities under certain conditions. Most of the 48 laboratories with latent capacity were more inclined to perform services to the society or the private/public sector than technological production. Such services include advising companies and government in the field of Bioeconomy, providing analyses of materials and components and even creating certifications for products. However, several barriers compromise the consolidation of these capabilities.

### ***3.2 Barriers for Innovation and Services Related to Bioeconomy***

Since this paper characterizes a case study, the results obtained from the sample represent only the situation of DRC's laboratories acting in the field of Bioeconomy. Therefore, even though we shall compare our findings with others from the literature, it is important to note that only one other article [11] had a similar scope, also being conducted at UnB, specifically on its Support Centre for Technological Development (SCTD).

According to the interviewees, the “need for consumables or reagents” impacted their laboratory's capacity to supply continuous services to the society, especially due to their elevated costs. Similarly, as reported by the respondents, the necessity of

“equipment maintenance” made it difficult for their laboratories to perform certain types of analyses or services continuously to the private sector. However, that does not mean the laboratory’s equipment was not working or out of use. Instead, the lack of proper maintenance made it difficult for the laboratories to ensure the accuracy of their analyses to companies. Both of these topics are related to one of the reasons why laboratories seek to provide services or technology transfers, which is the attainment of necessary resources to carry on their research activities [12, 13].

Laboratories’ “need for physical space” appeared only in answers from the Institute of Chemistry and the Faculty of Technology. The appearance of this topic on the IC was related to the need for scaling up the activities in order to achieve what the respondents considered an adequate technological production or service provision. This topic’s presence on the FT, however, was mostly related to their current physical installation. The Department of Environmental Engineering, where our research took place, had increased its staff and activities over the years inside the FT. Such facilities had consequentially become too small to accommodate the Department, and the University was taking action to reallocate them into a new building.

The “lack of equipment” was one of the most frequent topics cited in our sample (17 times), and it brings some relevant considerations to our study. It was observed that this topic’s mention on the IC was usually related to the need for scaling up processes of technology production or service provision (much like the category “need for physical space”). Respondents from the IC also stated that sometimes companies reach out to the laboratories requesting types of analyses that require specific equipment that is not available. Interestingly, the IC has at its disposal an Analytical Centre (Central Analítica do Instituto de Química—CAIQ), a laboratory located on the IC’s facilities with a pool of equipment and personnel dedicated to operating them. It seems, however, that CAIQ is not enough for IC’s researchers to develop their full potential for innovation and services and is more often used to assist them in their academic work.

To other institutes and faculties, on the other hand, the “lack of equipment” seems to impact both the provision of services/innovation and their academic work. However, the fourth question in our survey (main equipment in use at the laboratory) showed that several of the equipment listed by a laboratory as a necessity was usually available in other laboratories on the campus. This shows that researchers on the same campus often do not know other laboratories’ work and installations, and a result that was corroborated by our sixth question (research collaboration), which showed that cooperation between institutes and faculties within the same university are less frequent than within institutes or between different universities. For example, no laboratory outside the Institute of Chemistry cited any use of IC’s Analytical Centre (CAIQ).

The topic “bureaucratic problems”, which appeared nine times across our sample, encompassed both the slow internal processes of the University and the lack of preparation that professors-researchers have to deal with them. This last aspect also appears in other studies about technology transfer [12–14]. When it comes to this dimension, our interviewees demonstrated some frustration with UnB’s bureaucracy (although there were also positive opinions towards its institutions dedicated to technology

transfer and research support). For example, some respondents have reported that it takes at least six months for the university to approve the necessary arrangements for the laboratory to provide services to a firm, a reality that was also described in another study conducted on UnB [11]. The respondents disclosed their previous experiences with know-how and technology transfer, stating that some companies were not willing to wait for the extensive time it takes for cooperation between the private sector and university to be approved. Costa and Cunha [12] explain that small-medium enterprises (SMEs) often find this bureaucracy inadequate and lack the proper stimuli to invest in innovation. Bigger enterprises, on the other hand, may choose to execute their research and development internally, whilst international companies may simply opt to import technologies.

The category “need for laboratory technicians” was another barrier to the laboratories’ latent capacity, appearing with the highest absolute frequency in the sample. According to the interviewees, personnel that works on the laboratories is most often needed to execute research activities, being impossible to allocate the researchers to perform external services. As stated by previous studies [12, 13], the Brazilian Governmental policy for evaluation of higher education institutes may contribute to this issue, since the number of researchers’ publications are more relevant to their professional evaluation than work developed in cooperation with companies (a scenario also seen in Argentina [14]).

Barra et al. [15] have studied correlations between academic excellence, local knowledge spillovers and innovation in Europe. Their study shows a possible trade-off between academic impact/reputation and appropriation of scientific knowledge/innovation by local firms, since they had found negative correlations between a number of publications per university staff and local innovation. Barletta et al. also found similar results in Argentina [14], by observing a negative correlation of scientific production (i.e. papers) and technological transfers. The authors also found a negative correlation between public funding and technology transfer, whilst the same type of funding was positively correlated with scientific productivity. Barletta et al. argued that the design of public scientific funding in Argentina mostly targets researchers with higher levels of publications, failing to provide incentives for scientists to cooperate with firms [14], similar to the manner Brazilian scientific policy is structured.

Interestingly, several respondents stated that performing analyses of food, produce, environmental components or microorganisms on a producer or company’s request would provide data that could be used in their researches. Likewise, a study conducted in the United States [16] found positive correlations between scientific publications and innovation developed in partnerships of small firms and universities. This indicates that interactions between the private sector and universities produce both scientific papers and patent deposits, and one form of knowledge output does not necessarily crowd out the other. Such a result, however, may be due to greater maturity of the United States’ Universities when it comes to innovation and interaction with firms.

Furthermore, the interactions between firms and university researchers may also bring positive knowledge spillovers between both sectors. For example, cooperation

with laboratories may contribute to a company's human resource improvement and ability to carry out research and development. Those characteristics have a role in a firm's capacity to absorb new technologies, a relevant aspect of technology transfer [11, 12, 14, 17, 18].

From the laboratories' point of view, such interactions are also advantageous. For instance, a researcher may develop new technology without understanding how to increase its production in scale or how to insert it in the market. Cooperating with companies can help improve the scientists' understanding of their own researches applicability [14]. The improvement of a laboratory's ability to create functional prototypes or marketable products consequentially contributes to further attract new firms for possible partnerships [17].

Another intriguing aspect observed in this study is that most of the researchers seemed more inclined to interact with firms, government and society through service provision, instead of other mechanisms such as technology licensing. Yet, most of the literature on technology transfer from universities seems to deal with patent deposits and their licensing to companies. Our study might be indicating that other forms of cooperation between universities and firms/society are undervalued in this field. Indeed, broad research conducted in Brazil [18] suggested that the relevance of patents to technological transfer varied according to the technology type. For example, transferring processes and techniques to the industry usually did not involve patents, being instead correlated to consulting activities. Even considering their entire sample, "only 14.1% of respondents pointed to the use of patents to transfer technology" [18].

### **3.3 *Limitations of the Study***

Although the methodology adopted in this study was useful to reveal the current situation of innovation of DRC's laboratories in the field of Bioeconomy, more steps would be needed for an in-depth analysis. Our research managed to capture six categories of barriers that possibly hinder Bioeconomy innovation and the provision of services. However, there may be other issues that could impact such laboratories' capacities. Other works [12, 13], for example, suggest that divergences between academic and firm cultures are hindrances to university-company cooperation, a topic that did not appear in our sample.

Also, our study does not address how each topic is related to one another. For instance, the "need for equipment maintenance" and "need for laboratory consumables or reagents" could be related to a hidden underlying factor. Factor analysis is a statistical tool widely used by Marketing, Psychology and Health Sciences [19–22] and could be applied to estimate possible relationships among the categories. It would be necessary, however, to create a more detailed survey encompassing the categories presented in this study and others taken from the academic literature in order to use factor analysis. Scussel and Demo [6] used a similar methodology to propose a scale that measures the relationship between costumers and luxury brands.

Finally, our study indicates a large latent Bioeconomy capacity of Darcy Ribeiro Campus's laboratories, especially when it comes to providing services to the society and the private/public sector. However, we have only obtained information from the suppliers of such services. Only by assessing the actual demand for what the university offers can we truly estimate its Bioeconomy potential.

## 4 Conclusion

The scope of this study was to perform a descriptive analysis of the current situation of Darcy Ribeiro Campus's laboratories when it comes to innovation and service provision in the field of Bioeconomy. Our survey revealed that several laboratories had the latent potential for these activities, and respondents were more inclined to cooperate with companies and society by providing services than through technology transfer to firms. Six categories of obstacles to the realization of this potential emerged from the answers. We highlight that the constant requirement for researchers to publish academic results may be undermining their capacity/availability to innovate in the paths adopted to transfer the scientific knowledge from university to society. Furthermore, narrowing the relationship between academics and companies may contribute to both the sector's intrinsic abilities to generate innovation. It is also important to note that, although our study indicates a large latent capacity of DRC's laboratories in the field of Bioeconomy, we have only surveyed the laboratories themselves (i.e. the suppliers of products and services). New studies considering society's demands for such products and services will help to improve our understanding of UnB's true potential in the field of Bioeconomy.

**Acknowledgements** We would like to thank the researchers from UnB's Darcy Ribeiro Campus for their availability and disposition to contribute to this work. This study was funded by *Projeto Brasilia 2060*, executed by the Brazilian Institute for Information in Science and Technology (IBICT).

## References

1. European Commission: A sustainable Bioeconomy for Europe: strengthening the connection between economy, society and the environment. Brussels (2018)
2. Brasil: Estratégia nacional de ciência, tecnologia e inovação 2016–2022. MCTIC, Brasília (2016)
3. Brasil: Plano de ação em ciência, tecnologia e inovação em bioeconomia. MCTIC, Brasília (2018)
4. Organisation for Economic Co-operation and Development: The Bioeconomy to 2030: Designing a Policy Agenda. OECD Publishing (2009)
5. Bardin, L.: Content Analysis. Livraria Martins Fontes, São Paulo (1977)
6. Scussel, F., Demo, G.: Os aspectos relacionais do consumo de luxo no Brasil: o desenvolvimento da escala de percepção de relacionamento de consumidores de luxo e a análise da influência

- da personalidade de marca sobre a percepção de relacionamento com marcas de moda de luxo. *Braz. Bus. Rev.* **16**(2), 174–190 (2018)
7. Francis, J.J., et al.: What is an adequate sample size? Operationalising data saturation for theory-based interview studies. *Psychol. Health* **25**, 1229–1245 (2010)
  8. Seramim, R. J., Walter, S. A.: What does Bardin say that authors do not show? Study of Brazilian scientific productions from 1997 to 2015. *Adm. Ens. PESQ* **18**, 241–269 (May, 2017)
  9. Campos, C. J. G., Turato, E. R.: Content analysis in studies using the clinical–qualitative method: application and perspectives. *Rev. Lat. -am. ENF* **17**, 259–264 (March, 2009)
  10. Santos, F.M.: Análise de conteúdo: a visão de Laurence Bardin. *Rev. Eletrôn. Edu.* **6**, 383–387 (2012)
  11. Ferreira, C. L. D., Ghesti, G. F., Braga, P. R. S.: Desafios para o processo de transferência de tecnologia na Universidade de Brasília. *Cad. Prospec. Salvador* **10**, 341–355 (July, 2017)
  12. Costa, V. M. G., Cunha, J. C.: A universidade e a capacitação tecnológica das empresas *Rev. Adm. Contemp.* **5**, 61–81 (January, 2001)
  13. Closs, L.Q., Ferreira, G.C.: University-industry technology transfer in the Brazilian context: a review of scientific studies published from 2005 to 2009. *Gest. Prod.* **19**, 419–432 (2012)
  14. Barletta, F., Yoguel, G., Pereira, M., Rodríguez, S.: Exploring scientific productivity and transfer activities: evidence from Argentinean ICT research groups. *Res. Policy* **46**, 1361–1369 (2017)
  15. Barra, C., Mayetta, O.W., Zotti, R.: Academic excellence, local knowledge spillovers and innovation in Europe. *Reg. Stud.* **53**(7), 1058–1069 (2019)
  16. Audretsch, D. B., Link, A. N., Hasselt, M.: Knowledge begets knowledge: university knowledge spillovers and the output of scientific papers from U.S. Small Business Innovation Research (SBIR) projects. *Scientometrics* **121**, 1367–1383 (October, 2019)
  17. Pereira, M. F., Melo, P. A., Dalmau, M. B., Harger, C. A.: Transferência de conhecimentos científicos e tecnológicos da universidade para o segmento empresarial. *RAI* **6**, 128–144 (September, 2009)
  18. Póvoa, L.M.C., Rapini, M.S.: Technology transfer from universities and public research institutes to firms in Brazil: what is transferred and how the transfer is carried out. *Sci. Publ. Policy* **37**(2), 147–159 (2010)
  19. Auerswald, M., Moshagen, M.: How to determine the number of factors to retain in exploratory factor analysis: a comparison of extraction methods under realistic conditions. *Psychol. Methods* **24**, 468–491 (2019)
  20. Clevers, E., et al.: Factor analysis defines distinct upper and lower gastrointestinal symptom groups compatible with rome iv criteria in a population-based study. *Clin. Gastroenterol. H.* **16**, 1252–1259 (2018)
  21. Calobrace, M.B., et al.: Risk factor analysis for capsular contracture: a 10-year sientra study using round, smooth, and textured implants for breast augmentation. *Plast. Reconstr. Surg.* **141**, 20S–28S (2018)
  22. Hooker, J.L., et al.: Psychometric analysis of the repetitive behavior scale-revised using confirmatory factor analysis in children with autism. *Autism Res.* **12**, 1399–1410 (2019)



# A Proposal for Modeling of the Management of Talent Recruitment and Training in Peruvian Sports Centers



Arturo Laredo , Luzmila Pro Concepcion ,  
and Nestor Mamani-Macedo 

**Abstract** This study was determined by the need of entities of the Peruvian state to know whether relevant institutions are properly implementing a sports management process at the national level because attracted and recruited sports talents mostly arrive by their own free will, and many such talents drop out during their training path. This research was conducted using qualitative and quantitative methods, with a descriptive approach where instruments such as interviews and observation were applied to coaches, physical education teachers, athletes, and professional personnel involved in sports management. This study aimed at designing a sports management model based on information technology to help integrate the management indicators, which allowed the identification of more talented athletes, to reinforce the skills of such athletes and guide them to international competitions and tournaments. In this manner, the early dropout of talented athletes can be avoided.

**Keywords** IT model · Sports management · Sport management indicators

## 1 Introduction

Sports have always been considered important, similar to other disciplines, because it facilitates the acquisition of different individual skills, such as motor skills, in addition to the learning skills; further, engaging in sports improves the health of the population. Thus, government entities must focus on sports disciplines, and sports

---

A. Laredo · L. P. Concepcion  
Faculty of Systems and Computer Engineering, Universidad Nacional Mayor de San Marcos,  
Lima 15000, Peru  
e-mail: [alaredom@unmsm.edu.pe](mailto:alaredom@unmsm.edu.pe)

L. P. Concepcion  
e-mail: [lproc@unmsm.edu.pe](mailto:lproc@unmsm.edu.pe)

N. Mamani-Macedo (✉)  
Faculty of Mathematical Sciences, Universidad Nacional Mayor de San Marcos, Lima 15000, Peru  
e-mail: [nmamani@unmsm.edu.pe](mailto:nmamani@unmsm.edu.pe)

© The Editor(s) (if applicable) and The Author(s), under exclusive license  
to Springer Nature Switzerland AG 2021

Y. Iano et al. (eds.), *Proceedings of the 5th Brazilian Technology Symposium*,  
Smart Innovation, Systems and Technologies 202,  
[https://doi.org/10.1007/978-3-030-57566-3\\_50](https://doi.org/10.1007/978-3-030-57566-3_50)

institutions must implement a responsible sports management (SM) system, using indicators that facilitate talent identification among the youth participating in high-level competitions. To properly implement an SM system, information technologies (IT) must be used.

## 2 Theoretical Foundation

There are few studies on the use of IT in relation to sports management and similar topics, such as the impact of IT on the effectiveness and efficiency of SM models. Rodríguez [1] provides a relationship between information and communication technologies (ICTs) and sports. There is an insufficient amount of documentation on SM models; consequently, each country designs the best possible structure and technology adaptation for sports management in its own manner [2, 3]. Given the scarcity of literature on SM using IT models, studies have been found on technological innovation originally intended for different functions and applied in other scientific fields, such as medicine [4, 5]. Nevertheless, there is no doubt that the ICTs tools allow obtaining relevant data about sports [6], although some argue that their use is not yet significant [7].

### 2.1 *Theoretical Models Used to Optimize SM in Attracting Talent*

Factors such as performance levels, skills, human resource capabilities, and their level of commitment and identity toward the institution are important for sports managers [8] because the sports performance largely relies on it. Thus, an SM model aware of these factors based on quality and continuous improvement allows identifying policies improving sports activities, which information might be necessary for state agencies regards three aspects: the political, processes, and the total quality [3]. Information management model for sports organization: a model aimed at the implementation and development of five components (human capital, organizational memoirs, the operation and integration of institution members, information centers, and ICTs) that constitute a continuous improvement process in information management [9–13].

### 2.2 *IT Applications for SM*

The following technologies can be used to generate an SM database:

- **Business-to-business (B2B):** technology that allows connecting the application services of two companies at a minimum cost, improving revenue stream of both. [10]

- **Motion capture:** is a live movement recording, recreating such movement on a digital model using computer images [12].
- **Big data:** describes the large volume of data—both structured and unstructured—that floods a business on a day-to-day basis [12].
- **Cloud computing:** allows the user to access a catalog of standardized services to meet their business needs in a flexible and adaptive manner [13].

### 3 Problematic Situation

Rodríguez [1] argues that the negative results related to the use of ICTs in SM are due, among others, to the reluctance of coaches and athletes to take advantage of these technologies to improve their performance. Slusarczyk [2] considers that the poor use of ICTs, as in sports, produces major organizational gaps because the people in charge of business management are generally not familiar with the technology. Currently, the Peruvian Sports Institute (IPD) only implements information systems for administration and not for SM because of a lack of knowledge of the standard systems.

**General Problem:** There are few models of SM using IT that accurately measure SM processes and data in their entirety and in an efficient and timely manner to attract, develop, and produce more sports talents. All processes are aimed at recruitment, selection, training, promotion, and high competition. This is a challenge faced every day by entities that are dedicated to training, development, and competition in sports disciplines.

**Specific Problems:**

- Inadequate use of ICTs by those involved in sports recruitment and training, and the lack of a model of relevant indicators to measure talents that are not discovered at an early age in an efficient manner.
- A lack of policies and strategies by the public entities that deal with sports development.
- A lack of an SM model with adequate indicators to measure talents that are not discovered at an early age in an effective manner.

### 4 Methodology

This study comprises applied research that uses a pre-experimental design for which we created the necessary conditions or adapted existing ones to clarify the characteristics and relations of the optimal IT resources required to integrate and support SM processes. The research objective is to design an SM model based on IT, indicators, and implementation using qualitative and quantitative methods, as shown next in the phases of the methodology used.

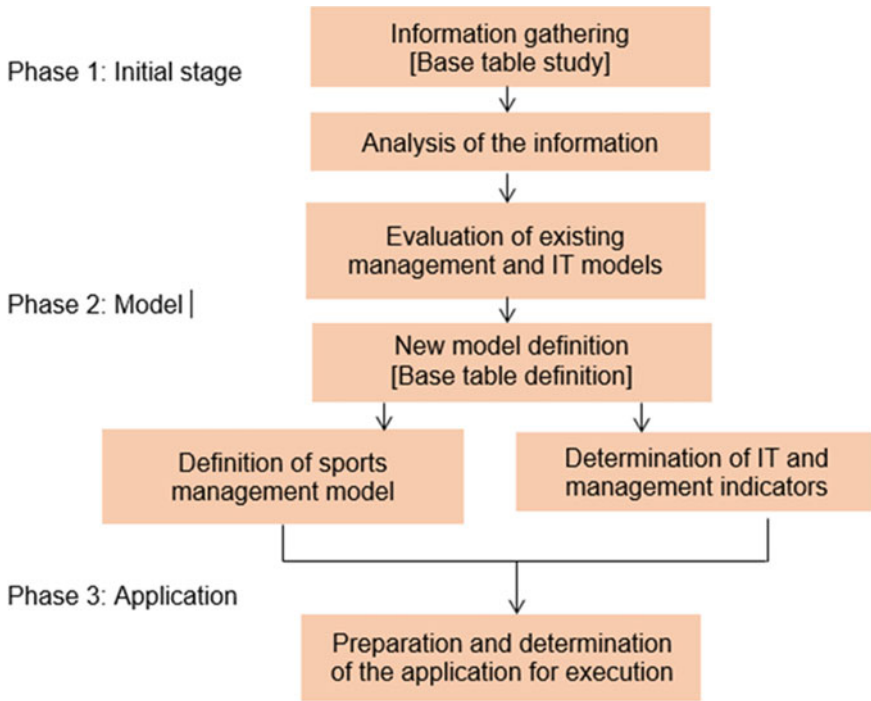


**Fig. 1** Research methodology for defining a sports management model using information technology applications for sports management

Six IT program procedures used in Phase 1 of the SM Model during the “Information Collection and Analysis” activities are chosen as shown in Fig. 1. Based on this, a management model using IT applications and SM evaluation elements is proposed, as shown in Table 1.

Figure 2 shows the IT tools used for model validation:

- **Motion capture technology:** a mobile application that captures bone height through scanning; speed through video recordings; the distance between two points.
- **Telepsychology:** Instant Message (IM) mobile/desktop applications for interactive evaluations.
- **Big data and Cloud computing:** for data storage and analysis.
- **Biomedical technology:** a medical calculator system (mobile/desktop application) about metrics and equations of people healthcare.

**Table 1** Evaluation of the sports management model based on IT applications

Evaluation elements	IT applications					
	B2B	Motion capture technology	Big data	Cloud computing	Telepsychology	Biomedical technology
Content distribution	10	10	10	10	5	5
Strategy management without considering the talent acquisition model	10	10			10	
Athlete tracking			10		10	
Measure mental health					10	9
Measure physical performance		6	8	5	8	10
Availability of information	10	10	10	10	8	8

## 5 Validation

After having completed the SM model based on IT applications, we adapted the model to the Experimental Sports Educational Center of the IPD (CEDE) in June 2018. Subsequently, we assessed the model through the indicators shown by the different applications and compared the current state against the post-implementation state (after six months).

## 6 Discussion

Table 2 shows that the number of athletes referred with projection highly competitive to receive support from their federations in the two periods increased by 14%. On the other hand, the number of specialists using data capture technology increased by 9%. The indicators number of athletes evaluated and psychologically supported and the number of athletes whose training can be sponsored was zero in June 2018 and 5% and 10% of the total in December 2018, respectively. This was due to the use of telepsychology and data capture technologies through smartphones with installed applications that measured with greater accuracy and transmitted the information in seconds to the server, thereby considerably minimizing the time previously used by

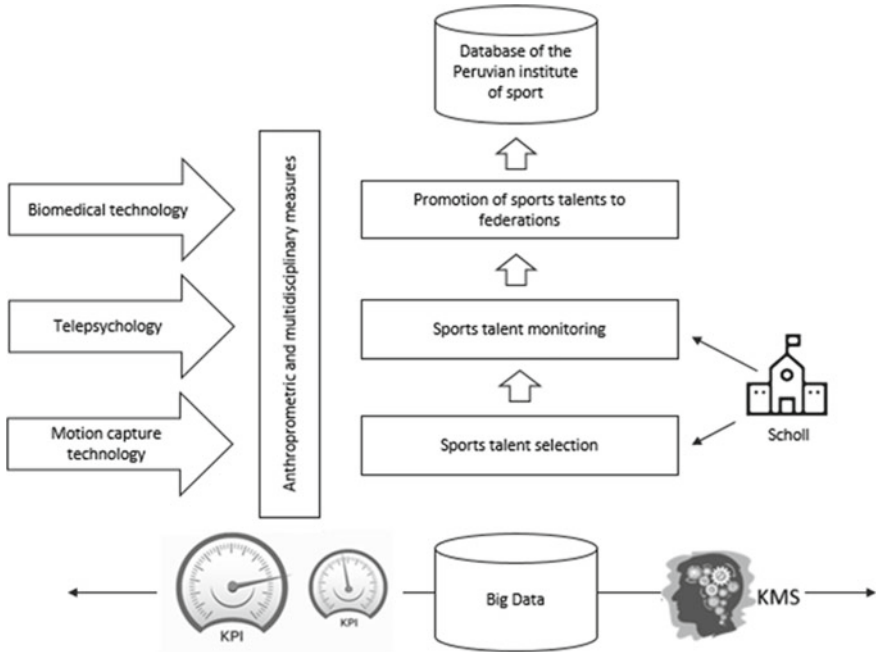


Fig. 2 Information technology applications selected for the model

trainers to evaluate each applicant. With relation to synergy indicators, the number of athletes subsidized (with a grant) by IPD increased by 7%, and the number of athletes registered for international competitions increased by 12% from June 2018 to December 2018. In the same period, the number of athletes with economic and social support from the IPD and the Ministry of Education went from 0 to 4%. This was due to the use of biomedical technology and economic and social applications that were measured with accuracy data of applicants.

In the present model proposed for SM at the CEDE-IPD (Fig. 3), we established three main management processes: **selection** (attracting sports talents), **training** (follow-up and monitoring), and **projection** (athletes are referred to federations, clubs, or sports centers); subsequently, the athletes are to be qualified as high-performance athletes that are directly supported by the state and/or sponsors. Similarly, we designed a set of indicators per sports process: **effectiveness Indicators** for the selection phase and **efficiency and synergy indicators** for the training phase as described by the indicators in Table 2. The “sports strategies” will address the model execution according to the geographical areas that each federation prioritizes to execute.

Based on the SM indicators, we integrated these technologies into a new SM model wherein the new evaluation criteria used from other disciplines that converge with the health and psychology of athletes have supported better analysis and decision making through the use of multi-disciplinary information. Further, another finding is

**Table 2** Six-month comparison of the indicator evaluation

Indicators	Jun-18		Dec-18		% Increase <sup>a</sup>
<i>Effectiveness</i>					
Number of applicants	57	% <sup>b</sup>	78	% <sup>c</sup>	
Number of candidates evaluated based on the anthropometric characteristics, nutrition, social, economic, cultural, and psychological data	0	–	78	100%	–
Number of applicants visually evaluated by the coach	57	100%	0	–	–
<i>Efficiency</i>					
Number of athletes referred for projection (federations)	12	21%	27	35%	14%
Number of athletes evaluated and psychologically supported	0	–	13	17%	17%
Number of athletes whose training can be sponsored	0	–	4	5%	5%
Number of specialists using data capture technology	1	2%	8	10%	9%
<i>Synergy</i>					
Number of athletes subsidized by the Peruvian Sports Institute	4	7%	11	14%	7%
Number of athletes registered for international competitions	10	18%	23	29%	12%
Number of athletes benefiting from economic and social support from the Peruvian Sports Institute and the Ministry of Education (MINEDU)	0	–	3	4%	4%

<sup>a</sup>The percentage of increase from June 2018 until December 2018

<sup>b</sup>The percentage of the total number of applicants in June 2018

<sup>c</sup>The percentage of the total number of applicants in December 2018

that the number of data provided to CEDE physical education teachers for evaluating the recruitment and selection processes of sports talent is greater and better addressed in relation to the processes of talent analysis.

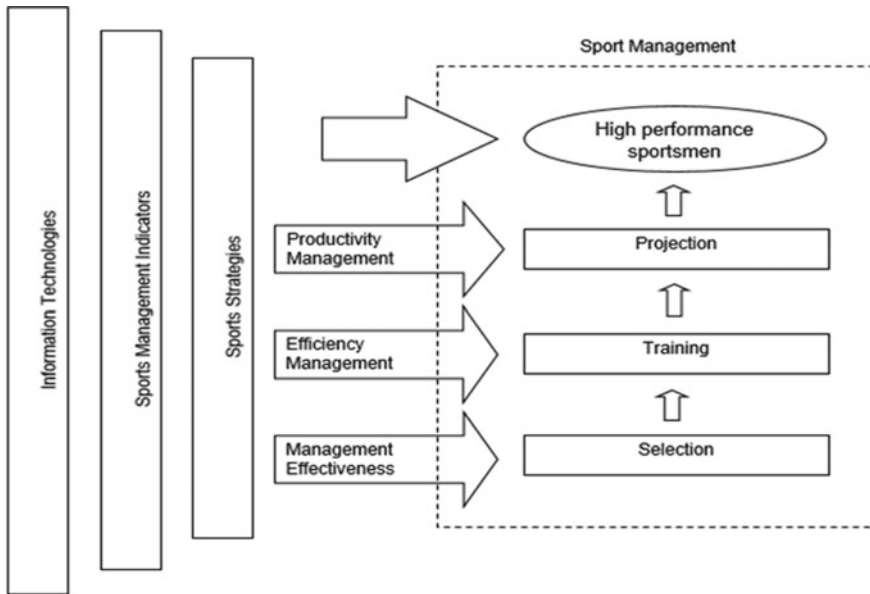


**Fig. 3** Proposed model for sports management in the experimental sports school or college

## 7 Conclusions and Recommendations

This work proposes a sports management model with the help of cutting-edge IT technologies that can be used in the recruitment of talent athletes by the Peruvian government. To operationalize the model, we define a set of indicators about effectiveness, efficiency, and synergy. The model was validated in a real scenario getting significant improvements in the results benefiting the athletes.

As future work we will develop productivity Indicators for the “Projection” phase, these indicators will be customized according to each type of sports discipline. Likewise, the model will be applied to other educational centers specialized in high competition sports that exist in some regional governments of Peru to receive feedback and improve the model itself.

## References







1. Rodríguez, Q.M.: Information and communication technologies (ITC) in physical education. *Theor. Rev.* **1**(1), 75–86 (2015)
2. Slusarczyk, A. M.: Analysis of Business and ICT Strategies. *Área de Innovación y Desarrollo p. 3c Empresa* **5**(1), 44 (2016)
3. Moreno, P.Y.: Modelo de gestión deportiva para el municipio de Quibdó. *Elsevier* **5**(12), 75–194 (2014)



4. Carballo, M., Barrero M., Villalazón, A.: FIMAN: Sistema Computarizado para Analisis de Movimientos Digitales. Investigación y Desarrollo (2016)
5. García, X., Salguero, A., Molinero, O., De la Vega, R., Ruiz, R., Márquez, S.: El papel del perfil resiliente y las estrategias de afrontamiento sobre el estrés-recuperación del deportista de competición. *Kronos* **14**(1) (2015)
6. Tiching: Las TIC en la Educación Física (2013). Available from: <http://blog.tiching.com/las-tic-en-la-educacion-fisica/>
7. Alvarado, P. C.: Uso de las TICs por parte de los profesores de Educación Física. *Lecturas educación física y deportes, Revista Digital.* EFDeportes.com. Año 22-Nº230 (July, 2017)
8. Núñez, R.G., Zueck, M.C., Marín, R., Soto, M.C.: Modelo gerencial para potenciar la práctica deportiva y recreativas. *Revista Española de Educación Física y Deportes* **420**, 25–38 (2018)
9. Cantos, M., Reyes, J.: El nuevo modelo de Gestión Pedagógica y su impacto en las escuelas de educación básica del cantón Cañar, Ecuador. *Revista Killkana Sociales* **2**(4) (December, 2018)
10. CYSEND: B2B API para recarga de móviles (21 March, 2019). Available from: <https://www.cysend.com/merchant/es/b2b-api-para-recarga-movil>
11. Arteneo. Captura de movimiento o motion capture: ¿cómo funciona? (25 January, 2515/2019). Available from: <https://www.arteneo.com/blog/captura-de-movimientos-motion-capture-como-funciona/>
12. Ramírez, N. L.: *Campeones de la Transformación Digital: 10 líderes españoles* Madrid: Profit Editorial (2018)
13. Moreno, M.: Computación en la nube. *CEMA* **566**, 1–17 (2015)

# Mentoring Process: An Assessment of Career, Psychosocial Functions and Mentor Role Model



Neusa Maria Bastos Fernandes dos Santos , Mariana Juer , Igor Polezi Munhoz , Alessandra Cristina Santos Akkari , Rodrigo Guimarães Motta , and Marianna Konyosi Miyashiro 

**Abstract** This work has focused on studying the relationships between mentor and mentee, as well as exploring the mentoring process as a current organizational demand and the perspectives of these actors regarding mentoring functions. So, a unique case study was developed, using as a model a large multinational company in the housewares sector that has an official mentoring program for young talent. Two research instruments were applied, which addressed the expectations of the mentees and the assumptions of the mentors regarding career functions, psychosocial functions, mentor role models and confidence present in the relationship, and then a statistic treatment was performed using the SPSS software. It was observed that although the expectations of program mentors and mentees are not entirely compatible, no program dysfunction was observed. There are no different expectations clearly evidenced among peers, but differentiation in levels. It is suggested a new look at how to accompany and train the participants in the mentoring process, or even to define the pairs in order to avoid possible disagreements that may cause frustrations.

**Keyword** Mentoring process · Mentor · Mentee · Career

## 1 Introduction

Mentoring emerged as a tool for personal and professional development and growth in companies in the 1970s and has been evolving with changes in the world of

---

N. M. B. F. dos Santos · M. Juer · R. G. Motta · M. K. Miyashiro  
Pontifical Catholic University of Sao Paulo (PUC-SP), Sao Paulo, Brazil  
e-mail: [admneusa@pucsp.br](mailto:admneusa@pucsp.br)

I. P. Munhoz (✉)  
Federal Institute of Education, Science and Technology of Sao Paulo (IFSP), Sao Paulo, Brazil  
e-mail: [igor.munhoz@ifsp.edu.br](mailto:igor.munhoz@ifsp.edu.br)

A. C. S. Akkari  
Mackenzie Presbyterian University, Campinas, Brazil

© The Editor(s) (if applicable) and The Author(s), under exclusive license to Springer Nature Switzerland AG 2021

515

Y. Iano et al. (eds.), *Proceedings of the 5th Brazilian Technology Symposium*, Smart Innovation, Systems and Technologies 202, [https://doi.org/10.1007/978-3-030-57566-3\\_51](https://doi.org/10.1007/978-3-030-57566-3_51)

work [1]. Nowadays, the mentoring process has become a critical tool for supporting and leveraging successful careers, particularly for interns and junior professionals entering the job market [2].

In recent decades, the concept of work has changed not only from the perspective of those who occupy the posts, but also the type of work performed and the format of how it is performed. In this scenario of change, outsourcing is another fact to be considered, as it has already become a visible element today, even though there is a debate about how much this could mean a deterioration of working conditions [3].

If in the 1980s, professionals wanted to move up the hierarchy until they reached the highest possible step in the organization where they began their careers, today's intellectual workers have more choices, more demands and more challenges ahead. From this point, temporary and part-time jobs increased. The individual is not expected to spend his entire life in a corporation, as this may sound like resignation. Careers are less limited to traditional barriers, more flexible according to profiles, and more directed to projects and temporary tasks, which implies greater responsibility for professionals for their own careers [3, 4].

It is in this context of dynamism and rapid evolution of organizational paradigms that evolve concepts of development of individuals to achieve success by organizations. So, a new set of mental models is needed, which migrates the thinking of command and control to coordinate and cultivate it. In this sense, there is expanding coaching, as evidenced by the dozens of books and articles on the subject published, mostly in the United States, Australia, Canada, and England. However, there are other modalities of intervention, such as the mentoring to be studied in this article, which is confounded, even because the authors' distinctions on the topics were not consensual [5].

Ensher and Murphy [1] state that although mentoring studies have advanced, there is the criticism to be made about their development. The first concerns the use of research results in corporations. Human resources professionals and managers do not appear to access research material published in academic journals. Many of these studies have been compiled into books, but, according to the authors, only a few more recent books draw a parallel between the academic theoretical universe and practice. The second criticism concerns the content of studies conducted over the past ten years, which focuses on conducting questionnaires and research to describe the nature and benefits of mentoring, even though it is so difficult to quantify the richness of these relationships.

Therefore, the aim of this paper was to study mentoring relationships between mentors and mentees from career, psychosocial functions, and mentor role model perspective. This research aims to contribute to both academia and the corporate universe by seeking a better understanding of mentee expectations and mentor assumptions about mentoring functions, as well as the level of confidence in the mentoring process.

## 2 Theoretical Framework

Mentoring, as a field of academic study, is among the literature on career, leadership, and development of leaders. In the late 1970s, the psychologist Levinson applied, in the United States, a survey among successful professionals from various areas and all stressed the importance at some point in their careers of the figure of a mentor as a deciding factor [1].

Thus, mentoring becomes an essential theme in current labor relations and its main objective is to provide greater job satisfaction by helping in the development and improvement of relationships in this environment and the pursuit of the desired results for professional growth. It is noteworthy that individuals do not depend on their companies to participate in a mentoring relationship [6].

Many definitions of what becomes a mentor have been created without consensus among the authors of the subject. Thus Chandler and Kram [6] adopt the definition of Ragins which will also be adopted in this article: individuals with advanced experience and knowledge who are committed to providing support and upward mobility to their proteges' careers.

The role of the mentor is not to indicate the right paths, but to raise questions, open possibilities and the mentor should define the path to be taken in order to win a challenge. It is interesting to note that some authors refer to the junior professional who receives help from the most experienced, the mentor, as a protégé, a word of French origin [1, 6].

The success of a formal mentoring relationship rests on a constant exchange between mentor and mentee, in which developmental experience involves responsibility and effort on both sides [4]. Appreciation and connection between the parties in formal relations play an essential role in their willingness to devote time and energy to the development of the process. While these factors naturally occur in informal relationships, the same may not occur in formal relationships.

Although Burke [7] has shown that mentors can have around fifteen different functions, the current literature has pointed to two essential functions, which have consequences [8], being the career functions and psychosocial functions. Young and Perrewé [9] noted that mentors value relationships more in which mentee behavior is career-oriented, and mentee places more emphasis on behaviors related to mentors' psychosocial issues. When each other meets common expectations, the perception of effectiveness in the relationship's results and the level of trust increase [10].

## 3 Methodology

The expectations and assumptions of the parties involved in the young talent mentoring program of a housewares sector multinational, present in more than 170 countries, with around 60 manufacturing units and technology centers in 12 countries, were assessed. The company has a formal mentoring program with clear objectives

to develop leadership within the organization. Although the organization has formal mentoring programs in all countries where it operates, this project focuses on the mentor-mentee relationships involved in the youth talent program in Brazil.

This research was comprised of two adapted questionnaires by Ensher and Murphy [1]. The first was divided into three sets of questions about mentoring functions (career, psychosocial and mentor role model) and compares expectations of the mentee versus assumptions of the mentor. Mentor and mentee evaluated each question by giving a note regarding the perception of what actually happened in the relationship and another on what they consider to be the ideal. The second questionnaire had a set of questions about trust and also contemplated the real and the ideal scenario, which made it possible to draw a parallel between the trust the mentee and the mentor feel, as well as the level of trust they believe is necessary versus reported actual confidence. The questionnaire on mentoring functions (career, emotional and mentor role model) consisted of 5-point Likert scales; and the 4-point Likert confidence questionnaire.

The instrument was developed in a digital platform and, at the beginning of the questionnaire, each respondent was informed about the academic objective of the research as well as the guarantee of anonymity giving the choice of participation or not as requested by the Research Ethics Committee of Pontifical Catholic University of São Paulo (PUC-SP).

Results were evaluated using the Statistical Package for Social Science (SPSS) version 13.0. The Cronbach's alpha coefficient for each dimension (career, emotional, mentor role model and confidence) for the real and ideal scenario was calculated, according to the assessment of mentors and mentees. Cronbach's alpha coefficient measures the internal consistency of the scale, that is, how much the questions on one scale correlate with the other questions on the same scale. In this exploratory study, Cronbach's alpha coefficients above 0.5 were considered satisfactory [11].

To compare the assessments of mentors and mentees for the real and the ideal scenario, assessing the dispersion of responses and the existence or otherwise of atypical responses, the Boxplot of mean scores for each dimension was developed. The same methodology was used to compare the perceptions of female versus male minds.

Finally, to assess the relationships between mentor and mentee evaluations for the ideal and the real scenario, scatter plots were developed for each of the combinations relevant to mentoring functions and confidence.

## 4 Results and Discussion

Of the 34 pairs who received the questionnaires, 18 questionnaires from mentors and 23 from mentees were answered. Regarding the mentor/mentee pair, 14 complete answers were obtained. Cronbach's alpha was higher than 0.547 (0.715 average) for each dimension and for the real and ideal scenario according to the evaluation of the mentors and mentees, allowing to consider the average scores of the questions that constitute each dimension.

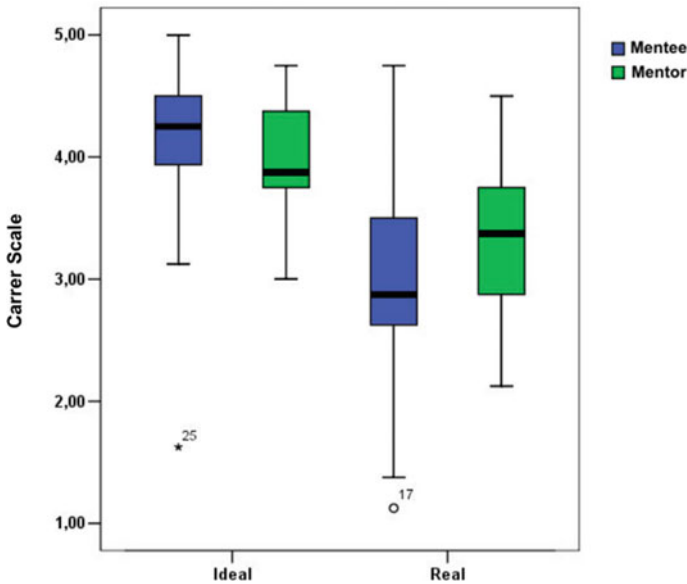
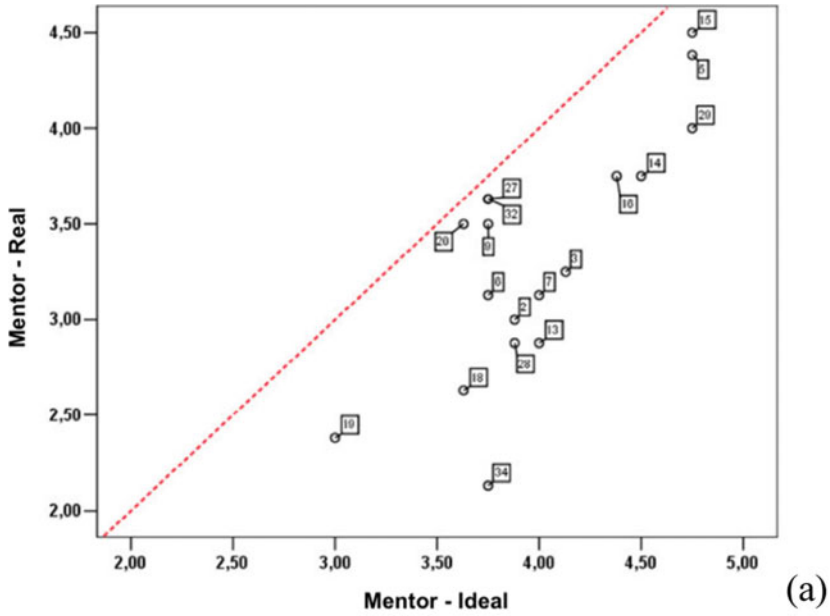


Fig. 1 Career scale Boxplot for mentors and mentees, considering the real and ideal scenario

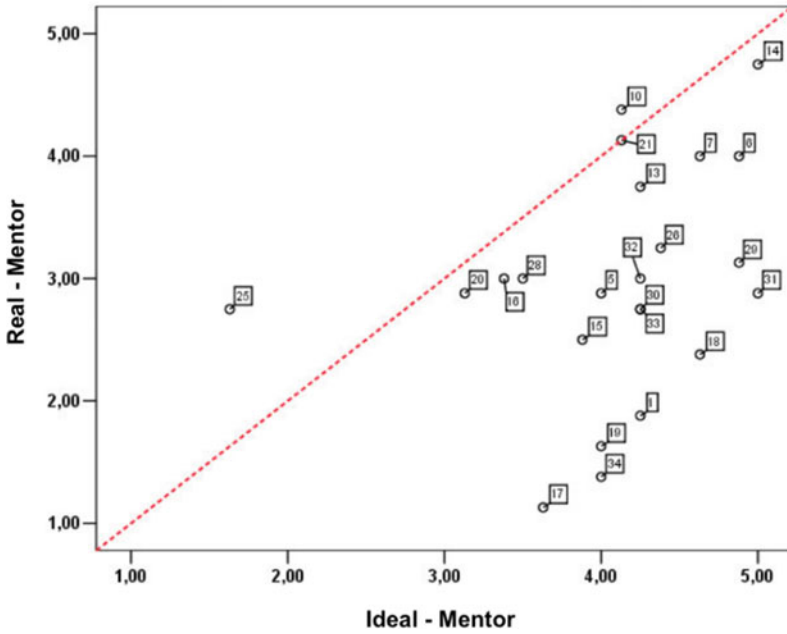
Figure 1 presents the career scale Boxplot for mentors and mentees, considering the real and ideal scenario. For the career ladder, in general, mentors and mentees value the real scenario as less than ideal. Moreover, it turns out that the ideal of mentees is slightly higher than the ideal of mentors. However, the reality of the mentees is slightly lower than that of the mentors; that is, both recognize that, with regard to mentor career support, mentors perform less than optimally. However, mentors believe that they are doing better support than they really are, according to their mentees.

In fact, Fig. 2 assesses the relationship between the real and ideal scenario for (a) mentors and for (b) mentees, considering the career scale. It is observed that all mentors consider the actual scenario to be less than ideal. All study participants understand that, for the career, the mentor should ideally provide at least medium support. Evaluating the real scenario, it is noted that only in three cases is the career support between good and great, but in the three cases, it is the same mentor (5, 15 and 29). Most mentees find that the support the mentor provides for their careers is less than optimal support. However, there is a mentee who considers the actual support to be the ideal and two mentees who consider the real to be greater than the ideal. All mentees believe that ideal career support should be at least medium; and most believe that it must be between good and great.

In fact, research published by Nature Reviews Cancer with scientific mentors has pointed to mentoring as a tool that aims to help young scientists identify their strengths and weaknesses so that they can make appropriate career choices and explore their potential, as well contribute to the ethical aspect and integrity in the scientific field. Through scientific mentorship, it was possible to achieve more collaborative environments, with resource sharing and research honesty [12].



(a)



(b)

Fig. 2 Relationship between the real and ideal scenario for **a** mentors and for **b** mentees, considering the career scale

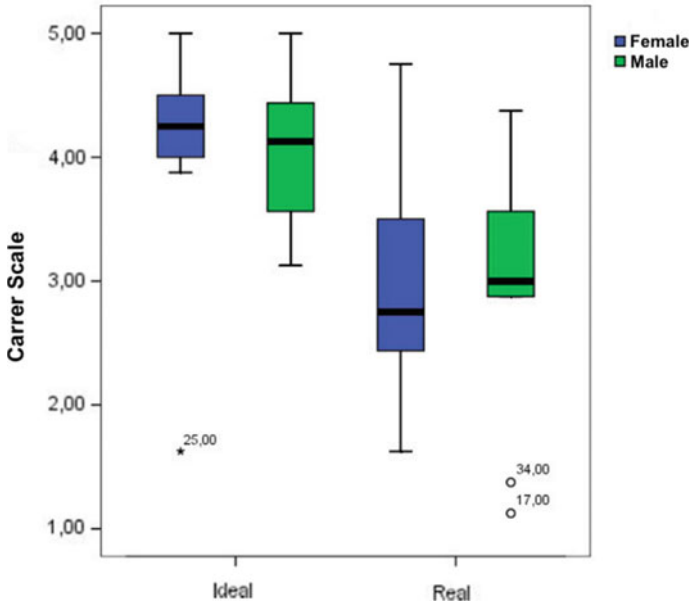


**Fig. 3** Boxplot of average career scale scores for mentees, according to gender, considering the real and ideal scenario

Figure 3 shows the Boxplot of average career scale scores for mentees, according to gender, considering the actual and ideal scenario. For the career scale, there is a difference between females and males in the ideal scenario only in relation to variability, because, in this scenario, men present greater variability. In the real scenario, women exhibit greater variability and a slightly lower perception of support than men.

Other work in the literature [13], when analyzing the success rate of the mentoring process by gender, found that the success ratings did not differ by mentor/mentee gender, so that the perception of success increased with increasing frequency of mentor-mentee interactions.

It is noted that for emotional scale (Fig. 4) there is great variability between female and male. Also, in the ideal scenario, the expectations of male are slightly lower than those of female. In the real scenario, female are even more dissatisfied than male.

Interestingly, other work in the literature [14], dealing with socio-emotional issues involved in the mentoring process with a sample of refugees and migrants, pointed out that the mentoring process acts as a tool for social inclusion, developing friendship between mentor and mentee.



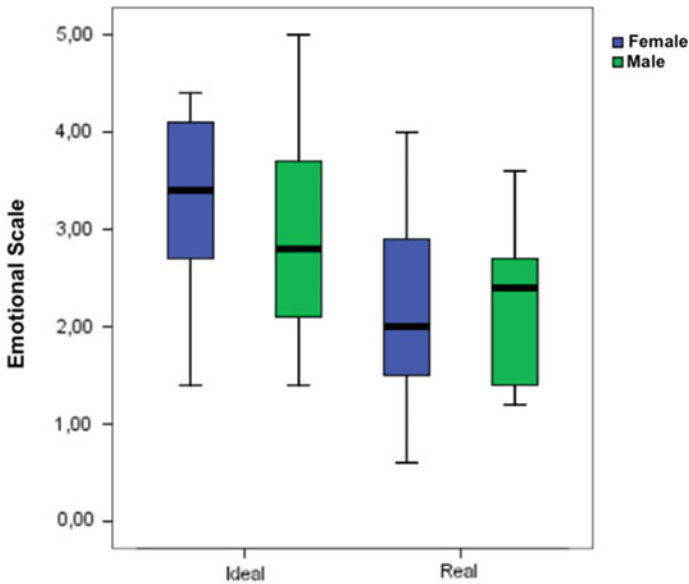


**Fig. 4** Emotional scale Boxplot for mentees, according to gender, considering the real and ideal scenario

Figure 5 shows the mentor role model scale Boxplot for mentors and mentees, considering the actual and ideal scenario. For the role of the mentor model role, there is great variability of the real scenario, especially for the mentees. There is an interesting divergence of opinion regarding the role played by mentors in evaluating their own mentors and mentees. Both recognize that the real role is less than ideal, but the mentee's assessment of mentors is superior to that of mentors in their self-assessment.

In this sense, it is interesting to note that the work of Esbenshade et al. [13], with 138 mentor-mentee peers, pointed out that 78.2% of mentors found that the mentoring process helped them succeed as professionals and 92% reported that it helped in overall career development.

Figure 6 shows the Boxplot of the mean scores of the confidence for mentors and mentees, considering the real and ideal scenario. It was observed that for confidence scale there is great variability of the actual scenario for the minds. Overall, mentors and mentees report to the real scenario a reasonable level of trust in the partner, close to their expectations, although still below them. Their assessments of the real scenario are similar, but the ideal scenario of the minds is superior to that of the mentors, that is, there is a divergence of opinion about the necessary trust in relationships.

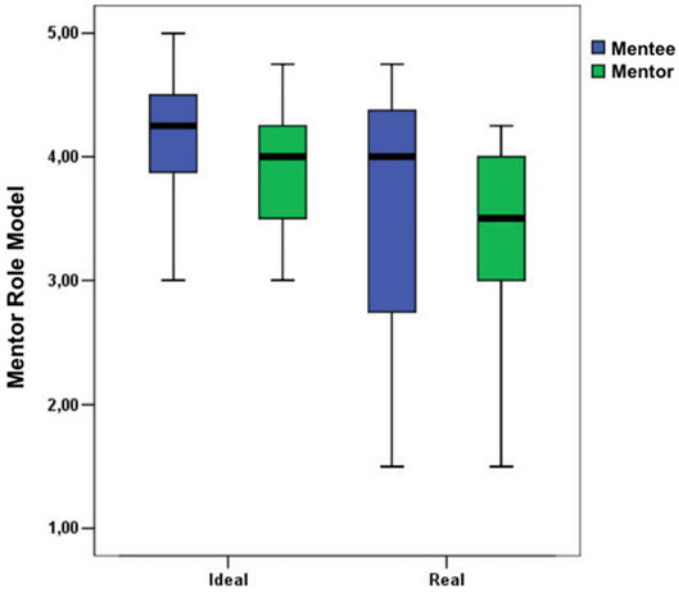


Fig. 5 Mentor role model scale Boxplot for mentors and mentees, considering the real and ideal scenario

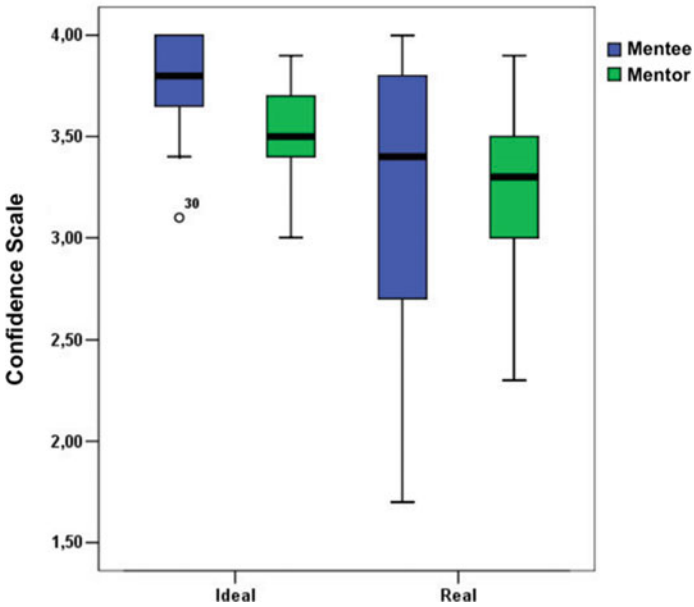


Fig. 6 Confidence scale Boxplot for mentors and mentees, considering the real and ideal scenario

## 5 Conclusion

It was observed that mentees have high expectations for both career and mentor role models in the mentoring process. In this study, for the confidence scale, there is great variability of the real scenario for the mentees. In general, mentors and mentees report to the real scenario a reasonable level of trust in their partner, close to their expectations. A divergence of views was observed regarding the necessary trust in relationships. There is a healthy level of trust between peers, but can still improve. Regarding roles, although there is no consensus between mentee expectations and mentor assumptions, the results are positive.

Thus, this study pointed to a positive outcome of the program, showing the presence of mentoring functions and the existence of the trust, but the lack of consensus regarding the role of the process is apparent.

It is suggested a new look at how to accompany and train the participants in the mentoring process, or even to define the pairs in order to avoid possible disagreements that may cause frustrations. Finally, studies that bring organizations closer to academia are necessary to enable the evolution of mentoring to develop and improve relationships within organizations.






## References

1. Ensher, E.A., Murphy, S.E.: *Power Mentoring: How Successful Mentors and Protégés Get the Most Out of their Relationships*. Jossey-Bass, San Francisco (2005)
2. Johnson, M.O., Gandhi, M.: A mentor training program improves mentoring competency for researchers working with early-career investigators from underrepresented backgrounds. *Adv. Health Sci. Educ. Theory Pract.* **20**(3), 683–689 (2015)
3. Maloni, M., Gligor, D., Chermie, R., Boyd, E.: Supervisor and mentoring effects on work-family conflict in logistics. *Int. J. Phys. Distrib. Logist. Manage.* **49**(6), 644–661 (2019)
4. Lankau, M.J., Riordan, C.M., Thomas, C.T.: The effects of similarity and linking in formal relationships between mentors and protégés. *J. Vocat. Behav. Athens, GA* **67**, 252–265 (2005)
5. Krausz, R.R.: *Coaching executivo: a conquista da liderança*. Nobel, São Paulo (2007)
6. Chandler, D. E., Kram, K. E.: Mentoring and developmental networks in the new career context. In: Gunz, H., Peiperl, M. *Handbook of Career Studies* Sage Publications, Thousand Oaks (2007)
7. Burke, R.J.: Mentors in Organizations. *Group Organ. Stud.* **9**, 353–372 (1984)
8. Santos, N.M.B.F.: Programas de mentoring: aprendendo com a realidade canadense. *Rio Grande: Interfaces Brasil/Canadá* **7**, 251–265 (2007)
9. Young, A.M., Perrewé, P.L.: What did you expect? An examination of career-related support and social support among mentors and protégés. *J. Manag.* **26**(4), 611–632 (2000)
10. Mancuso, C.A., Berman, J.R., Robbins, L., Paget, S.A.: What mentors tell us about acknowledging effort and sustaining academic research mentoring: a qualitative study. *J. Contin. Educ. Health Prof.* **39**(1), 29–35 (2019)
11. Robinson, J.P., Shaver, P.R., Wrightsman, L.S.: *Measures of Personality and Social Psychological Attitudes*. Academic Press, San Diego, San Diego (1991)
12. Clynes, M., Corbett, A., Overbaugh, J.: Why we need good mentoring. *Nat. Rev. Cancer* **19**(9), 489–493 (2019)

13. Esbenschade, A. J., Kahalley, L. S., Baertschiger, R. Dasgupta, R., et al.: Mentors' perspectives on the successes and challenges of mentoring in the COG Young Investigator mentorship program: a report from the Children's Oncology Group. *Pediatr. Blood Cancer* **66**(10) (2019)
14. Preston, J.M., Prieto-Flores, Ò., Rhodes, J.E.: Mentoring in context: a comparative study of youth mentoring programs in the United States and continental Europe. *Youth Soc.* **51**(7), 900–914 (2018)

# Compensation Program: A Quantitative Study of the Top Management Team's Level of Knowledge and Satisfaction



Neusa Maria Bastos Fernandes dos Santos , Rafael Maia Chagas ,  
Alessandra Cristina Santos Akkari , Igor Polezi Munhoz ,  
Fernando Fukunaga , and Ligia Kaori Matsumoto Hirano 

**Abstract** This article aimed to evaluate the level of knowledge and the degree of satisfaction of the top management team (TMT) of a global holding company regarding compensation policies and programs. Thus, a questionnaire was developed and applied to 55 professionals who hold managerial positions in the target company. The instrument was divided into three parts, encompassing demographic data, knowledge level and degree of satisfaction. The data treatment included the application of statistical tests (chi-square, Fisher significance, Spearman correlation, and multiple linear regression), obtaining a correlation between the level of knowledge and the degree of satisfaction with compensation policies and programs. However, no influence of demographic profile on the degree of satisfaction of TMT members was observed. The results showed that there is evidence that the degree of satisfaction is directly related to the level of knowledge about the company's compensation program, despite being a weak correlation ( $\rho = 0.4020$ ). Moreover, the level of knowledge and degree of satisfaction is independent of the area of activity ( $p = 0.469$  and  $p = 0.615$ , respectively) and the different hierarchical levels ( $p = 0.824$  and  $p = 0.957$ , respectively) of TMT members. Also, variable compensation proved to be the most important measure within the definitions of a compensation program ( $R = 0.7760$ ), including the level of knowledge as a measure. This paper points to the need for future studies that address ways to improve corporate transparency regarding compensation programs.

**Keyword** Compensation program · Satisfaction · Top management team

---

N. M. B. F. dos Santos · R. M. Chagas · F. Fukunaga · L. K. M. Hirano  
Pontifical Catholic University of Sao Paulo (PUC-SP), Sao Paulo, Brazil  
e-mail: [admneusa@pucsp.br](mailto:admneusa@pucsp.br)

A. C. S. Akkari  
Mackenzie Presbyterian University, Campinas, Brazil

I. P. Munhoz (✉)  
Federal Institute of Education, Science and Technology of Sao Paulo (IFSP), Sao Paulo, Brazil  
e-mail: [igor.munhoz@ifsp.edu.br](mailto:igor.munhoz@ifsp.edu.br)

## 1 Introduction

The issue of remuneration within companies has gained importance and great attention from academic studies in recent years, mainly considering the analysis of their amounts (excessive or not), the architecture of total remuneration programs and relationships of conflicts between agents. Usually, studies on compensation focused on the company's strategic level (top management team—TMT) relate the company's financial performance and the individual performance of professionals occupying these levels [1].

In addition to performance reviews, other factors may influence the success of full compensation programs, such as the professional profile and level of knowledge of the eligible about the component items of the programs. Within the components of a total compensation program, three main factors are identified: fixed compensation, variable compensation (short and long term) and benefits, and the impact on satisfaction may or may not be equal [2].

Other factors may influence the degree of satisfaction of professionals of the corporate management team, which would not necessarily be linked to financial remuneration, such as career development, level of knowledge about the total remuneration program itself, hierarchical level, area of activity, age group, time in company, gender, education, and place of operation [3].

For an analysis that covers factors other than the most commonly studied, a survey was conducted in a multinational company in the logistics segment. Additionally, a literature review on the subject found that academic research on compensation programs in companies is infrequent and, when conducted, have quantitative objectives related to the earning capacity of professionals and impacts on companies.

Therefore, the objective of this study was to evaluate the level of knowledge and satisfaction of TMT members regarding the company's compensation policies and programs, as well as to identify the sociodemographic profile of the professionals and to analyze correlations.

## 2 Theoretical Framework

The concept of job satisfaction has been the subject of studies since the mid-1930s, due to the models proposed by Taylor and Fayol and the appreciation of the human factor. For these two scholars, motivation and job satisfaction would result from premiums and salary improvements; for Elton Mayo, workers had their own goals and objectives. Many studies have attempted to conceptualize job satisfaction and motivation, however, a widespread concept would be Locke's (1976) conceptualizing job satisfaction as "an emotional state, positive or pleasure, resulting from work or your work experiences" [4].

Recently, other concepts have brought to light a multifactorial sense of worker motivation as the instrument presented by [5], which is based on five dimensions

(satisfaction with colleagues, satisfaction with management, satisfaction with salary, and satisfaction with promotions, satisfaction with the nature of the work).

The compensation program of executives is a topic that has gained great importance and discussion in recent decades. Jensen and Murphy [6] argue that changes in the economy and global operating environment of companies as the main responsible for this relevance and transformations.

In the 1970s, the executive compensation structure was basically a monthly salary and bonuses tied to corporate accounting results, treated individually and without details of the professional's valuation metrics and parameters.

Over the next ten years, no major changes in executive compensation programs were observed, with the 1980s being the period of major acquisitions and mergers, one of the main responsibilities of executives to operationalize these movements [7].

It was in the 1990s that executive compensation programs underwent profound changes, linked to their structure. Long-term incentives as a form of variable remuneration payment have gained widespread popularity in publicly traded companies [8]. Another item that makes up the compensation program, and which companies maintained their structures, was the short-term reward, such as bonuses and PLR payment linked to financial results.

In a contemporary view, the 2000s were marked by events involving large companies in accounting scandals. Backed by fraudulent accounting and forged income statements, these companies were in surplus shares and, after uncovered irregularities plunged into bankruptcy [7]. Pointed out as one of the causes of the situation, executive compensation systems have been criticized for benefiting short-term results, lack of concern about business continuity and errors in the communication process (both internal and external) [8].

Additionally, according to Murphy [9], there is great heterogeneity in remuneration practices. However, executive programs often contain four components that are often not fully known to the employee, namely base salary, annual bonus (linked to accounting performance), and long-term actions and incentives (including restrictive action plans and bonuses based on multi-year accounting results).

### 3 Methodology

To assess the level of knowledge about company compensation policies and programs and degree of satisfaction of TMT members, as well as to identify the sociodemographic profile of the professionals, a survey was conducted, which included the application of a questionnaire to a logistic company in Brazil featuring a case study. The study company belongs to is the main provider of moving, warehousing and transportation services in Brazil. This organization is part of a global holding company whose main business is courier services, commercial banking, express delivery, freight management, and logistics solutions. With German-origin capital, the logistics solutions division is present in 60 countries with 120,000 employees.

In Brazil, it has business units in all regions (11 states) and serves the automotive, chemical, energy, consumer goods, pharmaceutical and health, and technology segments.

The questionnaire was sent electronically accompanied by an invitation letter and informed consent, presenting the study and its objectives as well as the guarantee of anonymity, giving the choice of participation or not as requested by the Research Ethics Committee of Pontifical Catholic University of São Paulo (PUC-SP).

The instrument applied had thirty questions, divided into three parts, and was sent at random, without identification and without differentiation between the regions of the country, to 70 TMT professionals from the study model company

The first part of the questionnaire included 12 questions about sociodemographic data.

The second part addressed ten questions to measure the level of knowledge about the company's compensation policies and programs. There were three answer options for each question: "no", "partially" and "yes". In order to measure this level, a point-based counting method was developed, based on the Likert method [10], and the alternative "no" represented 1 point, the alternative "partially" represented 2 points and the alternative "yes" represented 3 points. The sum of the points obtained represented the level of knowledge through direct proportion.

The third part addressed eight statements to measure the degree of satisfaction of TMT members in relation to the company's compensation policy and program. A 5-point Likert scale and the same scoring method were applied [10]. The sum of the points obtained represented the degree of satisfaction with the policy and total compensation program practiced by the company through direct proportion. In obtaining the results, the following hypotheses were tested:

*H1*: The different hierarchical levels and the different areas of activity are equally aware of remuneration policies and programs.

*H2*: Different hierarchical levels and different areas of activity are equally satisfied with compensation policies and programs.

*H3*: There is a direct correlation between the level of knowledge and the degree of satisfaction.

To confirm or reject the above hypotheses, Fisher's statistical significance test was applied between the score obtained in the Likert scale-based score, by hierarchical level and area.

Descriptive statistics were contemplated with the distribution of variables in absolute and relative frequency tables according to the stratification of hierarchical levels and areas of activity. For the purpose of classifying the level of knowledge and degree of satisfaction with the company's compensation policy, the Likert scale indices for these variables were distributed in percentiles (25, 50 and 75).

The assessment of the association between the degree of knowledge and level of satisfaction and the areas of practice and functional hierarchy was obtained by applying the chi-square test, after classification according to the cutoff value (75th percentile), and by the non-parametric Kruskal-Wallis analysis, comparing the absolute indices of each of the dependent variables.



The correlation between the degree of satisfaction and level of knowledge was obtained by applying the Spearman correlation coefficient for ordinal samples. The relationship between demographic variables and the degree of satisfaction and level of knowledge was assessed by contingency tables using the chi-square test to verify differences in frequency distribution between groups.

In order to verify the influence of remuneration components on the participants' satisfaction level, a multiple linear regression model with step-by-step variables input was used, based on the absolute values of the answers to the questions included in the third part of the questionnaire.

For all statistical evaluations, SPSS software (version 18.0, IBM Inc., USA) and a significance level of 5% were used.

## 4 Results and Discussion

Among the 70 questionnaires sent, 55 were completed, which characterized the research sample. Regarding the characterization of the sample, 56.4% of the participants are aged between 30 and 40 years and 7.3% between 50 and 60 years. In addition, most of them are graduated in business administration (43.6%), have a specialization degree (72.7%) and work in the southeastern region of the country (70.9%). Also, the respondents were mostly male (87.3%).

Regarding the level of knowledge, the minimum score obtained was 12 and the maximum was 30. Also, the minimum score obtained was 18 and the maximum 39 for the degree of satisfaction for the TMT members.

To classify the knowledge levels and satisfaction levels, in relation to the compensation program, the 25pc, 50pc, and 75pc percentile cuts were used. Thus, for the level of knowledge it was obtained 17 points (25pc—low knowledge), 21 points (50pc—moderate knowledge) and 23 points (75pc—high knowledge). For the degree of satisfaction, it was obtained 24 points (25pc—low satisfaction), 31 points (50pc—moderate satisfaction) and 35 points (75pc—high satisfaction).

Table 1 presents the general results of the application of the questionnaires with the absolute numbers of the universe, unanswered questionnaires, research sample, minimum and maximum score in relation to the level of knowledge and degree of satisfaction, besides the points that represent the distribution in percentiles (25, 50 and 75).

From the test of statistical significance obtained results of  $p > 0.05$  ( $p = 0.824$  and  $p = 0.957$ ) and showed that there was no statistical significance when comparing the level of knowledge and degree of satisfaction (respectively) between the hierarchical levels. Also, it was demonstrated that there was no statistical significance ( $p = 0.469$  and  $p = 0.615$ ) when comparing the level of knowledge and degree of satisfaction (respectively) between the internal areas of the study target company, confirming Hypothesis 1 and 2.

**Table 1** General data and score that delimits the percentiles in relation to the level of knowledge and degree of satisfaction regarding the compensation policies and program, considering the responses of TMT members

	Knowledge level	Degree of satisfaction	
Universe	70	70	
Did not answer	15	15	
Research Sample	55	55	
Minimum score	12	18	
Maximum score	30	39	
Percentiles			
25pc	17	24	Low knowledge and satisfaction
50pc	21	31	Moderate knowledge and satisfaction
75pc	23	35	High knowledge and satisfaction

In fact, Lawler [11] addresses the employee's "high involvement approach" to the business and encourages the creation of an environment in which individuals care about company performance, have the information they need to influence it and, as a result, are rewarded. To contribute to these actions, employees must have knowledge about the policies and compensation program applied by the company. However, the results found showed that even at different hierarchical levels or areas of expertise the level of knowledge and degree of satisfaction with the compensation policies and the program is the same, that is, there is no statistical significance that differ the level of knowledge and degree of satisfaction by hierarchical level and by area of activity. Even when we grouped the areas into two larger groups (operating areas and support areas) there was no statistical significance ( $p = 0.281$  and  $p = 0.280$ , respectively).

The correlation assessment between the level of knowledge and degree of satisfaction of compensation policies and the program was found to be significantly weak positive (0.402), thus confirming Hypothesis 3. Once verified that it is a significant correlation, we proceed to analyze the magnitude of this association, estimated to be 40.24%, that is, about 40% of the satisfaction index variation occurs concomitantly with variations of the index of knowledge, a poor correlation.

Corroborating this result, a weak correlation between TMT member's knowledge of compensation policies and program and their degree of satisfaction was observed characterized by the Spearman correlation test ( $\rho = 0.4020$ ).

Thus, statistically, a correlation was found between knowledge of compensation policies and programs and the degree of satisfaction, corroborating studies in the literature that point to the participation of knowledge in strategic compensation approaches. However, this correlation was characterized as weak by the Spearman correlation test ( $\rho = 0.4020$ ), i.e., there are factors of greater relevance to the

strategic approach to remuneration. The study of Steiner et al. [12] found that job satisfaction is often influenced by factors that go beyond remuneration and effort.

In fact, Wood and Picarelli [13] stated that the strategic approach to remuneration reflects the reality of companies operating in the globalized and competitive world, and considered the entire organizational context, from company strategy, structure and management style. Thus, knowledge about compensation policies and programs becomes a critical factor for the use of the strategic approach.

Assessing the level of knowledge of an organization's TMT members about compensation policies and programs can identify the transparency and/or interest of this group regarding this topic. The communication process of policies and programs is essential to ensure their successful implementation, as it ensures a full understanding of the compensation model and the gains it establishes. The communication strategy can be composed of two strands: first, show employees the value of the total compensation package (salary, benefits, bonuses, retirement plan, etc.); second, explain the business context and be transparent by comparing the total compensation package with the companies used in salary surveys and studies [7].

Hipólito [2] states that among the relevant points of the compensation strategy, the profile of the TMT members is one of them. This profile may facilitate or hinder the performance of compensation (satisfaction) policies and programs. However, it is noteworthy that, in addition to the profile of the TMT members, another relevant point for the success of companies' compensation policies and programs is the alignment between the human resources area and the other areas. In fact, the role of the human resources area within the organization has a great influence on this alignment [14].

Considering the results obtained on the measures that satisfy TMT members in relation to the compensation program, it was observed that short-term variable remuneration was cited as the most relevant measure of total compensation programs ( $R = 0.7760$ ), followed by fixed remuneration ( $R = 0.8760$ ), job structure and professional development ( $R = 0.9160$ ), benefits ( $R = 0.9370$ ) and level of knowledge of the policies and program applied ( $R = 0.9460$ ).

It was also found that regarding age, the level of knowledge is lower in the range of 30–40 years, which is repeated in the degree of satisfaction.

Considering the time in the current position, the level of knowledge is lower in the range of 5–10 years and the degree of satisfaction is lower in the range of 1–3 years. Regarding the number of direct reports, the level of knowledge is lower for those with 10–15 employees and the level of satisfaction is lower for those with 15–20.

From a survey with data of 21,670 participants, found that according to the increase of the promotion of these individuals in the organization, their satisfaction decreased. However, with age, these individuals became more satisfied as they changed companies. In this dynamic, the work pointed to the importance of remuneration [15].

## 5 Conclusion

Based on the objectives of assessing the level of knowledge and the degree of satisfaction of the TMT members of companies in the logistics sector located in Brazil, by hierarchy and area of activity, in relation to the compensation program, there are the findings listed below.

First, it was observed that the level of knowledge regarding the compensation policies and the program was not influenced by the hierarchical level or area of activity and was below the 75th percentile, which meant a low/moderate level of knowledge. Still, the degree of satisfaction regarding the compensation policies and the program was not influenced by the hierarchical level or the area of activity and was below the 75th percentile, which meant dissatisfaction in a significant portion of the population studied.

The level of knowledge about the variable remuneration influences TMT member's satisfaction, although it is weak. Items related to the sociodemographic profile of the TMT members do not show an influence on the level of knowledge and the degree of satisfaction about the compensation policies and program.

Therefore, it was identified the need for future studies that refer to ways to improve the transparency of companies in relation to compensation programs, determining whether this situation is inherent in the business communication process or refers to the cultural attitude of employees not to seek the necessary information. Another point to be researched is the alignment between the compensation program and the expectations of the TMT members, analyzed under the spectrum that these factors may be related.

## References

1. Clot, S., Grolleau, G., Méral, P.: Payments vs. compensation for ecosystem services: do words have a voice in the design of environmental conservation programs. *Ecol. Econ.* **135**, 299–303 (2017)
2. Hipólito, J.M.: *Administração salarial: a remuneração por competências como diferencial competitivo*. Atlas, São Paulo (2001)
3. Frey, B., Oberholzer-Gee, F.: The cost of price incentives: an empirical analysis of motivation crowding-out. *Am. Econ. Rev.* **87**(4), 746–755 (1997)
4. Thaler, R.H.: Mental accounting matters. *J. Behav. Decis. Mak.* **12**, 183–206 (1999)
5. Siqueira, M.M.M.: Medidas do comportamento organizacional: ferramentas de diagnóstico e de gestão. Porto Alegre: Artmed **16**, 265–273 (2008)
6. Jensen, M.C., Murphy, K.J.: Performance pay and top-management incentives. *J. Polit. Econ.* **98**(2), 225–264 (1990)
7. Jensen, M. C., Murphy, K. J., Wruck, E. G.: Remuneration: where we've been we got to here, what are de problems and how to fix them. Negotiation, Organizations and Market Research Paper Series, Harvard Business School (2004). Jensen, M. C., Murphy, K. J., Wruck, E. G.: Remuneration: where we've been we got to here, what are de problems and how to fix them. Negotiation, Organizations and Market Research Paper Series, Harvard Business School (2004)
8. Bebchuk, L.A., Fried, J.M., Walker, D.I.: Executive compensation in America: optimal contracting or extraction of rents?. National Bureau of Economic Research, Cambridge (2001)

9. Murphy, K. J.: Executive compensation. In: Ashenfelter, O., Card, D. (eds.) *Handbook of labor economics*, 3rd edn. North Holland, Amsterdam (1998)
10. Stefano, N., Righi, A. W., Lisboa, M. G., Godoy, L. P.: Utilização das dimensão de qualidade e escala de likert para medir a satisfação dos clientes de uma empresa prestadora de serviços. *Anais do XXVII Encontro Nacional de Engenharia de Produção* (2007)
11. Lawler, E.E.: Paying the person: a better approach to management. *Human Resource Manage. Rev.* **1**(2), 145–154 (1991)
12. Steiner, E., Russel, S., Vizek, A., Warlick, A.: Crew in the West Coast groundfish catch share program: changes in compensation and job satisfaction. *J. Coast. Manage.* **46**(6), 656–676 (2018)
13. Wood, T., Picarelli, V.: *Remuneração Estratégica*, 1st edn. Atlas, São Paulo (1996)
14. Urbancová, H., Šnýdrová, M.: Remuneration and employee benefits in organizations in the Czech Republic. *Acta Universitatis Agriculturae et Silviculturae Mendelianae Brunensis* **65**(1), 357–368 (2017)
15. Riza, S.D., Ganzach, Y., Liu, Y.: Time and job satisfaction: a longitudinal study of the differential roles of age and tenure. *J. Manag.* **44**(7), 2558–2579 (2018)

# Physical Ergonomics Applied to the Administrative Sector and the Factory Floor: The Case of a Food Industry



Kélvn Santos Aguiar , Maria Thereza de Moraes Gomes Rosa ,  
Luiz Vicente Figueira de Mello Filho , João Carlos Gabriel ,  
and Alessandra Cristina Santos Akkari 

**Abstract** There is an increase in the number of individuals with disorders related to the spine and such dysfunction is classified as the second most common factor of leave in companies. Thus, this work is based on physical ergonomics and its relationship with musculoskeletal diseases alleged by workers of a multinational food industry, which was used as a study model. This research was conducted in the administrative area and on the factory floor of the model company, applying the validated Portuguese version of the Nordic Musculoskeletal Questionnaire, as well as observational methods, which aimed to better understand the processes of the industry regarding ergonomic scratches. Among the results, a difference was observed between the distributions of the body regions with the highest incidence of pain, so that, in the body sector, the discomforts were located mostly in the neck (75%), while in the factory pain was found mainly in the upper limbs, shoulders (40%), hip (14%), ankle/feet (14%) and upper back (14%). The observations made in loco corroborate the data obtained by the research instrument since there was excess load lifting (factory), excessive static work, repetition of tasks, improper posture, among others. As an optimization proposal, it is suggested the creation of a work gymnastics program and the use of quick massage, so that workers can perform better in their daily routines based on well-being, health, and safety.

**Keywords** Physical ergonomics · Musculoskeletal diseases · Food industry

---

K. S. Aguiar · M. T. de Moraes Gomes Rosa · L. V. F. de Mello Filho · J. C. Gabriel ·  
A. C. S. Akkari (✉)  
Mackenzie Presbyterian University, Campinas, Brazil  
e-mail: [alessandra.akkari@mackenzie.br](mailto:alessandra.akkari@mackenzie.br)

© The Editor(s) (if applicable) and The Author(s), under exclusive license to Springer Nature Switzerland AG 2021  
Y. Iano et al. (eds.), *Proceedings of the 5th Brazilian Technology Symposium*, Smart Innovation, Systems and Technologies 202,  
[https://doi.org/10.1007/978-3-030-57566-3\\_53](https://doi.org/10.1007/978-3-030-57566-3_53)

## 1 Introduction

In order to avoid displacements and employee health hazards, organizations should consider a holistic view of the process, with companies always abiding by the Regulatory Standards to ensure the well-being of people within organizations, following Ergonomic precepts. In this sense, it is of great value to understand and evaluate, in different work environments, how physical workload influences workers' lives regarding welfare, safety, production effectiveness, and other aspects.

Given a historical context, it is possible to observe an increase in the number of people with spinal dysfunction caused by the working conditions. In fact, musculoskeletal disorders have the highest statistical indices, being the second most common reason for work leaves [1].

Brazil has a number of 10% of the total chronic health problems occupied by low back pain, which is the disease that most invalidates the population. In the international scenario, especially in the United States, it is the eleventh reason for hospitalization, which affects people between 20 and 45 years old, thus disabling them to perform activities, and the most affected victims are usually men in the age range 35 years old. May be cited as the positions of greatest risk of developing such dysfunction, general service workers, truck drivers, domestic workers, mechanics, garbage, nursing assistants, and construction workers [2].

Ensuring the well-being, health, and safety of workers, as recommended by Ergonomics, collaborates to optimize levels of productivity, quality, and efficiency in performing tasks, enabling the employee to achieve personal satisfaction, as well as reach with the success of organizational objectives [3, 4].

In light of the above, the present work aims to evaluate aspects of physical ergonomics in the organizational environment, using as a study model a food industry.

## 2 Background

Ergonomics is the area of knowledge that relates to the interconnections between humans and other elements of a system, aiming to achieve an optimization of human well-being and overall system performance. Analyzing the domains of specialization of Ergonomics, there is the interaction between different fields of action and disciplines, encompassing the social, organizational, environmental, biological, among others.

Focusing on the physical ergonomics domain, it can be observed that this is somewhat related to the areas of human anatomy, physiology, anthropometry, and biomechanics. Some of the most interesting subjects to address include material handling, posture at work, skeletal muscle disorders, and repetitive movements [5].

Every activity performed by workers during their work hours implies the performance of effort, which can be mental or physical. The importance of knowing the limits of each worker is latent so that there is no physical and/or mental overload,

avoiding weaknesses and damage in different ways to the worker and the organization [6].

Physical workload refers to the physical requirements that an employee is exposed to during his or her workday. To improve understanding of the physical workload, it is necessary to evaluate the physical efforts to which the worker is subjected, so that by analyzing the energy consumption and heart rate of a collaborator one can infer the degree of difficulty to perform a particular task [7, 8].

The sector that covers the food industry, which includes food products and also drinks generally, corresponds to approximately 25% of the accidents that occurred in the industry between 2010 and 2012 in Brazil. This number can still be analyzed in relation to the whole, indicating representativeness of about 6.5% of the total accidents that occurred in recent years. Thus, it is noted the importance and needs for ergonomics to be considered in industries and companies in general, especially in the food industry, since the numbers indicate high rates of occupational accidents. In this type of company, occupational hazards are the biggest candidates to cause environmental discomfort due to poor working environment or operational processes [9].

Environmental risks may include, for example, factors related to lighting, noise, physical exertion, task repetition, radiation, monotony, improper posture requirements, humidity, and substances that may harm the employees' body, among others.

Besides chemical and biological risk, another type of environmental risk (Brazilian Regulatory Standard 09) extremely important to be analyzed in the food industry, and which was the main object of study of this work, are the ergonomic risks, including postures, lifting/loading of loads, task repetition, static work, etc. This situation can increase the degree of absenteeism in this type of organization.

Therefore, this paper aims to evaluate aspects of physical ergonomics in the organizational environment, using as a model the Brazilian plant of the food industry.

### 3 Methodology

This is descriptive exploratory research and, as for the procedures, a case study was developed, which was applied in the Brazilian plant of the food industry. The large food industry was chosen mainly because it is a reference in its market, so that, besides the plant located in the state of Sao Paulo (Brazil), the company has other production plants in the U.S., China, and France. The industry operates in the market for flavor enhancers for seasonings, sauces, etc.

The present study considered the plant operators in their different divisions of the factory floor, as well as analyzing the professionals in the administrative sector, in order to allow a comparative study. Many aspects that influence the physical workload of employees were analyzed, such as lifting loads, static positions during the workday, breaks, postures, height/conditions of the work, among others. Therefore, the observational method was applied in the part-time journey of different



areas. The non-participatory, systematic, and semi-structured method was chosen so that a previous script was developed from some observation categories. On the first day, 80 min were used for analysis in the factory sector, considering the pulp, dryer, and mixture lines. On the second day, 40 min of analysis were devoted to the administrative sector.

Also, the workers were submitted to the validated Portuguese version of the Nordic Musculoskeletal Questionnaire (QNSO—*Questionario Nordico de Sintomas Osteomusculares*), after signing the Informed Consent Form. The QNSO instrument has been validated in Portuguese [10] and represents the Brazilian version of the Nordic Musculoskeletal Questionnaire (NMQ) [11] which has been widely applied to assess the nature and severity of self-rated musculoskeletal symptoms.

The questionnaire was developed and sent electronically to the company's employees, in agreement with area managers. In the email, it was explained about the exclusively academic objective of the study, the contact of the responsible researcher was informed and it was also explained about the guarantee of the anonymity of the participant, giving the employee the option to respond or not to the instrument according to the general guidelines of the Research Ethics Committee of Mackenzie Presbyterian University.

In the data treatment, the characterization of the sample was developed and the descriptive statistics were applied (Fig. 1).

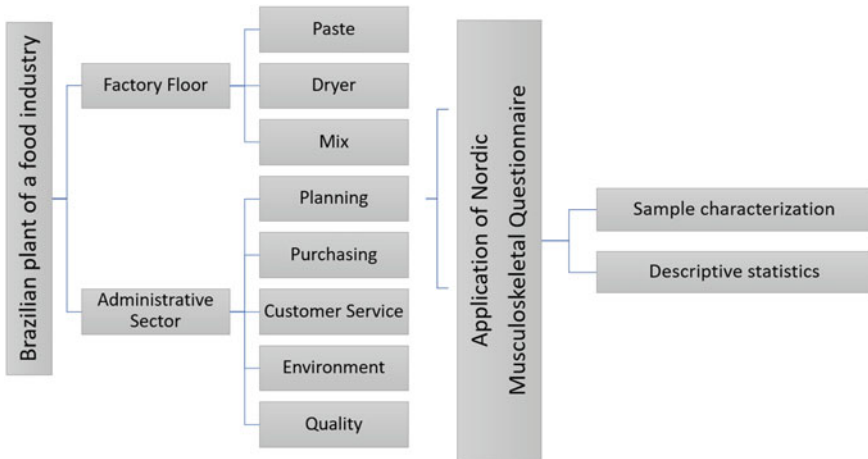


Fig. 1 Representative diagram of the methodological approach developed for this study

### 4 Results and Discussion

The sample obtained in the present study referred to 20 people, divided equally between the factory floor and administrative sector, with greater representation of males, as shown in Fig. 2.

With a 30% representation in the sample (Fig. 3), the most predominant age group is between 30 and 35 years old, and within this percentage, 66.7% of the employees were in the administrative sector and the rest in the factory. When the sample was analyzed, it was noticed that 60% of the employees who are younger, in their 20s and 25s, are in the administrative sector, being distributed in the purchasing, marketing, and planning areas. All respondents are over 45 years old is in the factory, centralized in the quality control sector.

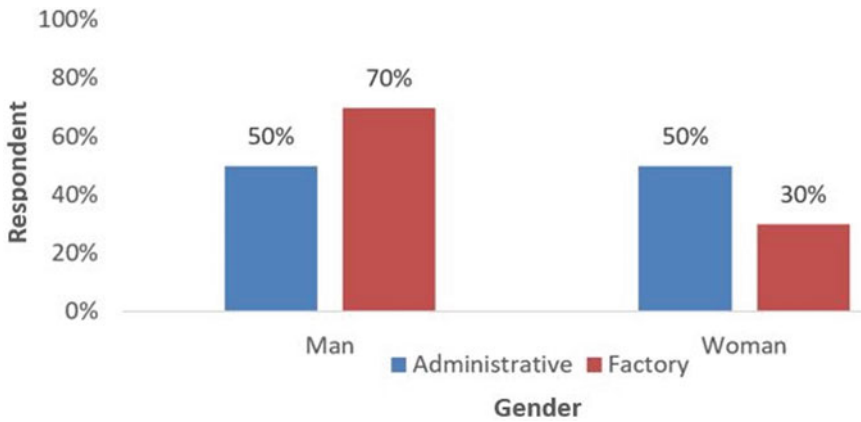


Fig. 2 Respondents by gender, considering the administrative sector and factory floor

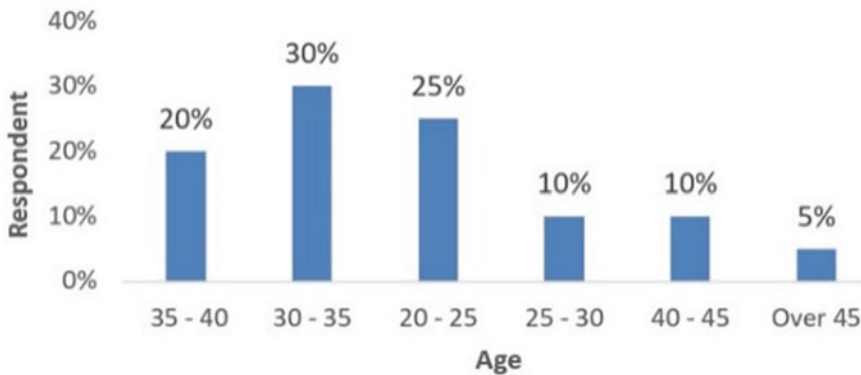


Fig. 3 Respondents by age, considering the administrative and factory sector

### 4.1 Data Analysis: Factory Floor and Administrative Sector

The analysis of the data collected from the application of the QNSO indicated that 70% of the respondents claimed that they felt pain, tingling or numbness in at least one of the body parts, in the last 12 months, and the shoulders received the highest rate of complaints with a representativity percentage of 43% (Fig. 4a). In fact, the work of Santos et al. [12] also pointed to the shoulders as the region with the highest incidence of pain for the shop floor worker. This result is in line with the observations made in the food industry since it was possible to notice inadequate postures for lifting loads.

It was observed that the layout of some sectors of the factory can be a major cause of injury to workers since the present format of machine distributions requires manual efforts, which are not fundamental to the activities. For example, the package is sealed manually and then the operator forwards the finished product for inspection. Inspection equipment could be moved closer to the sealing area as according to the current layout the operator must travel a distance of approximately 12 m to reach the specific location. Each package (with the finished product) is about 25 kg. Therefore, the more optimized the layout, the lower the physical effort of cargo transportation.

The observational analysis made it possible to identify a wrong degree of inclination of the worker's spine (30°) when compared to that recommended in the literature, which directs the lifting of the load so that the spine is at an angle of 90° to the ground to decrease the incidence of force on the vertebrae. Some examples of future problems that may arise from such practices would be back pain, which according to the National Institute of Social Security (INSS), is the factor that most generates work leave. When poor posture is practiced frequently, besides generating discomfort, it can promote problems in the muscles and joints [8].

Another point of note is that the worker needs to lower himself to feed the equipment with raw material in the system, requiring physical effort to pick up the raw material, lower it, and have to place it inside the intended compartment. In order to avoid this physical exertion, it is recommended to use a workstation that has a height adaptable to the employee, thus improving their well-being and decreasing the frequency/incidence of the shoulder, back, knee problems.

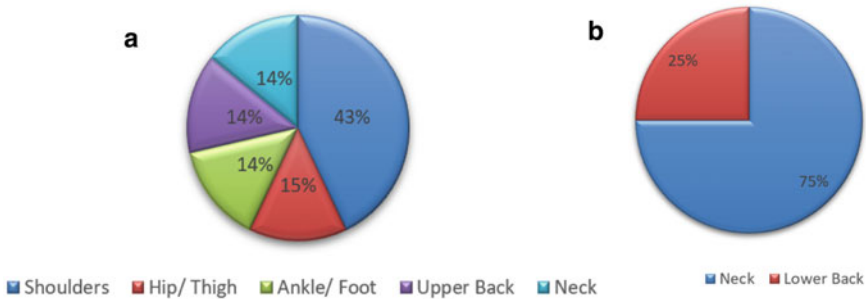


Fig. 4 Respondents who reported pain in the last 12 months, according to the body region and considering a factory floor and b administrative sector

Regarding their work or personal routines, 70% of respondents claimed that at no time did the pains described prevent them from practicing their daily activities (both personal and professional) in the last twelve months. The remaining participants (30%) answered that they were prevented, at some point, from practicing activities that are part of their routines, that is, they were impacted in some way.

When analyzed by gender, it is possible to observe that the female sample presented the highest percentage of affirmative answers in relation to the impacts and impediments of performing their routines, with a percentage of approximately 67%. In contrast, the male sample unanimously reported that they were not prevented from practicing their personal or routine professional activities due to the declared pain. It is also noteworthy that the age groups that were prevented from performing any of the activities present in their routines were between 20 and 25 years and between 40 and 45 years. The area with the most limitations due to pain was quality control.

It was also noted that 70% of people responded that they had not been to medical appointments in the last 12 months. On the other hand, it is observed that of the percentage that went to some consultation during the period, 67% were women.

Thus, it was found that women are more susceptible to pain in the workplace, increasing the likelihood of impacting their routines. In fact, a study with the Brazilian insurance company Sul América found that women are the most affected with back pain, which may have direct impacts on their productivity in the organization. The study was conducted between May 2013 and March 2016, with the participation of more than 13,000 policyholders, and the female population had the highest percentage of back pain (68.5%) and maybe related to hormonal variation [13].

It was observed that 70% of people said they did not feel any kind of problem/pain in the week before the questionnaire was applied. Looking at the 30% who said they felt some kind of problem, most were women (67%).

Also noteworthy is the excess of static work in the sector, i.e., through the on-site analysis it was noticed that during the activities execution the operators are always standing, generating fatigue, besides possible problems with repetitive movements.

After applying the QNSO instrument to the administrative sector, it was possible to notice that 80% of the respondents felt pain, tingling, or numbness in at least one part of the body in the last 12 months. Of all body parts analyzed, the one with the highest pain complaint rate in the last 12 months was the neck, with 75% (Fig. 4b).

When analyzing work or personal routines, 80% of respondents said they were never influenced by the pain described above. The remaining participants (20%) stated that they were prevented at some point from practicing activities that are part of their routines, that is, they were impacted in some way.

This observation is in line with the analysis made using the observational method, since it was possible to verify an inadequate positioning of the spine during the workday, especially of employees who use laptops. The workers begin their activities in an acceptable position, however, as time goes by, there is a relaxation so that they begin to tilt their body forward, tending the neck and affecting the spine. Analyzing in a general scenario, the factor of bad posture in the administrative sector (mainly),

due to the use of laptops and microcomputers, has been increasing more and more, causing more workers to leave the company when analyzed.

## ***4.2 Comparison Between the Analyzed Sectors***

The administrative sector presented a percentage of 10% more than the factory when studying the occurrence of pain in the body parts in the last 12 months. Analyzing the locations of pain reported by employees, in the administrative sector, the pain was felt more centrally in one or two regions (especially in the neck), while in the factory, the pain was more distributed, according to respondents' reports. This fact can be understood since, in the administrative sector, the postures that are required of the various functions are very similar, bringing similar consequences to their employees.

On the other hand, in the factory, there are quite different functions, requiring different rhythms, repetitions, and postures, which can, therefore, generate more dispersed pain, depending on the types of activities that will be performed by each employee.

Noting the number of respondents who claimed to have been prevented from performing any of their routine activities, it is noteworthy that in the administrative sector only 20% of respondents gave affirmative answers. When analyzed in the factory floor sector, there was an increase of 10%, thus reaching a percentage of 30%. In the administrative area, most of the pain is caused by poor posture during the workday, especially by people who use laptops. In the factory, besides the postures, there is another factor that further aggravates the situation of workers, the lifting/loading of cargo.

## **5 Conclusion**

During the case study developed in the Brazilian plant of the large food industry, it was noticed a diverse sample of gender and age, presenting a higher concentration in the range between 20 and 40 years. The sample (20) was equally divided, with 50% of the sample composed of administrative staff and the remainder by factory staff. A factory floor and administrative sector are reported to suffer from bad postures, having long-term consequences as well as some short and medium-term discomfort. However, the factory sector has an aggravating factor, since, besides the bad postures and the static and repetitive works, there is the load lifting/loading factor, impacting the distances in the food industry. As an optimization proposal, it is suggested the development of an occupational gymnastics program, so that the workers can perform better in their daily routines, predicting some future injuries to occur. Another improvement proposal, preventing muscle injuries, is the creation of the culture of quick massage during work hours.

## References

1. Hyunjin, B., Songa, S., Leea, D., Pyoa, S., Shinb, D., Leeb, G.: Musculoskeletal diseases of heavy industrial workers. *Phys. Ther. Rehabil. Sci.* **6**(2), 71–76 (2017)
2. Lax, M.: Occupational health in central New York state: a publicly funded occupational disease outpatient clinic 25 years later. *Rev. Bras. Occupat. Health* **38**(127), 149–161 (2013)
3. Kuijjer, P.P., van der Beek, A.J., van Dieën, J.H., Visser, B., Frings-Dresen, M.H.: Effect of job rotation on need for recovery, musculoskeletal complaints, and sick leave due to musculoskeletal complaints: a prospective study among refuse collectors. *Am. J. Ind. Med.* **47**(5), 394–402 (2005)
4. Gornostaeva, Z., Kushnaryova, I., Alekhina, E.: Increasing the Competitiveness of Small Business Companies on the Basis of the Modern Information Platform. In: Popkova, E. G., Ostrovskaya, V. N (eds.) *Perspectives on the Use of New Information and Communication Technology (ICT) in the Modern Economy* vol. 726, pp. 207–216 (2019)
5. Monteiro, M.S., Alexandre, N.M.C., Rodrigues, C.M.: Musculoskeletal, work-skeletal, work and lifestyle diseases among style workers of a public health institution. *J. Nurs. Sch. USP* **40**(1), 20–25 (2006)
6. Pinto, N.F., Murofuse, N.T., Carvalho, M.: Process and workloads and workers' health in sericulture: a review. *Rev. Bras. Occupat. Health* **40**(132), 237–247 (2015)
7. Taelman, J., Vandeput, S., Vlemincx, E., Spaepen, A., Van Huffel, S.: Instantaneous changes in heart rate regulation due to mental load in simulated office work. *Eur. J. Appl. Physiol.* **111**, 1497–1505 (2011)
8. Widanarko, B., Legg, S., Stevenson, M., Devereux, J., Eng, A., Mannetje, A., Cheng, S., Pearce, N.: Prevalence and work-related risk factors for reduced activities and absenteeism due to low back symptoms. *Appl. Ergon.* **43**(4), 727–737 (2012)
9. Vasconcelos, F.M., Maia, L.R., Almeida Neto, J.A., Rodrigues, L.B.: Risks in the workplace in the bakery sector: a case study in two cookie industries. *Gest. Prod.* **22**(3), 565–589 (2015)
10. Pinheiro, F. A., Troccoli, B. T., OAK, C. N.: Validation of the nordic musculoskeletal questionnaire as a measure of morbidity. *J. Public Health* **36**, 307–312 (2002)
11. Kuorinka, I., Jonsson, B., Kilbom, A., Vinterberg, H., Biering-Sorensen, F., Andersson, G., et al.: Standardised Nordic questionnaire for the analysis of musculoskeletal symptoms. *Appl. Ergon.* **18**, 233–237 (1987)
12. Santos, V.M., Santos, J. W., Alsina, O. L. S., Monteiro, L. F.: Application of the musculoskeletal Nordic questionnaire to estimate the prevalence of work-related musculoskeletal disorders in workers under temporal pressure. In: XXXVIII National Meeting of Production Engineering, Curitiba (2015)
13. Vitta, A., Canonici, A.A., Conti, M.H.S., Simeao, S.F.A.P.: Prevalence and factors associated with musculoskeletal pain in professionals with sedentary activities. *Physiotherapist Mov.* **25**(2), 273–280 (2012)

# Evaluation of Illuminance in Workplace: A Case Study on the Production of Multicolored Self-adhesive



Wellingtânia Domingos Dias , Taciana Ramos Luz ,  
and Meinhard Sesselmann 

**Abstract** Adequate lighting is important for the productivity, efficiency, and quality of a process line. Its evaluation is indispensable to keep mistakes and consequently accidents from happening as well as preventing the occurrence of physical and psychological complications for the employee. It is known that work in the industrial sector alone can be exhausting, just like any other production process which may demand a work rate with high productivity and concentration requirements. In the case of the production of multicolored self-adhesive labels, the lighting of the workplace comes across as essential for the correct configuration of colors to be used in the productive process likewise the visualization and differentiation of the various colors during the final inspection product. The goal is to assure the best product quality and a most satisfied client, being that this is the most compelling factor when the wish is to keep oneself competitive on the market. This paper has as its goal the development of a case study based on the analysis of the illuminance on workstations at a factory where multicolored self-adhesive labels are produced. The study started with the identification of variables relating to how the level of illuminance on the referred production sector meets the expected standards reported by the NBR 8995-1/2013 ABNT regulation. In this context and in the light of the evaluation of the variable correctional actions were then proposed in furtherance to better the final product quality control inspection, alongside providing greater visual comfort to the employees, minimizing health jeopardy.

**Keywords** Illuminance · Industrial environment · Workstations

---

W. D. Dias (✉) · T. R. Luz · M. Sesselmann

Post Graduate Department of Mechanical Engineering, Bioengineering Laboratory, Federal University of Minas Gerais, 6627 Presidente Antônio Carlos Ave, Belo Horizonte, MG 31270-901, Brazil

e-mail: [wellingtaniad@gmail.com](mailto:wellingtaniad@gmail.com)

T. R. Luz

e-mail: [tacianaluz@gmail.com](mailto:tacianaluz@gmail.com)

M. Sesselmann

e-mail: [meinhard@ufmg.br](mailto:meinhard@ufmg.br)

© The Editor(s) (if applicable) and The Author(s), under exclusive license to Springer Nature Switzerland AG 2021

Y. Iano et al. (eds.), *Proceedings of the 5th Brazilian Technology Symposium*, Smart Innovation, Systems and Technologies 202, [https://doi.org/10.1007/978-3-030-57566-3\\_54](https://doi.org/10.1007/978-3-030-57566-3_54)

## 1 Introduction

The lighting of workspace is a preponderant factor for the composition and spatial perception and may provoke various forms of sensations upon individuals, e.g., fatigue, drowsiness, visual discomfort, irritability. On the whole, the level of lighting directly affects the work done in particular spaces, which justifies the importance of planning lighting projects through.

According to Truccolo [1], poorly dimensioned lighting projects in which the final illuminance does not meet the truly desired environment requirements may reduce the employee performance drastically and, in some cases, risk their health as well as the final product quality. Iida [2] mentions that light is essential at the workplace and reinforces productivity and final product quality as a result of the employee's satisfaction and comfort.

On the other hand, a well-planned industrial lighting project improves the working environment, increases the safety of employees, provides better productivity, reduces operational costs, and, consequently, contributes to the preservation of the environment since the saving in energy consumption is taken into account.

In order to carry out an industrial lighting project compatible with the employees' needs, it is necessary to conduct ergonomic analysis aimed at correcting and preventing problems that might affect the quality of life in the workplace. Although the company may target their goals toward the optimization of productivity, this process ought not to put the health of the employees under jeopardy. For this reason, the implementation of given ergonomic actions may be seen as necessary; according to Falzon [3], the ergonomics must balance the companies goals like efficiency, productivity, reliability, quality, and durability; with the employee's goals as safety, health, comfort, satisfaction, and interest in work.

Likewise, it is important to emphasize that the industrial environment should be appropriate to the standards in force, including those concerning the lighting [4]. The Brazilian Association for Technical Standards [5], in specific the NBR 8995-1 rule, establishes the lighting requirements for indoor working environments beneficial to the workers to perform their visual tasks in an efficient manner, safely, and comfortably. Still, with regard to the rules, the lighting in a specific direction may reveal yet unseen details of a visual task, leading to better visibility and a more prompt problem-solving. This scenario is particularly important for tasks involving fine texturing, e.g., engraving and embossing of paper.

The way to achieve an efficient but low-price industrial lighting ranges from defining the level of illuminance required at the work environment for choosing the more suitable types of lamps available and their degree of cost-saving. These steps result in calculations which will, thus, lead to the required amount of lighting instruments needed to supply the desired level of illuminance.

For the activities in the multicolored tags production, the regulation recommends an average of 500 lx illuminance for printing and cutting automatic processes; 1500 lx for multicolored printing color inspection; 1000 lx for typesetting; and 500 lx for rewinding and shipping.



Dos Santos et al. [6] state that the brightest the lighting, the better the visual acuity. Nonetheless, excessive lighting may degrade vision and even cause injury. Overly lit objects may be even more difficult to observe than the ones with non-sufficient lighting shone upon. Nevertheless, if there is a rapid increase in lighting whenever the eyes are still adapting to low luminosity, there may be reduced visual acuity.

To each adaptation circumstance, there is an optimal level of lighting. As relative contrast is reduced, luminous intensity must be increased to maintain the acuity. The greater the contrast, the clearer the stimulus is perceived. Theoretically, the maximum contrast is represented by the instance in which the lighting is maximum on the stimulus and non-existent throughout the adjacent region. It is an almost never found instance in practice [6].

### ***1.1 Objective***

To evaluate the level of illuminance, while acknowledging NBR 8995-1 Brazilian standard within an industrial-worksite, at which the activities of printing, “typesetting” and “inspection” of multicolored self-adhesive labels are carried out.

## **2 Methodology**

The present work was developed from the evaluation of illuminance in the worksite of the production of multicolored self-adhesive labels. Under this perspective, the following parameters were considered:

- Level of illuminance in the industrial environment adopted in accordance with the Brazilian standard NBR 8915-1, which takes into account the activities carried out in this worksite—evaluated under the ergonomics perspective.
- Practical confirmation by collecting data with a lux meter and comparing the levels of illuminance collected to the ones listed on the standard in order to resolve any doubts as to the correctness of the illuminance used in the working environment.

The present work was carried out, from August to November of the year 2017, in a company located in the metro area of Belo Horizonte-Brazil that produces multicolored self-adhesive labels.

The company demand emerged from the need to perform improvements in the work environment and to promote the employees’ welfare, as well as to meet quality certifications.

Regarding the evaluation of the levels of illuminance, a study case was carried out within the production sector of the company, comprises 14 workstations.

In order to evaluate exposure to illuminance, “NBR 8995-1/2013: Lighting of Workstations” recommendations were followed. A digital thermo-hygro-anemometer-lux meter by the brand Lutron, model LM8000, serial AB33174,

equipped with a light detector for more accurate data collection, and with spectral responses within 0 and 20.000 lx, was used to verify the lighting parameters.

In effectuation of the measurements of the amount of light of the surroundings, some care was taken regarding known factors which could lead the data collection into mistaken responses.

As stated in NBR ISO 8995-1, another aspect worthy of the companies' attention, besides the gross amount of light in a given horizontal or vertical plane, it is the uniformity of light that covers not only the activities carried out in the production line but also the others have done around. According to Vianna and Gonçalves [7], the industrial work requires a light uniformity to avoid visual problems due to the contrast between light and dark lighting, where employees must make constant visual adjustments.

Other aspects to be considered are mutability, color reproduction index, and the color temperature. Mutability, flexibility, or versatility of light refers to the system's ability to adjust the lighting in accordance with the different needs specific to the environment. Color reproduction is the variation that is observed from the color vision of the objects under the illuminant study, in relation to a standard illuminant. The index of color reproduction is essential in industrial sheds, depending on the activity field, as in the printing industries, among others. Color temperature—warm, cool, and neutral, measured in Kelvin ( $K$ ) scale, is also a normative requirement.

For Vianna and Gonçalves [7], warm color sources are not advisable for manufacturing or office environments, once are observed a decrease in the pace of work by the employees. For these production environments, cool or neutral light sources are recommended. The company sector where the measurements were taken has only artificial lighting; therefore, it was of no need the data collection in several daylight times and/or on different seasons.

Fourteen workstations were evaluated, and the results of illuminance evaluation were compared with the minimums reported by NBR 8995-1/2013 standard. The data were collected; the illuminance level average values of each workstation were obtained. This way, forty-two measurements were performed in each workstation during the time interval of 10 a.m. through 11 a.m. of one single day in September/2017. All evaluations of the workstations' lighting were performed during a normal working day.

For the data analysis, Microsoft Excel software was used. After collecting the numbers, calculation of averages was made with the aid of spreadsheets in order to compare the illuminance levels among the workstations' values and weigh out whether they were in accordance with the minimum requirements of NBR 8995-1/2013 standards.

Table 1 shows the required levels of illuminance recommended by standard NBR ISO 8995-1 for workstations according to the nature of the activity carried out in the company under study.

Illuminance levels were registered after lux meter calibration and stabilization, the latter being passive of taking either short or long periods of time depending on variations on luminosity around the points of data collection. At each of these points, three admeasurements were collected.

**Table 1** Recommended illuminance for workstations by standard NBR ISO 8998-1

Environment—manufacturing	Min illuminance (lx)
Printing	500
Typesetting	1000
Color inspection in multicolored printing	1500
Rewinding	500
Shipping	300

In order to define the location of the measurement points, the task area—by definition, the partial area of the workstation within which the visual task is carried out— was imaginarily divided into contiguous and identical squares, each of which with the dimension of about 20 cm of side length—indicated number for small areas [8]. The gauging is done in the center of each of these squares during the printing of the adhesive labels; and the measurements for the illuminance levels on the surroundings of the task areas were done through a strip range of at least 0.5 m of width within the employee’s field of vision.

### 3 Results and Discussion

In the analysis of the company operations phase, visit was arranged in order to collect information on the production process and to embrace aspects with reference to the number of employees, workload, type of machinery run, and the sequence of production flow. Next, three visits to each company sector were scheduled and performed, comprising offices and production sectors altogether.

Observations and notes were held on the activities of workers who run the printing machinery, before with the preparation and during the actual process, as well as the “typesetting” and “color inspection” activities.

As by the analysis of the work environment conditions, despite the artificial lighting permanently on, it was detected that the environment luminosity was not the most adequate and did not offer good comfort conditions and thus employee welfare required by this production process. Besides, the darker shade of walls and shelves contributed to the darkening of the surroundings.

As for the spatial distribution, walls and shelves were located close to the machinery, which can be responsible for the casting of shadows that may cause harm to the employees’ eyes, mainly during the typesetting and color inspection processes.

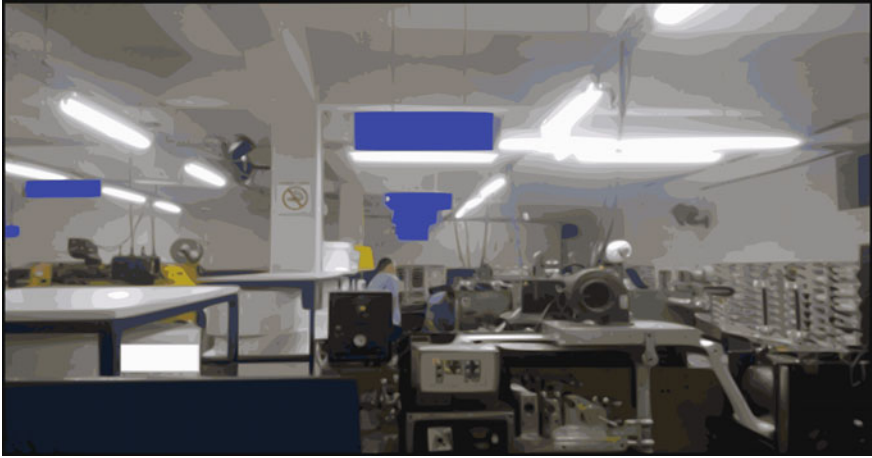


**Fig. 1** Representative image of the spatial distribution of the machinery in the production sector areas

As pre-diagnosis, one might be accurate on saying that the disposition of machinery (see Fig. 1) did not was framed well within the set spacing limits between machinery and spare supplies shelves, according to the Regulatory Standard 12: Machines and Equipment [9]. Printing machines were positioned too close to each other and too close to walls, hindering maintenance. Due to this fact, it was found out that, during the processes of typesetting and color inspection of tags, the lighting presented was not adequate, compromising visualization of tasks by workers and generating greater visual effort. Therefore, the focus of the analysis revolves around the adequacy of lighting in the task area for the typesetting and tag color inspection processes.

The lighting equipment was arranged in a localized configuration. This can be described as a setting in which the light incites predominantly on a preferred direction; the lamps are centered above and around the task area, providing high illumination in a workstation or on a machine. However, the inspection workstation, which demands lighting strictly necessary for a thorough visual examination, during and after the printing of the multicolored labels, was not found to be lit by localized configuration. Nevertheless, the activity station requires a 1500 lx illuminance is required.

**Table 2** Results for the factor illuminance on workstations at the company under study

Production sector	Number of workstations	Average illuminance
Printing	7	343.55
Typesetting	6	363.20
Inspection	4	309.25
Rewinding	3	397.56
Shipping	3	215.67
Total average		325.85

### 3.1 Illuminance Measurements

The collected data were submitted to analysis and are separated on the following by activity sector—printing, typesetting, inspection, rewinding, shipping. The admeasurements found were compared to the advised minimum values indicated by the ABNT NBR ISO/CIE 8995-1:2013 standard, in order to verify conformity.

The evaluation of illuminance on the workstations of the company under study resulted in an average general level of 325.85 lx. Table 2 presents the average results for the illuminance factor.

Based on Table 2, one can note that there was a significant variation of artificial illuminance on areas where workstations were set. Therefore, it was possible to observe that, for evaluation of illuminance, the physical environment exerts great influence.

After the establishment of lighting patterns according to the norm to the industrial environment values, it was possible the comparison with the average values measured in each workstation (see Table 3).

With respect to points where an efficient illuminance is indispensable, the work of the inspection presented the lowest average illuminance value. Data shown in Fig. 2 makes clear that the workstations are not in conformity with the minimum illuminance levels standards, with the exception of the shipping workstations, which display levels a bit higher than the minimum uniformity range. As demonstrated, the works need correction in order to reach adequacy to the norm.

The levels of illuminance at workstations were lower than the minimum established by the NBR 8995-1/2013 standard, which indicates the company must adopt

**Table 3** Comparison between results for the factor illuminance at the company under study and the values indicated by the ABNT NBR ISO/CIE 8995-1 2013 standard

Production sector	E—average illuminance measurements (lx)	Illuminance (lx)	Uniformity (0.7)
Printing	343.55	500	350
Typesetting	363.20	1000	700
Inspection	309.25	1500	1050
Rewinding	397.56	500	350
Shipping	215.67	300	210

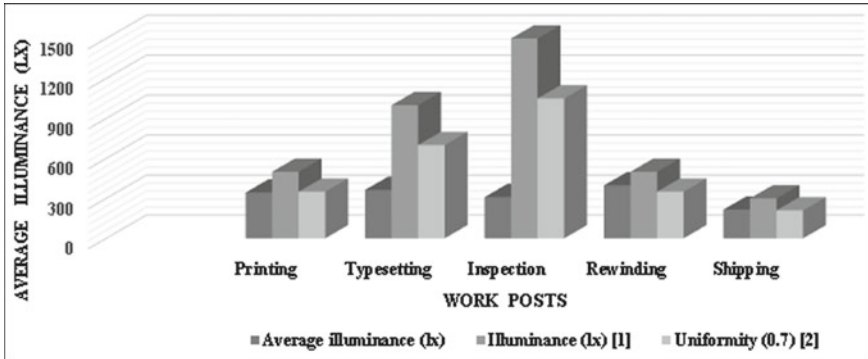


**Fig. 2** Graph—conditions of illuminance around workstations at the company under study. Average illuminance refers to the average values obtained from data collected at the workstations ( $x$ ); illuminance (lx) ( $Y$ ) [1] and uniformity (0.7) [2] refer to the standard values extracted from the norm

correctional actions to minimize or mitigate this fact. The present results resemble those from De Oliveira et al. [10], who analyzed the lighting in a wood workshop; the workstations, with the exception of only two, displayed levels of illuminance insufficient for the activities carried out. It is known that below the minimum limit recommended; the meager lighting may cause visual fatigue, excessive effort and can induce mistakes. Therefore, it was suggested that the wood workshop held adjustments in the lighting system of the working environment.

In a study of Von Bommel et al. [11] performed in a metallurgical company, results revealed that increasing illuminance from 300 lx to 500 lx could generate an increase in productivity of between 3 and 11%; that is, the increase in illuminance in the workplace brought improvements in task performance, reduction of waste, and diminishing of number of accidents.

Following the same lead, Juslen et al. [12] examined the influence of lighting in the employees' work pace and in the quality of work in the sector of assembly of electrical devices. Results showed that the work pace in the environment with 1.200 lx is 9% faster than that performed under the 800 lx detected during winter.

Based on a study done by IESNA [13], it could be observed that the accident recidivism factor decreased by 30% when the lighting increased from 65 to 170 lx. Such results demonstrate that there is a positive relationship between the increase in illuminance and productivity.

On the other hand, Akbari et al. [14], from the Pearson correlation coefficient calculated in his study, detected that the amount of lighting has no influence over human productivity in an automotive parts' assembly unit and even changes in lighting have no influence whatsoever over the productivity of employees from other units. This study is an exception; given that others such as one authored by Anizar et al. [15] about a cigarettes' industry were able to conclude that there actually is a correlation between the amount of imperfect cigarette paper that goes through inspection with the poor lighting at the lamination station, causing a decrease in employee performance and in how much they are centered on the task they carry out.

### 3.2 *Suggested Corrective Actions*

Correctional actions were suggested to the multicolored self-adhesive labels company in order to provide greater employee welfare, as well as optimized services and an increase in final product quality. The study by Rangkooy et al. [16] reiterated that illuminance-related correctional actions by many times are not efficient in a first instance; therefore, a second and more beneficial suggestion for the lighting design was made.

The adequacy proposals were: improving the company's lighting design, maintenance factor application done by trained professionals, performing maintenance on the lighting system and on the surfaces at the work sectors—the adoption of light colors for flooring, walls, and ceiling—and adjustment of physical arrangement.

As for the labels' inspection activity, color is a paramount factor of quality, and, therefore, when improving the lighting at the workstations the worker's emotional state is benefited, besides the reduction of individual work overload. Consequently, there are great improvements in product quality for the final consumer.

## 4 **Conclusions**

With respect to the quantitative illuminance evaluation, it is concluded that all the workstations in the industry of multicolored self-adhesive labels display average levels of illuminance lower than the minimum required by the Brazilian standard for the lighting of work environments.

This company demands a greater visual accuracy by workers when observing the color quality of labels in resonance to the product's final quality.

The field survey results show the existence of illuminance values in nonconformity with the NBR 8995/2013 standards in all workstations analyzed, which may be impairing the final product quality. In the meantime, it is up to the company to arrange the necessary corrections according to the standards referenced above, seeking minimization or mitigation of this wronged factor.

In the view of the foregoing, it is concluded that the characteristics of a work environment may alter the quality of the job carried out by the employee as well as the final product quality, being that a workstation must be adequate to guarantee to service quality offered by the employees together with their health. The company must provide a pleasant environment mounted with maximum protection and security, in order to favor the common welfare between company and collaborator.

So as to improve the company lighting system design project, a maintenance factor must be applied, embedded by trained professional, performing maintenance on the lighting system and on the surfaces throughout the work sectors, adopting light colors for flooring, walls, and ceiling, in addition to adjusting the physical arrangement.

**Acknowledgements** The authors thank the Federal University of Minas Gerais (UFMG) and the Brazilian National Council for Scientific and Technological Development (CNPq) for all financial support and the company that gave us the opportunity to study.

## References

1. Truccolo, L. J.: Análise dos riscos de acidentes no setor de produção em uma empresa de produção de móveis escolares. Monograph (Specialization)—Occupational Safety Engineering Course, Federal Technological University of Paraná, Medianeira, 69 f. (2013)
2. Iida, I.: Ergonomia: projeto e produção, 2nd edn. Edgar Blucher Publisher, São Paulo (2005)
3. Falzon, P. (ed.): Ergonomia. Edgar Blucher Publisher, São Paulo, p. 640 (2007)
4. Padilla, J. R.: Iluminação industrial, alternativas para melhorar sua eficiência energética e facilitar a manutenção. Revista Lumière Electric ed. 157. Iluminação Industrial, Editora Lumière, Eletron—PR, pp. 102–108 (2011)
5. ABNT: Associação Brasileira de Normas Técnicas. NBR ISO NBR ISO/CIE 8995-1. Iluminância de interiores. Rio de Janeiro, ABNT (2013)
6. Dos Santos, A., Leta, F., Veloso, M.: Fatores de risco industrial causados por diferentes percepções de cores devido à diferença de iluminantes. Revista Produção Online **5**(1) (2005)
7. Vianna, N. S., Gonçalves, J. C.: Iluminação e Arquitetura. Geros s/c Ltda, 2th edn. SP, São Paulo (2001)
8. Nogueira, A.: (a) Procedimento de trabalho DSA UASO-PE 14\_02 L. Determinação dos níveis de iluminância. (b) Ficha de Registo de Medição de Níveis Iluminância DSA UASO-IM 22\_01 L. Determinação dos níveis de iluminância. (c) Folha de cálculo em EXCEL da Iluminância e Uniformidade DSA UASO-IM 55\_03 L. Occupational Air and Health Unit of the Department of Environmental Health of INSA (2009)
9. ABNT: Associação Brasileira de Normas Técnicas. NR-12: Máquinas e Equipamentos. Rio de Janeiro (2009)
10. De Oliveira, F. N., De Sousa, L. S., Gadelha, L. F.: Análise da iluminância em postos de trabalho de uma marcenaria na cidade de Tabuleiro do Norte-CE. XXXVI National Meeting of Production Engineering (2016)
11. Bommel, J.W., Van Der Beld, G.L., Ooyen, M.H.F.: Industrial Lighting and Productivity. Philips Lighting, The Netherlands (2002)
12. Juslen, H., Wouters, M., Tenner, A.: The influence of controllable task-lighting on productivity: a field study in a factory. Appl. Ergon. **38**, 39–44 (2007). <https://doi.org/10.1016/j.apergo.2006.01.005>
13. Rea, M. S.: The IESNA Lighting Handbook, 9th edn. Illuminating Engineering Society of North America, New York (2000)
14. Akbari, I. J., Dehghan, H., Azmooh, H., Forouharmajd, F.: Relationship between lighting and noise levels and productivity of the occupants in automotive assembly industry Hindawi. Publishing Corporation. J. Environ. Public Health **527078**, 5 (2013). <https://doi.org/10.1155/2013/527078>
15. Anizar, K., Syahputri, R. M., Sari, I. R., Hardianti, D. A.: Changing lamp type and position to improve lighting quality. In: IOP Conference on Series: Earth and Environmental Science, p. 126 (2018). <https://doi.org/10.1088/1755-1315/126/1/012050>
16. Rangkooy, H. A., Mazaheri, A. H., Salehi, M. M. A., Khshmirz, A. F.: Assessment and design of illumination in a steel manufacturing company in Ahvaz, Iran. Jundishapur J. Health Sci. **9**(4) (October, 2017). <https://doi.org/10.5812/jjhs.64051>



# Smart City: A Qualitative Reflection of How the Intelligence Concept with Effective Ethics Procedures Applied to the Urban Territory Can Effectively Contribute to Mitigate the Corruption Process and Illicit Economy Markets



Kelem Christine Pereira Jordão , David Bianchini , Yuzo Iano , Ana Carolina Borges Monteiro , and Reinaldo Padilha França 

**Abstract** The public corruption and illicit market correspond to the greatest global challenges to be overcome by governments worldwide (Transparency International 2017). According to the Corruption Perceptions Index 2017, for 180 countries/territories studied, most of them are making little or no progress in ending corruption in the public sector. The public money laundered affects direct investments in infrastructure to improve the city's performance. The corruption encourages directly the illicit activities formation and the Organization for Economic Cooperation and Development (OECD) estimates that hundreds of billions of dollars of revenue from illicit activities are handled globally every year and was identified in the context of National Risk Assessments as part of the major risks that could affect countries in development. These practices have generated negative effects in society and the cities are the context in which all these issues occur. Then, this paper has aimed to conduct a qualitative reflection of how smart cities, which represent efficiency and effectiveness places, can contribute through your intelligent environment to mitigate the corruption process and illicit market operations.

---

K. C. P. Jordão (✉) · D. Bianchini · Y. Iano · A. C. Borges Monteiro · R. Padilha França  
School of Electrical and Computer Engineering (FEEC), University of Campinas—UNICAMP,  
Av. Albert Einstein, 400, Barão Geraldo, Campinas, SP, Brazil  
e-mail: [kelemjordao@gmail.com](mailto:kelemjordao@gmail.com)

D. Bianchini  
e-mail: [davidesperantista@gmail.com](mailto:davidesperantista@gmail.com)

Y. Iano  
e-mail: [yuzo@decom.fee.unicamp.br](mailto:yuzo@decom.fee.unicamp.br)

A. C. Borges Monteiro  
e-mail: [monteiro@decom.fee.unicamp.br](mailto:monteiro@decom.fee.unicamp.br)

R. Padilha França  
e-mail: [padilha@decom.fee.unicamp.br](mailto:padilha@decom.fee.unicamp.br)

**Keywords** Smart City model · Corruption · Illicit market · Indicators · Ethical · Social · Technical · Digital aspects

## 1 Introduction

Periodically, within a Republican State, mayors are democratically elected in order to start a new cycle for public management. They are chosen by a popular vote where it can be through voluntary or compulsory population participation. The elected administrator has a period of four years as mayor to administrate de city, where it can be renewed for a new period of time if approved again by popular vote. In theory, a public administrator is chosen through the proposal's comparative analysis that better meets the city's challenges and priorities. The proposals can be exemplified for improving the inhabitant's life quality, maximize the use of the city budget, maximize the service quality provided to the city minimizing expenses, leveraging investments and innovation, providing economic growth and social development for the municipality, as well as the political, professional and social candidate's background. Political alliances between parties are established during an electoral process, in order to strengthen candidates in the competition to assume the city hall; however, the elected public administrator must have a political maturity to continue successful programs of the previous administration, independent of the predecessor political party. Once elected, the public administrator has with responsibility, among the growth and development strategies of the municipality, the provision, and maintenance of public services that guarantee the dynamics of a city's urban systems, such as water, electricity, collection and adequate treatment urban transport, sanitation, gas, telecommunications [1].

Basically, there are three municipality processual steps to contract the provision and maintenance of public services: contracting, supervision, and payment. The contracting is carried out mostly through bidding processes, where companies that provide services or products, submit proposals that meet the city requirements. Once the service or product has been contracted by the city hall, the public technical staff is responsible to supervise the services or good provided, having as parameter the requirements set in the agreement, attesting the delivery veracity. Finally, once the service or goods have been delivered in compliance with the agreement requirements, the payment occurs as previously established between the city hall and the supplier [1–3].

## 2 The Public Corruption: The Typical Corruption Model Found in Cities

Even though there isn't a single model of public corruption, which may occur through an inadequate supply, over-fledged or non-existent goods or services, the first characteristic observed when studied the corruption in cities corresponded to the mapping

(by corrupt management) strategic functions in public operations that may be manipulated or fraudulent. Once identified, it is strategic to designate trusted person participants of a corruption network, in order to operationalize the irregularities, regardless of the corruption scheme to be established. Therefore, a second characteristic is identified: managers' appointment (commissioned) in municipalities' strategic positions without technical skill or experience to the function [3, 4].

The urban systems in a city (transport, water supply, energy, sanitation, garbage, etc.) are carried out through bidding processes established by the city hall. For this, two usually procedures are used: (1) the "invitation letter," for relatively low purchases (when compared to other expenses purchase of the city hall) where is not required a technical acquisition evaluation; (2) the "price evaluation" for purchases goods and services with expressive values that require a technical staff analyze. Though the "invitation letter" procedure, companies are invited by the city hall to submit proposals, instead of the "price evaluation" procedure, where companies specialized submit their proposals to attend the service [3–5].

The fraudulent method usually used by a corruption network (composed of public administrators, commissioners, and private companies) is forging the participation of competing for companies in a bidding process, by sending documentation of "non-existent (ghost) companies" or inactive companies. This action has the purpose of reinforcing the company proposal that already has a previously established agreement with the corrupt public administration. The second method most used and identified in the study corresponds to fictitious bidding processes assembled and conducted improperly by the public administration and public commissioners. A third method identified corresponds to bids under extremely specific technical conditions, making it difficult for other companies to submit a proposal, benefiting only the company(s) that already has a pre-established agreement with corrupt management. All methods aim to establish, within the formal and legal stages of procurement, the company that will benefit a corruption scheme [3–5].

Thus, the third characteristic identified the city corruption corresponding to the list of companies participating in a bidding process. All participants must be carefully verified and confirmed through documentary analysis, direct contact and companies visit the veracity of all participants. A technical commission must be formed by specialists, with the objective of identifying any irregularities that may generate suspicion. The company registration, the fee collection, and invoices issuance must also be carefully checked to ensure the proper companies' functionality, confirming it physically and legally existence [3, 5, 6].

Once established a corruption company to supply with services or goods the urban system by the corruption administration, the charge of them will be made through the payment of the invoice. The invoice payment (overprice or an irregular invoice) is divided between the members of the scheme, being paid through cash, in order do not establish a banking link between the supplier and the public administration that can be traced later through breach of bank secrecy.

Another feature mapped out in the city corruption scheme is regarding the formation of specialized gangs to defraud public biddings, set up vicious contests, cover illegalities, encouraging the development of illicit markets, and contribution actively

to the municipality impoverishment [3]. The municipality impoverishment affects directly investments to develop and improves the city's performance, affects the new job generation, resources to social, cultural and educational projects, and accumulates money for the city.

A corruption administration affects indirectly the population's perception of what is being done with all taxes and duties payments, reinforcing a distrust and insecurity environment of the public administration toward the inhabitants of the city. In a distrusting environment, which the population feels robbed by the public administration, becomes a viable alternative for them, search for markets with cheaper prices and paying taxes free. It is established with that, one of the other ways, for illicit markets operation [7].

### **3 Illicit Markets: Working Against the City Prosperity**

The illicit market is the existence, combined or isolated, of one or more categories of goods classified as forbidden by the government and being consumed individually or in society. The illicit markets are classified in five categories of human life, including social (trafficking of illegal drugs, persons and arms); commercial (stifling innovation and legitimate entrepreneurship); economic (distorting markets, diverting revenues and legitimate employment to illicit ends); environmental (trade in endangered and protected wildlife, timber, and toxic waste); and health (counterfeit pharmaceuticals, drug dependency, pollution) [8]. The sectors most affected by illegal markets are clothing, medicines, electron electronics, and auto parts.

Like any business, the illicit markets look for making profit and face the same market challenges to have a competitive sale cost (as a structured supply chain, capilarity logistics/ distribution, production scale, and supplier's diversity), but it not incurs the research and development cost, a safety workforce, compliance production, environmental aspects, and safety products regulations. Basically, an illicit market demand (through the consumers perspective) is driven by aspects related to the economic situation and consequently, budget constraints, product itself, price and quality perceived, individual consumer characteristics (attitude toward illicit markets), and finally by the institutional environment in which the consumer operates (risk of discovery and jurisdictions penalties, criminal laws and how efficiently and frequently this law are applied by the authorities to combat the issue). Through the supply perspective, illicit markets are driven by marketing opportunity, technological and logistics distribution challenges associated with an undertaking and the risk involved. The globalization economic is another aspect that potentially, foment, and viability this market (mainly with as counterfeit products around the world) through of easy access to resources, technology progress, and the rapid growth of e-commerce trade (supported by the rapid increase of different devices) [8].

Additional of that, the illicit markets touch directly the city when increase of disorder caused by irregular occupancy of the public space by drugs consumers, illegal street market causing (besides the illegal commerce) an unsafety and insecurity

place for citizens, public and private immobile devaluation, economic inhibition, facilitating the degradation of social environment in the city, affecting the innovation, the employment creating, an economic growth long term and explore incorrectly the environment and ecological sustainability [8].

Much of the concepts and technologies used by a Smart City can combat the corruption process formulation and the illicit markets, through a cultural and organizational cities changes [9].

The Smart City concept can organize and discipline the citizens routine through a city workflow process (interconnectivity between news and existing process), government transparency, a bottom-up and top-down culture between the population and administration, a efficient cultural and social education about the illegal and risk situation involving the population, rescue of the city to citizens (valorization of what is produced locally in the city itself), intensify the use of all kind of devices to control the routine of the place and the population (cameras, sensors, police application, etc.), and by the efficiency that the place will systemic and gradually present, etc. [10].

## 4 Smart City Concept and Technologies

The concept of Smart City is becoming more and more relevant for academics, policymakers, and governments, by the consistent changes generated in the urban territory related to the functionality and improvement of numerals systems existed in the city [11]. Some recent research has been proposing a Smart City model, suggesting understanding and quantify the different offers and demands existed in the Same City related with infrastructure, technologies, and social/cultural aspects, to provide specific solutions to transform the city without losing this systemic urban and unit vision [10].

The Smart City model promotes to work, plan, and organize the city through sub-centers (or subgroups), without losing their systemic and unit vision, identifying their existing and necessary infrastructure, investing to develop a digital network and mapping the social and cultural population aspects. This model reflects the idea that a Smart City—where people, technology, and process are connected—can only enjoy all efficiency of technology capability available, when developing aspects of your social and cultural intellectuality, as a tool that differences them of a simple city [12]. In this context, telecommunications systems with a low level of abstraction and low computational consumption are essential to connect people and systems and favor the implementation of Internet of things (IoT) to people's daily lives [13]. In addition, new methodologies related to the environment and health are also part of the concept of smart cities, because through innovative methodologies blood tests can be performed through computers and their results sent to doctors easily and quickly regardless of income and place where the patient is located [14–16]. Thus, the premise of this Smart City model is your citizens, as a key to connect, explore,

suggest, and increase the dynamic of urban territory, achieving the efficiency, efficacy, and synergy among process, systems and devices available.

The proposal of this concept has structured the analysis of the city no longer in a macroscale, where the territory is visualized in its totality, but in a microscale, where the local planning and the identity of the studied place are rescued, aiming at to the individual perception of the needs and challenges of each sub-center of the city [17]. Some essential characteristics are observed and planned on this microscale:

**Operational aspects:** Smart Cities, in contrast to centrally planned cities, are organized on a decentralized model (sub-centers or subgroups) but connected to each center composing a unique city [10]. In the meantime, it should seek to explore concepts in the territory that will work to increase the density and their multi-centricity—since the subcenters are generators of employment, infrastructure optimization, housing, education, health, security, etc., within the same city—providing the better use of existing empty spaces in regions provided with urban infrastructure and thus minimizing the need for new investments in infrastructure to meet the demand of the city. When well-worked the subgroups density, it also promotes a more efficient urban mobility system when it is planned to integrate the territory. This is possible by identifying and connecting the existing multi-centers within the territory, by exploiting with the better performance the use of collective public transport and by providing alternatives for mobility, which are accepted in the daily life of the population by transmitting security, reliability, and practicality. Examples are the cycle paths implemented to link the dynamics of the city (residential areas with commercial areas, universities, industrial, etc., and not just segregated bicycle paths in neighborhoods, squares, and parks) and the use of walking as an alternative modal, sharing of vehicles, etc. Such a change in behavior will naturally contribute to reducing the number of vehicles on the street, thereby reducing congestion extensions, and increasing the accessibility and use of alternative modes. Significant gains in air quality in cities by reducing the emission of gaseous pollutants, consequently improving air quality by reducing the level of greenhouse gas emissions per capita [18].

**Social aspects:** Each subgroup should be closely linked to the development of knowledge, research, innovation, culture, arts, economics, technology, of the place studied and have in these areas their raw material to differentiate them from others by stimulating the creation of ideas, building a culture of knowledge and intelligence in all segments of the sub-center and thus rescuing the strengthening of the city's competitive advantages as a larger group [19]. The intelligent city possesses in its DNA concepts and elements sustained by the creativity of individuals, companies, capital, institutions of knowledge, academia, governments, educated and productive population, etc. [20]. It is through the contributions promoted by the creativity that a city can maintain its identity, develop its characteristics, and stimulate its potential toward differentiation and competitiveness even in the face of globalized competition. This is only possible by encouraging creativity, providing access to new and varied knowledge, as well as respect for diversity and differences as they are sources for creativity and innovation. Ideas that are connected to new technologies in a constant

and growing act within the territory, improving the quality of life of its inhabitants and working to decrease budget constraints [21].

Digital aspects: Once the sub-centers have been identified, it is also intended to complement the organization of sites by promoting interconnection between existing systems (commerce, security, public administration, infrastructure use, health, work, education, environment, transportation, etc.) by making intensive use of digital technologies (applications, sensors, citizen services, etc.), thereby promoting efficiency in services provided, process improvement, agility, quality, within the territory, services, and citizen [11]. They promote to their inhabitants, through interconnectivity, a community digital space with the construction of networks of knowledge, and providing spaces where the exchange of information and experiences occurs. These are the ones that enable the participatory innovation process conducted by citizens, employees, and end-users [22]. A resume of all aspects of a Smart City model is described in Table 1.

**Table 1** Characteristics of a Smart City model

Aspects	Smart City characteristics
Infrastructure	<ul style="list-style-type: none"> <li>• Compact (can be by neighborhood and not by city), dense and multi-centralized)</li> <li>• Growth and internal improvement, not its expansion</li> <li>• Rational and work to make better use of available resources</li> <li>• Work better on issues related to waste</li> <li>• Reduced pollution rates due to better management of urban mobility</li> </ul>
Social	<ul style="list-style-type: none"> <li>• Community directly involved and active with city life</li> <li>• Intimately committed to the development of the knowledge and knowledge of its inhabitants</li> <li>• Valuing the culture of knowledge and intelligence, to strengthen the competitive advantages of the territory</li> <li>• Creativity is the DNA of the city</li> <li>• They can identify their identity, develop them, and stimulate their growth toward differentiation and competitiveness</li> <li>• Incentives to creation, providing access to new knowledge and diversity</li> <li>• Ideas that are connected to new technologies in a constant and growing act within the territory, improving the quality of life of its inhabitants</li> <li>• Communities in which it exercises the articulation, cooperation, tolerance, and multiculturalism around the objectives and common responsibility in the city</li> </ul>
Digital	<ul style="list-style-type: none"> <li>• Massive Internet access</li> <li>• Open data and transparency as a strategy for citizen engagement</li> <li>• The citizen involvement of all levels of social class</li> <li>• Collaborative digital platforms, increasing the likelihood of innovation</li> <li>• The citizens are oriented to provide ideas, through a participatory plan of innovation, independent learning, feedback</li> <li>• Information is provided in real-time to the citizen, giving him greater participation in decision making, and therefore more conscious, participatory and collaborative</li> </ul>

## 5 The Natural Inhibitor of Corruption and Illicit Markets Potentialized Through the Smart City Concept

The intangibles aspects have become the major economic asset of countries, whether they are developed, emerging, or underdevelopment. The intangibles aspects are everything that will create knowledge of its inhabitants, in which it values the culture of intelligence, to strengthen the competitive advantages of the territory, stimulates growth toward differentiation and competitiveness, encourages creation by providing access to the new, diversity. It will result in research, innovation, developing goods and services, which allow adapted throughout several sectors of an economy and society, being appointed as one factor to avoid the prosperity of corruption organization and illicit markets through the decrease possibility of manipulation and fraudulent operations and the decrease customer interest channel of illicit products. How much more a nation is intellectually developed, more your citizens will look for practices structured that reflect order, discipline, organization, and prosperity [23].

The nations that historically invested in intangible aspects are naturally nations that have overcome different adversities and are located as the most developed countries globally. The intellectual knowledge is one of three pillars of a Smart City model, where is directly related to the social and cultural aspects of citizens. According to the Smart City model, the intellectual knowledge is responsible for promoting the city creativity, developing characteristics and stimulate its potential toward differentiation and competitiveness even in the face of globalized competition, and minimizing the social discrepancies, being, therefore, an important and natural inhibitor for corruption process and illicit markets [21].

Another aspect observed with the use of a Smart City model is the rescue of the city to your citizens. A common characteristic observed—independent of localization, economic, or development level—is the citizens are more and more mistreating their cities, aggravated by an exponential increase of cars, people, pollution, noises, insecurity, unhealthy, unsustainable, among others; that result in a city without a quality life and citizens that do not care and want to be there. Barcelona City during the process of transformation that led it to become one of the most respected intelligent cities in the world, understood that it needed to rescue the history of the neighborhoods where its citizens lived. This was done by sectorizing the city into 12 subcenters. For each subgroup was identified its advantages and disadvantages of infrastructures, it was mapped the characteristics that rescued the identity of each of the sub-centralities mapped. Its culture, the DNA interconnects the citizens and the region. It was mapped the regions that had urban voids, taking advantage of these regions to be populated, using the available infrastructure. Each subcenter should be self-sustaining in employment, housing, schools, hospitals, culture, leisure, supermarkets, to reduce the daily displacement between the regions of the city. These actions rescued the interest of the citizens by the place where they live, in the city. Citizens started to have idle time, which of course was occupied by the diversity of cultural and social options that the subcenter provided. The consumer practices were



reduced, and the interest in the diversity of offers of leisure that the city offered was increased [8].

Finally, natural inhibition is related to digital aspects, directly related to the diversity and dynamism of technology used by a Smart City model. The interconnection between urban systems promote the efficiency of the urban services (information about goods and services), improving the businesses efficiency (helping locate sellers), when enlarge the market scope (facilitating convenient delivery), lower operate barriers and cost (allows goods to be purchased easily), intensifying competitions and reducing cost (facilitating price comparisons), process improvement, promoting a agility and quality of services and reducing traditional commerce channels [9]. In order to support all kinds of technology adopted by a city, it is mandatory which has workflows structured and process well done defined. Without it, any technology (for more efficient and promising it can be) will fail by the technology itself. Additionality of this, workflows structured, and process well done defined naturally has the power to inhibit the corruption network formulation.

Another positive aspect promoted by the Smart City model is related to the diversity of data collected and analyzed never did before. The blockchain technology is an example of it, being studied their use to mitigate government corruption process, supply chain management (combating the pirated), smart contracting and financial transactions, through the decentralized validation of the numerous transactions in process flow (blocks) [24]. With all the city being monitored by digital technologies (applications, sensors, citizen services, among others), the number of data collected and mainly the information provided by this data certainly will show new ways to solve old issues. According to ACDE, information is still an essential key for designing and implement effective policies and measures to combat illicit markets [25].

However, data will not fix the problems existing in a city by itself. It is necessary to have new models of administration, that supported by information never observed before and can signal for simple and efficient solutions.

## 6 An Ethic Governance Proposal

Today's administrations bring problem-solving models that need to be reviewed against the new possibilities offered by future Smart Cities. According to Wind et al. [26]: "When the world changes significantly, there is a risk of a model completely irrelevant to the new situation." In this way, the context offered by new management tools based on information and communication technologies (TIC) that incorporate ad hoc networks, powerful databases and efficient data monitoring results in the possibility of innovating in the investment of new forms of energy generation, in the dynamics of education, health, safety, etc. All of this leads to a change in the mental models that structure managerial decisions. However, it is worth noting the observation [27] of the risk that exists to a world that, depending so much on collecting

large amounts of information and desire for quick decisions, loses the context of its sources.

Therefore, it is important to do not rely exclusively on the power of the new tools offered by TICs, as regards the new models that need to be created. Just as the current bureaucracy was not enough to overcome the problems seen at the beginning of this work, the simple fact of giving more efficiency to technological resources ends up reproducing “controls” similar to those that generated the problems described. In this context, Smart Cities should not only emphasize technological solutions in the information field and its processing, which would lead to a technocracy. The risk is to give life to all kinds of data, which postman alert and classify [27] as garbage information, that no more responding to human concerns and it being little useful to give a coherent direction to the solution of worldly problems. In this context is proposed—as a methodological way to solve the problems pointed out, which can’t increase in these new environments of the Smart Cities—a new concept of Governance, as presented by Melo, apud Santos [28]: “The ‘modus operandi’ of government policies which includes, among others, issues related to political-institutional format of decision processes, an appropriate definition of public/private mix policies with a participation decentralized, and new mechanisms for financing policies programs with a global reach”. However, this “modus operandi” needs to discuss the ethical dimension from a different perspective, a little bit singular. This ethical, in a pragmatic and realistic way, must rescue the right and fair conduct to be applied to any organization or society, driving for what is the correct to do in the cities in order to transform them in intelligent and sustainable, but fundamentally human places.

The ethics inclusion, as an effective dimension in a Smart City governance, would elevate the city into the condition of true human abode. The Smart Cities could be the carry of principles and values that would guide citizens to establish a new civilization paradigm, which Boff refers to the future with the look of “caution.” And who would be responsible for “care” in a Smart Cities model? It is necessary to overcome the actual model where public administration has the responsibility to monopolizing the directives to regulate the citizen’s life [1].

The Brazilian Cities Statute Guideline, for example [29], must be followed by public administration to elaborate on the urban city policy. In this document, it is stressed that all actions must be focused on ensuring a fair city to all citizens, where the poor and rich can enjoy the benefits of urbanization. In order to follow this aspiration, Rezende explains [22] that cities depend on their public managers to municipal planning and city management, but also is not limited to them. Any kind of strategic, multiannual, fundamentally or master plan of the city must be attended by a committee of citizens, private and public administration. However how to ensure that all involved (citizens, public and private administration) commit, feel responsible and accountable, in the greater objective of achieving effective quality in the governance of CISH, and the necessary “care” with the population, which encompasses the many situations of vulnerability and risk that exist? It is in this space of accomplishment that the numerous problems described at the beginning of this work find space for existence, and only more efficiency in data collection and mining would not be

enough, it becomes essential to be explicit as the data can be used by those who possess it, its limits and possibilities.

Thus, in practice, Hans Jonas's warning [30] when referring to ethics should be rescued here, and that: "Ethics must exist because of men act, and ethics exist to order their actions and regulate their power to act. Its existence is all the more necessary; therefore, the greater the powers of action which it has to regulate." In this context, it is then necessary to clarify the field of action in which ethics will become one of the forces that will concretize a Smart City that will guide its decisions through ethics.

Firstly, it is necessary to define the ethical guidelines that will guide the *modus operandi* according to the values and principles that point to the good of all. Within this framework, you can consider t [31] the approach that points out some general ethical principles that result in ethical attitudes committed to society and thus consistent with the goals desired here. They would be personalized principle, in which the valuation of the human person is practiced; principle of guidance for the common good, as a stimulus for each one to go beyond private interests, and to search for what is good for society as a whole; principle of order of responsibility, in order to prioritize actions that, depending on the responsibility of each one, be guided by what is most achievable and within its reach; principle of managers' prudence, where decision-making does not distance itself from a safe analysis in which ethical, conviction (deontology, treaty of duties), and responsibility (teleology, study of human ends) are elements of reflection given the complexity of the real.

Once the guiding principles have been defined, it is necessary to create conditions so that they can manifest themselves in the decision process, in the face of practical problems, when people are confronted with the need to guide their behavior through norms that are more appropriate or worthy of being fulfilled. From these assumptions, it is important to continuously develop ethical awareness through educational actions. In what concerns the governance of a Smart City, it is suggested at this point that the guidance should consider the categorical imperative of Kant, which according to Vázquez [32] is the supreme expression of the commandment of reason and is thus prescribed: "Age so that you may want the motive that led you to act to be a universal law."

Finally, acting in a way that establishes a management model guided by ethics include practical actions such as the creation of communication centers, citizenship, and ethics, whose dynamics can establish a dialogue between managers, businessman, and citizens, creating ways to encourage citizen participation. And, in particular, this citizen participation that is not limited to the Civil Councils linked to political positions, and, with this, it prevents that it happens to be effectively away from the population in a general way [1].

The presence of ombudsmen capable of establishing fair paths to blind spots in administrative processes as a whole; external ethical audits, which can go beyond the techno-administrative visions, but can enlarge the look to what differs from the established principles; foster a culture of ethical and transparent management. A transparent government where all citizens can have access not only to legislation in each area of government, but also to their flows and processes, freeing this citizen

from being held hostage by verbal information from servants or from written and slow protocols and inefficient [1–6].

## 7 Conclusions

Regardless of all challenges involved to combat corruption schemes and illicit markets around the world, it is notorious the need to reinforcing designing policies to address those issues. Even in the face of this challenging scenario, the Smart City is opening one more channel to mitigate the corruption and illicit markets through citizen involvement, considering to be the key to drive this chain.

Those positives opportunities that can be exercised, like the economy is stimulated by the drop unemployment rate (when each subgroup exercise to be self-sufficient with all kind or service and product to supply your subgroup), by the use of data (big data) and new technologies to mitigate the corruption scheme, by the government transparency and the population involvement to decide and supervision the main investments and decision to the city; by decrease, the number of accidents in transit when reduce the number of trips daily, reduce the congestions and increasing the accessibility and use of alternative modes, and consequently, the air quality is significantly improved; by the new city mobility will win bike and pedestrian adepts, that naturality improve the city space; by the decreasing number of accidents, it means that reduce the cost with hospital care and disability insurance, reducing the economy's expenses with these aspects; by the society is more interactive with the governments, and the governments with the society (bottom up/ top down), promoting an exchange of feedbacks about the efficiency of the services provided, process improvement, agility, quality, within the territory.

Finally, the citizens understanding that it is part of the city, as responsible to keep the system operating and the order established and will work to keep this perception in each subgroup that they are inserted.

**Acknowledgements** The authors would like to thank the Coordination of Superior Level Staff Improvement (CAPES), and National Council for Scientific and Technological Development (CNPq).

## References

1. Lopes, N. V. M.: Smart Governance for Cities: Perspectives and Experiences. Springer Nature (2020)
2. Mehmood, R., Katib, S. S. I., Chlamtac, I.: Smart Infrastructure and Applications. Springer International Publishing (2020)
3. Chizzotti, A., Chizzotti, A., Trevisan, A., Verillo, J., Ianhez, J.: The fight against corruption in prefectures in Brazil. Ateliê Editorial, Sao Paulo (2003)

4. Shan, M., Le, Y., Chan, A. P., Hu, Y.: Principal causes of corruption in the public construction sector. In: *Corruption in the Public Construction Sector*, pp. 49–77. Springer, Singapore (2020)
5. Shan, M., Le, Y., Chan, A. P., Hu, Y.: Corruption in construction: a global review. In: *Corruption in the Public Construction Sector*, pp. 9–22. Springer, Singapore (2020)
6. Ryder, N., Pasculli, L.: *Corruption, Integrity and the Law: Global Regulatory Challenges* (2020)
7. Atkinson, C. L.: *Theme-Based Book Review: Public-Sector Corruption* (2019)
8. FIESP.: *Transnational illicit markets in São Paulo: the transnational criminal economy/FIESP. FIESP, São Paulo* (2017)
9. Hanna, R.: Technology beats corruption. *Science* **355**(6322), 244–245 (2017)
10. Jordão, K. C. P.: *Intelligent Cities: A Proposal for the Transformation of Brazilian Cities* (2016)
11. Panhan, A. M., Mendes, L. D. S., Breda, G. D.: *Building Smart Cities*, vol. 1, 1st edn, p. 149. Appris, Curitiba (2016)
12. Song, H., Srinivasan, R., Sookoor, T., Jeschke, S.: *Smart Cities: Foundations, Principles, and Applications*. Wiley (2017)
13. Padilha, R., Iano, Y., Monteiro, A. C. B., Arthur, R., Estrela, V. V.: Betterment proposal to multipath fading channels potential to MIMO systems. In: *Brazilian Technology Symposium*, pp. 115–130. Springer, Cham (2018)
14. Monteiro, A. C. B., Iano, Y., França, R. P., Arthur, R., Estrela, V. V.: A comparative study between methodologies based on the hough transform and watershed transform on the blood cell count. In: *Brazilian Technology Symposium*, pp. 65–78. Springer, Cham (2018)
15. Monteiro, A. C. B., Iano, Y., França, R. P., Arthur, R.: Methodology of high accuracy, sensitivity and specificity in the counts of erythrocytes and leukocytes in blood smear images. In: *Brazilian Technology Symposium*, pp. 79–90. Springer, Cham (2018)
16. França, R. P., Iano, Y., Monteiro, A. C. B., Arthur, R.: Potential proposal to improve data transmission in healthcare systems. In: *Deep Learning Techniques for Biomedical and Health Informatics*, pp. 267–283. Academic Press (2020)
17. Kneib, É.: *Project and City: Centralities and Urban Mobility*, vol. 2, p. 324 (2014)
18. Crainic, T. G., Gendreau, M., Potvin, J. Y.: Intelligent freight-transportation systems: assessment and the contribution of operations research. *Transport. Res. Montréal* **Part C**, 541–557 (2008)
19. Komninos, N.: *The Age of Intelligent Cities: Smart Environments and Innovations-for-all Strategies*, vol. 1, 1st edn, p. 298. Routledge, London (2014)
20. Fachinelli, A. C., D’arisbo, A. E. D. M.: The importance of social innovation and the creative economy as an indicator for sustainable development. *Int. J. Knowl. Eng.* **3**(5), 276–293 (2014)
21. Landry, C.: *The Creative City, A Toolkit for Urban Innovators*, vol. 1, 2nd edn, p. 352. Comedia, London (2012)
22. Rezende, D. A.: *Planning of Municipal Information and Strategies for the Digital City: Guide for Projects in Prefectures and Public Organizations*. Atlas, São Paulo (2012)
23. Fernandes, R., Gama, R. A.: *Territorial Creativity in Portugal: From the Indicators to the Creative Territories*, pp. 1–12. FLUC Geografia, Coimbra (2012)
24. Puii, T.: How Bitcoin’s Blockchain Could Mark the End to Corruption. *ZME Science* (2015)
25. OECD Workshop.: *Assessing the Harms Posed by Illicit Trade and the Illegal Economy for Global Supply Chain Integrity, Economic Growth and Market Security* (March, 2018). <https://www.oecd.org/governance/risk/Illicit%20Trade%20Workshop%2026%20October%202012-rev.pdf>
26. Wind, Y. J., Crook, C., Gunther, R.: *The power of Mental Models*. Bookmark (2009)
27. Postman, N.: *Technology: The Surrender of Culture to Technology* (1994)
28. Santos, M. H. C.: *Governance, and Democracy: Creation of Governance Capacity and Executive-Legislative Relations in Post-Constitutional Brazil* (April, 2018). <http://egov.ufsc.br/portal/conteudo/governabilidade-governan%C3%A7a-e-democracia-cria%C3%A7%C3%A3o-de-capacidade-governativa-e-rela%C3%A7%C3%B5es-execut>
29. Federal Senate: *Statute of the City*. (April, 2018). <https://www2.senado.leg.br/bdsf/bitstream/handle/id/70317/000070317.pdf?sequence=6>

30. Jonas, H.: *The Principle of Responsibility: a Test of an Ethics for Technological Civilization* (2006)
31. Pineda, E. S., Cárdenas, J. A.: *Ética en las Organizaciones*. McGraw-Hill (2007)
32. Vázquez, A. S.: *Ethic* (2006)

# A Discussion of the Challenges Small Towns Face in Reaching the Promising Scenario of Electronic Government Intelligent Cities



Valéria Sueli Reis , Yuzo Iano , Gabriel Gomes de Oliveira ,  
Telmo C. Lustosa , Mauro A. S. Miranda , Odair dos Santos Mesquita ,  
Ana Carolina Borges Monteiro , and Reinaldo Padilha França 

**Abstract** This work aims to total the reality of cities through some Brazilian electronic data e-Gov, and other research conducted and counteracted with the latest assumptions proposed by smart cities governance models (CI) and intelligent governance (IG) increasingly imposed by the information society and network, realizing the new social engineering of collaboratively and ICT. Data were collected through reports of their research and also the theoretical literature review concerning the issue. This paper presents a discussion in order to clarify how the small municipalities still need to mature to achieve a reality of smart city governance.

---

V. S. Reis · Y. Iano · G. Gomes de Oliveira (✉) · T. C. Lustosa · M. A. S. Miranda ·  
O. dos Santos Mesquita · A. C. Borges Monteiro · R. Padilha França  
School of Electrical and Computer Engineering (FEEC), University of Campinas—UNICAMP,  
Av. Albert Einstein-400, Barão Geraldo, Campinas, SP, Brazil  
e-mail: [oliveiragomesgabriel@ieee.org](mailto:oliveiragomesgabriel@ieee.org)

V. S. Reis  
e-mail: [Valeriareeis@gmail.com](mailto:Valeriareeis@gmail.com)

Y. Iano  
e-mail: [yuzo@decom.fee.unicamp.br](mailto:yuzo@decom.fee.unicamp.br)

T. C. Lustosa  
e-mail: [telmoclustosa@gmail.com](mailto:telmoclustosa@gmail.com)

M. A. S. Miranda  
e-mail: [mauro\\_miranda\\_@hotmail.com](mailto:mauro_miranda_@hotmail.com)

O. dos Santos Mesquita  
e-mail: [odair.s.mesquita@gmail.com](mailto:odair.s.mesquita@gmail.com)

A. C. Borges Monteiro  
e-mail: [monteiro@decom.fee.unicamp.br](mailto:monteiro@decom.fee.unicamp.br)

R. Padilha França  
e-mail: [padilha@decom.fee.unicamp.br](mailto:padilha@decom.fee.unicamp.br)

**Keywords** Innovation in public service · Service design · E-governance · E-gov · Smart city

## 1 Introduction

Forms of public–private cooperation and its strengthening are perhaps one of the best advantages arising and improving the success and knowledge about smart city models (CI). Therefore, there is no governance without innovation, and innovation emphasizes collaborative elements, partnership, integration, new arrangements for solutions to the old problems of municipal governance.

The evaluation of public policies is prevalent factor for evolution to occur in the efficiency of government, and as a result of advances in e-government, we used in this article some references in the latest research carried out as Tic e-Gov operated by CGI.br, ENAP service search data public, and IEGM of São Paulo Court of Auditors, on the municipal, state and federal government initiatives, and we will explore some aspects revealed, as well as other researchers at the national level dealing with the municipal electronic governance.

In the early 2000s, the governance of Brazilian cities was still under strong influence of the precepts of NPM (theory of New Public Management) that brought to public administration its load control and efficiency, inspired by the private management, where the electronic government had their space and growth in the modernization of information systems and general computerization of departments and municipal departments. Innovation was not feared or reflection in this period was disenfranchised almost or totally, the values that focused in this phase are the quality as far as possible, and often questionable, the economic viability that much focus still on the bidding process, and immediatism efficiency.

But cities still in need of solutions to their problems of governance, we can score the areas of finance, human and regulatory resources, secondly, but no less problematic, the negative impact on key areas of provision of services to the population: health, basic education, infrastructure, social welfare, urban mobility.

In the way of governance/e-government to think of smart city, opened the scope of possibilities that are still strongly supported by the use of Information and Communication Technology (ICT), but with intelligence element that requires smart government, smart servers, active and socially intelligent citizens, and intelligent technological solutions, we will discuss intelligent governance (GI) who resort, for example, autonomous systems, sensing and Internet of Things (IoT), knowledge management and innovation, intelligent platforms, big data, analytics, service design, health services with quality and low cost, telecommunication systems with low memory consumption. All this must be done for that the objectives and interests should be aligned between the people and resources that make up the city [1–6]. This definition of [7], among several, and several authors who defined smart cities, contemplates broadly: Smart cities are those that well realize the vision of the future in various aspects—economy, people, governance, mobility, environment, and quality of life



and are built on the intelligent combination of decisive action, independent, and aware of the actors who work in them and generate public value.

In the municipality of context, we would enter in your smartest stage when the management follows an integrated, real-time manner, exposure data, and relevant information and value-added services to citizens and businesses. It is based on shared intelligence by all actors of the city and the city's platform a facilitator of collaborative solutions [8].

## 2 Methodology

This survey carried out a bibliographic review focusing on data that were collected through reports of academic research, governmental data, and also the theoretical literature review concerning the issue.

### 2.1 *Policy Brief Analysis of the Municipalities to the Challenges for CI and GI*

We go forward with the legislation in some aspects such as LAI<sup>1</sup> [9] and Law 139/2009<sup>2</sup> [10, 11]. That enabled access from several municipalities toward transparency and look at its governance, providing information, but this legal/political framework must evolve more, and we justify with data later.

The base decisions should be distributed, shared, transparent, and democratic, within the representative democracy we live, expanding participatory democracy with the presence of citizen, government relationship expansion with the local community, with business, with institutions that contribute municipal management.

More consultations with society, more ears. It is not for the smart city closed management, individual decisions, solutions that do not add public value or without social interest or generate waste, by a requirement of the information society itself, although it is obviously the exception to the willingness of data, open data, and information security, which is a big challenge, among others, to municipal IT governance, and obligation of social welfare and the city's quality of life that must be shared and liable for all and the intelligent management cannot do without this support, even as local governments increasingly suffer from the scarcity of resources, and increase in expenditure.

Brazil's cities suffer from the limitation of income, many survive only with two recipes, namely the property tax and the annual transfer of National Fund of Municipalities (FNM), being held hostage for most of the period of funding parliamentarians and transfers from the federal government having difficulties to have qualified

---

<sup>1</sup>Law No. 12,527 of November 18, 2011, known as the Law of Access to Public Information, (LAI).

<sup>2</sup>Complementary Law No. 131 commonly called Transparency Law (2000), as amended by Law.

human resources, qualifying servers and a tract of continuous training, and that directly suffers the impact of change management (managers) which compromises the continuity of the plans and projects.

Having a recurring difficulty of working with deadlines and schedules of projects and deliveries, showing the absence of a culture of deadlines. Smart cities plans represent a set of actions that stir the political and economic structures established in the municipality and strongly questioned its internal organization.

According to [8], the need to revisit the federal pact in Brazil is illustrated, in terms that balance the investment needs and funding and access to financial resources. At the same time propose new forms of organization for more horizontal municipal administrations, more integrated, more open to the participation of society, and new work processes. In this scenario, the ICTs should play an important role in making these changes [2, 8].

## ***2.2 Smart City and Implies a New Insight into the Governance of the City***

So, it is necessary to think about the theme of governance of cities with integrator based, sustainable and efficient, and also in tune with the needs of communities and citizens, that meets the improvement of the value of services and quality of urban life, where it is necessary to present a brief historical tour, especially with regard to technology applied in municipal management, being relevant to deal with the impact of e-government on small municipalities.

With the democratization process in Brazil from the Citizen Constitution of 1988 [12], the Brazilian public administration is moving forward with parallel legislation to the maturing of the democratic principles of management and incorporating the principles of private management (NPM) in Brazil clearly demonstrated from the 90s [12–16]. More detail about the evolution of public administration models, the phase that is characterized today in management is the bureaucratic model Weberian that is characterized by strong bureaucracy and government inflexibility; it is a regimented government marked by formality, impartiality, and professionalism; this phase it is important to stress that we inherited over control and attachment information. The next phase recorded in theory comes the era of managerialism.<sup>3</sup> Because there, in 2000, already we have the LRF Fiscal Responsibility Law [16].<sup>4</sup> However, there is criticism of this influence, it does not include a vision of participatory citizen able to citizenship, but as a user/client, and in this respect there is the theory of NPS—New Public Service that favors all public commitment to the fact that

---

<sup>3</sup>Related to transparency, accountability of rulers, as well as the accountability of rulers for their actions.

<sup>4</sup>LRF Fiscal Responsibility Law (LRF)—(Complementary Law No. 101 of 04 May 2000.

investment e-government, where the government has to be open to citizens to exercise participation. In these last two phases, the concepts of accountability, accountability (accountability), transparency, citizen engagement, democratic governance, and network governance or digital, now have strength, the 2000s to the present.

As well as some federal laws that encouraged good practice in municipalities (LAI, LRF, Law transparency, Cities Statute, this one suggests various instruments of governance, underused and unknown to many managers/cities), TCU's initiatives and other ministries, and finally on the efforts and growing more isolated initiatives, the need a national plan for smart cities, would be important.

Despite some initiatives by the federal government, such as Dec. 9319, the Brazilian Strategy for Digital Transformation, E-Digital, should also reflect the medium term in the cities in order to make investments and technological innovation and development in cities.

Moving forward in our analysis, in the first phase of e-government in the municipalities, there is a focus on improving internal processes and subsequent investments for relations with citizens, according to ENAP [17] are legal frameworks reflecting in governance actions e-government and municipalities.

### ***2.3 The Facts to the Data: Some Aspects of Electronic Data Governance in Small Towns***

To the specifics of municipalities with up to 100,000 inhabitants, covering 97% of the cities contingent in Brazil, we noted the lack of research studies and more compliant models to this city's profile, so relevant if it does, this article explicitly within the logic evaluation of public policies, recent survey data, such as Tic gov 2017 that may show aspects that demonstrate the use of ICT and to reflect in greater transparency, citizen participation, open data, sustainability, and security.

The first information is that only 23% of cities between cities up to 100 thousand inhabitants have smart cities plans. According to the results of research, Tic gov only 18% of all Brazilian municipalities had a project or smart city project. The municipality must tow your regular planning mechanism as a master plan, multi-year plan (PPA), and make adjustments in the legislation with a view to regulation that allows GI CI and actions.

The second base and as a gateway that is 92% of these municipalities have a website; Only 52% of these municipalities have their own IT industry, demonstrating the high degree of outsourcing of IT services, and only one in four municipalities with up to 10,000 inhabitants also has a department focused on ICT [18, 19].

About infrastructure data networks, there has been increased use of cable and fiber optic connections to 87% of these connections in the range of municipalities with up to 100,000 inhabitants and 77% those with up to 10,000 inhabitants. Regarding what is available information and services on the portals and municipal sites, according to Table 1 (derived from the websites Tic and Gov 2017).

**Table 1** Services on the websites of municipalities with up to 100,000 inhabitants

City halls, by type of service available on the website, location, and size (2017)	More than 10 thousand to 1000 thousand inhabitants (%)
Download documents or forms	84
Fill or send forms on the website	58
Electronic invoicing issue (e-Invoicing)	61
Consult ongoing administrative or judicial processes	47
Issuing documents such as licenses, certificates, permissions, and others	44
Register or enroll, for example, in competitions, courses in schools	33
Schedule appointments, consultations, services, among others	21
Make payments such as fees and taxes	25

There was growth in the provision of some services in the municipal sites, however, they are not those configured as transactional, payment services, the opening of new enterprises, fines payment, or requisition of personal documents. Other transactional services such as possibilities for payments of fees, taxes, and registration or enrollment in competitions, courses, and schools were less frequent on the websites of municipalities, except the capitals with the highest proportion of the supply of these resources.

The more common in municipal websites, for example, is the possibility of downloading documents or forms. Of the nine services indicated in the survey only three were offered for more than half of the municipalities that have a site, they are: download documents or forms with 84%; fill and send a form with 58%, and issue electronic invoices with 61% incidence. In this scenario, there is the difficulty of municipalities to provide online services and potentiating the digitization of public services.

For this information, have posted positive indicators, most public accounts or rendering of accounts with 98%, purchasing, procurement, or electronic procurement to 93%. Some content, however, as documents with plans and goals and results, and even public service catalog are less publicized, which can be configured as an obstacle for society to access information and track the progress of public policies and actions of the public sector organizations.

The catalog services, quoted at least 59% should improve this ratio with that service user code provides that demand more imperative charter services in its Art. 7, starting next year. This instrument is important for citizens to know what to look for and have available the services provided by the city.

About half of the municipalities (49%) claimed to have done electronic auction and this most common practice in the capital (88%) and in cities with over 500,000 inhabitants (90%). Therefore, the potential benefits of electronic trading, as the expansion of

competition and increased transparency and social control, are not being incorporated into part of Brazilian municipalities.

Another important feature, 47% of the municipalities in this size have an online ombudsman. The ombudsman is one of empowering instruments of citizen participation, described in the main initiatives of the Federal Government as the Access to Information Act, 2011, and most exalted in the recent public service user code.

The ombudsman is an instrument important for citizens can demand their rights with regard to public services, and the expansion of institutional channels for participation via the Internet is another important challenge of smart governance. One of the dimensions associated with digital government policies is a government to adopt measures that consider the demands of society in times of definition and evaluation of public policies [20].

Addressing solely on the municipalities of SP, it exposed the initiative of the court, in the state of São Paulo is a ruler marking out the municipalities in its governance [21, 22] and measures the knowledge and use of Information Technology resources in favor of society.

This index collects information about computer usage policy, information security, staff training, and transparency. The average rating of municipalities was in 2017 with the average +C on a scale of A, B + B, C+, and C.

Classification:

- A Highly effective
- B Effective
- B+ Very effective
- C+ In adaptation phase
- C Low level of adjustment.

Where IEG-C + M is greater than or equal to 50% and less than 60% of the maximum score. St. Paul of the municipalities is still undergoing adjustments to its electronic services and e-governance [23–29]. The Municipal Index of Technology Governance i-Gov Information IT/TCESP makes up the Effectiveness Index of Municipal Management—IEGM IEGM/TCESP [30, 31], as shown in Fig. 1.

The Munich research—Profile of municipalities conducted by IBGE and published with 2017 results [31–36], we highlight results that address sustainability and security. These illustrate how natural disasters have affected the Brazilian cities such as over 48% of the municipalities have been affected by drought, (2706 municipalities). 1726 were affected by flooding; 1515 by floods; 1093 by accelerated erosion and 833 by landslides. And yet, 59% of the municipalities do not have any kind of natural disaster prevention tool and only 14.7% of Brazilian municipalities, 821 municipalities have some contingency plan or protection. It makes us reflect on the potential of emerging technologies and advances in tools for prevention and assistance to these problems. Obviously, there is an important context to be faced with a smart and challenging vision, which is not only social inequality, but also regional disparities, political and economic that befall our country.

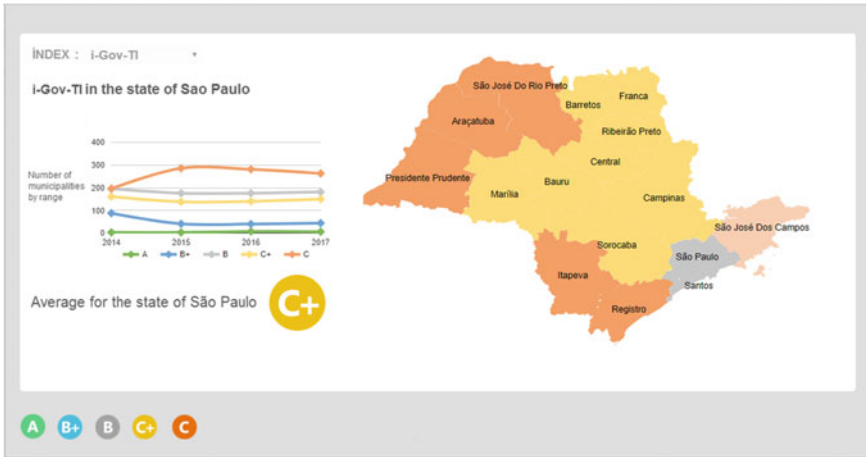


Fig. 1 Municipal index of governance of information technology I-Gov IT/TCESP [27]

### 3 Results and Discussion

Despite the different levels of appropriation of intelligent governance between municipalities, these are in the intensive process of computerization/digitalization and all feature some website. Most acts of transparency are performed so that it meets the legal instruments (laws), and there are few services geared to citizens that they can expand their arch action or intervention in public administration, with the majority of services refer to the collection of taxes (Building urban land tax, electronic invoice, tax on services).

It also points out the importance of governance models that includes the subjective nature of the project actions as leadership and culture change within the municipal government. With the same focus on service, design can be applied to the empowerment of this governance and alignment of goals together stakeholders, citizens, and generate public value. The initial plan, the evaluation, and correction of routes, deployment of smart governance is not an end in itself, be a major challenge, the discontinuities of the municipal administrations.

However, e-government is an eminent contemporary need to municipalities with their local conditions, economic and social needs in the face of opportunities and advancement in technology. The theoretical references, models and empirical experiences and new Tic's, denote that there are great possibilities for the deployment of smart e-government systems or maturation of existing initiatives in municipalities, citizens, and generate public value.

The initial plan, the evaluation, and correction of routes, deployment of smart governance is not an end in itself, be a major challenge, the discontinuities of the municipal administrations. However, e-government is an eminent contemporary need to municipalities with their local conditions, economic and social needs in the face of opportunities and advancement in technology.

The theoretical references, models and empirical experiences and new Tic's, denote that there are great possibilities for the deployment of smart e-government systems or maturation of existing initiatives in municipalities, citizens, and generate public value. The initial plan, the evaluation, and correction of routes, deployment of smart governance is not an end in itself, be a major challenge, the discontinuities of the municipal administrations.

However, e-government is an eminent contemporary need to municipalities with their local conditions, economic and social needs in the face of opportunities and advancement in technology. The theoretical references, models and empirical experiences and new Tic's, denote that there are great possibilities for the deployment of smart e-government systems or maturation of existing initiatives in municipalities.

With discontinuities of the municipal administrations. However, e-government is an eminent contemporary need to municipalities with their local conditions, economic and social needs in the face of opportunities and advancement in technology. The theoretical references, models and empirical experiences and new Tic's, denote that there are great possibilities for the deployment of smart e-government systems or maturation of existing initiatives in municipalities—the discontinuities of the municipal administrations.

However, e-government is an eminent contemporary need to municipalities with their local conditions, economic and social needs in the face of opportunities and advancement in technology. The theoretical references, models and empirical experiences and new Tic's, denote that there are great possibilities for the deployment of smart e-government systems or maturation of existing initiatives in municipalities.

## 4 Conclusions

Smart cities are urban spaces capable of promoting economic development and increasing people's quality of life. Given this, it is possible to see that smart municipalities have a lot to offer to society, since the use of technologies capable of making cities more intelligent directly influence the way society lives and behaves in urban environments, considering the applications and other government digital platforms that make urban management more efficient and still carrying out planned development projects, with the aim of making cities increasingly humanized.

It is important to highlight that the concept of smart cities cannot be an end in itself; it must allow society to develop in a more educated way, rescuing local culture and generating jobs and growth opportunities in the most varied sectors of life.

Smart cities are based on the union of public, private, and civil society efforts to create a planned infrastructure, providing for the use of technology and the effective participation of the community in decision making, based on the union of efforts of the public, private, and civil society sectors. Smart cities use digital technologies to optimize resources, reduce costs, connect people and, mainly, improve the quality of public and private services, always focusing on users.

Thus, it is possible to transform large cities into smart urban centers. Just prioritize people and the quality of living in the spaces. Since the need for investment in technologies that allow the development of projects, with a focus on bringing communities and the environment closer together, connecting people and opportunities, strengthening the economy, and promoting business, are crucial factors that overcome the challenges faced for cities that are not yet considered smart.

## References

1. Caragliu, A., Del Bo, C., Nijkamp, P.: Smart cities in Europe. *J. Urban Technol.* **18**(2), 65–82 (2011)
2. França, R. P., Iano, Y., Monteiro, A. C. B., Arthur, R.: Improvement of the transmission of information for ICT techniques through CBEDE methodology. In: *Utilizing Educational Data Mining Techniques for Improved Learning: Emerging Research and Opportunities* (pp. 13–34). IGI Global (2020)
3. França, R. P., Iano, Y., Monteiro, A. C. B., Arthur, R.: Intelligent applications of WSN in the World: a technological and literary background. In: *Handbook of Wireless Sensor Networks: Issues and Challenges in Current Scenario's* (pp. 13–34). Springer (2020)
4. Padilha, R., Iano, Y., Monteiro, A. C. B., Arthur, R., Estrela, V. V.: Betterment proposal to multipath fading channels potential to MIMO systems. In: *Brazilian Technology Symposium* (pp. 115–130). Springer, Cham (2018)
5. Monteiro, A. C. B., Iano, Y., França, R. P., Arthur, R., Estrela, V. V.: A comparative study between methodologies based on the hough transform and watershed transform on the blood cell count. In: *Brazilian Technology Symposium* (pp. 65–78). Springer, Cham (2018)
6. Monteiro, A. C. B., Iano, Y., França, R. P., Arthur, R.: Methodology of high accuracy, sensitivity and specificity in the counts of erythrocytes and leukocytes in blood smear images. In: *Brazilian Technology Symposium* (pp. 79–90). Springer, Cham (2018)
7. Giffinger, R., Gudrun, H.: Smarter cities ranking: an effective instrument for the positioning of cities? *ACE: architecture. City Environ.* **12**, 7–25 (2010)
8. Cunha, M. A., Przybilovicz, E., Macaya, J. F. M., Burgos, F.: Smart cities [electronic resource]: digital transformation of city. Program Public Administration and Citizenship-PGPC, St. Paul, p. 161. ISBN: 978-85-87426-29-1 (2016)
9. Brazil: Law on Access to Public Information. Law No. 12,527, of 18 of November 2011. Presidency. Civil House. Subchefia for Legal Affairs. Brasília (2011)
10. Brazil: Decree No. 6932 of 11 August 2009. Brasília: Official Gazette [of] the Federative Republic of Brazil, 2009 Brasil. Law No. Law 11.079/04 of 30 December 2004. Brasília: Official Gazette of [the] Federal Republic of Brazil (2004)
11. Brazil: Transparency law. Complementary Law No. 131 of 27 May 2009. President of the Republic. Civil House. Subchefia for Legal Affairs. Brasília (2009)
12. Brazil: the Presidency. Constitution of the Federative Republic of Brazil 1988 to October 5 (1988)
13. Denhardt, R. B.: *Theories of Public Administration*, 6th edn, p. 367. Cengage Learning, São Paulo (2012). ISBN 978-85-221-1081-0
14. Perry, J.L.: Democracy, and the new public service. *Am. Rev. Public Adm.* **37**(1), 3–16 (2007). <https://doi.org/10.1177/0275074006296091>
15. Tsukumo, A. N., Pepper, M. F., Teracine, E.: Information technology providing new directions for Public Administration. III Seminar, Democracy, Law and Public Management Theme III—New Directions for Public Management. Brasília (24–25 November, 2011)
16. Brazil: Federal Law No. 13 460 of 26 June 2017. Provides for participation, protect and defend the rights of the user of public services of the public administration (2017). Available in: [http://www.planalto.gov.br/ccivil\\_03/\\_ato2015-2018/2017/lei/113460.htm](http://www.planalto.gov.br/ccivil_03/_ato2015-2018/2017/lei/113460.htm)



17. Brazil: Fiscal Responsibility Law. Complementary Law No. 101 of 04 May 2000. President of the Republic. Civil House. Subchefia for Legal Affairs. Brasília (2000)
18. ENAP: Research on utility services from the federal government. Brasília: Enap, pp. 10–11, p. 75. YI. (Enap notebooks, 55) (2018). Accessed September 10, 2019. <http://www.enap.gov.br/>
19. Studies Center of the Technologies of Information and Communication (Cetic.br). ICT Government Electronic (2017). Available at: <https://cetic.br/tics/governo/2017/prefeituras/E2/>
20. Organization for Economic Cooperation and Development—OECD. Review of the digital government of Brazil: Towards the transformation type of the public sector (2018)
21. Bolivar, M. P. R., Meijer, A. J.: Smart governance: using a literature review and empirical analysis to build a model research. *Social Science Computer Review* 0894439315611088, first published on (29 October, 2015). <http://doi.org/10.1177/0894439315611088>
22. Castells, M.: *The network society. The information age: economy, society, and culture*, vol. 1. Paz e Terra, São Paulo (1999)
23. Dunleavy, P., Margetts, H.: *Design Principles for Digital Essentially Governance* (2015)
24. Margetts, H., Dunleavy, P.: The second wave of digital-era governance: a quasi-government paradigm is on the Web. *Phil. Trans. R. Soc. A* **371**(1987), 20120382 (2013)
25. Meijer, A., Bolívar, M.P.R.: Governing the smart city: a review of the literature on smart urban governance. *Int. Rev. Admin. Sci.* **82**(2), 392–408 (2016)
26. Meijer, A. J., Gil-Garcia, J. R., Bolivar, M. P. R.: Smart city research contextual conditions, governance models, and public value assessment. *Soc. Sci. Comput. Rev.* 0894439315618890 (2015)
27. Savoldelli, et al.: Understanding the e-government paradox: learning from literature and practice on barriers to adoption. *Gov. Inf. Q.* **31**, 63–71 (2014)
28. Meijer, A., Bekkers, V.: The meta theory of e-government: creating some order in the fragmented
29. Letaifa, S.B.: How to strategize smart cities: Revealing the SMART model Elsevier. *J. Bus. Res.* **68**, 1414–1419 (2015)
30. [www.governodigital.gov.br/documentos-e-arquivos/digital-gov-review-brazil-portu-gues.pdf/view](http://www.governodigital.gov.br/documentos-e-arquivos/digital-gov-review-brazil-portu-gues.pdf/view)
31. TCESP, IEGM/TCESP: Effectiveness Index of Municipal Management (2017). <https://iegm.tce.sp.gov.br/respostas.html>
32. ECA-SP. <https://iegm.tce.sp.gov.br/>
33. IBGE: Profile of Brazilian municipalities: 2017/IBGE, Coordination of Social indicators population. IBGE, Rio de Janeiro (2017). <http://portalods.com.br/wp-content/uploads/2018/07/perfil-dos-municipios-brasileiros-2017-IBGE.pdf>
34. Weiss, M. C., Bernardes, R. C., Consoni, F. L.: Smart cities as a new practice for the management of services and urban infrastructure: the experience of Porto Alegre. *Metropolis, Rev. Bras. Gest. Urban* 7(3), 310–324 (EPUB) (18 September, 2015). ISSN 2175–3369. <http://dx.doi.org/10.1590/2175-3369.007.003.AO01>
35. Brazil, Decree No. 7724 of 16 May 2012. Regulates Law No. 12,527, of November 18, 2011, which provides for access to information under item XXXIII of art. 5, item II, § 3 of art. 37 and § 2 of art. 216 constitution. Official Gazette of [the] Federative Republic of Brazil. Brasília, DF, Extra Edition, vol. 94, p. 1 (16 May, 2012)
36. Ministry of Science, Technology, Innovation, and Communications—MCTIC: Brazilian Digital Transformation Strategy—E-digital (2018). <http://www.mctic.gov.br/mctic/export/sites/institucional/estrategiadigital.pdf>